![TUM logo]

TECHNISCHE UNIVERSITÄT MÜNCHEN

TUM School of Engineering and Design

Motion Comfort:

Physical-Geometric Optimization of the Vehicle Interior to Enable Non-Driving-Related Tasks in Automated Driving Scenarios with the Focus on Motion Sickness Mitigation

Dominique Kevin Bohrmann

Acknowledgment/Danksagung

Abstract

Within the irresistible development of transportation, automated vehicles will play a crucial role in far-seeing mobility concepts and might change the way people are traveling in future. Among the major aspects of future road transportation is the promise of increasing one's efficiency while being driven. To achieve this challenging goal, non-driving-related tasks (NDRTs) such as eating, texting, working, or relaxing during the journey have to be met by automated vehicles. According to future interior concepts, the vehicle becomes a new living space with several innovative features for enabling and supporting such activities. The primary weakness of the described development, however, is the human itself. Many occupants react with symptoms which can include pallor, dizziness, headache, sweating, or vomiting while performing visually demanding NDRTs when being exposed to mechanical vibrations. This phenomenon of the human organism has been known for many centuries and given the term kinetosis (motion sickness or in this particular case carsickness). Different factors contribute to the likelihood of experiencing such symptoms. In fact, interindividual susceptibility constitutes one of the main human-related aspects which are essential for the occurrence of motion sickness. Furthermore, the duration and type of motion stimuli determine the nature and severity of symptoms as well. To prevent motion sickness in automated vehicles, it is mandatory to understand how various vehicle characteristics affect the prevalence of the physiological syndrome. To this end, the current elaboration addresses three main research areas linked to this particular issue in human-machine-collaboration. As a first priority, vehicle-related treatments of the interior are investigated. To ensure viable transferability of results, vehicle driving experiments were carried out on a test track. Among the key determinants observed were the effects of seat configuration and vision. The analyses indicated that reclined postures lead to a significant decrease in motion sickness symptoms. This effect already becomes apparent due to slight backrest adjustments while extended inclination angles provide further advantages in motion sickness mitigation, at least for people who are highly sensitive to motion sickness. To evaluate the recommended backrest inclination regarding subjective comfort, further investigations had been conducted on a dynamic simulator. Here, the participants were exposed to synthetic noise and measured road signals when being in different sitting and lying positions. As a result, improvements in motion comfort by means of extended backrest inclinations can be observed. Furthermore, fundamental biomechanical differences in head motion as a result of backrest inclination are reported. Furthermore, the positive effect of outside view and interior light stimulation to alleviate motion sickness can be stated. Both effects are present even if visually demanding NDRTs had to be performed during the entire trial. Given that motion sickness is evaluated mostly by subjective measures the second research question addresses aspects of physiological and behavioural objectification. Even if no ubiquitous criterion could be detected, the change in heart rate and core body temperature shows sensitivity to motion sickness. The third research question examined the change in human performance due to expressions of malaise and nausea. Here, only tendencies in the relationship between motion sickness and human performance e.g., reaction time or ability to concentrate, can be reported.

Zusammenfassung

Mit der Entwicklung des automatisierten Fahrens wird sich die Mobilität der Zukunft nachhaltig verändern. Der Fahrer wird zum Passagier und kann sich während der Reise fahrfremden Tätigkeiten, wie Essen, Entspannen, Lesen oder gar Arbeiten zuwenden. Um die Bedarfe und Anforderungen dieser neuen Nutzungsszenarien zu erfüllen, muss jedoch das Fahrzeug sowie dessen Innenraumkonzept nach anderen Prämissen gestaltet und entwickelt werden. Es gilt den Menschen in den Fokus der Entwicklung zu stellen, da dieser besondere Wünsche, aber auch Restriktionen mit sich bringt, die essenziell für die beschriebene Fahrzeugautomatisierung sind. Beispielsweise reagieren viele Insassen mit Symptomen von Blässe, Schwindel, Kopfschmerzen, Schwitzen sowie Erbrechen, wenn sie visuell beanspruchenden Nebentätigkeiten während der Fahrt im Automobil nachgehen. Dieses Phänomen des menschlichen Organismus ist bereits heute weitreichend unter dem Fachterminus Kinetose (Reisekrankheit oder auch Motion Sickness) bekannt. Durch die steigende Fahrzeugautomation beziehungsweise den damit einhergehenden neuen Nutzungsszenarien ist jedoch mit einer Zunahme der Prävalenz von Kinetose zu rechnen. Um entsprechende Manifestationen in automatisierten Fahrzeugen vorzubeugen, gilt es die Wirkzusammenhänge verschiedener Fahrzeugeigenschaften auf Passagiere bei fahrfremden Tätigkeiten zu erforschen und zu verstehen. Die folgende Ausarbeitung befasst sich daher mit drei Forschungsbereichen, die mit diesem Thema der Mensch-Maschine-Kollaboration einhergehen und von besonderer Relevanz sind. Der Fokus liegt auf den physikalisch-geometrischen Merkmalen des Fahrzeuginnenraums, die sich mit steigender Automation voraussichtlich ändern werden und zur Beeinflussung von Reisekrankheit beitragen können. Um eine angemessene Übertragbarkeit der Ergebnisse zu gewährleisten, werden reale Fahrversuche auf einer Teststrecke durchgeführt. Unter anderem werden die Auswirkungen verschiedener Sitzkonfigurationen und visueller Stimulationen unter Bedingungen definierter Nebentätigkeiten untersucht. Es zeigt sich, dass eine zurückgelehnte Körperhaltung zu einer signifikanten Linderung von Reisekrankheit führt. Dieser Effekt wird bereits durch geringfügige Anpassungen der Rückenlehne deutlich. Um die empfohlenen Anpassungen der Sitzlehne hinsichtlich des subjektiven Komforts zu bewerten, werden weitere Untersuchungen auf einem dynamischen Fahrsimulator durchgeführt. Hier werden die Probanden synthetischen Rauschsignalen sowie aufgezeichneten Stuckerfahrten in unterschiedlichen Sitz- und Liegepositionen ausgesetzt. Infolgedessen können Verbesserungen des Bewegungskomforts durch eine stark zurückgelehnte Liegepostion beobachtet werden. Weiterhin werden im Zuge der Simulatoruntersuchung grundlegende biomechanische Unterschiede in der Kopfbewegung als Resultat der veränderten Körperlage beschrieben. Der Einfluss des peripheren Sichtfeldes sowie der gezielten Animation der Innenraumbeleuchtung zeigt sich in Realfahrten ebenfalls als kinetosemildernd. Die beiden untergeordneten Forschungsgegenstände definieren sich über die Objektivierung sowie die potenzielle Veränderung der Leistungsfähigkeit bei eintretender Reisekrankheit. In beiden Fällen sind zwar signifikante Ergebnisse und systematische Korrelationen erkennbar, jedoch ist eine generalisierbare Aussage aufgrund der speziellen Versuchsaufbauten, der hohen Inter- und Intraindividualität sowie der begrenzten Datengrundlage nicht ohne Weiteres möglich.

Contents

List of Figures

Chapter 8

Chapter 9

Chapter 12

List of Tables

List of Abbreviations

		A
ACC	Adaptive cruise control	
ACh	Acetylcholine	
ACTH	Adrenocorticotropic hormone	
ADH	Antidiuretic hormone	
AIC	Akaike-Information-Criterion	
AMPA	α-amino-3-hydroxy-5-methyl-4-isoxazolepropionic acid receptor	
AVOR	Angular vestibulo-ocular reflex	
AVP	Arginine vasopressin	
		B
B	Respiratory cycles per minute	
BIC	Bayesian-Information-Criterion	
bpm	Beats per minute	
		C
CAN	Controller Area Network	
CCR	Cervico-collic reflex	
CGRP	Calcitonin gene-related protein	
		D
DA	Dopamine	
DoF	Degrees of freedom	
		E
ECG	Electrocardiogram	
EDA	Electrodermal activity	
e.g.	Exempli gratia	
ENK	Enkephalin	
Eq.	Equation	
		F
Fig.	Figure	
FMS	Fast Motion Sickness Scale	
		G
GABA	γ-aminobutyric acid	
GIF	Gravitoinertial force	
Glu	Glutamate	
Gly	Glycine	
		H
H	Transfer function	

HF	High frequency
hGH	Growth hormone
HMI	Human-Machine-Interface
hPRL	Prolactin
HR	Heart rate
HRV	Heart-rate-variability
Hz	Hertz

I

i.e.	Id est
ISO	International Organization for Standardization

K

KA	Kainic acid
km/h	Kilometer per hour

L

LCD	Liquid crystal display
LDT	Lateraldorsal tegmental nuclei
LED	Light-emitting diode
LF	Low frequency
LME	Linear-mixed-effects
Log Likl.	Log-Likelihood ratio

M

M	Mean
MN	Motorneurons
ms	Milliseconds
MSAQ	Motion Sickness Assessment Questionnaire
MSI	Motion Sickness Incidence
MSSQ	Motion Sickness Susceptibility Questionnaire

N

n	Number of
NA	Noradrenaline
NDRTs	Non-driving-related tasks
NMDA	N-methyl-D-aspartic acid
NN	Interbeat intervals
NVH	Noise Vibrations Harshness

O

ODD	Operational design domain
OKR	Optokinetic reflex

X

		P
PCRF	Parvocellular reticular formation	
PPT	Penduculopontine tegmental nuclei	
PSD	Power spectral density	
PWM	Pulse width modulation	
		Q
Q-Q	Quantile-Quantile	
		R
RMSSD	Root mean square of successive differences	
r_{xx}	Autocorrelation	
r_{xy}	Cross-Correlation	
		S
s	Seconds	
SAE	Society of Automobile Engineers	
SD	Standard deviation	
SDBB	Standard deviation of the respiratory cycle lengths	
SDNN	Standard deviation of interbeat intervals	
SgRP	Seat reference point	
SP	Substance	
sps	Sample per seconds	
ST	Somatostatin	
STFT	Short-Time Fourier Transformation	
		T
Tab.	Table	
TVOR	Translational vestibulo-ocular reflex	
		U
U.K.	United Kingdom	
U.S.	United States	
		V
VCR	Vestibulo-collic reflex	
VDI	Verein Deutscher Ingenieure	
VI	Vomiting Index	
VIF	Variance Inflation Factor	
VLF	Very low frequency	
VSR	Vestibulo-spinal reflexes	
		Additional Character
µm	Micrometer	
5-HT3	Serotonin	

Glossary

	A
Abdomen	The abdomen is also known as the stomach and is defined as the anatomical region between the thorax and the pelvis.
Agonist, Antagonist	Whereas an agonist binds to the receptor and initiates an effect within the cell, an antagonist, on the other hand, may bind to the same receptor but does not produce a response. Even more, instead, it blocks that receptor to a natural agonist. (Pleuvry, 2004)
Anorexia nervosa	Anorexia nervosa is defined as an eating disorder (Jacobi & Paul, 1991).
Anteroposterior	Anteroposterior comprises the terms anterior as well as posterior and means from front to back.
Area postrema	The area postrema is located at the caudal end of the rhomboid fossa in the brainstem and belongs to the vomiting center (Longatti et al., 2015).
Aura	An aura is a human perceptual disturbance mainly experienced in cases of epilepsy and migraine (Goadsby, 2007).
Axis-at-lantis joint (C1-C2)	The atlantoaxial joint is part of the upper neck between the first and second cervical vertebrae (Forbes & Das, 2021).

	C
Cardiac sphincter	The cardiac sphincter is defined as the muscular ring embracing the opening between the esophagus and the stomach (Merendino & Dillard, 1955).
Cerebellovestibular tract	The cerebellovestibular tract is a bundle of nerve fibers that runs from the cerebellum to the vestibular nuclei (Walberg, 1972).
Cerebral cortex	The cerebral cortex is the outermost layer of neural tissue of the human brain.
Cervical nerves	The cervical nerves are the spinal nerves from the cervical vertebrae in the eponymous segment of the spinal cord (Waxenbaum et al., 2021).
Cochlea	The cochlea is a part of the inner ear that resembles the shape of a snail shell and is the receptor field for the perception of hearing.
Cupula	The cupula is a gelatinous mass that overlies the hair cells of the ampullary crista of the semicircular canals in the inner ear (see chapter 3.2.1).

D	
Diaphragm	The diaphragm is a thin sheet of muscle between the thorax and the abdomen (Merrell & Kardon, 2013).
E	
Endolymph	The endolymph is a potassium-rich fluid contained in the membranous labyrinth of the inner ear (see chapter 3.2.1).
Epithelium	The epithelium is a membranous tissue that comprises protective layers of cells. It mainly covers internal and external surfaces of the body including its organs or blood vessels. (See chapter 3.2.1)
Excitatory neurons	Excitatory neurons increase the likelihood that the respective neuron will increase its firing rate (see chapter 3.2.1).
Exteroception	Exteroception means that the organism is sensitive to stimuli originating outside of the body (see chapter 3.2.3 and Araujo et al., 2015).
Extracranial	Extracranial means outside the bony dome that houses and protects the brain (Lokossou et al., 2020).
G	
Ganglion	A ganglion is a bundle of nerve cells that especially appears outside the brain or spine (see also Boycott & Wässle, 1974).
Gastric	Gastric is a medical term and is related to the stomach.
Glial cells	Glial, or also known as Neuroglial cells, provide major support for the nervous system and are also involved in homeostatic functions (Araque & Navarrete, 2010).
Gynecotropism	Gynecotropism describes the increased occurrence of certain diseases and (hereditary) syndromes in women.
H	
Homeostasis	Homeostasis describes the regulation of steady internal, physical, and chemical variables to maintain a stable metabolic equilibrium (Asarian et al., 2012).
Hyperglycemia	Hyperglycemia is the medical term for high levels of sugar, or glucose, in the blood (Giugliano et al., 2008).
Hypothalamus	The hypothalamus is a part in the front of the brain that links the nervous system to the glands in the body and controls its functions.

Hypotension	Hypotension is low blood pressure, which is defined as the force of blood pushing against the walls of the arteries as the heart pumps (Simjanoska et al., 2018).
Hypothermia	Hypothermia is a drop in body temperature below 35 °C, in which shivering and mental confusion occur as side effects (Reuler, 1978).
Hypoxia	Hypoxia is a condition in which the body or some regions of the body parts are deprived of adequate oxygen supply (Brahimi-Horn et al., 2007).

I

Inflammation	Inflammation is defined as a systemic reaction of the human organism to injury or infection (L. Chen et al., 2018).
Inhibitory	Inhibition is the counterpart to the excitatory effect and means stopping or slowing down (see chapter 3.2.1).
Interoception	Interoception is defined as the sense that provides information of the internal state of the body (see chapter 3.2.3 and Araujo et al., 2015).
Ipsilateral	Ipsilateral means to be located on the same side of the body.
Isovergence plane	Vergence is defined as movements by the eyeballs toward or away from each other, while an isovergence surface of fixation is built on the restriction that the position of each eye was constrained to a plane (Mok et al., 1992).

L

Luteinizing hormone	The Luteinizing hormone is one essential element that controls the reproductive system and is produced by the pituitary gland (Nedresky & Singh, 2021).

M

Macula (saccular/utricular)	The macula utricular and saccular are the two otolith organs in the inner ear and are relevant for sensing linear motion (see chapter 3.2.1).
Mastocytosis	Mastocytosis is a form of mast cell disease (Akin, 2020).
Mediolateral	Mediolateral describes a direction from side to side or in some cases from median to lateral.
Medulla	The medulla is the technical term for bone marrow.

Muscarinic neurotransmitters	Muscarinic neurotransmitters are acetylcholine receptors that play important roles in the parasympathetic nervous system (Enz, 2007).

N

Neurohumoral transmission	Neurohumoral transmission is a process to manipulate the postsynaptic cell by released chemical agents (Middlekauff & Mark, 1998).
Nystagmus	Nystagmus is a vision condition of involuntary rhythmic eye movements, which is often associated with balance (see chapter 3.2.5).

O

Ophthalmoplegia	Ophthalmoplegia denotes paralysis of the ocular muscles (Lavin, 2014).
Otoconia	Otoconia are small calcium carbonate crystals located in the inner ear (top layer of the macula organs) and are involved in linear motion sensing (see chapter 3.2.1).

P

Parasagittal plane	Parasagittal is an anatomical expression, in which the body is split into unequal parts of left and right (see also the sagittal plane).
Parvocellular reticular formation	The reticular formation is a part of the brainstem, which forces sensory and motor functions as well as consciousness, while parvocellular pathways are particularly essential for vision (C.-S. J. Liu et al., 2006).
Pathogenesis	Pathogenesis is a technical term that describes the development of a disease.
Peptidergic	Peptidergic refers to nerve cells, in which neural impulses are transmitted through peptide molecules (Hatton, 2009).
Perilymph	The perilymph is an extracellular fluid, which fills the space within the bony structure and the membranous labyrinth of the inner ear (see chapter 3.2.1).
Perpendicular	A perpendicular axis points orthogonal (90°) to another line or surface.
Photophobia	Photophobia, or also known as light sensitivity, is the technical term that describes the intolerance of light (Katz & Digre, 2016).

Pituitary gland	The pituitary gland is a tiny organ located in the brain that is important in regulating and controlling vital body functions (Zaidi et al., 2020).
Plasmalemma	The plasmalemma is also known as a cell membrane, which covers the cytoplasm and regulates the flux of elements into or out of the cell (Herrnberger, 2015).
Proprioception	Proprioception is the sense of joint and limb positioning and relevant for sensing self-movement (see chapter 3.2.3 and Tuthill & Azim, 2018).
Protrusion	A protrusion is an anatomical tissue or excrescence that sticks out from a surface (see also Mogilner, 2006).

S

Sagittal plane	The sagittal plane describes the deviation of the human body in the longitudinal direction.
Single-nucleotide polymorphism	Single-nucleotide polymorphism is a single base-pair difference in the sequence of the DNA at a specific position in the genome (Brody, 2016).
Spatial frequency	Spatial frequency, as the reciprocal value of the wavelength, is essential to all kinds of imaging and addresses the number of pairing bars imaged within a certain distance on the innermost layer of the eyeballs (Diener et al., 1976).
Spatio-temporal	Spatial-temporal qualities manage information of space and time.
Stroma	The stroma is a matrix of chloroplasts that builds supportive tissue of an epithelial organ (Silberstein, 2001).
Sui generis	Suis generis is a Latin expression of not being like anyone or anything else.
Supraspinal	Supraspinal describes the areas above the spine.

T

Tachygastria	Tachygastria is a technical term that describes an increased frequency of contractions of the stomach.
Trabeculae	Trabeculae is a rod-shaped structure that separates organs into separate parts and anchors a framework of cells within a body (see also Lozupone & Favia, 1990).
Transverse	Transverse means being across or in a crosswise direction.

Trigeminovascular system	The trigeminovascular system is involved in the origin of migraine and consists of neurons that innervate cerebral blood vessels (Moskowitz, 1984).

V

Vasoconstriction	Vasoconstriction describes the effect of narrowing or constriction of the blood vessels (van Someren, 2011).
Vasodilatation	Vasodilatation describes the dilation or widening of the lumen of a blood vessel (Aschoff, 1944).
Vertebrobasilar vasculature	Vertebrobasilar describes the posterior portion of the brain, which is fed through the vertebral and basilar arteries, while vasculature is the technical term of vessel system (see also Akgun et al., 2013).
Visuovestibular	Visuovestibular combines vision and vestibular system, mostly relevant for (self-) motion perception.

1 Motivation

The world´s automotive industry has fundamentally changed the way people live by enabling almost unlimited mobility all around the world (Maxton & Wormald, 2009). Although this sector has grown into a firmly established economic entity within the capital markets, it has been deeply impacted by a series of unprecedented changes. "The car of the future must be networked, autonomous, emissions-free, and deliver the possibility of shared mobility", stated Ola Källenius, Chairman of the Board of Management of Daimler AG at the Consumer Electronics Show 2017 in Las Vegas (Daimler AG, 2016). This ambitious target leads to multiple and substantial transformations, which affect crucial parts of the car designing process. Among several trends that are going to shape the mobility of tomorrow, the increasing level of automation is considered to be one of the most challenging developments in the history of car manufacturing (Langheim, 2016).

Concerning the actual nature of active vehicle safety systems, the intervention of automation does not fully replace the responsibility of the driver in controlling at least parts of the driving task (SAE J3016:2021-04). To maintain safe vehicle control, the role of humans, either as an operator, monitor, supervisor, or at the very least as a passenger needs to be specified. Within the SAE J3016 taxonomy, concise definitions for six levels of driving automation, ranging from no driving automation (level 0) to full automation (level 5), deals with the degree of human engagement by addressing responsibilities at any given time. The following illustrations (see Fig. 1-1 and Tab. 1-1) describe the allocation of those responsibilities that go along with increasing road vehicle automation.

Level 0	Level 1	Level 2	Level 3	Level 4	Level 5
No Driving Automation	Driver Assistance	Partial Driving Automation	Conditional Driving Automation	High Driving Automation	Full Driving Automation

DRIVER SUPPORT FEATURES	AUTOMATED DRIVING FEATURES
The human driver constantly supervises the support features and monitors the driving environment	The automated driving system monitors the driving environment and can drive the vehicle (under limited conditions for L3/L4)

Fig. 1-1: Taxonomy of road vehicle automation.
Based on SAE J3016:2021-04; IPG Automotive (2021);
background-images modified from Daimler AG (2020): converted into a vector graphic

Tab. 1-1: Driver´s role in the SAE J3016 taxonomy.
Based on Seppelt et al. (2018)

SAE J3016	Vehicle Control Task[*]					Supervise Automation[*]		
	Longitudin. (Brake and Accelerate)	Lateral (Steer)	Monitor the environment	Monitor vehicle performance	Respond in an emergency	Monitor autom. performance	Respond to vehicle messages	Decide on automation use based on ODD[**]
Level 0	X	X	X	X	X			
Level 1	X	X	X	X	X	X	X	X
Level 2			X	X	X	X	X	X
Level 3					X		X	X
Level 4								X
Level 5								

* When automation has been engaged and is active; ** Operational Design Domain

Although today, advanced driver assistance systems, such as *adaptive cruise control* (ACC), emergency braking, or active lane-keeping assist, are available in modern vehicles, fully or at least highly automated driving (level 4 and 5) promise additional socioeconomic benefits (Bengler et al., 2021; Brenner & Herrmann, 2018). For example, Anderson et al. (2016) and Bagloee et al. (2016) emphasize that autonomous driving avoids accidents, promotes social justice, increases road capacity, optimizes land usage, and avoids environmental damage by lower vehicle emissions and better fuel economy.

1.1 User Expectations on Increasing Road Vehicle Automation

Apart from the aforementioned socioeconomic impacts, automated driving promises further individual advantages. From the user perspective, it is expected that autonomous driving is likely to increase comfort and productivity by allowing the passenger to engage in *non-driving-related tasks* (NDRTs) such as working, eating, reading, watching movies, or just resting (T. Becker et al., 2018; Hecht et al., 2020). Until today, NDRTs, or also known as secondary tasks, are included in the vehicle design with lower priority because of their side effects of distraction from the actual task of driving (Smyth et al., 2020; Y. Yang et al., 2019). In the future, when the control transfer of driving allows more freedom for all passengers, the vehicle design might change in a way that NDRTs are becoming more present within interior concepts (Diels & Bos, 2015; Golowko et al., 2017). This assumption is reinforced by many researchers (Herzberger et al., 2019; Schoettle & Sivak, 2014). In fact, according to investigations from Kyriakidis et al. (2015), drivers are willing to spend more time on complex NDRTs as the vehicle automation level rises. Especially, when drivers are no longer forced to constantly control or even monitor the trajectory of the vehicle, as it is in SAE automation level 4 and 5, visually demanding activities are more likely to occur in which the subject´s gaze deviates from the vehicle surroundings. Fig. 1-2 illustrates the results of the corresponding internet-based survey across 109 countries. The 5,000 respondents are representative of society's preference regarding NDRTs with increasing road vehicle automation.
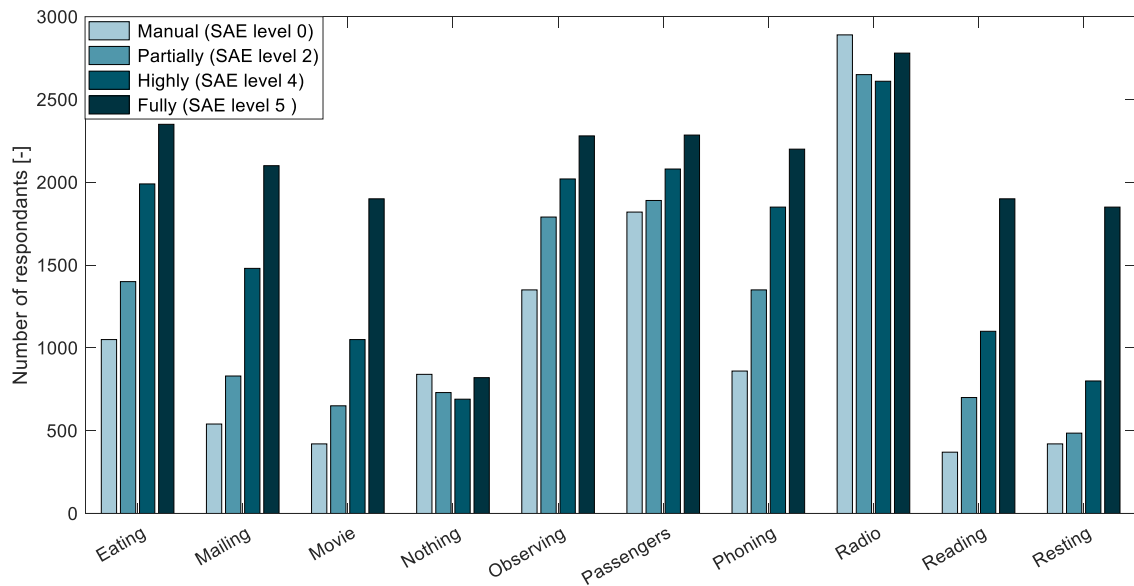
Fig. 1-2: Preference on NDRTs coming along with road vehicle automation.
Based on Kyriakidis et al. (2015)

To meet those various demands and user expectations, innovative interior concepts might be obliged, for example, to enable occupants to interact more easily with each other (Diels & Bos, 2016). Already in 2015 the Mercedes-Benz F015 show car and its immersive user interface illustrated some of these ideas and allowed a preview of the vision of future vehicle interior design (see Fig. 1-3). Within the transformation from a manual driver´s workplace to the next level of living space on wheels (Smyth et al., 2020), seating concepts may flexibly and situationally adapt to different individual preferences. Given that the automation is activated, the steering wheel can disappear into the dashboard and the pedals can move away from their original position to enable more space in the footwell. Empathic interfaces will allow operating vehicle functions by voice, gaze, or gesture control. Through digital devices, like screens being integrated into the door panel of the vehicle, entertainment, working, and reading seem to be possible in almost every condition.

Advanced User Interfaces are installed in the door panels

Vis-à-vis seating simplifies in-vehicle communication

Digital devices enable working and entertaining

Geometric adjustments allow new seat designs
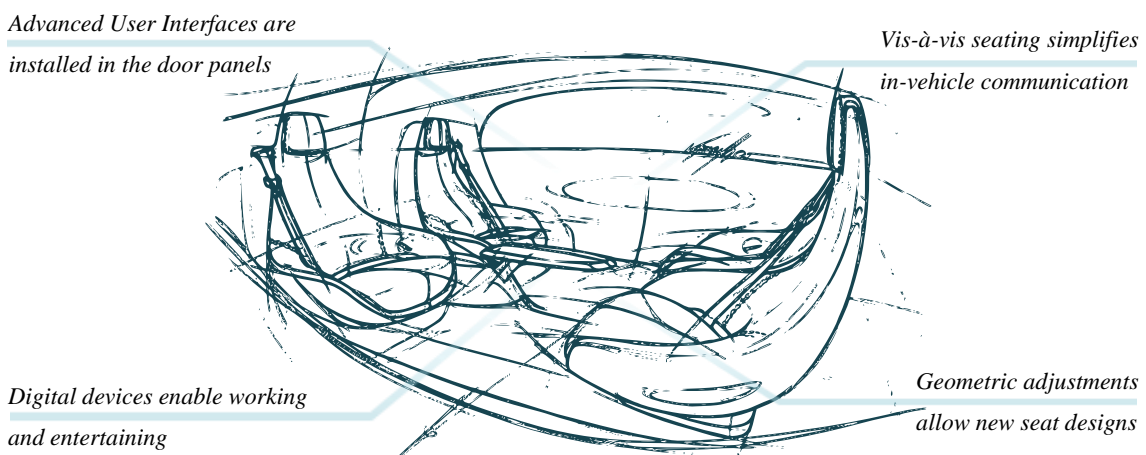
Fig. 1-3: Vehicle interior concept of the Mercedes-Benz F015.
Modified from Daimler AG (2020): converted into a vector graphic, colour changed and labeling added

3

Along with this accelerating evolution, research on human factors becomes increasingly important (Carsten & Martens, 2019; Nordhoff et al., 2019; Strömberg et al., 2019; Winter & Hancock, 2021; Woopen et al., 2018; Y. Yang et al., 2020). In particular, since the reservations on the benefits of driving automation still are ubiquitous and influenced by user acceptance (P. Liu et al., 2019; P. Liu & Xu, 2019; Roche-Cerasi, 2019).

1.2   Human Characteristics as Restraining Factor of Vehicle Automation

The physiological manifestation called motion sickness (also known as kinetosis - Greek: κινειν kīneîn, "to move") is one of the oldest protective reactions of the human organism and a widely experienced and well-documented phenomenon. Motion sickness in vehicles, or specified as carsickness, occurs when perception sensors of the human body are confronted with passive movements under conditions where incongruent motion perception information is present (Reason & Brand, 1975). This is mainly due to the loss of visual interaction with the actual outside world (Schmäl, 2013). Almost 70 % of the population has ever suffered from carsickness and it is expected to increase by use cases of highly automated or autonomous driving (Diels & Bos, 2016; Sivak & Schoettle, 2015; Wada, 2016).

For human perception, the visual and vestibular sensory channels are arguably the most relevant ones to provide information that is essential for driving (Lachenmayr et al., 1996; Rockwell, 1972). By assuming that in future occupants are going to be involved in visual activities, information about vehicle movements is then mostly perceived by vestibular inputs. Therefore, a lack of anticipation and increasing discrepancy between integrated sensory afferents with the prediction model provided by the internal neural store of the human brain results in not being in control of the actual and future vehicle dynamics (see chapter 3.2.6). In fact, this leads to the aforementioned increased risk of suffering from motion sickness. The unpleasant physiological expressions that come along with motion sickness, in turn, can prevent the driver from activating the automation, negatively affect customer acceptance, and, therefore, may limit the described potential of rising road vehicle automation (Sivak & Schoettle, 2015; Wada, 2016). Even if occupants do not undergo the cardinal symptoms of motion sickness, moderate manifestations might be already sufficient to influence the user experience (Cowings et al., 2001). By assuming that automated motion-control algorithms need to be designed in such a way that the prevalence of motion sickness is reduced to a minimum, it is evident that the expected decrease of traffic congestion might be affected by this tailored driving style. Due to the momentary nature of daily traffic situations, the majority of road accidents are linked to human errors while automated driving with its transition from controlling to monitoring may reduce the likelihood and severity of collisions by taking the driver out of the loop (Diels & Bos, 2016). Unfortunately, motion sickness may decrease individual performance, which might affect the ability to make an appropriate context-based decision e.g., during the take-over request from automated to manual control in an SAE level 3 driving mode (Britton & Arshad, 2019; Matsangas et al., 2014; Muth et al., 2006; Smyth et al., 2018). Furthermore, the after-effects of motion sickness like dizziness and exhaustion may also influence subsequent safety-relevant situations (Diels et al., 2016).

Although it is known that sensory and sensomotoric inputs play a major role in the development of the physiological syndrome, there are several theories regarding the etiology of motion sickness (Dobie, 2019, pp. 93–108). Consequently, some principles and underlying mechanisms have yet to be fully understood and, thus, demonstrate important research capability (Hromatka et al., 2015). Indeed, many researchers emphasize the importance of motion sickness research (Bronstein et al., 2020; Classen et al., 2021; Smyth et al., 2020), which can be evaluated by analyzing the emerging development of active patent families in the topic of carsickness (see Fig. 1-4).
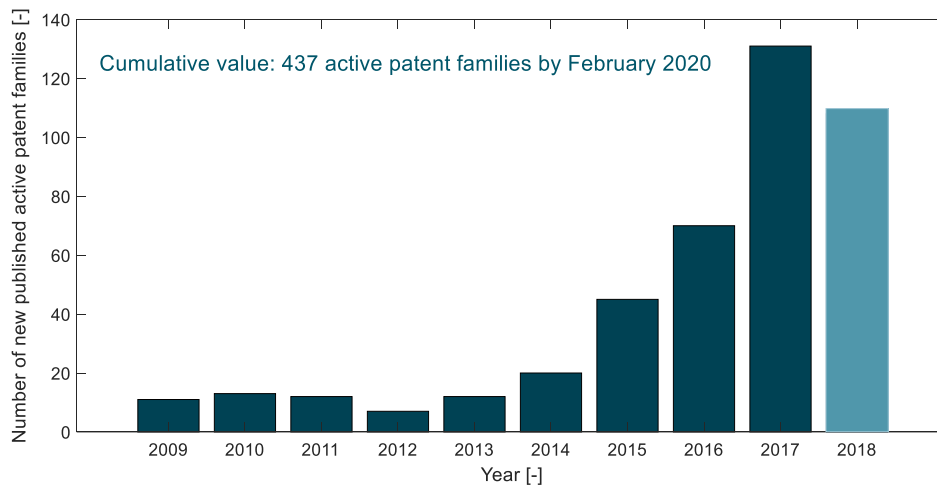
Fig. 1-4: Development of active patent families in the field of carsickness.
Based on ORBIS - Daimler AG (2020)

2 Outline and Structure

The current elaboration is divided into two main sections. Firstly, the theoretical part in which the framework of motion comfort and the criteria for the experimental setup are described. The second part includes the experiments, which tackle the research questions identified in relation to motion comfort based on four driving investigations and one additional simulator study. A summary of the entire structure is shown in Fig. 2-1.

At the beginning of the first section, basic information about the types and forms of motion sickness is described (see chapter 3.1). To understand the etiology of the physiological syndrome, the initial mechanism of perception including the functionality of the three motion senses as well as the corresponding neural processes and reflexes are presented. This information forms the foundation for different motion sickness theories that are described at the end of chapter 3.2. In the subsequent chapter 3.3, the physiological diagnostics and human responses that emerge within motion sickness are discussed. As motion sickness has been clearly defined at this juncture, dependencies and influencing factors are demonstrated accordingly. Next, three main motion sickness-related variables are highlighted, which are essential for the study design and the interpretation of its results. The first predictor reveals human-related findings, which are summarized in chapter 3.4 and contribute to the selection of subjects. The physical motion characteristic and the referring interaction to the subjective comfort feeling describe the exogenous input variable, which is relevant for the test setup (see chapters 3.5 and 3.6).

Subsequently, the outcome variable referring to the human organism e.g., the quantification of motion sickness, is described. At the end of the theoretical section, categories of countermeasures to avoid motion sickness are presented. From chapter 4 on, the focus shifts to the self-conducted examinations on motion comfort. Even if the aim of the five investigations addresses individual research topics, each experiment is linked closely with its neighbouring examination. Overall, three crucial areas can be identified, whereas adjustments of the vehicle interior to avoid motion sickness are particularly salient here. The subordinate research topics belong to the field of performance and objectification. In the area of motion sickness treatments, the results are clustered into vehicle-related physical-geometric countermeasures (see chapters 5 to 8) and further non-vehicle-related influencing factors (see chapter 9). The results of performance and objectification are summarized across all investigations and discussed in chapter 10. In order to collect deeper knowledge about motion comfort in advanced interior concepts, additional analyses with a biomechanical study (see chapter 11) accompanied by a multibody and several vision simulations were carried out too. Within chapters 12 to 15 the collected results are analyzed, discussed, and summarized in terms of carsickness and motion comfort. For further information concerning the structure and content of the conducted research investigations, please refer to chapter 4.
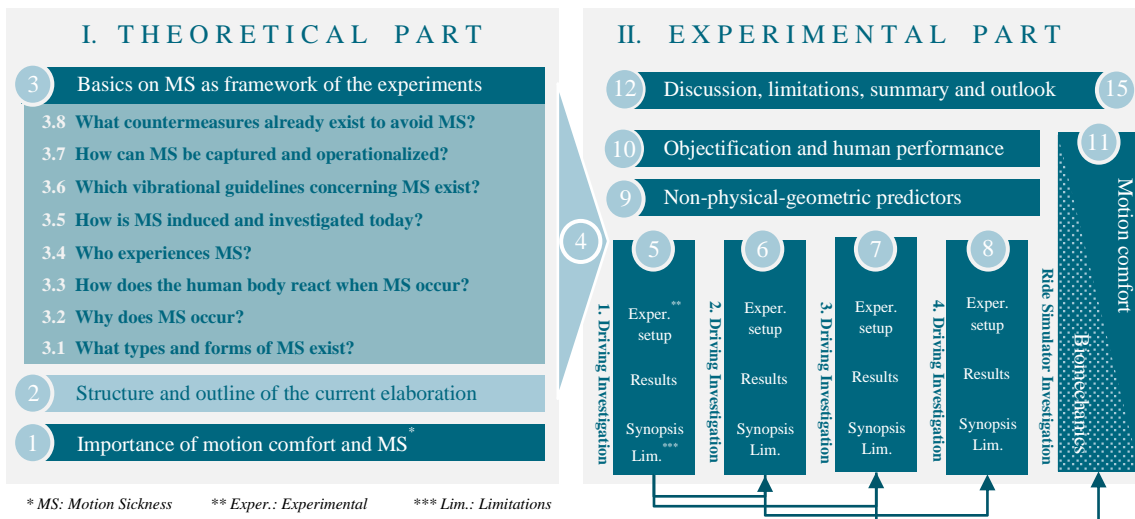
Fig. 2-1: Structure of the current elaboration.

3 Motion Sickness – A Natural Physiological Reaction

Circa 400 B.C., Hippocrates noted the common experience that traveling under passive motion conditions can lead to negative effects on human´s well-being (Braccesi & Cianetti, 2011; Megighian & Martini, 1980). Several centuries later, in 1881, Irwin introduced the term motion sickness. One famous incidence of nausea and vomiting during traveling has been reported in Napoleon´s war against Egypt in 1798 - 1801, where soldiers with high susceptibility to kinetosis were unable to engage in battle as a result of the after-effects of riding a camel (Huppert et al., 2017; Waldfahrer, 2008). Towards the assumption of naming, motion sickness is a natural response of the human organism to a peculiar motion stimulus, which, in turn, does not fulfill the requirements of a true sickness per definition of sui generis (Schmäl, 2013).

Until the dissemination of road transportation, the common expressions of motion sickness were mainly limited to syndromes of seasickness (Dobie, 2019, p. 52; Money, 1970). With increasing digitalization, further types of motion sickness have developed, for example in conditions where immersive artificial environments occur. Therefore, depending on the origin of stimuli, motion sickness can be divided into subgroups of physically induced forms of sea-, air-, train-, or carsickness and visually induced types like simulator or cybersickness (Benson, 2002, pp. 1066–1071; Förstberg, 2000b; Keshavarz et al., 2014). In cases of visual motion stimuli combined with the absence of expected vestibular inputs, for example in fixed-base simulators, researchers have defined the terms pseudokinetosis or pseudo motion sickness (Schmäl & Stoll, 2000). Apart from the common forms of motion sickness, extraordinary observations indicate that a small number of people have experienced malaise just by sleeping in waterbeds (Waldfahrer, 2008). Even during winter sports, forms of motion sickness have been reported. The so-called ski sickness with its pathophysiology-related vestibular overstimulation during dynamic cornering has been mentioned in previous studies (Häusler, 1995).

3.1 Forms of Transportation-Related Physically Induced Motion Sickness

In general, the severity and characteristics of motion sickness concerning different passive transportation modes depend on several variables, such as the origin of stimuli, duration of exposure, or the individual constitution of subjects (see chapters 3.4 to 3.6). Therefore, the following descriptions of motion sickness occurrence must be interpreted as indicators which are influenced by the prevailing selection of the experimental setup.

3.1.1 Seasickness

Seasickness is still an important issue in the maritime industry (A. Koch et al., 2016). In 1988, Lawther & Griffin surveyed the number of people suffering from seasickness while crossing the English Channel. Among 20,000 passengers, 7 % reported cardinal symptoms of seasickness. As many as 21 % showed slight manifestations in any unpleasant form of discomfort and malaise. By analyzing the body posture of passengers during the predominant low-frequency vertical-pitch oscillation, Lawther & Griffin (1986) just as Golding et al. (1995) discovered that lying down results in less seasickness than sitting upright. Given that seasickness increases with the magnitude, it was unexpected that stabilizers, which can reduce low-frequency roll motion, did not show the ability to improve the performance in a simulator examination (Morrison et al., 1991).

3.1.2 Airsickness

According to a survey by Rubin (1942), 11 % of trainee pilots suffered from feelings of malaise and nausea at a U.S. Air Force flying training detachment. Bagshaw & Stott (1985) reported an initial ratio of prevalence in airsickness of 20 - 30 % in pilot training with a decrease in malaise as adaption occurs (see also chapter 3.8.2). Apart from pilots, further risk groups among whom airsickness frequently emerges are engineers in maritime reconnaissance aircraft where extensive flight durations are carried out at low altitudes (Benson, 2002, p. 1066).

Due to the increasing likelihood of turbulent air layers in lower flights, as they occur during starting and landing maneuvers, a more critical situation is stated, which is characterized by low-frequency aircraft motion with high magnitudes (Money, 1970; Turner et al., 2000). In general, a much higher incidence of airsickness is to be assumed for military flights since typical maneuvers lead to high acceleration forces (Waldfahrer, 2008). Conversely, kinetosis among air passengers in civilian airplanes is expected to be more seldom, even though, here also a fraction of almost 100 % is reported during hurricane penetration, while the number of incidences decreases with the size of the aircraft (Lederer & Kidera, 1954 as cited in Dobie, 2019, p. 39). Within examinations by Turner et al. (2000), 923 passengers were surveyed on commercial airline flights about the prevalence of motion sickness. In summary, 0.5 % of the passengers vomited, 8 % showed symptoms of nausea, and 16 % reported symptoms of illness during the flight. Additional results are shown in Fig. 3-1, where Dobie et al. (2001) present the ratio of U.S. children reporting nausea and vomiting concerning different transportation modes. Here, traveling with airplanes indicates a high incidence of motion sickness. Potential inconsistencies with other examinations can be attributed to the frequency of experience based on the different transportation modes or to the simple fact that children show particular sensitivity to motion sickness compared to elderly people (see chapter 3.4.2).

3.1.3 Trainsickness

In general, it is reported that motion sickness occurs less in passively tilted trains than in actively tilted ones (Bromberg, 1996; Persson, 2008). In fact, with the development of tilting trains, the railway industry was suddenly faced with the implications of motion sickness. Before this technology was developed, motion sickness in non-tilting trains only amounted to less than 5 % of all passengers (Kaplan, 1964; Ueno et al., 1986). Due to the Coriolis cross-coupling motions in tilting trains, to compensate the centripetal force during turns, passengers complain about nausea and malaise more often (B. Cohen et al., 2011; Donohew & Griffin, 2007; Förstberg et al., 1998; Kufver & Förstberg, 2001). First, strong benefits were expected with active tilting suspensions. Indeed, by a cabin´s rotation of 8° trains can pass curves at an enhanced speed of up to 21 % while the thrusts of centrifugal acceleration on the cabin´s passengers during turning are reduced (B. Cohen et al., 2011). As a result, it had been considered that within this new evolution of rail journey the ride comfort reaches at least the same level as it is maintained in the original non-tilting trains. However, as mentioned, the coupled stimuli and time delay of actuators dramatically increased the number of people suffering from motion sickness up to 30 % (Bertolini et al., 2017; Ueno et al., 1986).

3.1.4 Carsickness

Given that this work focuses on the impact of increasing road vehicle automation on human factors, the severity of motion sickness when driving in buses or automobiles is of special relevance. Fundamental research had been conducted by Turner & Griffin (1999b), where both researchers evaluated 3,256 travelers on mainland U.K. bus or coach journeys. In summary, 28 % of the passengers verbalized expressions denoting illness, 12 % of nausea, while 1 % vomited during the journey.

Already in 1976, Fukuda discovered that the posture of a bus driver inclines toward the center of the curve when initiating turning, while the head and trunk of the passengers in the same bus incline toward the opposite direction, due to centrifugal forces. As a result, the bus driver, in contrast to the passengers, aligns his body with the up-coming force. With reference to this investigation, an indicator of motion sickness can be identified by passengers with increasing post rotational nystagmus (Fukuda, 1976). This natural anticipatory behaviour is one explanation why drivers do not get car-sick (Wada et al., 2012; Wada & Yoshida, 2016). In general, it is expected that around 3 - 4 % of passengers are affected frequently by expressions of kinetosis (Waldfahrer, 2008). Furthermore, about two-thirds of people traveling by car have experienced at least minor symptoms of motion sickness in the past (A. Koch et al., 2018). A survey by E. A. Schmidt et al. (2020) with 4,479 participants showed that 46 % of car occupants were treated for expressions of carsickness in the past five years, while 59 % have experienced the physiological syndrome at least once during the course of their lives.

In 2013, Perrin et al. investigated requirements provoking motion sickness in 85 rally car co-drivers of whom 21 participants were women. The subjects surveyed their experience with carsickness. By analyzing typical situations in which motion sickness principally occurs reading a book during driving exposure and sitting on the rear seat were most frequently cited as examples of when this occurred. Interestingly, changes of landscape recorded by the peripheral vision of the co-drivers were recognized only by 31 % during the task of reading. This effect, however, does not draw a clear picture in terms of motion sickness within the elaboration. Even if heterogeneity was observed within environmental conditions, Perrin et al. (2013) found clear subjective risk factors provoking motion sickness with stress, on-board smells, and on-board temperature. Overall, stress response might impact the neurochemistry of motion sickness concerning individual susceptibility (Grunfeld & Gresty, 1998; Zwerling, 1947). To quantify the occurrence of motion sickness with increasing road vehicle automation, Sivak & Schoettle (2015) constructed a survey performed by 3,255 adults in the U.S., China, India, Japan, the U.K., and Australia. The data indicates that approximately 6 - 10 % of respondents in the U.S., China, and India would expect often, usually, or always manifestations of motion sickness. In Japan, the U.K, and Australia the percentage ranges between 4 and 7 %. Furthermore, 6 - 12 % of Americans riding in automated vehicles would be expected to experience severe or at least moderate manifestations of carsickness at some time during their journey. Similar results can be found for the Chinese. In comparison, Indians show the greatest likelihood of experiencing moderate to severe expressions of carsickness with 8 - 17 % of all rides that are attributed to some kind of nauseogenic manifestations.

The values that are given in Fig. 3-1 illustrate average scores of young children from the U.S., ranging from 9 - 18 years, showing their experience of motion sickness under different transportation modes. It must be mentioned that the number of traveling experiences made in trains and cruise ships is considerably lower than for the remaining motion conditions (Persson, 2008). One additional and fundamental limitation had also been noted by Persson (2008) who postulated that the results by Dobie et al. (2001) take the average over nonlinear scales, which might lead to incorrect evaluations.
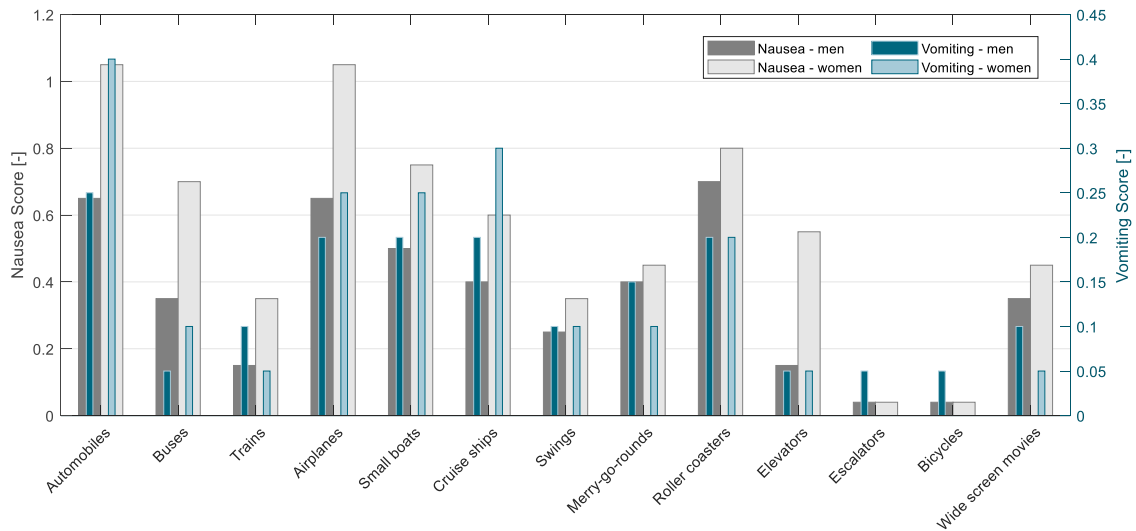
(0=never, 1=rarely, 2=frequently, 3=always)
Fig. 3-1: Average nausea and vomiting experience in U.S. children.
Based on Dobie et al. (2001)

3.1.5 Space Motion Sickness

Not only does physically induced motion sickness occur under passive motion stimuli on earth, it is increasingly being reported that also astronauts in space are suffering from motion sickness within the first three days of orbital flight (Heer & Paloski, 2006; Lackner & DiZio, 2006). This is due to the lack of gravity force, which leads to unaccustomed perception signals detected by the apparatus of equilibrium, or better known as the vestibular system (Russomano et al., 2019; Thornton & Bonato, 2017, pp. 31–54; Wotring, 2012). Until that time, the workload has to be reduced due to the inability to fulfill operational tasks (Dobie, 2019, p. 44; Jennings et al., 1988). The technical term space adaption syndrome, also known as space motion sickness, reports symptoms of kinetosis like cold sweating, nausea, or vomiting, which is experienced by almost two-third of the crewmembers in space (J. R. Davis et al., 1988; Lackner & DiZio, 2006). Since typical manifestations are limited to mild symptoms of the central nervous system, the space adaption syndrome is considered not to be involved in gastrointestinal complaints, as it is reported by other forms of kinetosis (Wotring, 2012).

3.2 Etiology of Motion Sickness and its Relationship to Human Perception

To understand the principles of motion sickness, the pivotal role of perception with its receptors and the neural network must be considered in the first instance. Perception is defined as the process of recognizing, organizing, and interpreting sensory information to represent a mental model of the surrounding world (Bos & Bles, 2002; Reason, 1978). In fact, human perception rather differentiates between subjects and is affected by physical just as mental abilities, body posture, and duration of exposure (J. J. Arnold & Griffin, 2018; Beard, 2012; Decker, 2009). However, principles like the Weber-Fechner law, which is explained in chapter 8.3, determine guidelines on the link between objective measurements and subjective sensation. Fig. 3-2 shows humans´ multisensory physiological system, which is involved in perception and provides the human apparatus with information about the vehicle dynamics interacting with the motion environment.

I Vision
II Audition
III Vestibular

IV Somatosensoric,
proprioception

V Haptic, tactile

Vehicle dynamics	Sensory channels				
	I	II	III	IV	V
Position (lateral and longitudinal)	X				
Velocity (longitudinal)	X	(X)			
Velocity, side slip angle (lateral)	X	(X)			
Acceleration (longitudinal)		(X)	X	(X)	X
Acceleration (lateral)		(X)	X	(X)	X
Angle (pitch, roll, yaw)	X				
Angular velocity (pitch, roll, yaw)	X		X		
Steering wheel angle	X			X	
Steering torque				X	X

Fig. 3-2: Sensory channels of a driver to gain motion perception.
Based on Decker (2009, p. 22); image: modified from Daimler AG (2020)

Driving activities, such as keeping the vehicle within the lane, can be subsectioned into a generalized information process consisting of perception, sensor fusion inclusive processing, and realization (Wolf, 2009, pp. 50–53). The individual characteristics are mainly influenced by the type of task and the possible control strategy. As outlined by Decker (2009), in the first level, five receptors accomplish the sensation apparatus of the human being to detect the actual state of self-motion in a moving environment. As previously stated, optokinetic signals from the visual sense deliver the most important information for perceiving motion characteristics in driving situations, such as the position and velocity of the vehicle (Rockwell, 1972; Wolf, 2009, p. 54). Accelerations, by contrast, are mainly perceived by the vestibular system. In general, independent sensory information of only one modality certainly might be insufficient for a suitable motion perception (Farkhatdinov et al., 2019b). Therefore, the visual and vestibular senses, with their high information retrieval, combined with tactile and audition inputs enable a proper representation of the external world.

According to Heißing et al. (2000), kinesthetic thresholds vary especially in angular stimuli since pitch and roll motion indicate thresholds between 0.1 - 0.2 $°/s^2$, whereas yaw motion shows a wider range of 0.05 - 5 $°/s^2$. Within translational motion, however, longitudinal (0.02 - 0.8 m/s^2), lateral (0.05 - 0.1 m/s^2), and vertical (0.02 - 0.05 m/s^2) directions show fewer differences in human sensitivity between each other (Bubb et al., 2015, p. 97). Even the stimulus itself contributes with its characteristics of frequency and magnitude to the perception performance (ISO 2631-1:1997-05). If single sensory inputs are absent, the internal weighting of the remaining senses adapts within the multisensory integration process to provide the highest possible accuracy in perception (see Fig. 3-3). Beyond the consideration of multisensory capturing, Fig. 3-3 points out the comparisons of single and multiple modality thresholds involving visual and body motion perception. Furthermore, regarding the SAE J182, the motor vehicle three-dimensional reference system, also known as the coordinate system, is described within this illustration. This generic representation provides fundamental directional information which is valid for the entire elaboration, especially for the experimental part from chapter 4 onwards.
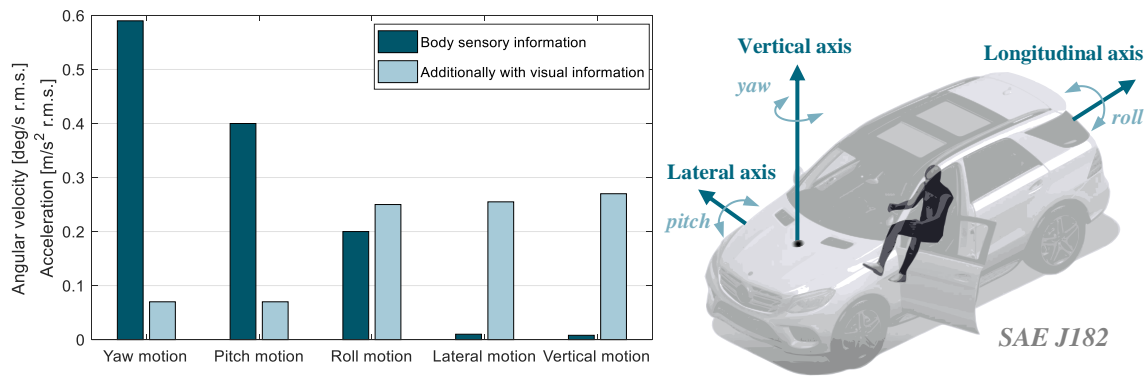
Fig. 3-3: Perception threshold depending on the type of sensory channel (left); vehicle coordinate system (right). Left: based on Muragushi et al. (2006); right: based on SAE J182:2020-11; image: modified from Daimler AG (2020)

The perception threshold of the body sensory information, or in more precise terms the haptic-kinesthetic system, seems to be comparatively low for vertical and lateral linear movements when they do not receive any visual information about the exogenous motion. The perception thresholds for pitch and yaw motion, however, are lower with combined motion sensation rather than with pure haptic-kinesthetic information. As a result, additional visual information leads to higher sensitivity in cases of vehicle movements characterized by distinct pitch and yaw motion, while contrary effects are reported for linear motion conditions.

In the case of straight-line driving, the command variable in steering torque equals zero. Remarkably, investigations have shown that drivers with moderate vehicle speed induce micro-oscillations in driving style, even on entirely straight routes (Timpe et al., 2000). This phenomenon can be explained by assessing Fig. 3-4, illustrating the steering wheel angle at which a noticeable perception event is stated. This evaluation is presented for different modalities. The calculation is based on an average mid-class vehicle with a dynamic visual resolution for the viewing angle of $\sigma_{min} \approx 2/s$ and a minimally perceptible acceleration of $b_{min} \approx 0.008$ m/s^2 (Bubb et al., 2015, p. 48; Lindsay & Norman, 1973; Stewart, 1971). Until the velocity of approximately 45 km/h, the visual sense shows greater sensitivity on lateral movements, whereas upon 45 km/h the kinesthetic receptors show higher sensitivity e.g., accuracy in motion sensing.
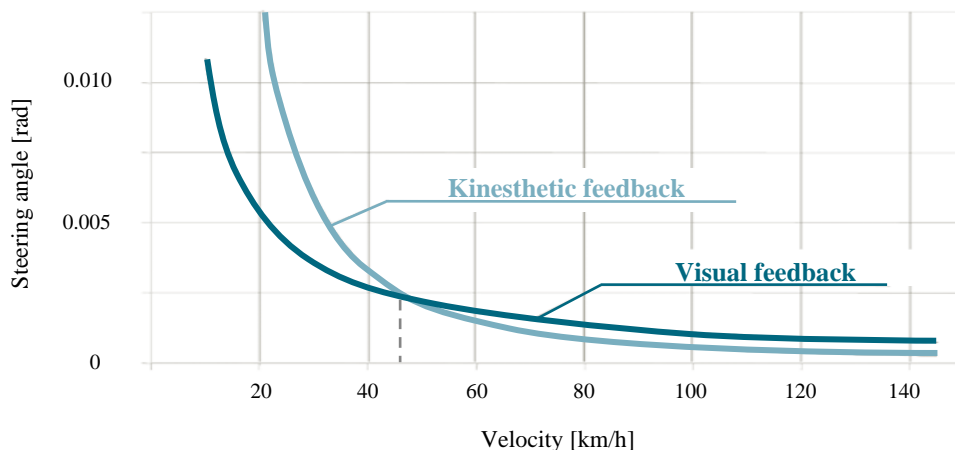
Fig. 3-4: Perception threshold as a function of velocity and human feedback system when applying lateral force. Modified from Bubb et al. (2015, p. 49): translated into English and colour changed

As visual NDRTs increase, such as expected during high-level automation modes, the amount of information provided by the human optokinetic sensor decreases. Consequently, the presence of the vestibular apparatus increases in such situations. This organ is already integrated into several fundamental regulating functions of the human body (Baker et al., 1985; Farkhatdinov et al., 2019b; Magnus, 1924). Indeed, the vestibular system is essential in stabilizing gaze as well as maintaining head and body posture by triggering an autonomic response, such as the vestibulo-ocular and the vestibulo-collic reflex (see chapter 3.2.5).

3.2.1   Vestibular System

The peripheral vestibular organs are essential for the development of motion sickness (Deepak et al., 2021; Kennedy et al., 1968; Money, 1970; Reason & Brand, 1975) and, consequently, play a major role in the current elaboration. Their main function involves revealing the detection and decomposition of forces acting on the head in space (Lee & Kaylie, 2013). Due to three senses, located in the semicircular canals, the human body can monitor angular motions, while two organs called otoliths (saccular and utricular) capture linear acceleration (Hamann, 1994). Neuron fibers codify and connect these five receptors with the brainstem and terminate in the vestibular nuclei (see chapter 3.2.4). Here, further perception inputs from somatosensory and visual senses are received. The frequency of physical stimuli in vestibular sensation ranges between 0 - 20 Hz (Goldberg et al., 2012, 83).

Anatomy of the Vestibular Labyrinth

Each inner ear consists of a cochlea, three tubes, and sacs-shaped channels, which build the bony structure of the vestibular system covered by the membranous labyrinth. Whereas the membranous is comprised of a potassium-rich extracellular fluid called endolymph, the interspace to the bony structure is filled by the more common sodium-rich perilymph, an extracellular fluid with less K^+ concentration. In general, the membranous and bony labyrinth are linked by connective-tissue trabeculae. As outlined by Iurato et al. in 1972, at the five receptors, however, a matrix of hair cells on top of a connective-tissue stroma, through which blood vessels and three types of nerve fibers penetrate, separate the epithelium from the sensory area, called neuroepithelium. The three types of nerve cells are separated into afferent fibers from bipolar cells of the vestibular ganglion, efferent fibers entering the brainstem, and autonomic fibers coming from the ipsilateral superior cervical ganglion. The semicircular canals with their curved ducts (tubes) enter the utricle and are arrayed approximately orthogonal to each other. Therefore, according to the orientation of the resulting planes, the semicircular tubes can be divided into one horizontal, also known as lateral, and two vertical (anterior and posterior) canals. Across the circular path, an endolymphatic continuity exists, interrupted at the ampullae (crista ampularis) by an equal density, elastic gelatinous structure at the neuroepithelium. This structure is called cupula and is fundamental in detecting angular head motion. (Goldberg et al., 2012, pp. 23–44)

In squirrel monkeys, for instance, the fluid volume in the lateral ampullae is about 50 % greater than in the lateral semicircular duct (Igarashi et al., 1981). Although there are interspecies variations, such as canal dimensions, the mechanical function of the labyrinth remains unchanged (Urciuoli et al., 2020). The structure of the labyrinth is illustrated on the left-hand side of the following Fig. 3-5. On the opposite side, the deflection of the cupula is shown as the major element for detecting angular motion. As previously mentioned, the crista ampularis is known as an essential element of the semicircular canals and is comprised of hair bundles, hair cells, and supporting cells.
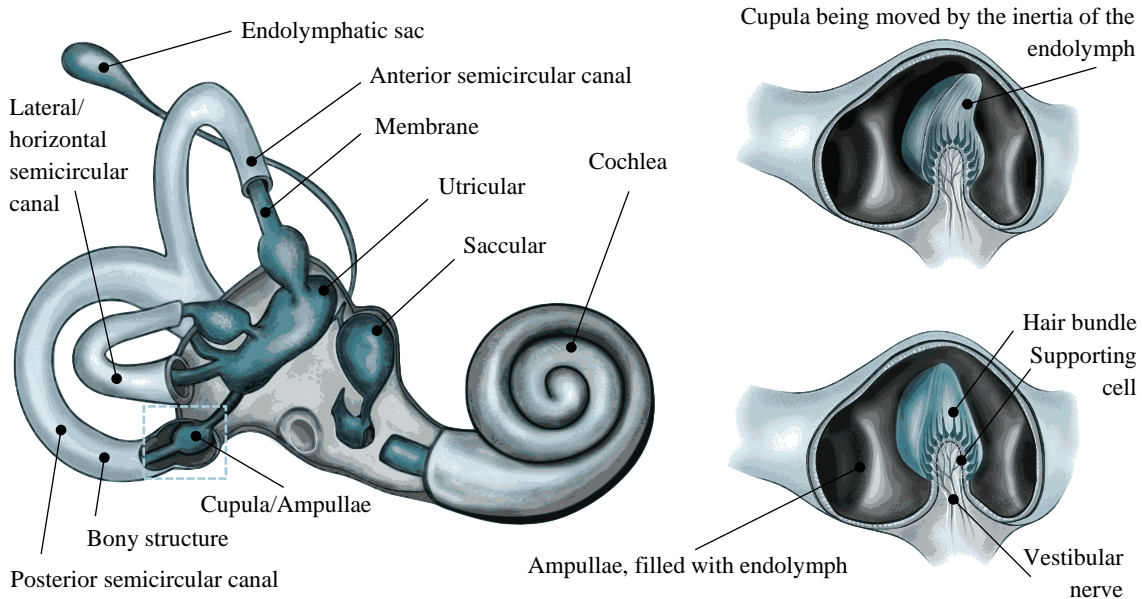
Fig. 3-5: Anatomy of the vestibular organ (left); mechanoreceptor of angular motion (right).
Based on Araújo et al. (2021)

Hair Cells as Mechanosensitive Receptors in Motion Sensation

An important element in motion sensation is attributed to hair cell projections, which respond to mechanical stimuli by a modulation in transmitter release. Within the process of converting physical force into an electrical signal, also known as the mechanoelectrical transduction process, a rigid, actin-based structure anchored into the cellular surface is required. This structure is called stereocilia or microvilli and couples physical displacement to depolarization of membrane potential by manipulating transduction channels as illustrated in Fig. 3-10. (McGrath et al., 2017)

Each hair bundle, consisting of 20 - 100 stereocilia, implies a polarization axis towards an eccentrically located, motile protrusions structure, called kinocilium (Goldberg, 2016, p. 1019). According to the mechanoelectrical mechanism, stereocilia are arranged to a scaling principle, in which the length of cilia successively decreases with distance to the kinocilium (see Fig. 3-6 - left). To transmit motion through the hair cell, an extracellular filament (tip link) joins a stereocilium to its next taller ranked unit (Kachar et al., 2000). Tip links are shown in Fig. 3-6 and are likely to be involved in the transduction process. According to Holt & Corey (2000), there are two models for hair cell adaption which are affected by tip link intervention (see A and B of Fig. 3-6).

14
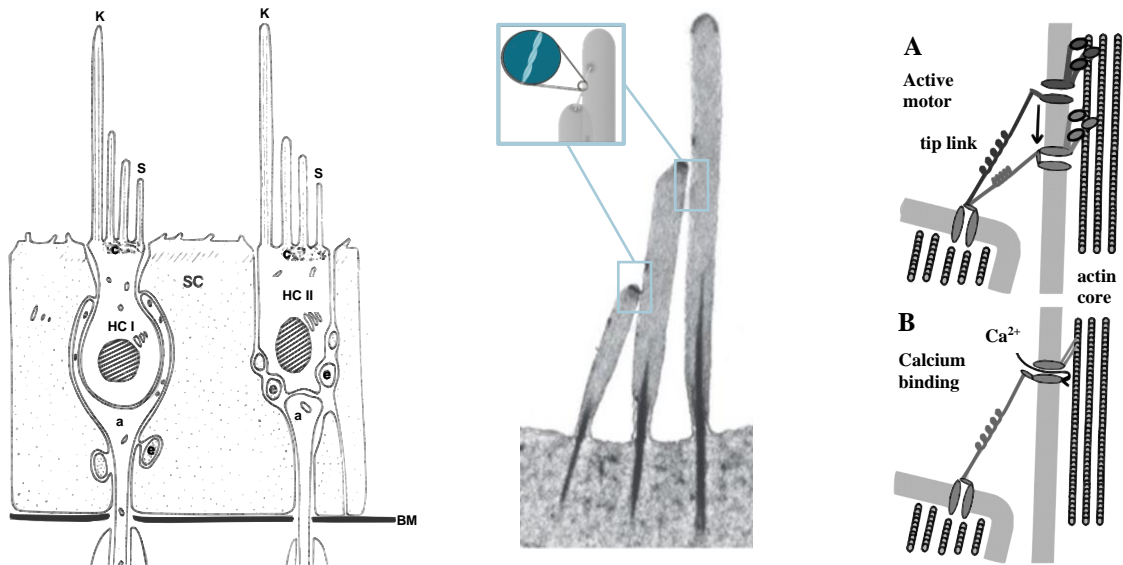
Fig. 3-6: Type I and type II hair cell (left); kinocilium and stereocilia (middle); tip link interaction (right). Left: modified from Lee & Kaylie (2013, p. 234): labeling changed; middle: Kachar et al. (2000); Fettiplace & Hackney (2006); right: modified from Holt & Corey (2000): labeling changed

Firstly, the active motor model, in which the motor complex is defined as a continuous effort of the upper tip link forced to increase its tension by climbing up the coupled stereocilium. In cases of positive deflection of hair bundles, the motor is unable to withstand the heightened tension and slips down the adjacent stereocilium, resulting in a decrease of tip-link tension and closure of channels. Furthermore, due to the flux of Ca^{2+} through open channels, the amount of slipping ratio increases. In fact, when the hair bundle is bent in the opposite direction, the motor complex can climb and regain tension while reopening channels. However, there is evidence that some mechanical properties, like the high stiffness of the cadherin element, might not fulfill the requirements of the described gating spring mechanism (Géléoc & Holt, 2003; Pickles et al., 1984). By contrast, due to intercellular extensions, the tip links are assumed to be more bendable and, thus, support the above-mentioned theory (Kachar et al., 2000; Vollrath et al., 2007).

In the second model, the calcium-dependent closure mechanism proposes that Ca^{2+} ions enter the stereocilia and dock onto or near the channel protein. Consequently, a closure of the channel is initiated, whereas negative deflection leads to a decrease in calcium concentration and reduction of channel inhibition. In response to persistent stereocilia bending, the cell receptor current declines or adapts through three different kinds of effects. Firstly, due to the decrease in sensitivity a greater deflection is required to open more channels. Secondly, an inactivation limits the number of channels available to be opened. Lastly, the stimulus-response relationship is shifted without a reduction in channel sensitivity. (Holt & Corey, 2000)

Each hair bundle in the cupula shows the same orientation, while the alignment within the otoliths builds a reversal line, representing the middle of the striola (Lee & Kaylie, 2013). The striola is a narrow section characterized by the change in hair cell polarization (Dimiccoli et al., 2013). In the utricular macula, the hair cells are oriented with their kinocilium facing the striola, whereas in the saccular the bundles are oppositely oriented with the kinocilium pointed away from the dividing line (Baloh & Honrubia, 1979).

The striola for both otoliths, saccular as well as utricular, are shown in Fig. 3-7.
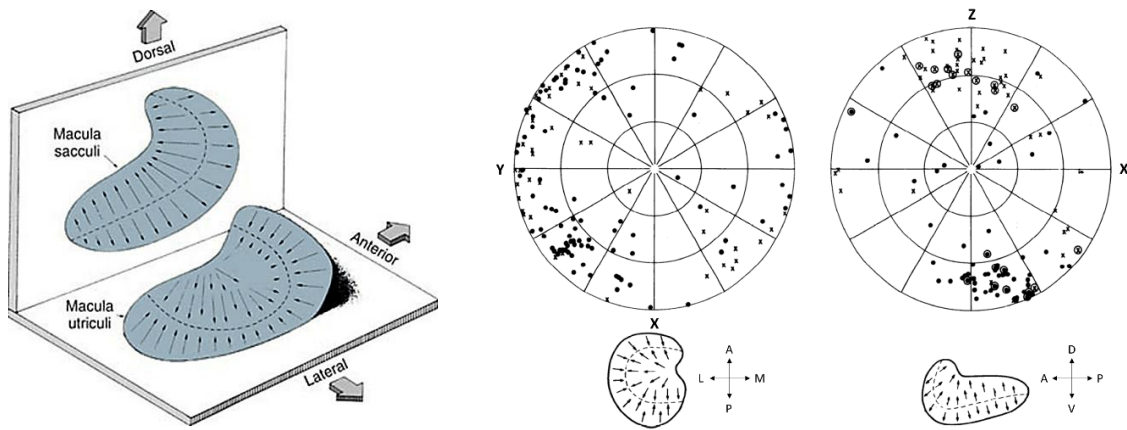
Fig. 3-7: Orientation of macula saccular and utricular (left); distribution of hair cells (right).
Left: modified from Clarke (2008): colour of macula organs changed; right: Fernández & Goldberg (1976a)

Directional properties are illustrated by a unit polarization vector of $v = (x, y, z)$, which refers to the coordinate system presented on the right-hand side of Fig. 3-7. As the heads tilt, a sinusoidal modulation of discharge is initiated that is proportional to the polarization and gravity vector. By applying matrix algebra and coordinate transformation, it is possible to decompose gravity force $(0,0,1)$ to head-fixed pitch (P) and roll (R) motion to estimate the force acting on the human receptors (F), which is given by the following equation with the transformed gravity vector $(\hat{g})$: (Fernández & Goldberg, 1976a)

$$F = v \cdot \hat{g} = x \cdot \sin P + y \cdot \sin R \cos P - z \cdot \cos R \cos P \qquad \text{Eq. 3-1}$$

As shown in Fig. 3-6, there are two different subtypes of hair cells located with almost equal ratios in the neuroepithelium of the vestibular organs (Burns & Stone, 2017). As outlined by Goldberg et al. (2012, pp. 28–42), the pyriform-shaped type I hair cell possesses a globular base, containing the nucleus and is innervated by a single calyx ending. By contrast, the type II hair cell with its cylindrical shape and bouton-like synapses owns a centrally located nucleus and is innervated by several afferent axons. Even if the functional differences between hair cells still have to be examined, evidence indicates that type I hair cells, especially those arranged centrally within the sensory neuroepithelium, are more sensitive to high-frequency head motions compared to type II hair cells (Burns & Stone, 2017; Contini et al., 2012; Eatock & Songer, 2011). One essential difference is related to recovery since only type II hair cells are replaced (Forge et al., 1993; R. R. Taylor et al., 2015).

Supporting cells, as an integral part of the sensory architecture, show similarities with epithelial and glial cells (Burns & Stone, 2017). They anchor hair cells with their microvilli into the sensory epithelium of the cupula and otolithic membranes. Furthermore, supporting cells are involved in the removal of dead hair cells and neurotransmitters from the extracellular space (Monzack & Cunningham, 2013; G. Wan et al., 2013). According to R. R. Taylor et al. (2015), new hair cells arise in supporting cells, which is relevant for the age-related degeneration process and, thus, for the change in sensitivity to motion sickness (see chapter 3.4.2).

Transduction Process in Semicircular Canals and Otolith Organs

The vestibular organ, as a typical hair-cell mechanoreceptor, senses angular motion during head rotation by the deformation of the cupula. Due to its inertia, the endolymph inside the canal duct lags behind the membranous structure, which initiates the described bending of hair cells located in the cupula (see Fig. 3-5 - right). For each semicircular canal on one side, there is a corresponding contralateral coplanar located one on either side of the head. Given that each canal renders acceleration within its plane of the duct, the pattern sensed by the mirrored canal responds with the opposite transducing answer. Therefore, this mechanism reveals a push-pull relationship (see Fig. 3-8). In fact, based on the side of the head (L: left, R: right) and the orientation of the channel duct (A: anterior, P: posterior, H: horizontal) three pairs (LHRH, LARP, LPRA) are referring to each other. (Goldberg et al., 2012, p. 78)
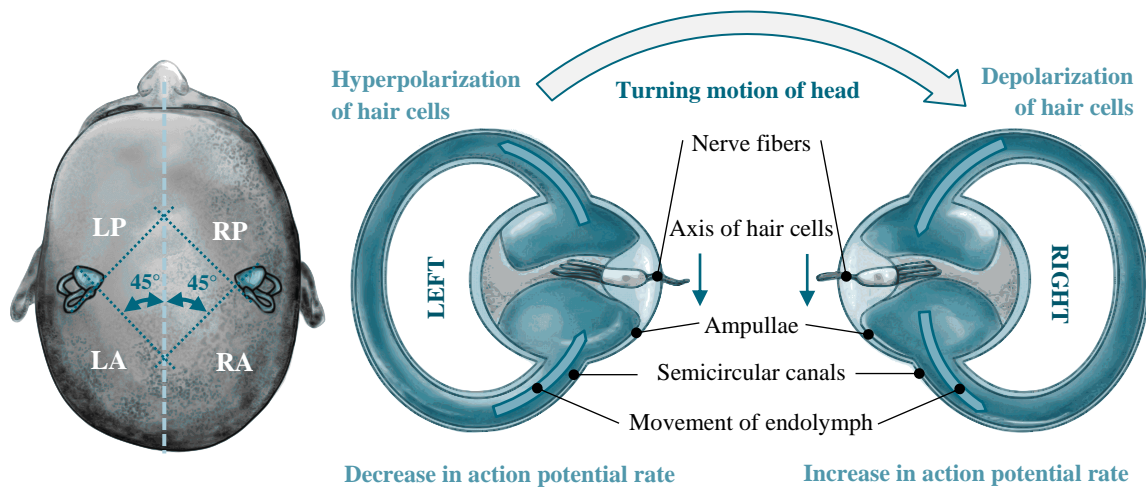
Fig. 3-8: Orientation of the vestibular organ (left); the push-pull relationship of opposing channel ducts (right). Left: based on Fetter (2010); right: based on Stanley (2015)

The previously mentioned flattened sensory epithelia sensing linear head motion and gravity force, which is called macula and located in otoliths neuroepithelium, shall be highlighted in the current section. The utricular macula has a horizontal orientation with an inclination angle of approximately 30°, whereas the saccular macula has a primarily parasagittal orientation (Fetter, 2010). Since the macula responds to linear forces parallel to its top surface, the utricular receptor predominantly senses in the transverse plane, while the saccular macula shows its sensitivity in the vertical direction to heave motion (Farkhatdinov et al., 2019a). Each macula consists of a 60 µm thin otolithic membrane with three layers (Kachar et al., 2000). Otoconia, small calcium carbonate crystals with a three times greater density of 2.7 g/cm^3 than the surrounding endolymph, are embedded in the top layer of the macula membrane (Money et al., 1971).

The displacement of the otoconia membrane forces stereocilia deflection and is initiated through a transient response of linear accelerations in the form of a tonic response of a tilting head. Underneath, there is a gelatinous rigid layer with a chaotic, fuzzy mass of cross-linked filaments. The third and lowest layer consists of strict vertical arranged filaments, attached to the apical surface of supporting cells. (Goldberg et al., 2012, pp. 94–104)

When taking the capability in shear into consideration, this layer shows the greatest influence in movements within the otoconial membrane that is illustrated in Fig. 3-9. In general, for motion sickness, the utricular appears to play a more important role in the ability to provoke symptoms of malaise than the saccular does (Beier et al., 2002; Helling et al., 2003; Hilbig et al., 2002; Schmäl, 2013).
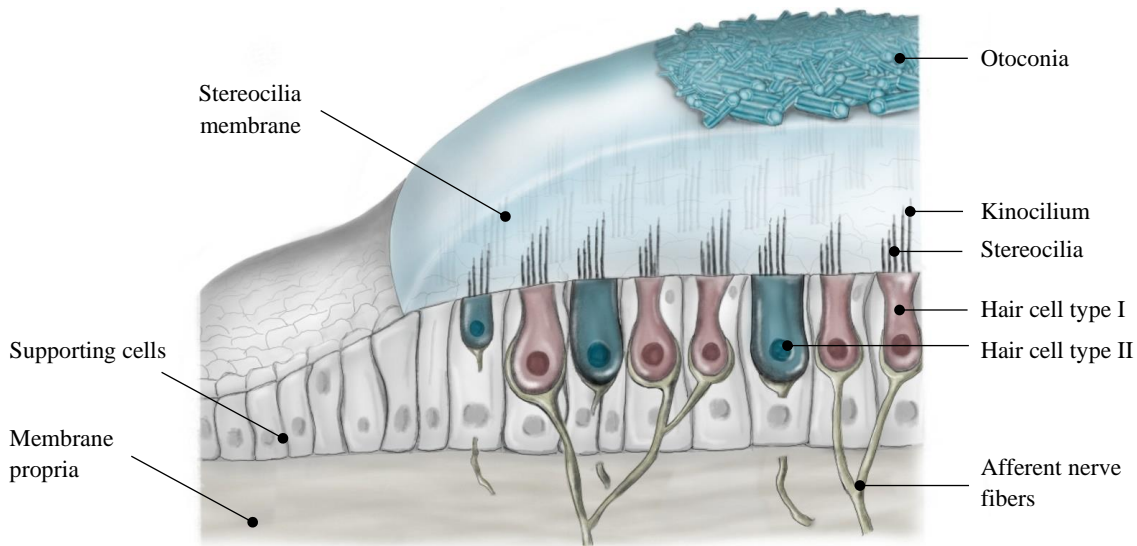
Fig. 3-9: Anatomy of the macula organ.
Based on Schünke et al. (2009)

Shearing stress in the hair bundles initiates six serial sequences in the aforementioned transduction process, which is presented on a consolidated basis, for instance, by Soto et al. (2013) or Goldberg (2016, pp. 1017–1028). Firstly, as a consequence of the stereocilia deflection, mechanoelectrical transducer channels are regulated (1). Already 100 nm of bending corresponds to almost 90 % of the response capacity (Fettiplace & Fuchs, 1999). Deflections towards kinocilium increase inward currents (excitation), whereas bending in the opposite direction causes a decrease in afferent discharge (inhibition) (Hudspeth & Corey, 1977; Wersäll & Bagger-Sjöbäck, 1974). To put it in more precise terms, voltage-sensitive K^+ and Ca^{2+} channels in the basolateral plasmalemma are activated (2), which lead to changes in receptor potential (3). In particular, the Ca^{2+} channels manipulate cellular processes, respective neurotransmitter discharge (4). The agonists and antagonists of several neurotransmitters modulate the efferent or the afferent synaptic input, either to the hair cell or to the afferent axon fiber. The main neurotransmitter of hair cell afferent synapses is glutamate, which is packaged in vesicles at the ribbon synapses to diffuse across the synaptic cleft to attach to postsynaptic *α-amino-3-hydroxy-5-methyl-4-isoxazole propionic acid* (AMPA) receptors. Also, interactions with further subtypes of ionotropic glutamate receptors, just as *N-methyl-D-aspartic acid* (NMDA), *kainic acid* (KA) receptors, and metabotropic receptors, influence neurotransmitter modulation. As a result, depolarization of the afferent terminal is initiated (5). Finally, the so-called spike encoder converts the postsynaptic depolarization into action potentials and, therefore, determines the firing rate (6). Despite the unidirectional peculiarity of the transduction process, the feedback mechanism enables regulation of the depolarization. Efferent neuronal synapses, by contrast, release acetylcholine as the primary neurotransmitter.

Inhibition on α9/α10 nicotinic (anchor) receptors in hair cells refers to the influx of calcium and activation of small-conductance calcium-activated potassium channels, which lead to a hyperpolarization of the hair cell and reduction in the distribution of particles (Faber & Sah, 2007). Fast synaptic actions on calyx endings are combined with slow efferent responses involving muscarinic or peptidergic neurotransmitters (Goldberg et al., 2012, p. 63). Typical cellular synaptic functions with respect to calcium channels are shown in Fig. 3-10.

"... The synaptic vesicles in the active zone are triggered to fuse to the plasma membrane following the entry of calcium via voltage-gated calcium channels (A). A calcium microdomain (B) results from both mobile and fixed calcium buffers (C) that restrict elevations in calcium concentration to the vicinity of open calcium channels. Putative interactions between the calcium channels and core complex proteins such as syntaxin hold the low-affinity calcium receptor of exocytosis (D) within the high-calcium plume of the microdomain. Cooperative binding of calcium to this receptor ... results in vesicle exocytosis and the release of neurotransmitter into the synaptic cleft (E). There diffusion, degradation, and active removal all shape the arrival of neurotransmitter at the postsynaptic receptors (F). Receptor affinity, kinetics, and desensitization in turn determine the postsynaptic potential. After fusion and release of neurotransmitter, vesicular membrane is recaptured in the process of endocytosis (G) that can occur through clathrin-mediated and non-clathrin-mediated pathways." Fuchs and Parsons (2006, p.254)

Fig. 3-10: Neurotransmitter and synaptical actions.
Based on Fuchs & Parsons (2006)

Afferent fibers, whether innverating from canal ducts or otoliths, differ in the spacing of their action potentials. Depending on the characteristics of the afterhyperpolarization pattern, afferents can be spread into regular or irregular variations. The following Tab. 3-1 from Goldberg et al. (2012, p. 76) provides information about the fundamental differences between those two.

Tab. 3-1: Comparison of regular and irregular discharging.
[1] Selection: Lysakowski et al. (1995); Yagi et al. (1977); Goldberg & Fernández (1977)
[2] Selection: Fernández & Goldberg (1976a); Goldberg et al. (1990)
[3] Selection: Goldberg & Fernández (1980); Marlinski et al. (2004)
[4] Selection: Ezure et al. (1983); Bronte-Stewart & Lisberger (1994)

Irregular Discharging	Regular Discharging
Thick and medium-sized axons ending as calyx and dimorphic terminals in the striola zone[1]	Medium-sized and thin axons ending as dimorphic and bouton terminals in the peripheral zone
Phasic-tonic response dynamics, including a sensitivity to the velocity of cupula (otoliths)[2]	Tonic response dynamics, resembling those expected of end-organ macromechanics
High sensitivity to angular or linear force[2]	Low sensitivity to angular or linear force
Large responses to electrical stimulation of efferent fibers[3]	Small responses to electrical stimulation of efferent fibers
Low thresholds to short shocks and large responses to constant galvanic currents, delivered via the perilymphatic space[4]	High threshold and small responses to the same galvanic stimuli

The static discharge property describes the number of spikes in the absence of external or internal physical stimuli. Resting charge of regular afferents range between 50 - 100 spikes/s, whereas irregular discharging and innervating otoliths, compare to canals, show lower firing rates (Estes et al., 1975; Fernández et al., 1972; Lysakowski et al., 1995).

The phenomenon of resting discharge comes with the advantage of allowing each fiber to respond bidirectionally to head motion, which leads to either an increase or a decrease in discharge properties. Furthermore, due to the resting value, the sensory threshold is eliminated. Therefore, resting discharge enables constant excitatory information for the brain to control crucial regulatory effectors. (Goldberg et al., 2012, pp. 70–76)

Macromechanics on Motion Sensation

Angular head motion induces internal forces resulting in fluid dynamics of the endolymph within the semicircular canals. The generated flow acts as an integrator since the bending of hair cells is proportional to the angular velocity. In fact, even if the physical process of motion detection within the semicircular canals is sensitive to acceleration, the neural output from the sensory system is related to the velocity of angular motion (Farkhatdinov et al., 2019b). The perceived stimuli are involved in peripheral and central mechanisms and lead to the so-called velocity storage, which is essential for the vestibulo-ocular reflex (see chapter 3.2.5) to maintain a stable gaze while moving (Curthoys, Markham & Curthoys, 1977; Obrist, 2011, p. 40; Rabbitt et al., 2009). To specify angular motion concerning the dynamics of the endolymph, the acting force needs to be decomposed for every individual semicircular duct. According to laboratory testing from Isu et al. (2001) on isolated Coriolis stimuli, the severity of nausea is proportional to the product of external angular stimuli and self-motion-induced head rotation. Due to the anatomical fact that the semicircular canals are not arranged perfectly rectangular to each other, the sensory nervous system has to adjust the vectorial summation of forces to assess a correct pattern of the real acting force (Blanks et al., 1975; Curthoys, Blanks & Markham, 1977; Isu et al., 2001). Therefore, two values for coordinate transformation, with and without adjustment by the nervous system, are shown in the following Tab. 3-2.

Tab. 3-2: Coordinate transformation of canal ducts. Based on Isu et al. (2001)

	LH	LA	LP	RH	RA	RP
α_*	**-9.2°**	-49.1°	34.3°	-170.8°	-130.9°	145.7°
β_*	**-21.9°**	-88.5°	-112.9°	-21.9°	-88.5°	-112.9°
Adjustment through the sensory nervous system						
α'_*	**-3.8°**	-59.8°	34.3°	-176.2°	-120.2°	145.7°
β'_*	**-15.0°**	-109.8°	-112.9°	-15.0°	-109.8°	-112.9°
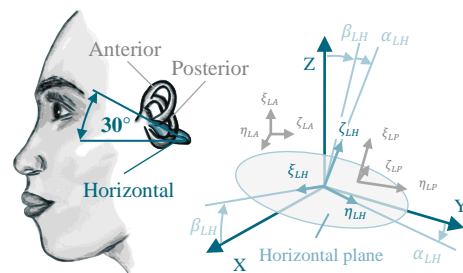
Fig. 3-11: Orientation of semicircular canals and coordinate transformation. Based on Isu et al. (2001); Fetter (2010)

By supposing angular motion upon the z-axis (ψ), the R_1 matrix represents the operator of the respective transformation to the head-fixed coordinate system.

Multidimensional forces lead to further adjustments, however, to decrease complexity, only a singular stimulus is applied in this case of application. To calculate the forces acting on every individual cupula, the head-fixed coordinate system must be rotated by angle β around the y-axis followed by a rotation of α around the x-axis (see Fig. 3-11).

$$R_1 = \begin{bmatrix} \cos \psi(t) & \sin \psi(t) & 0 \\ -\sin \psi(t) & \cos \psi(t) & 0 \\ 0 & 0 & 1 \end{bmatrix} \quad , \quad R_* = \begin{bmatrix} \cos \beta_* & 0 & -\sin \beta_* \\ \sin \alpha_* \sin \beta_* & \cos \alpha_* & \sin \alpha_* \cos \beta_* \\ \cos \alpha_* \sin \beta_* & -\sin \alpha_* & \cos \alpha_* \cos \beta_* \end{bmatrix} \qquad \text{Eq. 3-2}$$

The six resulting semicircular canal-fixed coordinates, summarized in Tab. 3-2, are defined as $O_*(\xi, \eta, \zeta)$. The presented coordinate transformation is based on the idea of Isu et al. (2001) and is adapted under consideration of matrix algebra with the matrices R_1 and R_* as follows:

$$\begin{pmatrix} \cos \beta_* \cdot [\cos \psi \cdot x + \sin \psi \cdot y] - \sin \beta_* \cdot z \\ \sin \alpha_* \sin \beta_* \cdot [\cos \psi \cdot x + \sin \psi \cdot y] + \cos \alpha_* \cdot [-\sin \psi \cdot x + \cos \psi \cdot y] + \sin \alpha_* \cos \beta_* \cdot z \\ \cos \alpha_* \sin \beta_* \cdot [\cos \psi \cdot x + \sin \psi \cdot y] + \sin \alpha_* \cdot [\sin \psi \cdot x - \cos \psi \cdot y] + \cos \alpha_* \cos \beta_* \cdot z \end{pmatrix} \quad \text{Eq. 3-3}$$

Given that cupula deflection is limited to the plane of the semicircular canal, the endolymph rotates only around the ζ-axis. For further mathematical description, the torsion pendulum model, first introduced by Steinhausen in 1931, offers a simple way to describe the physical behaviour of head rotation on canal dynamics. The general form of a temporal depending second-order differential equation is shown as follows:

$$M\ddot{x} + B\dot{x} + Kx = M\frac{d^2x}{dt^2} + B\frac{dx}{dt} + Kx = -f(t) \qquad \text{Eq. 3-4}$$

Based on that mathematical approach, the equation represents the relationship between head motion (ψ) and the displacement of the cupula with the respective interactions to the endolymph in the semicircular canals. In the application of canal duct dynamics, the endolymph mass ($M\ddot{x}$) and viscosity ($B\dot{x}$) as well as the cupular elasticity (Kx) are integrated, while Fig. 3-12 illustrates the background of the biophysical phenomenon. When humans rotate their heads abruptly while being initially in a static state, two reset forces resist rearward motion on the endolymph. (Obrist, 2011, pp. 15–20)

With respect to endolymphs viscosity, which shows similarities to the characteristics of water, a force called viscous drag (dF_D) is applied to the fluid elements initiated by the narrow structure of the labyrinth. Furthermore, the elasticity of the cupula produces counter-pressure on the moving elements as the second opponent force (dF_C). According to this assumption, it is obvious that physical characteristics of the endolymph, such as the density (ρ) and the viscosity (μ), as well as the elasticity of the cupula (k), influence the relationship between external force and deflection of hair cells. In addition to this, the geometry of the canal duct shows a strong impact on the mathematical expression. Here, the radius of curvature (R) with its cross-section area (A) along the streamline (l) is relevant. The cross-section along the canal duct (CD) is simplified as a constant value. Since Q is defined as the volume displacement of the endolymph, it is permitted, due to the law of fluid continuity, to express Q as displacement multiplied by the cross-section ($A_{CD}x_{CD} = A_{CUP}x_{CUP}$). (Goldberg et al., 2012, pp. 78–84)
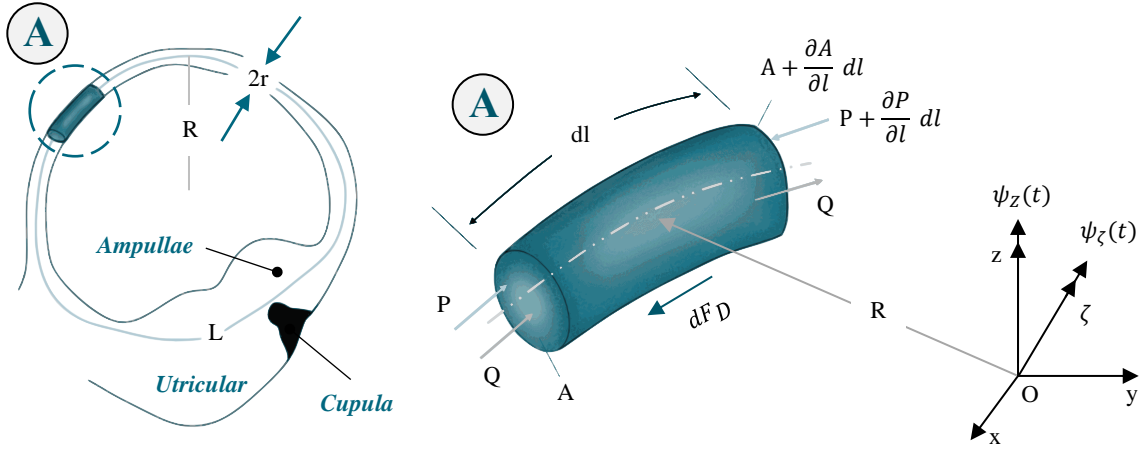
Fig. 3-12: Mechanical model of angular motion sensing.
Based on Goldberg et al. (2012, p. 80)

By applying Newton's second law in which the sum of the forces is equivalent to the acceleration of the element of mass, the fundamental idea of the torsion pendulum model is applied as it is formulated by Goldberg et al. (2012, pp. 78–84):

$$dm \cdot a(l) = \rho \cdot A(l) \cdot \left[a_x(l) + \frac{d^2x}{dt^2}(l) \right] dl = dF = dF_D + dF_C \qquad \text{Eq. 3-5}$$

Here, an important convention determines reactive force as $\frac{d^2x}{dt^2}(l)$, whereas internal force is represented as $a_x(l)$. According to the continuum mechanics of steady Hagen-Poiseuille flow in circular tubes, the viscous force is given as:

$$dF_D = \frac{-8 \cdot \mu \cdot \frac{dQ}{dt} \cdot dl}{A(l)} \qquad \text{Eq. 3-6}$$

To address the retention force by the stiffness of the cupula (k), as the reaction of the movement of endolymph elements, a proportional pressure (Δp) is obtained. According to Newton´s law of equilibrium, added by a multiplication of the cross-section area, the following equation contains the resulting force:

$$dF_C = -\frac{k \cdot Q \cdot A(l) \cdot dl}{L} \qquad \text{Eq. 3-7}$$

After utilizing the equations above, the linear ordinary differential equation for the semicircular canals are shown as follows:

$$\rho \cdot \frac{d^2Q}{dt^2} \cdot \oint_L \frac{dl}{A(l)} + 8 \cdot \pi \cdot \mu \cdot \frac{dQ}{dt} \cdot \oint_L \frac{dl}{A(l)^2} + k \cdot Q = -\rho \cdot \oint_L a_x(l) \cdot dl \qquad \text{Eq. 3-8}$$

$$\text{with } \oint dl = L \ , \ a_x(l) = R \cdot \psi_Z(t) \cdot O_*(\zeta) = R \cdot \psi_\zeta(t)$$

To simplify the calculation, the line integrals are only obtained over the length of the canal duct (L_{CD}) since the cross-section area in the ampullae is much larger than in the residual canal duct. The deductive equation determines two values, $\tau_1 = B/K$ and $\tau_2 = M/B$, which are essential for the behaviour of the fluid-mechanical system:

$$\tau_1 = \frac{8 \cdot \pi \cdot \mu \cdot L_{CD}}{k \cdot A_{CD}^2} \qquad , \qquad \tau_2 = \frac{\rho \cdot A_{CD}}{8 \cdot \pi \cdot \mu} \qquad \text{Eq. 3-9}$$

The short time-constant (τ_2) is obtained from the Navier-Stokes equation for viscous fluid and range mainly between 3 - 5 ms (L. Gastaldi, S. Pastorelli & M. Sorli, 2009; Lasker et al., 2008; Oman & Young, 1972; van Buskirk et al., 1976). The long time-constant (τ_1), however, shows great differences in the order of 4 - 20 s, whereas the main observations emphasize a value of 5.7 s (Goldberg et al., 2012, p. 83; L. Gastaldi, S. Pastorelli & M. Sorli, 2009; Lasker et al., 2008; Mueller & Verhagen, 1988; Salva et al.; van Buskirk et al., 1976). By considering these estimations, it becomes apparent that the system is characterized as overdamped (original from $B^2 \gg 4MK$ or in this case $\tau_1 \gg \tau_2$) (Asadi et al., 2016). Indeed, these two values describe fundamental characteristics of angular motion sensation and determine the corner-frequencies $f = 1/2\pi\tau$, which can be discerned in the Laplace domain e.g., the transfer function $H(s)$ and the bode plot, with:

$$H(s) = \frac{Ks}{(\tau_1 s + 1) \cdot (\tau_2 s + 1)}$$

Eq. 3-10
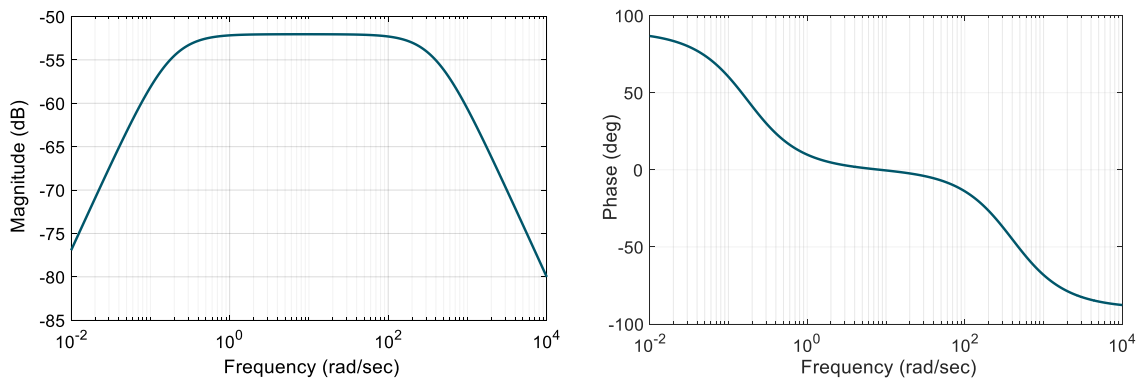
Fig. 3-13: Transfer function of angular motion sensing.

As illustrated in Fig. 3-13, the system comprises three individual characteristics depending on the frequency domain of external motion stimuli. Firstly, the low-frequency band in which the system reacts as an acceleration transducer. Secondly, in the mid-frequencies, the system approximates a velocity transducer, while, thirdly, in the high-frequency region, the characteristics change to a displacement transducer. In general, typical head movements fall in the range of 0.5 - 20 Hz, whereas high prevalence occurs around 2 - 5 Hz with peak velocities of 10 - 50 deg/s and peak accelerations of 500 - 1,000 deg/s², in which the system becomes an angular-velocity transducer (Armand & Minor, 2001; Baird et al., 1988; Goldberg & Fernández, 1971). Consequently, the semicircular canal functions show proportional reactions to the ratio of endolymph´s density and viscosity, independent of cupula elasticity (Goldberg et al., 2012, p. 83).

Otolith Organs - Sensation of Linear Motion

In addition to this, linear motion sensed by the otoliths is of special interest since many researchers emphasize the strong evidence of those motion patterns influencing motion sickness (Diamond & Markham, 1992; Helling et al., 2003). Interestingly, the head movement from nose-up posture to upright enhances greater feelings of nausea than movements in the opposite direction (Isu et al., 2001).

According to Goldberg et al. (2012, p. 95), two different kinds of stimuli occur in otoconial organs, while only shearing force is suitable for stimulation. In fact, compressional force pointed perpendicular to the macula plane seems to be ineffective. Concerning several simplifications, a second-order partial equation represents the biomechanical behaviour of the otoconial membrane (see the following equation based on Kondrachuk, 2001 and further developed by Goldberg et al., 2012):

$$\Delta\rho \cdot \frac{\partial^2 X}{\partial t^2} + \mu \cdot \frac{\partial^3 X}{\partial t \partial Z^2} + \frac{E}{2(1+\sigma)} \cdot \frac{\partial^2 X}{\partial Z^2} = \Delta\rho \cdot A_x(t) \equiv (\rho_{OL} - \rho_{ENDO}) \cdot (g_x(t) - a_x(t)) \qquad \text{Eq. 3-11}$$

This model is valid for accelerations smaller than 2 - 3 g in tonic units since until this value a linear relationship between acceleration and neural responses is ensured (Fernández et al., 1972; Fernández & Goldberg, 1976a; Jaeger & Haslwanter, 2004). X describes the shearing displacement of the gelatinous and columnar layers, which are considered as one combined layer. The value Z measures the height, starting from the surface of the neuroepithelium. On the right side of the equation, the difference in density between the otoconial layer and the endolymph is multiplied by the *gravitoinertial force* (GIF). The GIF is defined as the gravitational force (g) added by motion-induced stimuli (a), like the centripetal force that occurs during rotation. Similar to the model of the cupula sensation, physical coefficients of the gelatinous layer, such as viscosity (μ), Poisson´s ratio (σ), and elastic Young´s modulus (E), are obtained to characterize the mechanical behaviour of the otoconial membrane during linear motion. To estimate Young´s modulus, the time derivates are canceled and the GIF implies a constant force given that a steady-state displacement must be considered. The values of Poisson´s ratio ($\sigma = 0.5$) and density difference ($\Delta\rho = 0.33$ gm/cm^3) are taken over from previous experiments conducted by Steinhausen (1935) and Trincker (1962). By setting some additional boundary conditions, the equation can be solved and shows a value of approximately $E = 100$ dyne/cm^2. Lastly, the viscosity measured from efferent nerves provides the value $\mu = 1$. Since all necessary mechanical properties are known, the governed time constants can be determined ($Z_{max} = 10$ µm: top of the gelatinous layer): (Goldberg et al., 2012, pp. 101–103)

$$\tau_1 = \frac{8 \cdot \mu \cdot (1+\sigma)}{E} \approx 3 \cdot 10^{-3} \, ms \qquad , \qquad \tau_2 = \frac{\Delta\rho \cdot Z_{max}^2}{\mu} \approx 30 \, ms \qquad \text{Eq. 3-12}$$

Due to the high discrepancy between long- and short-time constants, the highly overdamped model of the otoconial membrane (sensory threshold by otoconia displacement of 0.005 g - Ormsby, 1974, p. 64) nearly behaves as a first-order system (Goldberg et al., 2012, p. 102). However, as a result of those approximations, the bode plots illustrated in Fig. 3-14 show several mathematical approaches with different system boundaries and assumptions. Fernández & Goldberg (1976b) just as Ringland & Stapleford (1972) described a first-order system with different time constants, whereas Young & Meiry (1968) postulated a model added by a neural processing term. The proposed models for linear motion sensation are valid for the vertical (heave), sagittal (surge), as well as for the lateral axis (sway) and are shown as follows (Asadi et al., 2016):

$$H(s) = \frac{1}{(\tau s + 1)} \qquad , \qquad H(s) = \frac{K(1 + \tau_a s)}{(\tau_L s + 1) \cdot (\tau_S s + 1)} \qquad \text{Eq. 3-13}$$
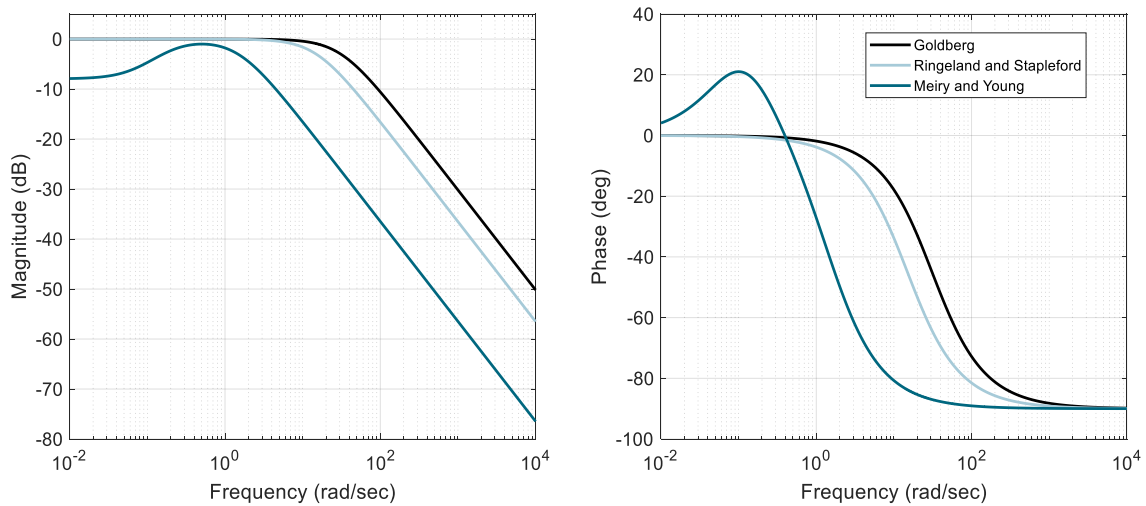
Fig. 3-14: Transfer function of linear motion sensing.

In both cases, cupula and otoconial deflection, further mathematical modeling of macromechanics was done by different researchers. The aim of those examinations, for instance, was to consider additional physiological parameters, like the curvature of the organs (Jaeger & Haslwanter, 2004). Even if these models provide increased accuracy, the main characteristics are congruent with the previously presented illustration (Obrist, 2011, p. 20). For this reason, further mathematical description is beyond the scope of this elaboration. Furthermore, micromechanics and consecutive neural processing provide deeper knowledge about the sensation of motion (Asadi et al., 2016). While mathematical descriptions of these processes are rejected here, some crucial human body reflexes, which are initiated by the vestibular sensory input, are presented in chapter 3.2.5.

3.2.2 Vision

Visual sensation with its ability to perceive and anticipate motion cues contributes to the etiology of motion sickness, especially in situations in which contrary visually-driven stimuli evoke the physiological perturbations (see chapter 3). Indeed, Bos et al. (2012) postulate that visual information about the upcoming trajectory enhances situation awareness and decreases the risk just as the severity of motion sickness. Their findings are based on virtual environmental examinations, in which an artificial earth-fixed reference marker was added by anticipatory visual cues of the upcoming trajectory. The importance of motion prediction can be confirmed by investigations of Golding et al. (2003), who ascertained a reduction of malaise in subjects who anticipated the upcoming motion and aligned their head within the GIF. As previously mentioned, this strategy is also reported by drivers who lean in the inner curve side before or at least during turning (Bronstein et al., 2020). If these compensational movements occur passively by external systems, as seen in tilting trains, latency and missing muscle activities somehow increase rather than avoid motion sickness (B. Cohen et al., 2011; Golding et al., 2003).

The sense organs concerned with visual perception in humans are the eyeballs, while their appropriate stimuli refer to light rays. When such light rays enter the eye, they fall on a neural sensitive tissue that covers the ball-shaped interior surface of three cross-section layers, which are illustrated by the detailed description of the eye anatomy in Fig. 3-15.

First of all, the rays have to pass the cornea and lens that filters, refracts, and focus light on the innermost layer. The lens, in addition to the iris, can adjust its size and shape to regulate the amount of light in order to bring objects into focus. The dynamic lens adaption leads to an adjustment of refractive power and is called accommodation. (Irsch & Guyton, 2009)
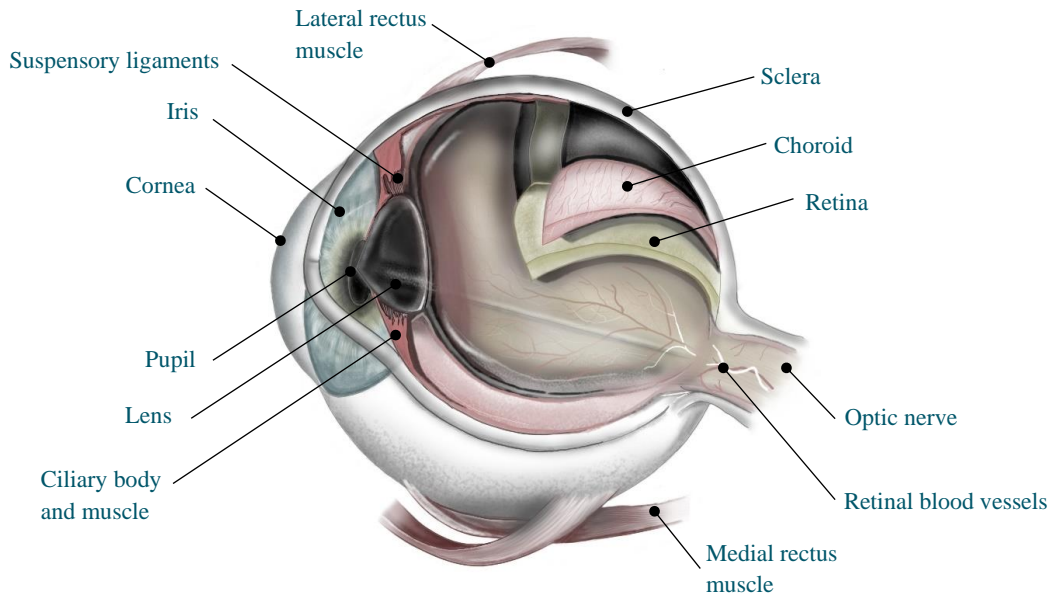
Fig. 3-15: Anatomy of the eyeball.
Based on Esquibel (2021); Malhotra et al. (2011)

The outmost layer, comprising the cornea and sclera, shapes the form of the eye and provides a tough covering to the external portion. The intermediate coating consists of a section called choroid that offers nourishment to the retina since this layer is populated with blood vessels. The retina, as the innermost layer, reveals nerve cells and neurons including two different types of photoreceptors, called rods and cones. While rods require very low light intensity to generate signals, cones need a higher amount of light since these receptors are involved in colour vision. The photosensitive rods show less visual acuity and low resolution, whereas cones provide an acute vision of images. The density distributions of both, retinal cones and rods, are illustrated in the following Fig. 3-16. (Irsch & Guyton, 2009; Löfgren et al., 2013)
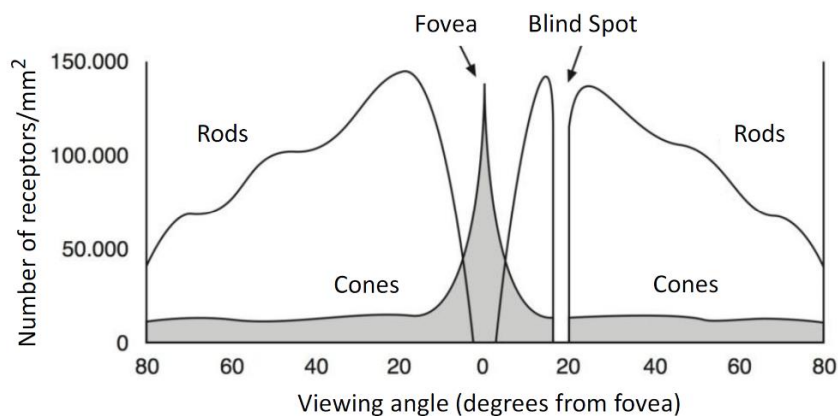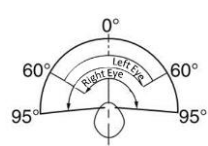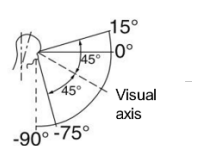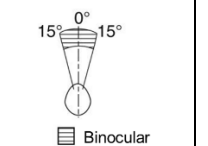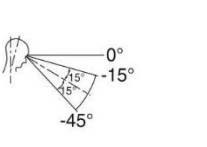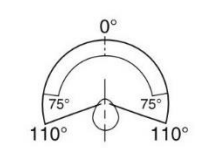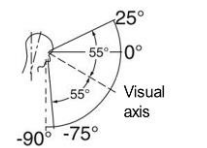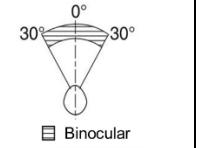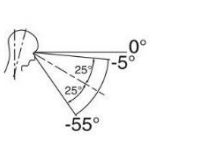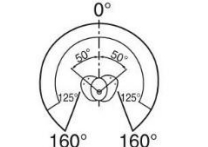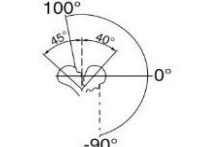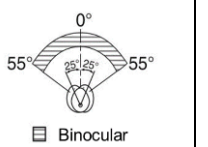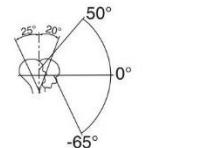
Fig. 3-16: Distribution of density of cones and rods across the retina.
Löfgren et al. (2013, p. 6)

The fovea is characterized as the area with the highest density of cones to enable an exceedingly high-quality image and colour resolution. This information is relevant for the brain to register objects in a concise manner. Since rods and fewer cones mainly occupy the periphery of the retina, this area is predominant in the perception of contrast and detection of motion. Tab. 3-3 contains some crucial aspects of monocular and binocular vision that determine characteristics of visual sensation and environmental motion capturing. (Bubb et al., 2015, pp. 81–91)

Tab. 3-3: Monocular and binocular vision.
Hudelmaier (2003, pp. 21–27); Schmidtke (1975, pp. 1984–1987) as cited in Bubb et al. (2015, p. 215)
Modified: translated into English

Eyes	*Head*	*Torso*	*Maximum range*		*Optimum range*	
			horizontal	*vertical*	*horizontal*	*vertical*
fix	fix	fix				
move	fix	fix				
move	move	fix				

The term binocular summation describes viewing with both eyes rather than using the better eye alone (Campbell & Green, 1965 as cited in Schneck et al., 2010). This improvement in visual performance is attributed to probability summation, but, moreover, may also refer to the neural summation of the signals from both eyes (Blake & Fox, 1973; Schneck et al., 2010). Furthermore, the researchers outlined that the degree of binocular summation depends on many factors. In cases of viewing conditions with poor contrast targets, for instance, an extended gain can be observed. Under these circumstances, however, other investigations have shown that binocular summation likewise depends on spatial frequency (Gagnon & Kline, 2003; Home, 1978; Pardhan, 1996).

According to Eckstein (2014c, pp. 42–44) visual ability is divided into visual range, field of vision, and field of view. The visual range covers the area which is captured by a fixed head and resting eye, while the field of vision allows eye movements without head movement. The field of view is the area of sharp viewing that mainly covers an opening angle of 4°. In real-life situations, the possible range of vision by turning torso and head is rarely exploited. In addition to the visual field, the direction of sight as well as the fixation rate show highly relevant properties in human perception. Drivers' eye movements, for instance, differ in most cases by less than 6°, while 90 % of eye fixations fall in a small bandwidth of (+/-) 4° around the point of aim (Rockwell, 1972).

As precisely outlined by Goldstein et al. (2002, pp. 183–366), visual sensation allows the categorization of objects by identifying and clustering colours, shapes, and spatio-temporal relationships. Some of these structures and elements, divided into monocular and binocular information, are illustrated in Tab. 3-4. Given that motion sickness arises under motion conditions, further analyses focus on dynamic circumstances, namely the optic flow and motion parallax.

Tab. 3-4: Dimensions of vision.
Based on Howard & Rogers (2002) as cited in Chatziastros (2003, p. 2)

MONOCULAR				BINOCULAR		
	Static	Perspective	*Texture, size of object*		**Convergence**	Dynamic
		Masking	*Transparency*			Static
		Illumination	*Shades*		**Disparity**	Position
		Atmospheric effects	*Dust, fog*			Orientation
						Temporary
		Focusing	*Accommodation*			Monocular occlusion
	Dynamic	**Optic flow**				
		Motion parallax				

The optic flow, first introduced by Gibson (1950), characterizes the relation of motion between the observer and the visible points in space projected on the image area. This phenomenon is defined as the transformation of surfaces of the enveloping optic domain during locomotion, also known as the gradient of locomotion (Bubb & Wohlfarter, 2012; Chatziastros, 2003, pp. 2–7; Goldstein et al., 2002, pp. 327–343). In short, optic flow represents visual changes in the respective scene, while the speed vectors of all visible objects are equivalent to the term visual field. The importance of optic flow to perception and self-motion, in particular during traveling, is uncontested. The bio-physiological process of regulating eye movements will be further discussed in chapter 3.2.5 where the optokinetic and vestibular-driven reflexes are presented.

The effect of motion parallax is illustrated on the left-hand side of Fig. 3-17, in which the velocity thresholds of perception are shown. It is to be stated that with increasing distance between an observer and target the threshold of perception increases (Bubb & Wohlfarter, 2012). In addition, it is evident that further properties e.g., the duration of visual input, also affect the ability of perception. Concerning investigations of Rockwell (1972), drivers´ eye fixations mainly range between 100 and 350 ms duration. Under circumstances in which NDRTs are expected to increase, this value might change significantly. Especially when thinking about the previously outlined process of sensation and accommodation, positive velocity shows greater thresholds for the same headway compared to cases of negative velocity (Todosiev, 1963, pp. 88–91). On the right-hand side of Fig. 3-17, the optic flow during perpendicular movement is depicted. Within this illustration, the arrows represent the relative displacement of three objects at different isovergence distances. The shadow rays indicate the angular displacement of objects that differ in distance and eccentricity (the reference point is the right eye of the observer).
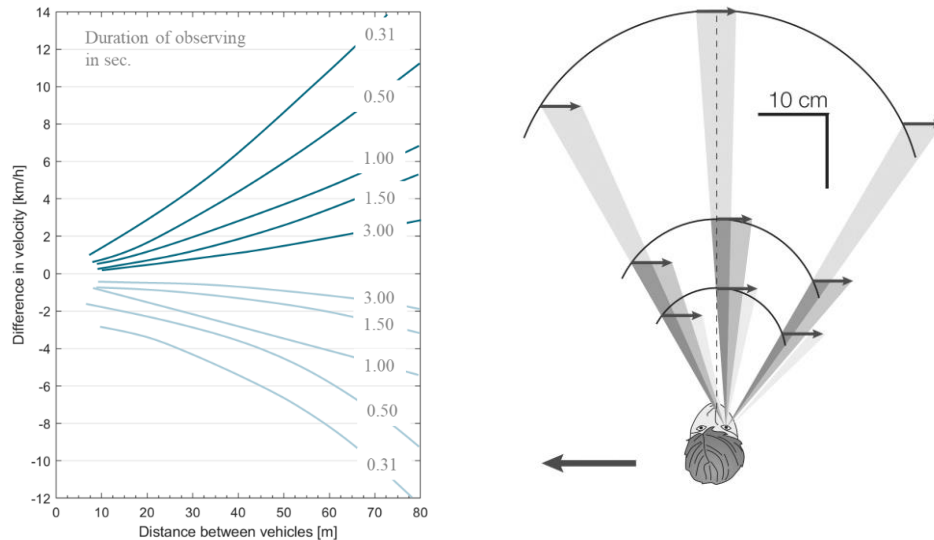
Fig. 3-17: Motion detection as function of velocity and distance (left); patterns of planar optic flow (right).
Left: based on Todosiev (1963, p. 89); right: Angelaki & Hess (2005)

3.2.3 Somatosensoric, Kinesthetic, and Haptic

As depictured in a consolidated manner by Yusof (2019, pp. 14–15), the somatosensory apparatus is a constituent element of the nervous system, which combines several modalities of somatic sensation. Somatic sensation can be divided into three subgroups of interoception, exteroception, and proprioception (Oman, 1998). The latter is involved in posture control, self-motion perception, and active movements of body parts (Tuthill & Azim, 2018). Due to control motor responses, conveyed by fused information of tendons, muscles, and joints with vestibular and visual cues, a change of body and head position can be achieved. Within the pathways of nonconsciousness proprioception, information about body posture and dynamics are rooted in muscles or tendons receptors and terminate in the ipsilateral cerebellum. Proprioceptive information, in particular of limb dynamics, diminish with age, which leads to a decrease in body posture control with side effects of overthrows (Proske & Gandevia, 2012). Exteroception with its sensation of taction, thermoception, and nociception also provides some kind of information about the external environment (Araujo et al., 2015). Whereas many researchers emphasize that the terms haptic and tactile are congruent, some authors postulate haptic to be a combination of kinesthetic and tactile information (Amemiya et al., 2013; Fitch et al., 2011; Gibson, 1962; Lederman & Jones, 2011; Tan, 2000). Tactile implies cutaneous input through stimuli of vibration, pressure, or touch, while the perception of muscle length or tension and joint angle refers to kinesthetic sensation. The interoception includes internal information such as provided from inner organs (Jacobs, 2011).

3.2.4 Neural Centers and Pathways Involved in Motion Sickness

Since the three main perception receptors have been previously described, their pathways and converging processes are included in the current chapter. To put this in more precise detail, the fundamental principles on the origin of the physiological syndrome refer to four essential neural structures and pathways, which are described by Benson (2002, p. 1064) and are highlighted in Fig. 3-18 through dark-petrol boxes and black arrows.

The light-petrol boxes and dotted arrows, by contrast, represent structures and pathways which might be involved in the development of the symptomatology but are not necessary for the origin of motion sickness. The dot-dash lines connect the physiological expressions (signs and symptoms) with the neural structures of the nervous system.

RECEPTORS   **CENTRAL NERVOUS SYSTEM**   **SIGNS / SYMPTOMS**

* AVP: arginine vasopressin
**PCRF: parvocellular reticular formation

Cerebral cortex limbic system

Retina

Vestibular cerebellum

Hypothalamus

Pituitary

Motion stimuli

Vestibular apparatus

Vestibular nuclei

Autonomic center

Proprioceptors

PCRF vomiting center**

NAUSEA
Dizziness
Somnolence
Headache
Depression
Performance decrement

Increased secretion
ADH/AVP*, ACTH, ADH, hPRL

SWEATING, PALLOR
Decreased gastric motility
Cardiovascular and respiratory changes

EMESIS

Fig. 3-18: Pathways involved in the development of motion sickness in humans.
Based on Benson (2002, p. 1064)

As summarized by Cullen (2012), the first and most important element is, among other things, involved in the conjunction of receptor inputs and is known as the vestibular nuclei. In synergy with the cerebellum, it is expected that both play a key role in mismatch comparison (see chapter 3.2.6). In particular, the cerebellum is relevant in the adaption of sensory rearrangements, which is an essential part of the eponymous theory. In terms of habituation, Robinson and colleagues discovered that the cerebellar cortex shows adaptive modification abilities within vestibulo-ocular control in cats (Robinson, 1976; Wolfe, 1968). Benson (2002, p. 1065) stated that due to the sedate development of motion sickness interacting with the persistence of signs after the withdrawal of nauseogenic stimuli, it is evident that the stimulation of autonomic centers arouses through the aggregation of neurohumoral agents. He, furthermore, concluded that the last essential component refers to the reiterated contraction of abdominal muscles and stimulation of the diaphragm as well as the relaxation of the cardiac sphincter and gastric stasis, or in other words emesis. Here, the zone of the *parvocellular reticular formation* (PCRF), also known as the vomiting center, is involved.

Even if the chemoreceptor trigger zone, which is located in the area postrema at the floor of the fourth ventricle on the upper surface of the medulla, is mandatory for vomiting provoked by drugs and toxins, it is not a crucial element of the neural structures within the physiological reaction of motion sickness (Cuomo-Granston & Drummond, 2010; B. J. Yates et al., 1994). Nevertheless, the chemoreceptor trigger zone receives indirect signals and information via cerebellum as cerebellovestibular conjunctions project to vestibular nuclei (Cuomo-Granston, 2009, p. 211). Due to the ablation experiments of Money & Wood (1970) neither of the following structures, namely the hypothalamus and the pituitary gland, are essential in provoking motion sickness. The cerebral cortex, however, seems to be involved, in the development of this physiological phenomenon at least to some extend.

In general, as mentioned by Cuomo-Granston (2009, p. 71), the cerebral cortex responds to stressful stimuli, while the thalamus, for instance, is sensible to afferent noise stimuli and the hypothalamus, by contrast, captures changes within the body and the carotid blood vessels as a result of vasodilatation.

When considering further typical synaptic mechanisms, the neurotransmitters histamine, acetylcholine, and noradrenaline are essential for the neural interactions and processes coming along with the physiological syndrome (Takeda et al., 2001). To better understand the biochemical properties that are involved in motion sickness, Fig. 3-19 illustrates the main entities associated with the neurotransmitters linked to the vestibular system. The light-petrol circles represent excitatory neurons and synapses, whereas dark-petrol-filled circles indicate inhibition. Abbreviations are listed in the eponymous table at the beginning of the current elaboration, while some acronyms are explained more precisely in the subsequent chapters.
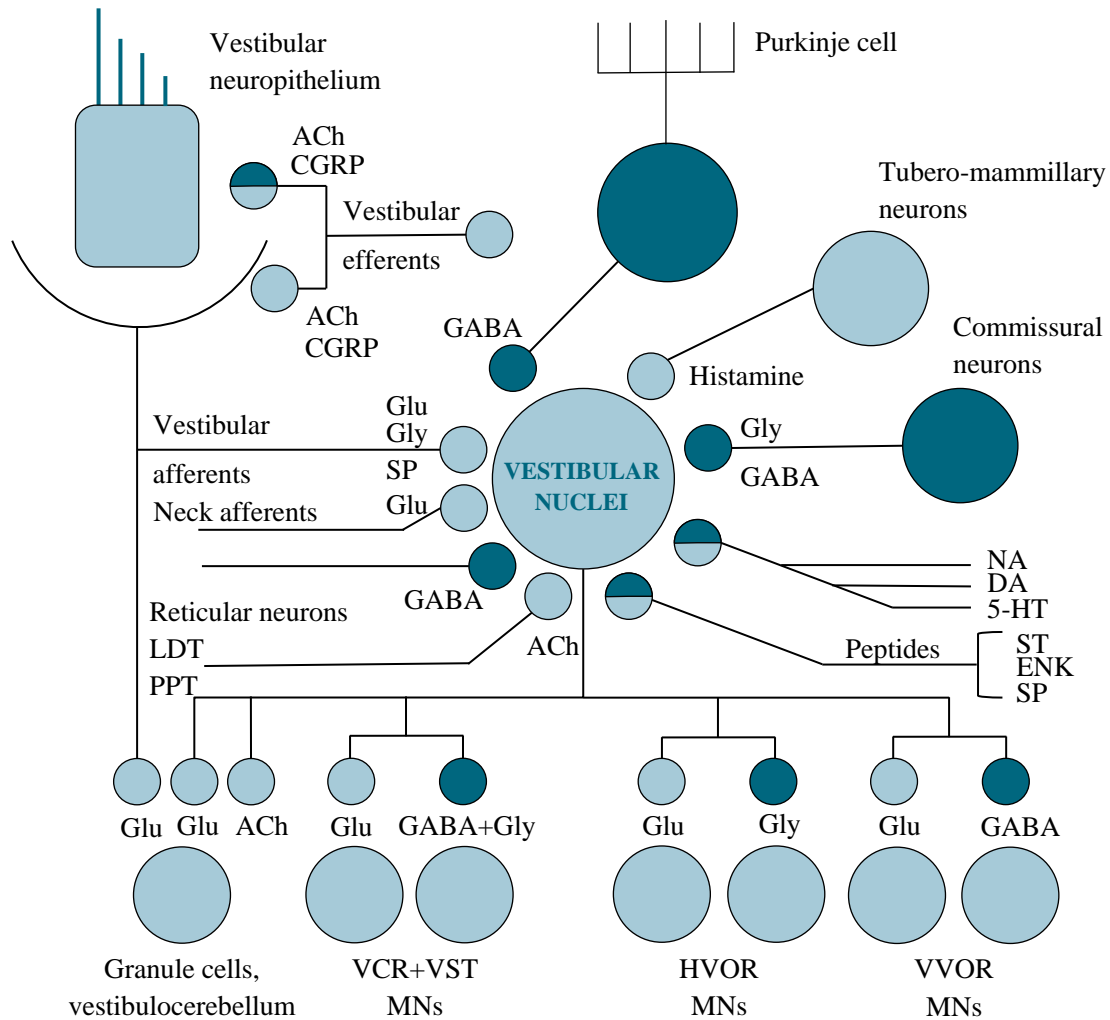
Fig. 3-19: Neurotransmitter involved in the development of motion sickness.
Based on Waele et al. (1995) as modified and cited in Goldberg et al. (2012, p. 199)

The importance according to motion sickness, as it is presented in the following, is due to the fact that cells origin in neurons of the vestibular nuclei could react to optokinetic input and joint stimuli (V. J. Wilson & Melvill Jones, 1979). Also, Purkinje's cell status within the cerebellum has been proven to distinguish between retinal and vestibular signals during physical dynamics (Lisberger & Fuchs, 1978).

3.2.5 Reflexes Maintaining Gaze and Postural Control

This chapter provides information about important sensory-motor reflexes to maintain postural, respectively head-neck, and gaze control. Walking, for instance, is elicited by such crucial motor reflexes and multisensory strategies. The following Fig. 3-20 illustrates recorded head acceleration in the sagittal plane during a typical walk.
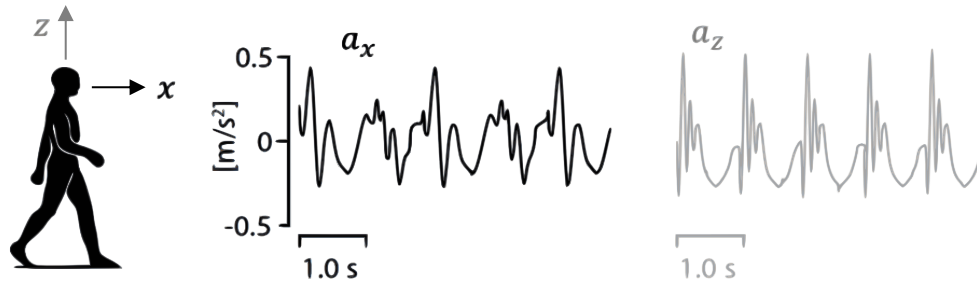
Fig. 3-20: Acceleration of head motion during walking.
Modified from Farkhatdinov et al. (2019a, p. 13): converted into a vector graphic, coordiante system added and colour of vertical motion changed

According to everyday experience, the respective oscillating motion pattern, as illustrated above, is not present in the subjective visual perception during walking. Due to oculomotor processing, straight visual information is perceived. According to Goldberg et al. (2012, pp. 231–240), here, three types of eye movements, namely smooth pursuit, vergence, and saccades, are mainly voluntarily initiated, whereas the *vestibulo-ocular* (VOR) and *optokinetic reflexes* (OKR) keep images stable on the retina during rotational and translational head movements. Compared to other reflexes, the OKR does not react to vestibular afferents. It is provoked by the motion of the visual world across the retina and complements the VOR during very-low-frequency head movements. In specific situations, for example, when co-drivers are looking out of the windshield during turning of the vehicle and are focusing on a visual target at the surrounding landscape (Bronstein et al., 2020), the two physiological functions take place simultaneously.

Furthermore, balance and posture control is needed to ensure an upright head and body position. In general, posture is defined as the overall configuration of the body with its segments, while postural control is described as the coordinated stabilization of all body parts (Riccio & Stoffregen, 1988; Stoffregen & Riccio, 1988). According to Cullen (2012), posture control relies on multisensory reafference from vision, proprioceptive inputs, and vestibular organs. In fact, the so-called *vestibulo-spinal reflexes* (VSR) are essential in coordinating head-neck movements with the trunk and body. The technical term VSR additionally implies motor output to the skeletal muscle below the neck, whereas the *vestibulo-collic* (VCR) and *cervico-collic reflexes* (CCR) contribute to head stabilization as described by Happee et al. (2017).

As illustrated in Fig. 3-21 the vestibular nuclei is the central element in the regulation of human body parts as well as in stabilization processes. As previously mentioned, vestibular afferents are not the only source of (self-)motion perception (Goldberg, 2016, p. 1010). Indeed, a distinguishing facet of vestibular processing is related to its multimodal sensory combination of input signals at the first stage of central processing.

Nonetheless, the focus will be placed on reflexes initiated by the vestibular system since the impact on balance is equally illustrated by its colloquial naming, the organ of equilibrium. Given that some kind of spinal stabilization is possible to achieve in sitting conditions in vehicles, the focus regarding postural-related reflexes is shifted exclusively to the VCR and CCR.
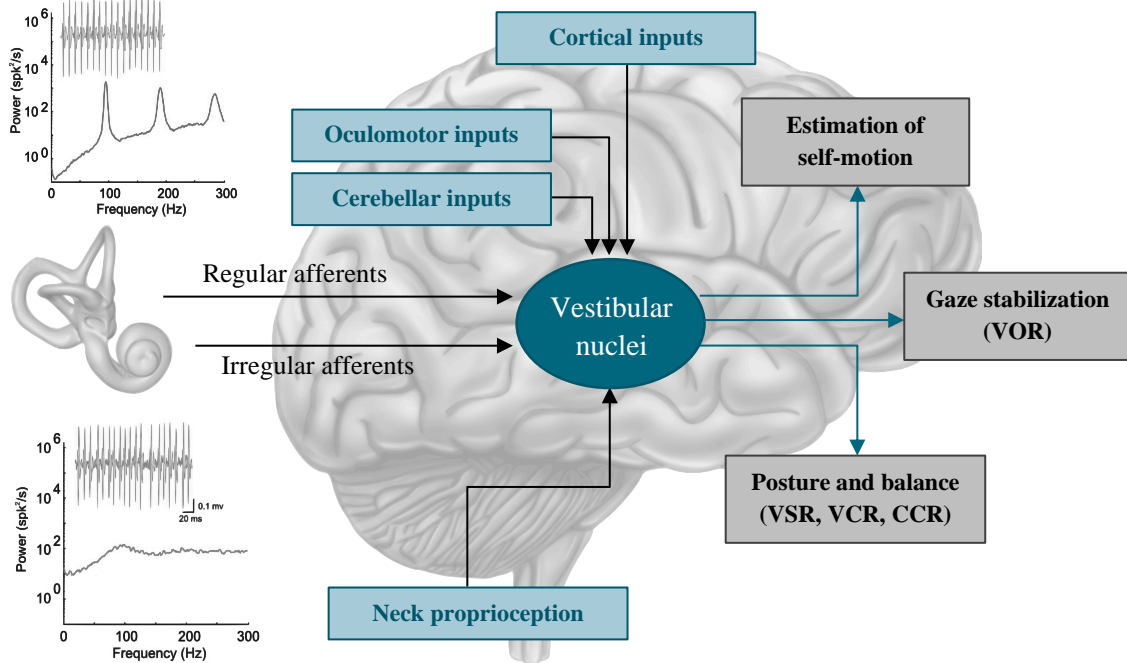
Fig. 3-21: Reflexes controlled by the vestibular nuclei.
Based on Cullen (2012); images: power plots - McGuinness (2014, p. 9), vestibular organ - Boselli (2021)

Vestibulo-Ocular Reflex to Maintain Stable View

To maintain a constant visual perception of the surrounded world, the vestibular and visual systems synergistically supplement each other in triggering eye movements. In fact, due to this interaction, steady images on the retina are achieved by keeping the line of sight in space, irrespective of whether head dynamics occur (Bronstein et al., 2020; Fetter, 2007; Somisetty & M Das, 2020). The VOR, as an essential part of this process, is driven by angular (AVOR) and translational (TVOR) motion, whereas in both conditions the eye rotation compensates for the complementary head movements. The latency between the beginning of head rotation and the subsequent eye movements in the opposite direction only lasts 5 - 6 ms (Cullen, 2012). However, a greater period of time (up to 10 ms) is observed by translational stimuli (Huterer & Cullen, 2002). Goldberg et al. (2012, p. 273) suggested that this increase in latency is due to the more complex polysynaptic pathways mediate by the TVOR. In any case, both subtypes refer to direct neuronal conjunctions. Within the AVOR, a three-neuron arc connects the vestibular nerve with the oculomotor nuclei and extraordinary fast muscle filaments (Szentagothai, 1950). The schematic representation of the AVOR involving neuronal structures and projections during rightward rotation in the horizontal plane is shown in Fig. 3-22.

1. Detection of rotation

Semicircular canal

RIGHT LEFT

Aducens internuclear interneurons

Vestibular nerve

Oculomotor nuclei

Scarpa´s ganglion

Oculomotor nerve

Vestibularis nucleus

2. Inhibition of extraocular muscles on one side

2. Excitation of extraocular muscles on the other side

Medial rectus muscle

Abducens nucleus

Lateral rectus muscle

Abducens nerve

EXCITATORY

INHIBITORY

3. Compensatory eye movement

Fig. 3-22: Pathway of the vestibulo-ocular reflex.
Based on Somisetty & M Das (2020); Obrist (2011, p. 9)

Under dynamic circumstances, saccadic eye movements readjust gaze to targets of interest in visual space. The neural control of saccades is regulated by step pulse commands which are monitored in muscle tension. Saccades can be voluntary, but also can occur unconsciously. For larger head rotations, a mechanism called nystagmus appears which is characterized by a combination of a slow-phase control strategy to reduce the gaze velocity error and a fast phase control strategy to maintain eye position within the oculomotor range. In the slow phase, eye movements in the same direction as the visual stimulus becomes apparent, whereas in the fast phase the eyes move in the opposite direction. A specific form of nystagmus occurs under visual stimulus on the retina and is known as optokinetic nystagmus. Further forms are evoked under different provoking stimuli, which, in fact, determine the terminology of the specific type of nystagmus e.g., vestibular or post-rotatory nystagmus. Saccades and nystagmus show great similarities such as the innervation by the identical premotor generator. According to Hepp et al. (1989), the difference is suggested within the neural input, which triggers the human control mechanism. In summary, the nature of nystagmus appears to be a reflexive combination of saccadic and smooth pursuit movements, which is controlled by the AVOR. As previously described in mathematical terms (see chapter 3.2.1), the semicircular canals, as high pass head-velocity sensors, provide physical information for the AVOR. Therefore, it is evident that also the AVOR compensates in mid and high-frequency ranges with characteristics of near-unity gain and a minimum phase close to zero. Referring to the biomechanical model of semicircular stimulation a long time constant of around 5.7 s represents the cupula rebound deflection. By considering the response of vestibular nuclei neurons, a time constant up to 20 s can be observed. (Goldberg et al., 2012, pp. 240–245)

The consecutive eye movements, produced by the AVOR, show the same lengthened behaviour. This central integrative network phenomenon is called velocity storage, in which the brain integrates the means of vestibular-nerve signals. In general, there is no inevitable visual stimulation needed for innervating this characteristic motion pattern. At exceptionally low frequency, the AVOR is mainly driven by the velocity storage mechanism integrator mediated by an indirect pathway, which is demonstrated in Fig. 3-23. (Raphan et al., 1979)

NI: Neural integrator
MN: Motorneurons

Neural integrator
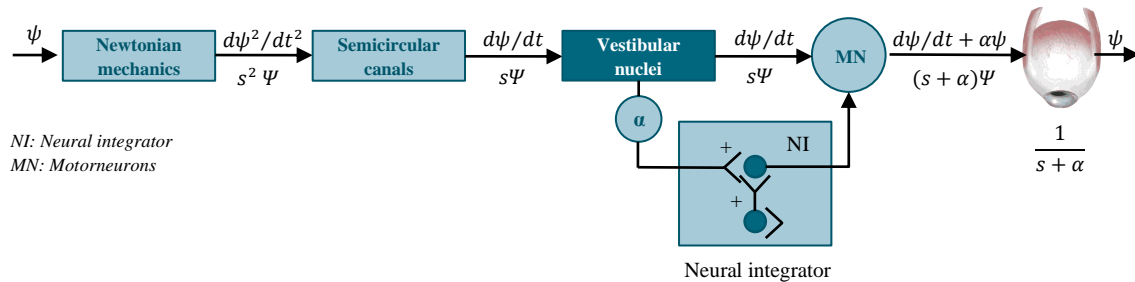
Fig. 3-23: Transfer function of the vestibulo-ocular reflex.
Based on Goldberg et al. (2012, p. 239)

In general, there is strong evidence that the velocity storage mechanism seems to be involved in the development of motion sickness (Clément & Reschke, 2018; Dai et al., 2003; Guo et al., 2017; Hoffer et al., 2003). In fact, according to the investigations of B. Cohen et al. (2003), motion sickness is influenced by the properties of the velocity storage mechanism concerning the GIF. This value had been previously described in chapter 3.2.1 and is defined in this particular case as the sum of linear accelerations acting on the human´s head-neck plant under consideration of the gravity force. The visuovestibular interaction does not only exist in physical motion conditions, since inadequate visual stimuli e.g., the occurrence of congenital nystagmus or external ophthalmoplegia, influence the vestibular function as well. This state of knowledge explains why vestibular patients report greater symptoms of vertigo during visual stimulation (Grunfeld et al., 2003; Okada et al., 1999; Seemungal et al., 2007). Furthermore, expanded time constants due to optokinetic exposure, which is represented through an extensive duration of optokinetic afternystagmus, occur in subjects with strong sickness symptoms (Guo et al., 2017). In 2003, Dai et al. postulated that motion sickness is associated with the spatio-temporal characteristics of velocity storage. The researchers proved conclusively that motion sickness is determined through the orientation properties of the velocity storage mechanism, which is liable to adjust the eye velocity vector towards the spatial vertical. As outlined by Nooij et al. (2018), other investigations such as from Laurens & Angelaki (2011) concluded that the velocity storage mechanism seems to contribute in a more general way to the estimation of the spatial vertical. The importance of this assumption will be explained in relation to etiology in chapter 3.2.7. In summary, further research needs to be carried out to understand the underlying mechanism between motion sickness and velocity storage (Nooij et al., 2018).

For rotational head movements, retinal stabilization can be achieved by a single eye rotation, whereas during translational movement, a single eye movement is insufficient in stabilizing the whole visual field (Goldberg et al., 2012, p. 7).

To address this issue, once again, the example of a co-driver looking out of the window is chosen and illustrated in the following Fig. 3-24.
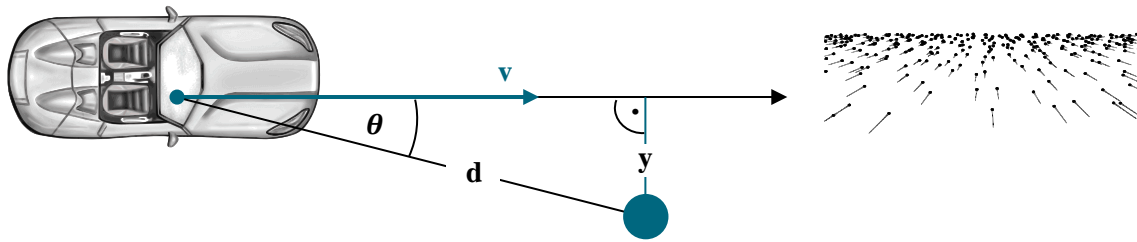
Fig. 3-24: The optic flow.
Left: based on Chatziastros (2003, p. 12); right: Chatziastros (2003, p. 6)

The velocity of optic flow, as described in chapter 3.2.2, follows the motion parallax theory that describes the dependency on eye-to-target distance and relative eye-to-target motion (Angelaki & Hess, 2001). In other words, proximal objects increase retinal image slip, whereas distant targets move less rapidly on the retina. While observing the center of the optic flow, neither movements nor visualization of motion parallax occur, which, in turn, can be seen on the right-hand side of Fig. 3-24 and is known as the focus of expansion in optic flow fields (Bubb & Wohlfarter, 2012; Warren et al., 2001). Gibson (1950) postulated that moving towards the center of target leads to an increasing gradient motion of visual cues which align themselves in the opposite direction, or more precisely, away or respectively nearer to the focus of expansion (Yusof, 2019, p. 13). The velocity of elements in the optic flow during linear translation in the horizontal plane is determined by the following equation (Chatziastros, 2003, p. 11):

$$\frac{d\theta}{dt} = (\sin \Theta)^2 \cdot \frac{v}{y}$$

Eq. 3-14

According to Fig. 3-24, v represents the translational velocity of the observer, while y describes the distance of the target perpendicular to the direction of movement. The value θ illustrates the angle between the direction of movement and eye-to-target distance (d). In consequence, the observer´s velocity concerning the distance between the environmental elements determines the behaviour of the optic flow. (Chatziastros, 2003, pp. 10–14)

Angelaki & Hess (2005) presented a more general form with respect to the fovea in which image stabilization is added by horizontal $\dot{\gamma}$ and vertical $\dot{\varphi}$ components of eye velocity during horizontal translation. Here as well, the focus will be placed on the flow velocity orthogonal to the optical axis in which parallel components are not considered:

$$\frac{d\gamma}{dt} = \frac{v}{d \cdot \cos\varphi} \cdot \sin(\theta - \gamma) \quad , \quad \frac{d\varphi}{dt} = \frac{v}{d} \cdot \sin(\varphi) \cdot \cos(\gamma - \theta)$$

Eq. 3-15

In cases of moving straight along the gaze line ($\theta = 0$, $\gamma = 0$, and $\varphi = 0$), the respective eye does not require any movement and, therefore, keeps in a stable position. Furthermore, no horizontal eye dynamics are initiated when turning the head along the direction of the target ($\gamma = \theta$). With an increasing eccentricity of the object´s location relative to the direction of the heading, a larger eye movement is needed to maintain a stable image on the fovea. (Angelaki & Hess, 2005)

As outlined by Angelaki & Hess (2005), arbitrary gaze direction requires horizontal and vertical eye movements, which typically differ in terms of their characteristics within each eye. In general, as opposed to the AVOR, the TVOR shows a strong relationship with target distance (Angelaki et al., 2000). Under near-viewing conditions, the gain of TVOR is underestimated (0.5), while objects far away (>1 m) tend to overcompensation (Liao et al., 2010). The main cues that contribute to the viewing distance in terms of scaling the TVOR amplitude are accommodation and vergence angle, whereas binocular disparities and textural cues show small effects (Busettini et al., 1991; Schwarz et al., 1989). Goldberg et al. (2012, pp. 271–273) concretized that the concerns about the distinction between translational motion and head tilt are solved by frequency segregation and canal input. Due to this information, the perception system can determine whether the otolith afference is the result of tilt or linear motion. In summary, the AVOR and TVOR, in synergy with visuomotor reflexes, ensure gaze stabilization by vestibular-driven inputs at high frequencies and visually driven eye movements at low frequencies (Goldberg et al., 2012, p. 274).

Head-Neck Stabilization Concerning CCR and VCR

As mentioned by Goldberg et al. (2012, p. 280), two different approaches define the current understanding of postural control. Firstly, the idea of multisensory strategies, in which internal programs evoke a pattern of muscular activity. These programs arise through experienced visual, vestibular, and somatosensory information, while their capability to adapt is related to redundant motor strategies and sensory inputs. The second perspective refers to the occurrence of motor reflexes to regulate posture tone and to ensure an upright body, trunk, and head-neck posture. Within this analysis, the focus will be on the characterization of passive feedback reflexes.

When the head moves in space, activation of canal and otolith afferents are transmitted to neurons in the vestibular nuclei and the reticular formatio to evoke motor reflexes like the VCR. As previously seen, vestibular-driven reflexes can be divided into angular evoked head rotations (AVCR) or linear head forces (LVCR). The provoked motor reflexes within the AVCR are in the same plane, while the direction of movement is inverse to the preceded head rotation. Here as well, direct, disynaptic excitatory and inhibitory pathways conjunct motoneurons, which are located in the neck, with ampullary axons. The LVCR is elicited by otolith organs, while the predominant activation of the utricular macula or saccular macula depends on the nature of stimuli. Most notably, the VCR neurons are suppressed during voluntary head movements, while this effect does not occur during passive head motions. (Goldberg et al., 2012, pp. 287–294)

The CCR is a stretch reflex and arises through proprioceptive muscle activation. Although the CCR originates in muscle spindles, its origin is assumed to be related to complex spinal pathways as well as supraspinal loops (Bolton et al., 2018; Keirstead & Rose, 1988). It aligns with the function of the VCR since the same neck muscles are controlled during compensatory head rotation (Goldberg et al., 2012, p. 294).

According to Dutia & Hunter (1985), the dynamic responses of CCR and VCR, in particular over the frequency range of 0.2 Hz, show strong similarities.

As shown in Fig. 3-25, both reflexes obtain negative feedback loops to keep the head stable by minimizing the angle between head and trunk. By applying the Laplace transformation, a system diagram of two feedback reflexes extended by mechanics of the head-neck system and voluntary head movements is shown. Here, the control is shrunken to yaw head motion (ψ) through the axis-at-lantis joint (C1-C2) (Peng et al., 1996).
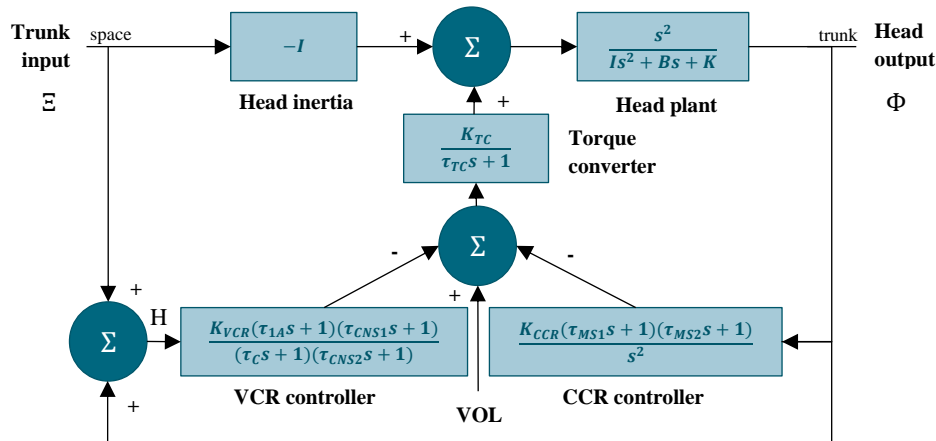
Fig. 3-25: Reflexes of head and neck stabilization.
Based on Goldberg & Cullen (2011); Peng et al. (1996)

As evident from the block diagram in Fig. 3-25, the position of the trunk in space (Ξ) as well as the voluntary motor command (*VOL*) constitute two input variables for the dynamic control system. Under circumstances in which CCR and trunk movements are absent, head-neck control acts as a conventional negative feedback system with a single input value. The output variable (Φ) refers to the neck angle, which is determined as the angular position of the head with respect to the trunk. To address the mechanical properties of the head-neck system, a transfer function called head plant (*P*) is included. Lastly, the low-pass torque converter (*T*), activated by the two negative feedback reflexes (VCR and CCR) in combination with voluntary motor commands, produces muscle activation to manipulate head-trunk position. By combining the paths shown in Fig. 3-25, the following equation is obtained:

$$-I \cdot P \cdot \Xi - VCR \cdot T \cdot P \cdot (\Xi + \Phi) - CCR \cdot T \cdot P \cdot \Phi = \Phi \qquad \text{Eq. 3-16}$$

While suppressing active motor commands and reflexes, the mechanics of head dynamics behave like a passive second-order differential system. Despite the postural tone of neck muscles, passive behaviour is characterized through the moment of inertia (*I*), viscosity (*B*), and elasticity (*K*). Whereas the moment of inertia depends on the geometry and density of the head concerning the eccentricity between the center of gravity and the rotation axis, the stiffness and viscosity are affected by the postural tone set by the central nervous system. Stiffness as well as viscosity show great inter-individual differences, which contribute to uncertainties in their estimation. It is confirmed that passive head mechanics constitute an underdamped system, which arises due to large head inertia. In fact, the value of viscosity must be at least three times greater to avoid head oscillation. (Goldberg & Cullen, 2011)

Mathematical transformation and substitution of the passive head plant through a general Laplace expression of a second-order, ordinary differential equation provide the following derivation:

$$\frac{\Phi}{\Xi} = \frac{-(I + VCR \cdot T)}{\frac{Is^2 + Bs + K}{s^2} + (VCR \cdot T + CCR \cdot T)}$$

<div align="right">Eq. 3-17</div>

To investigate the feedback loop of the VCR it seems to be beneficial to establish H, as the head position in space (H = Ξ + Φ), rather than utilizing the head-trunk ratio that is represented by the variable Φ. The necessitative human parameters for calculating the following chart are originated from Peng et al. (1996).
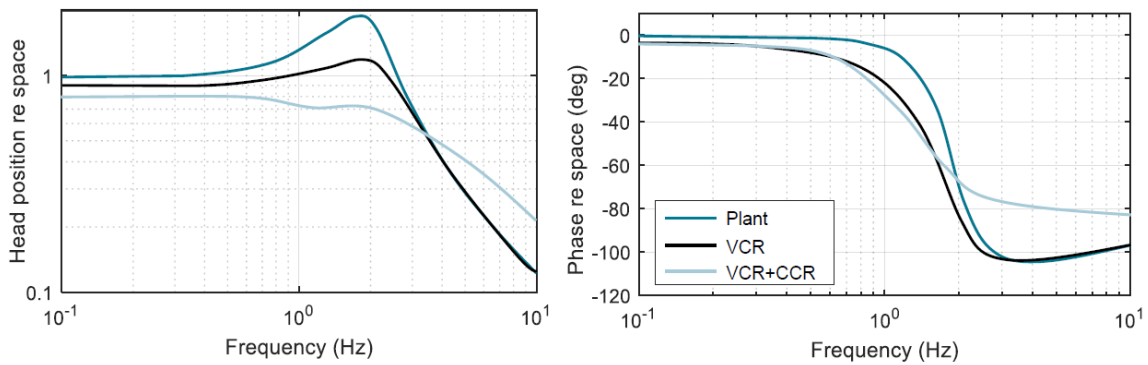
Fig. 3-26: Transfer function of head and neck stabilization.
Based on Goldberg & Cullen (2011)

As illustrated in the bode plot of Fig. 3-26, the calculated passive plant response constitutes a resonant peak around 2 Hz with gain reaching up to a maximum value of 1.83. Here, the CCR and VCR can curtail the maximum peak. However, these two reflexes are unable to maintain head stabilization during low-frequency neck or trunk incidents. Indeed, below 1 Hz stabilization is negligible. At higher frequencies, the moment of inertia, rather than activation of the negative feedback reflexes, is likely to damp head oscillation.

3.2.6 Sensory Rearrangement and Neural Mismatch Theory

One of the main implications underlying the crucial role of the vestibular organ on the etiology of motion sickness is based on the fact that people with labyrinthine laison are immune to pursuant symptoms (Money, 1970). Due to this finding, a theory of vestibular overstimulation has been established as the triggering factor of provoking motion sickness (Dobie, 2019, p. 9). Over the years, this theory has been disproven and replaced by the sensory conflict theory. According to Reason & Brand (1975), motion sickness occurs due to conflicts between the perception signals. The information provided by the three sensors is compared in the brain as described in the previous chapters. Already in 1931, Claremont postulated that seasickness is related to unaccustomed conflicts between senses originating in the vestibular, visual, and proprioceptive system. Nevertheless, according to Dobie (2019, pp. 93–108) as well as Oman & Cullen (2014), it took several elaborations, scientific debates, and research efforts until the taxonomy of inter-sensory cue conflict by Reason & Brand (1975) aroused.

In 1978, Reason elaborated on his assumption and published the neural mismatch model, which consists of two additional premises. Firstly, the sensory information of the relevant structures can vary between each other. Indeed, it is even more important that these receptor inputs differ from the sensory pattern of already experienced situations. The respective exposure history is linked to the neural store and attributed to activations of the cerebellum. Thus, the misalignment provoking motion sickness arises between the actual sensed and expected sensory information, rather than the variance between the current receptor signals (see Fig. 3-27). By way of example, the model provides an explanation for the great ability to adapt to nauseogenic stimuli, by which the motion sickness susceptibility is reduced. Among researchers and physicians the neural mismatch model, also known as sensory rearrangement theory, is arguably the most accepted approach to describe the etiology of motion sickness (A. Koch et al., 2018).
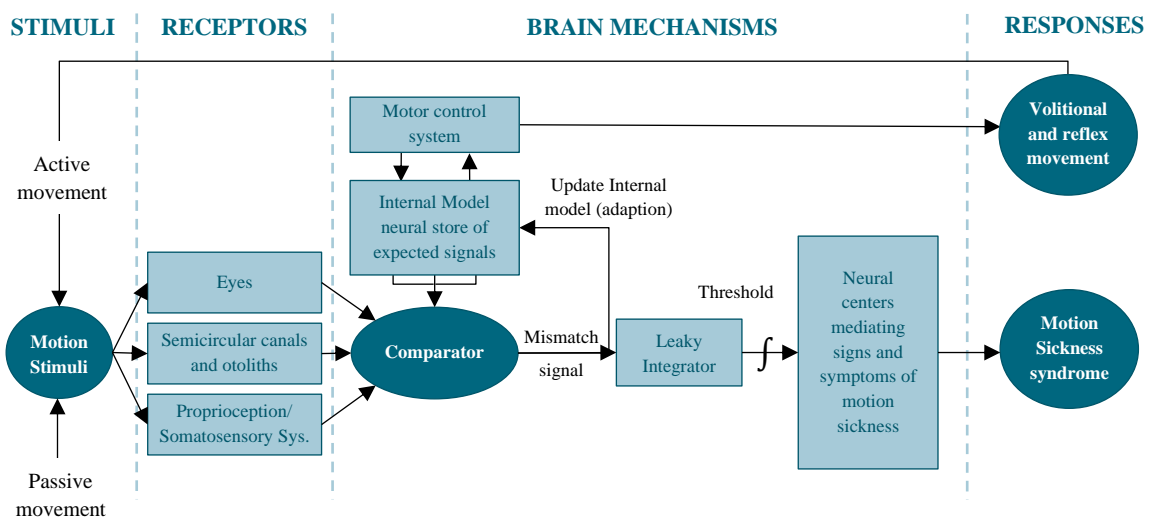
Fig. 3-27: The sensory rearrangement model.
Based on Dix & Hood (1984) as cited in Benson (2002, p. 1053)

The second premise encourages the assumption that the vestibular system has to be involved in the process of motion sickness in any manner. These situations occur either under physical-induced circumstances or in an indirect stimulation by visual-induced forms. To address these differences, Reason (1978) defined two main categories of sensory rearrangement: visual-vestibular (intersensory) and canal-otolith (intrasensory) conflicts. Furthermore, as shown in Tab. 3-5, three different subtypes of sensory status lead to six potential rearrangement scenarios.

Tab. 3-5: Type of conflict in the sensory rearrangement theory.
Based on Schmäl (2013)

Type of conflict	Category 1: Conflict between visual (A) and vestibular, propriocept. (B) signal	Category 2: Conflict between canal (A) and otolith (B) signal
Type 1 Input A and B simultaneously receive contradictory or uncorrelated information	Looking out of the rear windows of a moving vehicle	Low-frequency oscillation e.g., in Truck cabins

The table continues on the next page.

Tab. 3-5: Type of conflict in the sensory rearrangement theory *(continued)*.

Type 2 a		
Input A signals in the absence of the expected B signal	Operating a static car simulator with a moving visual display	Space motion sickness e.g., orbit flight
Type 2 b		
Input B signals in the absence of the expected A signal	Riding in a vehicle without any external visual reference e.g., in the rear of an ambulance car	Rotation about an earth-horizontal axis e.g., laboratory testing with rotation-chairs

3.2.7   Subjective Vertical

In 1998, Bles et al. proposed a modification of the aforementioned sensory rearrangement theory. The subjective vertical theory affirms the idea of a sensory conflict, however, instead of attributing several sensory rearrangements, the conflict only occurs between the sensed and the expected vertical. Fig. 3-28 illustrates the control-oriented approach, in which the efference copy and the estimated values are used to compare the actual sensed vertical and the expected one. The difference between these two values is equivalent to the motion sickness conflict. Therefore, the human regulation process provides suitable bio-mechanical information to deeply understand the mismatch theory. Furthermore, the researchers attribute their theoretical approach to postural control, which is linked to the theory of Riccio and Stoffregen described in the following chapter 3.2.8.
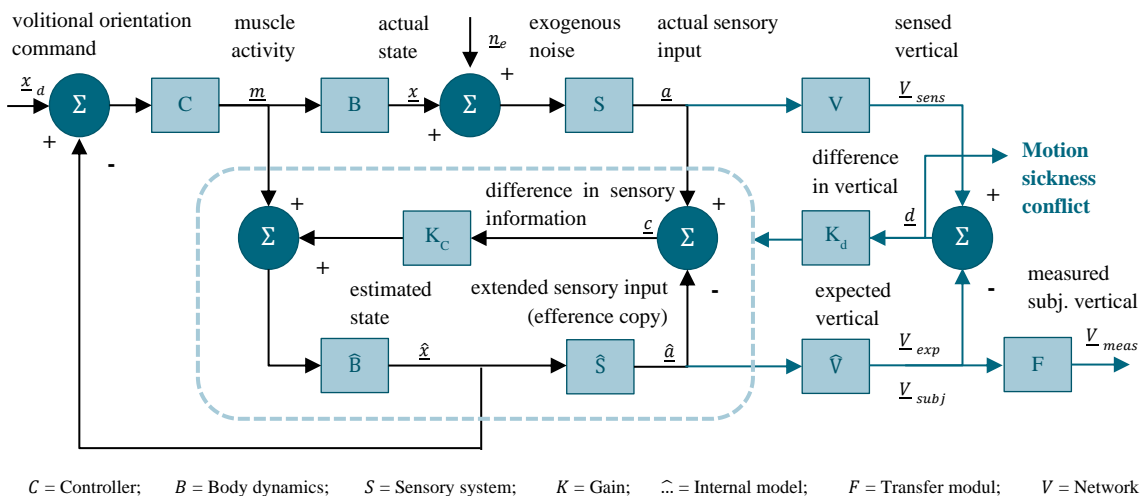
Fig. 3-28: The subjective vertical model.
Based on Bles et al (1998)

3.2.8   Postural Instability Theory

In 1991, the ecological psychologists Riccio & Stoffregen claimed that humans learn strategies to obtain their balance. Those learned strategies cannot be applied in unknown situations, where information through the human senses differs from an already stored pattern. In animal experiments, the researchers investigated if motion sickness occurs whenever the subjects found themselves in situations where they were unable to maintain their body control. Accordingly, the researchers concluded that the lack of balance is a key factor in the development of kinetosis.

The postural instability theory, as the counterpart to the sensory-related explanations, offers a different approach to the etiology of motion sickness. With respect to the existing theories, Riccio & Stoffregen (1991) argued that all conflict notions have to be considered as unproven reifications. However, both, the subjective vertical and the postural instability theory also underline the importance of the vestibular organ as the main sensory receptor for maintaining balance and contributing to the prevalence of motion sickness (Dobie, 2019, p. 108).

3.2.9   Poison Theory

In 1977, Treisman postulated an evolutionary hypothesis to explain the cause of motion sickness. As a result, this approach addresses the reason why the misalignment between the different perception signals, namely the vestibular apparatus, the eyes, and the somatosensory system, triggers cardiovascular and gastrointestinal symptoms. Within the poison theory, two main aspects refer to the physiological phenomenon. Firstly, by considering the cardinal symptoms, it is concluded that vomiting occurs to eliminate the ingested toxins, whereas, secondly, nausea and fatigue arise as a reminder to avoid future encounters with toxic material. According to Treisman, motion sickness is an accidental side effect of the early warning mechanism. However, as already outlined by Oman (2012), Treisman also suggested that motion sickness with its spatial orientation-emetic linkage is "so obviously disadvantageous that, if there were no positive reason for its presence, natural selection should have acted strongly to eliminate it".

In 2014, Lackner reiterates the weaknesses of the poison theory. For instance, there is a lack of explanation regarding the difference between passengers and drivers in the severity of carsickness. In addition, the poison theory is incapable of explaining the highly provoking nature of low-frequency vibrations. Furthermore, from an evolutionary point of view, nausea and vomiting limit the capability to move which decreases survival likelihood in escape situations. This would identify an extensive sensitivity to motion sickness as a disadvantage rather than a survival attribute.

As will be discussed in chapter 3.4.1, there is strong evidence that individual susceptibility to motion sickness refers to genetic aspects, which supports the idea of the poison theory (Bakwin, 1971; Klosterhalfen et al., 2005; Reavley et al., 2006). However, according to Oman (2012), there are several contrary aspects as well as limited experimental evidence on the poison theory. Therefore, it seems challenging to distinguish Treisman´s explanation from other adaptationist theories.

3.3   Physiological Diagnostics on Motion Sickness

Even if the vegetative symptomatology of the motion-induced illness is retching and vomiting, it is mostly preceded by a wide range of signs such as fatigue, lethargy, dizziness, cold sweating, facial pallor, increase in skin oxygen, flushing, drowsiness, headache, nausea, decreased gastric motility, tachygastria, hypotension, and cardiovascular complaints (Cuomo-Granston & Drummond, 2010; Flöchinger, 2012; Golding, 1992; Holmes et al., 2002; Marcus et al., 2005).

In some cases, increasing sensitivity to odors and loss of appetite can be observed (Bronstein et al., 2020). Several researchers emphasize that under nauseogenic motion exposure, changes of facial blood flow, as revealed by modification in skin colour, can be observed (Cuomo-Granston & Drummond, 2010; Drummond & Granston, 2004; Holmes et al., 2002). Across phases of eccentric vertical axis rotation, Kolev et al. (1997) measured the microcirculatory skin blood flow of subjects in which significant correlations to motion sickness occurred. These results, however, only had been observed when measures were applied at the forehead, not at the fingertip. In any case, facial vasodilatation shows potential in the early diagnosis of motion sickness, even before the first cardinal and severe symptoms are subjectively present or noticeable (Kolev et al., 1997). Pallor is characterized as a reduction of oxyhemoglobin in superficial membrane and is originated by vasoconstriction of internal (cutaneous) vessels associated with vasodilation of deeper regions with increasing muscle blood flow (Benson, 2002, p. 1052; Johnson et al., 1993). According to Golding (1992), the combination of sweating with pallor, as a result of motion sickness, is an aberration since the thermoregulatory increase of skin conductance is ordinarily linked with peripheral vasodilatation.

In general, the scope of symptoms within the two types of visual and physical induced motion sickness differ rarely between each other, even though disorientation and oculomotor incidents like eyestrain are more common in visual-provoking conditions (Keshavarz, Riecke, et al., 2015; Keshavarz et al., 2021; Lawson, 2014). Furthermore, K. M. Stanney et al. (1997) proposed that within the manifestations of visual-induced motion sickness, major physiological expressions also vary between each other. For example, in cases of cybersickness less nausea is perceived (K. M. Stanney et al., 1997). Overall, the severity of the polysymptomatic manifestation differs between individuals and depends on the type, duration, frequency, and amplitude of the provocative motion stimuli, as well as the individual susceptibility to motion sickness (McCauley et al., 1976; Money, 1970; William, 1881).

Furthermore, it is known that kinetosis is accompanied by increased excretion of pituitary hormones since those correlate with the severity of symptoms during exposure, as well as in the recovery phase (Benson, 2002, p. 1065). Due to investigations from Eversmann et al. (1978), *antidiuretic hormone* (ADH), *growth hormone* (hGH), *prolactin* (hPRL), and cortisol show a strong relationship to the motion-induced sickness, whereas serum levels of luteinizing hormones did not change significantly in consecutive sessions. Fig. 3-29 illustrates the results in the secretion of anterior and posterior pituitary hormones during cross-coupled motion stimuli, investigated by Eversmann et al. (1978). In fact, a swiveling chair was used with an angular velocity ranging from 15 to 215 °/s by which the participants simultaneously moved their heads in a predefined pattern during turning. The operationalization of motion sickness was achieved by using the subjective scaling principle of Miller & Graybiel (1970). The respective severity of motion sickness manifestations is presented by the gray area in the center of the following figure. The trial was only discontinued when a strong incidence of motion sickness i.e., retching or vomiting, occurred.
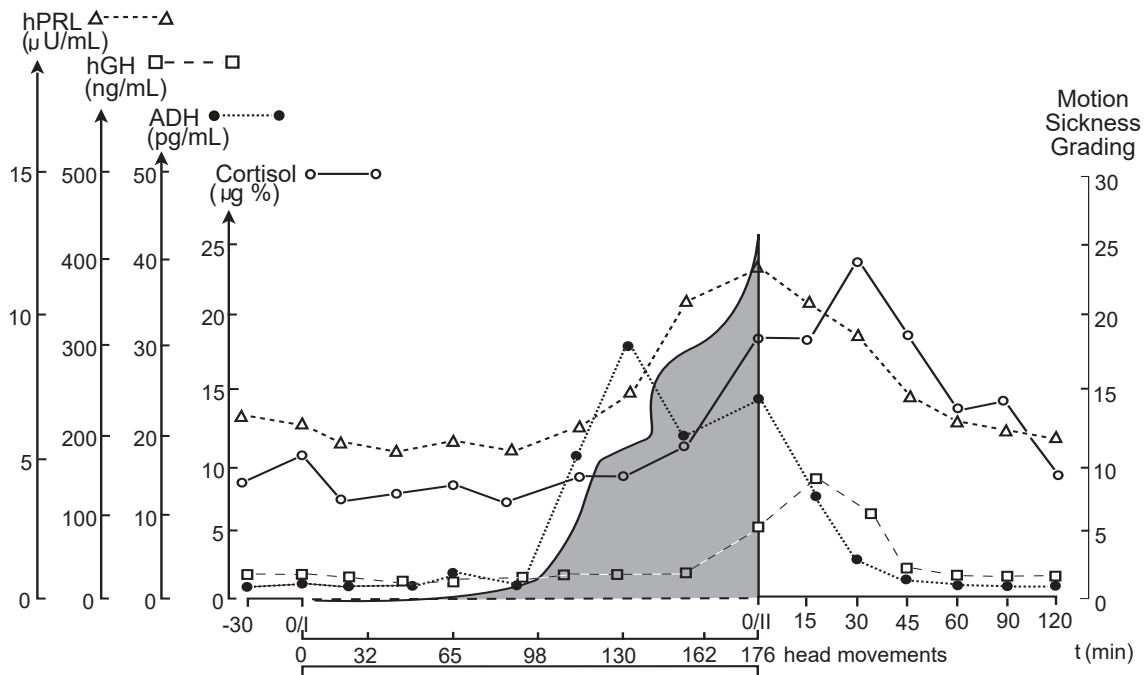
Fig. 3-29: Secretion as an indicator of motion sickness prevalence.
Modified from Eversmann et al. (1978) as cited in Benson (2002, p. 1051): English version

Within the wide range of conspicuous secretion, the antidiuretic hormone acts as the most sensitive indicator for motion sickness, whereas growth hormone, prolactin, and cortisol levels show greater delays and less evidence on predicting motion sickness. Compared to the baseline level, an ADH secretion level of up to 21 times greater was reported. As a result, the researchers concluded a decreased urinary excretion associated with high urine osmolality. This, however, is not accompanied by changes in serum osmolality (Graybiel et al., 1965; N. B. G. Taylor et al., 1957). Eversmann et al. (1978), furthermore, outlined that even if no correlation was found between intraindividual hormone prevalence and duration of exposure, inter-individual secretion levels correlate with the severity of motion sickness.

In 1985, Kohl carried out investigations to assess the influence of anti-motion sickness drugs on endocrine response. Here, predrug levels of *adrenocorticotropic hormone* (ACTH) and vasopressin acquired before experiencing the nauseogenic stimulus were twice as high in less-susceptible subjects. According to Kohl (1985), the chronic modulation of endocrine might be more effective than the blockade or stimulation of specific receptors, as it appears in common anti-motion sickness drugs.

Cardinal symptoms of motion sickness are mediated by peripheral pathways, while vomiting and nausea originate within the central nervous system (Takeda et al., 1986). This assumption is supported by Levine et al. (2000), who investigated the intake of *serotonin* (5-HT3) receptor antagonist with its anti-emetic nature during nauseogenic stimuli. As a result of their investigation, gastric tachyarrhythmia disappears due to the intake of this drug, while nausea just as malaise still occurs. The receptor antagonists inhibit the development of tachyarrhythmia and, therefore, act as gastric anti-dysrhythmic. By contrast, the receptor antagonist is unable to contain the disease of further motion sickness symptoms (Levine et al., 2000).

3.4 Individual Factors Influencing Motion Sickness Susceptibility

On average, one out of three individuals is affected and relatively susceptible to motion sickness (Hromatka et al., 2015). According to Schmäl & Stoll (2000), about 5 - 10 % of individuals are exceedingly sensitive, whereas 5 - 15 % are resistant to kinetosis stimuli. The rest reveals moderate sensitivity. Moreover, the researchers postulate that about 90 % of the population, living in industrialized countries, experienced motion sickness in any form at least once in a lifetime.

3.4.1 Ethnic Origin and Genetics

It is known that the inter- and intraindividual motion sickness susceptibility differs within subjects (Schmäl, 2013). However, some characteristics can be identified which lead to more or less sensitivity in experiencing motion sickness. Asians, for example, are more sensible to incongruent perception stimuli than Caucasians (Beard, 2012, p. 107; Klosterhalfen et al., 2005). Stern et al. (1993) and Stern & Koch (1996) emphasize corresponding results, presenting greater motion sickness occurrence in Chinese subjects compared to European- and African-Americans with no difference in tolerated exposure time during nauseogenic stimuli between the latter two. It seems obvious that ethnic differences are attributed to genetic reasons, however, despite high heritability, results on genetic factors are rare (Reavley et al., 2006). In 2015, Hromatka et al. evaluated genetic variants from a database of 80,494 individuals who were surveyed about their experiences regarding motion sickness in cars. They identified 35 single-nucleotide polymorphisms that could be attributed to carsickness, many of which are linked to genes responsible for postural control as well as the eye, ear, and cranial development. This finding underlines the importance of perception sensors in the motion-induced prevalence of kinetosis. Furthermore, other single-nucleotide polymorphisms had been identified to potentially affect the physiological reaction through nearby genes with their contribution to the nervous system, glucose homeostasis, or hypoxia (Hromatka et al., 2015). Nevertheless, at present, the reason why genes involved in glucose and insulin regulation affect the physiological reaction of kinetosis has not been sufficiently researched. A study by Mo et al. (2012) emphasized that hyperglycemia seems to be attributed to gastrointestinal symptoms of motion sickness. To put this into precise terms, within their investigation, subjects who reported motion-induced symptoms, like nausea and vomiting, showed lower levels of insulin than individuals without gastrointestinal manifestations.

Motion sickness, as a complex physio-psychological syndrome, is related to several comorbid phenotypes, including migraines, morning sickness, vertigo, postoperative as well as chemotherapy-induced nausea and vomiting (Covanis, 2006; Golding, 1998; Morrow, 1985; S. Yang et al., 2012). The investigations of Hromatka et al. (2015) strengthen this assumption due to the discovery of shared genetic factors between motion sickness and migraines as well as postoperative nausea. Further information on associated disorders will be presented in chapter 3.4.5.

3.4.2   Age

Children younger than 12 years show the highest incidence and sensibility to motion sickness (Bos et al., 2007; Dobie et al., 2001). In fact, Waldfahrer (2008) postulates that almost 80 % of children with the age of 8 are affected by motion sickness to some extent. This is due to the inconsistency in the development of the vestibular apparatus resulting in a sensorimotor oversensitivity during puberty (Huppert et al., 2019). A study by Huppert et al. (2019), examining a total of 3,744 young people in the range from 6 months to 18 years supported the effect of age on the severity of motion sickness and revealed that the mean age at which children experience motion sickness the first time was around five. Given that the utilization of perception sensory information for self-motion estimation in small children still has to be learned, motion sickness does not occur below the age of one (Huppert et al., 2019). As the degeneration of otoliths increases with age, the susceptibility to motion sickness correlates negatively with this biological degradation process (Dobie et al., 2001; Eulenburg et al., 2017; Zuniga et al., 2012). To put this into precise terms, during measurements of unilateral acoustic short tone bursts, which trigger ocular and cervical vestibular-evoked myogenic potentials by activating irregular otolith afferents, Zuniga et al. (2012) and Eulenburg et al. (2017) detected comparably larger blood-oxygen-level-dependent responses in cases of elderly subjects. This finding causes Zuniga et al. (2012) to assume "a mechanism of central sensitization for otolith perception to counterbalance the concurrent peripheral vestibular and somatosensory functional decline". Also, Schmäl (2013) postulates that beyond the age of 50, syndromes of motion sickness are seldom.

According to investigations from Lamb & Kwok (2015), this assumption can be supported, whereas in the respective experimental setup the effect of degeneration occurs only in subjects over 65 years. Within this observation, around 1,700 data sets of the general population in New Zealand and Australia were collected to assess a robust norm to quantify individual susceptibility to the physiological reaction in elderly people. According to the authors, there seems to be no reasonable suspicion to assume that the collected results differ between Europeans and Australians or rather New Zealanders in terms of their susceptibility.

Fig. 3-30 illustrates the results of the linear regression across all groups, in which a significant effect of age on the susceptibility score of motion sickness can be observed (*Motion Sickness Susceptibility Questionnaire* (MSSQ) – see chapter 3.7.1). However, when excluding the subjects over 65 years, age had no significant effect on MSSQ scores (Lamb & Kwok, 2015). This finding corresponds to the investigations of Oman (1998), who reported no differences between age, even though no adolescents or elderly subjects had been included in the investigation and experienced the provocative motion stimuli.
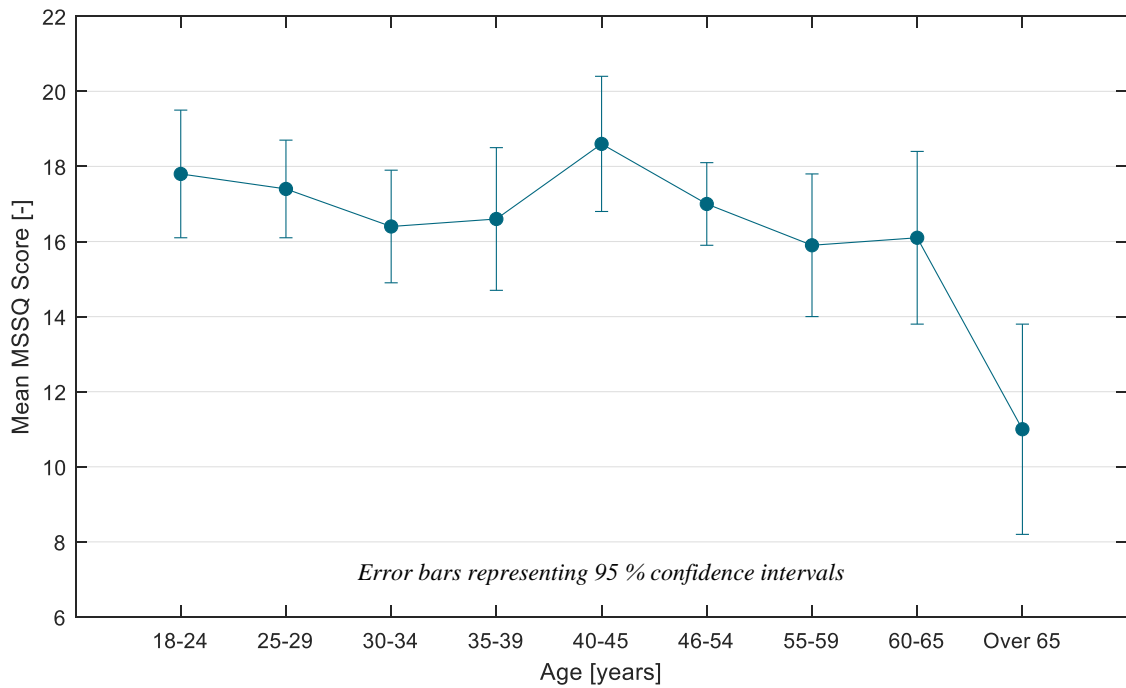
Fig. 3-30: Motion sickness susceptibility as function of age.
Based on Lamb & Kwok (2015)

3.4.3   Biological Gender

As reported in Tab. 3-6, females indicate significantly higher susceptibility scores than males, $t(1,692) = 10.9$, $p < .001$, with a medium effect size of Cohen´s d around 0.53 (Lamb & Kwok, 2015). Also, Park & Hu (1999) quantified a clear gynecotropism-ratio of 1.7:1, which strengthens the fact that women are more prone to experience kinetosis than men are, in particular during the menstrual cycle (Dobie et al., 2001; Flanagan et al., 2005; Golding et al., 2005; Grunfeld & Gresty, 1998; Lawther & Griffin, 1988; Matchock et al., 2008; Propper et al., 2018; Turner & Griffin, 1999a; Waldfahrer, 2008). In the study of Hromatka et al. (2015), some single-nucleotide polymorphisms showed up to three times stronger effects in women. In addition, the influence of biological gender also relates to the effectiveness of countermeasures, at least for the cardinal symptoms of nausea or vomiting, and their regulation by anti-emetic medicine (Klosterhalfen et al., 2005). However, there are also contradictions according to sex differences between other investigations (Classen et al., 2021; Fulvio et al., 2021; Paillard et al., 2013).

Tab. 3-6: Descriptive statistics of motion sickness susceptibility in age and biological gender.
Based on Lamb & Kwok (2015)

Variable	Descriptive Statistics			Percentiles		
	N	M	SD	25th	Median	75th
Age [years]	[-]	Score	Score	Score	Score	Score
Under 17	3	15.1	6.4	8.0	16.6	-
18-24	182	17.8	12.0	7.7	17.2	27.0
25-29	267	17.4	11.4	9.0	16.0	25.0

The table continues on the next page.

Tab. 3-6: Descriptive statistics of motion sickness susceptibility in age and biological gender *(continued)*.

30-34	226	16.4	11.1	7.4	16.0	24.0
35-39	177	16.6	12.1	6.8	15.0	24.9
40-45	208	18.6	12.2	9.0	17.0	26.8
46-54	366	17.0	12.1	6.4	15.7	26.0
55-59	138	15.9	12.2	5.6	13.3	23.2
60-65	95	16.1	12.5	6.0	13.5	25.5
Over 65	43	11.0	10.0	2.0	6.5	18.9
Gender	[-]	Score	Score	Score	Score	Score
Male	798	13.7	10.5	5.0	12.0	21.0
Female	898	19.8	12.2	10.0	19.0	28.5

3.4.4 Physical Constitution

Since motion sickness is related to perception, the individual ability of orientation under dynamic conditions, influenced by the practice of motoric demanding activities, is expected to be a relevant parameter in the development of the physiological reaction. This is true, however, incongruent results concerning the effect in motion sickness provocation are reported. Some researchers emphasize that aerobic exercises have been proven to decrease motion sickness resistance (Banta et al., 1987; Cheung et al., 1990; Rawat et al., 2002). Whinnery & Parnell (1987) found a relationship between intense susceptibility to motion sickness manifestations and long-term aerobic conditioning by reporting 52 % of aerobically fit subjects experienced motion sickness compared to 23 % of subjects with a lower level of aerobic fitness. Especially vomiting indicates a difference between the two groups of 31 % when exposed to a nauseogenic stimulus (Whinnery & Parnell, 1987). Investigations by Bethel (2021) did show some difference in motion sickness severity between the population of subjects who are engaged in recreational sports and physical activities compared to participants who are not. Cheung et al. (1990) conducted a longitudinal analysis of eleven healthy subjects with a sedentary lifestyle. The participants had to complete an aerobic fitness training program for two months with mainly four training sessions per week. As expected, the fitness program resulted in significantly higher aerobic fitness, quantified by improvements of VO_2max and endurance capacity as well as a decrease in body fat. Furthermore, the researchers detected a significant increase in susceptibility to motion sickness. The authors suggested an attribution to ACTH, which is indeed released in cases of motion sickness. As mentioned in chapter 3.3, the baseline ACTH level just as motion sickness triggered ACTH onset are higher in low-susceptible subjects, while ACTH secretion seems to be lower in acute stress situations for trained people (Kohl, 1985).

Conversely, among 125 shuttle crewmembers, no relationship between space motion sickness and aerobic fitness could be discovered. This, however, can be explained by limitations within the study design. (Jennings et al., 1988) Even more remarkable are the findings from Caillet et al. (2006), suggesting that the practice of sport before the age of 18 reduces the incidence of motion sickness. The effect within 1,829 students was even stronger, the more proprioceptive abilities were needed during the targeted physical activity.

3.4.5 Associated Disorders and Pathogenesis

The involvement of the vestibular apparatus in the origin of kinetosis can be explored by leveraging the fact that individuals with nonfunctioning vestibular organs are immune to motion sickness (Kennedy et al., 1968). This effect is not limited to human beings. In fact, all individuals owning intact labyrinths can experience the physiological syndrome together with its vegetative reactions (Oosterveld, 1995; W. D. Wilson, 1997). Even fishes can get seasick (Helling et al., 2003). Furthermore, it is well known that those with a high susceptibility to motion sickness show greater asymmetry in responses to caloric labyrinth stimuli (Benson, 2002, p. 1063). Therefore, it is not surprising that illnesses or imbalances of the vestibular system lead to high sensitivity to incongruent motion stimuli (Beier et al., 2002; Diamond & Markham, 1992; Nooij et al., 2011). The researchers suppose that initially, a misbalanced and incongruent sensitivity of the otoliths appears, but then is equilibrated by the vestibular apparatus and the neural network, as long as learned physiological motion patterns are present (Diamond & Markham, 1992; Nooij et al., 2011; Schmäl, 2013). Vestibular disturbances are common in the human population since 35 % of the U.S. Americans over 40 years were affected by at least some symptoms of dizziness, imbalance, or just deterioration of vestibular functions (Agrawal et al., 2009; Burns & Stone, 2017). Consequently, contrary effects between vestibular disturbances and age-related hair cell degeneration can be identified. However, here as well, intravestibular differences are present. For instance, aged macula exhibits less hair degeneration than it occurs with the cristae, in which a continuous decrease in vestibular ganglion neurons and supporting cells can be observed (Burns & Stone, 2017; Lopez et al., 2005; Richter, 1980; Slattery et al., 2014). This is only a general rule, because it has been reported that also elderly people form new otolith hair cells (R. R. Taylor et al., 2015).

An important but rare and poorly understood entity is the nature of the relationship between mainly visual induced-motion sickness and vection, which remains an essential research area according to self-motion perception (Keshavarz et al., 2018; Keshavarz, Riecke, et al., 2015; Lien et al., 2003; Nooij et al., 2018; Sawabe et al., 2017). A typical real-life self-experiment of vection can be conducted in train stations while sitting in a stationary wagon and observing the movement of a neighbouring train can cause a feeling of illusion that the own standing wagon is under dynamic (Keshavarz, Riecke, et al., 2015). In general, vection occurs when the human being senses illusory self-motion in the absence of congruent physical stimuli (Sawabe et al., 2017). According to Keshavarz, Riecke, et al. (2015), the association between visual-induced motion sickness and vection might be linked by the magnitude and type of sensory conflict. However, vection, as a stand-alone incident, seems to be an insufficient prerequisite to motion sickness. This conclusion is due to the fact that vection can occur without symptoms of malaise. By contrast, visual-induced motion sickness can also occur without any corresponding manifestation of vection (Keshavarz, Riecke, et al., 2015). Nonetheless, in general, many researchers postulate evidence on reporting visual-induced motion sickness with coupled expressions of vection, even if mainly weak correlations around r = 0.2 and only seldom high correlations with r = 0.7 appear (Diels et al., 2007; Golding et al., 2012; Keshavarz et al., 2011; Keshavarz, Riecke, et al., 2015; Nooij et al., 2017).

In 2017, Nooij et al. showed that visual-induced motion sickness increases with vection strength, but with high variations between subjects. In fact, subjects who experienced higher vection intensity were not inevitably more prone to visual-induced motion sickness, whereas stimuli that induce stronger vection refer to higher nauseogenic expressions. In this context, it is referred to chapter 3.2.5, in which the crucial visual-vestibular interactions are described. Indeed, the impact of the discharge of the velocity storage mechanism is, among other things, linked to the optokinetic stimulation and, therefore, important for the prevalence of motion sickness (Dai et al., 2007; Nooij et al., 2018; Raphan et al., 1979).

Given that diseases on labyrinth or otolith functions may also affect postural control, it is obligatory to assess the attribution between motion sickness and postural sway. In 2006, Bonnet et al. discovered instabilities and increased variance in displacements of the center of pressure among individuals who experienced motion sickness. The differences of disturbances occurred before the onset of nauseogenic stimuli. During exposure, instability increased for both, sick and well subjects. However, the amount of sway was greater for participants reporting symptoms of motion sickness. Y.-C. Chen et al. (2012) analyzed data on standing body sway before and after bouts of 15 amateur boxers. Since eight of 15 subjects reported motion sickness after the bout, statistically significant interactions occurred and, therefore, confirm the observation made by Bonnet et al. (2006). Overall, the researchers suggested that individual susceptibility to symptoms of malaise in boxers seems to be manifested in characteristic patterns of body sway. To investigate body sway coupled with imposed oscillatory motion of the illuminated environment, Walter et al. (2019) conducted a repeated measures examination with 30 women, who experienced visual motion stimuli by a surrounded moving room. As a result, the researchers concluded that humans can couple the dynamics of body sway with complex enforced motion, and that differences in the nature of its coupling are influencing the risk of motion sickness severity. In 2015, Lubeck et al. presented the participants motion and stationary images while measuring their postural sway and the severity of visual-induced motion sickness. Here, measures of postural sway are defined as path length, standard deviation, as well as short- and long-term scaling components of the center of pressure. Some of these parameters, namely the sway path length, the standard deviation and the short-term scaling components in the anteroposterior direction, increased significantly. This observation is, in contrast to the severity of visually-induced motion sickness, without significant differences between the two types of images. The researchers assumed that the increase in sway during exposure to stationary images can be explained by the nature of visual implications in steady-state conditions. The absence of vection within the motion images provide an explanation why sway was not greater when watching the dynamic images as compared to being exposed to the stationary scenarios (Lubeck et al., 2015).

Multiple studies found associations between motion sickness, mal de débarquement, increased self-motion, and visual sensitivity since the respective syndromes might have in common the poor ability to adapt to unknown motion conditions (Cha et al., 2008; Stoffregen et al., 2013; Tal et al., 2005; Tal et al., 2014).

Mal de débarquement is a disorder of false perception of movement after experiencing a strict periodic passive motion pattern, which sometimes leads to postural disorders (van Ombergen et al., 2016). Its etiology and true incidence have not been explored yet (Nwagwu et al., 2015). As this phenomenon is also known as sea legs or rocking dizziness, it is deduced that this disease mainly occurs after sea travel (Cha & Cui, 2013; Stoffregen et al., 2013). Many researchers reported the high incidence of mal de débarquement with numbers between 60 - 80 % (H. Cohen, 1996; Gordon et al., 1992; Gordon et al., 1995; Stoffregen et al., 2013; Tal et al., 2014; van Ombergen et al., 2016). Tal et al. (2014) postulated that 79 % of cases lasted less than six hours. This assumption is supported by Gordon et al. (1995) since 88 % of 116 subjects reported the same chronic alleviation of their disorder. Even though, pathological diseases can also lead to persistent postural disturbances lasting up to several years (Cha et al., 2008; Lewis, 2004; Teitelbaum, 2002; van Ombergen et al., 2016). Interestingly, individuals with high susceptibility to mal de débarquement may weigh sensory paths differently. Indeed, reliance on vestibular and visual inputs seems to be reduced, while, in consequence, the impact of the somatosensory system increases to facilitate postural control and balance (Nachum et al., 2004). Furthermore, a far-reaching association of mal de débarquement, headache, and migraine are reported, especially in cases of patients developing spontaneous symptoms of mal de débarquement (Cha et al., 2008; Cha & Cui, 2013).

Additionally, it is well known that migraine preposition shows a strong association to self-motion perception, vestibular symptoms, such as motion sickness, and comorbid maladies of nausea, headache, and photophobia (Baloh, 1997; Drummond, 2006; Drummond & Woodhouse, 1993; Grunfeld & Gresty, 1998; Susan King et al., 2019). In 1997, Baloh postulated that high sensitivity of motion sickness occurs in about two-thirds of patients with migraines. Kayan & Hood (1984) only received 50 % out of almost 400 migraine patients with motion sickness history. Furthermore, adolescents that show a history of malaise or headache, due to experience of motion sickness or migraine, are more prone to vomit from even slight head injuries (Jan et al., 1997). Given that the vegetative manifestation of headache, nausea, dizziness, drowsiness, and perceived body temperature regulation are typical maladies of migraine and motion sickness, it is expected that both syndromes share the same neural circuitry with their pathways from brainstem activation up to hypothalamus functions (Denuelle et al., 2007; Cuomo-Granston & Drummond, 2010). In particular, according to investigations of Bahra et al. (2001), activation of the brainstem during migraine without aura and activation of the hypothalamus were reported. Therefore, it is admissible to conclude that vasodilatation is provoked by neural activation originating from the brainstem (Bahra et al., 2001). Brainstem centers combine several functions, from flow-modulation of pain messages to other forms of sensory information to higher brain regions, through managing the general excitability of these cortical areas. In consequence, disturbance in brainstem processing is likely to affect several unpleasant symptoms, vegetative changes, and neurovascular attacks. Fig. 3-31 illustrates the work of Cuomo-Granston & Drummond (2010) and outlines the relationship between the two maladies including key structures in the brainstem that are involved in both pathologies. Within the illustration, the black arrows represent activation processes.
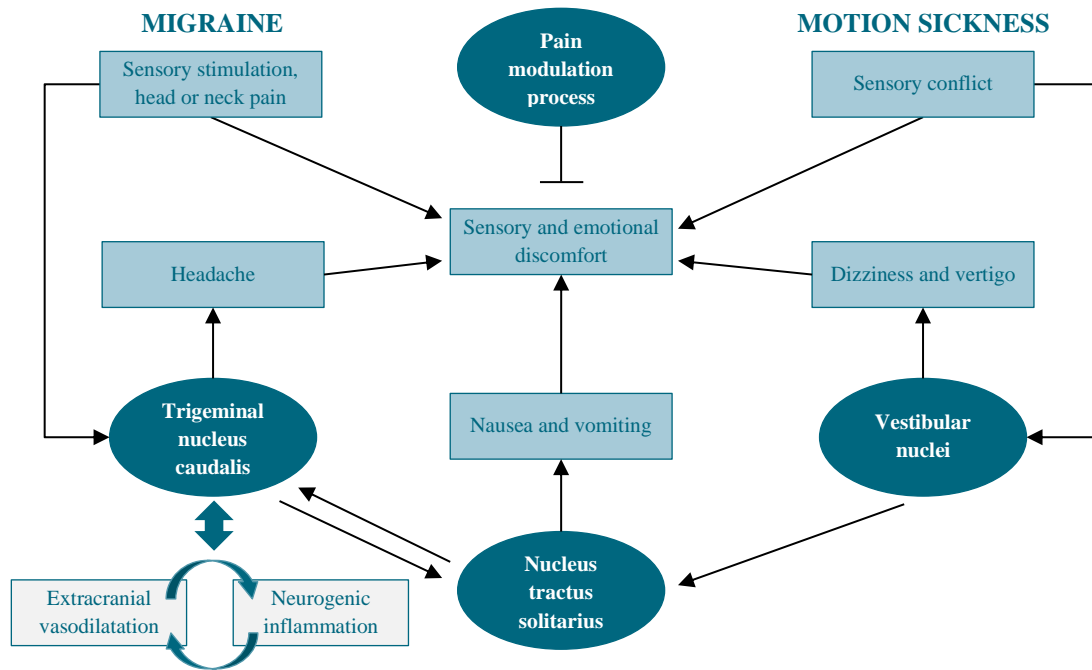
Fig. 3-31: Relationship of migraine and motion sickness including neural pathways and structures in the brainstem. Based on Cuomo-Granston & Drummond (2010)

Main structures associated with common symptoms of migraine and motion sickness include the trigeminal nucleus caudalis, the nucleus tractus solitarius, as well as the vestibular nuclei, which, in turn, is highlighted in chapter 3.2.4 of the current elaboration. Cuomo-Granston & Drummond (2010) described the neural processes associated with migraine and motion sickness as follows: First of all, the inhibition pain modulation process, represented by the flat terminal adjustment to the sensory and emotional discomfort box, can influence sensitivity on perception information and sensory signals. In cases of oversensitivity, symptoms are more likely to occur, whereas key brainstem nuclei are irritated. Once initiated, the neurogenic inflammation and extracranial vasodilation process are activated by the trigeminovascular system. This process involves a surge of vasoactive neurotransmitters and, therefore, provokes vasodilatation (Moskowitz, 1993). Through interactions between the trigeminal nucleus caudalis and the nucleus tractus solitarius symptoms of nausea, vomiting and headache arise. Notably, for assessing motion sickness, the link between the trigeminal nucleus caudalis and the vestibular nuclei alleviates the potential of vestibular disorders (Diagne et al., 2006). Furthermore, vestibular nuclei can be affected by trigeminovascular reflexes, which regulate blood flow through the cerebellar and vertebrobasilar vasculature (Vincent & Hadjikhani, 2007). In summary, the projections of the aforementioned structures to the hypothalamus, thalamus, limbic system, and cerebral cortex influence higher brain centers on brainstem processing and project to autonomic output pathways, which might affect motion sickness susceptibility (Marcus et al., 2005; Menétrey & Basbaum, 1987).

3.5   Types of Provocative Stimuli to Investigate Motion Sickness

The mechanism involved in nauseogenic stimuli is influenced by various human-related and environmental conditions. Therefore, a wide range of different experiments had been conducted to analyze treatments, predictors, or contributing factors on motion sickness.

Laboratory testing on physical-induced forms, like off-axis rotating drums, centrifuges, vertical-moving air, or seafaring simulators as well as simple swings or sleds were carried out as fundamental studies on motion sickness (Eversmann et al., 1978; Frett et al., 2020; Golding, 1992; Kuiper et al., 2020; Nooij & Bos, 2007; Stankovic et al., 2019; Takeda et al., 1986; Ventre-Dominey et al., 2008; Williamson et al., 2004). Furthermore, real-life investigations under rail, sea, air, or road conditions enable high resolution on practical relevance under its circumstances (Kuiper et al., 2018; Saruchi et al., 2018; Tal et al., 2016; Turner & Griffin, 1999a, 1999b; Ueno et al., 1986; Wada et al., 2018). One of the earliest settings for provoking nauseogenic stimulation was conducted on parabolic flights (Bagshaw & Stott, 1985; Hilbig et al., 2002). With the development of visual-induced motion sickness, pseudo-motion stimuli, such as vection illusion, became apparent more often in studies of kinetosis. Artificial environments with access to virtual reality, *liquid crystal display* (LCD) screens, high immersive projections, or simply moving surrounding rooms were obtained in these kinds of experiments (Curry et al., 2020; Nooij et al., 2018; K. Stanney et al., 2020; Sugita et al., 2007; Villard et al., 2008; Walter et al., 2019; Weech et al., 2020). Given that labyrinth function is involved in the origin of motion sickness, it is possible to bring on the physiological manifestation even by caloric vestibular stimulation (Costa et al., 1995; Mallinson, 2011; Preber, 1958). Mallinson (2011), for instance, carried out two prospective experiments with 321 patients, in which the researchers hypothesized that the caloric trigger provokes a signal mismatch between semicircular canals and the two otolith organs (macula saccular and utricular). Subjects who were incapable to suppress the resulting manifestations of the parasympathetic activation of nausea and malaise often suffer from comorbidities of kinetosis on a long-term basis. However, no evidence of sympathetic withdrawal can be provoked with this methodology (Costa et al., 1995). Typical caloric stimulation is initiated by in-ear water flow, in which the temperature is sequentially lowered until intolerable side effects occur (Costa et al., 1995). In general, it is well known that the presence of greater asymmetry in responses to caloric stimuli occurs in the group of subjects with high susceptibility to motion sickness (Benson, 2002, p. 1063). Even galvanic stimulation provides a proper insight into visual-vestibular interactions, such as ocular torsion and nystagmus properties (Pasquier et al., 2019; E. Schneider et al., 2002).

3.6 Mechanical Vibrations as Origin of Discomfort and Motion Sickness

Motion sickness, similar to general comfort, depends on motion characteristics, namely the magnitude, duration of exposure, frequency, and waveform (Mansfield, 2005, p. 8). Even if the subjective interpretation and sensation of those characteristics differ between individuals, many researchers insist that this issue of individuality can be broken down into focus areas, which are generalized to a substantial part of human comfort requirements. In fact, various experiments on vertical as well as horizontal oscillators, lifts, and swings were conducted to evaluate these fundamental guidelines (Benson, 2002, pp. 1055–1059). With regard to carsickness, this guidance seems to be beneficial since vehicle occupants are exposed to strong, predominant linear accelerations from longitudinal (fore-and-aft acceleration), lateral (cornering), and vertical (road surface) nature (Yusof, 2019, p. 19).

One of the most popular and representative laboratory investigations on motion sickness was carried out by O´Hanlon & McCauley (1974), who postulated that the symptomatic incidence of kinetosis can be described as a function of frequency, acceleration, and time by a two-dimensional normal distribution:

$$\text{MSI} = \frac{100}{2\pi\sigma_a\sigma_t\sqrt{1-\rho^2}} \int_{-\infty}^{log_{10}a} \int_{-\infty}^{log_{10}t} \exp\left\{\left(\frac{-1}{2(1-\rho^2)}\right)\left[\left(\frac{x-\mu_a(f)}{\sigma_a}\right)^2 - 2\rho\left(\frac{x-\mu_a(f)}{\sigma_a}\right)\left(\frac{y-\mu_t}{\sigma_t}\right) + \left(\frac{y-\mu_t}{\sigma_t}\right)^2\right]\right\}dydx = 100\,\phi(a,t)$$

Eq. 3-18

Within their study, 300 subjects were exposed to vertical oscillation for a total duration of two hours. The motion was accomplished by a gradual increase in input amplitude over a period of approximately 30 - 60 s, while motion frequencies were varied. The mathematical model was fitted to the discrete data points. The symptom rating was applied by using the *motion sickness incidence* (MSI) value, a 5-point Likert scale from "no symptoms" to "severe nausea, emesis is imminent". To quantify vibrations that oscillate about a fixed point, the methodology of the *root-mean-square* (r.m.s. - see chapter 3.6.2) was chosen, which is defined as the square root of the arithmetic mean of the squares applied to the set of values (Mansfield, 2005, p. 125). With respect to further calculations by McCauley et al. (1976), a three-dimensional representation of the motion sickness incidence in the vertical direction as a function of wave frequency and r.m.s. is attained, in which the frequency of maximum motion sickness sensitivity is estimated with 0.167 Hz (see Fig. 3-32).
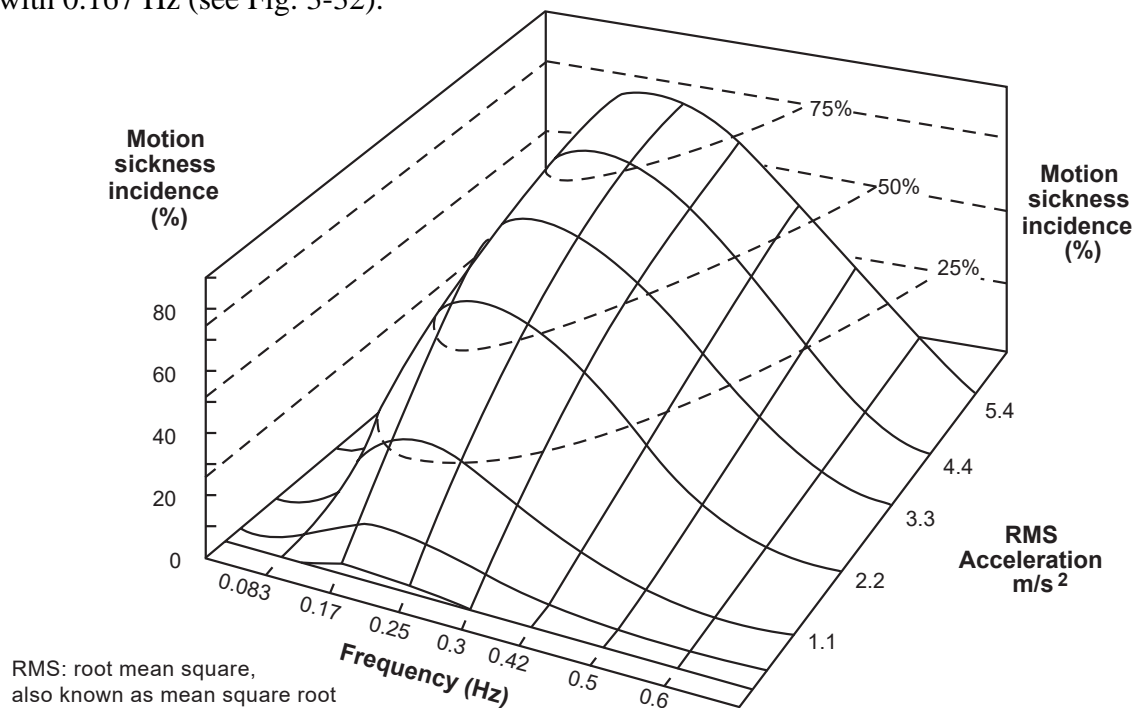
Fig. 3-32: Motion sickness sensitivity as function of frequency and r.m.s. during vertical wave motion pattern. Modified from McCauley et al. (1976, p. 39) as cited in Benson (2002, p.1059)

To understand why humans show high sensitivity to low-frequency motion, one explanation is related to the macromechanics of the vestibular system discussed in chapter 3.2.1.

With respect to the receptor bode plots and the domain of natural frequencies of active head motion, it is suggested by Benson (2002, p. 1059) that under low frequencies the human organism interprets otoliths sensation as a change in the head's orientation to gravity, while under specific circumstances canal information that is expected by the central nervous system did not occur (conflict 2B - see chapter 3.2.6). An alternative explanation was postulated by Stott (1986), who emphasized that the neural conflict occurs between the sensed low-frequency locomotor activity, which is interpreted over periods of more than about one second as gravito force, with the normal invariant pattern of sensory afference.

As discussed in chapter 3.1.3, with the implementation of tilting trains the ratio of occupants affected by motion sickness increased substantially. Until that time, most research was conducted in the vertical direction to address issues from aviation and maritime traveling (Dobie, 2019, pp. 69–91). Since then, research areas have been extended and intensified, especially in terms of combined lateral motion patterns occurring in high-speed tilting trains. With reference to this, a summary of respective investigations is shown in Tab. 3-7.

Tab. 3-7: Laboratory studies to identify motion sickness-related malaise in uniaxial and cross-coupled motion stimuli. Based on Beard (2012, p. 35)

Study	Frequency	Roll displacement	Roll acceleration	Earth-lateral acceleration	Lateral acceleration in the plane of the seat	Proportion of subjects to reach mild nausea
	Hz	± °	± °/s²	± m/s²	± m/s²	%
Howarth & Griffin (2003)	0.025	8	0.20	0	1.37	10
	0.050	8	0.79	0	1.37	10
	0.100	8	3.16	0	1.37	5
	0.200	8	12.63	0	1.37	15
	0.400	8	50.53	0	1.37	15
Donohew & Griffin (2004)	0.032	0	0	0.20	0.20	4
	0.050	0	0	0.31	0.31	10
	0.080	0	0	0.51	0.51	15
	0.125	0	0	0.79	0.79	30
	0.160	0	0	1.00	1.00	45
	0.200	0	0	1.26	1.26	55
	0.315	0	0	0.99	0.99	20
	0.50	0	0	0.63	0.63	35
	0.800	0	0	0.39	0.39	10
Donohew (2006)	0.050	1.83	0.18	0.31	0	25
	0.080	2.93	0.74	0.50	0	35
	0.125	4.58	2.83	0.79	0	20
	0.160	5.85	5.91	1.01	0	60
	0.200	7.30	11.53	1.26	0	75
	0.315	5.76	22.56	0.99	0	60
	0.500	3.67	36.22	0.63	0	45
	0.800	2.27	57.35	0.39	0	30

These findings were confirmed by several real-life observations, predominantly made in aircraft and seafaring exposures. A survey by Turner et al. (2000), for instance, investigated 923 passengers during commercial flights.

The results supported the assumption that vibrations in the lateral and vertical direction below 0.5 Hz correlate with malaise and nausea, while this guidance did not work in the longitudinal direction within this type of scenario. In general, with reference to the model of O´Hanlon & McCauley (1974), symptoms increase with magnitude in both, the lateral and vertical direction. Along with further investigations addressing different transportation modalities, 3,256 coach passengers reported that the severity of nausea increased while traveling on cross-country roads characterized by high magnitudes of lateral coach motion at a frequency below 0.5 Hz (Turner & Griffin, 1999b).

According to Cheung & Nakashima (2006), evidence from investigations indicates that real-life vertical motions, recorded during vehicle journeys, do not show extensive impact as a predictor of motion sickness. By contrast, low-frequency motion in the horizontal plane seems to determine the severity of motion sickness. Vertical vehicle accelerations, differing in peaks between 1.0 - 2.0 Hz, are mainly influenced by vehicle suspension and road conditions, while horizontal motion is rather affected by drivers, topography, and route than by vehicle characteristics (Griffin & Newman, 2004). Fig. 3-33 summarizes different publications regarding ride comfort and includes eigenfrequencies of the human body and outlines provoking stimuli that occur in different transportation systems.
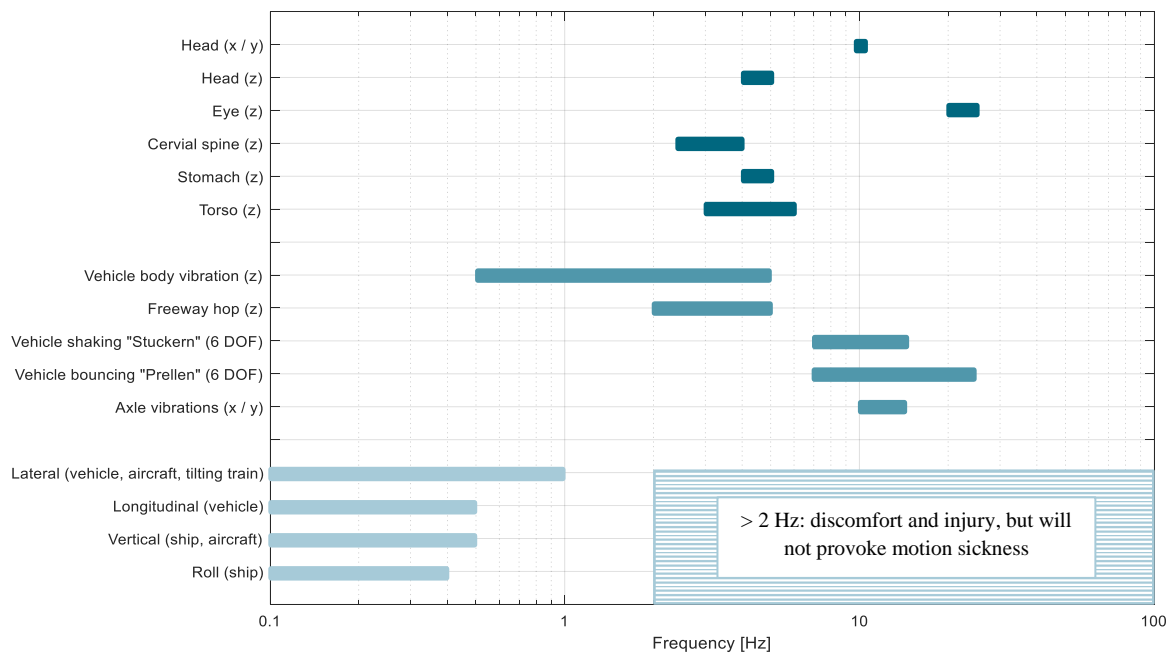
Fig. 3-33: Eigenfrequencies of human body parts, exogenous vehicle stimuli, and motion sickness frequencies occurring in several transportation modes. Based on Cheung & Nakashima (2006); Bubb et al. (2015, p. 488); Thomaier (2008, pp. 31–33)

3.6.1 Mechanical Human Whole-Body Vibration: ISO 2631 and VDI 2057

International and national standards provide guidance that describes the possible effects of vibration on human health, comfort, perception, and performance (ISO 2631-1:1997-05; VDI 2057-1:2017-08). Frequency weighting, as an integral part of those norms, connects information about the subjective human response to different vibration properties. This is essential given that the body shows differences in sensitivity across the frequency band.

For instance, subjects are more vulnerable to whole-body vibration at about 5 Hz, compared to higher frequencies of 50 Hz (Mansfield, 2005, p. 124). According to the ISO 2631-1 and the VDI 2057-1, there is not only one all-encompassing frequency weighting function available. A wide range of functions exists, depending on direction, application area, and the dimension of sensitivity. With respect to Fig. 3-34, the focus will shift to linear acceleration concerning motion sickness (W_f) and whole-body sitting comfort (W_k). While W_k is defined for all three coordinate axes, W_f only provides information about the z-axis. Furthermore, the motion sickness weighted function is only applicable to sitting or standing postures. Although there is evidence that roll and pitch motion, as well as recumbent postures, contribute to motion sickness, these implications are not represented in one of the standardized norms. In any event, until recently, this guidance was the most capable tool for linking subjective sensitivity with physical data sets.
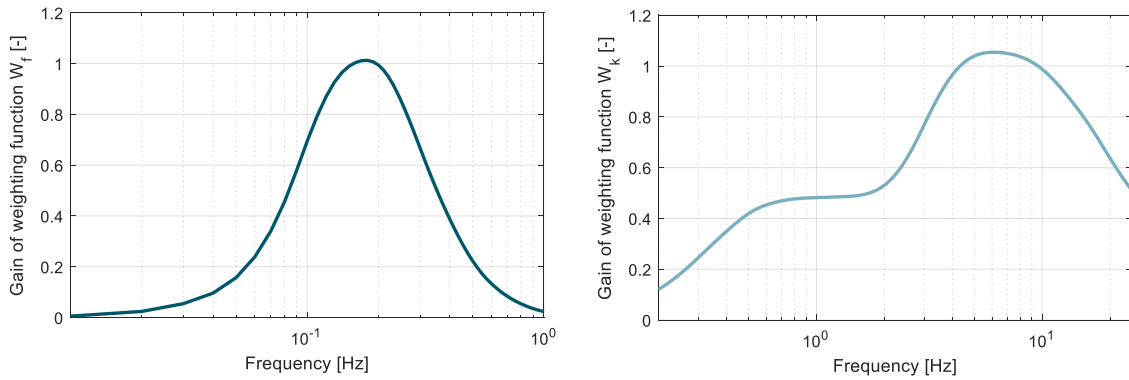
Fig. 3-34: Frequency weighted functions for motion sickness (left) and general discomfort in sitting position (right). Based on ISO 2631-1:1997-05

Mathematically, the application of a weighting function W_i is obtained as follows:

$$a_w = \sqrt{\sum_i (W_i \cdot a_i)^2} \qquad \text{Eq. 3-19}$$

The weighted r.m.s. acceleration a_{wT}, as the energy-equivalent quadratic mean value, can be applied to translational and rotational vibration and is calculated for the exposure period T:

$$a_{wT} = \sqrt{\frac{1}{T}\int_0^T a_w^2(t)\,dt} \quad , \quad a_{w\tau}(t) = \sqrt{\frac{1}{\tau}\int_{\xi=0}^t a_w^2(\xi)\cdot e^{\frac{\xi-t}{\tau}}\,d\xi} \qquad \text{Eq. 3-20}$$

The running r.m.s. acceleration $a_{w\tau}$ varies in time, while ξ is defined as the integration variable with τ as slow (1 s) or fast (0.125 s) time constant. The accumulated vibration value of the frequency-weighted accelerations in space a_{wv} can be determined as follows:

$$a_{wv} = \sqrt{k_x^2 \cdot a_{wx}^2 + k_y^2 \cdot a_{wy}^2 + k_z^2 \cdot a_{wz}^2} \qquad \text{Eq. 3-21}$$

The correction factors k_i for the different directions of vibrations range from 0.8 - 1.4, depending on the desired human response. (ISO 2631-1:1997-05)

Motion Sickness Dose Value

The two national and international standards per definition estimate the amount of motion sickness due to exposure to vertical linear motion. The respective *motion sickness dose value* (MSDV) is calculated by the following equation and it is postulated that this value is proportional to the incidence of nausea and malaise experienced by the human being.

$$MSDV_z = \sqrt{\int_0^T a_{W_f}^2(t)dt} \qquad , \qquad VI = k_m \cdot MSDV_z \qquad \text{Eq. 3-22}$$

The *vomiting incidence* (VI) provides further information about human responses, in tangible terms, the percentage of people who vomit. According to investigations of Lawther & Griffin (1987), about 30 % of the subjects vomited leading to the constant value of $k_m = 1/3$. However, the calculation of VI is only valid for a normally distributed, non-adapted group of adults (ISO 2631-1:1997-05). The exposure within the investigation differed between T = 20 min and 6 hours, while the prevalence of vomiting varied up to 70 % (Lawther & Griffin, 1987). Many researchers applied the weighting function in both, the longitudinal and lateral direction, and emphasized the importance of replacing the constant value of $k_m = \sqrt{2}$ in horizontal motion conditions (Förstberg, 2000a, p. 67; Golding et al., 1995; Golding & Markey, 1996; Griffin & Newman, 2004). Therefore, it is permitted to apply the frequency weighted function W_f in all translatory *degrees of freedom* (DoF) and, thereby, calculate the respective MSDVs.

Ride Comfort and Perception Threshold

The following Tab. 3-8 outlines the relationship between the total frequency-weighted acceleration a_{W_KT} and subjective perception when undergoing sinusoidal vibrations in a seated condition. Given that perception thresholds are influenced by age, sex, physical condition, situation awareness, and the kind of task being engaged in, the following table only provides approximations on perception and individual well-being. As a result, the general guidelines are not defined precisely with a claim of universal validity. (VDI 2057-1:2017-08)

Tab. 3-8: Perception and comfort rating as function of frequency weighted acceleration. Based on VDI 2057-1:2017-08

r.m.s. of frequency weighted acceleration a_{W_KT} [m/s²]	Description of perception under sinusoidal stimuli
< 0.01	Not perceptible
0.015	Threshold of perception
0.015 - 0.02	Barely perceptible
0.02 - 0.08	Easily perceptible
0.08 - 0.315	Strongly perceptible
> 0.315	Extremely perceptible

3.6.2 Basic Information about Signal Analysis

The parameters presented below have been applied in the current elaboration when it comes to the evaluation of large data sets.

Standard Deviation of the Root-Mean-Square

The aforementioned *root-mean-square* (r.m.s.) is defined as the arithmetic mean of the squares of a data set. More precisely, the r.m.s. represents the transmitted energy load during a certain exposure period (T). The standard deviation indicates the average amount of fluctuation between the individual measured values and the cumulative mean (Beucher, 2015, p. 505). To obtain the standard deviation (σ), the difference between the time signal and the r.m.s. is integrated using the square as follows:

$$\sigma(x) = \sqrt{\frac{\int_0^T \big(x(t) - r.m.s.(x)\big)^2 \, dt}{T}} \qquad \text{Eq. 3-23}$$

Cross-Correlation

The *cross-correlation* (r_{xy}) shows the degree of similarity between the input signal (x) and output signal (y) with different temporal delays. The cross-correlation, therefore, is a modification of the *autocorrelation* (r_{xx}), which compares a signal with itself. As can be seen in the following equation, the two-time signals are multiplied by each other for the calculation of r_{xy} followed by the integral of its result. The standardized form is defined as the correlation value that is calculated for all time steps (τ) and, thus, corresponds to a convolution. By comparing the discretized values of the cross-correlation, the time delay as well as the similarity of the two signals can be assessed: (Beucher, 2015, pp. 404–411)

$$r_{xy}(\tau) = \frac{\int_0^T x(t) \cdot y(t + \tau) \, dt}{\sqrt{\int_0^T x(t)^2 \, dt} \cdot \sqrt{\int_0^T y(t)^2 \, dt}} \qquad \text{Eq. 3-24}$$

In the present work, r_{xy} is used as a constant expression for the cross-correlation coefficient and is not intended to give any indication of the considered directions. Guidelines for the interpretation of the correlation coefficient are given by J. Cohen (1988, pp. 82–83) as follows:

- Small effect: $0.1 \leq |r_{xy}| < 0.3$
- Medium effect: $0.3 \leq |r_{xy}| < 0.5$
- Large effect: $|r_{xy}| > 0.5$

Power Spectral Density

The motion behaviour and characteristic in the frequency domain can be described by considering the *power spectral density* (PSD) and the transfer function.

The power spectral density indicates the distribution of power into frequency components. The statistical average of signals, as analyzed in terms of their frequency information, is called spectrum. The PSD, also written as $S_{xx}(f)$, is calculated according to the Wiener Chintschin theorem as a Fourier transformation of the autocorrelation function (r_{xx}), analogous to the following equation: (Beucher, 2015, pp. 427–450)

$$S_{xx}(f) = \int_{-\infty}^{\infty} r_{xx}(t) \cdot e^{-j2\pi ft} \, dt \qquad \text{Eq. 3-25}$$

Here, r_{xx} is calculated according to the previous equation of the cross-correlation, however, y(t) is replaced by x(t) in compliance with the nomenclature. The discrete Fourier transformation is used to implement the power spectral density. To achieve an optimal spectral power density, the frequency of the signal has to be an exact multiple of the frequency resolution. In fact, the time duration and spectral bandwidth of a signal can not be arbitrarily small at the same time (Beucher, 2015, p. 195). Due to those guidelines and requirements in data analyses, the signal is windowed in the time series to avoid artifacts in the frequency domain. In this work, the Hamming window is used as it is described and applied by Armand & Minor (2001):

$$w(t) = 0.54 - 0.46 \cdot \cos\left(\frac{2\pi t}{T - 1}\right) \qquad \text{Eq. 3-26}$$

Transfer Function

The *transfer function* (H) is a representation of an input-output relation for a linear system (Eckstein, 2014b, p. 59). Here, the behaviour of humans is approximated to be a linear time-invariant dynamical system. In the current elaboration, the transfer function represents the relationship between the output signal of the head or headrest and the applied input signal in the frequency domain for different motion stimuli (see chapter 11). The transfer function is calculated as follows:
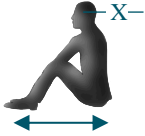
$$|H(f)| = \sqrt{\frac{S_{yy}(f)}{S_{xx}(f)}} \qquad \text{Eq. 3-27}$$

To analyze body motion in all translational and angular directions, researchers used a 6x6 matrix of transfer functions (Mutschler, 2007, p. 48). This methodology allows the observation of interaction effects between directions, which is essential since uniaxial excitations can cause body motion in multiaxial directions.

3.6.3   Direction of Stimuli and Body Posture

As previously mentioned in chapter 3.1.1, under specific circumstances, motion sickness is affected by body posture. According to laboratory investigations of Golding and colleagues (1995), horizontal motion appears to be twice as nauseogenic as vertical motion. Moreover, there was no crucial difference in motion sickness occurrence by manipulating posture in vertical motion conditions. Tab. 3-9 illustrates the results of two consecutive experiments, in which sinusoidal motion with a maximum peak intensity of 3.6 m/s^2 and a frequency of 0.35 Hz was applied.

Tab. 3-9: Laboratory testing: motion sickness influenced by uniaxial motion direction and posture. Based on Golding et al. (1995)

The ratio of time to nausea	2.5 - 1.8	1.2	1.0	0.5
Body posture				
Direction (Axis)	*Upright* Longitudinal (x)	*Supine* Vertical (x)	*Upright* Vertical (z)	*Supine* Longitudinal (z)

p < .05 (n=12); p < .0001 (n=28)   *p < .001 (n=12)*

The results imply that motion direction with respect to the gravity vector does not show a great and powerful impact on the severity of motion sickness. If low-frequency motion with predominance in the longitudinal direction (x-axis) occurs, higher nauseogenic expressions are observed. Also, in 1986, Benson et al. concluded that movements in the footward direction are more readily perceived than movements in the opposite direction.

3.7   Multidimensional Measurements of Motion Sickness

Research has been focused on methodologies for the quantification of human physio-psychological expressions for many decades. However, until recently, in many research areas evidence on predictors was still scarce. In terms of motion sickness, subjective measures, such as standardized questionnaires, appear to be the most appropriate tool for detecting the physiological syndrome. By contrast, objective measures, namely physiological and behavioural information, act in a more adjuvant manner. In this chapter, all three categories are discussed, while the questionnaires which were utilized can be found in the appendix.

3.7.1   Subjective Measurements

There are several questionnaires and metrics assessing different characteristics associated with motion sickness. Before measuring the severity of the corresponding maladies, the individual susceptibility of the test sample has to be considered in the study design, or at least in the conclusion and interpretation of results. In fact, different types of questionnaires, such as the Motion Sickness History, Motion Sickness Susceptibility or its short-form, are available (Golding, 1998, 2006; Griffin & Howarth, 2000; Reason & Brand, 1975). Even questionnaires for obtaining subforms of motion sickness were developed to increase accuracy in evaluating subjects' ability and affinity to experience, for instance, visual-induced kinetosis (Golding et al., 2021; Keshavarz et al., 2019). Concerning validity, reliability, purchase costs, and setting economy, the *Motion Sickness Susceptibility Questionnaire* (MSSQ) in the short-form was chosen (Golding, 2006). This indicator has been established as the standard questionnaire to evaluate individual motion sickness vulnerability and is recommended by many researchers (Asawavichienjinda & Patarapak, 2019; Catanzariti et al., 2016; Pan et al., 2020).

In any case, some researchers postulate few limitations with the MSSQ. For instance, from the perspective of Lamb & Kwok (2015), the sample size seems to be quite small (n = 257) and overrepresents adolescents and females, which potentially skews actual susceptibility within the general population.

With reference to Golding (2006), the MSSQ-short covers past motion sickness experiences of the respondents when traveling by cars, buses, trains, boats, or swings and sitting on roundabouts in playgrounds. The evaluation includes experiences gained during childhood (before the age of 12) and as an adult (past 10 years). The questionnaire is designed as a 4-point Likert scale ranging from 0 (never felt sick) to 3 (frequently felt sick), while there is also a possibility to mark types of transportation that have never been used. Both scores, based on experience until the age of 12 (MSA) and the past 10 years (MSB) are accumulated and calculated as follows:

$$MSA \text{ or } MSB = \frac{Total\ sickness\ score * 9}{9 - \sum number\ of\ types\ not\ experienced} \qquad \text{Eq. 3-28}$$

The total MSSQ score can range from 0 to 54 and is designed by the unweighted summation of the MSA and MSB. Fig. 3-35 illustrates the measured data on the left-hand side, whereas on the opposite side a polynomial approximation of the total score is shown.
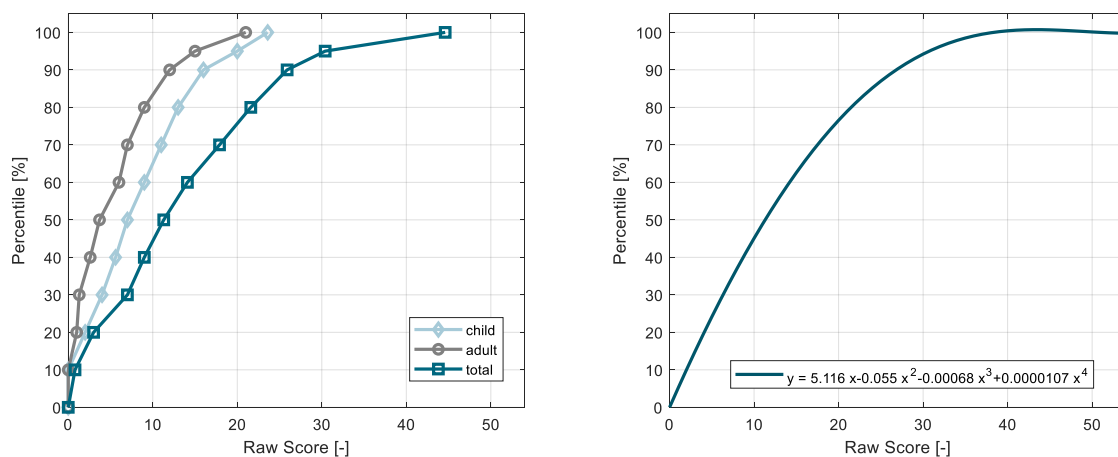
Fig. 3-35: Cumulative motion sickness susceptibility rating (left); mathematical approximation (right). Based on Golding (2006)

As outlined by Stone (2017, p. 25), to enable a reliable evaluation of motion sickness symptoms a selection of different questionnaires, such as the Pensacola Diagnostic Index by Graybiel et al. (1968), the Misery Scale by Bos et al. (2005), or the Pensacola Motion Sickness Questionnaire and its derivative forms by Kellogg et al. (1965) and Kennedy et al. (1993) were used in the past. With reference to chapter 3.4.5, motion sickness refers to associated disorders, which offers further opportunities to utilize related questionnaires e.g., the Dizziness Handicap Inventory, to assess motion sickness (Henriques et al., 2014; Susan King et al., 2019). In some cases, the Simulator Sickness Questionnaire by Kennedy et al. (1993) was also used in physical-induced motion conditions. Lastly, modifications and combinations of existing questionnaires are utilized in different examinations (Brietzke et al., 2021; Kato & Kitazaki, 2006; Perrin et al., 2013; Wada et al., 2012).

With the equivalent quality criteria that had been applied for evaluating susceptibility, the recent questionnaire of Gianaros et al. (2001) is stated as the most appropriate tool for measuring motion sickness severity under dynamic physical conditions. The *Motion Sickness Assessment Questionnaire* (MSAQ) is a multidimensional approach for assessing individual motion sickness severity. The questionnaire consists of 16 items covering the major dimensions of the polysymptomatology, while these items are clustered into four subscales reflecting gastrointestinal, central, peripheral, and sopite (from the Latin sopire: to lull, to put to sleep) symptoms (A. Koch et al., 2018). The MSAQ, as described by Gianaros et al. (2001), offers a detailed analysis by using a 9-point Likert scale ranging from 1 (not at all) to 9 (severe) for the individual items. Scores of subscale or in total ranging from 11.1 % (no symptoms) to 100 % (maximum expression) are calculated as follows:

$$Overall\ MSAQ\ score = \frac{Total\ points\ from\ all\ items}{144} * 100 \qquad \text{Eq. 3-29}$$

$$Subscale\ MSAQ\ score = \frac{Total\ points\ of\ all\ subscale\ items}{Total\ numbers\ of\ all\ subscale\ items * 9} * 100 \qquad \text{Eq. 3-30}$$

Additionally, in 2011, Keshavarz & Hecht postulated the *Fast Motion Sickness Scale* (FMS) with a simple arbitrary spectrum from 0 (no sickness) to 20 (frank sickness). The participants had to rate their actual state of well-being verbally, which enabled a frequent assessment of motion sickness without disturbing the trial of exposure. However, the limitation is clear since the multidimensional symptomatology of motion sickness is simplified or, more precisely, neglected.

3.7.2 Objective Measurements

In the context of motion sickness, several measures have been investigated, but, like the wide range and complexity of its origin already suggests, inter- and intraindividual differences lead to diverse and contrary results between the subjects concerning their expression of the physiological syndrome (Cowings et al., 1990; Gianaros et al., 2003; Hemingway, 1944; Jones et al., 2019). Before now, a reliable and valid quantification resolution to measure motion sickness remained unattainable. However, as previously outlined, implications including cardiovascular and gastrointestinal diseases, ocular, and posture imbalances, as well as changes in hormone and neuropeptide secretion can possibly occur. Some of these expressions have already been discussed in chapter 3.3, while a revised summary of physiological correlates and autonomic responses, reported during physical-induced motion sickness, is illustrated in the appendix (Dobie, 2019, pp. 14–16; Nicogossian & Parker, 1982, p. 143). In line with the objectives of the current research, the focus will shift to non-invasive and reliable measurements, which can be assessed in vehicle environments without disturbing the actual test design. Even if there is a strong consensus regarding clinical study findings in gastrointestinal measures, such as changes in gastric tachyarrhythmia, this measurement is highly vulnerable to artifacts and dynamic perturbations (Hu et al., 1991). Therefore, cardiovascular (heart rate, blood pressure or circulation) and cardiorespiratory (respiration rate) measures concerning thermoregulation are of special interest and are presented in the current chapter.

Physiological Measurements

According to Gianaros et al. (2003), a decrease in cardiac parasympathetic activity, namely respiratory sinus arrhythmia, is over time associated with motion sickness severity. This finding is in line with previous investigations that emphasized the inhibition of the sympathetic nervous system while maintaining parasympathetic activity during nauseogenic stimuli (Hasler et al., 1995; Kohl & Homick, 1983; Uijtdehaage et al., 1992). By contrast, an increase in electrodermal activity and plasma catecholamine as well as the decrease in heart period variability e.g., reduction in mean successive differences in R-R intervals, suspects that motion sickness is mediated by sympathetic activation rather than parasympathetic stimulation (Doweck et al., 1997; Golding, 1992; Hu et al., 1991; K. L. Koch et al., 1990; Kohl, 1993). Holmes & Griffin (2001) found a significant correlation between the development of motion sickness and the rise of heart rate, while studies of Mullen et al. (1998) contradicted the theory that heart rate serves as a reliable indicator to quantify motion sickness. The researchers were unable to find supporting evidence for a strong association neither to heart rate nor to respiratory indicators. However, changes in respiration patterns are not only due to human respondents as a result of nauseogenic stimuli, it, furthermore, reveals as an intentional strategy to avoid the physiological syndrome (Denise et al., 2009). Conscious respiration control is known to influence heart rate variability and, therefore, the state of the autonomic nervous system (Horn, 2003, p. 46). Consequently, values associated with respiratory impact are governed by the fundamental issue of causality. By analyzing blood pressure, heart rate, and body temperature divergent resolutions are found (Cowings et al., 1990; Graybiel & Lackner, 1980; Nalivaiko et al., 2015). Cowings et al. (1990), in contrast to Graybiel and colleagues, who emphasized, "biofeedback control of the physiological variables studied is not likely to prevent the expression of motion sickness symptomatology", finds a stable individual autonomic response to the physiological syndrome. Furthermore, there is strong evidence for the close link between nausea and thermoregulation since several investigations encourage the idea of motion sickness potentiating hypothermia (Cheung et al., 2011; Cheung & Hofer, 2001; Mekjavic et al., 2001; Nobel et al., 2010). In experiments from Nalivaiko et al. (2014), rectal core temperature differed around 0.3 °C between subjects experiencing motion sickness and control subjects. Within their investigation, strong evidence was found that biological mechanisms that are responsible for the nauseogenic-induced hypothermia also include cutaneous vasodilation, increase skin conductance, and reduce thermogenesis. Furthermore, in 2014, Farmer et al. pointed out that the occurrence of salivation leads to the deduction of increasing activity of the peripheral nervous system.

Behavioural Measurements and Performance Testing

Behavioural responses associated with motion sickness are linked to vegetative and deep neurophysiological activations. Especially sopite syndromes are typically represented by yawning, blinking, or staring in a state of apathy and sleepiness (Matsangas & McCauley, 2014). In fact, with increasing salivation forced swallowing is visible, while exaggerated exhaling and mimic changes are frequent concomitants in this state of well-being.

Since increasing skin conductance is commonly associated with motion sickness, wiping sweat from the forehead is a quite often seen incident (Golding, 1992). Expressions of anxiety and loss of motivation are mainly observed indirectly (Dobie, 2019, pp. 14–16; Graybiel & Knepton, 1976; Money, 1970). Furthermore, deterioration of muscular coordination and psychomotor performance as well as anorexia, the unusual sensitivity to repulsive sights or odors, could be examined through pursuant testing before, after, or during the exposure of nauseogenic stimuli (Pasquier et al., 2019). Given that motion sickness is associated with motor control permutations, standardized tests concerning motor coordination and balance, like posturography, can be conducted to generate objective data sets (Koslucher et al., 2014; Laboissière et al., 2015; Walter et al., 2019).

3.8   Prophylaxis and Treatments on Motion Sickness

Treatments to suppress and mitigate motion sickness include pharmacological substances, behavioural strategies, and, for this special case, vehicle-related solutions. For the sake of completeness, the pharmacological treatments are only alluded to by reference to a selection of medication (see appendix), whereby the focus of this work will be placed on the two other solutions, especially when it comes to the experimental part.

3.8.1   Pharmacological Treatments

Pharmacological medications have a limited range of use in daily life, although, in extraordinary situations, it is the most common method to avoid motion sickness (Dobie, 2019, p. 183). Lawther & Griffin (1988) surveyed 2,000 passengers during sea-going ferries, of which 26 % had taken anti-motion sickness drugs. However, pharmacological treatments are not limited to seafaring environmental conditions. For instance, 13 % of Rallye co-drivers reported taking anti-motion sickness drugs during their trial sessions (Perrin et al., 2013). In general, motion sickness drugs are accompanied by side effects of neural suppression and sedation, which are likely to affect individual performance and mental awareness (B. Yates et al., 1998). Other adverse effects potentially include headache, dry mouth, stomach pains, gastrointestinal responses, muscular weakness, and impairment of the ocular system (A. Koch et al., 2018). Medication to avoid motion sickness also has in common that its most effectiveness occurs when the pharmacological drugs had been taken before exposure rather than during the occurrence of the first symptoms (Murdin et al., 2011; Schmäl, 2013). In 1993, Takeda et al. postulated that anti-motion sickness medications could be clustered into three classes of effects, which:
- reduce incongruent neural information by a blockade of sensory inputs,
- accelerate the acquisition of habituation to a new pattern of sensory inputs, and
- block the onset of vegetative symptoms.

As previously outlined in chapter 3.2.4, the neurotransmitters histamine, acetylcholine, and noradrenaline are fundamental in the origin of motion sickness and, consequently, relevant for drug-related prevention (Schmäl, 2013). Even if less efficacious than competing drugs, antihistamines are attributed to a long half-life period and a safe operation, which makes it the most common and presently available medication on clinically used motion sickness prevention (B. Yates et al., 1998).

Histamine acts through three types of receptors, H_1 and H_2 (postsynaptic) as well as H_3 (presynaptic), and mediates the firing rate in afferent axons, which arises in the neuroepithelium of the semicircular canals (Shupak & Gordon, 2006; Zimatkin & Anichtchik, 1999). Promethazine, dimenhydrinate, cyclizine, meclizine, and cinnarizine are common drugs with central anticholinergic effects and act as a histamine H_1-receptor antagonist (Benson, 2002, p. 1075; Mitchelson, 1992a, 1992b). Furthermore, flunarizine, which had been mainly investigated in squirrel monkeys, blocks calcium channels and affects neural signal processes to reduce motion sickness portability (Cheung et al., 1992). In general, antihistamines in motion sickness, for at least 5,184 analyzed subjects, show an effectiveness rate of almost 70 % (Wood, 1966). Scopolamine, an anticholinergics (acetylcholine antagonist) acting on muscarinic receptors in the central nervous system, is still one of the most effective pharmacological agents in clinical use for treating motion sickness (Cheung et al., 1992). Recent studies, carried out by Stankovic et al. (2019), have shown that intranasal scopolamine, by contrast to the common administration of anti-motion sickness drugs, shows potential in rapid relieving of symptoms. The expected advantage is linked to its short elimination half-life and need-based administration.

In summary, the main categories in preventing motion sickness consist of antihistamines, scopolamine, and amphetamine medications, in which dosage and duration of actions differ between each other. Moreover, dopamine and serotonin receptor antagonists are only two among several more transdermal patches, tablets, injections, or tablet solutions to avoid motion sickness. (Schmäl, 2013; Soto et al., 2013) By contrast, the dopamine antagonist metoclopramide as well as some assertive antiemetic, such as the serotonin antagonist ondansetron, have proven to be ineffective in alleviating motion sickness (A. Koch et al., 2018). Furthermore, according to the investigations of McIntosh (1998), psychological factors are likely to influence motion sickness severity, whereby placebo plays a major role across the entire range of subjects. Almost 45 % of patients benefit from placebos and, thus, they appear not to have a negligible effect in kinetosis treatment.

3.8.2 Behavioural Treatments

In addition to the described medication possibilities, non-pharmacological countermeasures to avoid or at least alleviate motion sickness exists. Some of those suggestions include nutrition-related and behavioural recommendations as well as environmental enhancements.

Nutrition-Related Solutions

In 1992, effects of food ingestion on vection-induced motion sickness were examined by Uijtdehaage et al., in which 46 participants were assigned either in the group of food intake or a no-meal group. The results suggest that the food-related enhancement in cardiac parasympathetic tone effectively suppresses motion sickness responses. Furthermore, Levine et al. (2004) discovered that "liquid protein-predominant meals were most effective in suppressing both the development of gastric tachyarrhythmia and the entire spectrum of motion sickness symptoms, including nausea".

Given that vitamin C is known as a histamine agent and the intake of this supplement has proven to reduce nausea in persons with mastocytosis, it is imperative to carry out investigations to evaluate its influence on motion sickness symptoms (A. Koch et al., 2016). According to Jarisch and colleagues (2014), high doses of vitamin C seem to be effective in suppressing motion-induced sickness, particularly in younger subjects and adolescents. Compared to the above-mentioned pharmacological treatments, vitamin C does not have adverse side effects such as dizziness, headache, or drowsiness (Jarisch et al., 2014; A. Koch et al., 2016). Application of ginger (up to 2,000 mg), before the actual motion stimuli onset, has proven to alleviate nausea, tachygastria, and plasma vasopressin (Lien et al., 2003). Furthermore, according to Lien et al. (2003), ginger extended the latency before nausea occurs and abbreviated the recovery time. Extracellular glucose concentration shows a strong relationship to the neurotransmitter glutamate, which is released from the central pathways of vagal afferent neurons (S. Wan & Browning, 2008). This is combined with the ability of changes in blood glucose concentration to modulate gastrointestinal response, especially stomach motor functions (Schvarcz et al., 1997). Hence, a detailed investigation regarding glucose level and motion sickness had been carried out by Mo et al. in 2012. The researchers recommended that a stable glucose level is likely to relieve gastrointestinal symptoms in the physiological syndrome, while acute hyperglycemia is linked to the severity of gastrointestinal manifestations. By contrast, alcohol and fermented nutrition e.g., red wine, cheese, or hung beef, shows interaction to H_1 and H_2 histamine receptors and, therefore, promote the risk of suffering from motion sickness (Zimatkin & Anichtchik, 1999). According to Golding et al. (2011), nicotine increases the severity of motion sickness, while its deprivation provides effective protection against the respective symptoms. The corresponding effectiveness as a treatment to avoid motion sickness seems to be almost equivalent to half of the effect of the previously mentioned pharmacological countermeasures (Golding et al., 2011). Furthermore, the researchers emphasized that this finding explains why temporary nicotine withdrawal preoperatively leads to an increased tolerance to sickness for postoperative nausea and vomiting by habitual smokers, whereas non-smokers show an elevated risk of suffering from these symptoms.

Behavioural Recommendations and Environmental Optimizations

There are two main strategies to manipulate the incidence of motion sickness by either improving individual tolerance to provocative motion stimuli or diminishing the intensity and characteristics of the motion pattern (Benson, 2002, p. 1072). The provocative motion properties are already described in chapter 3.6. The most consistent and high-quality evidence on motion sickness prevention can be found in extensive habituation programs, often called motion sickness desensitization exercises (Bagshaw & Stott, 1985; Bertolini & Straumann, 2016; Dai et al., 2011; Domeyer et al., 2013; A. Koch et al., 2018; Lackner, 2014; Riccio & Stoffregen, 1991; Smyth, Jennings, et al., 2021; Tal et al., 2013). Especially in military conditions, selection and habitation programs with success rates exceeding 85 % are a common tool to ensure a fully operational team (Benson, 2002, pp. 1067–1074; Bronstein et al., 2020; Dobie, 2019, pp. 177–179).

Fig. 3-36 illustrates representative progress of resistance to motion sickness in 45 trainee paratroopers participating in a consecutive daily desensitization program.
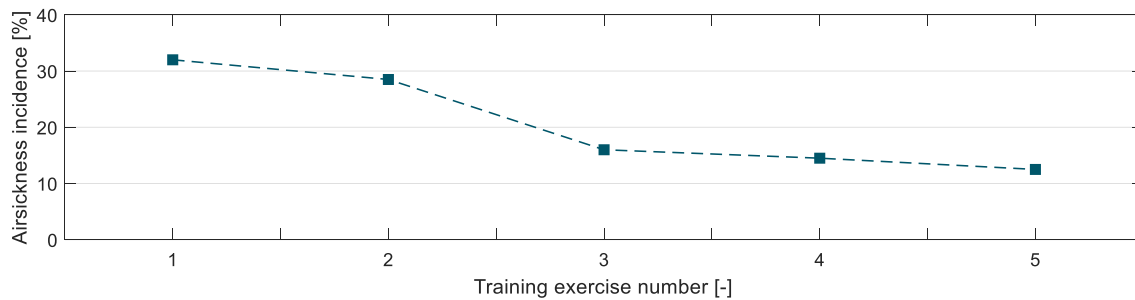
Fig. 3-36: Habituation effect in airsickness of paratrooper flight training.
Based on Antuñano & Hernandez (1989)

Although habituation seems to be quite effective, according to Schmäl (2013), at least 5 % of the population experiencing motion sickness show no signs of adaptation.

The second strategy is related to the reduction of provocative stimuli concerning the intersensory and intravestibular mismatch theory, explained in chapter 3.2.6. Here, behavioural implications are demonstrated, while the respective technical adjustment will be discussed in the next part of the current chapter. Firstly, it is mandated that low frequency and cross-coupled motion have to be limited to a minimum by avoiding movements outside the axes of motion. If angular stimuli are present, sitting close to the pitch, yaw, and roll pole seems to be worthwhile (Waldfahrer, 2008). As a result, provocative head motion is going to be diminished. Moreover, according to Brainard & Gresham (2014), it is valuable to synchronize vision with the other two motion senses, respectively the vestibular one. This can be achieved by visually focusing the horizon or a distant obstacle during passive motion on ships, in buses, trains, or vehicles. If the outside view is limited, closing eyes is strongly recommended (Brainard & Gresham, 2014). Additionally, if possible, intervention through actively taking the driving task and steering control synchronizes actual receptor inputs with the experienced neural pattern (Benson, 2002, p. 1073). Under these circumstances, it is reported that less motion sickness occurs in subjects who anticipate the upcoming trajectory and, as a result of that, actively misaligned their head with the gravito-internal force during turning (Golding et al., 2003; Kuiper et al., 2020; Wada et al., 2012).

Apart from the described low-frequency motion, high-frequent noise stimuli also affect the severity of motion sickness, especially under visual-induced circumstances in simulator or laboratory conditions. In 2015, during chair rotation, while high-frequency vibration to the head was applied, a reduction up to 25 % in motion sickness severity could be observed (Bos, 2015). Further investigations, in which high-frequency seat noise was initiated by a vibrating device attached to the bottom of the chair, showed a reduction in motion sickness of almost 35 %, however, without showing statistical significancies (D'Amour et al., 2017). In summary, high-frequency vibration and exogenous noise stimuli seem to influence vestibular processing and promise to be a potential treatment against motion sickness (Keshavarz, 2016). In addition, non-motion environmental conditions also provide opportunities to further dampen motion sickness severity.

Firstly, odors that are perceived as pleasant are likely to reduce motion sickness, whereas unpleasant rated odors do not show any robust impact on the development of symptoms (Keshavarz, Stelzmann, et al., 2015; Paillard et al., 2014). The link between olfactory and motion sickness is comprehensible since its increasing sensitivity is already mentioned as a side effect of motion sickness (see chapter 3.3). Moreover, Keshavarz & Hecht (2014) carried out investigations in a static simulator and observed the potential impact of music and airflow on the subject's well-being. Within their study, the researchers discovered that pleasant music and constant airflow, provided by stationary fans, seem to be an effective and affordable way to avoid motion sickness. Furthermore, the surrounding temperature, however without statistical significance, correlates with motion sickness severity (J. T. Arnold et al., 2019). In combination with active deep diaphragmatic breathing, individual manipulation of the autonomic nervous system with the ability to minimize motion sickness can be achieved (Denise et al., 2009). There are many other solutions such as acupuncture as well as acupressure, transcranial magnetic stimulation, or transcutaneous electrical nerve stimulation with a contradicting nature in alleviating motion sickness (Cha, Deblieck & Wu, 2016; Cha, Urbano & Pariseau, 2016; Chu et al., 2012; Chu et al., 2013; B. Yates et al., 1998). Those solutions are beyond the scope of the current work, this is why they are not explored in further detail within this analysis.

3.8.3   Carsickness-Related Treatments

Although carsickness is mainly initiated by provocative longitudinal and lateral motion, active suspension systems, which are predominantly relevant in regulating vertical and angular motion, show evidence of reducing motion sickness in passengers (DiZio et al., 2018). In fact, according to Shyrokau et al. (2015), vehicle suspension systems are forced to eliminate vehicle disturbances targeting an improvement of motion comfort. In 2014, Bär equipped his vehicle prototype with an active roll suspension system to compensate for lateral motion that is initiated through long cornering and, consequently, reduces postural and head disturbances. Already at that time, the potential for motion sickness prevention was mentioned, but, until recently, has not been entirely researched. Besides vehicle dynamics, aspects of the vehicle interior, such as sitting direction (Salter et al., 2019) or backrest inclination (Vogel et al., 1982), are investigated as well and will be displayed in the consecutive chapters in more detail. In addition, auxiliary display positioning and visual conditions have been observed with respect to the vehicle interior (Kuiper et al., 2018; Probst et al., 1982). In both investigations, the outside view is likely to minimize motion sickness. To increase visual information, Karjanto et al. (2018) evaluated a peripheral visual feedforward system in an automated vehicle. Moving LED stripes, adjusted on the frame of the screen positioned in front, provided the passenger with information about the upcoming trajectory. The results suggested that the additional visual information led to a substantial improvement in kinetosis manifestations, whereas the subjects' mental workload remained unchanged. In 2021, Winkel et al. investigated augmented visual environments in cars, however without promising results in reducing carsickness. Finally, there are several anti-motion sickness devices available for purchase, such as glasses representing an artificial horizon in the peripheral visual field. However, there is a fundamental lack of evidence on their efficiency in mitigating motion sickness.

4 Scope of Work

In chapter 1.1 it is shown that increasing road vehicle automation with its promise of usability improvement by facilitating NDRTs during vehicle journeys is inextricably linked to the heightened risk of vehicle occupants suffering from motion sickness. Prior to this, with the exception of sleeping, there was no convenient way to completely avoid motion sickness symptoms in all cases without willing to accept potential side effects of drowsiness or lethargy (Dobie, 2019, p. 214). Therefore, the aim of this work pertains to countermeasures on motion sickness to enable visually demanding activities while being shuttled. To identify non-pharmacological treatments, basic research, for instance from Griffin (1990), provides fundamental information about influencing factors that are likely to manipulate the occurrence of motion sickness. Furthermore, those aspects are essential for the experimental designs conducted in this elaboration and are presented in Fig. 4-1.
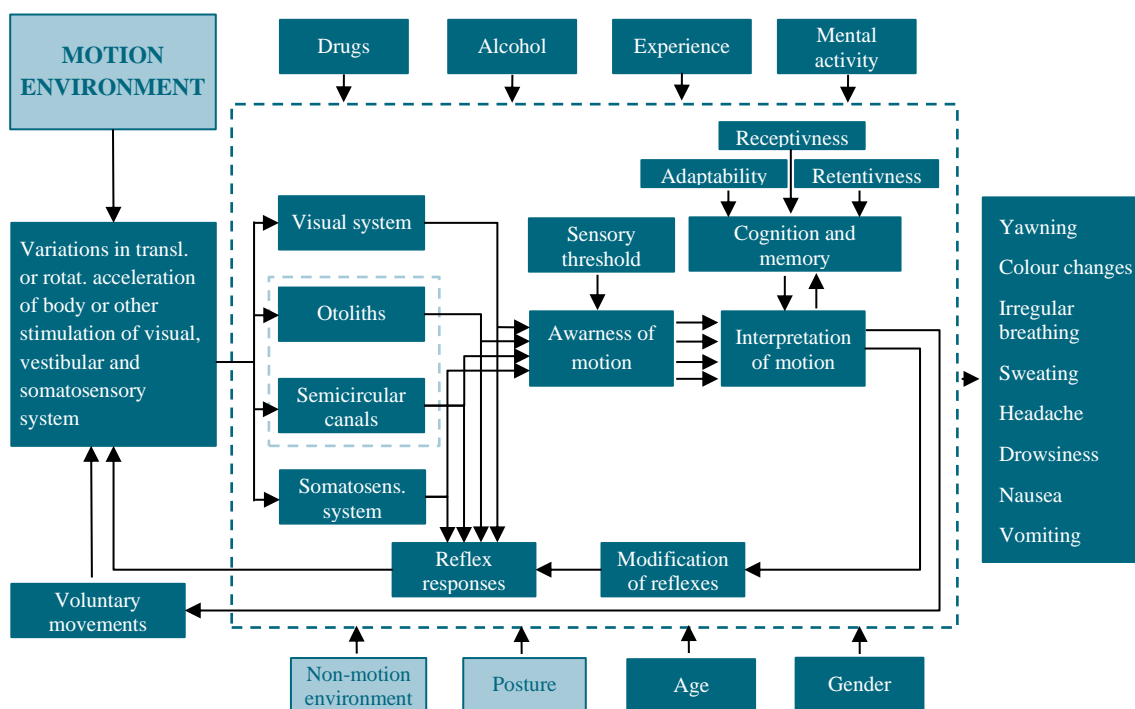
Fig. 4-1: Exogenous and human-related factors contributing to motion sickness.
Based on Griffin (1990) as cited in Förstberg (2000b, p. 25)

Human-related factors e.g., biological gender, age, and experience, are relevant for subjects recruiting but do not contribute to vehicle-related solutions in mitigating motion sickness. By contrast, posture, motion in addition to non-motion environmental conditions, and mental activity, which is influenced by the HMI and the task that has to be performed, are worthwhile vehicle-related aspects determining user experience in an automated vehicle. In general, all influencing factors, which are shown in the model above, either have to be manipulated or standardized within the experimental setup.

With the development of future vehicle design guidelines, apart from motion sickness treatments, further aspects of general motion comfort have to be considered as well. Moreover, if motion sickness occurs, it is clear that discomfort is present. Conversely, countermeasures to avoid motion sickness do not consequently coincide with a status of well-being and providing a suitable feeling of comfort.

70

Therefore, inferential investigations to evaluate motion sickness treatments in terms of motion comfort are also included in the scope of work. Lastly, with subordinate priority, objectification and performance capability are investigated. Given that motion sickness is accompanied by side and after-effects leading to expressions of malaise and nausea, those research targets address safety-relevant aspects occurring with vehicle automation.

4.1 Research Potential in Motion Sickness Treatments

In general, the current work concentrates on physical-geometric aspects of the vehicle interior, while the definition of occupant´s posture, as the basis of vehicle´s cabin dimension, is elementary and, therefore, the very first research step in this elaboration. The idea of proposing supine postures as a countermeasure to motion sickness is already demonstrated by previous investigations (Golding et al., 1995; Golding & Kerguelen, 1992; Griffin, 1990, p. 31; Manning & Stewart, 1949), some of which are described in chapter 3.6.3. However, most of these experiments were conducted in motion simulators and aircraft or seafaring environments with clear oscillatory and generic motion patterns. Therefore, the natural characteristic of stochastic multiaxial motions that occur in real-life vehicle driving was not represented. Even investigations carried out under road conditions were overshadowed by predominant uniaxial strong artificial driving maneuvers, which do not allow an unexamined transferability of results (Probst et al., 1982; Vogel et al., 1982). In fact, when considering the study of Vogel et al. (1982), it is unclear whether a reclined posture provides the same anti-emetic effect as reported in supine postures. Also, the test setup did not represent a real-life scenario (device for head fixation) or addressed situations in which vehicle occupants are engaged in visually demanding NDRTs as expected in the near future.

As an extension to the supine paradigm, the seating orientation shall increase the potential of vehicle usage by allowing the occupants to sit face to face with each other. Traveling rearwards is expected to increase the likelihood of motion sickness (Wada, 2016), however, clear evidence on the prevalence of symptoms when facing against the driving direction is rare. Kuiper et al. provided support to this implication, by demonstrating that the ability to predict anticipatory cues of future vehicle motion leads to less motion sickness compared to situations when the motion was unpredictable (Kuiper et al., 2018; Kuiper et al., 2020). This finding is in line with the conclusion of Turner & Griffin (1999a) who emphasized that observing the road ahead increases the opportunity to anticipate the future trajectory and, therefore, helps to reduce motion sickness. In 2019, Salter et al. investigated the likelihood of motion sickness when traveling rearward compared to the conventional forward sitting condition. The researchers chose two different kinds of test tracks to simulate motorway and urban areas. The participants reported, especially under urban driving conditions, a significant increase in motion sickness when traveling backward. Since the participants were only instructed to carry out typical office tasks, inter- and intraindividual differences in the characteristics of activity may influence the nauseogenic stimuli and, therefore, also affect the overall result in motion sickness responses. The seats were rotated around the z-axis but did not show any manipulation in backrest angle (rotation around the y-axis in the sagittal plane).

As highlighted in the previous sections, vision seems to be one of the main keys to manipulate motion sickness. To provide suitable visual information about the motion surrounding, for instance, due to an optimization of in-vehicle display position (Kuiper et al., 2018), general outside view (Perrin et al., 2013; Probst et al., 1982), as well as artificial visual stimulation using digital devices (Meschtscherjakov et al., 2019; Miksch et al., 2016; Mu et al., 2020; Winkel et al., 2021), have been investigated in real-test driving scenarios. The described inventions, however, are limited to digital in-car or mobile devices. A more holistic approach seems to be rewarding by using existing vehicle interior components to stimulate the visual apparatus. When incongruent information appears, Perrin et al. (2013) emphasize that the presence of optic flow increases the likelihood of motion sickness, while the findings and opinions of Meschtscherjakov et al. (2019) in relation to the impact of optic flow are to the contrary of this. Consequently, the optic flow seems to provide an appropriate research target when it comes to a new, innovative, and promising approach to alleviate carsickness.

4.1.1 Human-Related Research Questions on Motion Sickness Methodology

To address the previously mentioned research topics, the following questions form the basic framework for the examinations which had been conducted in this elaboration. In addition to the field of treatments to alleviate motion sickness, also more general topics do take part in the research scope. However, those questions are considered with lower priority:

1. Is it possible to quantify individual carsickness by objective measurements?
2. Does carsickness affect human concentration and reaction time?
3. Which non-vehicle-related parameters affect the severity of carsickness and, thus, are relevant for the test design?

4.1.2 Vehicle-Related Research Questions on Motion Sickness Treatments

The main research questions addressing motion sickness countermeasures are based on situations in which occupants are driven in the rear of a vehicle while performing visually demanding NDRTs:

4. Is it possible to manipulate carsickness in subjects by adjusting the vehicle interior?
5. In fact, do supine postures influence carsickness?
6. If supine postures are likely to decrease the severity of carsickness, to what extent does the backrest inclination need to be adjusted?
7. Do vis-à-vis seating positions increase the prevalence of carsickness?
8. What is the impact of outside view on carsickness when being engaged in visually demanding activities?
9. Moreover, is it possible to increase visual perception by manipulating in-vehicle lighting systems to reduce carsickness?
10. Are the findings regarding vehicle-related countermeasures on carsickness congruent with the already presented etiological theories?

4.1.3 Further Research Questions Regarding Motion Comfort

Finally, after the different seating configurations are investigated in terms of their motion sickness prevalence, analysis regarding general comfort is conducted. This is essential since motion sickness is only one element that contributes to motion comfort. Given that the benefit of increasing road vehicle automation is, among other aspects, related to improvements in quality of time by facilitating complex NDRTs, user acceptance and motion comfort are highly relevant for the successful introduction of this technology (see chapter 1.1). In consequence, the following questions address this additional issue:

11. How is the feeling of comfort and the user acceptance with respect to innovative seating configurations?
12. How does human body vibration change when manipulating seat configurations?

4.2 Overview of Investigations

Within the current elaboration, physical-geometric properties of the vehicle interior design influencing motion sickness and comfort are categorized as seating configuration and visual conditions. While seating configurations can be divided into backrest angle and sitting direction, visual conditions include aspects of outside view and interior lighting. In addition to chapter 2, the following Fig. 4-2 provides a more precise overview of the main investigations (column) which had been carried out to examine motion comfort with regard to automated driving scenarios. For each real-test driving investigation, the motion exposure and the source of predefined NDRTs were not manipulated and, therefore, kept constant across the respective test trials.
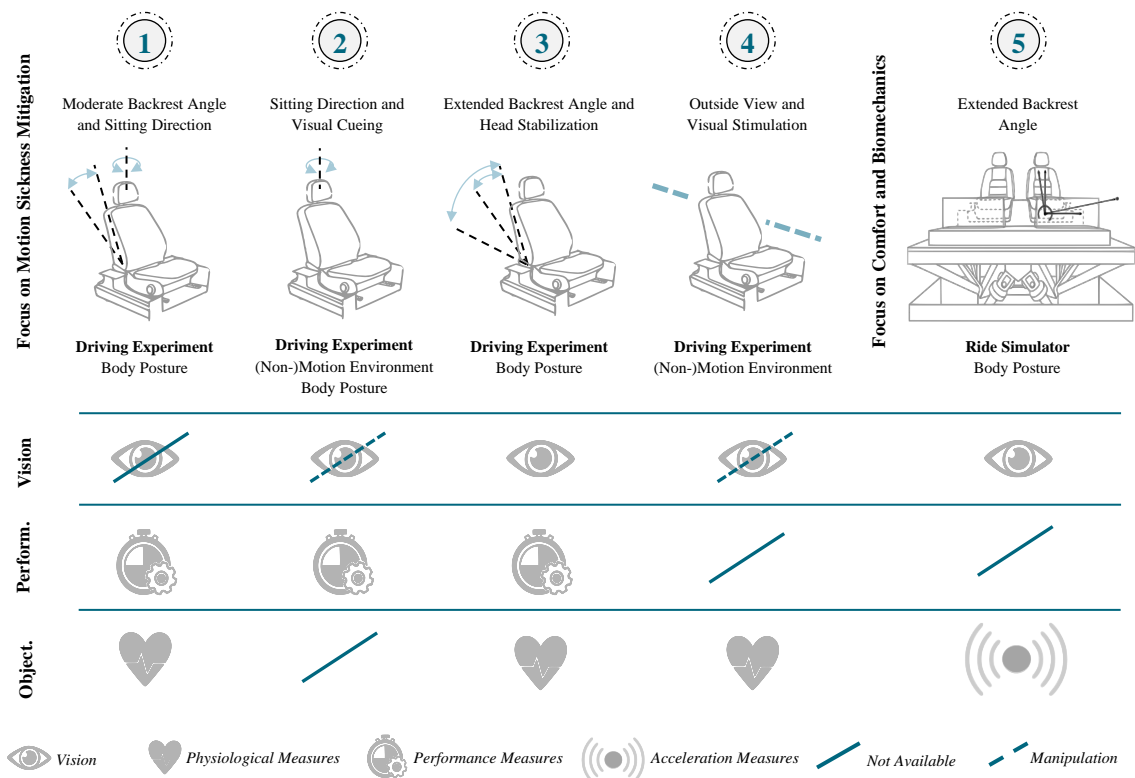
Fig. 4-2: Investigations of the current elaboration.
Images: Ride Simulator and seat modified from Daimler AG (2020)

Based on the fact that carsickness belongs to the group of motion-induced incidence of kinetosis, investigations took place in real-test driving environments with standardized vehicle motions. To ensure repetitive physical inputs, driving events were carried out at a test track without fluctuations in traffic density. Furthermore, a dynamic simulator was chosen for biomechanical analysis as the most appropriate environment for standardized motion stimuli. Additionally, aspects of subjective motion comfort were examined here.

In the following chapters, the four real-test driving experiments addressing the main research questions on motion sickness treatments by physical-geometric adjustments of the vehicle interior are presented. Here, the study design and several important environmental conditions are illustrated. Subsequently, consolidated answers regarding non-vehicle-related predictors of the four investigations are outlined, followed by the subordinate findings concerning objectification and performance measures. Lastly, the impact of backrest inclination on subjective comfort and head dynamics is discussed by analyzing the results of the Ride Simulator investigation.

5 First Investigation – Moderate Backrest Angle and Sitting Direction

The first driving study[1] was carried out in March 2018 with the aim of exclusively examining the impact of today´s serial seat constitutions on the severity of carsickness while performing targeted visually demanding NDRTs. Focus was taken on the manipulation of vestibular and somatosensory input rather than on visual sensory information. The digital device used in all experiments was a 9.7-inch tablet, which was attached to the vehicle structure and not held by the individual itself. The subjects were driven in a 2x2 mixed design on the test track of Mercedes-Benz AG in Sindelfingen.

5.1 Participants

Subjects were recruited from a panel of Daimler employees and people from the area of Stuttgart. Within the selection process, it was ensured that none of the subscribers had vestibular or gastrointestinal diseases (see chapter 3.4.5). To construct equal groups, the potential participants were asked within a cover letter about their susceptibility to motion sickness from 0 (not at all) to 20 (highly susceptible). Since the study aimed to evaluate motion sickness, responses with scores below the value of 3 were not invited and excluded from this type of investigation. The final categorization in terms of susceptibility was obtained due to the MSSQ short score (see chapter 3.7.1), which did not differ significantly between the two groups (M = 12.80, SD = 8.21). Using the software *GPower* and considering a high effect size, the mandatory sample size was defined, so that finally n = 25 subjects aged 21- 56 years (M = 42.46, SD = 11.96), of whom 21 were male and four females, participated in this investigation. Each subject was asked to conduct two exposures with a time interval of at least one day between them to facilitate recovery.

---

[1] The experiment was designed and conducted with the assistance of K. Lehnert (2018) as part of her Master´s thesis. Major results of the first investigation are published in Bohrmann et al. (2018a, 2018b); Bohrmann (2019); Bohrmann & Bengler (2020).

The participants were randomized to the grouping factor of sitting direction using the restriction of equal group size without significant difference in susceptibility, biological gender, or age (see Tab. 5-1). The repetition factor sitting position (backrest angle) was varied within the test subjects so that the same number of subjects first passed the reclined position after experiencing the upright sitting condition or vice versa (see Fig. 5-1).

Tab. 5-1: Constitution of test sample – first investigation.

	Group A Forward	Group B Rearward	p-value
N (females / males)	13 (2/11)	12 (2/10)	.52
Mean age ± SD	38.25 ± 12.21	46.67 ± 10.31	.39
Mean MSSQ short score ± SD	12.69 ± 6.25	13.00 ± 10.23	.92

Fig. 5-1: Experimental seating conditions – first investigation.
Modified from Bohrmann et al. (2018b)

The reclined posture was defined with a 38° backrest angle (52° set up inclination) due to previous ergonomic examinations on rear-seat vehicle occupants (Kilincsoy et al., 2014) and further restrictions on vehicle safety. The upright sitting position was determined by the standard driving posture with 23° backrest angle (Bubb et al., 2015, p. 363). According to ethical standards, all participants were informed about the purpose and the procedures prior to participating in the investigation. In addition to the written part of the informed consent, which had to be signed as a prerequisite for the start of the trial, the participants were also verbally reminded about their ability to discontinue the test procedure at any given time without any recourse. To ensure that participants did not exceed the bounds of acceptable kinetosis manifestations, an internal abort criterion was defined, of which the participants were not aware. Consequently, if subjects reported an FMS value beyond the value of 12, the trial directly was stopped by the examiner. None of the subjects were paid, which precluded the risk of any conflict of interest.

5.2 Procedure

Measurements took place between 7:30 am and 6:00 pm, while the external air temperatures differed in total between 1 and 15 °C. Since the test track provides limited access only to licensed drivers, subjects were picked up by the examiner with the experimental vehicle (see chapter 5.3) at the main gate of the Mercedes-Benz plant. The subjects then were brought to the preparation room next to the test track. While being shuttled, participants sat on the co-driver seat to avoid non-study-related nauseogenic expressions. As outlined in Fig. 5-2, the test procedure consisted of three main sequences, of which only the second part took place in the vehicle.

The preparation and follow-up phase of the measurement, by contrast, were conducted in the preparation room next to the test track. Here, a 5-minute baseline measurement of physiological parameters was captured, followed by the pre-questionnaire that covered demographics, the actual status of health, and the candidate´s opinion on automated driving as well as their susceptibility to motion sickness (measured by the MSSQ short - see chapter 3.7.1). Before re-entering the vehicle, it had been ensured that all subjects were sufficiently aware of the risks associated with participation. While the subjects took their seat in the rear of the experimental vehicle, the technical setup was installed and adjusted by the examiner in a way that guaranteed a comfortable usage of the tablet.

The total driving exposure was divided into four identical 5-minute rounds with short breaks between each other (see chapter 5.4). During this break, the participants were asked about their actual state of health by rating the FMS. Furthermore, if the verbally reported score did not reach the value of 12, the participants were asked whether they want to stop or continue the experiment. The inside temperature was logged and the predefined task for the next round was configured on the tablet. During that time, the participants performed the bdpq test for one minute (see chapter 5.2.2). The vehicle stops occurred at the same predefined spot on the test track and lasted exactly three minutes. Once they had completed the last trial, subjects were driven back to the collection point at the preparation room, where they recovered from potential motion sickness expressions and answered the follow-up questionnaire (incl. the MSAQ - see chapter 3.7.1) to evaluate the severity of motion sickness.
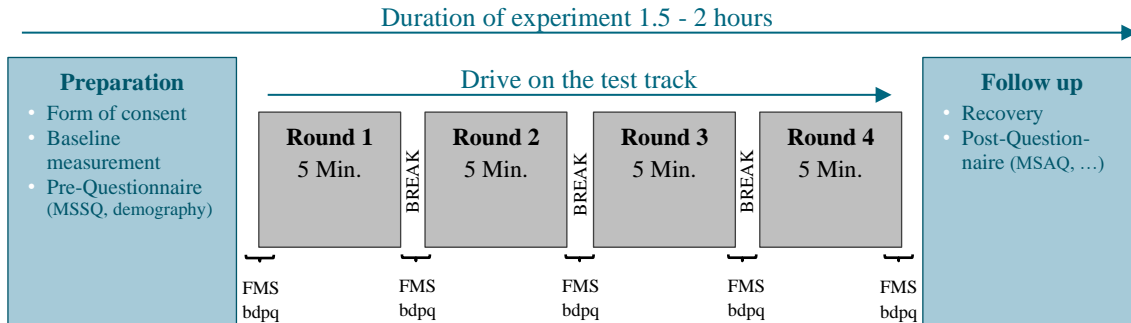
Fig. 5-2: Plan of procedure – first investigation.

During the entire journey, all subjects were monitored by the co-driver to capture motion sickness-related patterns of physiological behaviour, such as yawning, swallowing, or wiping sweat from their forehead. Moreover, if necessary, corrective action was possible to take before the participant's health problem occurred. The real-time monitoring video was included within the framework of the physiological user interface at the front display to the co-driver, where respiration rate, *electrocardiogram* (ECG) as well as the core body temperature of the occupants were presented.

5.2.1 Physiological Measurements

To analyze the previously mentioned physiological parameters in terms of their sensitivity to capture motion sickness manifestations, ultra-short-term sequences of three minutes were applied, whereby very-low-frequency analysis had not been considered within the current elaboration (Baek et al., 2015).

Each of these sequences had been defined to take place immediately before the query of the FMS to link the objective measure with the subjective evaluation. To calculate cardiac cycle lengths, the raw data series were filtered by a commonly used algorithm for this purpose (Fenzl & Schlegel, 2010; Gerteis, 2014, p. 35). According to Marchant-Forde et al. (2004), this filter is predestined to identify and exclude type four and five artifacts from the time series. Here, the values are compared with their adjacent reference point to identify excessive deviations between each other. To put this into more precise terms, the mean and median of a sub-data set consisting of ten surrounding intervals were determined for every raw value. Each data point outside of the interquartile range was captured as an outlier and had then to be eliminated. Subsequently, the raw values were compared to the moving average. If the individual data point deviated more than 30 % from the subset average, it had to be replaced. The sliding calculation empowered statistical parameters to adapt to the variance and dynamics of the data set (Schega et al., 2010). Therefore, large independence according to extreme data points and high robustness against artifact-related distortions had been achieved due to the upstream calculation of the medians. Finally, to avoid errors of artifact accumulation, also known as data drift, a visual review was carried out by the examiner. As extended criteria, more than 5 % of the values had to be identified as artifacts in at least one of the four intervals. Even if violations of the described requirements occurred in six subjects, only three data sets were proven to be inadequate for the evaluation and excluded from the data frame of the consecutive analysis. In general, the ECG data represents the gold standard for measuring and calculating neurocardiac responses, such as the heart rate or its variability (Zink et al., 2015). The physiological activity was recorded with a high resolution of 2048 *samples per second* (sps) by using the *NeXus-10* device (version V2015B1), while this data was post-processed in the *BioTrace+* Software and then transferred to *R Studio* as well as *MATLAB 2019/20b* to estimate the subsequent parameters.

As mentioned by Bombardini et al. (2008), *heart rate* (HR) is defined as the number of heartbeats per minute and, under consideration of the *cardiac cycle lengths* (NN_i), mathematically described as follows:

$$HR = \frac{60000}{\frac{1}{n}\sum_{i=1}^{n} NN_i}$$

<div align="right">Eq. 5-1</div>

Furthermore, *heart rate variability* (HRV), as the variance of the time intervals between consecutive heartbeats, can be derived from the ECG data as well. Contrary to universal expectations, a healthy heart rhythm is not characterized by homeostatic oscillations. The beats rather show a more complex, non-linear, and chaotic behaviour (Goldberger, 1991). Elementary statistical variables are either calculated in the time-domain, which enables a description of variance within the interbeat interval, or in the frequency-domain to quantify the allocation of energy by applying the Fourier transformation and calculating the PSD (Shaffer & Ginsberg, 2017). Both opportunities had been considered for this investigation, whereas non-linear measurements e.g., Poincare plots or detrended fluctuation analysis, are not part of this elaboration. For further information about frequency analysis see chapter 3.6.2.

The first value calculated in the time domain is known as the *standard deviation of interbeat intervals* (SDNN) and is defined as follows (Fenzl & Schlegel, 2010):

$$SDNN = \sqrt{\frac{1}{n}\sum_{i=1}^{n}\left(NN_i - (\overline{NN})\right)^2}$$

Eq. 5-2

The *r.m.s. of successive NN interval differences* (RMSSD) reflect the beat-to-beat fluctuation in the heart rate. Taking into account the above-mentioned healthy heartbeat paradigm, higher RMSSD values imply a suitable regeneration capacity. This parameter is an important criterion due to its resistance against respiration and baroreceptor reflex disturbances. Compared with the SDNN, the RMSSD is known to be more sensitive to the peripheral nervous system and is calculated as follows: (Hill & Siebenbrock, 2009)

$$RMSSD = \sqrt{\frac{1}{n-1}\sum_{i=1}^{n}(NN_{i+1} - NN_i)^2}$$

Eq. 5-3

To further evaluate the cardiac sympathovagal regulation of the human organism, bands of *very low frequency* (VLF) < 0.04 Hz, *low frequency* (LF) 0.04 - 0.15 Hz, and *high frequency* (HF) 0.15 - 0.4 Hz spectrum are defined. While the LF band is influenced by longer-term fluctuations of interbeat intervals, the HF band, in turn, shows a severe relationship with the RMSSD and represents predominant transient changes (Horn, 2003). According to several researchers, the ratio of LF to HF spectrum is capable of quantifying the activity of the autonomic nervous system (Pagani et al., 1984; Rosenberg et al., 2017). Higher ratio values indicate a shift to sympathetic dominance, while lower values correspond to the incidence of the parasympathetic system. However, due to the complexity of the non-linear neurocardiac nerve activity, the LF/HF ratio seems to not always reflect a clear index of the human autonomic balance (Billman, 2013).

The same technical equipment was applied to measure respiration, whereas the sampling rate of this channel was only 32 sps. The *respiratory cycles per minute* (B), as well as the standard deviation of the respiratory cycle lengths (SDBB), were determined analogously to the previously described analyses of the ECG data. The core body temperature was measured using an in-ear wearable called *cosinuss° one* with a sample rate of 100 sps. In contrast to the other physiological measures, here, the post-processing was less complex. Indeed, the nature of those data points in the time domain did not show oscillating patterns, which had to be converted into characteristic frequency-related parameters.
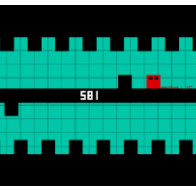
5.2.2 Performance Testing and NDRTs

To analyze the impact of motion sickness on performance, the bdpq test, as a modification of the standardized d2-R attention and stress test, was chosen (Brickenkmap et al., 2010). The participants had to perform this test for exactly one minute before and after the trials as well as during the breaks. This standardized task aimed to identify the actual power of concentration while the participants had to identify a certain pattern of "b" and "q" in a randomly arranged sequence of letters (see appendix).

The quantification of performance was calculated as the correct operations minus the omission and the confusion errors. This method had also been applied by Jarosch & Bengler (2019) when investigating performance in conditionally automated driving.

In order to generate a standardized and nauseogenic provoking stimulus that also provides the opportunity to investigate the effect of mental employment, four different NDRTs were defined which had to be performed during the ride (see Tab. 5-2). The order of tasks was randomized among the participants according to the Latin square method, which had also been used in other studies (Golding & Kerguelen, 1992). Over the two measurements, the order of tasks was kept unchanged to enhance comparability within the repetition factor of backrest inclination.

Tab. 5-2: Description of non-driving-related tasks – first investigation.

Movie	With the lowest mental effort, four videos of different European landscapes with inconspicuous background music were available. The subjects were able to choose between one of them. To ensure equal visual stimuli, the dynamic of content and image change was equivalent for all videos. Image on the right: (Lueg, 2019)	
Quiz	As a quiz "Who Wants to Be a Millionaire" was chosen and downloaded from the App Store. Even if this secondary task required some kind of mental reflection, it did not necessarily need permanent visual monitoring. In consequence, this activity was assumed to be only slightly stressful. Image on the right: (Sony Pictures, 2018)	
Reading	Reading is a mentally demanding activity that had proven to be quite nauseogenic when being performed during vehicle trips (Sivak & Schoettle, 2015). It is characterized by a continuous recording of letters in combin. with a high attention and concentration level. The subjects had the chance to decide between five novels, in which the font size had been equalized between each other. Image on the right: (Stephen King, 2015; Pasini, 2019)	
Game	The game "Flip Run" is considered to be highly demanding in the visual and mental domains. The red token continuously moves along a horizontal line, while the target of the player is to avoid passing rectangular obstacles by changing the side the token is on. This is done by tapping on the screen. A random change of background colour and turning of the graphical user interface gradually increase with time. Each time the token hits an obstacle, the game had to be restarted. Image on the right based on: (Olofsson, 2015)	

5.3 Experimental Vehicle and Setup

Initially, a test vehicle that fulfilled the demands in flexible seat adjustments had to be defined. By analyzing different vehicle types, a mini-van was selected and identified as providing the best vehicle platform for the purpose of this examination. The 2018 modified Mercedes-Benz V-class (O 447) was equipped with series seats in the rear and two different mounting brackets. Both ensured a standardized condition for the tablet positioning. For the reclined sitting position, a stable metal rod was installed between the vehicle floor and the roof frame of the c-pillar, to which a height-adjustable and swiveling clamping system (mounting bracket) was attached (see Fig. 5-4). Consequently, the digital device could be individually adjusted (6 DoF) in such a way that the head could be positioned in a stable manner on the headrest for the entire duration of the trial. Within this construction, care was taken to comply with vehicle safety requirements.

The rear seats, for instance, included integral seatbelts, which ensured a suitable belt routing even in reclined postures. For the upright sitting condition, another bracket was attached in front of the subject. Here, the tablet was adjusted near the beltline of the vehicle, which guaranteed a natural head position for all users. This scenario is based on today´s experience when people are sitting in buses, trains, or even when being co-driver and working during their journey. Assuming that in the future the driver is also able to engage in visual-demanding tasks, it is obvious that the same behaviour is visible, especially when using personal devices like smartphones or notebooks. When working instead of observing the environment, the head is slightly bent at the cervical joint and the field of view is mostly limited to the point of interest and the vehicle interior in the periphery. An exemplary *RAMSIS* visualization of such observations or even assumptions for future scenarios when being in a highly automated vehicle is shown in Fig. 5-3.

Fig. 5-3: Vision simulation representing NDRTs in upright sitting condition i.e. working on a laptop: 95th male (left); 5th female (middle); head-neck bending at cervical joint sitting upright (right) – first investigation. Modified from Daimler AG (2020)

Regarding those illustrations, restricting visual information is shown, which might also lead to the suppression of natural reflexes like the VOR that is described in chapter 3.2.5 (Bronstein et al., 2020). As mentioned, the first study concentrates on manipulation of the vestibular organ during multiaxial vehicle movements, whereas the visual orientation of the vehicle trajectory is excluded to avoid involuntary interaction effects. The elimination of external visual information was achieved by covering the vehicle windows with prototype plates. To prevent subjects from monitoring the route through the windshield, a partition between the cockpit and the rear was created using a black curtain. The interior lighting was switched on throughout the entire journey. Fig. 5-4 illustrates the test setup when sitting rearwards and monitoring the tablet while being in the reclined position.
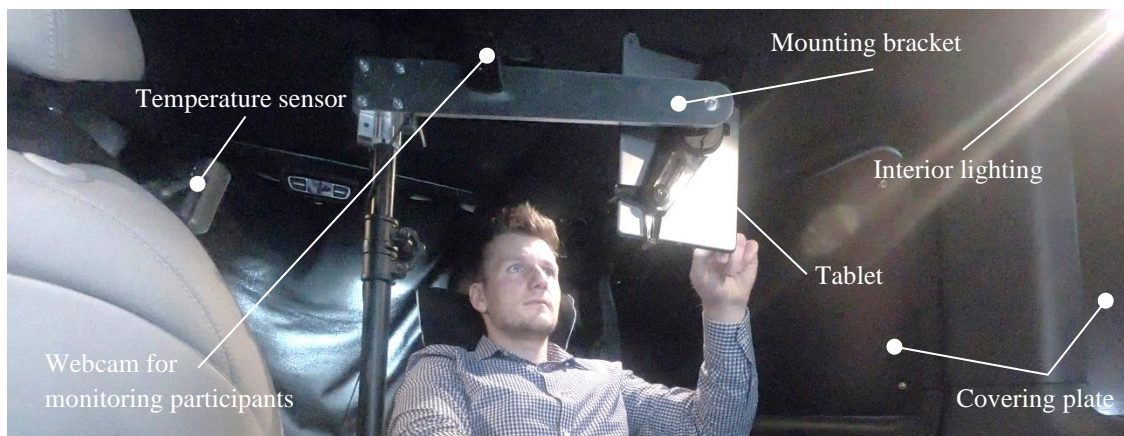
Fig. 5-4: Experimental setup: sitting rearward in a reclined position – first investigation.

5.4   Test Route of Driving Events

According to Griffin & Newman (2004), low-frequency vehicle acceleration in the horizontal plane (longitudinal and vertical direction) is affected to a greater extent by the driving style of individual subjects than by differences between vehicles. Therefore, a trained driver was deployed throughout all investigations to ensure reliable and recurring vehicle dynamics in terms of speed, acceleration, and driving duration. Vertical motion, however, is mainly influenced by vehicle suspension and road surface with peaks between 1.0 and 2.0 Hz (Griffin & Newman, 2004). Consequently, besides the driver limitation, a 2.3 km/round test track in Sindelfingen ("Einfahrbahn") was designed with seven sequences of characteristic vehicle maneuvers and route characteristics (see Fig. 5-5). For instance, traffic congestions were simulated through high-frequency fore-and-aft vehicle motions. The resulting motion profile can be characterized as a start-stop maneuver representing the daily ride in rural areas (Diels et al., 2016).
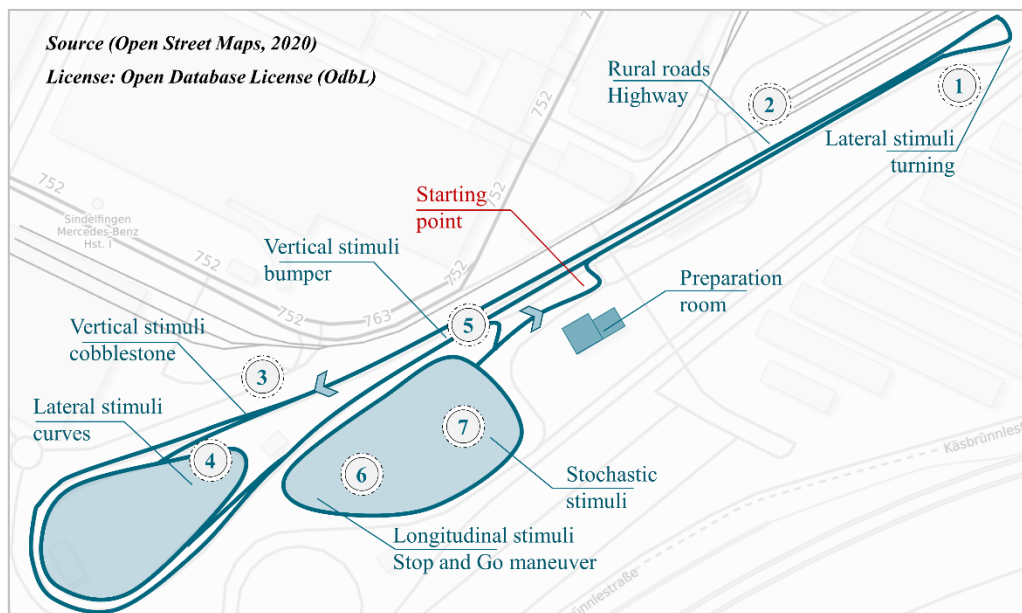
Fig. 5-5: Test track with characteristic maneuvers and route sections during one round – first investigation.
Open Street Maps (2020)

To generate an adequate nauseogenic stimulus with the purpose of identifying and evaluating countermeasures to carsickness, several levers of the respective experimental setup needed to be defined. Firstly, the duration of exposure had to be long enough to manifest at least slight symptoms of motion sickness. However, limitations regarding time effort had to be considered as well. Here, the total time of a 20-minute journey was considered to be acceptable. The second important lever was the strength of physical stimuli e.g., the characteristic of vehicle maneuver. As opposed to investigations of Probst et al. (1982), where the brakes of the test vehicle had to recover after every second trial due to overheating, the premise of this examination was to apply a strong but realistic pattern of vehicle acceleration. Throughout the journey, vehicle motions were captured using the *Xsens MTw* tri-axial accelerometer with a sample rate of 75 Hz, which was located at the vehicle floor next to the seat attachment structure. To illustrate the test procedure, in the first instance Fig. 5-6 shows the distribution of acceleration recorded during one representative lap.

The applied colour convention, in which longitudinal motion is presented in petrol, lateral one in red, and vertical motion grey, has a universal validity for motion description in this work.
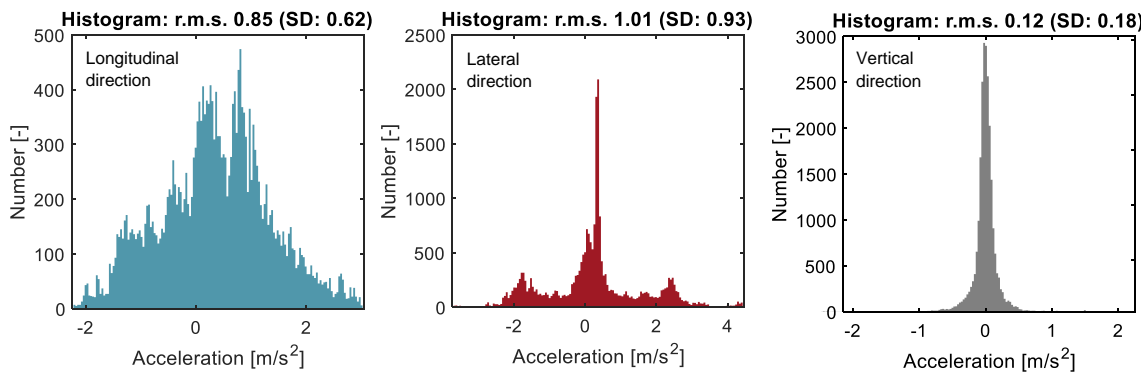
Fig. 5-6: Distribution of translatory accelerations measured on the vehicle ground – first investigation.

The longitudinal acceleration, for instance, ranged between -2.2 and 3.0 m/s^2 and addressed with this profile the guidance of the development of ACC systems that are published in the ISO 15622. Heinrich (2016, p. 66) examined logging data of real-life vehicle motions, by which the aforementioned approach aiming to apply realistic accelerations can be confirmed. Intricately linked to the characteristic of maneuver is the frequency of its events. While in traffic congestions up to five start-stop maneuvers per kilometer are common (Heinrich, 2016, p. 77), in this investigation a higher density in motion events was chosen as it is shown in Fig. 5-7. Moreover, in the time domain, the aggregated MSDVs are presented as well. The left-hand side of Fig. 5-7 shows the power distribution of the vehicle accelerations before and after applying the motion sickness weighting function that has been described in chapter 3.6.1. Further information about the PSD is presented in chapter 3.6.2. Due to the fact that it took almost 30 *seconds* (s) from the location of breaking to the starting point of the next round, the time-domain exceeded the 5-minute barrier.
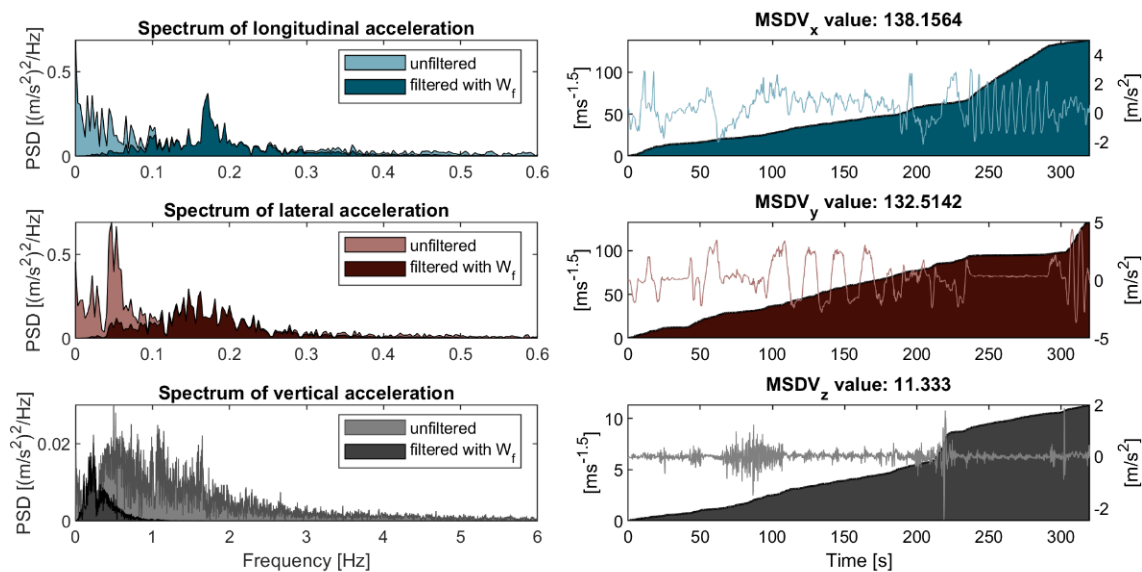
Fig. 5-7: PSD of filtered and unfiltered vehicle acceleration (left);
vehicle acceleration, and MSDV (right) – first investigation.

The conclusion of Griffin & Newman (2004), Karjanto et al. (2018) as well as Cheung & Nakashima (2006) can be confirmed that the MSDV for vertical vehicle acceleration is indeed smaller than the respective values in the longitudinal and lateral direction. This is predominantly associated with the passband of the weighting function W_f and the respectively low overall energy impact in the vertical direction.

5.5 Statistical Analysis

In addition to the previously mentioned physiological measures (see chapter 5.2.1), further subjective parameters were integrated into the analysis (see chapter 3.7.1). In contrast to most experiments, discontinuation and, therefore, the duration of exposure is treated as a quasi-objective dependent variable to measure motion sickness. Even if participants prematurely stopped their trial, the MSAQ and the FMS were applied and, therefore, integrated into the subsequent analysis. Here as well, all calculations were done using *R Studio* (the respective R packages are listed in the appendix) and *MATLAB 2019/20b*. The following description is also valid for the other driving investigations in a mixed test design that had been executed within this elaboration.

The 2x2 mixed test design with repeated measures and grouping factors requires a more advanced method to analyze the data set. Therefore, a multi-level approach of *linear mixed-effects* (LME) models with fixed and random coefficients were used for assessing the main research questions. Within fixed effects, all possible treatment conditions are present in the experiment, whereas random effects can be generalized beyond the treatment conditions. The general form of an LME model, for example, with a random intercept (b_{0j}) and a random slope (b_{1j}) within the first predictor (X) is shown as follows:

$$\begin{aligned} Y_{ij} &= (b_0 + u_{0j}) + (b_1 + u_{1j})X_{1ij} + b_2 X_{2ij} + \cdots + \varepsilon_{ij} \\ &= b_{0j} + b_{1j}X_{1ij} + b_2 X_{2ij} + b_{n(j)}X_{ni(j)} + \varepsilon_{ij} \end{aligned}$$

Eq. 5-4

The outcome (Y), also known as the dependent variable, is added by an error (ε). The index i represents a particular case of data set, whereas the j reflects the levels of the variable over which the intercept or slope varies. (Field et al., 2012, pp. 862–863)

5.5.1 Model Diagnosis and Initial Requirements

The construction of a suitable statistical regression model pursues the following steps. Firstly, a baseline model with fixed and random effects is designed. Afterwards, this model is stepwise extended by the forward selection method. (Field et al., 2012, p. 264)

In terms of model diagnosis, each calculation within the forward selection method is compared to the previous one using the *Akaike-Information-Criterion* (AIC), the *Bayesian-Information-Criterion* (BIC), and the *log-likelihood ratio* (Log Likl.). For all three of the criteria, it can be stated that the smaller the value is, the better the model fit. An exemplary illustration of their relationship is described by Field et al. (2012, p. 318) and outlined as shown in the following equation:

$$AIC = -2\ Log\ Likelihood + 2k \quad , \quad BIC = -2\ Log\ Likelihood + 2k\ln(n)$$

Eq. 5-5

In fact, the Log. Likl. statistic is based on the maximum-likelihood theory and gives the probability of correctly predicting outcomes in ratio to the probability of incorrectly predicted ones. The model shows a chi-square distribution (i.e. for categorical data) and is strongly linked to the other two criteria. Since the BIC is more conservative and corrects the number of parameters more strictly, this method is recommended for a large sample size with a small number of parameters. The AIC, by contrast, does not violate model extension that harshly. As a result, this method is more suitable for the current application and, thus, will be the leading criterion of the model comparison. (Field et al., 2012, p. 316, p. 868)

The AIC is based on the number of cases (n) and the sum of square errors of the model (SEE) added by the penalizing term, which includes the number of predictors (k):

$$AIC = n \ln\left(\frac{SEE}{n}\right) + 2k \qquad \text{Eq. 5-6}$$

Whenever the research target and the mathematical model selection were not congruent, hierarchical regressions or backward elimination within the stepwise method had been chosen. Those methods, moreover, are suitable for avoiding potential suppressor effects as they occurred in the fourth investigation (see chapter 8.4). (Field et al., 2012, pp. 263–265) For the hierarchical regression, the significant change in R^2 is calculated by using the F-Ratio as follows (Field, et al., 2012, pp. 249–252, p. 285):

$$F = \frac{(N - k - 1)R^2}{k(1 - R^2)} \qquad , \qquad R^2 = \frac{SS_M}{SS_T} \qquad \text{Eq. 5-7}$$

R^2 represents the ratio of the explained variance by the model (SS_M) to the baseline total sum of squares (SS_T), while N is the number of participants that are included in the model.

Regardless of which method had been used, the best model fit comparison then provided the final model, which had been further investigated within either contrast or post hoc analysis. However, before applying this method, the eligibility of the following requirements had to be checked:
- linearity between the metric predictors and the outcome (dependent variable),
- independency and normal distribution of the errors (residuals).

To inspect the distribution of data points, a *quantile-quantile* (Q-Q) plot (see Fig. 5-8 - left) and histogram (see Fig. 5-8 - middle) were calculated. The Q-Q plot illustrates the cumulative values that were measured during the trial against the cumulative probability of a normal distribution. The more the data points deviate from the ideal diagonal, the greater the probability of violating the assumption of normal distribution. By applying the *stat.desc* function, potential lack of symmetry (skew) and pointyness (kurtosis) were observed. In addition, the Shapiro-Wilk test for normality provided a suitable method to quantify whether the data points were normally distributed or not. To analyze the variable in terms of homogeneity of variance the Levene´s test was explored for the predictors. As a means of visualization, a graph of the residuals against the predicted (fitted) values was used (see Fig. 5-8 - right), in which a random array of dots equally distributed around zero indicated ideal homoscedasticity. (Field et al., 2012, pp. 171–190)
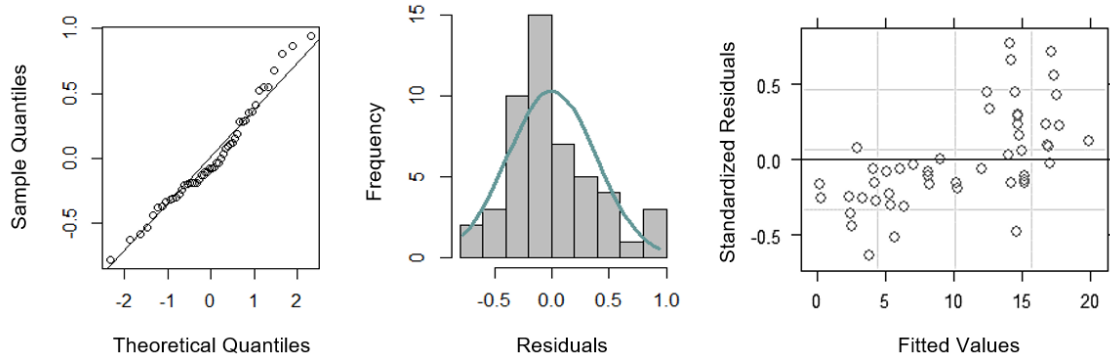
Fig. 5-8: Normal Q-Q (left); histogram of residuals (middle); residuals vs. fitted values (right) – model 7 in Tab. 5-3.

If the model consisted of more than one predictor, multicollinearity had to be examined by calculating bivariate correlations just as the *Variance Inflation Factor* (VIF). Multicollinearity exists when predictors show a strong relationship between each other, which, among other disadvantages, leads to an increase in standard errors of the slope coefficients and difficulty in assessing the individual importance of the predictors. As the main criterion, the largest VIF cannot be greater than ten. Particularly, if the mean VIF substantially exceeds the value of one, the results imply that the regression seems to be biased. Finally, the tolerance, as the reciprocal value of the VIF, has to be greater than 0.1. The assumption of independent errors was tested with the Durbin-Watson approach, which tests serial correlations between errors. (Field et al., 2012, pp. 272–276)

Concerning Field et al. (2012, pp. 312–320), for categorical outcomes, ordinal logistic regressions were applied. Within those models, the "equal slopes assumption" was defined to confirm the validity of the model. Since the assumption of linearity between the variables is violated for those parameters, the data set was transformed by using the logarithmic function. As a result, the probability of *Y* occurring given values of *X* was represented, whereby the resulting value varies between 0 and 1. The general form without random effects is shown as follows:

$$P(Y_i) = \frac{1}{1 + e^{-(b_0 + b_1 X_{1i} + \, \dots \, + b_n X_{ni})}} \qquad \text{Eq. 5-8}$$

A common way of interpreting logistic regression is reflected in the odds ratio. The odds probability of a particular event is defined as the probability of a certain event divided by its inverted probability. The proportionate change in odds (odds ratio) can be calculated by dividing the odds after a unit change in the predictor by the original odds. Here as well, the model fit has to be judged by using the above-mentioned criterion. Analogous to the previous diagnosis, the Log Likelihood assesses the basis of the fit:

$$Log\ Likelihood\ = \sum_{i=1}^{N} \left[Y_i \ln(P(Y_i)) + (1 - Y_i) \ln\big(1 - P(Y_i)\big) \right] \qquad \text{Eq. 5-9}$$

Given that there is contestation regarding the level of correspondence between predicted and observed values within the dependent variable, all three approaches to calculate the corresponding Pseudo R^2 are reported within the current analysis. Firstly, the calculation of Hosmer & Lemeshow (1989, p. 140) is presented:

$$R_L^2 = \frac{(-2 \, Log \, Likelihood_{Baseline}) - (-2 \, Log \, Likelihood_{New})}{-2 \, Log \, Likelihood_{Baseline}} \qquad \text{Eq. 5-10}$$

Around the same time Cox & Snell (1999, pp. 208–209) presented their approach, in which the researchers included the sample size (n) as follows:

$$R_{CS}^2 = 1 - exp\left(\frac{(-2 \, Log \, Likelihood_{New}) - (-2 \, Log \, Likelihood_{Baseline})}{n}\right) \qquad \text{Eq. 5-11}$$

The weakness of this calculation is due to the fact that the theoretical maximum of one never could be reached. Consequently, in 1991, Nagelkerke extended the model of Cox and Snell and introduced the following equation:

$$R_N^2 = \frac{R_{CS}^2}{1 - exp\left(-\frac{-2 \, Log \, Likelihood_{Baseline}}{n}\right)} \qquad \text{Eq. 5-12}$$

Even if the presented Pseudo R^2 differ in their mathematical constitution, conceptionally they show strong similarities and provide a solid basis for model comparison.

5.5.2 Outliers and Influential Cases

For the main analysis, standardized residuals and Cook-Distances methods were carried out. According to Field et al. (2012, p. 269), 95 % of the z-scores should lie between ± 1.96. Only in a few cases were more outliers identified than permissible. However, none of them showed the potential to interfere with the respective regression model (Cook's-D < 1). Therefore, no adjustment was necessary. An exemplary analysis from Tab. 5-3 is shown in the following Fig. 5-9.
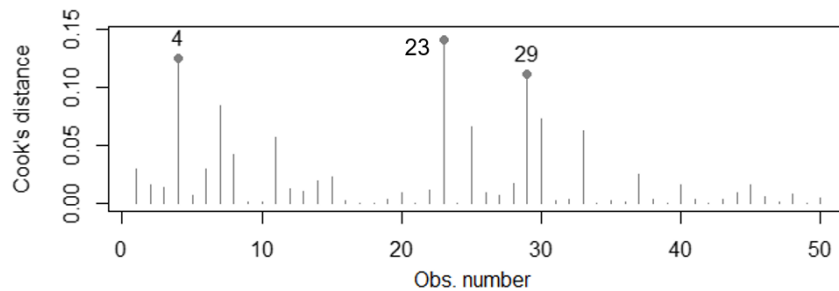
Fig. 5-9: Outlier analysis: Cook´s Distance – model 7 in Tab. 5-3.

5.6 Results

The first demonstration addresses the main research topic of seating configurations, while non-vehicle predictors will be further discussed in chapter 9. According to the previously mentioned methodology, an overview of the model comparison within the multiple regression (LME) and the max. FMS as the dependent variable is shown in Tab. 5-3.

The baseline model (1) was successively amplified by the predictor's backrest angle, seating direction, motion sickness susceptibility, and in-car temperature. The best model fit (4) then were analyzed by once again adding the remaining predictors and interaction terms. Finally, model 7 was found to be the preferred regression model based on the statistical quality criteria AIC, BIC, and Log Likl.

Tab. 5-3: Model comparison (LME): max. FMS – first investigation**.**

	Dependent Variable Max. FMS										
Model	(1)	(2)	(3)	(4)	(5)	(6)	**(7)**	(8)	(9)	(10)	(11)
Upright sitting		7.20*** (.95)				7.20*** (.96)	**7.20*** (.96)**	7.19*** (.98)	7.20*** (.97)	7.16*** (.98)	8.17*** (1.81)
Forward direction			-1.32 (1.67)			-1.32 (1.60)			-1.25 (1.45)		
MSSQ short				.21** (.10)			**.21** (.09)**		.21** (.09)	.21** (.09)	.25** (.11)
In-car temp.					.28 (.52)			.01 (.41)		.08 (.40)	
Interact. Sit.:MSSQ											-.08 (.12)
Constant	10.48*** (.83)	6.88*** (.93)	11.17*** (1.20)	7.76*** (1.51)	4.11 (12.04)	7.57*** (1.25)	**4.16*** (1.45)**	6.58 (9.36)	4.84*** (1.64)	2.27 (9.20)	3.68** (1.66)
Observ.	50	50	50	50	50	50	**50**	50	50	50	50
Log Likl.	-158.91	-143.51	-158.58	-156.66	-158.76	-143.15	**-140.90**	-143.51	-140.50	-140.88	-140.68
AIC	325.81	297.02	327.16	323.32	327.52	298.30	**293.80**	299.02	295.00	295.75	295.37
BIC	333.46	306.58	336.72	332.88	337.08	309.77	**305.27**	310.49	308.38	309.14	308.75

*p<.1; **p<.05; ***p<.01

In addition to the model comparison, the p-values and the parameters of the regression model i.e., the intercept (constant) and slope, are presented in Tab. 5-3. The values in brackets show the standard deviation of the adjusted mean. Since model 7 showed the best model fit, contrast analyses were obtained for this model to further evaluate the results of the multi-level modeling. Initially, subforms of the FMS and the MSAQ score for the entire sample are presented in Fig. 5-10.
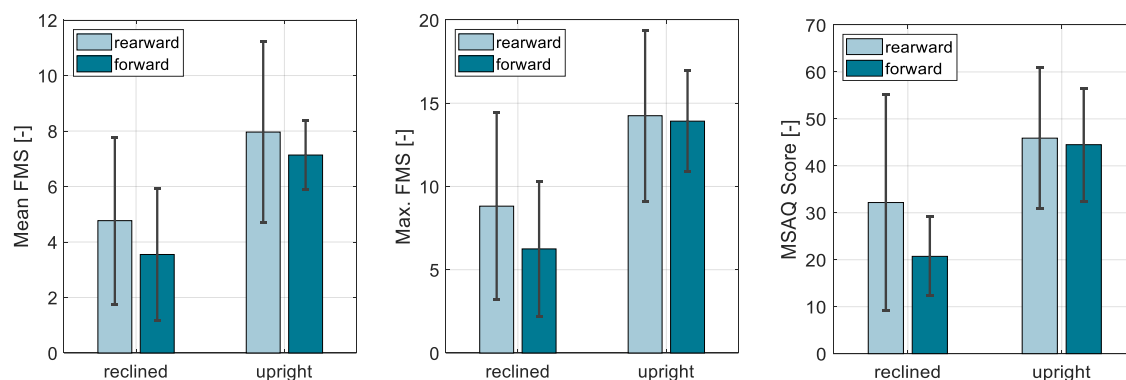
Fig. 5-10: Descriptive analysis: MSAQ score and FMS values – first investigation.

When analyzing the results of model 7, it is shown that the max. FMS value (b = 7.20, t(24) = 7.51, p < .01, r = .84) increased by almost eight points when changing the backrest angle from the reclined constitution to an upright position, while the rate of susceptibility, measured by the MSSQ, kept constant. The effect size of r = .84, which is linked to this predictor, is characterized to be very large. Next, an analysis with discontinuation as the main criterion was calculated. Whereas only 12 % of subjects stopped the trial in the reclined posture, 80 % did not finish the same procedure in the upright sitting position, $\chi^2(1) = 25.63$, p < .01 (see Fig. 5-11).

Tab. 5-4 summarizes the results of the ordinal logistic regression for the prediction of discontinuation (0 = no termination, 1 = termination) based on the sitting position i.e., the backrest angle. As mentioned in chapter 5.2.1, the odds ratio is reported to quantify this effect, while further statistical parameters of the regressions are outlined as well.

Tab. 5-4: Odds ratio analysis: sitting position – first investigation.

		95 % confidence interval of odds ratio		
	b (SD)	Lower barrier	Odds ratio	Upper barrier
Constant	-1.99 (.62)	.03	.14	.39
Sitting upright	3.38*** (.79)	7.02	29.33	166.62

R^2=.37 (Homer & Lemeshow), .20 (Cox & Snell), .44 (Nagelkerke), $\chi^2(1)$ = 25.63, p < .01; *p<.1; **p<.05; ***p<.01

Intuitively linked to the number of terminations is the duration of exposure. Constructing a new LME model with driving duration as dependent variable, the predictors backrest angle (b = -11.24, t(24) = -6.68, p < .01, r = .81) and MSSQ score (b = -0.33, t(23) = -2.44, p < .05, r = .45), once again, have shown to be the most reliable and sensitive parameters for the prediction of the criterion. Compared with the baseline model, the inclusion of these two predictors resulted in a significant improvement in explaining the time until the trial stopped, $\chi^2(1)$ = 32.99, p <.01. Moreover, neither the seat orientation nor the in-car temperature showed a significant influence on the model fit. The model indicates that the trial stopped for every person (under the same level of MSSQ score) 11 minutes earlier in the upright sitting position compared to the reclined condition (see Fig. 5-11). In fact, observing the subjects who did discontinue in both conditions, the average time of exposure in the reclined position was 4.5 times higher than it was in the upright position. By contrast, concerning the other significant parameter within the model analysis, the test duration is reduced by 20 s in the reclined position by each increasing unit of the MSSQ score.
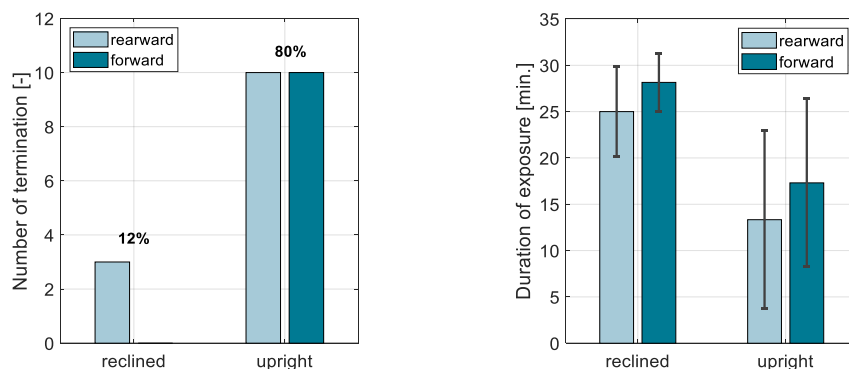
Fig. 5-11: Quasi-objective measurement: number of termination and duration of exposure – first investigation.

Setting the focus to the second parameter, the sitting direction is observed which had been manipulated as between condition. When being in a reclined position, every subscale within the MSAQ score showed greater values in the rearward sitting condition. By contrast, when analyzing the upright sitting posture, gastrointestinal and sopite syndromes were more present in the forward direction, while peripheral and central manifestations exhibited greater severity in the opposite direction. The participants were requested after every trial to report the amount of time until a total recovery of symptoms was achieved.

Tab. 5-5 illustrates the results of the multilevel modeling. Indeed, the duration of symptoms did not show any significant model improvements by adding predictors when analyzing the entire test sample. By observing only the participants facing forward, the backrest angle showed statistical tendencies in predicting recovery time.

Tab. 5-5: Time to recover – first investigation.

	Dependent Variable Duration of symptoms, time to recover					*Only forward-facing seat*	
Model	(1)	(2)	(3)	(4)		(1)	**(2)**
Upright sitting		.75 (.45)					**1.24[*] (.61)**
Forward direction			.04 (.59)				
MSSQ short				-.00 (.04)			
Constant	1.71[***] (.29)	1.34[***] (.37)	1.69[***] (.44)	1.73[***] (.56)		1.73[***] (.32)	**1.08[**] (.44)**
Observations	44	44	44	44		25	**25**
Log Likl.	-85.89	-84.50	-85.89	-85.89		-49.90	**-44.80**
AIC	179.79	179.00	181.78	181.79		101.80	**99.60**
BIC	186.93	187.92	190.70	190.71		106.68	**105.69**

*p<.1; **p<.05; ***p<.01

In addition to this, subgroups were defined to further examine the sitting direction in more detail. The following Fig. 5-12 illustrates, firstly, the overall recovery time with the above-described phenomenon and, secondly, the mean FMS as well as the MSAQ score measured in the subgroup of participants, who did not discontinue any of the two trials.
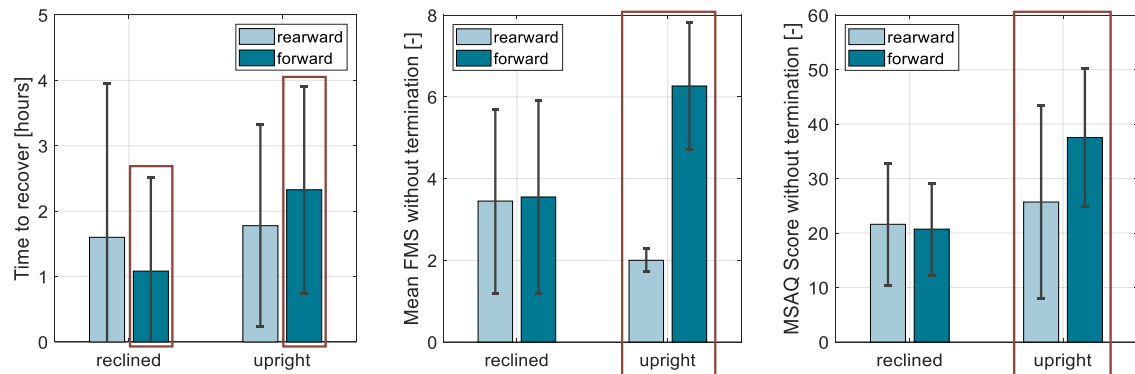
Fig. 5-12: Descriptive analysis: subgroup without termination – first investigation.

Within the upright sitting condition, the direction of driving had become a significant effect, FMS: $b = 4.27$, $t(19) = 3.45$, $p < .01$, $r = .62$, whereas in the reclined position sitting direction did not show any significant impact on the subgroup of non-discontinuers. In fact, the FMS as well as the MSAQ score show the same characteristic pattern indicating greater nauseogenic expressions when sitting in the forward direction and being upright.

By evaluating the nauseogenic nature of the applied driving events, start-stop maneuvers are the only condition that showed a significant difference as a result of backrest manipulation, $\chi^2(1) = 3.66$, $p = .06$ (see also Bohrmann & Bengler, 2020). Overall, fore-and-aft motion was subjectively rated to be the most critical scenario that had been associated with carsickness.

No other maneuver or road condition within the trial showed a comparable score. Furthermore, 68 % of all participants reported in the open questionnaire that they had experienced less head motion in the reclined position. In addition, they also mentioned this effect to be the main reason for the potential differences in motion sickness severity. To evaluate this assumption in more detail, a multibody simulation[2] was carried out to illustrate the biomechanical behaviour of vehicle occupants sitting upright against being in a reclined position. The focus was placed on longitudinal motion i.e., an impulse-like force intending to represent a short braking maneuver. In fact, due to restrictions of the simulation environment a generic approach had been chosen in order to outline the aforementioned qualitative statements and the observations made during the experiment.

5.7   Simulation - Biomechanics of a Strong Generic Braking Maneuver

In this specific case of application, the *Mathematical Dynamical Model* (MADYMO) solver with its multibody simulation tool was used. This software usually is applied in the area of vehicle safety, in which high accelerations and short sequences are calculated to simulate the passenger´s motion behaviour. A multibody is modeled by rigid ellipsoids which are connected with their neighbouring ones by joints. The degrees of free motion of the individual rigid body are restricted by its connection characteristic. Each body is defined by its mass, moment of inertia, and the position of its center of gravity, while its contact behaviour is described as a function of force via penetration. The simulation environment comprised a Hybrid III 50th percentile ellipsoid human body model and a vehicle seat consisting of six high-order elements. To the seat cushion, a high friction characteristic of 0.9 was applied to prevent the dummy from slipping off the seat at the slightest braking force. The applied postures were determined by the standard driving position (23° backrest angle) and the executive seating position (42° backrest angle), the maximum permitted backrest angle in the rear of existing series vehicles (see Fig. 5-13).
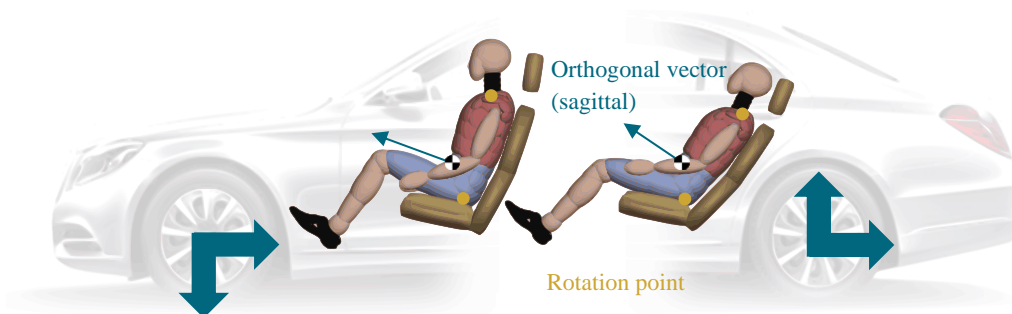
Fig. 5-13: Biomechanical illustration of a sitting and reclined posture – multibody simulation. Modified from Bohrmann (2019)

The corresponding load case circumvented potential disturbances and interacting effects with the seat structure e.g., its shape and material property, due to the forced dummy movement away from the back- and headrest. Fig. 5-14 shows the discretized visualization of the longitudinal dummy motion including its head displacement.

---

[2] The simulation was conducted with the assistance of C. Maier (2018) as part of his bachelor´s thesis. The results are published in Bohrmann, Just, et al. (2020); Bohrmann, Koch, et al. (2020).
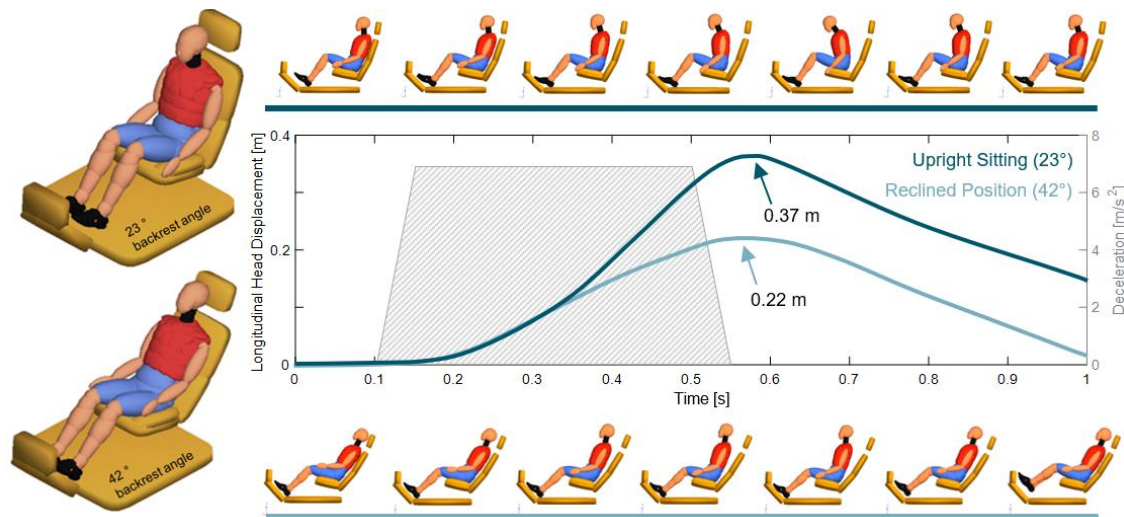
Fig. 5-14: Results of longitudinal head motion during an impulse-like braking maneuver – multibody simulation.

As presented in the upper series of images, the upright sitting condition with a 23° backrest angle is characterized through an initial slipping behaviour of the dummy on the seat cushion accompanied by a torso pitch rotation around the hip point away from the seat structure. In general, the maximum head displacement in the longitudinal direction is reached after approximately 0.6 s with 0.37 m away from its original starting position. Since the deceleration of 7 m/s^2 was only applied for 350 *milliseconds* (ms), the upper body then returns to its initial position from the beginning of the simulation. The reclined position with a 42° backrest angle shows in general congruent head motion, even though the maximum longitudinal displacement differs from the upright sitting condition that had been presented before. The greatest longitudinal head displacement captured within the reclined posture is 0.22 m, whereas this position kept for a longer time than it has been observed before in the 23° backrest condition. Finally, the reverse movement is initiated with the legs lifting up from the vehicle floor. The observations made within this simulation are in accordance with previous calculations e.g., the start-stop maneuver illustrated in Bohrmann, Koch et al. (2020). Nonetheless, it must be stated that especially the initial phase and maximum longitudinal head displacement are affected by boundary conditions of the simulation such as the strength and duration of the applied force or the proper dummy positioning. Thus, the results can be used only in a qualitative manner.

5.8   Discussion, Synopsis, and Further Research Questions

Throughout all calculations, the FMS just as the MSAQ score represents congruent information, in which the impact of sitting direction on the severity of carsickness seems to be less effective than the manipulation of backrest inclination. More precisely, the effect of posterior torso rotation (dorsal) around the lateral axis in the sagittal plane leads to a significant and powerful improvement in motion sickness prevention (in line with Vogel et al., 1982 and Golding et al., 1995), whereas the body rotation around the vertical axis generates diminished and inconsistent results. While significant deviations occurred in a small subgroup of non-discontinuers thereby indicating a higher incidence of motion sickness in the forward-facing position, the overall evaluation, however without significant effects, highlights that rearward sitting exhibited greater values of carsickness.

According to the interviews, video material, and human body simulation, it is concluded that the reason for the significant impact of reclined postures is due to the reduction in active head stabilization as well as a dampened head motion, which, in turn, might lead to a reduced level of postural instability (see chapter 3.2.8). This effect seems to be particularly present in longitudinal motion, which has been identified as quite nauseogenic. Furthermore, when considering the second significant predictor, it is shown that the body posture shows a higher effect size and a larger slope than the individual motion sickness susceptibility. This assumption, however, is biased due to the limited variability in motion sickness sensitivity as a prerequisite for participation in the examination. More detailed information about this human-related predictor is discussed and summarized in chapters 9 and 12. Within the qualitative questionnaire, subjects were surveyed and asked about recommendations to further adjust the seating configuration concerning motion comfort. By analyzing these statements, it has been mentioned that lateral support of the headrest is desired. Furthermore, participants were unable to define whether the 38° backrest angle felt like a sitting or lying position. It is presumed that this finding is due to the large angle between the torso and the femur. Finally, it has to be stated that these results are based on a situation in which participants had to perform visually demanding NDRTs in the rear of a visually encapsulated mini-van.

Limitations and Consequent Research Questions Regarding Motion Sickness

As already postulated by Festner et al. (2016), future automated driving scenarios show the potential that vehicle dynamics are perceived differently when being engaged in NDRTs compared to the situation of manual driving in which the vehicle trajectory is constantly monitored. Indeed, perception is influenced by the surrounding view (see chapter 3.2) and, therefore, may affect the beneficial impact of a reclined position due to the modification of vision. Since the first investigation was conducted without any outside view, the results have to be evaluated with uncovered vehicle windows as well. Even if the experiment of Vogel et al. (1982) included a mechanical device for stabilizing the head in an upright position, under different conditions this approach perhaps produces similar comfort ratings as reported in the reclined position. Furthermore, it still awaits to be answered whether a greater inclination angle leads to an even better comfort level or vice versa. Since the impact of sitting orientation on carsickness remains unspecified, analysis with this variable as the repetition factor would appear to be a beneficial pursuit.

6   Second Investigation – Sitting Direction and Visual Cueing

The following examination[3] addresses two main aspects that were identified as limitations of the first experiment. Firstly, the sitting direction was designated as being the main factor as a repetition condition in the current study design, while, secondly, anticipatory visual cues in the periphery of the field of vision are included as the between condition.

---

[3] The experiment was designed and conducted with the assistance of L. Gottselig (2019) as part of her Master´s thesis.

In contrast to the discrete performance measurement obtained in the first investigation, here, a continuous reaction test was conducted that had to be performed during the entire ride. To achieve suitable comparability between these two investigations, the recent study design shows strong similarities to the original trial e.g., test track and vehicle dynamics.

6.1 Participants

The total sample included n = 24 subjects aged between 20 and 62 years (M = 38.21, SD = 12.69). As illustrated in Fig. 6-1, significant differences in the age distribution between the two visual conditions were found, F = 11.55, p < .01. However, when analyzing the current test sample, the MSSQ scores did not differ significantly by age, F = .95, p = .34. Thus, the difference in age distribution between the experimental groups is interpreted as an acceptable imbalance for the purpose of motion sickness examination. The average MSSQ score (M = 17.98, SD = 12.68) is about 5.18 points higher than that of the sample in the first investigation. The motion sickness susceptibility was evenly distributed over the experimental conditions, F = 0.32, p = .58. Overall, 17 males and seven females took part in the study, while only one subject had already participated in the initial investigation. Within the experimental conditions, the distribution of biological gender did not differ significantly between each other, χ^2 (1) = 2.52, p = .11.
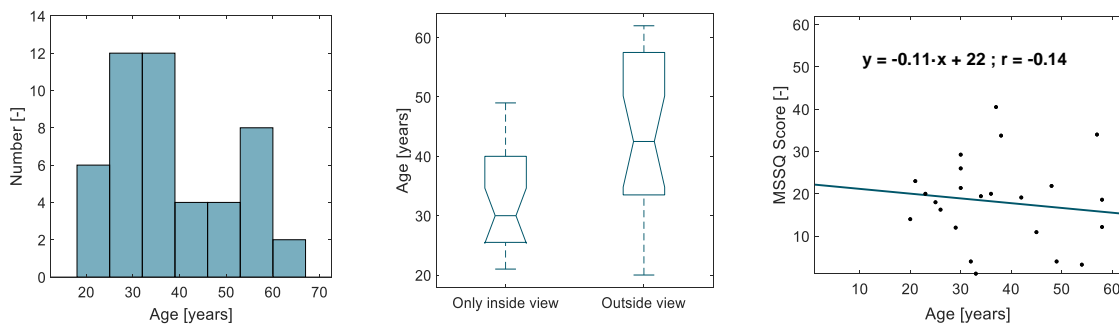
Fig. 6-1: Test sample: distribution of age (left); experimental condition (middle); regression between MSSQ score and age (right) – second investigation.

6.2 Procedure

The measurements stage of the procedure took place between 7:30 am and 6:00 pm in March 2019 at the same test track as previously described in chapter 5.4., with outside temperatures varying from 2 to 17 °C. The general course of study was identical to the first investigation and based on a 2-step repetition factor of seat orientation (forward vs. rearward) as well as a 2-step grouping factor of visual cueing (only inside view vs. outside view). The subjects were divided by randomization under the restriction of equal group sizes and MSSQ characteristics to the grouping factor of vision. To avoid repetition effects, the seat alignment was varied within the test subjects, so that the same number of subjects first experienced either the forward or backward condition. The seat was adjusted in the reclined position, as it has been described in the first investigation. The participants were instructed to carry out the NDRTs continuously and not to actively take their eyes off the digital device. Compliance with this requirement was ensured by the investigator based on the camera data.

Performance Testing and NDRTs

Due to the fact that reading in a moving vehicle is considered to be highly nauseogenic (see chapter 5.2.2), this task was selected as the main NDRT to simulate a realistic automated driving scenario in which motion sickness might occur. As the interaction with displays is likely to be an important criterion within future vehicle interior designs, the feasibility of performing the task on a tablet was a prerequisite. Consequently, the reading task was carried out on the same digital device that had been utilized in the preparation phase. In fact, during the preparation period, there was time for a training session to practice all of the tasks which the participants had to perform. The test trial lasted until the subjects reliably mastered the task.

While reading on a tablet, a performance test was simultaneously conducted during the entire drive. The purpose of this test was to measure the reaction time of occupants in situations, in which motion sickness increases over time. The subjects were instructed to react to an acoustic signal by pressing any button on a keyboard in front of them. The distance of this keyboard was individually adjustable and approximately an arm's length away so that accessibility was guaranteed for all subjects when being in the reclined position. There was a total of six acoustic signals per lap with time intervals of 45 to 60 s between them. The subjects were instructed to interrupt the reading task immediately when the sound signal occurred and react as quickly as possible by pressing the button. After that, the subjects continued with the reading task. It was carefully ensured that suitable freedom of movement was accomplished during the journey, which was essential for the operation of the reaction task. This is why no physiological measurement with its hardware application was conducted in this investigation.

6.3   Update of the Experimental Vehicle

Here as well, the V-class had been used as the experimental vehicle, however, an additional pillow with side pads to stabilize the upper body e.g., the head and neck area, was added to the headrest. This adjustment addressed predominantly lateral motion and was made because of the suggestions participants mentioned in the previous investigation. The adjustable mounting bracket on the backside of the co-driver seat that had been used in the first investigation as well as an additional table, securely fixed to the vehicle structure, was utilized to attach the keyboard. In addition, the clamping system for the tablet, which had been used for the reclined position within the first investigation, was also used in the current setting. Regardless of the direction the seat was facing, the masking effect created by the tablet was similar. Furthermore, it was ensured that the tablet and keyboard were equally accessible in both sitting conditions. Before starting the journey, the position and angle of the keyboard were adjusted individually to compensate for differences in the subject´s anthropometry. Once the setup was defined for the first trial, the relevant parameters were transferred to the setting of the next trial with the opposite sitting direction. An exemplary representation of the test setup with extreme values of the keyboard inclination is shown in Fig. 6-2.

Fig. 6-2: Experimental setup of reaction task: keyboard positioning – second investigation.

Given that visual information, even if only apparent in the periphery, is the second main research target of the study, it is important to deal with vehicle characteristics that show an impact on this parameter. Concerning the SAE J1100, the belt height measured from the seating reference point (SgRP) is defined by the H25 value and relevant for all-round visibility, or better known as panoramic or surrounding view. As shown in Fig. 6-3, the H25 value of the V-class differs in the longitudinal direction, which resulted in the general requirement that the head of every subject had to be positioned at the same longitudinal point, whether facing forward or rearward. This requirement was already valid in the first examination due to equalizing vehicle dynamics that act on the subject´s head, but, within the update of vision, was reaffirmed and consequently applied.
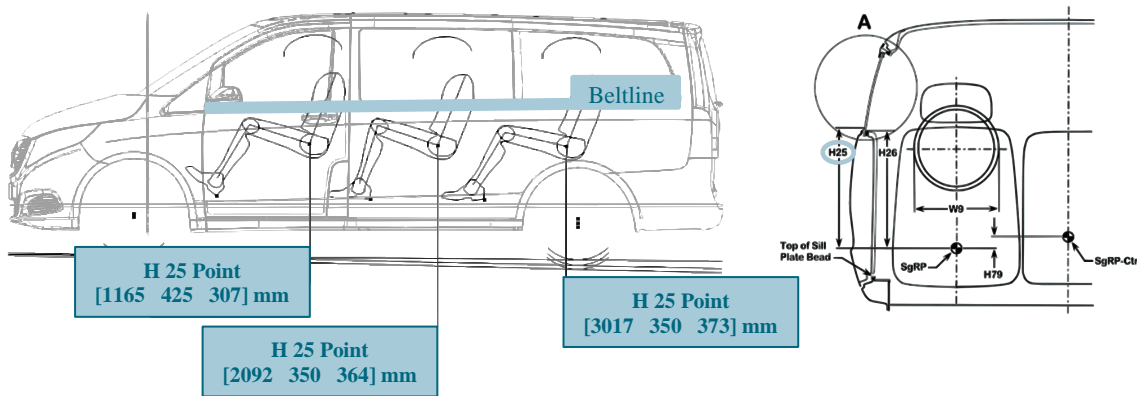
Fig. 6-3: Vehicle dimension with focus on the beltline (H25).
Left: modified from Daimler AG (2020); right: modified from SAE J1100:2009-11

The seat height (H30), which will be discussed more precisely in chapter 7.2, represents an additional important parameter in terms of vision. Since the vehicle was equipped with standard seats in the second row, the H30 value of 395 mm was constant for every participant. Consequently, inter-individuality in anthropometry e.g., the torso length, was not compensated and led to differences in the surrounding view. Nevertheless, the overall circumferential visibility was comparatively appropriate for every subject due to the typical vehicle's interior dimensions of a mini-van. This also holds true when being in a slightly reclined position (see Fig. 7-4 and Fig. 12-3).

6.4 Results

Several hypotheses and research questions were formulated to build the backbone of the second main examination, in which LME methods were applied as well. Within this elaboration, motion sickness expressions were treated as dependent variables, while the sitting direction was included as an independent one. As seen in the first investigation, one opportunity to capture motion sickness is utilized by the FMS value that was queried four times during the entire exposure. Due to further calculations, the delta value between the first and last inquiry, the maximum, the mean as well as the last FMS scores are criteria for consideration, for which individual models were created. In the following LME calculation, the mean value represents the effect that became apparent in all subtypes of the FMS (see Tab. 6-1).

Tab. 6-1: Model comparison (LME): mean FMS – second investigation.

Model	Dependent Variable Mean FMS
	(1)	(2)	(3)	**(4)**	(5)	(6)	(7)	(8)	(9)	(10)
Outside view		-1.39 (1.68)					-1.12 (1.56)			
Forward direction			-.21 (.68)					-.21 (.68)		
MSSQ short				**.17** (.08)**			.16** (.08)	17** (.08)	17** (.08)	17** (.08)
Age					-.08 (.07)				-.06 (.06)	
Gender female						-.31 (1.88)				-.54 (1.77)
Constant	4.38*** (.84)	5.08*** (1.19)	4.49*** (.92)	**1.34 (1.61)**	7.36*** (2.65)	4.29*** (1.01)	1.99 (1.84)	1.45 (1.66)	3.83 (3.02)	1.40 (1.63)
Observ.	48	48	48	**48**	48	48	48	48	48	48
Log Likl.	-130.20	-129.85	-130.15	**-127.98**	-129.49	-130.19	-127.71	-127.93	-127.49	-127.93
AIC	268.40	269.70	270.30	**265.96**	268.99	270.37	267.41	267.86	266.98	267.86
BIC	275.89	279.05	279.66	**275.32**	278.35	279.73	278.64	279.08	279.20	279.09

*p<.1; **p<.05; ***p<.01

The single predictor model 4 shows the best model fit, while neither the seat orientation nor the view condition did significantly improve the model fit. Fig. 6-4 shows several FMS parameters depending on the level of vision for both expressions of sitting direction.
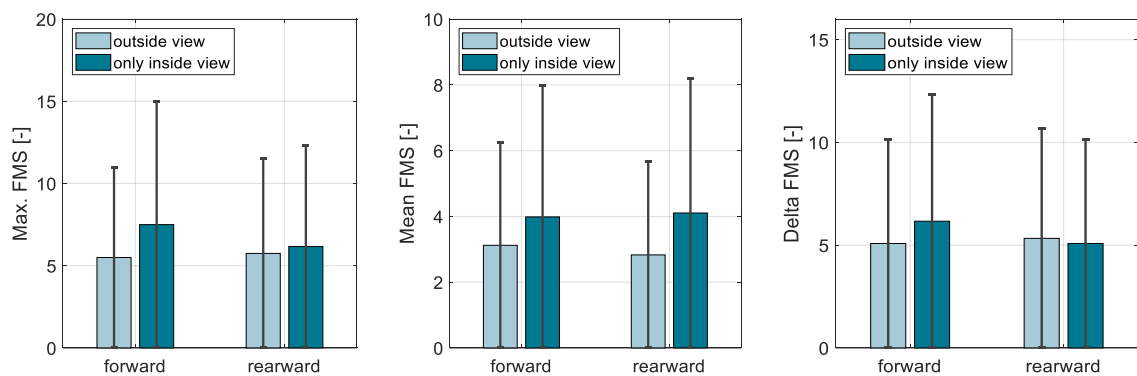
Fig. 6-4: Descriptive analysis: FMS values – second investigation.

In addition to the FMS, motion sickness was also operationalized using the MSAQ score with its subscales (see Fig. 6-5). Both subscales, the sopite and peripheral one, will be for use in the later stages of analysis. In fact, when investigating the change in performance level (see chapter 10.2) all MSAQ subscales are integrated into the LME model.
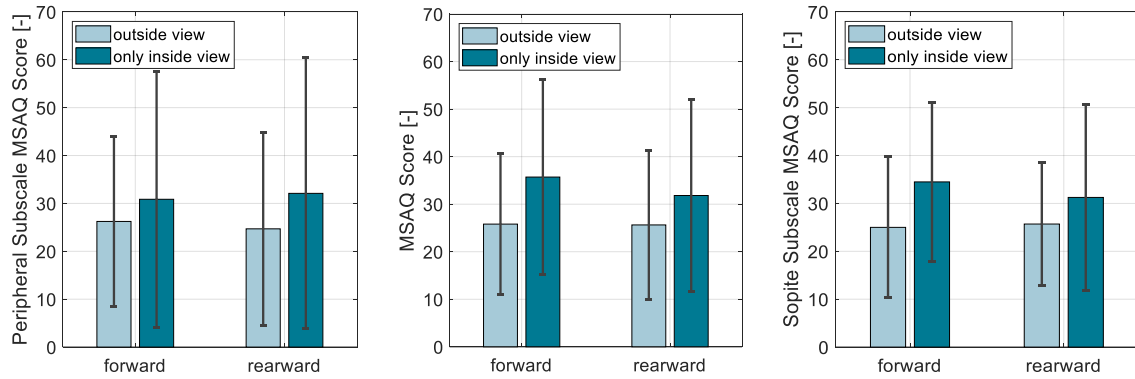
Fig. 6-5: Descriptive analysis: MSAQ score incl. subscales – second investigation.

When analyzing the MSAQ score, here as well, no significant model improvement by means of the experimental conditions occurred. This is the reason why also a hierarchical LME model was built, in which the sitting direction (b = 2.02, t(23) = 0.73, p = .47, r = .15) and view condition (b = -8.04, t(22) = -1.21, p = .23, r = .25) are integrated. Given that in this investigation greater distribution in motion sickness susceptibility is present, a detailed analysis of subgroups seems to be beneficial. This is particularly important due to the characteristic pattern, that occurred in Fig. 6-4 and Fig. 6-5. Under the assumption of constant sitting direction, the outside view showed on average less motion sickness than the condition of a limited surrounding view. Therefore, instead of analyzing the entire sample size, the main effects were examined with subgroups constructed by the method of median split and termination rate. However, only the subgroups of termination are presented due to missing significant results within the median split approach. Fig. 6-6 illustrates the MSAQ scores for both subgroups as well as the distribution of terminations.
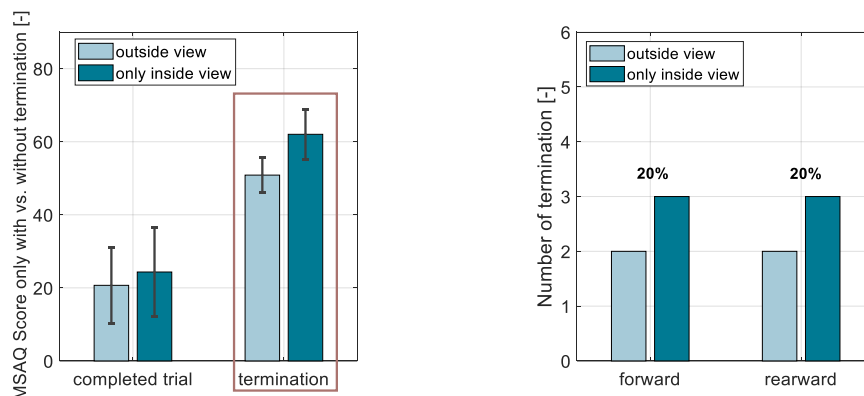
Fig. 6-6: Quasi-objective analysis: number of termination – second investigation.

There was a total of 10 test terminations (20 % of all journeys). The number of discontinuers in the repetition factor was equal, whereas a more detailed analysis reveals that the group of termination comprised four double-dropouts and two single dropouts, one sitting forward and the other one rearward.

With reference to Tab. 6-2, the best model fit of the dropout group showed a significant main effect of vision, $b = -11.36$, $t(4) = -2.82$, $p < .05$, $r = .82$. Corresponding results of the FMS with its mean value can be reported with $b = -4.39$, $t(4) = -2.51$, $p < .05$, $r = .78$.

Tab. 6-2: Model comparison (LME): MSAQ score for the subgroup of discontinuation – second investigation.

Model	Dependent Variable MSAQ Score - only discontinuation					
	(1)	**(2)**	(3)	(4)	(5)	(6)
Outside view		-11.36** (3.96)				
Forward direction			-2.10 (5.43)			
MSSQ short				-.28 (.40)		
Age					-.38 (.59)	
Gender female						-1.91 (5.94)
Constant	57.77*** (2.58)	**62.03** (2.50)**	58.62*** (3.84)	64.24*** (9.94)	70.78** (20.68)	58.14*** (3.25)
Observations	10	**10**	10	10	10	10
Log Likl.	-34.66	**-31.22**	-34.57	-34.37	-34.41	-34.60
AIC	77.32	**77.43**	79.14	78.73	78.82	79.19
BIC	78.53	**73.94**	80.65	80.25	80.33	80.71

*p<.1; **p<.05; ***p<.01*

Qualitative Analysis

After the two exposures, the subjects were asked to retrospectively assess their ability to perform the required NDRTs. While predominantly negative statements appeared in the "only inside view" condition, the "outside view" situation, by contrast, showed comparatively better ratings (see Fig. 6-7 - left). As previously stated, further results about the impact of carsickness on individual performance are discussed in chapter 10.2.
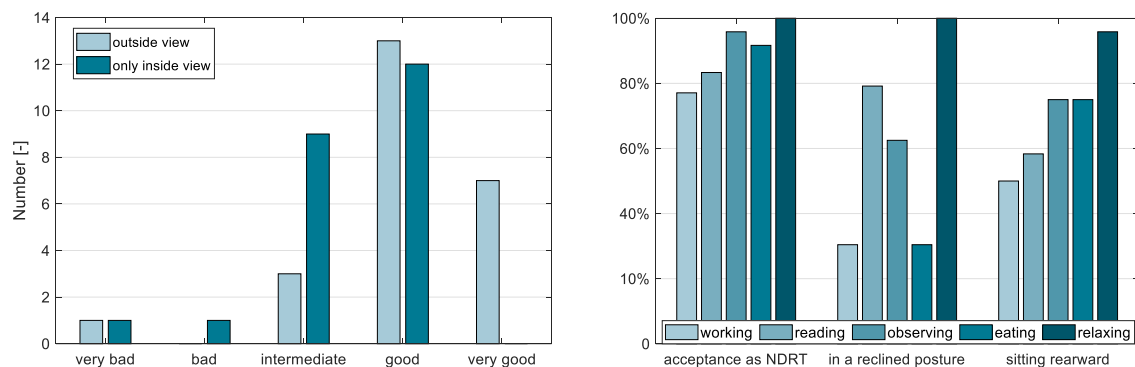
Fig. 6-7: Qualitative analysis: performance quality depending on vision (left); acceptance on NDRTs in different sitting positions (right) – second investigation.

Furthermore, the subjects were surveyed about their opinion on NDRTs and their usage during an automated driving scenario (see Fig. 6-7 - right). Taking these statements with respect to backrest angle and sitting direction into account, it is shown that in particular working, eating, and observing in one form or another, show differences between general acceptance and the situation of performing these NDRTs in a reclined posture.

On the whole, relaxation showed the highest ratings, no matter which sitting condition is chosen. Reading, with the third-best general rating of around 83 %, shall be highlighted here since also the acceptance when being in a reclined position shows an almost unchanged value of 80 %. When changing the sitting direction, however, the acceptance decreases down to 58 %. One-half of the subjects are willing to accept the task of working and 75 % eating in an autonomous vehicle while sitting against the driving direction.

6.5   Discussion, Synopsis, and Further Research Questions

Under consideration of the entire sample size, the individual susceptibility is identified as the only significantly meaningful variable influencing the motion sickness severity within the second investigation. However, when analyzing the descriptive visualization of the experimental conditions, "only inside view", especially when sitting forward, seems to be more nauseogenic and provokes greater symptoms of carsickness than the condition "outside view". This observation is congruent throughout all operationalization parameters regarding motion sickness. As a result, vision, even if only for the subgroup of discontinues with statistical significance, seems to affect the prevalence of carsickness. Therefore, the importance of the external view, as already had been mentioned by other researchers (e.g. Kuiper et al., 2018), can be confirmed. It is stated that vision is at least not irrelevant for the development of carsickness when being engaged in visually demanding NDRTs. It might have been expected that visual stimulation in the periphery of the visual field would distract from secondary activities. Observing the subjective statements, however, this assumption does not seem to be the case. Even more, according to the qualitative questionnaire, the encapsulated condition (only inside view) shows worse values in the concentration scale. This prominence might also be attributed to the group distribution given that the visual condition was manipulated as a between factor within the study design. Furthermore, it is evident that the incidence of carsickness might superimpose the pure effect of vision as a variable to concentration. When being in a reclined position, seat orientation does not show any significant impact on either the FMS or the MSAQ scores. This result confirms the conclusion researched in the first investigation. Nevertheless, regarding the qualitative analysis, it is of particular interest to expand the scope of work and observing also aspects besides motion sickness.

Limitations and Consequent Research Questions Regarding Motion Comfort

Combining the results of the first two studies, the reclined posture with the opportunity to see the outside environment defines the optimum setup for carrying out visually demanding NDRTs, such as reading. These findings are based on research tackling exclusively aspects of carsickness. By including user acceptance and their preference, for instance, working is undesirable when being in a supine position (see Fig. 6-7 - right). Therefore, the compatibility of user acceptance and motion sickness prevention e.g., a maximum of head stabilization, needs to be the aim of the consecutive work. Furthermore, due to the visual covering setup in the first investigation, the validity of its results should be examined and evaluated under more realistic vision circumstances.

7   Third Investigation – Extended Seat Configuration

To meet the unexplored limitations described in the first two investigations, an additional driving study in a repeated measures design was conducted in June 2019. The outside temperature ranged between 13 to 29 °C, while the in-car temperature was kept constant around 22 °C. The participants experienced three different sitting configurations in the rear of the modified V-class, whereby the seat was positioned in the driving direction for all conditions. Furthermore, the windows were kept uncovered throughout the entire test setup, whereas the applied vehicle dynamics were similar to the first two investigations.

7.1   Participants

The sample of the third investigation included eleven healthy subjects with an equal distribution in biological gender (five females and six males) and an average age of 37 (SD = 11.88). From the originally twelve subjects, one participant prematurely terminated the investigation as a result of strong symptoms experienced in the second trial (upright sitting). The average MSSQ score was 15.25 points with a standard deviation of 12.47. Although almost half of the total sample belonged to a less susceptible group (< 15 MSSQ score), a wide range in motion sickness susceptibility was reported. For instance, one participant stated a maximum MSSQ score of 40.07, while another participant had never experienced motion sickness before. This, with respect to the aim of investigating inadequate distribution, is the result of the unpleasant aftereffects of motion sickness and the high frequency of the required participation within the eligibility criteria.

7.2   Update of the Experimental Vehicle

Since the main focus of this examination was to investigate future seating concepts in terms of motion sickness mitigation, the serial equipment of the V-class did not provide a suitable range of sitting configurations. Indeed, to attain increasing motion comfort, the extended seat configuration aimed to achieve a comfortable and stable position with a maximum of joints relaxation. Here, the technical term zero-gravity position, which occurs in astronauts during weightlessness in space (Bubb et al., 2015, p. 362), provided a suitable guideline for the purpose of this work. To enable such extended postures a seat bracket was designed and integrated into the V-class, which is illustrated in Fig. 7-1.
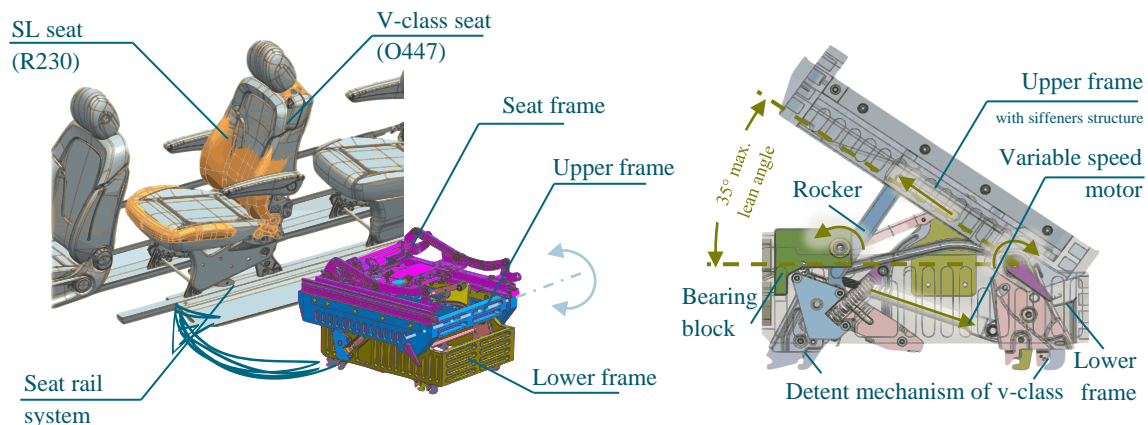
Fig. 7-1: Construction of seat bracket – third investigation.
Modified from Daimler AG (2020)

The lower frame was anchored into the seat rails of the vehicle. A Mercedes-Benz SL driver seat was attached to the upper frame with an integrated seat belt system. This was essential in terms of occupational safety. In fact, a common belt attachment on the b-pillar would lead to an inadequate strap position in supine positions. In general, the seat belt detachment increases with the backrest´s inclination, resulting in the necessity to utilize the integrated belt system. This is only one among other advantages regarding safety and comfort that are accompanied with integral seats, some of which are further described by Eckstein (2014c, p. 235). Finally, an adjustable footrest was integrated into the upper frame to support the legs of the vehicle occupants when being in supine positions.

The seat bracket enables a pitch rotation of the entire seat structure. This is due to an electric linear drive system that can change the angle between the upper and lower frame. Consequently, the seat cushion provides axial support up to 35°, while the backrest position can be adjusted up to a horizontal position by its serial function. The fully electrical SL seat was preconfigured in such a way that a comparable seat height (H30) of 393 mm to a serial seat configuration could be guaranteed. Fig. 7-2 illustrates this essential parameter of vehicle dimensions, which is described in the SAE J1100.
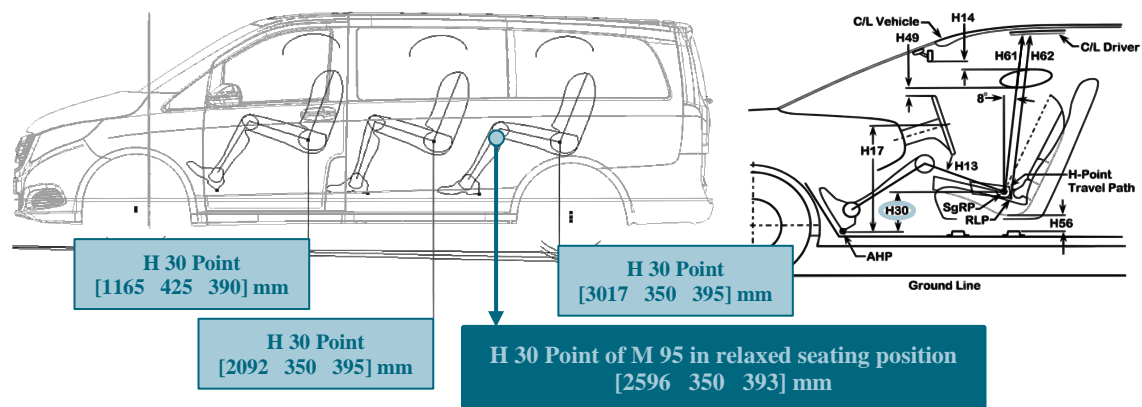
Fig. 7-2: Vehicle dimension with focus on the seat height (H30).
Left: modified from Daimler AG (2020); right: modified from SAE J1100:2009-11

The consecutive simulations depend on these values and, therefore, represent the state of vision that was experienced with the third investigation. Both the seat bracket and the attachment of the seat structure were approved by the Mercedes-Benz safety department.

7.3 Procedure and Experimental Setup

In contrast to the other driving investigations, here only one experimental condition was manipulated. In comparison with the first study, the rotation of the subject´s torso was greater and no longer limited to the setup of a series vehicle. Upon closer inspection, it is noticeable that a rotation of the upper body around the transverse axis is inevitably associated with changes in the range of vision. Indeed, this study included the additional part of outside view, which provided information about motion perception. To illustrate this effect, a simulation via *RAMSIS* was conducted. Here, images with an overall 190° range of vision (see Tab. 3-3) are shown according to the eyepoint of a 95th mannequin. Firstly, in Fig. 7-3, the standard driving posture was defined with a backrest angle of 23°.

However, contrary to the first investigation, a head-neck brace was worn by the participants to stabilize the head-neck plant when being in the upright sitting position. The main question that arose with this approach was whether this might be able to decrease motion sickness as it has been observed in the reclined position.
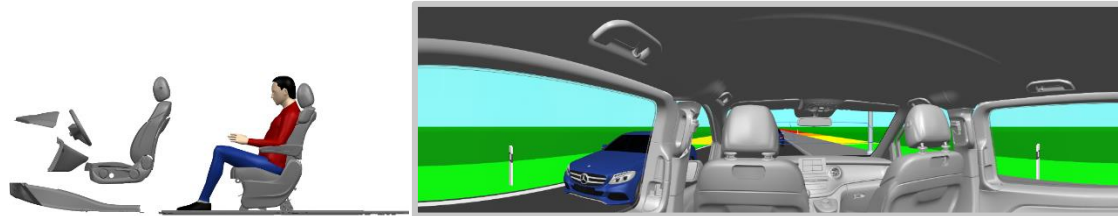
Fig. 7-3: Field of vision of an upright sitting 95th mannequin with 23° backrest angle – vision simulation.
Modified from Daimler AG (2020)

The second position addressed the results of the participants' query, in which low acceptance of reclined postures occurred while performing physically active and visually demanding activities during a vehicle journey. To provide head stabilization without provoking a feeling of being in a supine position, two main seat adjustments were applied. Firstly, the backrest was set up to only a 35° inclination angle. In fact, this was 3° less than in the original test. Secondly, to compensate for the more upright sitting position, a wedge pillow for the seat and a footrest were added (see Fig. 7-4). The resulting increase in inclination improved axial support to the occupant´s body and aimed to provide better head support. The disadvantage of this configuration was the deviation from the universal comfort values of human joint angles (Lorenz, 2011, p. 4; S. Schmidt et al., 2014).
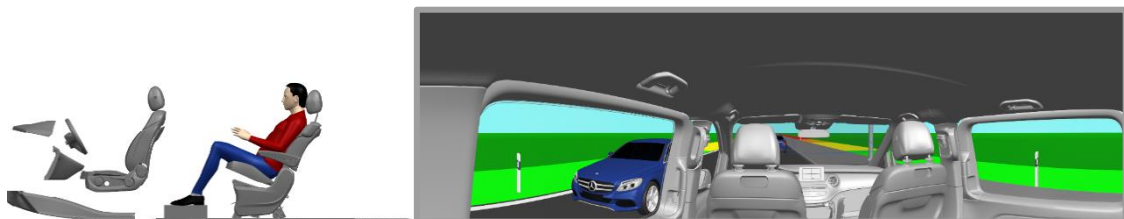
Fig. 7-4: Field of vision of a reclined sitting 95th mannequin with 35° backrest angle – vision simulation.
Modified from Daimler AG (2020)

Inspired by the previously mentioned zero-gravity position, a lying posture was defined as the third experimental condition. The backrest angle was set to 62° and the seat cushion was adjusted to 35° inclination angle (see Fig. 7-5). As a result, an angle of 117° between the torso and femur was achieved, whereas the lower body was positioned differently compared with the original zero-gravity model. This adjustment had been made, due to recommendations collected during the pre-tests.
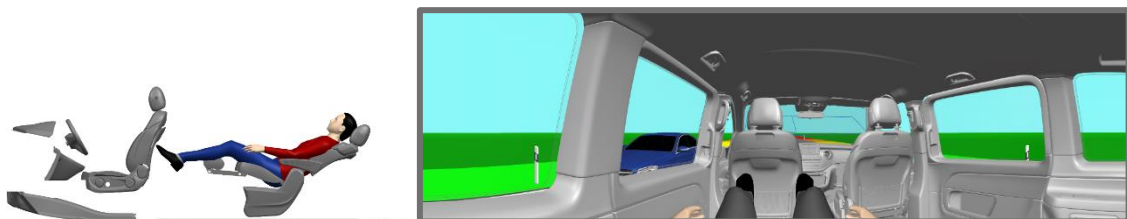
Fig. 7-5: Field of vision of a lying 95th mannequin with 62° backrest angle – vision simulation.
Modified from Daimler AG (2020)

The previous images shown above are intended to illustrate the change in visual range and outside view through an increased backrest angle. Anthropometry was treated as a constant factor and, therefore, was not manipulated within the simulation. If the ratio of H25 to H30 would be greater, the small female (5th percentile) is strongly recommended as the human model to be used to investigate the maximum lean angle until the outside view is limited. In this application, however, the small female had sufficient all-round visibility in every position, so that any human model could be used for this investigation. In fact, the leverage of the trunk length is reduced to a minimum when lying in a total flat backrest configuration, like it is almost achieved in the third position (see Fig. 7-5). Further analysis, also with respect to anthropometry, will be discussed later.

Physiological Measurement

Compared with previous physiological measurements, here discrete sensing of oxygen saturation and heart rate were conducted during the breaks. Using the *PULOX PO-200*, pulse oximetry was used, which is based on the fact that the blood pigment shows different colours depending on the status of hemoglobin. Oxygen-laden hemoglobin is bright red and absorbs red light, while unsaturated one appears dark red to bluish and absorbs light in the infrared range. To measure these differences a light source on one side of the pulse oximeter is used. It emits red light with a wavelength of 660 nm and infrared light with a wavelength of 940 nm. There is a photodetector on the other side of the pulse oximeter that measures the amount of light arriving on the other side of the finger. From these measured values, the absorption level of blood and tissue can be determined so that the saturation of oxygen within the blood vessels is permitted to be evaluated. (Patent No. US 9,392,970 B2, 2016) The heart rate was measured by the pulse and describes the pressure fluctuation originating from heart activity.

Performance Testing and NDRTs

In the previous studies, performance examinations were carried while being on the test track. The characteristics of detection within those tests can be divided into continuous and discrete measurements. The current investigation focuses on a discrete pre-post comparison of a more complex reaction test. Both trials were performed in the examination room immediately before and after the journey, while its exposure lasted exactly two minutes. The test was conducted on the tablet. The participants needed to press the upper or lower part of the screen, depending on the actual state of the changing colour pattern represented on the tablet screen. Latency and errors were then recorded and calculated to a cumulative performance score. The predefined NDRTs are obtained from the previous applications described in chapter 5.2.2. The participants played the game "Flip Run" and as a second activity, they watched a movie in a quasi-randomized order by applying the Latin square method. Since subjects had to attend on three occasions care was taken to present the most exciting tasks during these four opportunities. Even though the game had been firmly proven to induce carsickness, it was also of entertaining nature (see chapter 9.6 for additional information in relation to this finding).

7.4   Results

To examine the impact of the head-neck brace, a pilot study with five volunteers was carried out. Camera data were collected as well as accelerometers were attached to the head and the cabin of the vehicle. Isolated vehicle maneuvers were performed to understand the general behaviour of head dynamics when wearing the supporting device. In order to minimize disturbing effects, each subject participated in a repeated measures design. The test run was carried out twice, one trial with and the second one without the device or vice versa. A generic motion profile was chosen to identify directional influences. As a representative example, the analysis of a preliminary test is illustrated below in Fig. 7-6.
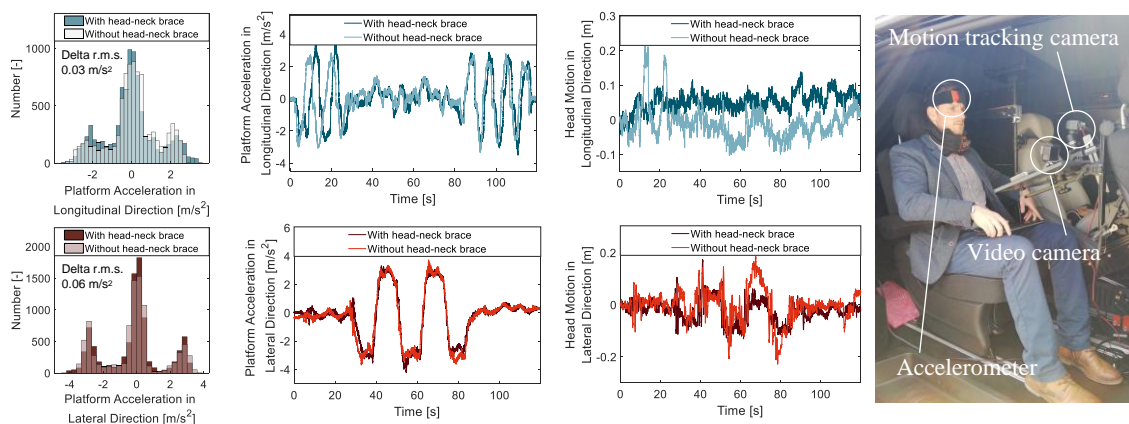
Fig. 7-6: Impressions of stabilization due to the head-neck brace – third investigation.

When analyzing the driving profiles and their distribution of acceleration for both trials, only slight differences occurred between each other. In consequence, it can be stated that the applied input parameters are similar for the experimental condition. While only partial reductions in longitudinal head motion due to the head-neck brace were noticeable, lateral motion showed over the entire trial greater dampening effects. Nonetheless, stabilization can be observed for every direction. This conclusion can be confirmed by analyzing the head acceleration, by which a maneuver-based reduction in r.m.s. due to head-neck brace in lateral (e.g. 0.16 m/s^2) and longitudinal (e.g. 0.2 m/s^2) direction occurred. Taking the qualitative video data into account, a form of pendulum behaviour of the upper body was recognized when wearing the head-beck brace. In light of the fact that this was a preparatory study with a limited number of samples, further analyses were rejected.

To evaluate the main research question of the third investigation, various parameters concerning motion sickness operationalization are reported to capture a complete impression of the outcome i.e., the nauseogenic manifestations. Due to less complexity in study design, a simple non-parametric pairwise method had to be applied to evaluate inferential statistics. Motion sickness, for instance, represented through the MSAQ score, showed a significant impact of backrest inclination by applying the Chi-square test, $\chi^2(2) = 15.21$, $p < .01$. Tukey post hoc multi comparison analysis revealed a significant difference between the upright sitting and the reclined position ($z = 3.44$, $p < .01$) as well as between the upright sitting and the lying position ($z = -4.47$, $p < .01$). Between the two supine postures(reclined vs. lying), no significant difference could be observed ($z = -1.03$, $p = .56$).

Fig. 7-7 summarizes the results of the extended backrest inclination and the use of a head-neck brace on the severity of motion sickness. The frame colour of the vision simulation in Fig. 7-3 to Fig. 7-5 is congruent to the bar illustration.
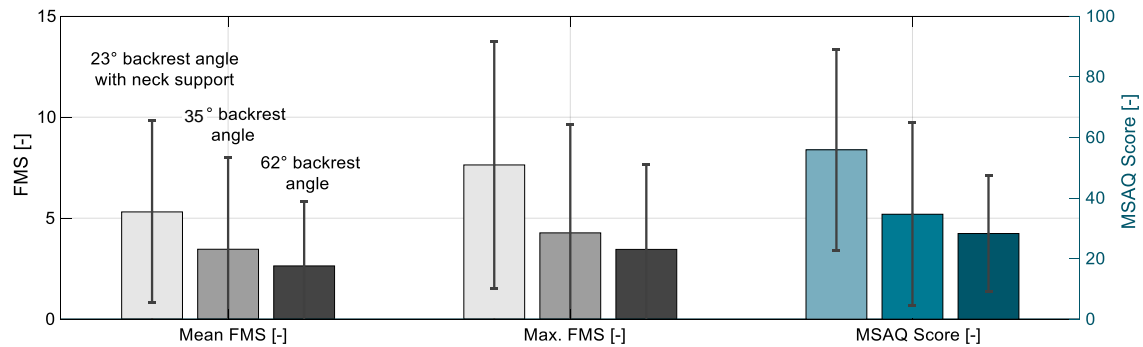
Fig. 7-7: Descriptive analysis: MSAQ score and FMS values for all sitting conditions – third investigation.

By evaluating the number of terminations, statistically, every set up in backrest inclination increases the likelihood of discontinuation by almost 10 %. To be more precise, three aborts occurred when sitting upright, while two terminations were present in the reclined position and only one discontinuer was recorded in the lying position. Due to the inhomogeneous distribution in susceptibility, the MSSQ data were dichotomized to apply the median split method (see Fig. 7-8). Two groups were created - one consisting of highly susceptible subjects and the other consisting of insusceptible subjects.
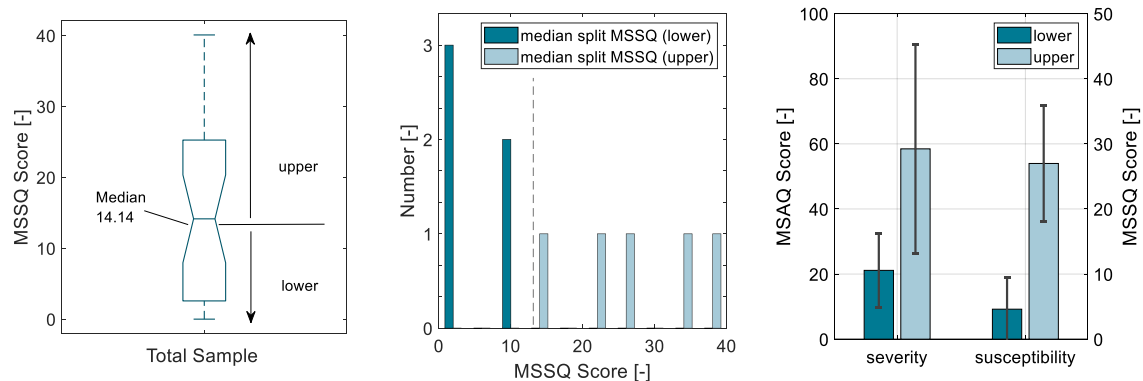
Fig. 7-8: Setup of median split method – third investigation.

The incidence of carsickness differed between the susceptible and insusceptible groups and correlates with the MSSQ score (see Fig. 7-8 - right). Fig. 7-9 provides information about the main effect of body posture on individuals' well-being i.e., carsickness, for both.
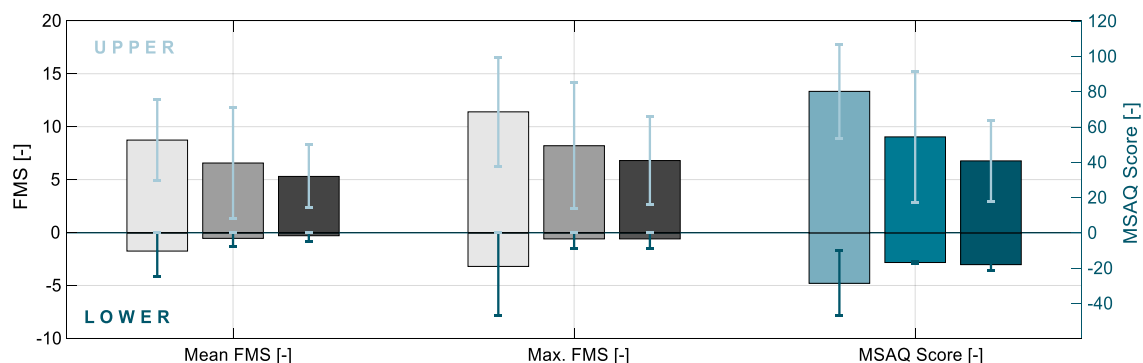
Fig. 7-9: Median split method: MSAQ score and FMS values for all sitting conditions – third investigation.

When considering the insusceptible subgroup (lower), a trend of increased nauseogenic manifestation within the upright position can be discovered. By contrast, both the reclined and lying positions show almost no differences between each other with the standard deviation within this subgroup being noticeably small. The highly susceptible group (upper) demonstrated a constant decrease in motion sickness with every change (increase) in backrest inclination. This effect is particularly outlined by the MSAQ score.

7.5   Discussion, Synopsis, Further Results, and Research Questions

The median split method is predestined to clarify the main effect of backrest inclination on motion sickness and additionally shows the importance of susceptibility as an essential parameter in study design to observe motion sickness treatments. A deeper analysis of individuals' susceptibility and its influence on the characteristics of motion sickness is discussed in chapter 9.1. On the whole, it has been shown that an extended backrest inclination leads to further improvements in motion sickness mitigation. In fact, when analyzing the qualitative questionnaire regarding motion comfort and general well-being in vehicle environments, nine of eleven subjects were "very satisfied" with traveling in the lying position. The remaining two subjects stated that they were "satisfied" or "neutral". When asking the subjects for suggestions on improvements for this position, the participants rated the experienced body posture as shown in Fig. 7-10:
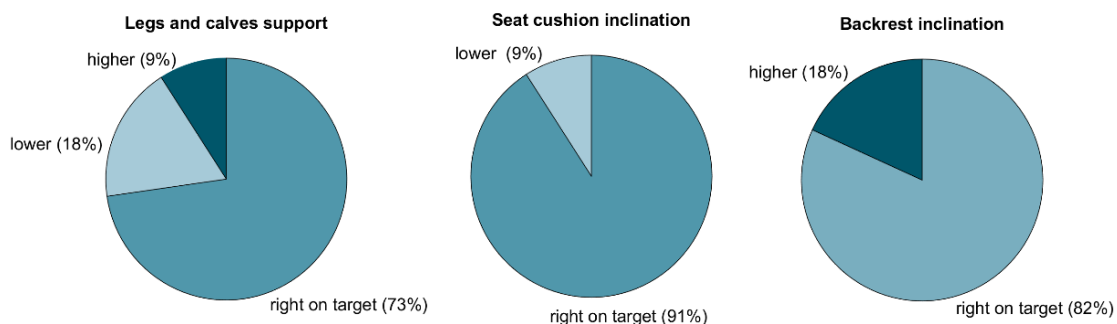
Fig. 7-10: Preference on seat adjustment in the lying position – third investigation.

Stabilization of the head in the upright sitting condition accompanied by a reduction in motion sickness could not be achieved using this approach. Although almost 45 % of the participants mentioned that they had experienced stabilizing effects to some extent when wearing the head-neck brace, nobody would want to use this for their own private use. The possibility of a suitable surrounding view of the vehicle environment, regardless of whether being in an automated vehicle or as a passenger in a manual driving mode, appears to be an essential criterion for the well-being of vehicle occupants. The participants rated the importance of the surrounding view on a 5-point Likert scale from "not important" to "very important" as follows: "slightly unimportant" (two) with 9 %, "somehow important" (four) with 36 %, and "very important" (five) with 55 %. Within the vehicle setup, sufficient all-round visibility was guaranteed regardless of which posture was selected. This was also reflected in the assessment of the belt height (H25), in which 91 % of the respondents surveyed this value as "right on target". Only one participant rated the belt height in the upright condition as "too high", whereas in the lying position the H25 value was considered to be "too low".

When observing the overall rating of the outside view, a deterioration with increasing backrest inclination can be recognized. In the upright sitting and the reclined posture, the outside view was rated on a 5-point Likert scale with an average value of four, whereas in the lying position on average one point less was achieved.

External Validity and Further Research Questions Concerning Motion Sickness

Although visually demanding activities had to be carried out during the journey, as examined in the second investigation, the effectiveness of the peripheral view on motion sickness cannot be denied. Moreover, the all-round view is not only relevant in terms of motion sickness, but it is also an essential part of the user experience and acceptance within automated vehicles. Given that the results of the lying position were collected in an experimental setup in which sufficient visibility was ensured, the external validity of the result has to be assessed by further simulations. The first parameter was attributed to adjustments of the eye point, initiated by a change in seat height or anthropometry, but without changing the cabin design of the V-class. Lowering the eyepoint of the 95th male from 443 to 258 mm the horizon is only slightly visible. In fact, if the seat bracket and the trunk length of the occupant in total reduce the head position in the vertical direction by 185 mm, the horizon of the surroundings can no longer be seen (see Fig. 7-11).

Fig. 7-11: Lying position with a lower H30 value: 95th mannequin with 62° backrest angle – vision simulation. Modified from Daimler AG (2020)

The second experimental condition addressed different vehicle types. The simulation of a short female (5th mannequin - east) sitting in the driver seat of a limousine showed to be a realistic and rewarding approach. With respect to other vehicle designs, and under consideration of the given seat structure, the short female is unable to see the outside horizon when being in the lying position. Even the tall male (95th mannequin - west) has limited access to an adequate panoramic view. Here, the observation of the outside horizon is also not received. Both simulations are presented in the following Fig. 7-12.
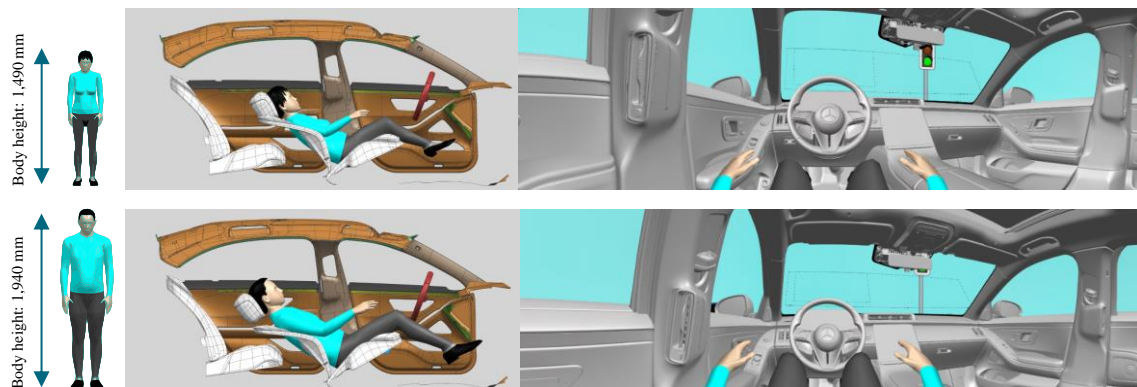
Fig. 7-12: Lying position on driver seat in a limousine: 5th female (top); 95th male (down) – vision simulation. Modified from Daimler AG (2020)

As previously stated, the impact of body and trunk length on the vertical eye point decreases with increasing backrest inclination. Regarding the simulations above, the question arises whether the potentially missing view can be replaced or supported by an artificial representation of the actual vehicle dynamics. By reducing the visual information to the relevant parameters of the passive motion environment, a lack of individuals' panoramic view could be theoretically offset and, therefore, show the ability to decrease the sensory conflict described in chapters 3.2.6 and 3.2.7.

8 Fourth Investigation – Outside View and Visual Stimulation

Referring to the model of Griffin (see Fig. 4-1), motion sickness can be influenced by more variables than the human posture. The motion environment, for instance, makes a decisive contribution to the severity of motion sickness. DiZio et al. (2018) had already pursued the idea of manipulating the experienced motion by compensating the unevenness of the road surface through an active in-car suspension system. The subsequent reduction of vibration load led to a decrease in sensory mismatch and, therefore, reduced motion sickness. Apart from this consideration of avoidance of nauseogenic mechanical motion stimuli, providing optimal assistance in perceived motion information offers another alternative for improving human well-being during the journey i.e., reducing carsickness. In fact, humans generate situation awareness by connecting and interpreting several sensory information (see chapter 3.2). Here, vision as a highly sensitive input variable shows great potential in manipulating motion perception and, as already outlined in the second investigation, could potentially be relevant when it comes to mitigating motion sickness. A proper motion cue representation shows different methodical approaches. From an anticipatory trajectory planning through an artificial earth-fixed horizon to an actual motion demonstration of the passive transportation system - countermeasures common to these three approaches contain some level of visual portrayal. The anticipatory estimate, whose considerable potential in motion sickness reduction had been investigated by Karjanto et al. (2018), requires a long-time forecast of the future vehicle trajectory. The earth-fixed visualization, if provided by a digital device, equally needs a proper motion preview, whereas only short durations in foresight are necessary. In cases of mechanical equalization, similar to what can be seen in anti-motion sickness glasses, no forecast of the upcoming motion is necessary. Evidence of the effectiveness in avoiding the physiological syndrome by presenting stable reference obstacles has, until now, only been promoted in simulators (Bos et al., 2012). In the vehicle environment, the efficiency in motion sickness mitigation has been lacking to date and needs to be proven in the near future. Both of the approaches which have already been described address roll, pitch, and yaw motion as well as lateral accelerations. However, given that longitudinal motion has proven to be of great nauseogenic nature, another form of representation has to be displayed. Analogous to previous thoughts (DE 10 2014 210 170 A1, 2015), a more dynamic approach which epitomizes visual cues intended to simulate the optic flow is indispensable. As stated in chapter 3.2.5, the interaction of vestibular and ocular reactions through the VOR and the velocity storage are likely to influence motion sickness (B. Cohen et al., 2003).

Consequently, this work[4] aims to evaluate the effectiveness of dynamic vehicle motion visualization to avoid or at least reduce carsickness of passengers who are performing visually demanding NDRTs.

8.1 Participants

In line with previous investigations, subjects were recruited based on their individual motion sickness susceptibility, biological gender, and age. Each participant was assigned to the grouping factor of vision (outside view vs. only inside view) with the restriction of equal distribution in the relevant recruiting parameters mentioned above. The rank order of the repetition factor i.e., LED stimulation, was counterbalanced to avoid potential habituation effects. The established eligibility requirements of exclusion such as pregnancy, cardiovascular diseases, gastrointestinal disorders, migraine or vestibular impairments, as well as the stipulated break between the two driving exposures of at least one night of sleep were also applied in this investigation. Three subjects had to be excluded from the analysis due to visual disorders, lack of recovery, and scheduling difficulties. Ultimately, the total sample consisted of 23 healthy participants of which 14 were males and nine females. The average age was 42.57 with a standard deviation of $\pm$ 14.12, whereas the overall MSSQ score revealed 16.15 (SD = 8.38). When analyzing the distribution within the two groups, neither individuals' age, $t(41) = -0.26$, $p = .80$, nor their susceptibility rate, $t(42) = 0.2$, $p = .84$, varied significantly between each other. Regarding biological gender, there was no significant distinction between the groups, $\chi^2(1) = 0.004$, $p = .95$, or within the MSSQ distribution, $t(38) = -1.09$, $p = .28$. Furthermore, order effects and time between trials were observed within this investigation, whereby the individual's recovery time has to be considered here. On average, there were 5.3 ± 4.7 nights between the two exposures, while the mean number of days between the two measurements did not vary significantly between the groups, $t(43) = -0.04$, $p = .96$, nor within subjects, $t(22) = 0.56$, $p = .58$.

8.2 Procedure

In December 2019, a 2x2 mixed test design study was conducted at the test track of Mercedes-Benz AG in Sindelfingen with an average outside temperature of 7.5 °C ($\pm$ 3 °C). The study design was developed along similar lines to the second investigation, in which a 2-step grouping factor of vision was examined. However, in contrast to that study, the repetition factor provided some further visual stimulus instead of changing the direction of sitting. Concerning the common standards of study design, the visual stimulus was randomized within the two groups. To avoid influences of expectations, the participants were not informed during the instruction about the visualization and its functionality or purpose. They were rather directed to focus on the NDRTs, whereby its compliance was monitored by the examiner during the entire journey.

---

[4] The experiment was designed and conducted with the assistance of A. Bruder (2020) as part of her Master´s thesis. Major results of the fourth investigation are submitted to the Journal IEEE Transactions on Intelligent Transportation Systems in October 2020.

Due to this requirement, it was ensured that the participants perceived the visual stimulus only in the periphery of their range of vision, instead of actively focusing on the light installation. As previous studies have explored, posture reveals a strong impact on the development of motion sickness. Based on this conclusion, a one-for-all valid specification of backrest angle, seat cushion height, and sitting direction was defined. To guarantee comparability, the reclined position of the first investigation was chosen. As the predefined task, the participants either had to read a particular e-book or conducted the previously explained reaction game called "Flip Run". The overall procedure applied in the fourth investigation is equivalent to the three reference studies before, however, without conducting performance measures.

Physiological Measurement

Analogous to the already utilized objective measurements, *NeXus-10* with the respective *BioTrace+* software was chosen to measure the heart rate and *electrodermal activity* (EDA) of the participants. While heart rate, determined through the ECG data, has been previously measured, EDA was found to be a new parameter to quantify motion sickness. EDA measures the changes in electrical potential between different parts of the skin, which represents neurally mediated effects of sweating. Since the degree of sweatiness is a major item within the MSAQ its utility in objectification can be emphasized. However, compared to other sympathetic effector synapses, EDA is resistant to neural fluctuations in adrenaline and noradrenaline levels (LaCaille et al., 2013), which might be misleading in terms of motion sickness detection. Due to data loss as a result of dropping electrodes, the EDA data set is highly volatile and, consequently, is not discussed in the current work.

8.3 Update of the Experimental Vehicle and Motion Profile

Given that humans are more sensitive to exogenous motion in the periphery of their range of vision (Fademrecht et al., 2016; Otten & Wittkowske, 2014, p. 28), it seems to be beneficial to present additional visual motion information in the side panel of the vehicle cabin. In fact, two stripes of RGBW-*light-emitting diodes* (LEDs) with a total length of 2 m and consisting of 120 LEDs were installed on each side of the vehicle´s beltline and the cabin´s ceiling. The stationary light animation consisted of 30 active LEDs followed by a threefold longer sequence of deactivated ones. To compute the visual animation, Teensy 3.2 OcotWS2811 adaptors, a USB-based microcontroller development system consisting of a 3.3 Volt ARM Cortex M-4 CPU with 72 MHz (frequency) and 64 KB (RAM) were used and installed into the rear of the V-class. The programming was executed by an additional Linux-based computer, which was linked to the microcontrollers and compatible with the Arduino framework with its libraries. To connect the LED animation with the actual vehicle motion, information from the *Body Controller Area Network* (Body-CAN) was integrated into the technical framework. The electric power supply was ensured by an additional 200 Ah 12 Volt lead-gel battery with a digital charging indicator. Fig. 8-1 shows the technical setup (left) and the active LED stripes with their characteristic pattern of motion visualization (right).
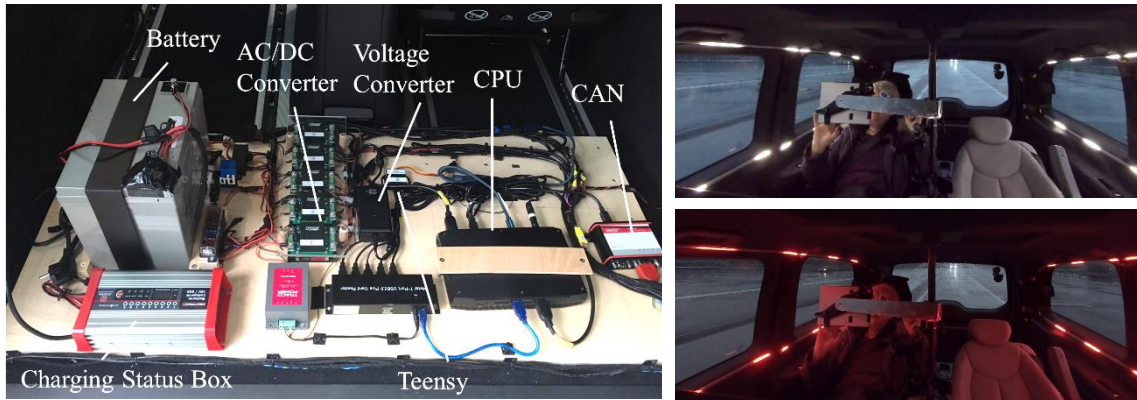
Fig. 8-1: Technical setup (left); LED animation during acceleration and deceleration (right) – fourth investigation.

Characteristics of Motion Visualization

Karjanto et al. (2018) proposed that detailed information of the vehicle dynamics shall be presented intuitively to gain the most possible information density regarding the exogenous vibrational load. With respect to this suggestion, the vehicle motion data provided by the Body-CAN was processed and rendered by the LED light animation in order to represent the actual state of driving in a simple way. Indeed, an immersive impression of movement was initiated through a dedicated activation of LEDs in a way that a smooth transition of the characteristic lighting pattern was perceived. The running direction of the LED lights was programmed with reference to the optic flow (see chapters 3.2.2 and 3.2.5). In fact, a forward-moving vehicle was equipped with an LED motion simulation flowing from the front to the rear, while backward vehicle motion showed the reciprocal LED direction. Vehicle velocity reveals a major part in representing the interaction with the outside world. As seen in Fig. 3-4, perception thresholds under low-speed conditions are influenced by visual information, whereby this effect explains the increasing likelihood of vection in these situations. Given that motion sickness can be provoked through feelings of vection, it was essential to support the human apparatus with precise motion information under low-speed vehicle conditions. Therefore, a velocity-related assumption was formulated, in which a linear behaviour of LED and vehicle motion under low-speed conditions was required. With increasing velocity, however, the impact of visual information decreases, while kinesthetic and vestibular information achieve an even greater presence. Concerning multi-modal-interaction, a maximum of 20 ms time delay between the vehicle Body-CAN information and its respective LED representation was embraced throughout the entire velocity spectrum to ensure the required synchronization of perception modalities (Altinsoy et al., 2001). Regarding the lateral eccentricity between the observer and the LED panels, the motion parallax paradigm indicates that both velocities claim not to be in an exact one-to-one relationship. Nevertheless, due to the nature of visualization, every representation of LED movement is exclusively linked to the actual motion of the vehicle and, thus, leads to a congruent sensation between the vestibular and visual modality. Based on technical requirements, an upper boundary condition in LED motion (1.5 m/s) was defined, which affects the saturation behaviour between the LED and vehicle motion at high-speed conditions. The corresponding graphs of the velocity ratio are shown in Fig. 8-2.
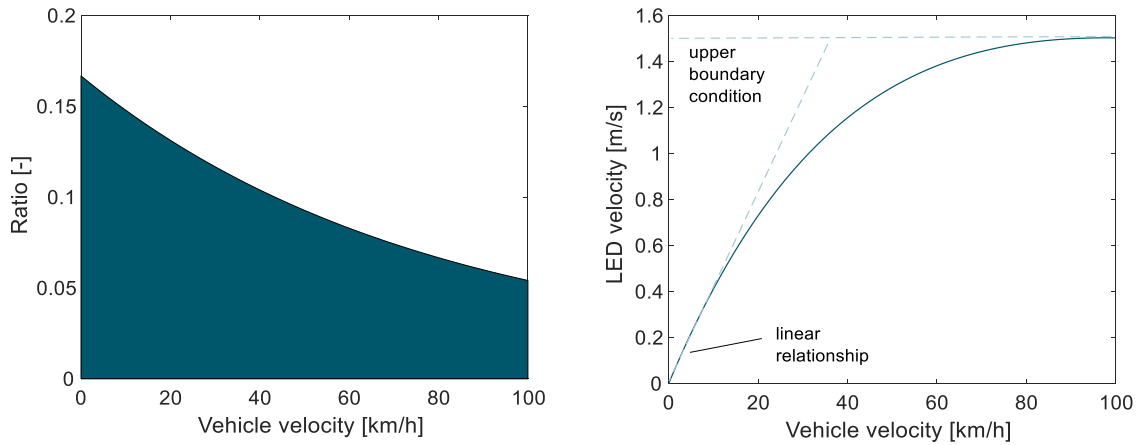
Fig. 8-2: Ratio between vehicle and LED velocity – fourth investigation.

The following equation mathematically describes the above-presented ratio between vehicle and LED pattern velocity:

$$y(x) = (S - (S - y_0) \cdot e^{(-k \cdot x)}) \cdot \frac{1}{6} \qquad \text{Eq. 8-1}$$

To meet the accompanying requirements, the lower limit was defined by the value $y_0 = 0.07$ and $S = 1.0$ with an attenuation constant (k) of 0.013. These parameters were evaluated in terms of pleasantness by iterations during several explorative examinations with the participation of five experts in the field of user interaction.

Even if acceleration is predominantly captured by the vestibular system, the change in vehicle velocity is integrated into the visual animation for synchronizing the different motion input signals and compensating for the static visual content. In contrast to the prominent demonstration of vehicle velocity, its change is subliminally presented through adjustments of LED colour and brightness. The colour change is characterized as being either white or red, depending on whether the vehicle accelerates or decelerates (see Fig. 8-1). To be precise, from positive values (acceleration) up to a range of -0.5 m/s² (deceleration), the colour of the LED light was purely white. The reason for the negative threshold is due to the natural longitudinal braking behaviour of the combustion engine, which would lead to flickering effects of the LEDs when setting the threshold to 0 m/s². Consequently, values between 0.0 m/s² and -0.49 m/s² were also achieved by not actively braking the vehicle but just letting the car roll, which was not desired to be visualized in the same manner as active braking action. To ensure a pleasant user experience, a smooth transition from white to red or vice versa had been implemented. In fact, between the range from -0.5 m/s² to -1.5 m/s² a hysteresis was programmed. Decelerations above the value of -1.5 m/s² were presented solely in red, while this colour is used since it is already known from daily traffic situations and subconsciously associated with braking maneuvers (Matthews et al., 2004). To achieve a suitable LED-dimming algorithm a non-linear change in LED brightness had to be realized due to the conclusion of Weber and Fechner, who postulated that the intensity of psychological sensation is proportional to the logarithm of the stimulus intensity (Weber-Fechner law, see Stevens 1957):

$$P = k \cdot \ln(S) \qquad , \qquad \frac{\Delta S}{S} = k \qquad \text{Eq. 8-2}$$

S is the value of the standard stimulus, whereas ΔS reflects the threshold of a just noticeable difference. The scaling constant k depends on the stimulus-specific units and is known as the Weber fraction, while the perceived magnitude is expressed by P. In 1961, Stevens introduced his power law, in which he postulated that perception intensity is a power function of the stimulus (Stevens, 1961). He extended the given formula by the exponent b, also known as the power value, which is dependent on the sensory dimension that is being described. Finally, the value I describes the physical stimulus intensity, which leads to the following equation:

$$P = k \cdot I^b$$

Eq. 8-3

Tab. 8-1 and Fig. 8-3 show the power-law relationship for the stimuli brightness, electric shock, and length, by illustrating the effect of different use cases with their respective exponents. For the present study, the perception of brightness of an extended target requires a power-law exponent of $b = 0.33$.

Tab. 8-1: List of different exponents within the power law.
Based on Stevens (1961)

Use Case	Exponent
Brightness	**0.33**
Vibration (250 Hz fingertip)	0.60
Loudness (3000 Hz)	0.67
Vibration (60 Hz fingertip)	0.95
Apparent length	**1.00**
Heaviness	1.45
Muscle contraction	1.70
Electric shock	**3.50**
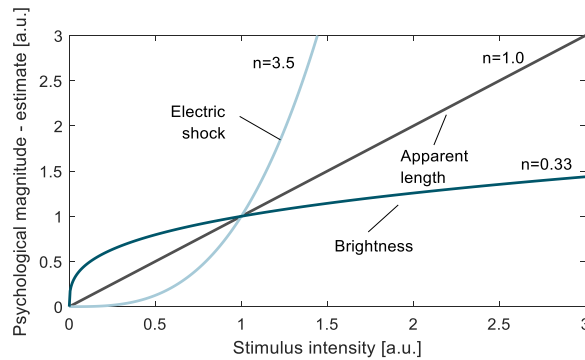
Fig. 8-3: Weber-Fechner law.

Applying Steven´s power law with the inverted exponent value set to $\frac{1}{0.33}$, the raw (original) calculation of brightness as a function of the vehicle acceleration is shown in Fig. 8-4 with the light petrol colour scheme. The light intensity can be arranged from 0 to 255 within the *pulse width modulation* (PWM) method (Narra & Zinger, 2004). As the LEDs are not supposed to be switched off when the vehicle is not accelerated, an offset value of $c = 10$ PWM was iteratively determined and defined as suitable for the perception experience.

As shown on the left-hand side of Fig. 8-4, most accelerations are operating in the range of ± 2 m/s² (up to a maximum of ± 3.5 m/s²), which, in turn, do not result in a noticeable change in LED brightness within the original function (see Fig. 8-4 - right). Therefore, a linear behaviour was added to ensure this predefined adaption in visualization as intended. Furthermore, to stay within the limits of the technical specifications of the LEDs, the specific scaling constant was set to $k = 0.3$. The resulting function of the dimming behaviour is defined as follows:

$$y = k \cdot (a + 3)^b + c$$

Eq. 8-4
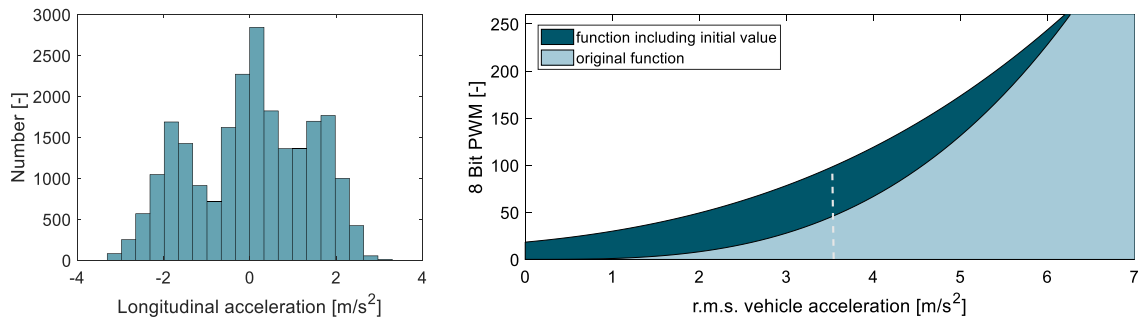
Fig. 8-4: Distribution of longitudinal vehicle acceleration (left);
brightness of LED as a function of r.m.s. acc (right) – fourth investigation.

Analogous to previous investigations, the driving event was subsectioned into four identical 5-minute rounds with partial driving maneuvers. In this case, however, a paradigm shift to a predominant fore-and-aft motion pattern had been conducted. The primary reason for this adjustment was due to the above-described animation of longitudinal motion, whereas a representation of lateral and roll motion was not included in the LED algorithm. As demonstrated in the right part of Fig. 8-5, the section of lateral motion was replaced by further start-stop maneuvers with a major power distribution of motion between 0.1 and 0.2 Hz (see chapter 3.6.1).
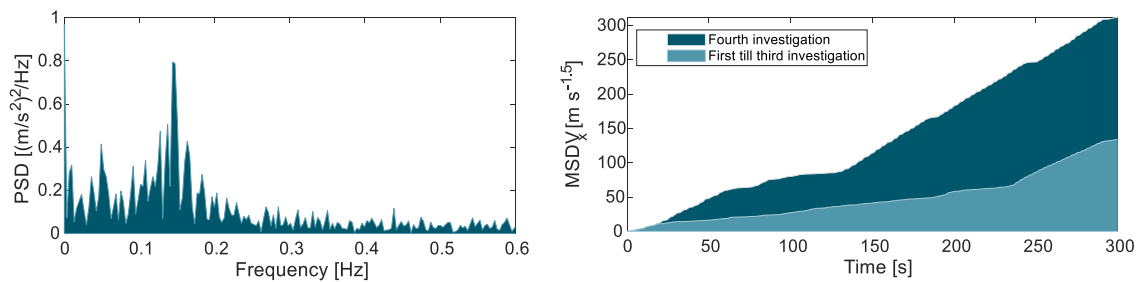
Fig. 8-5: PSD of longitudinal vehicle acceleration (left);
$MSDV_x$ across all test conditions – fourth investigation.

8.4 Results

The participants' state of motion sickness expression is operationalized and presented through the delta and mean FMS as well as the MSAQ score in Fig. 8-6.
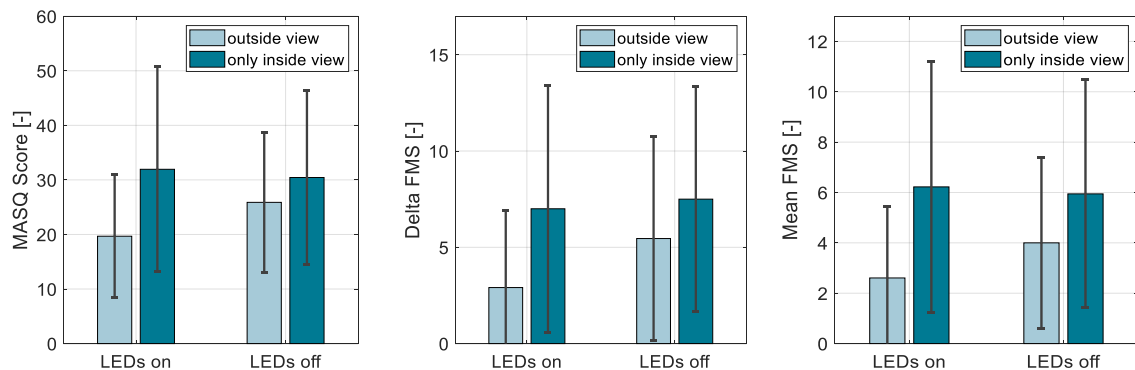
Fig. 8-6: Descriptive analysis: MSAQ score and FMS values – fourth investigation.

Analyzing the delta FMS results in Tab. 8-2, the LED condition (b = 2.71, t(19) = 2.39, p < .05, r = .48) as well as the view condition (b = 4.33, t(21) = 2.16, p < .05, r = .43) showed significant effects on the severity of motion sickness. Even if the interaction term did not improve significantly the model fit, $\chi^2(1) = 2.17$, p = .14 (model 9 vs. 10), the integration as predictor does have an impact on the main effects of outside view and LED animation. Both statistical significancies increased, which can be explained by the phenomenon called suppressor effect (Field et al., 2012, p. 265). Furthermore, a detailed inspection of the results revealed that the mean change in FMS score due to LED activation was greater for the group with the ability to see the outside environment compared to the inside view condition. This result, however, does only show statistical tendencies when applying the Wilcoxon signed-rank test (V = 5, p = .07). The LED condition resulting in a small change in FMS scores varied between the subgroups of the inside view group, while there was no significant difference in between (V = 18, p = .33).

Tab. 8-2: Model comparison (LME): delta FMS – fourth investigation.

Model	Dependent Variable Delta FMS									
	(1)	(2)	(3)	(4)	(5)	(6)	(7)	(8)	**(9)**	(10)
LED off		-1.48[*] (.86)						2.54[*] (1.25)	**2.71[**] (2.33)**	1.55[*] (.81)
Inside view			3.07 (2.08)					4.25[*] (2.01)	**4.33[**] (2.00)**	3.22[*] (1.81)
MSSQ short				.31[**] (.11)				.31[**] (.11)	**.31[***] (.11)**	.31[***] (.11)
Gender female					-1.19 (2.22)					
Age						-.08 (.08)				
Day of Measur.							-1.65[*] (.85)		**-1.77[**] (.78)**	-1.72[**] (.81)
Interact. LED: View								-2.04 (1.73)	**-2.20 (1.57)**	
Constant	5.78[***] (1.08)	5.04[***] (1.17)	4.18[**] (1.50)	.80 (2.04)	6.25[***] (1.39)	9.26[**] (3.44)	6.60[***] (1.17)	-2.24 (2.29)	**-1.44 (2.33)**	-.89 (2.27)
Observ.	46	46	46	46	46	46	46	46	**46**	46
Log Likl.	-136.42	-134.98	-135.33	-133.02	-136.27	-135.84	-134.59	-129.19	**-126.58**	-127.67
AIC	282.83	281.96	282.67	278.05	284.53	283.69	281.19	276.38	**273.16**	273.33
BIC	291.98	292.93	293.64	289.02	295.50	294.66	292.16	292.84	**291.45**	289.79

*p<.1; **p<.05; ***p<.01

In summary, the experiment was discontinued twelve times by nine different subjects, while main terminations occurred during the inside view condition with nine intermitted trial events (by six subjects). By contrast, there were three discontinuations by three different subjects in the outside view condition. Regarding the repetition factor, equal distribution of termination (n = 6) with and without visual stimulus appeared. Only three participants quit the experiment on both days before the 20-minute ride was over. The accumulated results are shown in Fig. 8-7.
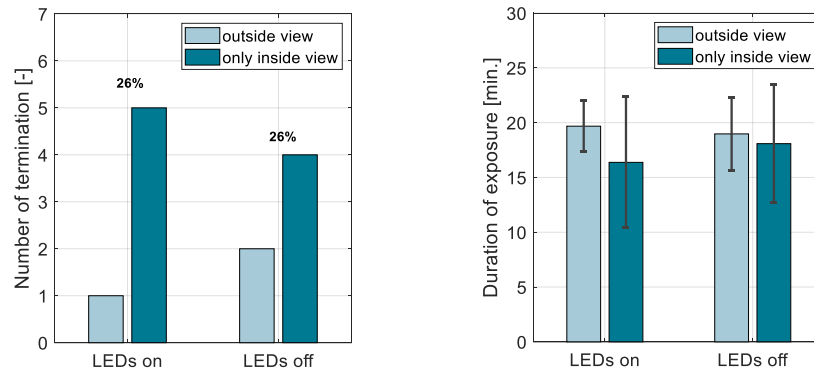
Fig. 8-7: Quasi-objective measurement: number of termination and duration of exposure – fourth investigation.

Taking a closer look at the people who discontinued in at least one of the two trials further results can be collected. Hence, Tab. 8-3 shows the average driving duration for the subgroup of discontinuers compared to the total sample.

Tab. 8-3: Driving duration: Comparison of total sample and subgroup of discontinuers fourth investigation.

Viewing Condition	LED Condition	Mean driving duration all subjects [min]	Mean driving duration discontinuers [min]
Outside	On	19.68 ± 2.33	17.81 ± 4.47
Outside	Off	18.97 ± 3.35	15.22 ± 5.19
Only Inside	On	16.38 ± 5.99	12.27 ± 6.19
Only Inside	Off	18.08 ± 5.40	15.71 ± 7.11

No statistically significant effect of either view condition ($F(1, 7) = 1.26$, $p = .30$) or LED condition ($F(1, 7) = 0.16$, $p = .70$) could be observed between the driving durations of discontinuers. Moreover, the interaction term between LED and view condition did not show any significance in terms of driving duration ($F(1, 7) = 0.64$, $p = .45$). When observing the whole sample, the mean duration of exposure neither varied significantly due to view nor to LED manipulation.

In the group of discontinuers, no significant effect could be detected, whereas the sample of non-discontinuers showed a significantly lower FMS value when turning on the LED visualization, $b = 1.93$, $t(13) = 3.88$, $p < .01$, $r = 0.73$, (see Fig. 8-8 and Tab. 8-4).
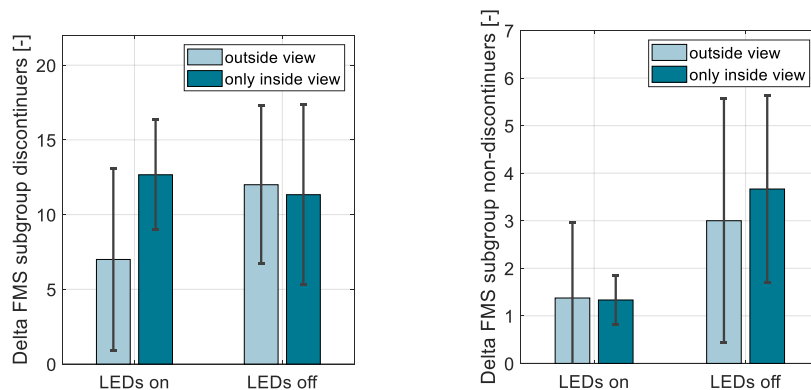
Fig. 8-8: Comparison of subgroups: discontinuers and non-discontinuers – fourth investigation.

Tab. 8-4: Model comparison (LME): delta FMS for the subgroup of non-discontinuers – fourth investigation.

Model										
	Dependent Variable — Delta FMS - subjects who did not discontinue the experiment									
	(1)	(2)	(3)	(4)	(5)	(6)	(7)	(8)	(9)	(10)
LED off		1.93*** (.50)						1.63** (.67)	1.93** (.51)	2.02*** (.48)
Inside view			.31 (.84)					-.04 (1.01)		
MSSQ short				.07 (.06)					.07 (.06)	
Gender female					-.85 (.81)					
Age						.00 (.03)				
Day of Measur.							-.36 (.72)			-.65 (.48)
Interact. LED: View								-.71 (1.02)		
Constant	2.32*** (.41)	1.36** (.49)	2.19** (.55)	1.30 (.96)	2.69*** (.53)	2.12 (1.41)	2.50*** (.55)	-1.38* (1.17)	.33 (1.01)	-1.63*** (.53)
Observ.	28	28	28	28	28	28	28	28	28	28
Log Likl.	-59.02	-53.63	-58.95	-58.31	-58.45	-59.01	-58.89	-53.29	-52.92	-52.68
AIC	128.05	119.27	129.90	128.62	128.90	130.15	129.79	122.58	119.85	119.37
BIC	134.71	127.27	137.90	136.62	136.89	137.78	137.78	133.24	129.17	128.70

*$p<.1$; **$p<.05$; ***$p<.01$

No other parameter including view condition, susceptibility, day of measurement, or biological gender had a significant effect on the occurrence of motion sickness in the subgroup of non-discontinuers. Furthermore, no interaction effect between LED condition and view condition can be identified. Since significant effects occurred in the subgroup of non-discontinuers, it seems appropriate to assess the composition of this sample. Fig. 8-9 illustrates the distribution of susceptibility and reveals that, compared with the results of the previous investigations, the MSSQ score did not strongly differ within the two subgroups of termination. Nevertheless, here as well, strong correlations between the severity of motion sickness and the individual susceptibility are observed on the right side of Fig. 8-9. Both subgroups indicate almost a similar range between the lower and upper whisker, while the interquartile range demonstrates stronger differences between the discontinuers and the non-discontinuers.
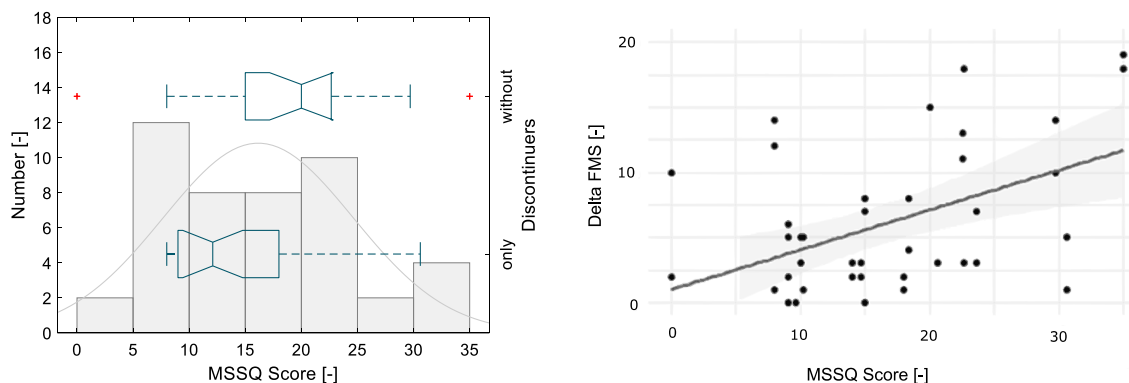
Fig. 8-9: Distribution of MSSQ score (left); MSSQ score as predictor of delta FMS (right) – fourth investigation.

Qualitative Analysis

The following Tab. 8-5 shows the subjective evaluation of the dynamic visual stimulus. The participants were asked to rate the effectiveness regarding motion sickness mitigation while performing visually demanding NRDTs. Five participants (22 %) found the stimulus to be very helpful, seven (30 %) felt it was rather helpful, while nine (39 %) stated the stimulus as neutral (neither helpful nor disturbing). Two subjects (9 %), both in the cover interior group (only inside view), perceived the LEDs as very disturbing. As outlined by Tab. 8-5, the extreme evaluations concerning the effectiveness of the vehicle motion visualization predominantly originate in subjects with relatively high susceptibility scores.

Tab. 8-5: Qualitative analysis: subjective evaluation on LED animation as countermeasure on motion sickness fourth investigation.

Viewing Condition	Very disturbing	Rather disturbing	Neutral	Rather helpful	Very helpful
Outside	0	0	4	4	3
Only Inside	2	0	5	3	2
Total	9%	0%	39%	30%	22%
MSSQ Score	17.50 (± 24.75)	/	13.65 (± 7.53)	15.98 (± 7.60)	20.34 (± 3.69)

When evaluating the reason for the subjective assessment, ten out of twelve participants in the upper median rating group, who valued the LEDs as rather or very helpful, mentioned that the visualization increased their ability of orientation by providing further immersive feedback of the vehicle dynamics. One of the other two subjects stated a positive sub-conscious effect of perception, while the other participant mentioned being positively distracted by the LED animation, which was helpful in the mitigation of motion sickness. Even though each subject with a neutral rating noticed the visual stimulus, neither a positive effect nor a negative one was mentioned by this group. The two negative ratings, however, indicated a disturbing influence of the visual animation causing sensory overload, nervousness, negative distraction, and aberration. By evaluating the simple question, whether the participants are willing to activate the LEDs during an autonomous ride, 13 subjects answered positively (seven outside view and six inside view) whereas ten participants (four outside view and six inside view) expressed a preference for them to be switched off.

8.5 Discussion and Synopsis

The overall results imply that LED motion feedback of the actual vehicle dynamics can mitigate carsickness. This effect, however, was greater within the subgroup of non-discontinuers. One reason might be due to the universal abort criterion, in which termination of experiments has to be carried out at the same state of nausea. Therefore, the resulting FMS score in both exposures is likely to be similar, which, consequently, might lead to a certain degree of leveling of the resulting motion sickness scores. In the post hoc evaluation, lower motion sickness ratings predominantly occurred when being in the outside view condition and turning on the LED animation.

Therefore, it is suggested that the visual feedback system, at least as presented in this investigation, predominantly supports, but does not replace the optic flow with its visual stimulation. In addition to the investigation of Karjanto et al. (2018), who found a significant reduction in motion sickness due to utilizing a feedforward system, it is shown that, apart from an anticipatory approach, the actual state of motion is likely to influence motion sickness as well. This is also true for situations in which visually demanding NDRTs were performed. The great volatility in the subjective rating of the LED animation is in line with the investigation of Huysduynen et al. (2017), who found strong individuality in acceptance to ambient light feedback systems covering driving experience. Even if the effect might be influenced by user expectations and individual preference, the polarizing nature of the LED rating is seen especially by those who are prone to experience motion sickness. Effects of interior lighting animation with the purpose to alleviate carsickness were also examined by the German Aerospace Center (Hainich et al., 2021). In their latest examination, anticipatory light cues of the upcoming turn were presented while this HMI prototype was proven to be effective in mitigating motion sickness within the group of susceptible participants. By contrast, the approach of Winkel et al. (2021) shows strong similarities to the current elaboration. The researchers presented visual information of the actual vehicle dynamics by using a head-mounted display, however, without identifying potential in alleviating motion sickness.

The main effect of the outside view is in line with the results presented in the previous study and is strengthened through the distribution of termination with the respective mean driving duration. In fact, the number of discontinued trials was three times higher in the encapsulated condition (inside view) than it occurred in the outside view condition. This is only one representation of the overall tendency in manipulating motion sickness as the result of different surrounding view conditions. In general, the subjective motion sickness rating showed slightly a lower amount of significances and effect sizes for the outside view compared with the LED animation. This mismatch can be explained due to the limited forward view for all subjects participating in this investigation. The test vehicle was equipped with three monitors in front of the subjects for both view conditions, while only in the inside view condition total masking of the front view was realized. Griffin & Newman (2004) postulated that being in a vehicle without panoramic view resulted in similar motion sickness occurrence as it is reported in a vehicle with a covered forward view, regardless of the ability to see the surrounding through the side window.

9   Further Non-Physical-Geometric Predictors

The current chapter tackles further non-vehicle-related predictors, which were analyzed within the four real-life driving investigations. The results are clustered, while in most instances only one representative application is presented unless inconsistencies between the studies are present. In this particular case, the total conclusion of the relevant results is discussed and compared with each other if necessary. Firstly, human-related predictors will be presented, followed by research findings on the methodical part of the study design with the focus on non-motion environments (see Fig. 4-1).

9.1   Motion Sickness Susceptibility

As previously mentioned in various results of the multi-level models, especially when applying the forward selection method, the MSSQ score is identified as one of the most sensitive predictors in terms of motion sickness occurrence. Since the distribution of the MSSQ scores was controlled individually by the conditions of participation, differences in susceptibility between the four different examinations are visible (see Fig. 9-1).
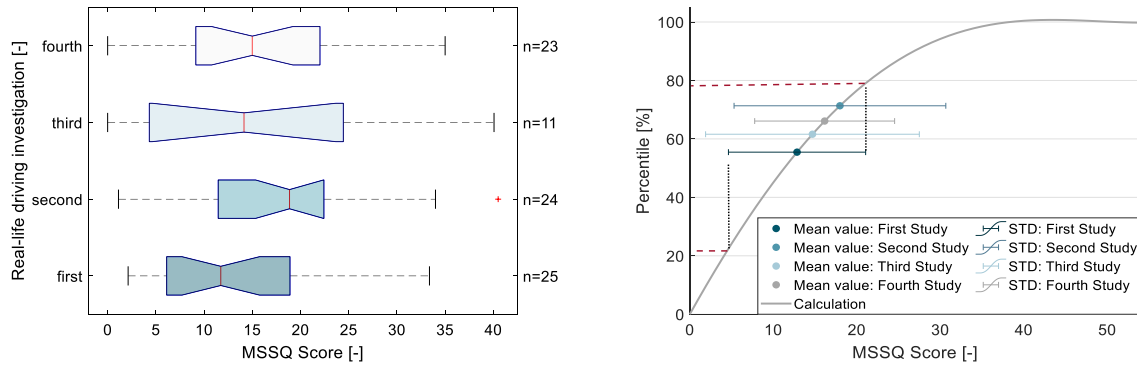
Fig. 9-1: Meta-analysis: distribution of MSSQ scores (left);
percentile analysis of MSSQ scores (right) – all investigations.

Tab. 9-1 reveals the MSSQ score results of the inferential statistics in motion sickness prediction for the four different studies. Due to the reduction in complexity, only the MSAQ score as the operationalized value for the total sample is presented, while some specific applications will be discussed in more detail.

Tab. 9-1: Meta-analysis: MSSQ scores as predictors for the MSAQ score – all investigations.

| | Observ. | Model fit | Dependent Variable MSAQ Score | | | |
			df	test	p-value	r-value
First investigation	50	best	23	t=2.11	.05**	.40
Second investigation	**48**	**best**	**22**	**t=3.05**	**< .01***	**.42**
Third investigation	33	/	27	t=-4.47	< .01***	.65
Fourth investigation	46	best	20	t=2.72	.01***	.52

*p<.1; **p<.05; ***p<.01

Whenever a multivariate procedure is applied, the best model fit is achieved when the individual susceptibility is included as one of the main predictors. This phenomenon is in common with every study presented above. The effect size, here outlined through the r-value, shows a consistent picture across the four investigations, in particular, when bearing in mind the variance in MSSQ score distribution between the different samples (see Fig. 9-1).

In none of the studies can an interaction effect be observed as it is clearly illustrated through the results of the second investigation. The following Fig. 9-2 shows the severity of motion sickness (MSAQ score) as a function of susceptibility (MSSQ score). Whilst on the left-hand side the total sample is represented, on the right-hand side, both stages of vision are compared with each other. It is outlined that individual susceptibility and incidence of motion sickness strongly correlate with each other. This effect seems to be greater in the more nauseogenic condition of the inside view (grey), compared to the outside view condition (black).
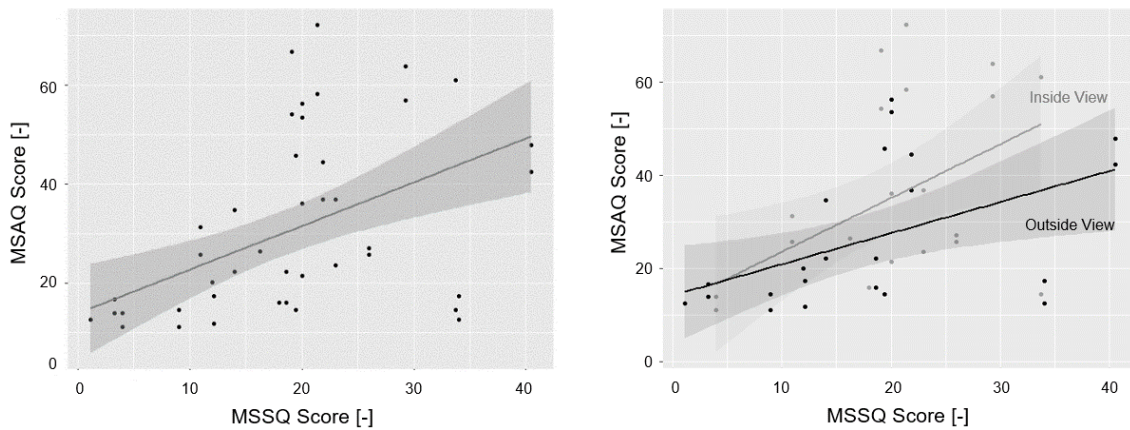
Fig. 9-2: Exemplary illustration of regression between MSAQ score and MSSQ score:
total sample (left); for both stages of vision (right) – second investigation.

9.2   Expectations on Motion Sickness Occurrence

Due to the high sensitivity to placebo effects (see chapter 3.8.1) the individual expectation regarding motion sickness was recorded in a categorical form in the second investigation. Because it has to be assumed that the experience of motion sickness investigation influences the general expectation on the occurrence of symptoms, the questionnaire was utilized before the first and second trial. Interestingly, no change in expectation occurred so that only one value was assigned to each participant (0 = expect no motion sickness, 1 = expect motion sickness symptoms).

Fig. 9-3 illustrates the distribution of MSSQ scores across the two groups of motion sickness expectations. The mean MSSQ score is about 9.5 points higher in the group of subjects who expect motion sickness symptoms compared to the other group who did not anticipate any decrease in motion comfort. The respective result of motion sickness severity, here represented through the MSAQ score, is shown on the left side of Fig. 9-3. A similar pattern occurred when analyzing the ability of surrounding view as the manipulated variable, instead of outlining the sitting direction.
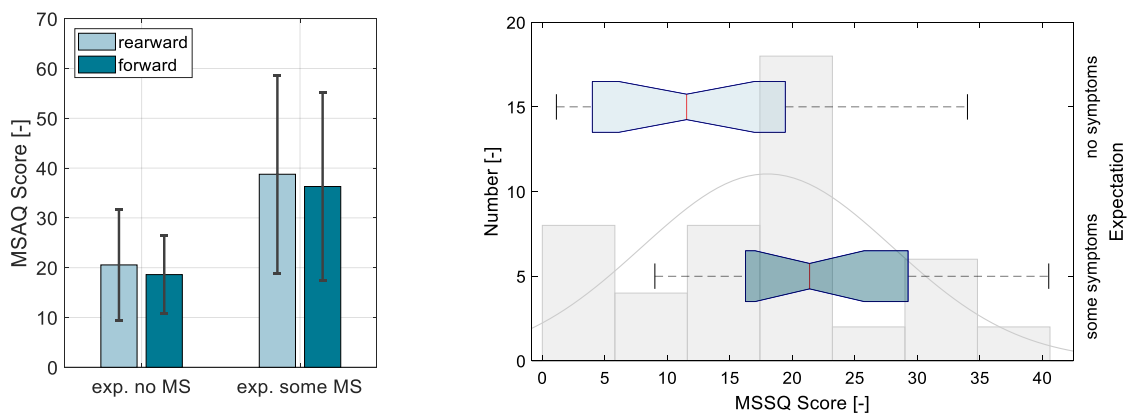
Fig. 9-3: Expectation on motion sickness as predictor of motion sickness (left);
distribution of MSSQ score for both groups of expectation – second investigation.

The results in motion sickness occurrence differed between the two groups. Indeed, the severity of symptoms was almost twice as high within the group of participants who expect at least slight symptoms of motion sickness through the examination. Including the predictor of expectation in the LME modeling, the lowest AIC and BIC could be achieved in combination with the MSSQ score, while the interaction term did not further improve the model fit. Despite the common origin of the two parameters (expectation and susceptibility), of which use is based on previous experience, the model was proven not to show any multicollinearity. The post hoc analysis revealed the following statistical impact of expectation on the MSAQ score: $b = 4.75$, $t(23) = -2.04$, $p < .1$, $r = .39$.

9.3 Habituation

As already outlined in chapter 3.8.2, habituation has been verifiably proven to be a suitable countermeasure to motion sickness. In the field of examinations with the purpose of identifying treatments to further avoid or at least reduce motion sickness in autonomous driving scenarios, this phenomenon is considered to be an important disturbance variable. The potential order effect had been controlled by the randomization and is afterwards analyzed as part of the conclusion within the driving investigations.

In most cases only slight effects appeared, whereas in the fourth investigation the strongest expressions of habituation had been identified. Therefore, the results of the fourth investigation will be assessed in this section, while the following Fig. 9-4 illustrates the expressions of motion sickness severity for both steps of measurement.
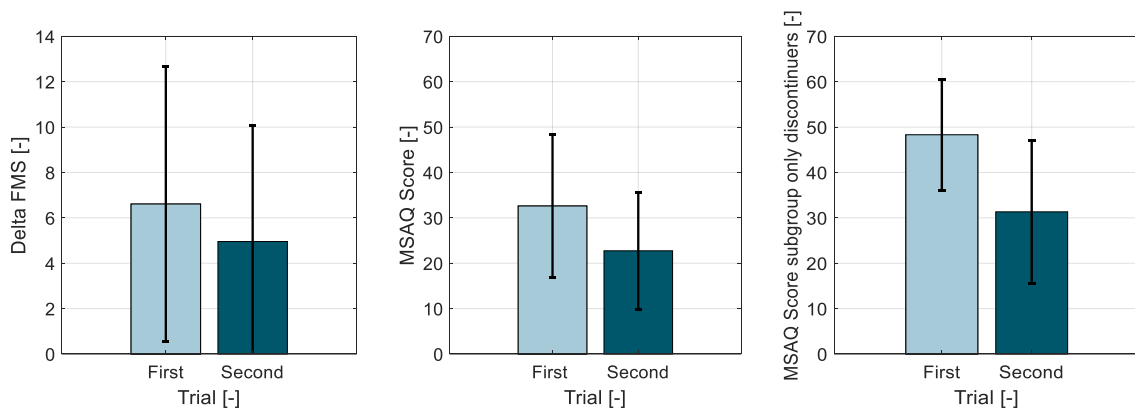
Fig. 9-4: Habituation as disturbance effect in motion sickness examinations – fourth investigation.

The significant effect of habituation can be operationalized through the delta FMS value, $\chi^2(1) = 4.56$, $p < .05$ and the MSAQ score, $\chi^2(1) = 12.04$, $p < .01$. In particular, the subgroup of discontinuers was responsible for the segmentation, $\chi^2(1) = 8.43$, $p < .01$. This measurable order effect tended to be perceptible by the participants themselves. While 22 % of the subjects indicated that motion sickness symptoms felt more intense on their second trial, 65 % rated the first exposure as the more critical day of measurement. The remaining 13 % had no preference and rated the two measurements as being equal in terms of motion sickness occurrence. In the second study, for instance, 43 % rated the first trial to be worse, whereas 24 % felt in the second exposure greater symptoms of motion sickness. 33 % did not recognize any difference between the two trials.

9.4 Duration of Exposure

Given that the FMS offers a fast and convenient way to frequently detect individuals' well-being, this value is suitable for investigating the progress of motion sickness during the test trial without creating severe interferences. In the original application, the FMS was obtained more often than it was conducted in the current four real-life driving investigations. A 5-minute section from break to break was obtained and assumed to be the best trade-off between sampling rate and avoidance of interruptions. The reduction of interruptions is important because visually and mentally demanding NDRTs had to be performed conscientiously and functioned as a trigger for inducing motion sickness symptoms.

Fig. 9-5 shows the results of the FMS values only for the completed trials within all driving examinations. It has to be mentioned that the samples were kept constant over time, but differed between the investigations. In particular in studies with high rates of discontinuation, as observed in the first investigation, a great number of subjects were rejected from this evaluation. Nevertheless, when taking a closer look at those individuals, the same characteristic pattern as it is shown in the following Fig. 9-5 becomes apparent.
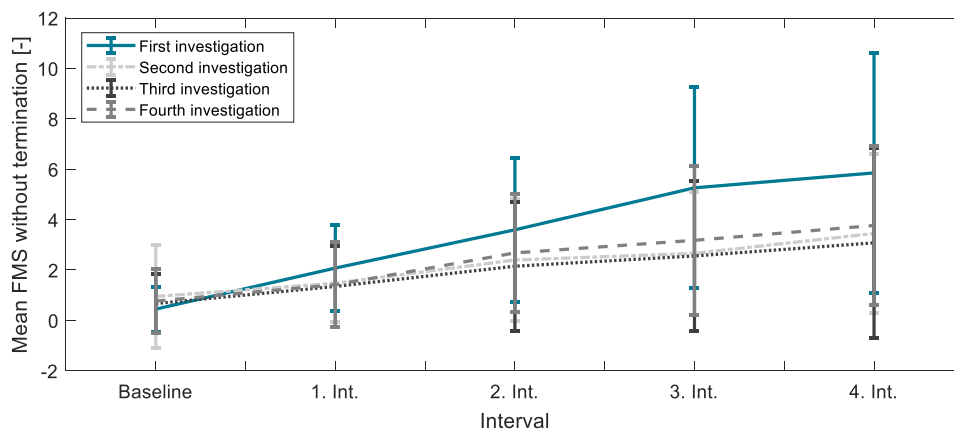
Fig. 9-5: Meta-analysis: increasing motion sickness severity per time-interval – all investigations.

An extensive variance of FMS evaluation within every interval of measurement is observed, whereas a uniform trend over time is discernible across all investigations. As a basic principle, it can be stated that the mean value increases with the duration of exposure, even if temporary plateaus are reached. A particular strong rise was recorded in the primary stages of the first investigation. The increase of FMS referenced to the baseline measurement for the first investigation is demonstrated below (see Tab. 9-2).

Tab. 9-2: Inferential statistics: FMS/interval – first investigation.

				Dependent Variable FMS (interval to baseline)		
	Observ.	b	df	t-value	p-value	r-value
First interval	27 (135)	1.63	4	2.04	.11	.67
Second interval	27 (135)	3.14	4	3.94	.02**	.87
Third interval	27 (135)	4.81	4	6.03	< .01***	.94
Fourth interval	27 (135)	5.41	4	6.77	< .01***	.95

*p<.1; **p<.05; ***p<.01

Even if the first stages do not show significant results, the effect size turns into relatively high values. Moreover, with every time interval, an increase in statistical performance can be achieved. Those results are clearly illustrated in the following Fig. 9-6.
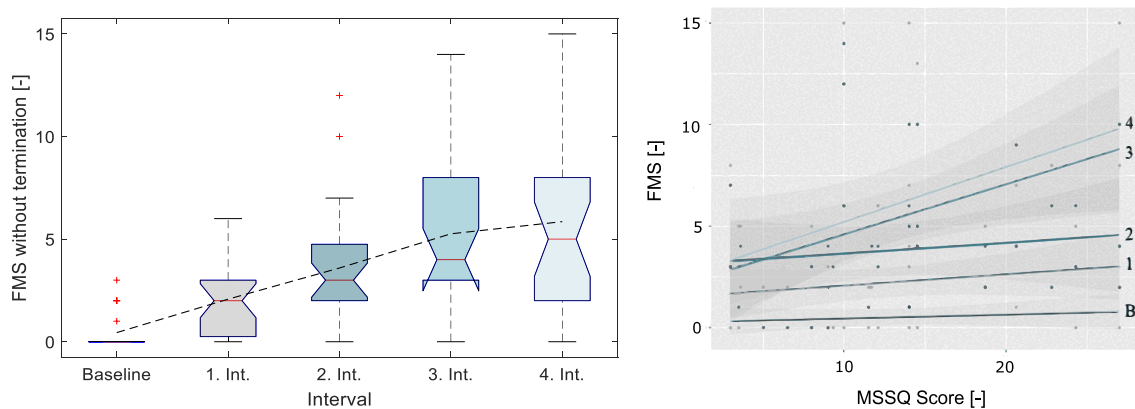
Fig. 9-6: Variance of FMS per time-interval (left);
regression between FMS and MSSQ score across all intervals (right) – first investigation.

By observing the boxplots, it appears that the interquartile range and, therefore, the variance of motion sickness symptoms across the sample increases with time. This observation is attributed to the inter-individuality in motion sickness susceptibility. Indeed, the effect of susceptibility, which was previously discussed in chapter 9.1, and the development of motion sickness over time is furthermore illustrated on the right side of Fig. 9-6. In fact, even if a limited number of samples are presented here, the impact of duration is more present in subjects who are exceedingly prone to experience motion sickness symptoms. Therefore, it is expected that the influence of time would have been even stronger within the subgroup of discontinuers. Due to the lack of data quantity, no additional analysis was made to tackle this observation.

9.5   In-Vehicle Temperature

The temperature was measured during the breaks to match the subjective rating of the participants´ well-being (FMS) with a discrete value of vehicle air and temperature conditioning. Although the premise was to keep the in-vehicle temperature constant during the trial and across the two measurements, certain fluctuations could not be completely eliminated. Regarding the following illustration, however, it is demonstrated that the mean temperature did not vary much over time. Only slight drifting especially occurred in the first stage. Moreover, except in the fourth investigation, the overall in-vehicle temperature showed a narrow temperature band from 22.1 to 23.8 °C across the first three investigations. The systematic difference in the average temperature between the fourth and the other investigations can be explained by the strong dissimilarities between the outside temperature. Only the last investigation was conducted in winter, while the remaining examinations took place in spring, summer, and fall. Analogous to the previous illustration, Fig. 9-7 summarizes the change of in-vehicle temperature over time for every driving experiment.
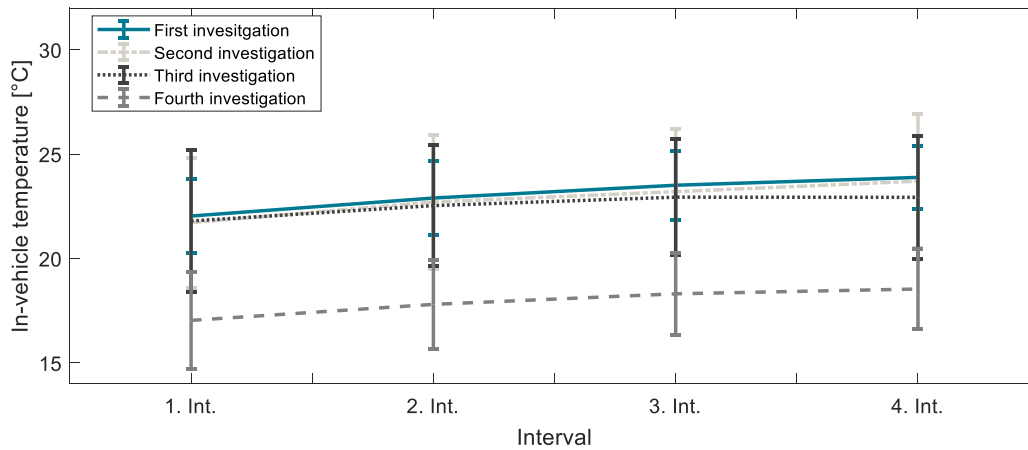
Fig. 9-7: Meta-analysis: change of in-vehicle temperature – all investigations.

Since the cabin temperature was not actively manipulated, no systematic comparison is possible and, thus, only indications can be derived from the integration of this parameter into the multi-level models. Due to the standardizing approach, it is hardly surprising that if any, only small effects were registered. Nevertheless, the results of the forward selection method within the second examination, in which the temperature was identified as the second-best single predictor for the MSAQ score, is presented in Tab. 9-3.

Tab. 9-3: Model comparison (LME): temperature as predictor of MSAQ score – second investigation.

	Dependent Variable MSAQ Score											
Model	(1)	(2)	(3)	(4)	(5)	(6)	**(7)**	(8)	(9)	(10)	(11)	(12)
Outside view		-8.05 (6.63)						-6.64 (5.69)				
MSSQ short			-.88** (.29)					.86*** (.29)	.88*** (.29)	.83*** (.29)	.91*** (.30)	.80** (.31)
Age				.39 (.26)						-.29 (.23)		
Gender female					2.62 (7.50)						-1.78 (6.58)	
Forward direction						2.02 (2.77)			2.02 (2.80)			
Interior temp.							**1.62* (.83)**					1.02 (.83)
Constant	29.75*** (3.38)	33.77*** (4.69)	13.85** (5.96)	44.58*** (10.46)	28.98*** (4.05)	28.74*** (3.69)	**-7.08 (19.27)**	17.67** (6.70)	12.84** (6.19)	26.06** (11.04)	14.05** (6.06)	-7.85 (18.71)
Observ.	48	48	48	48	48	48	**48**	48	48	48	48	48
Log Likl.	-197.6	-196.8	-193.5	-196.5	-197.5	-197.3	**-195.8**	-192.8	-193.2	-192.6	-193.5	-192.8
AIC	403.13	403.64	396.99	402.91	405.00	404.58	**401.59**	397.58	398.44	397.25	398.91	397.65
BIC	410.62	413.00	406.34	412.27	414.36	413.94	**410.95**	408.81	409.67	408.47	410.14	408.88

*p<.1; **p<.05; ***p<.01

Considering the previously mentioned limitations, the vehicle temperature requires further research since this parameter reveals the potential to cause less motion sickness. Until now, only presumptions could be obtained from the actual state of the data set, although, as shown above, statistical tendencies are identified. Those implications are congruent with previous findings outlined by Perrin et al. (2013), whereby it is to be stated that also interactions with time might be the reason for this promising result.

9.6   Distraction

As already indicated by the analysis of the fourth investigation, distraction had been argued to be able to influence motion sickness severity. Whether the distraction is likely to reduce or rather increase symptoms is highly debatable. Even if some researchers emphasize the positive effect on motion sickness treatment, concrete evidence on this topic is still rare (Bos, 2015; Keshavarz & Hecht, 2014). This is why the characteristics of NDRTs are analyzed in the current chapter in more detail.

Non-Driving-Related Tasks (NDRTs)

The subjects had to perform visually demanding NDRTs during their journey. Those predefined tasks had been selected from four different clusters. They were chosen, on the one hand, to guarantee a passionate execution and, on the other hand, to distinguish relevant characteristics of visually related motion sickness provocation. Already Isu et al. (2014) discovered a 2.7 times stronger expression of motion sickness when watching a video during the journey as it occurs in an ordinary ride without performing secondary tasks. Furthermore, the researchers maintain book-reading to be 25 % more nauseogenic than watching a movie. This general tendency can be supported by the conclusion of the subjective rating within the first investigation.

All subjects were interviewed after the first and second trial, on one hand, which secondary activity felt pleasant, and on the other hand, which one was the most unpleasant activity during the ride (multiple answers were allowed). Moreover, the respondents had to justify their decision (see Fig. 9-8).
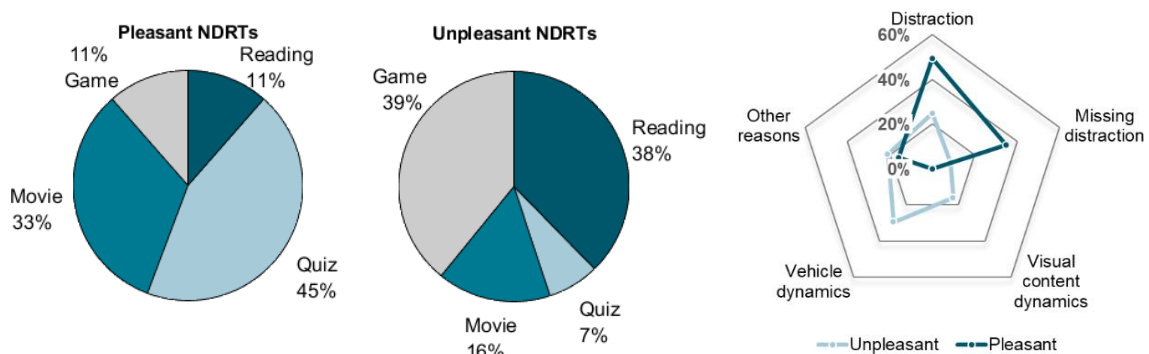
Fig. 9-8: Qualitative analysis on NDRTs: pleasant (left); unpleasant (middle); reasons (right) – first investigation.

When observing the preference in NDRTs, quite a uniform picture emerged, in which reading and gaming were identified as the activities with the highest ability to provoke motion sickness. Watching a movie and playing a quiz, by contrast, are two activities that are pleasant and less provoking in terms of motion sickness. The inconsistency regarding the impact of distraction on the severity of motion sickness is also visible in the responses of the participants and confirms previous evaluations of other researchers. Furthermore, vehicle motion is not only stated to provoke feelings of motion sickness but also affect the ability to perform visually demanding NDRTs by generating disturbing shaking conditions.

10 Performance and Objective Measures

Different kinds of tests were carried out to examine the influence of motion sickness on individual performance. Since the research focus was not placed on this part, the results of performance are only mentioned in passing. In the first investigation, the bdpq test was used, which had been conducted during the four breaks. In the subsequent investigation, a continuous measurement was performed during the trial, whereas another type of experiment was carried out in the third investigation, which was characterized by a pre-post comparison.

10.1 Bdpq Test

Analogous to the evaluation of driving duration, a complete and exhaustive data set of all time steps is necessary to evaluate the change in performance over time. Therefore, only the part of the sample that had completed both trials was considered in the upcoming illustrations of the bdpq test. Apart from the objective value, which is demonstrated on the left side of Fig. 10-1, perceived capabilities were assessed as illustrated on the right-hand side. Even if a significant decrease in performance occurred between the first and second interval of the objective measurement, $b = -8.65$, $t(59) = -0.92$, $p < .01$, $r = .45$, the integration of this parameter in the multiple regression did not substantially improve the model fit, $\chi^2(1) = 0.52$, $p = .47$.
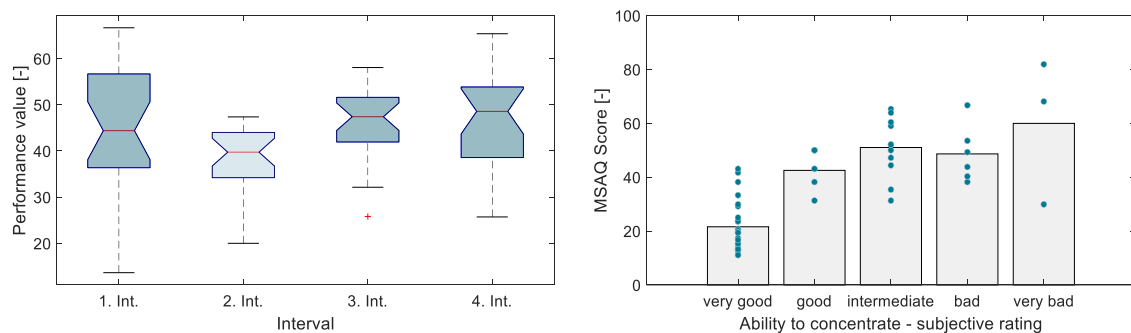
Fig. 10-1: Objective bdpq value across all intervals (left);
subjective assessment of concentration ability (right) – first investigation.

By contrast, the subjective ability to concentrate and perform the desired task, which was surveyed after the exposure, showed a strong negative correlation with the severity of motion sickness, $\chi^2(1) = 41.27$, $p < .01$ (see Fig. 10-1 - right).

In order to analyze the performance in more detail, the mean value of the bdpq test was calculated for the entire sample and treated as the dependent variable in the LME model. For one participant no measurement is available since the discontinuation occurred in the first round and the respective motion sickness expressions were so severe that no bdpq test could be carried out. As shown in Tab. 10-1 and by analyzing the respective mean bdpq value, no statistical significance occurred when including the severity of motion sickness in the LME model. Due to the aim of the first investigation, the sitting configuration was additionally included in the analysis. However, here as well, no improvement in the model fit could be observed.

Tab. 10-1: Model comparison (LME): bdpq-value – first investigation.

	Dependent Variable bdpq - value			
Model	**(1)**	(2)	(3)	(4)
Sitting upright		-1.23 (2.10)		
Forward direction			6.04 (3.57)	
MSAQ Score				-.05 (.07)
Constant	**40.88*** (1.86)**	41.52*** (2.16)	37.73*** (2.59)	42.73*** (3.21)
Observations	**49**	49	49	49
Log Likl.	**-180.65**	-180.48	-179.24	-180.39
AIC	**367.31**	370.95	368.47	368.79
BIC	**372.98**	380.41	377.93	376.35

*p<.1; **p<.05; ***p<.01

Nevertheless, because motion sickness severity and human posture are inextricably linked to each other, it is not surprising that at least the subjective ability of performance was significantly influenced by the backrest inclination during the first investigation, $\chi^2(1) = 27.27$, p < .01. In addition, Tab. 10-2 shows the odds ratio of the subjective performance level and its change as a result of the backrest angle (sitting position).

Tab. 10-2: Odds ratio: performance influenced by the sitting position – first investigation.

		95 % confidence interval of odds ratio		
	b (SD)	Lower barrier	Odds ratio	Upper barrier
Backrest angle	3.49*** (.80)	.01	.03	.13

R^2=.21 (Homer & Lemeshow), .43 (Cox & Snell), .46 (Nagelkerke), $\chi^2(1) = 27.27$, p < .01;   *p<.1; **p<.05; ***p<.01

10.2 Reaction Time During the Trial

The second performance test was carried out parallel with the visually demanding NDRTs during the second investigation. Given that the test track was split into different vehicle maneuvers with characteristic motion patterns, interaction with the body movement and, as a result, the reaction time within the trial is conceivable. Nevertheless, due to standardization, this misalignment is equivalent for all subjects during their two trials.

Tab. 10-3 illustrates the results of the LME models, in which several demographic and motion sickness-related parameters are integrated as predictors in the multiple regression calculation. Considering the maximum reaction time, as presented below, some kind of relationship to the peripheral MSAQ score appeared, b = 4.76, t(23) = -2.04, p < .1, r = .39. Extending the analysis by its mean value, a similar conclusion can be provided, b = 3.80, t(23) = -1.99, p < .1, r = .39. Turning to a more detailed observation, an even stronger relationship within the subgroup of discontinuers (n = 10) appears. Albeit there is a quite small sample size, between the mean FMS and the average reaction time a high effect size is to be reported, b = 88.29, t(3) = -2.67, p < .1, r = .83 (see Fig. 10-2 - left). Tendencies of learning effects occurred, when comparing the first and second trials with each other (see Fig. 10-2 - right).

Tab. 10-3: Model comparison (LME): max. reaction time – second investigation.

Model	(1)	(2)	(3)	(4)	(5)	(6)	(7)	(8)	(9)	(10)
				Dependent Variable Max. Reaction Time						
Outside view		-128.05 (114.73)								
Forward direction			-25.99 (72.07)							
MSAQ Total				3.24 (2.95)						
MSAQ Central					1.56 (3.15)					
MSAQ Gastro						1.55 (2.18)				
MSAQ Periph.							4.76* (2.33)			
MSAQ Sopite								3.62 (2.92)		
Mean FMS									17.49 (11.73)	
Max FMS										9.44 (9.10)
Constant	1292.9*** (58.27)	1356.9*** (81.13)	1305.9*** (69.05)	1196.5*** (105.12)	1248.9*** (106.04)	1241.5*** (92.80)	**1157.5***** **(89.43)**	1187.7*** (103.93)	1216.3*** (76.49)	1233.9*** (80.82)
Observ.	48	48	48	48	48	48	**48**	48	48	48
Log Likl.	-343.91	-343.28	-343.84	-343.29	-343.79	-343.66	**-341.99**	-343.17	-342.79	-343.37
AIC	695.82	696.56	697.69	696.58	697.59	697.32	**693.98**	696.34	695.58	696.73
BIC	703.31	705.91	707.04	705.93	706.94	706.67	**703.34**	705.69	704.94	706.09

*$p<.1$; **$p<.05$; ***$p<.01$

On average, the participants entered the button on the keyboard 60 ms earlier during the second trial. Due to the randomization within the examination setup, order effects of sitting direction can be excluded as the reason for this effect. When including all data points into a regression model to represent the development of performance over time, the previously described learning effect among others is included in the following function of $y = -1.5 \cdot x + 1,180$. Therefore, an average improvement of 30 ms from the beginning to the end of the trial could be observed, regardless of motion sickness, biological gender, sitting, or visual effects.
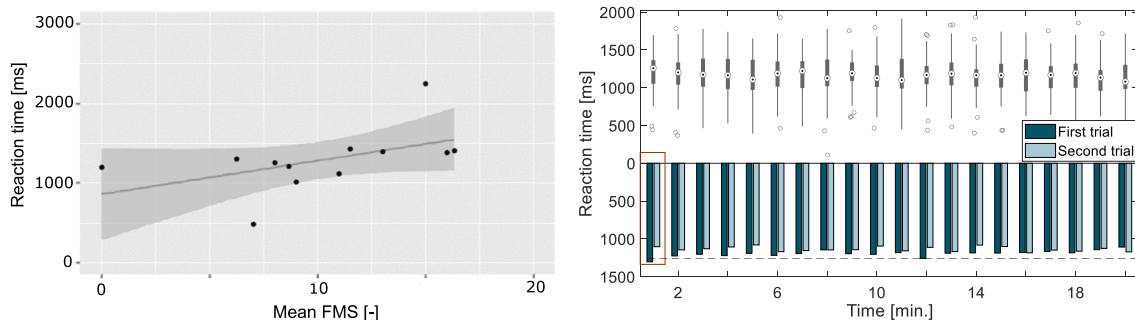
Fig. 10-2: Regression between reaction time and FMS for subgroup of discontinuers (left); reaction time per minute for both trials (right) – second investigation.

The first measurement of each trial is likely to be biased due to the potential risk of being extensively engaged in the original task and, as a result of that, mentally not aware of reacting to the sound signal. Indeed, sometimes subjects forgot about their mission to perform a reaction test during the journey, which led to extended neural processing as the acoustic signal sounded for the first time during the trial. This presumption is strengthened by two observations. Firstly, the greatest value of reaction time is recorded during the first minute of the primary trial. Secondly, the learning effect and the change in reaction time between the two trials show the highest potential at the beginning of the trial since here the hazard of oblivion is greatest. Observing this difference, it was revealed to be the best improvement of reaction time across the entire measurement.

10.3 Pre-Post Comparison

Given that in every trial the accuracy of the short-time vigilance test was rated consistently with 100 %, the calculation of an additional performance value had been deemed as unnecessary. Therefore, the reaction time was revealed as the only criterion for the pre-post diagnostics. As a reference, the overall average in reaction time across all subjects was determined with 417 ms ($\pm$ 79) in the pre-condition and 421 ms ($\pm$ 81) in the post-condition. Three parameters concerning motion sickness occurrence are demonstrated below in Fig. 10-3, applied with the median split method.
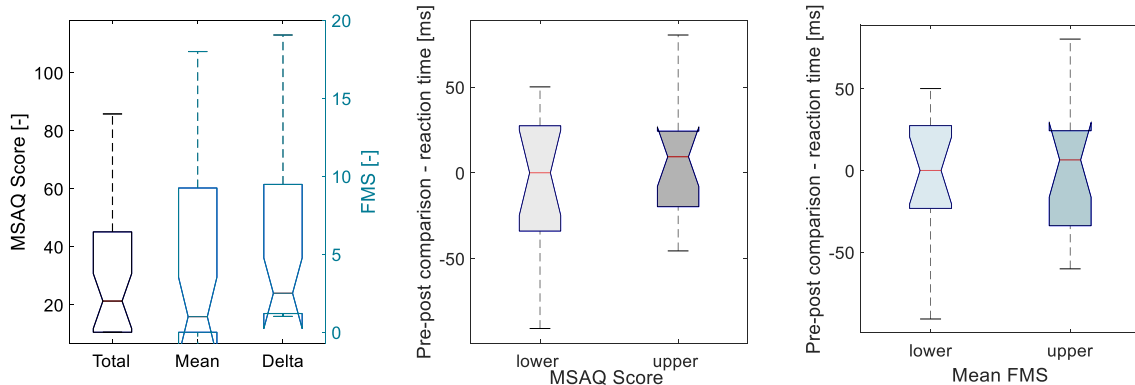
Fig. 10-3: Pre-post comparisons of reaction time: total sample (left); median split for MSAQ score (middle); median split for mean FMS (right) – third investigation.

It is shown that the change in reaction time slightly varied between the upper and lower median groups. A constant pattern of pre-post variation in reaction time was revealed for both parameters, in which an average difference of 14 ms for the MSAQ score and 16 ms for the FMS, as grouping factor, were observed. Based on this data, a negligible average improvement of only 3 to 4 % can be detected. Nevertheless, a consistent phenomenon could be discovered, especially when considering the distribution of reaction time across the different sitting conditions (see Fig. 10-4).

Despite the fact that it is reasonable to expect the upright sitting condition with the greatest deteriorations in reaction time, the reclined position is identified to be the only condition with a decrease in performance when comparing the pre-post results. However, when considering the median subgroups, a uniform negative correlation between motion sickness severity and reaction time was identified.
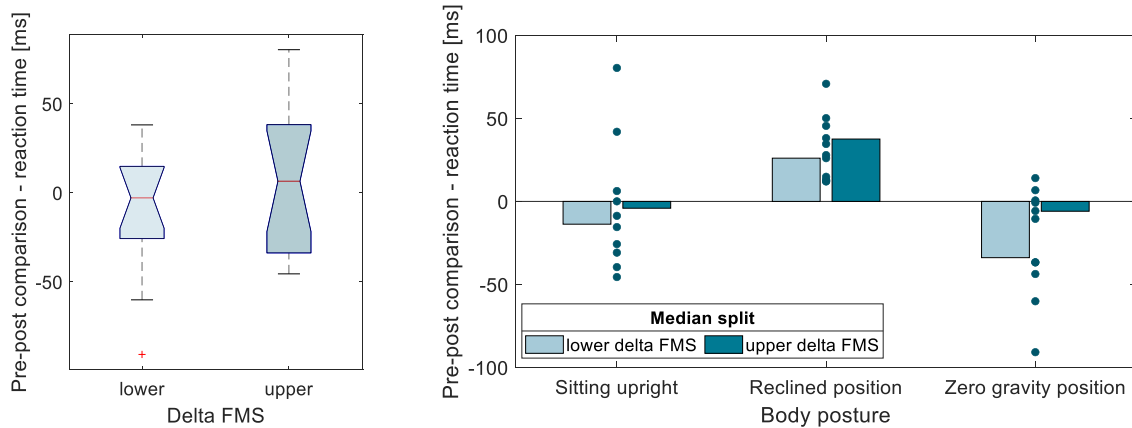
Fig. 10-4: Pre-post comparison of reaction time: median split for delta FMS (left); median split for delta FMS across all sitting conditions (right) – third investigation.

In principle, there are two opposing effects, which have to be considered when interpreting the above-shown results. On one hand, learning effects support the individual achievement potential, while on the other hand, raising expressions of motion sickness and exhaustion are likely to deflate the ability to perform in a focused and clear-minded manner. Overall, the external validity within this conclusion is undermined since the test sample is quite small and the short-time vigilance test was carried out as a pure generic approach. Even though, with positive reinforcement through previous investigations, some tendencies of loss in performance due to motion sickness occurrence are perceived.

10.4 Discussion and Synopsis of Performance Measures

Concerning the first investigation, the objective performance value, even if only operationalized through the bdpq test, is revealed to be incongruent with the perceived performance level. As a consequence, in situations of severe motion sickness, subjects might be still able to concentrate, at least for a short period of time, and fulfill tasks in a reasonable manner. Considering the short-time vigilance and reaction test, the impact of motion sickness occurred, which supports the subjective estimation on the loss of individual performance with increasing malaise. Nevertheless, only slight differences were recorded between the subgroups with strong and less motion sickness symptoms. Although the participants practiced the performance tests during the preparation phase, learning effects during the trials are discernible by the examiner. In any event, within this context, it has to be mentioned that these distinctions retain their validity only in these specific use cases. Performance is a multivariate parameter that is comprised of several dimensions which makes general conclusions exceedingly difficult.

10.5 Physiological Measures

To investigate the ability of motion sickness objectification, partial regressions between each of the six physiological parameters recorded in the first examination and the expression of motion sickness severity were obtained. As a dependent variable, the MSAQ score was chosen while the mathematical model was performed twice with and without controlling the variance of further variables, such as the subject´s individuality.

An average value for the baseline measurement as well as for each of the four intervals was determined. Likewise, with additional control of the time factor, the characteristics of the parameters were checked at all times with respect to their relationship with the respective FMS value. The resulting correlation coefficients and their p-values did not show any significance. Finally, the difference between the baseline value and the last recorded value was calculated for each test subject. The consecutive delta value was then checked for a significant relationship as follows (see Tab. 10-4 and Fig. 10-5).

Tab. 10-4: Correlation analysis of physiological parameters and MSAQ score – first investigation.

Stat. parameters	Δ HR	Δ SDNN	Δ RMSSD	Δ LF/HF	Δ B	Δ SDBB	Δ T
			Dependent Variable MSAQ Score				
Correlation	$r_S=.27$	$r_S=.05$	$r_S= -.06$	$r_S= -.11$	$r_S= -.02$	$r_S=.06$	$r_S=.45$
p-value	$p=.06^*$	$p=.72$	$p=.68$	$p=.44$	$p=.88$	$p=.66$	$p<.01^{***}$
p-value (par. cor.)	$p=.03^{**}$	$p=.35$	$p=.72$	$p=.20$	$p=.81$	$p=.32$	$p=.02^{**}$
Observation	47	47	47	47	47	47	40

$^*p<.1; ^{**}p<.05; ^{***}p<.01$
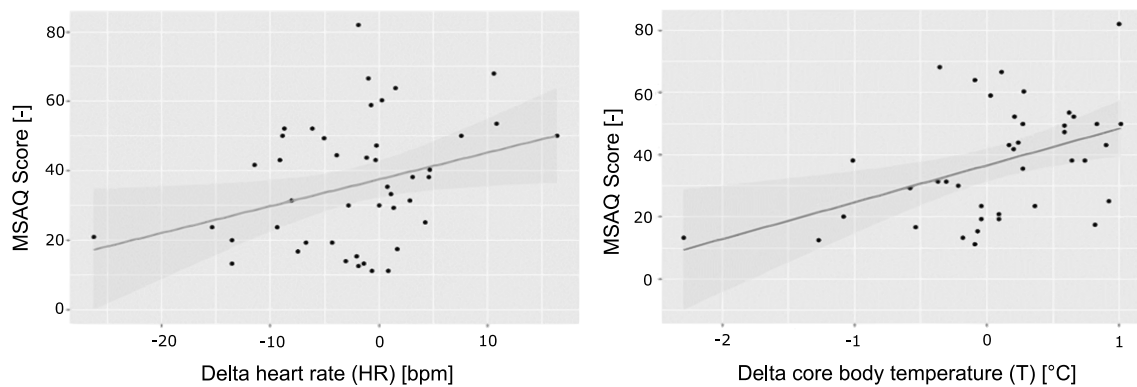
Fig. 10-5: Regression with MSAQ score: delta heart rate (left); delta core temperature (right) – first investigation.

There was a moderate but significant correlation between the amount of pre-post comparison of the *core body temperature* (T) and the MSAQ value, r = .45, p < .01. In addition, a tendency in cardiovascular parameters i.e., the delta *heart rate* (HR), was also identified as relevant, r = .27, p = .06. When applying a partial linear regression, given the variables individual susceptibility and subject-ID, slight changes in p-values can be observed for both parameters. While the statistical quality criteria increased with heart rate (p = .03), the p-value of the core body temperature decreased (p = .02).

Due to the promising results collected in the first investigation, ECG data were recorded in the latest real driving experiment as well. Consequently, further analyses on HR in terms of motion sickness prediction were conducted. The average baseline HR over all samples was 72 (± 10) bpm while the latest measurement shows an average reduction in HR of 0.7 (± 5) bpm. Regarding the previous investigation, the general conclusion can be supported, in which greater motion sickness expressions lead to higher changes in heart rate (here: inverse). This observation, however, does not show a significant effect for the total sample, $\chi^2(1) = 2.53$, p = .11 (delta FMS), nor for the subgroup of non-discontinuers, $\chi^2(1) = 0.13$, p = .72 (delta FMS) within the hierarchical model construction.

Considering the subgroup of discontinuers, this relationship turned out to have great significance for the FMS parameters, $\chi^2(1) = 9.12$, $p < .01$ (see Tab. 10-5). The contrast analysis specified the model improvement by the following parameters: $b = 1.5$, $t(8) = 3.25$, $p < .01$, $r = .75$.

Tab. 10-5: Model comparison (LME): delta HR of discontinuers – fourth investigation.

	Observ.	AIC	BIC	Log Likl.	L.Ratio	p-value
		Dependent Variable Delta HR - only discontinuers				
Baseline	18	99.69	104.14	-44.84		
+ delta FMS	**18**	**92.57**	**79.92**	**-40.29**	**9.12**	**< .01*****
+ MSAQ	18	93.68	99.91	-39.84	.89	.34

*p<.1; **p<.05; ***p<.01*

In the third investigation, pulse and oxygen saturation were measured four times during and one time before the journeys. Due to some technical problems, just a few data sets had to be excluded from the analysis. Since the method of pre-post comparison has been proven to be most suitable for the physiological comparison in terms of motion sickness prediction, delta values between the baseline and the latest measurement were calculated. Here, the median split method with the criterion of motion sickness severity was obtained and integrated into an LME model with the two physiological parameters as dependent variables. As a result, neither for the pulse, $t(19) = 0.92$, $p = .39$, $r = .21$, nor for the oxygen saturation $t(18) = 0.01$, $p = .92$, $r < .01$, the integration of the MSSQ median split subgroups showed a significant effect or increased the model fit.

Then, the mathematical models were extended by the grouping factor of sitting configuration, in which the MSAQ median split method was applied as well. The following Fig. 10-6 illustrates the change in oxygen saturation and pulse concerning the different body postures (boxplots). For each position, a comparison between the two subgroups of the median split method (bar plots) is shown.
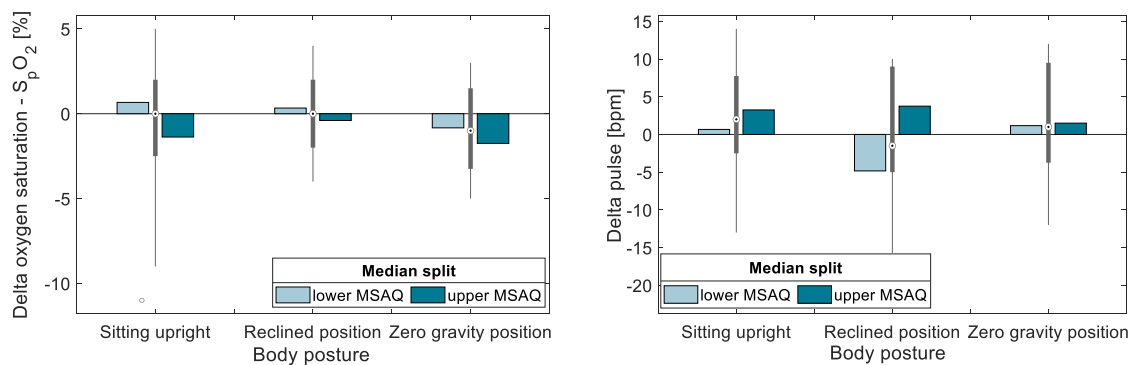
Fig. 10-6: Median split method: delta oxygen saturation (left); delta pulse (right) – third investigation.

When evaluating the oxygen saturation, a characteristic pattern is recognizable, in which the subjects, who show less motion sickness, are in comparison characterized with a greater reduction in the pre-post comparison throughout all conditions. This behaviour is also observed within the variation of pulse, here, however, with an inverse direction.

In the upright sitting position as well as in the reclined posture the strongest differences between the two subgroups are visible, whereas in the zero-gravity position only slight tendencies occurred. Tab. 10-6 summarizes the results of both physiological parameters and their difference across the three body postures and the motion sickness severity.

Tab. 10-6: Inferential statistics: delta oxygen saturation and delta pulse – third investigation.

Sitting position	Observ.	Dependent Variable Oxygen Saturation (pre-post comparison)				
		df	t-value	p-value	Bonfer.	r-value
Sitting upright	11	8.7	.89	.40	.99	.29
Reclined position	11	8.2	.44	.67	.99	.15
Zero-gravity position	9	3.4	-.07	.94	.99	.04

Sitting position	Observ.	Dependent Variable Pulse (pre-post comparison)				
		df	t-value	p-value	Bonfer.	r-value
Sitting upright	11	4.6	-.50	.64	.99	.23
Reclined position	10	8.0	-1.53	.16	.49	.48
Zero-gravity position	9	3.4	-.22	.84	.99	.12

*$p<.1$; **$p<.05$; ***$p<.01$

As a result of the small sample size, no statistical significance could be observed. Considering the Bonferroni post hoc evaluation, only the variation of the pulse between the two subgroups within the reclined posture does not show a p-value of .99. Considering the r-values, this observation turned out to be a medium effect. However, besides the descriptive analysis, no further reliable conclusions can be made by this limited data set.

10.6 Behavioural Measures

In the first investigation, the behaviour of the participants during the journey was not only monitored but further integrated into a separate analysis with the aim of predicting and objectifying motion sickness. Fig. 10-7 demonstrates the frequency of individual behaviour patterns across all subjects that occurred during the journey. Here, three characteristics are predominantly visible: audible exhalation, looking up and away from the task, and swallowing loudly.
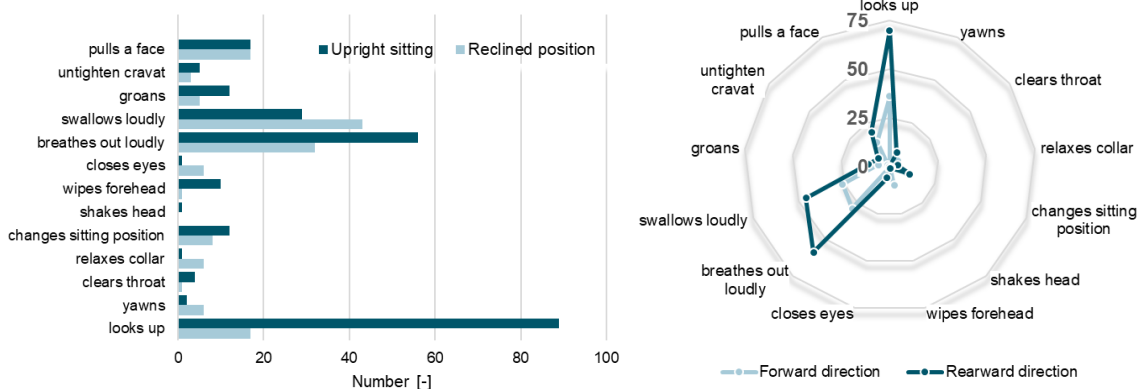
Fig. 10-7: Qualitative analysis: behavioural measures clustered upon backrest inclination (left); clustered upon sitting direction (right) – first investigation.

For a more detailed analysis, an individual behaviour score was calculated for each person. Then, potential influences of seating conditions and duration of exposure were examined by applying an LME model. The results are presented in Tab. 10-7.

Tab. 10-7: Model comparison (LME): score of behaviour – first investigation.

Model	Dependent Variable Behaviour Events				
	(1)	(2)	(3)	(4)	(5)
Time		.44[*] (.23)			.44[*] (.23)
Upright sitting			1.19[*] (.65)		1.19[*] (.66)
Forward direction				-.26 (.72)	
Constant	**5.24[***]** **(.34)**	4.14[***] (.67)	4.63[***] (.47)	5.42[***] (.58)	3.53[***] (.74)
Observations	**140**	140	140	140	140
Log Likl.	**-364.97**	-363.13	-363.37	-364.90	-361.54
AIC	**737.94**	736.27	736.74	739.80	735.07
BIC	**749.70**	750.98	751.44	754.51	752.72

*p<.1; **p<.05; ***p<.01

Although no statistical significance could be identified, strong tendencies of time, $\chi^2(1) = 3.67$, p = .06, and seating position, $\chi^2(1) = 3.20$, p = .07, became apparent. In consequence, when sitting in the upright position, events within the behaviour cluster increased with time, whereas under time control, the correlation to motion sickness severity did not show any significant result, p = .76, r = .03 (MSAQ score). Therefore, it is not clear whether the increase of behavioural patterns occurs as a result of exhaustion, sitting posture, or is associated with motion sickness. Also, here, it is not explicitly clear if the behavioural observations are an expression of motion sickness or even more a strategy to avoid appearing maladies.

11 Ride Simulator – Comfort and Biomechanics

As previously mentioned, countermeasures to avoid motion sickness do not necessarily imply general motion comfort. The endorsement of anti-motion sickness guidance e.g., the reclined posture, therefore, had to be carried out through additional experiments in which user acceptance and individual well-being were an integral part of the investigation[5]. Even though the multibody simulation does give a proper insight about longitudinal head dynamics under strong and quasi-static force, the behaviour of head motion under stochastic shaking conditions, such as those occurring during constant travel scenarios with steady speed characteristics, has so far not been sufficiently taken into account. Therefore, a more holistic approach is mandatory to understand the general influence of backrest rotation on head dynamics. To meet both research questions, a comparative investigation involving generic motion patterns and real-life driving data was executed. Within the scope of work, objective measures as well as subjective parameters were collected during a simulator investigation, in which head dynamics and perceived comfort levels were captured.

---

[5] The experiment was conducted with the assistance of T. Koch (2020) as part of his research project.

11.1 Experimental Setup

The Ride Simulator of Mercedes-Benz AG was used to investigate weak to medium stochastic and periodic stimuli as well as road excitation in order to evaluate their influence on the subjective feeling of comfort. In comparison to various studies that examine seat configurations concerning automated or autonomous driving in static laboratory environments (Reed et al., 2019a; Y. Yang et al., 2019), the Ride Simulator offers the possibility to investigate comfort perception under dynamic and reliable conditions. As it is illustrated in Fig. 11-1, the Ride Simulator comprises a hexapod system with a platform and seat bracket on top. The control system allows, within the kinematic limits, a wide range of movements in all rotational and translational directions (6 DoF). As a result, through simultaneously multi-axial actuator control, longitudinal, lateral, and vertical motion as well as roll, pitch, and yaw rotation is educible.
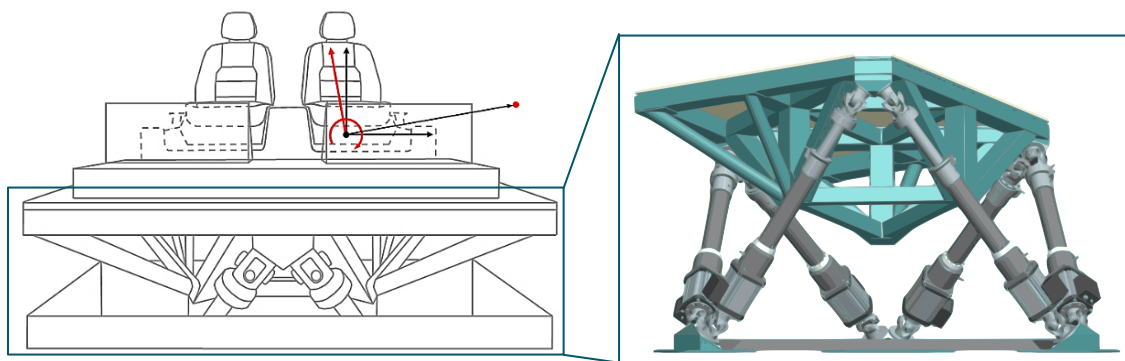
Fig. 11-1: Technical setup: hexapod and platform – Ride Simulator.
Modified from Daimler AG (2020)

Accelerations were measured at the participant´s head, headrest, and simulator platform using the already described *Xsens MTw* tri-axial sensors with a sample rate of 75 Hz. The coordinate system was congruent to the previously outlined SAE J182 and is illustrated in Fig. 11-2. The head orientation was calibrated to the vehicle coordinate system, regardless of which body posture was taken. From this initial position, the reference values were frozen to a head-fixed coordinate system. The platform sensor was attached to the rolling pole, which was located in the center of the seat bracket.

Fig. 11-2: Experimental setup incl. coordinate-system – Ride Simulator.
Bohrmann, Koch, et al. (2020)

11.1.1 Postprocessing of the Recorded Acceleration Data Set

Data processing was mandatory since transmission errors of constant deviation, data drift, and outliers occurred within the data recording. To remove potential baseline noise, which is represented through data drifting and offset values, a high-pass filter was used analogously to the investigations of Kreiman and colleagues (Kreiman et al., 2001; Kreiman et al., 2010). In their work, an elliptical high pass filter with 60 dB stopband attenuation was used. Since low frequencies are particularly relevant for head motion and kinetosis, the target was to find the minimum corner frequency at which a suitable data quality is achieved. The sensor drift had already been eliminated by a value of 0.01 Hz. Fig. 11-4 illustrates this effect since the constant offset of approximately 0.5 m/s^2 just as the data drift of -0.3 m/s^2 over a period of 70 s were eliminated by the application of the high pass filter. Outliers, as the third relevant error coming along with the transmission of the sensor signals to the measuring station, had to be addressed by another processing method. Given that this type of error only affected individual time steps, the mean value of the adjacent time increments was used for replacing an incorrect value. This adjustment was important to ensure equal length vectors for the consecutive data calculation. To guarantee a reliable detection of all outliers without picking wholesome data points, a data processing test described by Grubbs was used. As a prerequisite for the application of this method a normal distribution of the data set is required (Grubbs, 1969).

As a representative, the following Fig. 11-3 shows the head acceleration in the lateral direction of a randomly picked participant and the respective distribution highlighted with the model fit parameters. As the criterion for the evaluation of the most probable distribution the log-likelihood and the AIC parameters (see chapter 5.5.1) were determined. The respective MATLAB function (fitmethis) had been chosen and proven to fulfill the required properties (Castro de, 2020). Since in most cases, white noise was programmed as the input characteristic, it is not surprising that all relevant data sets were proven to show a normal distribution.
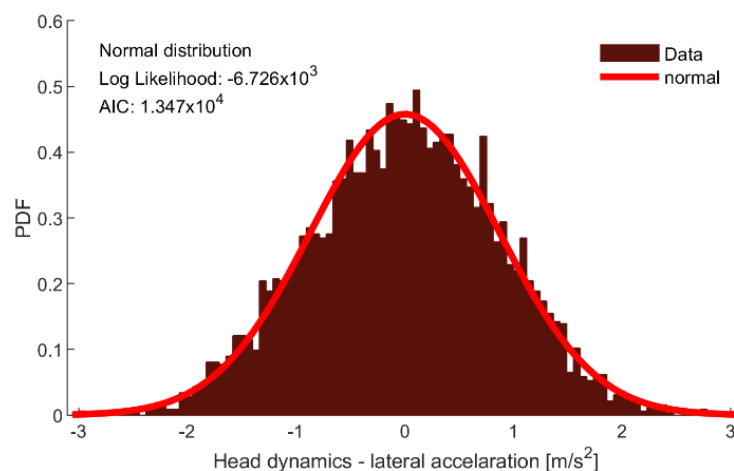
Fig. 11-3: Exemplary histogram of recorded head motion in lateral direction – Ride Simulator.

The total data processing including the outlier analysis by Grubbs and the application of the high pass filter is demonstrated in Fig. 11-4. It is shown that every outlier is detected (black) without erroneously recognizing regular values.
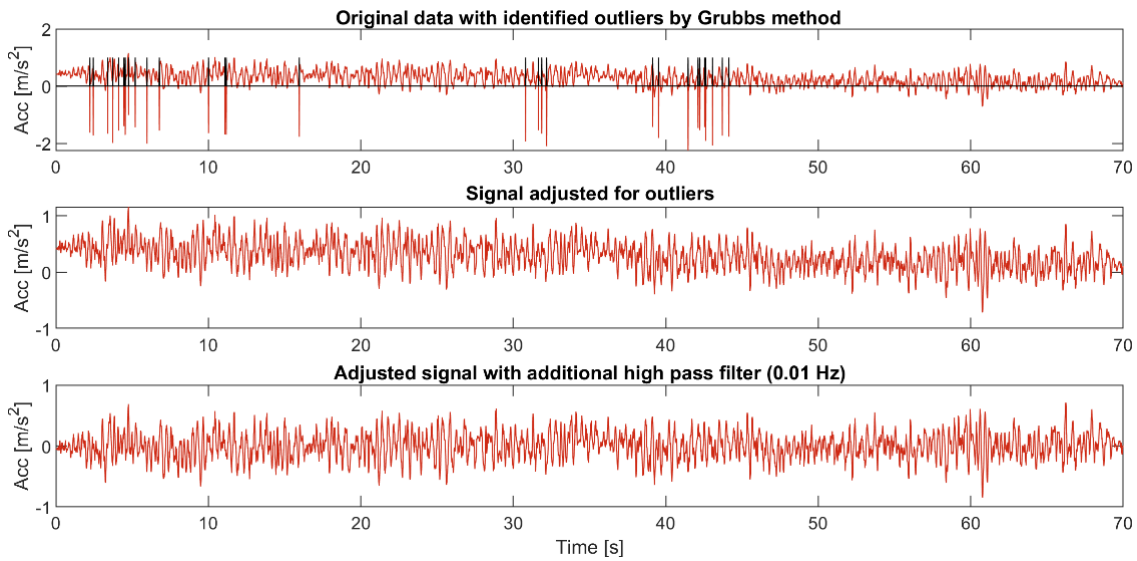
Fig. 11-4: Data post-processing – Ride Simulator.

11.1.2 Motion Stimuli

The predominant motion pattern applied during the ride was characterized as a uniaxial noise signal. While the linear motion was obtained in all directions, isolated angular forces were only conducted in the longitudinal axis (roll motion).

To identify interaction effects across different motion characteristics, multiaxial forces (6 DoF) were integrated into the routine as well. The noise signals were excited in a frequency range of 0.2 to 25 Hz with three consecutive amplitudes of 0.25 m/s^2, 1 m/s^2 just as 2 m/s^2. The frequency range was chosen due to the Nyquist-Shannon-theorem (Beucher, 2015, p. 299) that determines the minimum required sample rate of the data recording. For the current application, this setting seemed to be sufficient since, for instance, Eckstein (2014b, p. 7) postulated that unevenness of a road surface leads to vertical excitation up to 30 Hz.

To investigate possible overlapping effects of head and vehicle motion, which had been recognized in the real-life driving examinations, multi-sine signals were additionally obtained. However, those were only applied in the lateral direction and comprised of superimposed sine signals between 0.5 and 15 Hz with amplitudes of 0.5 m/s^2, 1 m/s^2 as well as 2 m/s^2. Besides the synthetic generated motion pattern, micro, meso, and macro shaking stimuli, which were recorded during the ride of a Mercedes-Benz E-class (W213) at the test track in Sindelfingen, finalized the test procedure and, thus, the overall motion sequences. This realistic motion pattern of a rough country road allowed a reasonable calculation of the MSDV and increased the capability of an immersive comfort rating.

The following Fig. 11-5 outlines this procedure by illustrating the main parts of the experienced motion input. The data were recorded at the platform of the Ride Simulator and considered the hereafter referred colour-related coordinate system. The brightness of colour represents the three different kinds of amplitudes, whereas the colour itself indicates the direction of motion.
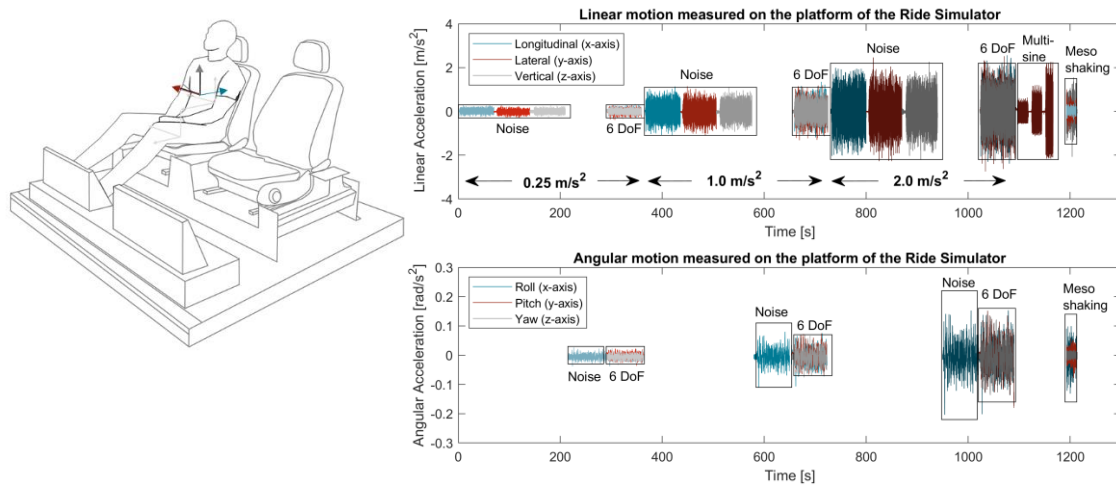
Fig. 11-5: Recorded platform motion – Ride Simulator.
Left: modified from Daimler AG (2020)

Angular and linear motion is pictured in different plots to improve the clarity of the presentation. In reality, both diagrams have to be superimposed to represent the actual experience produced during the trial on the Ride Simulator. Every ride lasted 21 minutes and had to be carried out several times in the repeated measures design by each participant.

11.2 Participants

In November 2019, 16 healthy subjects aging on average 36.6 years (±11.8) participated in the Ride Simulator study carried out at the Mercedes-Benz Driving Simulation Center. Within the acquisition of participants, the sample was preselected by the criterion of body height (1,792 ± 33.6 mm), to decrease anthropometry effects. The preselection aimed to represent the average 50th mannequin (1,813 - 1,817 mm) to identify clear biomechanical inferences. Furthermore, care had been taken to ensure that no participant had any history of vestibular or spinal disorders. In fact, from the original panel of 17 subjects, one participant did not complete the investigation due to a potential back injury.

The participants took part in a randomized three-step study design, in which the test trials were conducted immediately after each other. For the purpose of the investigation, three different sitting configurations were supposed to be evaluated by two females and 14 males. The first posture was defined by the standard driving position (23° backrest angle). The reclined posture showed a backrest inclination of 42°, which had already been investigated by the multibody simulation and is the most supine seating position available in the rear of actual series vehicles – known as executive seating position. The third configuration was influenced by the previous driving experiment and represents the main characteristics of the adjusted zero-gravity position (62° backrest angle). Here as well, just as applied in the experimental vehicle, the footrest was positioned significantly lower compared to the original recommendation of the NASA joint angles.

Fig. 11-6 illustrates all three sitting configurations utilized during the Ride Simulator examination.

Fig. 11-6: Experimental condition: sitting postures – Ride Simulator.
Bohrmann & Bengler (2020)

The participants took their place on a C-class (W205) driver's seat and were instructed by the examiner to hold their heads in a comfortable and stable position throughout the entire duration of the test trial. During the ride, NRDTs were retained as well, but, in contrast to the previous investigations, not with the objective to induce nauseogenic stimuli. Here, the purpose was to avoid involuntary head movements. Therefore, the subjects watched a movie on a tablet, which was positioned analogous to series screens on the backside of a driver or co-driver seat.

11.3 Subjective Comfort Rating

Before discussing the results of the participant´s evaluation, the generated motion stimuli have to be classified in terms of motion perception. Here, concerning chapter 3.6.1, the ISO 2631 with its comfort-related frequency weighting function W_k was utilized. Tab. 11-1 summarizes the itemized results according to the applied motion characteristics.

Tab. 11-1: Evaluation of applied motion stimuli: motion perception (ISO 2631) – Ride Simulator.

Motion Perception Frequency weighted acceleration a_{wT} [m/s^2] – ISO 2631 (W_k)										
[%]	Noise (u)	Perception	Noise (m)	Perception	[%]	Multisine	Perception	D	Shaking (me)	Perception
25	0.045	noticeable	0.078	noticeable	50	0.170	strongly noticeable	x	0.060	noticeable
100	0.200	strongly noticeable	0.345	a little un-comfortable	100	0.340	a little un-comfortable	y	0.120	strongly noticeable
200	0.400	a little un-comfortable	0.690	fairly un-comfortable	200	0.680	fairly un-comfortable	z	0.250	strongly noticeable

D = direction, u = uniaxial, m = multiaxial, me = meso

When observing the uniaxial noise signals, the same frequency band was applied in each of the three axes. In fact, the classification of the frequency-weighted platform acceleration is independent of the direction of motion. Thus, only three values representing the excitation strength were returned for the uniaxial noise signals. Since the same motion pattern was simultaneously applied to design the 6 DoF excitation, the root of the sum of the squares in all directions was obtained to calculate the above-shown frequency weighted r.m.s. value. Given that the multisine application was exclusively implemented in the lateral direction, here as well, only one parameter per amplitude is presented. Finally, the recorded real-life vehicle accelerations of a country-road journey were analyzed, even though, only the intermediate intensity (meso shaking) is illustrated here.

Each participant rated their feeling of comfort after being exposed to all three seating configurations. The overall rating of the three postures was carried out on a 5-point Likert scale from one to five, whereas five implies an optimal feeling of comfort. As a result, an average comfort value of 2.6 was achieved in the standard driving posture, whereas in the reclined position the average value reached one point higher. The best comfort rating occurred in the lying, or also known as the modified zero gravity position, with an average value of 4.3. In short, under dynamic conditions, increasing backrest angle leads to improvements in the subjective level of comfort. When applying the Nemenyi post hoc evaluation, a significant effect of posture and, consequently, backrest inclination could be observed between the upright and lying position, $\chi^2(2) = 12.5$, p < .01.

As previously mentioned, user interaction might change with an increasing degree of automation. The vehicle is becoming a new living space and the driver's seat is changing in a way that a wide range of NDRTs is going to be enhanced and supported. Considering various restrictions, such as occupant´s protection, it is important to offer to the user the best possible seat configuration for the respective application. For this purpose, NDRTs that are expected during a highly automated or autonomous journey were investigated in more detail. In fact, for each of these activities, the subjects had to choose from the three experienced seat configurations the most suitable one for the respective task. The results of the evaluation are shown in Fig. 11-7, while the associated colour-coding is defined as follows:

- standard driving position (gray),
- reclined sitting position (dark petrol), and
- lying position (light petrol).
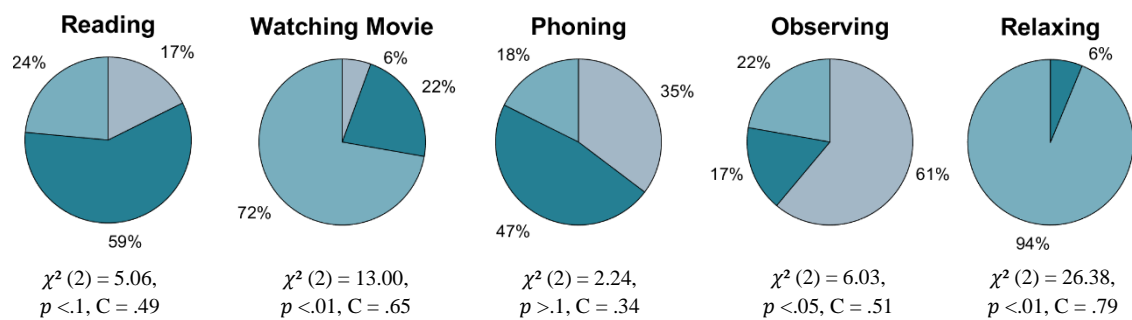
Fig. 11-7: Qualitative analysis: preference on seat configuration when performing NDRTs – Ride Simulator. Modified from Bohrmann & Bengler (2020)

An upright inclination of the backrest angle is preferred for activities in which the user seeks interaction with the outside world, for instance when observing the environment. In cases of passive activities, such as relaxing or watching movies, the preference is reversed. Here, supine postures are preferred. When analyzing reading, a compromise seems to exist between the everyday habit of being in an upright sitting position and the reclined posture, which leads to some kind of head stabilization under dynamic conditions. When talking on the phone, the results are diverse without statistical significance or clear tendencies in preferring one of the three seating configurations.

11.4 Objective Measures to Quantify Head Dynamics

When evaluating the data set, three main research questions were addressed to identify characteristic motion patterns:

- How much energy (force) is transferred from the platform to the subject's head?
- How much time does it take until the excitation runs from the platform to the head?
- Which frequencies are amplified or dampened by the oscillating system?

For each research question, specific analytical methods were utilized. The results are clustered into the type of motion excitation and are presented in the upcoming chapters.

11.4.1 Noise signal

To achieve a proper system identification of the human body, the uniaxial motion stimuli were initially observed. Due to technical issues, only 11 complete data sets were obtained for the objective analysis. Nevertheless, characteristics of head motion could be observed.

Root Mean Square

The mean values across all participants are intended to find differences between the three sitting conditions in the average amount of acceleration that is observed. The r.m.s. evaluation, as one of the most extensively used methods in data analysis, represents the equivalent of the transmitted energy between the input and output signal. The left part of the following Fig. 11-8 illustrates the mean r.m.s. values across all uniaxial head motion responses for one representative subject. It is striking that this subject experienced the highest average acceleration in the lying or at least reclined position, while the sitting posture showed constantly the lowest r.m.s. value. Extending the analysis from one subject to a more representative picture, the right side of Fig. 11-8 presents the vertical head response of the intermediate and strong excitation condition for the total sample.
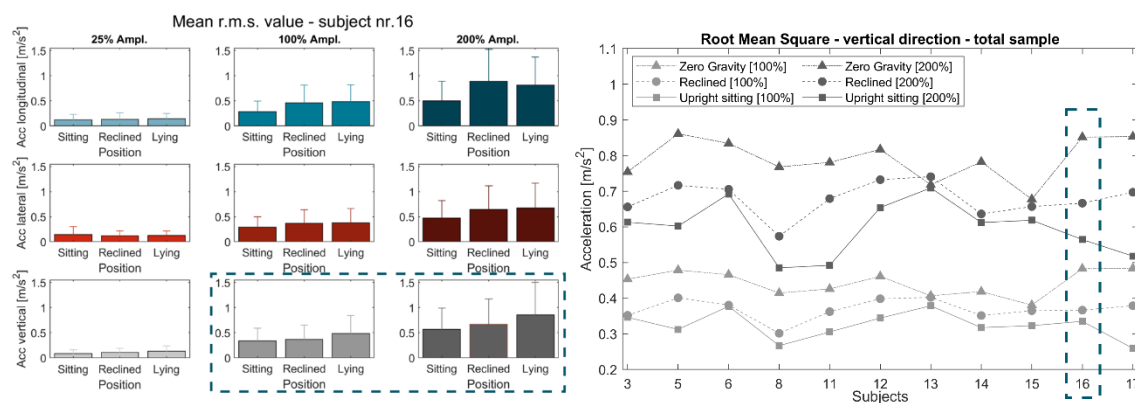
Fig. 11-8: Exemplary illustration of mean r.m.s. head motion (left); mean r.m.s. of vertical head motion for all subjects (right) – Ride Simulator.

Observing the sample-specific mean r.m.s. values, strong inter- and intraindividual variations can be recognized, whereas the overall behaviour across the sitting conditions revealed a unified picture. Indeed, humans showed within the manipulated position and excitation intensity similar reactions when considering the behaviour of the entire group.

Superimpose those mean values for all subjects, the bar plots within Fig. 11-9 emerge.

*p<.1; **p<.05; ***p<.01
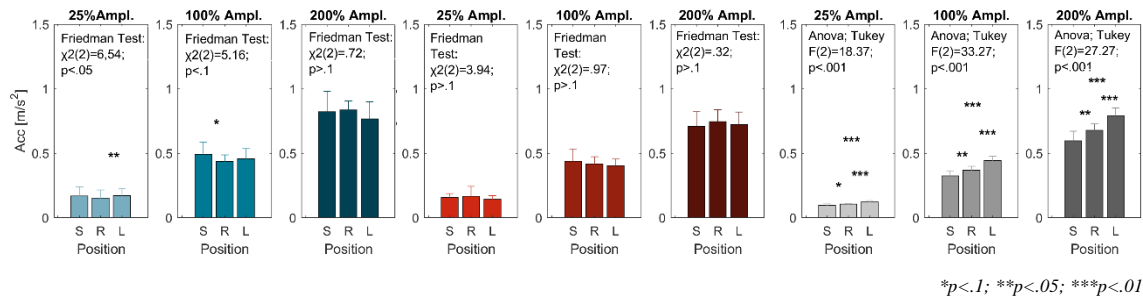
Fig. 11-9: Cumulative mean r.m.s. head motion – Ride Simulator.

In general, stronger excitations led to a significantly higher, but also non-linear reaction of the head acceleration. Across all excitation strengths, the comparatively highest average r.m.s. value was located in the longitudinal direction. Furthermore, neither in longitudinal nor in the lateral direction can substantial differences between sitting postures be observed. In the vertical direction, however, a significant impact of backrest inclination on the average r.m.s. value is visible. Both assumptions presupposed a constant intensity of motion stimuli.

Cross-Correlation

The cross-correlation has already been described in chapter 3.6.2 and addressed the research question according to the transfer time of the human-seat interaction system. As a result, two key parameters were deduced from this calculation. Firstly, the maximum correlation value r_{xy}, which indicates the uniformity between the platform signal and the head motion response. The second important value reveals the time step τ, in which the maximum correlation value occurred. This respective time delay represents the transmission period between the input and output signal. Fig. 11-10 shows a clear depiction of the individual results of the two values. The columns represent the three seating positions, while the lines indicate the strength of the stimulation.
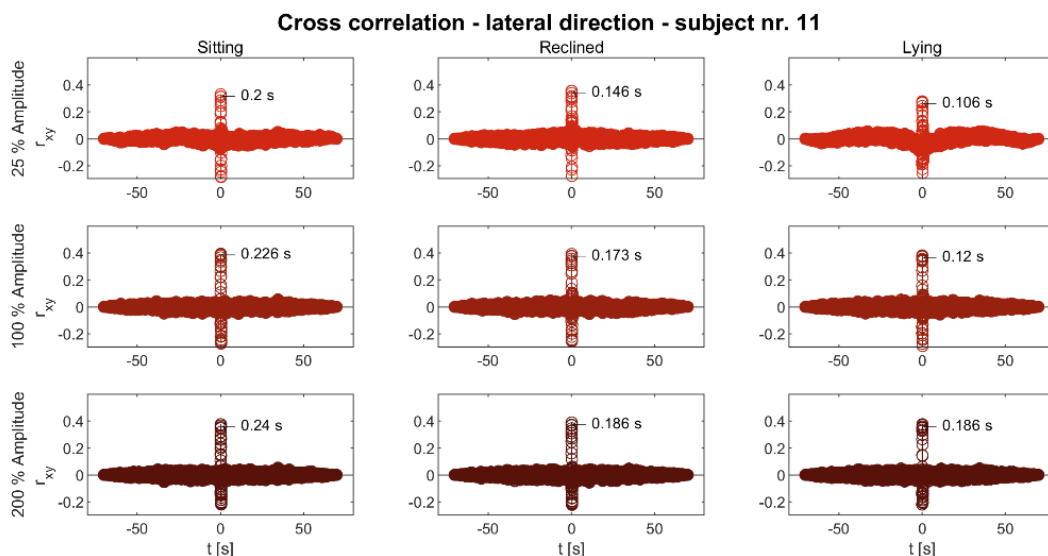
Fig. 11-10: Exemplary illustration of cross-correlation analysis in lateral direction – Ride Simulator.

The accumulated outcomes of the total sample are illustrated in the following Fig. 11-11. The first row demonstrates the results of the average cross-correlation value, whereas the second row displays the associated average time delay at the maximum point of cross-correlation. Considering all directions and intensities, the cross-correlation r_{xy} between the platform input and head response ranged between a value of 0.3 and 0.6. In consequence, a medium to high effect size can be assigned to their relationship. The cross-correlation and the respective time delays showed a recurring pattern within the longitudinal and lateral direction, regardless of the amount of motion intensity applied. In the vertical direction, however, the posture-related pattern in transmission time changed with excitation intensity. On average, the lowest correlation coefficient arose in the lateral direction, whereas the vertical motion pattern showed, by comparison, the greatest values.

*p<.1; **p<.05; ***p<.01
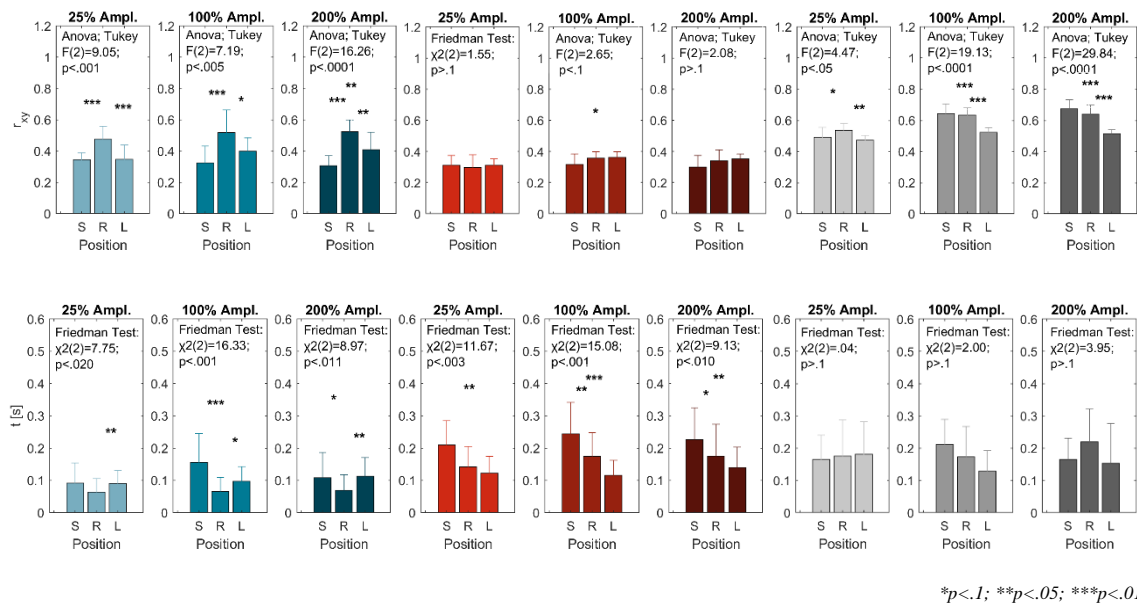
Fig. 11-11: Cumulative cross-correlation analysis:
cross-correlation value (top); time of max. cross-correlation (down) – Ride Simulator.

When analyzing the longitudinal direction, the reclined position showed overall the significantly lowest delay in transmission time, which is observed in approximately 80 % of the subjects (e.g. 100 % amplitude: Friedman Test $\chi^2(2) = 16.33$, p < .01; post hoc Nemenyi test: p < .01 - upright sitting vs. reclined and p < .1 - reclined vs. lying). When analyzing the results in terms of motion intensity, the lying position revealed between the 25 % and 200 % amplitude a significant effect of the excitation strength, whereas a similar effect could be observed in the sitting position between the 25 % and 100 % amplitude (lying position: Friedman test $\chi^2(2) = 10.64$, p < .01; post hoc Nemenyi test: p < .05 - 25 % vs. 200 %; sitting position: Friedman test $\chi^2(2) = 8.89$, p < .01; post hoc Nemenyi test: p < .05 - 25 % vs. 100 %). As already outlined, by comparing the pattern of time delay and correlation coefficient, it appears that there was an opposing behaviour between those two values. This is comprehensible since a high correlation coefficient implies congruent motion characteristics between the input and output signal and, therefore, an immediate motion transfer without great latencies between each other is concluded.

This observation, even if only at a slight expression, is also discernible in the lateral direction. Here as well, a significant change in latency with increasing excitation amplitude can be observed, even though in the reclined posture the post hoc evaluation did not show any significant effects. The total evaluation is presented in Tab. 11-2.

Tab. 11-2: Inferential statistics: time delay and cross-correlation – Ride Simulator.

Posture	Amplitude intensity – Transmission time delay τ *Friedman, Nemenyi post hoc test*					Amplitude intensity – Max. cross-correlation r_{xy} *Friedman, Nemenyi post hoc test*				
	χ^2	p-value	25 vs. 100	25 vs. 200	100 vs. 200	χ^2	p-value	25 vs. 100	25 vs. 200	100 vs. 200
Sitting	13.40	$< .01$	.05	.00	.54	0.8	.67	/	/	/
Reclined	5.24	.07	.54	.17	.74	7.8	.02	.02	.78	.11
Lying	9.50	$< .01$	.95	.03	.07	8.0	.02	.01	.33	.33

Given that some dedicated observations did not match at first glance with the theoretical model, the data sets were more closely examined to understand and resolve potential inconsistencies. First of all, it was ensured that no statistical calculations contained any errors. In the second step, the distribution of the data points was once again analyzed, in which some anomalies were detected. One of those is presented in Fig. 11-12. Here, the distribution of lateral transmission time in the upright sitting position for all execution strengths is illustrated. By comparing the three amplitudes with each other, anisotropy emerged for one subject exposed to the test trail characterized with the strongest motion stimuli (200 %). This is especially true when evaluating the regression coefficient, which dramatically dropped by including the data points of 200 % excitation with the outlier.
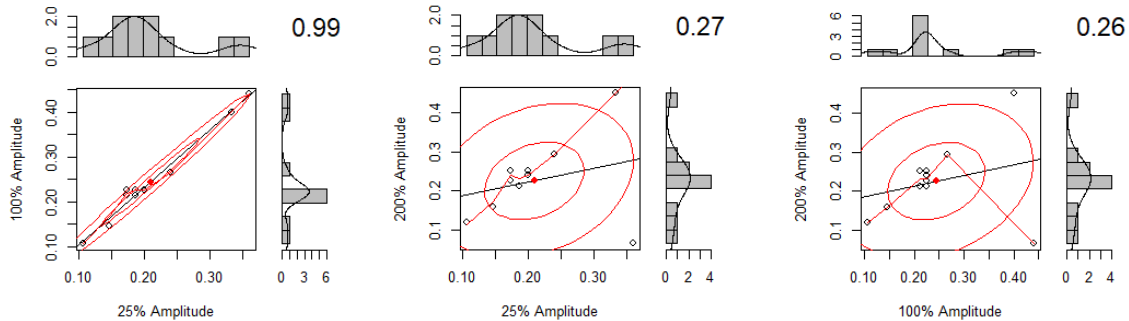
Fig. 11-12: Linear regression analysis of different magnitudes in lateral transmission time – Ride Simulator.

Excluding this particular subject from the total evaluation, a positive correlation between the time delay and the intensity of motion can be observed (25 % amplitude: 0.194 s, 100 % amplitude: 0.225 s, 200 % amplitude: 0.242 s). Thus, when considering the inter- and interindividual variations and potential anomalies across the different conditions, a coherent and uniform picture occurred.

When observing the transmission time between the platform and the head in the vertical direction, no posture-related similarities arose. In fact, across the different excitation strengths, different patterns of time delay occurred when analyzing the seat configurations with each other. Even though no significant effect can be observed for the transmission time, the r_{xy} mean value revealed some strong effects predominantly between the lying and the two other positions. Here as well, the effects of excitation strengths occurred, however, only between the low and the two stronger intensities. This effect became apparent within each of the three postures.

Power Spectral Density – PSD

Once findings in the time domain have been presented, the focus of this section considers results in the frequency domain. The power spectral density is intended to detect energy distribution along with the frequency range. The subplots within Fig. 11-13 are constructed in the same scheme as it is presented for the cross-correlation.
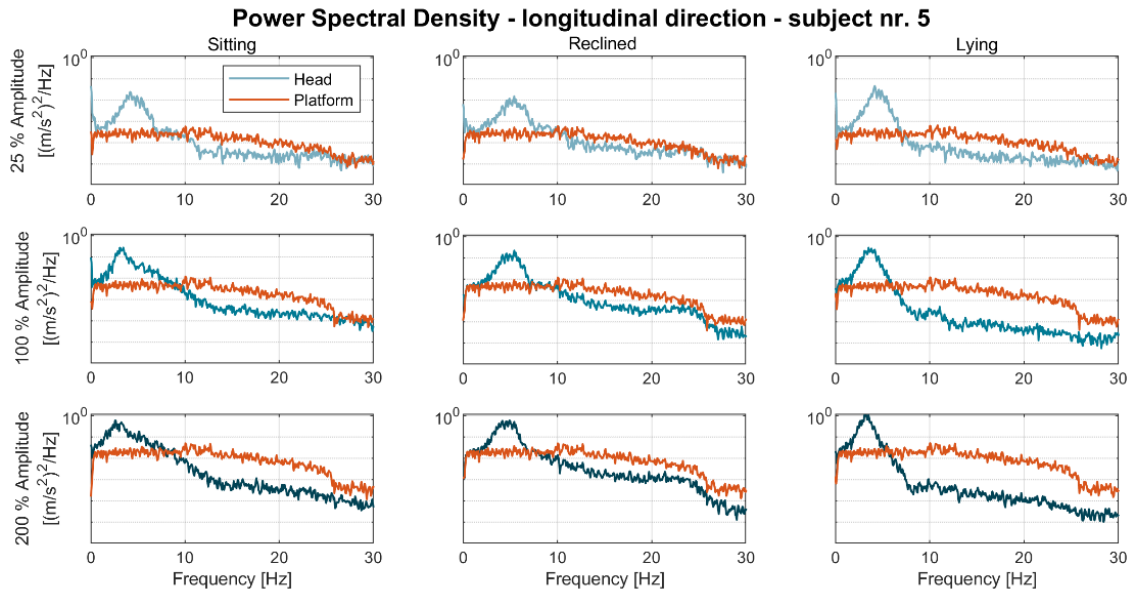
Fig. 11-13: Exemplary illustration of PSD analysis in longitudinal direction – Ride Simulator.

When observing the platform signals (orange), the frequency range of the generated input data was evident from 0.2 to 25 Hz. The gradient of the PSD reduction beyond the frequency of 25 Hz increased with amplitude intensity. As in the previous case of the cross-correlation value, two parameters were derived from the calculation above. On one hand, the peak power distribution was sought, while on the other hand, the associated frequency of this particular PSD value was determined. Since an equal white noise signal was applied, this peak frequency was likely to be approximated as the resonance frequency of the oscillating system.

To examine both parameters in a more representative way, once again, cumulative bar plots across the total sample are presented in Fig. 11-14. In the first place, the value of the ordinate (PSD) is visualized, while the consecutive results within the abscissa (frequency) are outlined below.

The figure continues on the next page.

*p<.1; **p<.05; ***p<.01
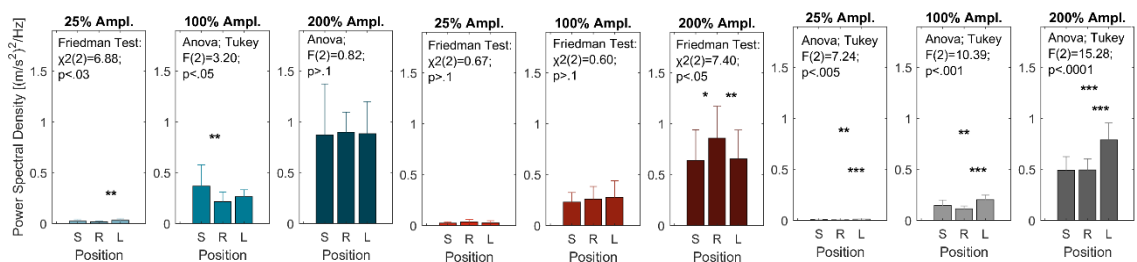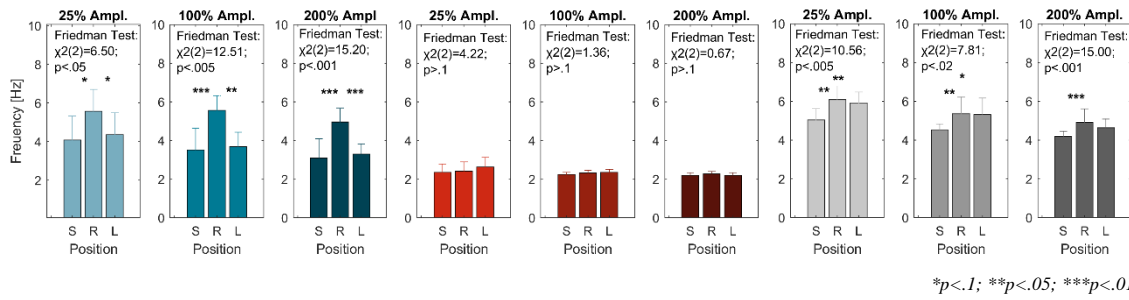
Fig. 11-14: Cumulative PSD analysis: max. PSD value (top);
eigenfrequency (down) – Ride Simulator.

In general, across all directions, stronger motion excitations led to lower resonance frequencies, whereas the peak power distribution of the head response showed counteracting effects, in which greater values occurred with increasing input amplitudes.

In the longitudinal direction, there was no overarching pattern of the peak PSD value, whereas posture-related significances occurred in the 25 % and 100 % excitation strength. By contrast, when examining the resonance frequencies, a uniform behaviour across all amplitude intensities arose (this observation is also valid in the other two directions). Further observations in the longitudinal direction imply that the reclined position showed the greatest maximum energy reaction across all postures. By analyzing the resonance frequencies, a constant behaviour is observed, in which significant p-values between the reclined and the other two postures occurred. It is assumed that the rigidity of the human oscillating system increased with backrest inclination due to the axial stiffness of the spine. Under this assumption, resonance frequencies shall accommodate higher values in supine postures. This was true for the reclined position. When analyzing the lying condition, a behaviour similar to the upright sitting position became apparent. At first glance, this observation seems not to be suited to the assumption of the relationship between longitudinal body stiffness and backrest tilt, however, when considering the actual head-neck bending of the subjects, a uniform cognition appeared. In fact, during the trial, the participants were faced with watching a movie on the tablet. In order to ensure the compliant execution of this task, the participants bent their heads in such a way that a comfortable forward view was guaranteed. Fig. 11-15 illustrates the change of vision (visual axis) due to increasing head-neck bending.

Fig. 11-15: Ramsis simulation of head-neck bending.
Modified from Daimler AG (2020)

Contrary to the schematic figure above, the subjects rested their heads continuously on the cushion of the headrest during the Ride Simulator examination. In any event, the consequent head-neck configuration identified similarities to the upright sitting position, which is visible in the resonance frequency of Fig. 11-14.

147

In the lateral direction, the resonance frequencies exhibited strikingly similar values. In consequence, consistent head motion as a result of the uniaxial noise input is concluded. This presumption is affirmed by video observations during the real-life driving and Ride Simulator investigations. Even if the movement pattern itself showed strong similarities, the peak energy indicated differences between the seat configurations as well as between the amplitude intensities.

Except for the 200 % amplitude in the lying position, the vertical excitation showed on average the highest resonance frequencies with the respective lowest peak energy compared to the other motion directions. Considering the inferential statistics, it is evident that the maximum PSD examination showed the lowest variance and the strongest significance in the vertical direction. This is comprehensible since, in general, vertical force does not initiate characteristic body motion (apart from some kind of head oscillation), but rather pursues the imposed motion characteristic. Indeed, especially supine postures are guided by a direct power transmission from the seat structure to the participant´s head.

Transfer Function

Cross-directional effects and interactions are likely to be analyzed by using the transfer function in a matrix arrangement of input and output signals. The principal diagonal represents the main effects for the identical motion direction of the input and output signal. To give a proper overview of the general motion behaviour across the entire sample, the transfer functions of all subjects were superimposed, so that an average value with a 75th and 95th percentile function can be displayed. The following Fig. 11-16 illustrates this method for the three different postures in the 200 % excitation condition.

Given that no uniaxial pitch or yaw motion was applied in this investigation, only four input rows are outlined. The output data, however, are fully utilized by a 6 DoF column-matrix. The different units between angular and translational motion may cause some distortions in the transfer function. This is the case, for instance, when observing "R_x Input" and "T_x Output". Although no transmission effects are to be expected here, there was a gain of almost 20 dB. By contrast, an effect is expected when analyzing "T_y Output". Here, a comprehensible amplification of up to 40 dB occurred. Consequently, transfer functions between angular and translational signals also provide substantial information but shall be considered more qualitatively.

Transfer function - Sitting position - 200% Ampl. (uniaxial) - 75% and 95% percentile

Transfer function - Reclined position - 200% Ampl. (uniaxial) - 75% and 95% percentile
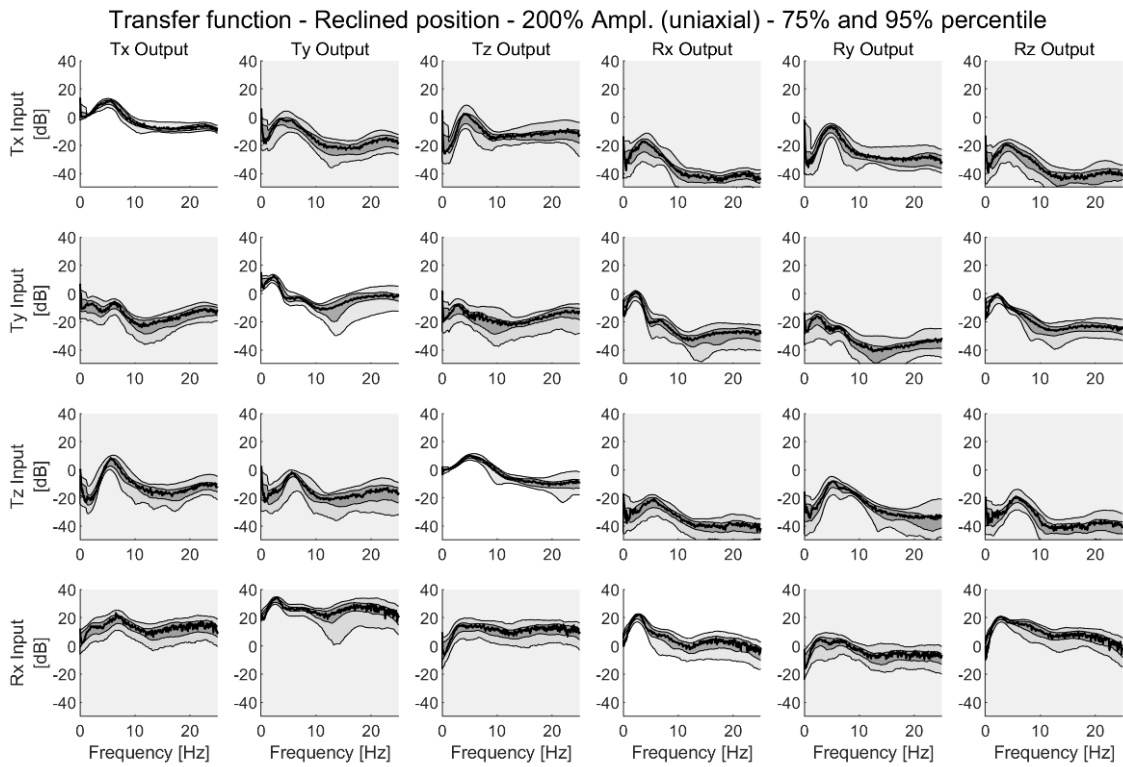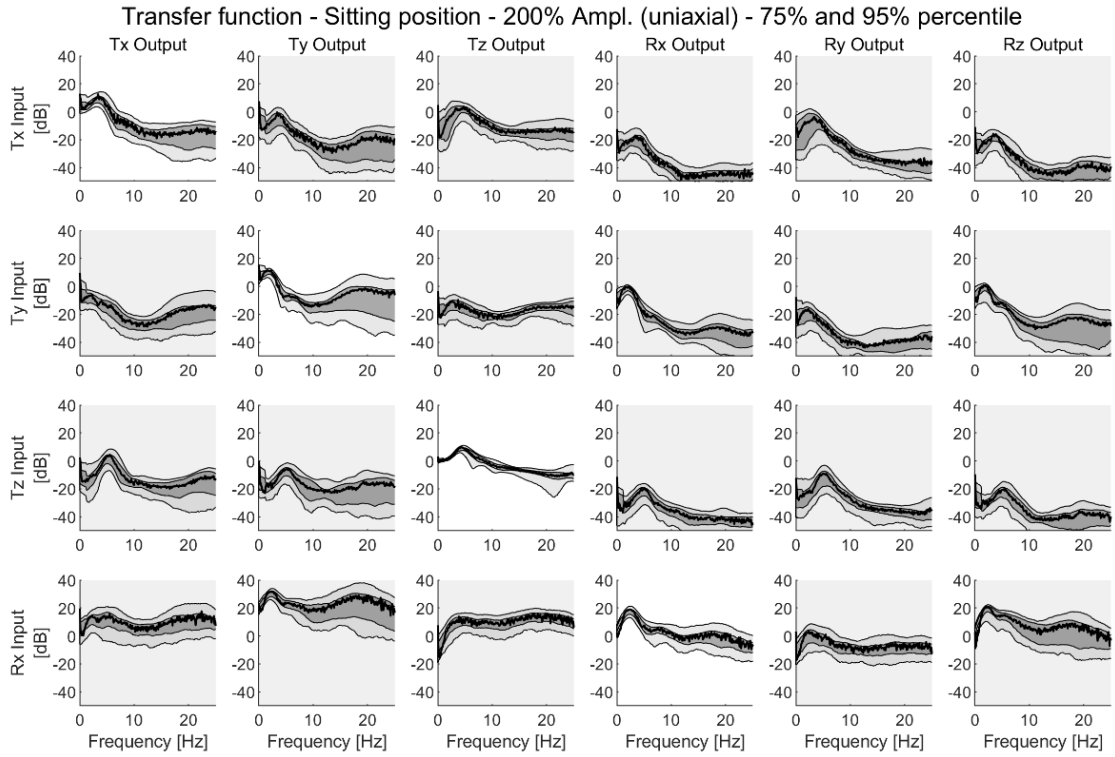
The figure continues on the next page.
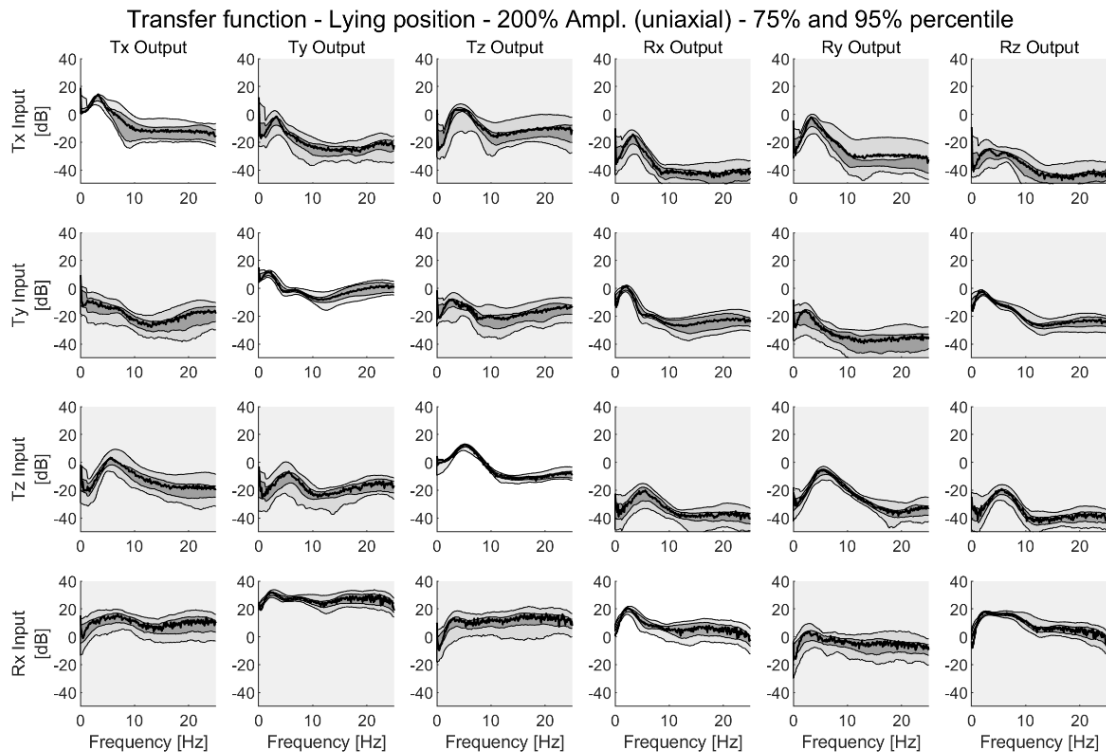
Fig. 11-16: Transfer function in 200 % ampl.: sitting position (top); reclined (middle); lying (down) Ride Simulator.

Many of the previous findings are also illustrated through the transfer function on a consolidated basis. Due to the designated scope of this analysis, however, only the most important observations with the focus of interaction terms are discussed in this chapter.

When analyzing longitudinal linear motion, interaction effects, characterized through pitch head motion, can be recognized across all seating configurations. The respective frequency, in which the maximum gain is observed, ranged between 4 to 6 Hz. Considering lateral motion, the interaction of roll and yaw head motion occurred. The two angular responses were comparatively strong, while the interindividual variance differed among the subject´s posture. In the sitting position, a wide scattering in higher frequencies is observed, whereas in the supine postures quite smaller percentiles across the total frequency band became apparent. Furthermore, when observing the magnitude (gain), the two angular responses were comparatively strong in the sitting position, while in the other positions yaw motion was slightly more present. In the vertical direction, strong interaction effects of head rotation around the lateral y-axis appeared. Therefore, it is expected that vertical force promoted the natural head oscillation. Examining the direct transmission from vertical input to heave head response, the overall narrowest scattering areas are found. While the lying position, in general, showed the smallest band of percentiles, both the reclined and sitting positions exhibited an exiguously wider range of interindividual variation. The only exception is found in longitudinal linear motion, which is attributed to the already described phenomenon of head-neck bending in the lying posture. When considering the input amplification within further transfer functions, some of which are illustrated in the appendix, it is to be stated that stronger excitation strength led to lower limit frequencies.

Based on the isolated angular excitation "R_x Input", the natural pendulum effect of the human body has to be considered here since the occupant's head showed a position-related offset to the pivot point of rotation. Hence, gain in lateral and yaw motion is observed when applying purely platform rotation around the longitudinal axis. For further analyses, the respective 6 DoF multiaxial as well as the remaining uniaxial applications are calculated accordingly and are available in the appendix.

Short-Time Fourier Transformation

The *short-time Fourier transformation* (STFT) is applied to simultaneously display the frequency and time domain. As presented in Fig. 11-17, this method allows the exact identification of striking events (frequency domain) along the period of measurement. The drawback of this method, however, reveals the limited representation of results.
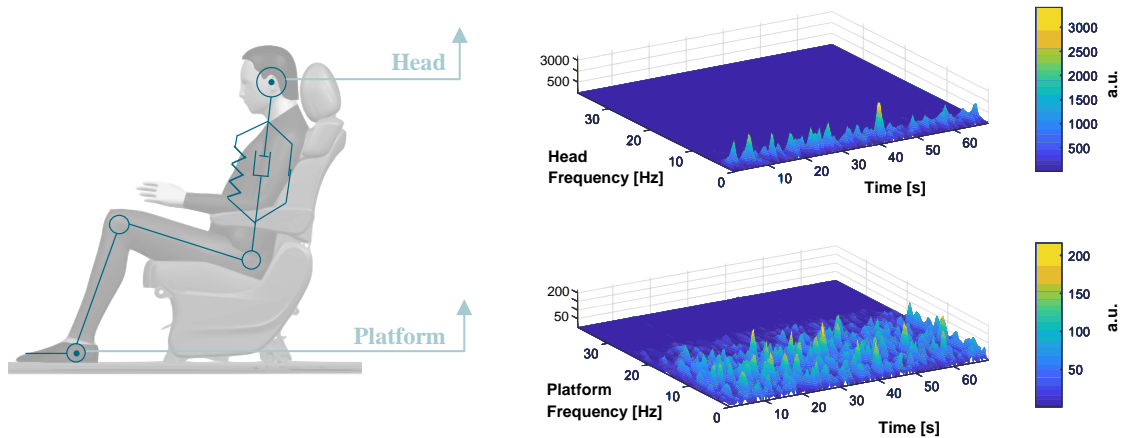
Fig. 11-17: Human body as an oscillating spring-damper system (left);
exemplary illustration of the transfer function in 200 % ampl. lateral motion (right) – Ride Simulator.
Left: Bohrmann, Koch, et al. (2020), based on Eckstein (2014b, p. 58)

The STFT (X_n) is calculated for a continuous-time signal $x(t)$ according to the following equation with the window function w and the frequency f (Giv, 2013).

$$X_n(\tau, f) = \int_{-\infty}^{\infty} x(t) \cdot w(t-\tau) \cdot e^{-j2\pi ft} \, dt \qquad \text{Eq. 11-1}$$

The frequency and the time resolution are determined by the width of the window. With respect to the uncertainty law, both resolutions, frequency as well as time domain, cannot be arbitrarily small at the same time (Udal & Kukk, 2012). Therefore, a compromise had been taken when applying the Hamming window, which is already described in chapter 3.6.2. When analyzing the individual STFTs, it is mandatory to contain a more universal and generalizable use case. As already identified with the examination of the transfer function, within vertical motion only a small amount of scattering is observed. Thus, the setup displayed on the left-hand side of Fig. 11-17 is chosen for the consecutive STFT analysis. A representative expression of the platform and head STFTs for all three seating postures are given in Fig. 11-18. Among others, the frequency range of motion input is clearly visible within this illustration as well.
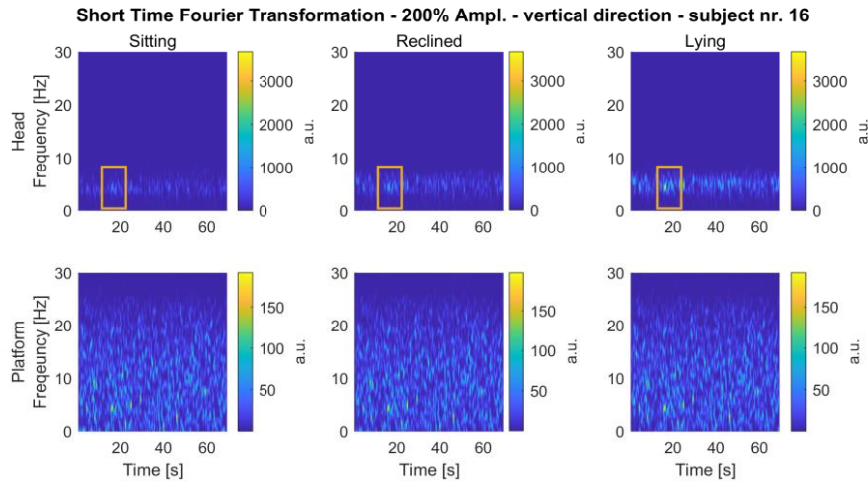
Fig. 11-18: Exemplary illustration of STFT in 200 % ampl. in vertical direction – Ride Simulator.

A distinct and uniform pattern emerged when observing the platform STFTs. Facing the corresponding head motion, several characteristics can be identified. In fact, an average increase of head motion energy with raising backrest inclination is detected. Similarly, as it is observed in Fig. 11-17 in which an anomaly around 40 s occurred, a characteristic and powerful head motion is identified in the vertical direction as well. This particular event is highlighted in Fig. 11-18 and emerged 18 s after starting the section. In fact, besides the variation of average energy load between the three postures, single pulse-like motion patterns were found to be more dominant in supine postures. This finding is in line with the results of the r.m.s. and PSD analysis, even if there is hardly any difference noticeable between the max. peak power distribution of the sitting and reclined position.

11.4.2 Multisine

The intensity-related three-step multisine function was obtained in the lateral direction to examine the potential upswing behaviour of the human body under various seating conditions. This application is based on observations made during the driving investigations and the associated statements by the participants. As it is presented in the previous chapter, by applying the STFT method a rapid overview of the head motion characteristics going along with the multisine condition is achieved (see Fig. 11-19).
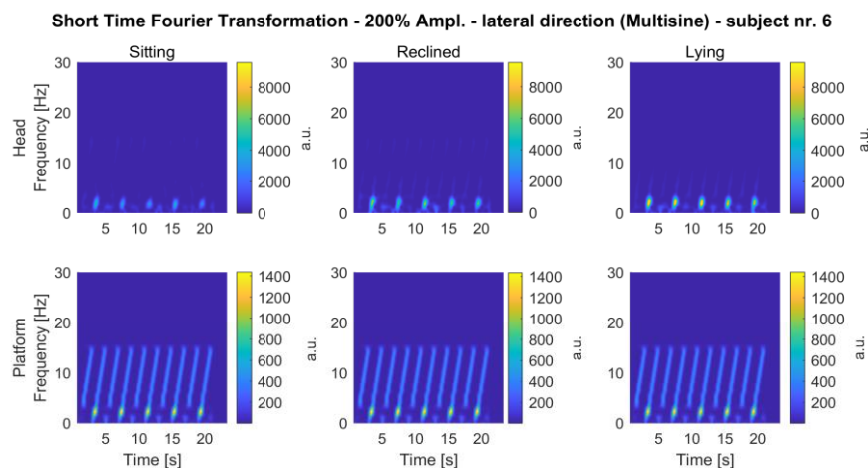
Fig. 11-19: Exemplary illustration of multisine STFT in 200 % ampl. in lateral direction – Ride Simulator.

152

When observing the second row of the STFT matrix, the unified energy input was also guaranteed through the replicated platform trajectory. In contrast to the uniaxial noise signal analysis, here, a strong correlation between backrest inclination and energy distribution of head response became apparent. For a more detailed examination, the cross-correlation and r.m.s. analyses were applied as well. Consequently, some selected representative excerpts, which contain the relevant findings, are presented in Fig. 11-20.
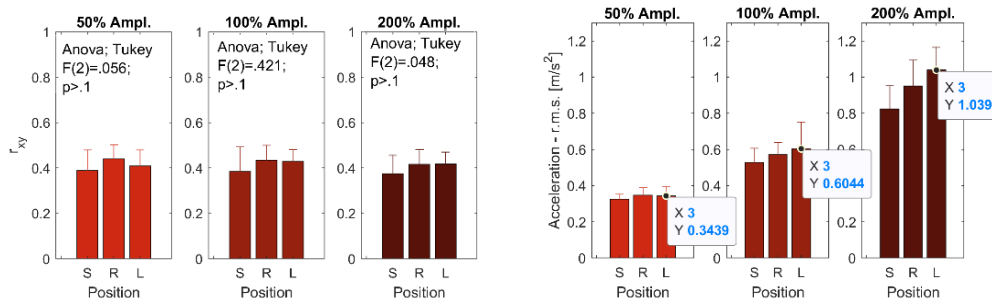
Fig. 11-20: Cumulative analysis of multisine stimuli:
max. cross-correlation (left), mean r.m.s. (right) – Ride Simulator.

Even if only the cross-correlation value itself is presented here, both relevant parameters revealed the same pattern as it is examined for the uniaxial noise application. Therefore, the already presented head egomotion during lateral force seems to be valid in oscillating motion environments as well. Alongside the commonalities, however, fundamental differences occurred when comparing the average energy of the head response. In the investigation of noise excitation, there was a reduction in the r.m.s. value for the lying position, while during oscillating movements a continuous increase with raising backrest inclination is observed. Therefore, the type of excitation is likely to influence the resulting head dynamics. For this reason, the recorded meso shaking data are additionally discussed in the consecutive chapter.

11.4.3 Meso Shaking

Given that the Ride Simulator does not have linear bearings to reproduce quasi-static movements, a real-life driving representation of an uneven and rough highway road (micro, meso, and macro shaking) was conducted. The simulator is capable of generating mainly vertical as well as angular motion that characterizes this particular type of motion pattern. The power distribution for the translational axes is shown in Fig. 11-21.
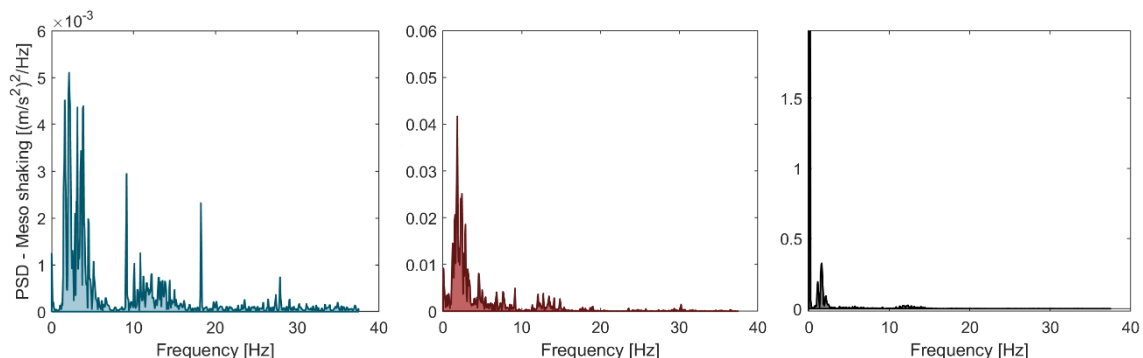
Fig. 11-21: PSD analysis of meso shaking stimuli – Ride Simulator.

Particularly in the vertical direction, high-energy motion occurred, whereas in the longitudinal direction the overall lowest power distribution was recorded. The greatest energy load arose in the lower frequency band, which might be of interest when observing motion sickness occurrence. Therefore, the MSDV value is determined for the platform just as the corresponding head motions, while the scope of work is limited to the translational accelerations concerning the ISO 2631. This had been done because pure translations are more likely to provoke motion sickness than pure rotations (Förstberg, 2000a, pp. 67–70; McCauley et al., 1976; Persson, 2008).

Motion Sickness Dose Value

The MSDV originally arose to examine the nauseogenic amount of the experienced vertical oscillation. Some researchers utilized this method for the evaluation of multiaxial motion in the same way as it is obtained in the previous driving studies. A cumulative representation of the MSDV results is shown in the following Fig. 11-22.
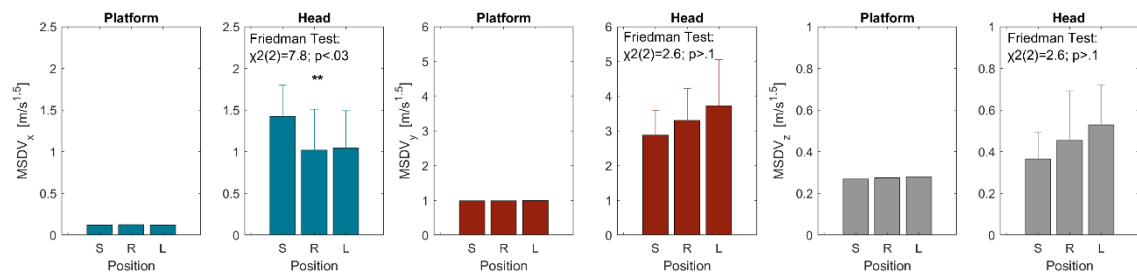
*p<.1; **p<.05; ***p<.01

Fig. 11-22: Cumulative MSDV analysis of meso shaking stimuli – Ride Simulator.

First of all, it becomes apparent that the platform MSDVs only showed negligible differences across the different seating configurations. Therefore, the uniformity of motion input is verified. In comparison to the platform evaluation, overall higher MSDV values arose in the head evaluation. In contrast to the homogeneous vertical and lateral behaviour, in which the backrest inclination and MSDV value correlated with each other, a conspicuous behaviour is observed in the longitudinal direction. For a more detailed analysis, Tab. 11-3 provides numerical information about the illustration above.

Tab. 11-3: MSDV analysis of meso shaking stimuli – Ride Simulator.

Position	$MSDV_x$ longitudinal [m/s$^{1.5}$]			$MSDV_y$ lateral [m/s$^{1.5}$]			$MSDV_z$ vertical [m/s$^{1.5}$]		
	Platf.	Head	Gain [-]	Platf.	Head	Gain [-]	Platf.	Head	Gain [-]
Sitting	0.124	1.424	11.48	0.984	2.873	2.92	0.269	0.365	1.36
Reclined	0.125	1.020	8.16	0.987	3.300	3.34	0.274	0.455	1.66
Lying	0.122	1.045	8.57	0.992	3.728	3.76	0.281	0.529	1.88

Gain is based on the greatest head MSDV value across the different body postures

The greatest amplification between the platform and head MSDV occurred during fore-and-aft motion characteristics. This finding supports the observation made in the real-life driving investigations, in which higher nauseogenic stimuli were observed in the upright sitting position, especially during longitudinal driving maneuvers.

The lowest levels of inequality were shown in the vertical direction, which is to be expected since the previous conclusions already have shown that coupling effects between the head and the motion underground mainly occur during heave movements and, consequently, lead to a uniform behaviour. The MSDV in the lateral direction showed the greatest nauseogenic stimulus. This is congruent with observations postulated by Yusof et al. (2020), who reported a six times higher MSDV value in lateral direction compared to the longitudinal results after exposure of an 8-minute ride. However, it has to be mentioned that here as well a synthetic route with 18 winding corners and speed limits up to 30 km/h was obtained.

11.4.4 Discussion and Synopsis

In the following, the already presented findings are summarized and interpreted to generate a holistic description of the head dynamics under posture manipulation. To do this in a structured manner, the translational axes are discussed individually.

Longitudinal Direction

Considering the video observations, it becomes apparent that some test subjects did not always lean their head against the seat structure when sitting in an upright position. In this particular situation, the longitudinal force is transmitted via the lower back and induces some kind of pendulum movement of the upper body. As a result, it takes some time to identify the platform excitation by a convenient head motion response. By contrast, the reclined position shows the shortest time delay when analyzing the transmission of motion from the platform to the head in the longitudinal direction. Observing this position in more detail, a unique characteristic can be observed, in which the participant´s spine and head-neck plant are in line with each other. As a consequence of this, a strong cranial and caudal stiffness in the direction of excitation occurs, which can be identified by the observation of the eigenfrequencies. This assumption is supported by the high correlation coefficient, which demonstrates the strong similarity between the platform and head motion characteristics. In addition, taking the transfer matrices into account, the narrowest percentiles occur in the reclined posture, followed by the lying position, while in the upright sitting condition the largest variance appears. In general, the narrower the percentiles, the more equal the behaviour of the test subjects. Uniformity arises especially when the freedom for voluntary movements is restricted or a strong cohesion across the spectrum of motion is observed. The percentile analysis confirms the results of the cross-correlation coefficients and the eigenfrequencies. In the lying position, the previously described head bending is determined and expected to cause a fairly long-time delay. The pattern shows similarities to the upright sitting position with its oscillating head motion response.

Lateral Direction

The transmission time and backrest inclination do correlate negatively with each other. Indeed, by inter- and extrapolating the three discrete measurements of seating configuration, it has to be stated that the flatter the posture of the participants, the shorter the time delay between the input and output signal. In the sitting position, the motion behaviour is expected to be influenced by the power transmission point. When applying a lateral impulse, the force is absorbed by the sluggishness of the free moveable upper body and only finds its way into a respective head response after a certain time delay. This effect seems to be quite strong since the greatest delay across all observations in lateral direction occurs here. When increasing the backrest inclination, the impact of gravity raises by pressing the subjects onto the backrest of the seating structure. As a result, more direct transmission is achieved, while the sluggishness of the torso plays a less important role. Including the correlation coefficients into the evaluation, it is recognizable that the lying position shows the highest value, even though this is clearly below the respective observations made in the longitudinal direction. The reason for this difference is attributable to the anatomy of the human body. The bending of the torso in the sagittal plane is obtained due to rotation around the hips in such a way that the head performs a quasi-linear movement, whereas in the coronal plane the human body does not have the freedom to induce a linear motion behaviour. Instead, especially in situations in which single-point support of the headrest is provided, head rotation around the vertical axis occurs. This phenomenon is visible in Fig. 11-16 when observing the transfer functions. When applying lateral motion, the pitch response seems to be systematically lower than the two angular responses of roll and yaw motion. Here as well, the smallest percentiles occur in the lying position, which indicates less variability in head motion when being in a supine posture.

Vertical Direction

When considering the r.m.s. evaluation, it can be clearly seen that the head experiences the highest average acceleration in the lying position. The lowest value is found in the sitting position, whereas the reclined posture is in between those two. In the sitting position, the stimulation has to be transmitted through the entire upper body and induces some kind of oscillating head motion, which explains why in comparison a more dampened head response is recorded. On this basis, a more direct motion transfer between the structure and the human body is observed in supine postures with increasing load on the headrest. The correlation coefficients, however, do not confirm this assumption since a strong negative correlation between the backrest angle and the uniformity between input and output signal became apparent. Therefore, it is expected that the sitting position is likely to best reflect the platform behaviour, despite the already mentioned damping effect. One explanation for this inconsistency is found in the transfer function and linked to the more intense head rotation components in the reclined and lying positions which deviates from the platform characteristics. However, since particular small percentiles are discernible in the supine postures, further systematic effects are expected.

Therefore, the connecting piece between the platform and the human being is analyzed in more detail when calculating the PSD for the headrest in vertical direction (see Fig. 11-23). In contrast to the previous illustration, here the application of percentiles is used to illustrate the general power distribution in the sitting, reclined, and lying conditions.
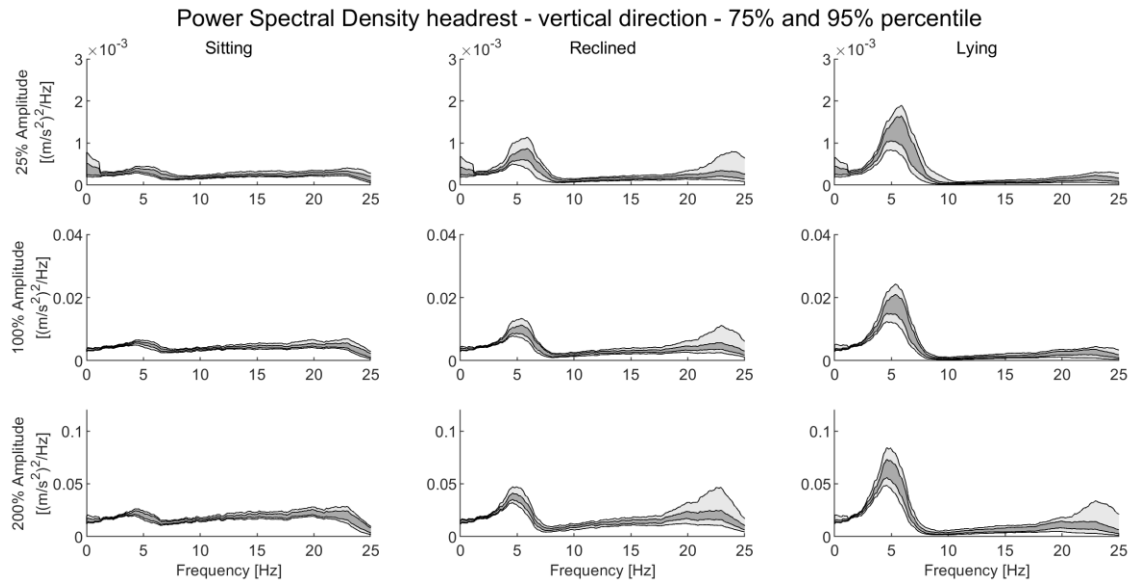
Fig. 11-23: PSD analysis of the headrest in vertical direction – Ride Simulator.

By analyzing the PSD evaluation of the headrest, an amplification of the vertical seat transmission behaviour with increasing backrest inclination and energy load is observed. The eigenfrequency of 5 Hz is dominant and might influence the behaviour of the head motion, especially in supine postures. In consequence, the primary assumption of a more direct head response in a lying or at least reclined position seems to be valid, but only in comparison to the instant connection point - the seat. Overall, this result is plausible since the biomechanical freedom of body movements is limited in the vertical direction and, therefore, a coupled movement between seat structure and humans is evident.

12 Superordinate Discussion

In addition to the study-related sections of discussion and synopsis, this chapter presents the results in a more interconnecting manner and addresses the cluster of research questions formulated in chapter 4 (a more strict representation is shown in chapter 14). Besides the methodical requirements in observing aspects of motion sickness (see chapter 12.1), countermeasures to avoid respective expressions of carsickness are analyzed (see chapter 12.2). Subsequently, some holistic approaches are presented, in which the impact of the already determined recommendations on future vehicle concepts are discussed (see chapter 12.3). To be more precise, the main question reveals whether the vehicle-related motion sickness treatments are also likely to increase general comfort or, if on the contrary, may limit the user experience. Furthermore, the underlying theoretical backgrounds were discussed to identify additional research topics. In the subsequent chapter, limitations of the work such as a restricted technical framework, shortage of human resources, or lacking external validity due to omitted field inquiries are presented.

12.1 Human-Related and Environmental Motion Sickness Factors

Firstly, the detection of motion sickness shall be highlighted. The FMS, MSAQ score as well as the number of terminations with the associated value of driving duration imply a smooth and consistent picture when it comes to a representation of motion sickness severity. Although the amount of termination seems to be a valid parameter in motion sickness detection, slight distortions and interaction terms with the subjective assessment are expected for participants who discontinued more than one trial. Since the criterion for abandoning was equally binding for both exposures, a quite similar value, especially for the maximum or last FMS, is to be assumed. Concerning the behavioural measures, it is to be stated that the identified characteristics are in line with previous examinations and are more of a supporting nature (Dobie, 2019, p. 16; A. Koch et al., 2018). Within the physiological measures, the pre-post comparison was the most promising method. In particular, heart rate and core body temperature are identified to be quite sensitive in motion sickness objectification. These results are in line with the observations presented in chapter 3.7.2. However, even if significant effects in those parameters arose, large inter- and intraindividual discrepancies in motion sickness expressions and emotional state might blur the systematic effects within the physiological data set (see also Smyth, Birrell, et al., 2021). To accomplish an objective quantification, clustering methods and multi-dimensional data processing might provide a suitable solution to eliminate individuality in nauseogenic responses. By considering future vehicle applications, data recording without physical contact between the sensor and the human being is required. This is why innovative methods and techniques with the aim of contactless physiological tracking have been more often investigated in the recent past (Pham Xuan et al., 2021).

Performance and Ability to Concentrate

Apart from the detection of motion sickness, the influence on performance constitutes another important issue. Three different kinds of reaction, short-time vigilance, and performance tests were carried out before, during, and after the exposure. Some statistically relevant effects were identified, which confirms the observations made by Bos et al. (2012), Matsangas et al. (2014), and Le et al. (2020) (see chapter 3). Even if during the construction of the statistical model the factor of time was controlled, the cause of change in performance cannot be determined with certainty. In fact, disturbances regarding ambitiousness, daily routine, or general weariness can influence the performance rating over time and, therefore, might superimpose the effect of motion sickness. Irrespective of whether the results can be assigned to motion sickness or not, the interpretation of the results does not allow an unverified transferability regarding vehicle safety. Even if differences in performance occur, those are quite small and only for some evaluations powerful. Furthermore, the applied test metrics display only a small and abstract form of the safety-relevant issues when it comes to increasing road vehicle automation. In addition to chapter 10.4, it is to be stated that transition as well as sustained attention during manual driving are only two of many situations that contribute to road safety. However, with the results collected in this elaboration, the importance of examining the impact of motion sickness on safety-relevant performance is underlined.

Inter- and Intraindividuality in Experiencing Motion Sickness

The individual susceptibility, measured through the MSSQ, is revealed to be one of the most sensitive predictors in terms of motion sickness prevalence. Subjects who are more prone to experiencing motion sickness show stronger expressions of malaise and nausea than participants with lower MSSQ scores. This result is consistent across all investigations and can be confirmed by several published research findings (see chapters 3.4 and 3.7.1). When it comes to sex and age no significant effect on motion sickness susceptibility or its symptoms can be reported within the four driving experiments. However, it is evident that the pre-selection of subjects does not only influence the statistical power of the MSSQ score as a predictor of motion sickness, but beyond that, it shows further skewed effects on demographic parameters. Therefore, due to the limited sample size, the irregular distribution, and the already mentioned pre-selection effect, the expected difference of the MSSQ scores across sex and age, which are found in the general population (e.g. Dobie 2019), might not be represented in the current test conditions. Consequently, the lack of representation of the total population diminishes the external validity of the presented findings. This trade-off was chosen deliberately since the focus was moved to countermeasures on motion sickness, while the criterion of a suitable susceptibility distribution regarding motion sickness had to be fulfilled.

Study Design and Meta-Analysis

Considering the above-mentioned strong inter- and intraindividual variances in motion sickness susceptibility with its associated expressions of malaise, nausea, and gastrointestinal diseases, it seems obvious to restrict the solution area by picking the same participants for all driving investigations. From a theoretical point of view, this approach eliminates individual disturbances, while potential order effects during the investigations are mitigated through randomization. This conclusion, however, is only partially true since motion sickness is strongly associated with placebo and habituation effects, as it has been observed in the fourth investigation. Multiple participations inevitably lead to some kind of general adaption, in particular, when only minor adjustments in study design had been made along with the subsequent investigations. Therefore, with the paradigm of a steady-state test sample, meta-analyses are predominantly valid in a qualitative manner. Only if some kind of leakage effect in participation is initiated, a suitable comparison between the different studies appears reasonable.

This issue raised the fundamental question of the most suitable study design with the aim of investigating motion sickness manifestations, independent of whether further examinations are planned or not. Three out of four real-life driving investigations were carried out in a mixed design, in which both methods between-subject design as well as repeated measures design were combined. In principle, focus had shifted to the repetition factor, whereby in most of the cases the between condition had been examined in the consecutive investigation as the new within-variable. This procedure permits an appropriate declaration of accuracy, whether the two studies indicate the same results or inconsistencies between those two become apparent.

As a result, looking towards all investigations, a consistent picture occurs, in which the neighbouring examinations provide at least similar tendencies for the independent variable in terms of motion sickness prediction. However, in this case too, the previously mentioned influencing factors on motion sickness, such as individual variability, contributed as disturbance factors in the meta-analysis. If people take part in several studies, it should be ensured that the period of time between the trials is long and the object of interest is incongruent between the measures to avoid any involuntary influencing effects of expectation (see chapter 9.2) or habituation like it is observed in Stelling et al. (2021). Considering the abort criterion, repeated measures show advantages since the participants can compare the trials with each other and stop at the same state of nauseogenic feeling. To avoid the aforementioned leveling effect in motion sickness evaluation, it is recommended to utilize multi-dimensional questionnaires, such as the MSAQ, rather than using a single item alone e.g., the FMS. If a between-subjects design is chosen, it is mandatory to ensure an equal distribution of motion sickness susceptibility between the groups. The MSSQ appears as a suitable selection criterion, although slight bias effects cannot completely be ruled out due to the subjective assessment as the basis for the determination. Even if repeated measures designs are recommended to investigate motion sickness, mixed and between methods are suitable, too. This recommendation is based on the fact that the error in the equality of susceptibility seems to be greater in most cases than the bias effect of habituation especially when only a two-step design is applied.

Characteristics of Non-Driving-Related Tasks

According to Fig. 4-1 motion sickness is influenced by more than human-related characteristics. Moreover, environmental and motion conditions contribute to the occurrence of motion sickness as well. Even if only qualitative surveys were conducted, the type of NDRTs has been proven to affect the nauseogenic nature of the driving event. Many characteristics such as mental workload, dynamics of content, size, and position of the displaying device appear to be important factors when it comes to the evaluation of motion sickness severity. Distraction, for instance, seems to be beneficial in reducing the likelihood of motion sickness, however, only if it is not of a visually demanding nature. This is the main reason why the quiz was rated better than the other tasks. When watching movies, less cognitive information processing without the necessity of following every detail of the storyline occurs. Here, it is possible to let one's mind wander, which also might decrease motion sickness provocation. Under this circumstance, the ambitiousness of execution is quite important, however, it has proven to be difficult to monitor and guarantee a compliant behaviour. When analyzing the interviews conducted immediately after the driving events, some factors could be identified that influence this behaviour. Besides the actual state of exhaustion, basic attitudes such as willingness and emotional relationship to the allocated task are just a few components that contribute to the multifactorial level of immersion. In consequence, the predefined NDRTs have to be chosen carefully. In this work, a wide range of visually demanding activities had been selected. This approach aimed to maintain some level of excitement and variation with the intention to improve individuals' drive to perform the desired task.

The disadvantage, in particular when considering gaming activities, is attributed to emotions which cannot be monitored and might affect the prevalence of motion sickness. Especially, when considering the physiological measures, emotions may superimpose the neuro-physiological reaction of the human organism that emerges as a result of the nauseogenic stimuli. In summary, a trade-off between diversity, validity, and attractiveness of the task has to be chosen. In this work, a balanced solution seems to be found, which ensures both a standardized nauseogenic stimuli but without providing only one monotonous and tedious type of task.

Exogenous Vibrational Load

As its name suggests, motion sickness is necessarily linked to the motion during which it is experienced, regardless of whether it is of a physical nature or only provided through visual stimulation. Particularly when it comes to carsickness, as a certain type of physical-induced kinetosis, the characteristics of motion are essential and quite complex. The variations of stimuli obtained in this elaboration range from using case-based real-life driving studies to a more generic approach of motion simulator investigations. Since the Ride Simulator examinations had only been carried out to validate seating configurations in terms of motion comfort, focus will be shifted to the vehicle-related driving scenarios. Those were carried out using a mixed methodological approach. In fact, singular driving events with strong but realistic accelerations were applied with the purpose of identifying unpleasant effects related to motion sickness. Therefore, the applied motion characteristics have been optimally mapped to real-life driving requirements, while their frequency of occurrence extends the normal amount that is observed in real life. As matter of fact, curvy roads were abstracted and represented by looping trajectories. Considering the recorded vehicle dynamics that are presented in chapters 5.4 and 8.3, in general, a steady state of motion sickness can be reported after 20-minute of driving. This particular observation is valid for the pre-selected sample, which is characterized by a high average susceptibility rate. To evaluate the experienced motion stimuli, the ISO 2631 provides, at least in parts, a conceivable tool to link the recorded data with subjective perception and comfort. By applying this norm, it is expected that motion sickness, even in vehicles, is induced only by vertical motion patterns. This assumption is made because the frequency weighted function is exclusively defined for this particular axis. When considering the findings of different researchers, who emphasized that motion sickness in tilting trains or vehicles is even more influenced by other motion characteristics, it is beneficial to take a closer look at the applied physical stimuli. Indeed, the essential question reveals the preference in relation to driving maneuvers that provoke motion sickness the most. Evaluating the subjective responses, it clearly demonstrates a strong nauseogenic nature during fore-and-aft motions. Even during journeys with constant speed on uneven roads, low-frequency head motions with the ability to provoke motion sickness show the greatest gain in the longitudinal direction. This observation is supported and quantified by the $MSDV_x$. The second critical motion stimulus is recorded in the lateral direction. This, on one hand, is derived from the participant's survey during the driving experiment and, on the other hand, confirmed by the associated $MSDV_y$ values.

Considering the uneven road condition, lateral accelerations reveals to be even more nauseogenic than longitudinal motion. In short, contrary to the ISO 2631, vertical motion seems to play a subordinate role in carsickness, while longitudinal as well as lateral motion might be important when it comes to motion sickness. Since these findings are linked to the track design and selected driving maneuvers, their generalization has limited coverage. However, two different kinds of motion stimuli with their respective subjective and objective evaluations show nearly the same results and tendencies. In particular, when comfort is to be examined in addition to motion sickness, the experimental setup in terms of physical excitation shall be designed in consideration of the use case and research issue. If, for example, the yaw movement of the head is aimed to be investigated, driving maneuvers, which induce the corresponding lateral impulse, have to be chosen. If, by contrast, motion characteristics with the best trade-off between reality and nauseogenic stimuli are required, the start-stop maneuver has been proven to be a suitable stimulus. In order to analyze head dynamics, a more generic approach is required in which synthetic and reproducible motion stimuli can be applied (see the hexapod simulator in chapter 11).

In summary, the investigations conducted at the test track have shown that examinations according to motion sickness require strong discipline concerning compliance and regulations of study design. Even factors that initially appear to be less relevant, such as the in-vehicle temperature, indicate slight tendencies in motion sickness prediction. Therefore, standardization is the key when it comes to motion sickness examinations. The design itself has to be adjusted to the research target. Investigations of treatments, for instance, require participants in which at least slight susceptibility rates are present, whereas for studies with relevance to identify the real-life probability of motion sickness occurrence, a representative sample is recommended. If a recurring stimulus pattern is used, care should be taken to internal models. If, for example, laps are driven several times on the same test track, it is advisable to let the participants experience the procedure once before the actual test begins. Otherwise, it might be expected that some prediction of the future stimuli develops during the course of study and, thus, may influence subjective motion sickness rating. This phenomenon is of special interest for situations, in which the human gaze and visual information are not controlled by the examiner.

12.2 Vehicle-Related Motion Sickness Treatments

The primary goal of this work comprises physical-geometric aspects of the vehicle interior to enable visually demanding NDRTs during highly automated driving scenarios. Firstly, it could be established that adjustments of the vehicle interior do indeed have strong effects regarding motion sickness. In fact, the main improvement in motion comfort had been achieved by optimizing the seat configuration. Here, two main aspects of seat adjustments had been scrutinized.

Direction of Sitting Orientation

Even if slightly turned seat configurations as well as sideways adjustments are also conceivable in the future, the focus was placed on forward and rearward seating.

As mentioned in the previous chapter, this variable had been analyzed in two investigations as a main and as an auxiliary condition. No reliable statistical significance could be found across the total sample neither in the first nor the second investigation. Taking a closer look at the first investigation, it can be observed that facing backward causes higher motion sickness expressions than sitting in the opposite direction. This homogenous output arises particularly in the reclined position, whereas in the upright sitting condition smaller differences emerge. Within this assumption, however, it is not entirely clear whether the small variations in the upright position is due to the actual motion sickness expression or influenced by the high amount of termination with the respective unification of motion sickness rating, for instance, initiated through the abort criterion (FMS ≥ 12). However, there is a prominent finding when analyzing only subjects, who did not discontinue the trial. Here, a significantly higher incidence of motion sickness in forward-facing conditions emerges (see Fig. 5-12). However, it is to be stated that this result is based on a quite small sample size, which leads to the conclusion that this finding is not of a representative nature. This is to be noted especially when analyzing the number of terminations in the reclined position because here every discontinuation occurred when sitting rearward.

Up until this point, the observations were based on the restriction of missing outside view and individuality since the sitting direction was manipulated as a between condition. By adding the second investigation and, therefore, the visual information into the examination of the sitting direction, a slightly different picture emerges. In the outside view condition, weak differences only in the mean FMS occurred, in which the forward sitting condition shows in average greater motion sickness expressions. Reconstructing the first examination by prohibiting the outside view, the presented observations above cannot be confirmed. When analyzing the maximum and delta FMS just as the MASQ score, forward sitting seems to be more nauseogenic than rearward supposing there is no visual cueing available and the participants are positioned in a reclined posture. In consequence, changes in sitting direction did not draw a clear picture and show a significant increase in motion sickness prevalence when performing visually demanding NDRTs. This is at least the case for the current test setup. In real-life situations, a more diverse portfolio of tasks, such as observing the surroundings or making phone calls, is expected. In particular, subjects who are extraordinarily sensitive to motion sickness with expectations to perceive stronger symptoms when sitting against the driving direction might be negatively affected by rearward driving (see chapter 9.2). This is likely to be the case since the results collected in this elaboration are not congruent with findings published by other researchers (Salter et al., 2019). Here, a significant increase in carsickness is observed when sitting against the driving direction. The discrepancy between the findings of the current elaboration and those results might be explained by the difference in study design. In fact, the influence of the seat orientation on the degree of malaise is strongly dependent on a multivariate framework such as expectation, experience, backrest inclination, outside view, or motion pattern. This is especially the case when fore-and-aft motion is dominant. Here the interaction between backrest inclination and sitting direction is reported by the participants. Indeed, rearward driving seems to be beneficial during braking maneuvers in terms of reduction in head dynamics.

Conversely, with respect to the postural instability and the sensory rearrangement theory, the learned motion pattern is expected to be more pronounced among forward driving scenarios than sitting rearward. Moreover, if the windows of the vehicle are uncovered, prediction of the future vehicle trajectory is possible when being in a forward-orientated sitting position. This, in fact, also contributes to improvements in motion perception. In summary, when taking into account the different results collected in this work as well as by other researchers and reviewing the sitting direction as part of future vehicle concepts, in the first place, no particular criticality can be identified. Especially when including further physical-geometric requirements with a more considerable influence, such as backrest inclination and outside view, the advantage of sitting across each other seems to outweigh the potential increase of motion sickness severity.

Backrest Inclination Angle

The second parameter of seat configuration addresses the pitch rotation of a human´s torso in the sagittal plane. Here, several backrest inclinations were investigated to find the most suitable position when performing visually demanding NDRTs. In general, the findings from previous examinations can be confirmed, in which supine positions lead to less motion sickness (see chapters 3.6.3 and 3.8.3). Considering the results of the third driving experiment, it can be maintained that an increase in backrest inclination leads to a decreasing likelihood of experiencing motion sickness symptoms. This relationship, however, does not indicate a proportional behaviour for the entire sample. Even if the best comfort and lowest motion sickness rating occurred in the lying position, this posture is neither necessary nor desired in all situations of undergoing NDRTs during a vehicle journey. This is the case when vehicle occupants are willing to perform active NDRTs, in which a more upright sitting position is required. Under these circumstances, only a reclined position is recommended as the best trade-off between individual preference and motion comfort. The effectiveness of a small change in the backrest inclination on motion sickness mitigation is presented in all of the first three driving experiments. Comparing the number of terminations in the first and second investigation, a consistent result with the same seat configuration can be reported. The gain of 8 % in the termination rate between those examinations can be explained by two main factors. According to the MSSQ score, the sample of the second investigation seems to be more prone to experience motion sickness than the first group. Another reason is attributed to the study design since the pre-defined NDRTs that had to be conducted during the second investigation reveals to be more nauseogenic than it is obtained in the first investigation.

The key point in mitigating motion sickness is found in the passive head support, while further aspects such as the direction of motion in relation to human´s plane, intra-vestibular effects, or the manipulation of the central nervous system due to a supine posture are likely to supplement the motion sickness prevention. This conclusion can be made, among others, since no improvements in motion sickness mitigation occurred when wearing the head-neck brace. Even if the device did not support the head entirely, as it is seen in supine postures, compared to the first investigation lower sickness levels would have arisen if head stabilization is the only contribution to motion sickness mitigation.

Nevertheless, the positive effect of suitable head support is unquestioned and has already been mentioned by some researchers (Manning & Stewart, 1949; Tyler & Bard, 1949), however, an explanation of why still is the subject of some debate between leading experts (Oman & Cullen, 2014). Concerning the r.m.s. values calculated at the Ride Simulator, no significant difference in motion perception could be identified when manipulating the backrest inclination. The amount of acceleration, which is recorded by the otoliths, appears to be quite similar, whereas head motion and the reflexes of postural stability, such as VSR, VCR, and CCR, are expected to be influenced by the change in posture. This might immediately affect the postural instability and, thus, the prevalence of motion sickness. In consequence, even if the otoliths are mainly sensitive to accelerations, it does not seem to be sufficient to collect only this parameter as the input variable for the sensory rearrangement theory. Active and passive motions, which can be separated by the human organism (Goldberg et al., 2012, p. 346; Oman & Cullen, 2014), as well as the attributed compensatory reflexes to stabilize the head-neck plant shall be collected and integrated into the modeling. That information is essential to identify and rebuild the reafference copy as an essential component of the sensory rearrangement theory. The body posture shows many interactions with several comfort-relevant parameters. One of them is a strong determinant of the severity of motion sickness and proved to be an integral part of this elaboration. It is referred to the crucial ocular sensory information system that provides information about the surrounding, called vision.

Vision and Surrounding View

Whereas in the second investigation no statistically significant effect of outside view on the motion sickness rating for the total sample can be reported, within the fourth real-driving experiment significant effects occurred. Nonetheless, a consistent tendency towards less motion sickness severity and the surrounding view became apparent in both vision examinations. In the latest investigation, for instance, the number of terminations was about three times higher in the inside view group compared to the subjects who were able to see the outside environment. However, compared to other investigations (Kuiper et al., 2018; Mu et al., 2020), the impact of vision seems to be quite less than expected. One explanation for this observation is due to the inclined seat configuration, which is proven to show strong effects on motion sickness mitigation. Therefore, the reclined position might have superimposed potential beneficial effects of vision, which would have become more noticeable in an upright sitting position, like it was obtained in comparable studies. Further mitigating effects have been caused by the study design, in which the subjects were asked to constantly focus on the visually demanding NDRTs. Considering daily situations, it is expected that occupants naturally search from time to time for visual contact with the outside world to instinctively increase motion perception. As a matter of fact, a better view of the environment reduces the sensory conflict and, thus, the likelihood of experiencing kinetosis. The real benefit of these investigations, however, leads to the conclusion that a subconscious perception of the peripheral visual information also seems to influence motion sickness. Nevertheless, this beneficial impact might not be as strong as it is during active observations of the environment.

The effect of visual perception when performing distracting NDRTs can be exploited by three interior adjustments. Firstly, the control of the occupant´s gaze can be adjusted by repositioning the in-vehicle displays. The second adjustment is linked to the general surrounding view, which is determined by the vehicle dimensions (prevailing the values of H30 and H25) and potential masking objects, such as front seats when sitting in the rear of the vehicle. The last and most innovative approach is described by active visual stimulation to support human perception.

Visual Stimulation of the Interior Lighting

The type and purpose of realization hardly know any bounds, while two main directions towards motion sickness mitigation can be identified. Hainich et al. (2021) and Karjanto et al. (2018), for instance, examined a lighting system in a vehicle prototype to allow anticipation of the future vehicle trajectory. This approach is based on foresight and, consequently, requires at least some kind of cognitive processing and mental awareness. By contrast, the representation of the actual motion characteristic is an integral part of motion perception. Observing the horizon, for example, is a typical countermeasure that motion-sensitive passengers are often instructed to do. The focus here is on a conscious reduction of the sensory conflict. However, if visually demanding secondary tasks have to be carried out, mental awareness is limited. In such situations, an LED feedback system to underline the actual vehicle dynamics seems to be beneficial in terms of motion sickness mitigation. Indeed, with respect to the fourth investigation, results showed significantly smaller changes in FMS scores with the LED animation in comparison to series equipment without any visual support. These results indicate that the visual animation is capable of underlining the optic flow resulting from the outside view, but does not provide an appropriate stimulus to replace the outside view. This may change when applying a different conversion factor between the LED and vehicle velocity. Even though, with the current implementation of parameters that were determined under physiological regulations, a human-centered approach was already chosen. Whether this animation represents the vehicle dynamics in the best suitable manner cannot be answered at this present moment in time. Considering the subjective evaluation regarding the pleasantness of the LED animation, it is notable that the extreme ratings occurred in subjects who are excessively sensitive to motion sickness. Therefore, effects, no matter if positive or negative, are associated with the LED animation, especially for the valuable group with high susceptibility rates. Concerning the motion profile that occurred during the fourth investigation, it has to be mentioned that focus was placed on longitudinal stimuli. The transferability from predominant uniaxial to multiaxial motions in the daily ride may decrease the effectiveness of the examined visualization. Even if contrary results are found by Winkel et al. (2021), in summary, both animation strategies identify the potential for mitigating motion sickness and disclose promising user acceptance. This is particularly true since learning effects are expected in not directly applicable motion visualizations e.g., the brightness as a representation of the intensity in acceleration. Even if it is not researched yet, under different circumstances, learning effects have shown promising results, such as reported in visuospatial training (Smyth, Jennings, et al., 2021).

12.3 Motion Comfort and Real-Life Feasibility of Supine Positions

If a maximum motion comfort is required, without considering specific NDRTs, a supine or lying posture is recommended. Since the progress of automation does not cease, a fundamental question arises. Is it possible to reach the extended body postures in serial vehicles of today or what needs to be done to enable such extended seating configurations? Various aspects contribute to this question, while only some of them are highlighted in this work.

Interior Design of Current Vehicle Concepts

First of all, the conceptional analysis of vehicle geometry is found to be an important restriction and is illustrated in Fig. 12-1. Here, the different assumptions, requirements, and limitations are outlined. Within the framework of a series limousine, a 95th mannequin was positioned in such a way that the customized zero-gravity position is optimally represented. To avoid collisions with the steering wheel and the dashboard (front panel), the legs were allocated in a lower position. This adjustment is advantageous for another reason namely because a similar position of the lower body has already been examined in the investigations presented in this elaboration. The headrest had to be moved manually since the final position is out of the adjustable range of the series function and, thus, does not meet the requirements of future non-nominal seat configurations. Researchers from the University of Michigan confirmed this issue by investigating new headrest designs for sitting in reclined positions (Reed et al., 2019a).

Steering wheel is not considered for high or full automation driving scenarios

Headrest is manually positioned to support human´s head and neck

No space for occupants sitting in the rear

Current serial seat does not fit the mannequin

Footrest has to be added to support the calves

Tight space between legs and instrument panel
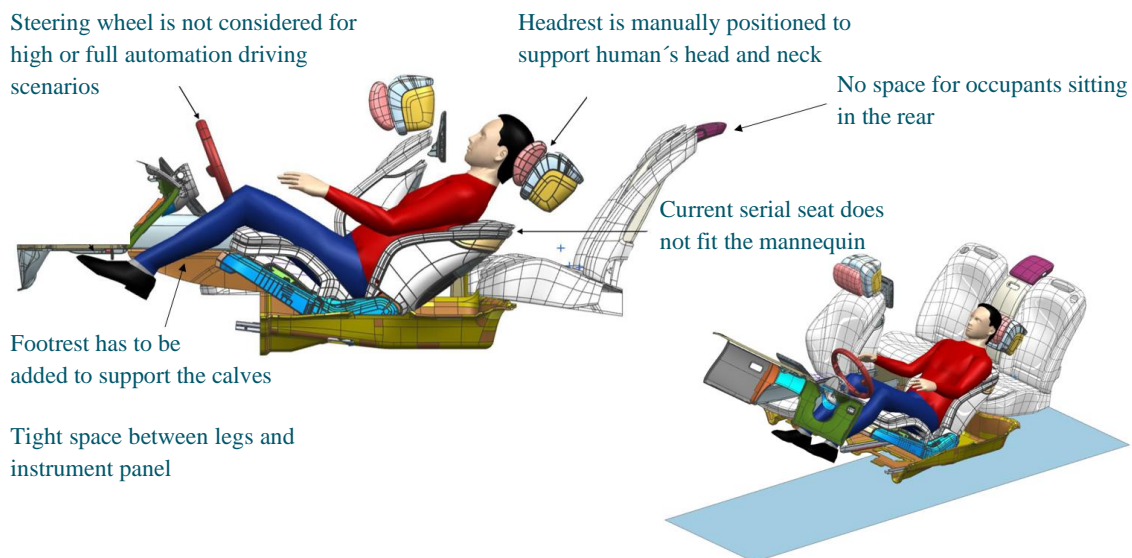
Fig. 12-1: Extended driver seat configuration in a series vehicle environment.
Modified from Daimler AG (2020)

Even if the backrest inclination could not be fully achieved the targeted 62°, a backrest angle of 58° seems to be possible. Especially, when considering SAE level 4 or 5 vehicles, it is expected that the steering wheel can disappear and provides more space for the legroom when being in a supine position. The final accomplished joint angles of the mannequin are shown as follows in Fig. 12-2.
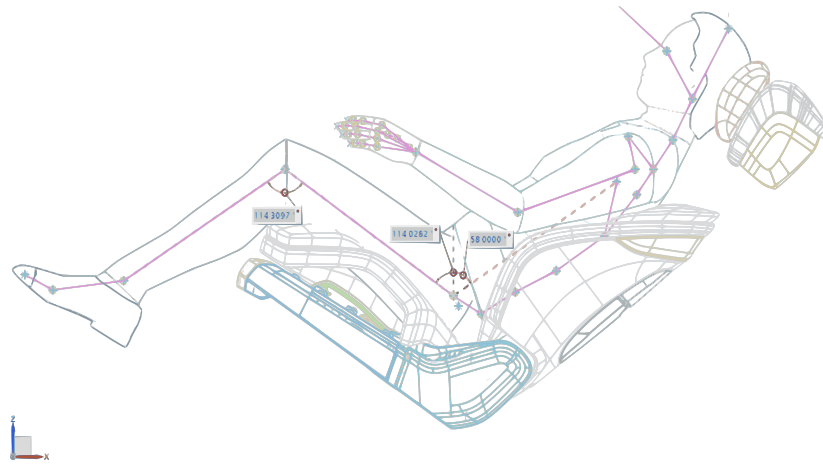
Fig. 12-2: Recommended joint angle of human body parts to enable a supine posture in series vehicles.
Modified from Daimler AG (2020)

Vehicle Safety and Human-Machine-Interface

The next important challenge is tackled by ensuring occupational safety no matter what sitting condition is taken. As it is obtained in the examination vehicle, the seat belt has to be attached to the seat structure to ensure a suitable belt routine in every backrest configuration. Furthermore, submarining as well as axial force on the spine are only some aspects that are of special interest and must be strictly avoided. The first ideas to address this safety issue are currently under examination while initial results are already published (J. Becker et al., 2020; Köhler et al., 2019; Reed et al., 2019b). Besides aspects of passive safety, also active safety contribution has to be investigated. Even if the supine position of 58° is assumed to be exclusively available for the driver seat in SAE level 4 or 5 automation, at least slightly reclined positions might be achievable also for SAE level 3 driving conditions. In terms of motion sickness mitigation, this adjustment is strongly recommended. When reclining the backrest angle of the first seating row, however, the time until the driver takes control of the vehicle e.g., as a result of an emergency situation, might increase due to the extended distance to the steering wheel. Therefore, regulations in terms of transition and the subsequent driving performance are to be integrated into the framework of an integral safety concept. Provided that such a position can be implemented under technical and regulatory circumstances, the HMI has to be designed in such a way that it can also be controlled and operated by the user in the supine posture. Control elements in the armrests and displays folding out from the vehicle roof are just a few ideas that have to be considered in future interior concepts.

Seat Design with Focus on the Headrest

When in a reclined position, the impact of the headrest on motion comfort is unquestioned. Moreover, with respect to the biomechanical behaviour of head motion, possible optimizations can be explored. Essential for a suitable vibration comfort in a supine posture is a soft and form-fitting surface of the headrest with lateral support. Here, it is recommended to design a concave-shaped headrest to ensure stable head positioning.

This is in particular important for supine positions, because the head pressure on the seat structure increases with backrest inclination. Consequently, less active head stabilization is present. If lateral oscillating force is applied, strong head motions are induced (see chapter 11.4). In other words, a flat backrest inclination enables an incomparable possibility of guiding and restricting head movements without the need for activating reflexes of the human head-neck plant. However, a reclined position comes with the disadvantages of having less vibrational comfort in the vertical direction while bearing in mind the human head resonance frequency and the vertical transmission behaviour of the headrest with the unpleasant overlay effects. Both resonating systems are oscillating around the frequency of 5 Hz, which is a typical peak frequency of an occupied seat (Eckstein, 2014b, p. 57; Seifert, 2016). As a countermeasure, shape as well as material adaptations are conceivable as methods of improving the mass-rigidity ratio. Furthermore, active compensating systems provide an additional solution to avoid the described vibrational phenomenon and solve the issue of resonance effects. Regardless of which approach is selected, cross-coupled head motions are to be imperatively avoided, not only for the sake of mitigating motion sickness (Persson, 2008) but also for the improvement in general comfort. In fact, when considering general comfort, research conducted by Fiorillo et al. (2021) has proven that shaped cushions improve the subjective comfort feeling and, thus, have to be considered for future seat designs as well.

Vehicle Dimensions and Dynamics

Another important contribution to motion comfort and motion sickness mitigation lies in the vehicle dimensions, or more precisely, the SgRP. Initially, it is stated that the vertical lever between the head and the pitch axis decreases with backrest inclination. If the longitudinal distance between the pitch axis and the head increases in a supine position, comparatively stronger heave movements arise. This effect depends on whether the first or second seat row is observed. Assuming that the driver or co-driver inclines his backrest, the head comes closer to the pitch axis, while in the second row a reversed behaviour is observed for longitudinal distance. Fig. 12-3 clearly illustrates changes of backrest inclination for the driver and co-driver position. The center of gravity is inspired by a typical sedan as described by Eckstein (2014a, p. 96).
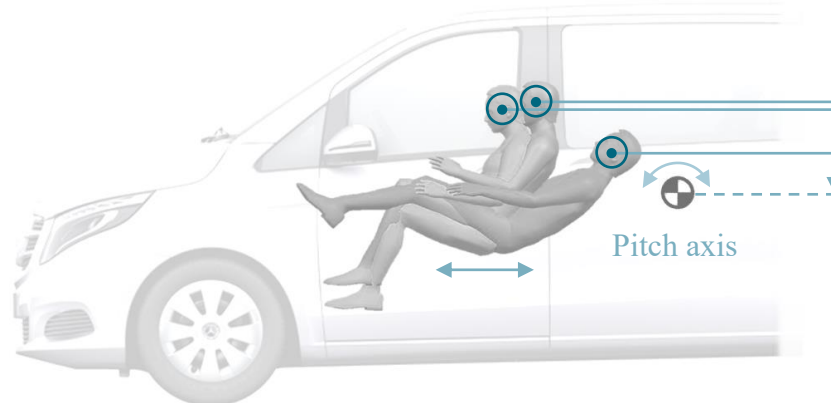
Fig. 12-3: Exemplary illustration of mechanical behaviour during backrest reclining.
Modified from Daimler AG (2020)

As a general rule, it is concluded that the smaller the SgRP (H30) the less the angular head motion is induced. At the first glance, this principle seems to be beneficial in terms of achieving comfort and mitigating motion sickness. In any case, the previously described effect of the outside view should be considered here as well (see Fig. 7-11).

Future Vehicle Concepts

In the future, additional conflicting goals such as powertrain electrification must be dealt with. A fully electric drive leads to, among other things, a better noise decoupling of the vehicle cabin compared to a vehicle with a classic combustion engine. This effect is predominantly noticeable when accelerating in low-speed conditions (Un-Noor et al., 2017). Given that noise reduction is an integral target of the NVH department of every automaker, it is expected that this development meets user desires and increases their comfort experience. This characteristic, however, comes along with unprecedented challenges. Since revving combustion engines give audible information about the actual vehicle dynamics (see Fig. 3-2), lack of motion perception might be the result when driving with electric vehicles. Especially while conducting visually demanding NDRTs, this information about vehicle acceleration seems to be of special interest. Furthermore, as outlined by Un-Noor et al. (2017), due to the immediate torque within electric powertrains, strong vehicle accelerations can be achieved. In consequence, the experienced motion patterns, which are stored in the neural network, have to be overwritten to regain motion perception and avoid symptoms of kinetosis. However, there is also an essential benefit in vehicle dimensions of future cars with the powertrain electrification. The missing engine block allows an increase in wheelbase (Luccarelli et al., 2014; Holder, 2021) and enlarges the vehicle cabin to enhance the recommended seat configurations. The cumulative assignment, therefore, is to find the ideal compromise between several human-related vehicle characteristics such as ride comfort, surrounding view, the usability of in-vehicle systems, powertrain performance, and occupant´s safety.

13 Limitations

With reference to chapter 3.1, it is described that motion sickness investigations are determined by several preconditions and assumptions. This chapter assesses the associated issues when it comes to the interpretation and external validity of the collected results by clustering the discussion into three main categories.

13.1 Limitations of the Real-Test Driving Examinations

Since all motion sickness-related examinations were conducted in a vehicle driving setting, some environmental parameters could not be controlled. Especially the weather with variations in lighting is important when analyzing vision and outside view. Within the fourth investigation, for instance, the intensity of the LED brightness did not adjust to the outside lighting conditions. This is why the illumination seemed brighter on cloudy than on sunny days.

Besides the interior lighting stimulation, outside view, in general, might be affected by environmental conditions, such as distraction initiated through passing vehicles on the test track. Since the measurements were conducted across the entire day, some variation in outside temperature is expected to have influenced the interior conditions. Therefore, changes in cabin temperature were logged throughout the entire journey. Albeit the oxygen saturation in the vehicle cabin, which probably has been decreased during the trial, no intense temperature fluctuation was captured. For instance, during the fourth investigation, a deviation from the mean temperature in a range from -1 to +3.1 °C with an average temperature change of +1.2 ± 1.01 °C across all sessions could be reported.

Even if the applied motion pattern was performed within the limits of the ACC system (ISO 15622:2018-09), no pure naturalistic approach had been chosen. Neither the original characteristic of motion nor the frequency of its events corresponds to reality in all forms. Moreover, when thinking about automated driving situations, future vehicle motions might differ from today's manual driving mode. This seems to be important since carsickness is highly influenced by the motion characteristic in which it is experienced. Because a human driver maintained the vehicle control during the studies, slight variations in the experienced dynamics across the measurements could not be excluded. However, to reduce the level of variation to a minimum, a trained driver with clear instructions carried out the predefined maneuvers in all investigations. Furthermore, no disturbing traffic on the test route occurred, which ensured a constant driving duration. The experimental vehicle, which is determining for the characteristics in vertical motion, kept the same across the entire driving events as well. This standardization, by contrast, implies disadvantages concerning the generalization of results and the human anticipation during the trial. In fact, due to the reproducible manner of stimuli (multiple driving rounds and repeated measures design), the participants were able to develop a suitable internal model of what was happing next. However, it is also expected that the predefined NDRTs obstruct this active mental behaviour.

The impact of the general nature of a test condition is not to be disregarded. In fact, when being in seafaring environments, for instance, suppression of the nauseogenic stimuli is not possible. As consequence, mental pressure which might reinforce motion sickness expressions is more likely to occur. For instance, in chapter 3.3 it is presented that cortisol, as an essential stress hormone, is somehow linked to motion sickness (S. Schneider et al., 2007). Moreover, Meissner et al. (2009) discovered the cortisol level to predict tolerance against nauseogenic stimuli in females. In consequence, the physical and mental format might have the same relevance as order effects or expectation and is to be treated as a disturbance variable in the interpretation of the collected results. Further human-related factors like duration of sleep, nutrition, and current level of mental or physical strain have been monitored at least in parts by the demographic questionnaire but were not controlled in the investigations.

To assess at least some meta-analyses, few participants took part in more than one examination. The benefit of a constant susceptibility rate, however, is impaired by the previously mentioned effects of habituation and expectation due to prior experience made in preceding studies.

The expectation, in general, is also affected by the circumstances that the participants had been previously informed about the purpose of the investigations i.e., the causation of carsickness. Especially in the third investigation, the small sample size is limiting the generalisability of the results. In fact, the median split method leads to a critical number of subjects for this particular application. Furthermore, the composition of the test sample across all investigations does not represent the distribution of motion sickness susceptibility in the population. Therefore, contrary effects in people who are not prone to experience motion sickness cannot be excluded. Moreover, the countermeasures have proven, on one hand, to decrease motion sickness severity in early stages and, on the other hand, to delay the time at which congruent expressions of nausea and malaise occur. Their effectiveness in situations with an already existing manifestation of motion sickness, however, was not yet researched. Even if missing evidence has to be stated, it is expected that those countermeasures are also effective in such situations. This assumption can be made since a few test subjects experienced symptoms in advanced stages and continued for some time the investigation (until they reached the abort criterion).

13.2 Limitations of the Biomechanical Examinations

In general, when analyzing the biomechanical behaviour, a distinction has to be made between the multibody simulation and the recorded head motion analysis that had been conducted on the Ride Simulator. The results of the strong braking maneuver conducted by the MADYMO multibody simulation are to be treated as principal analysis. This software, certainly, is originally used and validated for other use cases and, thus, may show some uncertainties in the generalization of results. For instance, the deceleration obtained within the simulation shows a more impulse-like nature than it becomes apparent in real-life braking maneuvers. Furthermore, only the passive human model was chosen without concerning active body reflexes like the CCR and VCR. However, the purpose of this analysis is fulfilled, in which the observations that had been emerged during the real-life driving experiments were reconstructed, visualized, and quantified. When comparing both results with each other, strong similarities in motion characteristics occur.

The main weaknesses associated with the Ride Simulator investigation are due to the limited variance in anthropometry, sample size, and the missing information about the individual´s head dimensions. To reduce the interindividual disturbances within this limited data set, the focus was placed on participants of the same body length of a 50th mannequin. Although it was possible to identify systematic characteristics in head motion, no quasi-static motions could be applied to the participants. Even if this kind of motion pattern does not allow a system identification, it better captures real-life driving conditions. Albeit the sampling rate of the accelerometers was quite small, it seemed to be an adequate representation of characteristic facets of head motion. However, regulating motor activities as well as the head position could not be captured with this method. Both pieces of information seem to be important to quantify and predict motion sickness.

13.3 Limitations Regarding Motion Comfort, Physiology, and Performance

The evaluation of subjective comfort is based on data gathered in the Ride Simulator investigation. Here, mostly noise stimuli occurred. In consequence, the issue of motion comfort was tackled in a more generic and holistic approach without considering the typical quasi-static vehicle motion of the daily ride. Moreover, no mockup or vehicle cabin was used which might affect the level of immersion. The findings and implications collected during this type of investigation were not validated by real driving experiments with longer durations and, therefore, have to be discussed critically.

Both subordinate research topics of objectification and performance had to obey the governing restrictions that come along with experiments on motion sickness treatments. For instance, the test setup of real driving events had shrunken the possibility and degrees of freedom of the experimental design within physiological measures. Besides this biased selection of physiological parameters, there are also important limitations within the applied measurements. Given that motion sickness correlates with hormone excretion, latencies in physiological manifestations such as respiratory and cardio-vascular expressions are obvious. Concerning the driving experiments, the measurements were stopped immediately after the trial ended or when extensive symptoms occurred. This had been done to initiate ad hoc initiatives with the purpose of curbing the unpleasant effects of motion sickness. This procedure is accompanied by potential data loss in physiological measures. To facilitate the practical use of objectification, the focus shall move to use cases of daily life. In fact, the main benefit reveals to the early recognition of motion sickness, even before the subjects are aware of the upcoming physiological expressions. For instance, during a long journey in an automated vehicle, potential countermeasures regarding motion sickness can be presented to the vehicle occupants, even before symptoms occur and the journey may have to be stopped. The findings determined within this work do not seem to be sensitive enough to fulfill this desire. Furthermore, cardio-vascular measures are affected by body posture (Horn, 2003, p. 41) and, therefore, might have limited evidence regarding motion sickness detection. Furthermore, the physiological parameters had been set into a relationship with subjective measures. In consequence, the evaluation of the objective measurement is based on the uncertainty in capturing actual motion sickness manifestations. Finally, the characteristics of NDRTs with their provoking emotions might have superimposed the physiological expressions of motion sickness and, thus, show the potential of blurring systematic results.

As previously outlined, motion sickness not only limits the user experience during journeys, moreover, it might be a safety-relevant issue of implementing further levels of road vehicle automation. The applied performance tests, on one hand, support this need for further investigations, however, but on the other hand, do not answer the question of the actual effect in real-life situations. More precisely, the testing did not capture long-time performance or aftereffects that commonly occur with motion sickness. Furthermore, opposite effects, like learning versus exhaustion, might superimpose manifestations on a physiological basis. Therefore, it is not clear whether significant effects are associated with expressions of carsickness or influenced by other attributes that also correlate with time e.g., personal involvement, ambitiousness, or exhaustion.

14 Summary and Conclusion

The idea of automated driving empowers new degrees of freedom in vehicle design and forces the evolution of its usage. Indeed, vehicle automation allows rethinking the conceptional design of future transportation. The vehicle is no longer exclusively a means of transportation. In the future, it promises to be a living space, office, or just a room that invites to relax. To enhance this ambitious goal, human-centered design including treatments on motion sickness has to be considered, in which the desires and restrictions of users built the core of the development. The current elaboration includes five investigations as well as additional simulations that address research on vehicle motion comfort with a strong focus on alleviating motion sickness. In fact, this work presents, among other findings, the possibility of mitigating carsickness through physical-geometric adjustments of the vehicle interior. Even if a significant reduction in motion sickness is evaluated, a complete exclusion of any symptoms for everybody has not been reached within this elaboration. Therefore, research in this domain is still a crucial object of interest when it comes to the successful introduction of automated vehicles in the near future. In the following, the main findings collected in this work are summarized concerning the research questions that have been formulated in chapter 4. In general, it has to be stated that the presented findings are strongly associated with the test setup, which leads to the assumption of shrunken generalizability.

14.1 Human-Related Research Findings on Motion Sickness Methodology

1. *Is it possible to quantify individual carsickness by objective measurements?*
   Correlations between physiological parameters i.e., predominantly the difference in heart rate and core body temperature, and carsickness are found. However, the criteria alone do not seem to be sensitive enough to represent the polysymptomatic nature of motion sickness for the majority of the population. Moreover, the evaluation of the physiological data set had been done on subjective measurements. This is an issue perse since the target of objective measures is, among other things, an unbiased detection of a particular variable of interest. When considering the behavioural observations, looking up, or in other words searching for the outside view, is a criterion that increases with the duration of driving and showed differences between the backrest inclinations. Even it is not clear whether this behaviour is related to the difference in body posture or is a compensational strategy to alleviate carsickness, it is recommended to treat it as a potential indicator of an increased likelihood of suffering from carsickness.

2. *Does carsickness affect human concentration and reaction time?*
   In general, there is no clear picture when it comes to objective evaluations as an indicator for the change in performance due to increasing carsickness. Although in some cases significant findings can be reported, their effect and relevance for daily life remain unanswered. When analyzing the qualitative questionnaires and the subjective evaluations, effects of carsickness on individual performance e.g., ability to concentrate, becomes apparent and seems to be relevant, at least for future research.

174

3. *Which non-vehicle-related parameters affect the severity of carsickness and, thus, are relevant for the test design?*

Beyond all examinations, the inter- and intraindividual susceptibility to motion sickness are highly relevant for the occurrence of malaise, nausea, and its kind of pathogenesis. In addition, it has been proven that carsickness strongly correlates with the duration of journey. This relationship is based on a steady-state condition and does not mandatory imply a linear behaviour between the severity of malaise and duration. The third important criterion does show at least some interactions with the vehicle. The driving maneuver and the road that is chosen substantially affect carsickness. To be more specific, low-frequency motion in the horizontal plane should be avoided. In particular, fore-and-aft vehicle motion as it occurs during stop-and-go traffic is the most critical scenario that fulfills these conditions. Thus, it is strongly recommended that in the future automated vehicles consider those requirements in their trajectory and route planning. Even though it is not sufficiently captured along all driving experiments, the characteristics and types of NDRT are highly relevant for carsickness, too. In fact, distraction, visual motion dynamics, state of immersion, personal involvement, and many other properties contribute to the nauseogenic nature of the task when being driven. Given that the samples within the examinations had not been randomly picked as it is necessary to represent the population, the ability to generalize results according to the effect of age and biological gender on carsickness is lacking. However, under this premise, no statistically relevant effect could be observed in neither case of these particular kinds of human-related characteristics.

14.2 Vehicle-Related Research Findings on Motion Sickness Treatments

4. *Is it possible to manipulate carsickness in subjects by adjusting the vehicle interior?*

Properties of the vehicle interior are extremely important when it comes to motion sickness treatments. A wide range of parameters manipulates carsickness and shows potential to support visually demanding NDRTs when being exposed to mechanical vibrations. Even variables that were intended to be standardized show slight effects on the severity of motion sickness (in-car temperature).

5. *In fact, do supine postures influence carsickness?*

Supine or even reclined body postures have proven to be one of the most effective treatments of the vehicle interior to avoid carsickness. This is especially true when being distracted from the outside world with a loss of visual information.

6. *If supine postures are likely to decrease the severity of carsickness, to what extent does the backrest inclination need to be adjusted?*

Firstly, it has to be ensured that the head is permanently stabilized by the headrest. This is already achieved by slight inclination angles of 35°. To increase axial head support, a heightened seat cushion is recommended. With seat adjustments up to 62° backrest angle, further reductions in carsickness can be achieved for vehicle occupants who are more sensitive to experiencing the physiological syndrome.

In consequence, it can be stated that the more supine the body posture, the less carsickness occurs.

7. *Do vis-à-vis seating positions increase the prevalence of carsickness?*
Rearward sitting with the ability to facilitate in-vehicle passenger communication is rather ineffective in manipulating motion sickness severity. This assumption, however, is linked to scenarios in which the occupants are visually distracted and do not monitor the motion environment. Furthermore, the results collected in this elaboration are predominantly superimposed by the backrest inclination.

8. *What is the impact of outside view on carsickness when being engaged in visually demanding activities?*
Although not significant in every manner, the ability of a surrounding view does make also a difference when being visually distracted. Besides the fact that outside view is known to be relevant for a suitable comfort level during a vehicle journey, it, even more, is important to decrease the risk of suffering from carsickness. While in the second investigation only slight effects could be observed, within the fourth study a stronger manifestation occurred. Here as well, superimposing effects of visual distraction and backrest inclination have to be stated. Under the adoption of this assumption, the impact of backrest inclination implies higher effect sizes and, therefore, might be more effective in avoiding carsickness when performing visually demanding NDRTs.

9. *Moreover, is it possible to increase visual perception by manipulating in-vehicle lighting systems to reduce carsickness?*
Interior lighting systems e.g., a prototypical LED animation, do indeed show potential in reducing carsickness. Within the current approach, the aim has been to represent the natural optic flow. This effect, even if it was not significant, tends to be influenced by the ability to see the outside environment. When considering only visual information, the LED animation seems to be slightly more effective in manipulating carsickness than the outside view is. As previously stated, interactions with body posture and tasks are present and determine the conclusion made in this work.

10. *Are the findings regarding vehicle-related countermeasures on carsickness congruent with the already presented etiological theories?*
The research findings have proven the justification of both the sensory rearrangement and the postural instability theories. The impact of outside view and LED animation clearly addresses the assumptions by Reason and Brandt (1978). Considering the first investigation, however, this seems to be insufficient since at least the external vehicle motion and the visual mismatch, by the loss of outside view, were equivalent for both backrest conditions. Here, the postural instability theory comes to play with the respective body reflexes (CCR, VCR, VSR). They seem to be influenced by active head support and decrease postural instability.

14.3 Further Research Findings Regarding Motion Comfort

11. *How is the feeling of comfort and the user acceptance with respect to innovative seating configurations?*
In general, improvement of motion comfort is reported with increasing backrest angle. This assumption is valid at least for generic motion patterns applied on a hexapod simulator (Ride Simulator). Taking NDRTs into account, a general conclusion can be made in which active tasks are more likely to be performed in a more upright position, whereas passive activities require supine positions.

12. *How does human body vibration change when manipulating seat configurations?*
With respect to the driving observations and the multibody simulation, it is confirmed that reclined positions lead to more head stability and less head displacement when being exposed to quasi-static longitudinal vehicle motion. Investigations conducted at the Ride Simulator gained deeper knowledge about the general head motion characteristics as a function of human body posture. Firstly, it is stated that the more supine the posture is, the more dominant the headrest becomes. Especially in the vertical direction, the resonance frequencies show that the actual design of seating structures can cause a fundamental issue when being in a lying position. Furthermore, a strong negative relationship between backrest angle and the time delay at which the head response is visible occurs.

14.4 Key Messages and Recommendations on Future Vehicle Interior Design

In addition to the above-mentioned research findings, this chapter focuses on interior design guidelines for future automated vehicles that drop out of the current elaboration. Hence, the following key messages have been formulated:

- Reclined and supine postures not only decrease the prevalence of carsickness, they are even more capable of increasing motion comfort. Ensuring a stable and continuous head support, also sitting against the driving direction does not intensively provoke kinetosis. The beneficial impact seems to compensate for potential negative effects that come along with rearward sitting as reported by other researchers.

- However, today´s seat structures and restraining systems are not capable of enabling such extended seat configurations in a comfortable and safe manner. For instance, the shape of the headrest, the limited adjustability of the seat structure, the missing lateral support of the upper body, or the belt routine are only a few examples that have to be solved in the future.

- Furthermore, in-vehicle HMI has to be redesigned to enable operation and control even when being in supine positions. In addition, the recommendation of a suitable surrounding view, for instance, determines the positioning of screens. Furthermore, masking obstacles shall be avoided. Lastly, the entire vehicle dimension concept is to be designed in such a way that outside view is possible in any given position. This can be achieved, among others, by a reduction of the H25 value.

- In the future, interior lighting will no longer be a means to an end. Even more, it is increasingly capable of enhancing user experience and motion perception by dedicated visual stimuli. Even if the presented approach did not match the desires of all users, the potential of ambient light as a catalyst of improvements in motion comfort has been identified.

15 Outlook

This elaboration presents research findings on mitigating carsickness for enhancing motion comfort within future automated vehicles. Even if some crucial conclusions had been made, nevertheless, there is still a wide range of research that awaits to be examined. For instance, in addition to the presented findings on treatments, performance, and objectification, also the everyday prevalence e.g., the relevance for autonomous driving, is only one topic among others that show potential for further research. Even if the findings on motion sickness treatments were collected during driving situations, a validation of these countermeasures is strongly recommended. Firstly, a more naturalistic test route characterized by a lower frequency of maneuver events and longer driving duration has to be defined. Secondly, it is recommended to choose a more diverse sample that also includes subjects who are more resistant to nauseogenic stimuli. Although some researchers emphasized that no statistical significance occurs in motion sickness towards different vehicle types (Turner & Griffin, 1999b), examinations across different chassis, suspension systems, powertrains, and cabin designs seem to be necessary. This is particularly true when considering future automated vehicle concepts. Active vehicle suspension systems with obstacle and road surface prediction, for instance, are likely to compensate specific vehicle motion by using the vehicle's predictability of road unevenness. Albeit this technological development intends to increase motion comfort, it is likewise conceivable that also motion sickness might increase with this technology. Even if DiZio et al. (2018) have already identified positive effects coming along with active safety systems, when considering the first introduction of tilting trains, by contrast, contrary effects with increasing kinetosis manifestations occurred (see chapter 3.1.3). In consequence, changes of motion characteristics, no matter due to suspension adjustment, rear-axle steering, or just through trajectory strategy, are fundamental research topics that have to be examined in terms of motion comfort (Jurisch et al., 2020).

Besides vertical and lateral vehicle motion, longitudinal characteristics also have to be considered. The increasing onset of electrified powertrains, for instance, leads to differences in the acceleration behaviour as it is experienced by today's vehicles with a combustion engine. Moreover, the missing engine sound decrease information about vehicle acceleration and, therefore, might affect the occurrence of motion sickness (Sawada et al., 2020). Future vehicle concepts demand a holistic human-centered design approach, in which the focus is on the experience and excitement of the journey. This paradigm shift is already visible in the latest serial vehicles of leading car manufacturers (Ernstberger et al., 2020) and has to be further intensified with future vehicle concepts.

For instance, slight changes in the interior design e.g., the backrest inclination, require several adaptations such as display and control element positioning as well as new occupational safety concepts.

Visual stimulation has been proven to show potential in motion sickness mitigation, albeit the invention presented in the current elaboration still is at a prototypical early stage. To improve the LED animation also for people who rated the visualization to be too intense, the characteristics of the light animation reveals to be a central research question in the future. Besides the need of optimizing the type and parameter of visualization, it is furthermore expected to achieve great learning effects. Therefore, longitudinal and panel analyses are recommended here. In addition, a fundamental question arises. In fact, it has to be examined which information about the surrounding motion environment is necessary to avoid motion sickness. Is it sufficient to see the sky through the sunroof or is it mandatory to have a stable look at the outside horizon? Or, even worse, do oncoming vehicles provide counterproductive information about passive motion perception?

When considering the requirements of the human body vibration, it has been shown that the ISO 2631, as it is now, does not sufficiently meet the demands of carsickness. Neither the direction of motion nor the impact of posture is concerned. Moreover, aspects of cross-coupled and angular motions, as well as jerk, shall be considered in the future. Beyond the topic of motion sickness, subjective sensation and objective measures have to be conducted to gain deeper knowledge about vibrational comfort. With reference to previous and current research, for instance from Bellem et al. (2016), Dettmann et al. (2021), Ossig et al. (2021), or D'Amore & Qiu (2021), it is recommended to further develop objective metrics to capture and evaluate general motion comfort with the purpose to design automated driving styles. When considering the current investigations, further research on head dynamics seems to be valuable. To collect corresponding information, motion capturing offers additional and previously unprecedented insights. Especially, when considering the paradigm of head support, the contact behaviour of the head and headrest describes a conceivable application for this method.

Given that the presented performance tests only provide information about a small range of individual capability, it will be necessary to carry out further investigations to clarify the vehicle-related pertinence. For instance, does the slight decrease in reaction time indicates a substantial impact on road safety? This is only one among several other fundamental questions that have to be answered when it comes to the dissemination of automated driving. Under these circumstances, a pre-warning system for detecting motion sickness in the early stages can be helpful to avoid hazards that occur with the physiological syndrome. Even if some significances occurred within the physiological measures, no all-encompassing parameter was identified. Therefore, a more holistic approach seems to be worthwhile that refers to a multidimensional model by combining biosignals, individual susceptibility as well as exogenous conditions such as mechanical vibration. With artificial intelligence, clustering, and neural network methods, further effort should be taken to eliminate leakage effects that occur in motion sickness prediction as a result of interindividuality. Initial research in this area has already been conducted and shows promising results (Islam et al., 2020; Y. Li et al., 2019).

16 Bibliography

Agrawal, Y., Carey, J. P., Della Santina, C. C., Schubert, M. C., & Minor, L. B. (2009). Disorders of balance and vestibular function in US adults: Data from the National Health and Nutrition Examination Survey, 2001-2004. *Archives of Internal Medicine*, *169*(10), 938–944. https://doi.org/10.1001/archinternmed.2009.66

Akgun, V., Battal, B., Bozkurt, Y., Oz, O., Hamcan, S., Sari, S., & Akgun, H. (2013). Normal anatomical features and variations of the vertebrobasilar circulation and its branches: An analysis with 64-detector row CT and 3T MR angiographies. *The Scientific World Journal*, *2013*, 620162. https://doi.org/10.1155/2013/620162

Akin, C. (2020). *Mastocytosis: A Comprehensive Guide* (1st ed.). Cham: Springer International Publishing. https://doi.org/10.1007/978-3-030-27820-5

Altinsoy, M. E., Blauert, J., & Treier, C. (2001). Inter-Modal Effects of Non-Simultaneous Stimulus Presentation. In A. Alippi (Ed.), *Proceedings of the 7th International Congress on Acoustics*. Retrieved from http://citeseerx.ist.psu.edu/viewdoc/download?doi=10.1.1.170.5006&rep=rep1&type=pdf on 6/2/2021

Amemiya, T., Hirota, K., & Ikei, Y. (2013). Tactile flow on seat pan modulates perceived forward velocity. In *2013 IEEE Symposium on 3D User Interfaces (3DUI)* (pp. 71–77). IEEE. https://doi.org/10.1109/3DUI.2013.6550200

Anderson, J., Kalra, N., Stanley, K., Sorensen, P., Samaras, C., & Oluwatola, O. (2016). *Autonomous Vehicle Technology: A Guide for Policymakers*: RAND Corporation. https://doi.org/10.7249/RR443-2

Angelaki, D. E., & Hess, B. J. M. (2001). Direction of heading and vestibular control of binocular eye movements. *Vision Research*, *41*(25-26), 3215–3228. https://doi.org/10.1016/s0042-6989(00)00304-7

Angelaki, D. E., & Hess, B. J. M. (2005). Self-motion-induced eye movements: Effects on visual acuity and navigation. *Nature Reviews. Neuroscience*, *6*(12), 966–976. https://doi.org/10.1038/nrn1804

Angelaki, D. E., McHenry, M. Q., & Hess, B. J. M. (2000). Primate translational vestibuloocular reflexes. 1st High-frequency dynamics and three-dimensional properties during lateral motion. *Journal of Neurophysiology*, *83*(3), 1637–1647. https://doi.org/10.1152/jn.2000.83.3.1637

Antuñano, M. J., & Hernandez, J. M. (1989). Incidence of airsickness among military parachutists. *Aviation, Space, and Environmental Medicine*, *60*(8), 792–797.

Araque, A., & Navarrete, M. (2010). Glial cells in neuronal network function. *Philosophical Transactions of the Royal Society of London. Series B, Biological Sciences*, *365*(1551), 2375–2381. https://doi.org/10.1098/rstb.2009.0313

Araujo, H. F., Kaplan, J. [Jonas], Damasio, H., & Damasio, A. (2015). Neural correlates of different self domains. *Brain and Behavior*, *5*(12), e00409. https://doi.org/10.1002/brb3.409

Araújo, M., Sampaio, A., & Oliveira, C. (2021). Anatomy And Physiology Of The Posterior Labyrinth [Webpage]. Retrieved from https://www.jaypeedigital.com /eReader/chapter/9789385999055/ch1 on 3/14/2021

Armand, M., & Minor, L. B. (2001). Relationship between time- and frequency-domain analyses of angular head movements in the squirrel monkey. *Journal of Computational Neuroscience*, *11*(3), 217–239. https://doi.org/10.1023/A:1013771014 232

Arnold, J. J., & Griffin, M. J. (2018). Equivalent comfort contours for fore-and-aft, lateral, and vertical whole-body vibration in the frequency range 1.0 to 10 Hz. *Ergonomics*, *61*(11), 1545–1559. https://doi.org/10.1080/00140139.2018.1517900

Arnold, J. T., O'Keeffe, K., McDaniel, C., Hodder, S., & Lloyd, A. (2019). Effect of virtual reality and whole-body heating on motion sickness severity: A combined and individual stressors approach. *Displays*, *60*, 18–23. https://doi.org/10.1016/j.displa.2019.08.007

Asadi, H., Mohamed, S., Lim, C. P., & Nahavandi, S. (2016). A review on otolith models in human perception. *Behavioural Brain Research*, *309*, 67–76. https://doi.org/10.1016/j.bbr.2016.03.043

Asarian, L., Gloy, V., & Geary, N. (2012). Homeostasis. In *Encyclopedia of Human Behavior* (pp. 324–333). Elsevier. https://doi.org/10.1016/B978-0-12-375000-6.00191-9

Asawavichienjinda, T., & Patarapak, S. (2019). Reliability of the Thai Version of the Motion Sickness Susceptibility Questionnaire Short-Form. *Aerospace Medicine and Human Performance*, *90*(1), 26–31. https://doi.org/10.3357/AMHP.5203.2019

Aschoff, J. (1944). Die Vasodilatation einer Extremität bei örtlicher Kälteeinwirkung. *Pflügers Archiv Für Die Gesamte Physiologie Des Menschen Und Der Tiere*, *248*(1-3), 178–182. https://doi.org/10.1007/BF01751522

Baek, H. J., Cho, C.-H., Cho, J., & Woo, J.-M. (2015). Reliability of ultra-short-term analysis as a surrogate of standard 5-min analysis of heart rate variability. *Telemedicine Journal and E-Health: The Official Journal of the American Telemedicine Association*, *21*(5), 404–414. https://doi.org/10.1089/tmj.2014.0104.

Bagloee, S. A., Tavana, M., Asadi, M., & Oliver, T. (2016). Autonomous vehicles: challenges, opportunities, and future implications for transportation policies. *Journal of Modern Transportation*, *24*(4), 284–303. https://doi.org/10.1007/s40534-016-0117-3

Bagshaw, M., & Stott, J. R. (1985). The desensitisation of chronically motion sick aircrew in the Royal Air Force. *Aviation, Space, and Environmental Medicine*, *56*(12), 1144–1151.

Bahra, A., Matharu, M. S., Buchel, C., Frackowiak, R. S., & Goadsby, P. J. (2001). Brainstem activation specific to migraine headache. *The Lancet*, *357*(9261), 1016–1017. https://doi.org/10.1016/S0140-6736(00)04250-1

Baird, R. A., Desmadryl, G., Fernández, C., & Goldberg, J. M. (1988). The vestibular nerve of the chinchilla. II. Relation between afferent response properties and peripheral innervation patterns in the semicircular canals. *Journal of Neurophysiology*, *60*(1), 182–203. https://doi.org/10.1152/jn.1988.60.1.182

Baker, J., Goldberg, J. M., & Peterson, B. (1985). Spatial and temporal response properties of the vestibulocollic reflex in decerebrate cats. *Journal of Neurophysiology*, *54*(3), 735–756. https://doi.org/10.1152/jn.1985.54.3.735

Bakwin, H. (1971). Car-sickness in twins. *Developmental Medicine and Child Neurology*, *13*(3), 310–312. https://doi.org/10.1111/j.1469-8749.1971.tb03267.x

Baloh, R. W. (1997). Neurotology of migraine. *Headache*, *37*(10), 615–621. https://doi.org/10.1046/j.1526-4610.1997.3710615.x

Baloh, R. W., & Honrubia, V. (1979). Clinical neurophysiology of the vestibular system. *Contemporary Neurology Series*, *18*, 1–21.

Banta, G. R., Ridley, W. C., McHugh, J., Grissett, J. D., & Guedry, F. E. (1987). Aerobic fitness and susceptibility to motion sickness. *Aviation, Space, and Environmental Medicine*, *58*(2), 105–108.

Bär, M. (2014). *Vorausschauende Fahrwerkregelung zur Reduktion der auf die Insassen wirkenden Querbeschleunigung* (Dissertation). Rheinwestfälische Hochschule (RWTH) Aachen University, Aachen, Germany.

Bates, D., Mächler, M., Bolker, B., & Walker, S. (2015). Fitting Linear Mixed-Effects Models Using lme4. *Journal of Statistical Software*, *67*(1). https://doi.org/10.18637/jss.v067.i01

Bates, D., Maechler, M., Davis, T. A., Oehlschlägel, J., & Riedy, Jason, R Core Team (2021). Matrix: Sparse and Dense Matrix Classes and Methods (R package version 1.3-3). Retrieved from https://cran.r-project.org/web/packages/Matrix/index.html on 5/29/2021

Beard, F. (2012). *Discomfort of seated persons exposed to low frequency lateral and roll motion* (Dissertation). University of Southampton, Southampton, United Kingdom.

Becker, J., D´Addetta, G., Wolkenstein, M., Bosma, F., Verhoeve, R., Sprenger, M., . . . Hamacher, M. (2020). Occupant Safety in Highly Automated Vehicles - Challenges of Rotating Seats in Future Crash Scenarios. *International Research Council on Biomechanics of Injury (IRCOBI)*, 381–397. Retrieved from http://www.ircobi.org/wordpress/downloads/irc20/pdf-files/51.pdf on 3/24/2021

Becker, T., Herrmann, F., Duwe, D., Stegmüller, S., Röckle, F., & Unger, N. (2018). *Enabling the value of time: Implikationen für die Innenraumgestaltung autonomer Fahrzeuge*. Stuttgart. Retrieved from Fraunhofer Institut für Arbeitswissenschaft und Organisation (IAO), Cordence Worldwide and Horvárt & Partner website: http://publica.fraunhofer.de/eprints/urn_nbn_de_0011-n-4970351.pdf
on 2/4/2021

Beier, M., Anken, R. H., & Rahmann, H. (2002). Influence of hypergravity on fish inner ear otoliths: 2. Incorporation of calcium and kinetotic behaviour. *Advances in Space Research: The Official Journal of the Committee on Space Research (CO-SPAR)*, *30*(4), 727–731. https://doi.org/10.1016/s0273-1177(02)00387-3

Bellem, H., Schönenberg, T., Krems, J. F., & Schrauf, M. (2016). Objective metrics of comfort: Developing a driving style for highly automated vehicles. *Transportation Research Part F: Traffic Psychology and Behaviour*, *41*, 45–54. https://doi.org/10.1016/j.trf.2016.05.005

Bengler, K., Dietmayer, K., Eckstein, L., Stiller, C., & Winner, H. (2021). Fahrerassistenzsysteme und Automatisiertes Fahren. In S. Pischinger & U. Seiffert (Eds.), *Vieweg Handbuch Kraftfahrzeugtechnik* (pp. 1009–1072). Wiesbaden: Springer Fachmedien. https://doi.org/10.1007/978-3-658-25557-2_8

Benson, A. J. (2002). Motion Sickness. In K. B. Pandoff & R. E. Burr (Eds.), *Medical Aspects of Harsh Environments* (2nd ed., pp. 1048–1083). U.S. Army Medical Department, Borden Institute. Washington, D.C., United States.

Benson, A. J., Spencer, M. B., & Stott, J. R. (1986). Thresholds for the detection of the direction of whole-body, linear movement in the horizontal plane. *Aviation, Space, and Environmental Medicine*, *57*(11), 1088–1096.

Bertolini, G., Durmaz, M. A., Ferrari, K., Küffer, A., Lambert, C., & Straumann, D. (2017). Determinants of Motion Sickness in Tilting Trains: Coriolis/cross-Coupling Stimuli and Tilt Delay. *Frontiers in Neurology*, *8*, 195. https://doi.org/10.3389/fneur.2017.00195

Bertolini, G., & Straumann, D. (2016). Moving in a Moving World: A Review on Vestibular Motion Sickness. *Frontiers in Neurology*, *7*, 14. https://doi.org/10.3389/fneur.2016.00014

Bethel, J. (2021). *A Comparison of Motion Sickness Susceptibility in Those Participating in Recreational Sport and Physical Activity Versus Those Participating in Competitive Sport and Physical Activities Chester Business School Personal Academic Tutor* (Dissertation). University of Chester, Chester, United Kingdom.

Beucher, O. (2015). *Signale und Systeme: Theorie, Simulation, Anwendung: Eine beispielorientierte Einführung mit MATLAB* (2nd ed.). Heidelberg: Springer Vieweg. https://doi.org/10.1007/978-3-662-45965-2

Billman, G. E. (2013). The LF/HF ratio does not accurately measure cardiac sympathovagal balance. *Frontiers in Physiology*, *4*. https://doi.org/10.3389/fphys.2013.00026

Blake, R., & Fox, R. (1973). The psychophysical inquiry into binocular summation. *Perception & Psychophysics*, *14*(1), 161–185. https://doi.org/10.3758/BF03198631

Blanks, R. H., Curthoys, I. S., & Markham, C. H. (1975). Planar relationships of the semicircular canals in man. *Acta Oto-Laryngologica*, *80*(3-4), 185–196. https://doi.org/10.3109/00016487509121318

Bles, W., Bos, J. E., Graaf, B. de, Groen, E., & Wertheim, A. H. (1998). Motion sickness: only one provocative conflict? *Brain Research Bulletin*, *47*(5), 481–487. https://doi.org/10.1016/s0361-9230(98)00115-4

Bohrmann, D. (2019). Probandenstudie - Vom Fahrer zum Passagier. *ATZ Extra*, *24*(S1), 36–39. https://doi.org/10.1007/s35778-019-0010-x

Bohrmann, D., & Bengler, K. (2020). Reclined Posture for Enabling Autonomous Driving. In T. Ahram, W. Karwowski, S. Pickl, & R. Taiar (Eds.), *Human Systems Engineering and Design II. IHSED 2019: Vol. 1026. Advances in Intelligent Systems and Computing* (pp. 169–175). Cham: Springer International Publishing. https://doi.org/10.1007/978-3-030-27928-8_26

Bohrmann, D., Fischer, S., & Strasdat, B. (2015), Volkswagen Aktiengesellschaft. DE 10 2014 210 170 A1. Verfahren zur Unterdrückung der Reisekrankheit in einem Kraftfahrzeug und Kraftfahrzeug zur Durchführung des Verfahrens. Deutsches Patent- und Markenamt.

Bohrmann, D., Just, W., Maier, C., & Bengler, K. (2020). Ergonomie 2.0 – Das Fahrzeug als neuer Lebensraum. In *VDI-Berichte: Vol. 2370. 8th VDI-Fachtagung Humanschwingungen: Vibrations- und Schwingungseinwirkungen auf den Menschen* (pp. 53–62). Düsseldorf: VDI Verlag. https://doi.org/10.51202/9783181023709-53

Bohrmann, D., Koch, T., Maier, C., Just, W., & Bengler, K. (2020). Motion Comfort: Human Factors of Automated Driving. In L. Eckstein & S. Pischinger (Eds.), *29th Aachen Colloquium Sustainable Moblity (digital event)* (pp. 1697–1708).

Bohrmann, D., Lehnert, K., Scholly, U., & Bengler, K. (2018a). Kinetosis as a Challenge of Future Mobility Concepts and Highly Automated Vehicles. In L. Eckstein & S. Pischinger (Eds.), *27th Aachen Colloquium Automobile and Engine Technology* (pp. 1309–1335).

Bohrmann, D., Lehnert, K., Scholly, U., & Bengler, K. (2018b). Der Mensch als bestimmender Faktor zukünftiger Mobilitätskonzepte: Physikalisch-geometrische Untersuchung zur Reduzierung kinetogener Ausprägungen im Zusammenhang fahrzeugspezifischer Nutzungsszenarien. In *VDI-Berichte: Vol. 2335. 34th VDI/VW Gemeinschaftstagung: Fahrerassistenzsysteme und automatisiertes Fahren* (pp. 345–359). Düsseldorf: VDI Verlag. https://doi.org/10.51202/978318 1023358-345

Bolton, P. S., Hammam, E., & Macefield, V. G. (2018). Neck movement but not neck position modulates skin sympathetic nerve activity supplying the lower limbs of humans. *Journal of Neurophysiology*, *119*(4), 1283–1290. https://doi.org/10.1152/jn.00043.2017

Bombardini, T., Gemignani, V., Bianchini, E., Venneri, L., Petersen, C., Pasanisi, E., . . . Picano, E. (2008). Diastolic time - frequency relation in the stress echo lab: Filling timing and flow at different heart rates. *Cardiovascular Ultrasound*, *6.* https://doi.org/10.1186/1476-7120-6-15

Bonnet, C. T., Faugloire, E., Riley, M. A., Bardy, B. G., & Stoffregen, T. A. (2006). Motion sickness preceded by unstable displacements of the center of pressure. *Human Movement Science*, *25*(6), 800–820. https://doi.org/10.1016/j.humov.2006.03.001

Bos, J. E. (2015). Less sickness with more motion and/or mental distraction. *Journal of Vestibular Research: Equilibrium & Orientation*, *25*(1), 23–33. https://doi.org/10.3233/VES-150541

Bos, J. E., & Bles, W. (2002). Theoretical considerations on canal-otolith interaction and an observer model. *Biological Cybernetics*, *86*(3), 191–207. https://doi.org/10.1007/s00422-001-0289-7

Bos, J. E., Damala, D., Lewis, C., Ganguly, A., & Turan, O. (2007). Susceptibility to seasickness. *Ergonomics*, *50*(6), 890–901. https://doi.org/10.1080/00140130701245512

Bos, J. E., Houben, M., & Lindenberg, J. (2012). Optimising human performance by reducing motion sickness and enhancing situation awareness with an artificial 3D Earth-fixed visual reference. In *Maritime Systems and Technologies conference (MAST Europe 2012)*.

Bos, J. E., MacKinnon, S. N., & Patterson, A. (2005). Motion sickness symptoms in a ship motion simulator: Effects of inside, outside, and no view. *Aviation, Space, and Environmental Medicine*, *76*(12), 1111–1118.

Boselli, F. (2021). Endolymphatic Flow in the Semicircular Canals - Micro-CT rendering of a human inner ear. Swiss Federal Institute of Technology in Zürich - Institute of Fluid Dynamics [Webpage]. Retrieved from https://ifd.ethz.ch/research/group-kleiser/inner-ear.html on 5/30/2021

Boycott, B. B., & Wässle, H. (1974). The morphological types of ganglion cells of the domestic cat's retina. *The Journal of Physiology*, *240*(2), 397–419. https://doi.org/10.1113/jphysiol.1974.sp010616

Braccesi, C., & Cianetti, F. (2011). Motion sickness. Part I: Development of a model for predicting motion sickness incidence. *International Journal of Human Factors Modelling and Simulation*, *2*(3), 163. https://doi.org/10.1504/IJHFMS.2011.044492

Brahimi-Horn, M. C., Chiche, J., & Pouysségur, J. (2007). Hypoxia and cancer. *Journal of Molecular Medicine*, *85*(12), 1301–1307. https://doi.org/10.1007/s00109-007-0281-3

Brainard, A., & Gresham, C. (2014). Prevention and treatment of motion sickness. *American Family Physician*, *90*(1), 41–46.

Brenner, W., & Herrmann, A. (2018). An Overview of Technology, Benefits and Impact of Automated and Autonomous Driving on the Automotive Industry. In C. Linnhoff-Popien, R. Schneider, & M. Zaddach (Eds.), *Digital Marketplaces Unleashed* (pp. 427–442). Berlin Heidelberg: Springer. https://doi.org/10.1007/978-3-662-49275-8_39

Brickenkmap, R., Schmidt-Atzert, L., & Liepmann, D. (2010). *Test d2 - Revision: d2-R; Aufmerksamkeits- und Konzentrationstest*. Göttingen.

Brietzke, A., Pham Xuan, R., Dettmann, A., & Bullinger, A. C. (2021). Influence of dynamic stimulation, visual perception and individual susceptibility to car sickness during controlled stop-and-go driving. In T. Bertram, S. Kabelac, T. Schmidt, & K. Stahl (Eds.), *Forschung im Ingenieurwesen*. Springer. https://doi.org/10.1007/s10010-021-00441-6

Britton, Z., & Arshad, Q. (2019). Vestibular and Multi-Sensory Influences Upon Self-Motion Perception and the Consequences for Human Behavior. *Frontiers in Neurology*, *10*, 63. https://doi.org/10.3389/fneur.2019.00063

Brody, T. (2016). Biomarkers. In *Clinical Trials* (pp. 377–419). Elsevier. https://doi.org/10.1016/B978-0-12-804217-5.00019-9

Bromberg, L. (1996). *Pourquoi vous avez mal au coeur* (No. 2556). Paris, France.

Bronstein, A. M., Golding, J. F., & Gresty, M. A. (2020). Visual Vertigo, Motion Sickness, and Disorientation in Vehicles. *Seminars in Neurology.* Advance online publication. https://doi.org/10.1055/s-0040-1701653

Bronte-Stewart, H. M., & Lisberger, S. G. (1994). Physiological properties of vestibular primary afferents that mediate motor learning and normal performance of the vestibulo-ocular reflex in monkeys. *The Journal of Neuroscience*, *14*(3), 1290–1308. https://doi.org/10.1523/JNEUROSCI.14-03-01290.1994

Bruder, A. (2020). *Effects of a Dynamic Visual Stimulus on the Development of Carsickness in a Real Driving Experiment* (Master´s thesis). German Sport University Cologne, Cologne, Germany.

Bubb, H., Bengler, K., Grünen, R. E., & Vollrath, M. (2015). *Automobilergonomie*. Wiesbaden: Springer Fachmedien. https://doi.org/10.1007/978-3-8348-2297-0

Bubb, H., & Wohlfarter, M. (2012). Eye-Tracking Data Analysis and Neuroergonomics. In M. Fafrowicz, T. Marek, W. Karwowski, & D. Schmorrow (Eds.), *Ergonomics Design & Mgt. Theory & Applications. Neuroadaptive Systems* (pp. 255–311). Boca Raton and London, New York: CRC Press. https://doi.org/10.1201/b13019-14

Burns, J. C., & Stone, J. S. (2017). Development and regeneration of vestibular hair cells in mammals. *Seminars in Cell & Developmental Biology*, *65*, 96–105. https://doi.org/10.1016/j.semcdb.2016.11.001

Busettini, C., Miles, F. A., & Schwarz, U. (1991). Ocular responses to translation and their dependence on viewing distance. 2nd Motion of the scene. *Journal of Neurophysiology*, *66*(3), 865–878. https://doi.org/10.1152/jn.1991.66.3.865

Caillet, G., Bosser, G., Gauchard, G. C., Chau, N., Benamghar, L., & Perrin, P. P. (2006). Effect of sporting activity practice on susceptibility to motion sickness. *Brain Research Bulletin*, *69*(3), 288–293. https://doi.org/10.1016/j.brainresbull.2006.01.001

Campbell, F. W., & Green, D. G. (1965). Monocular versus binocular visual acuity. *Nature*, *208*(5006), 191–192. https://doi.org/10.1038/208191a0

Carsten, O., & Martens, M. H. (2019). How can humans understand their automated cars? HMI principles, problems and solutions. *Cognition, Technology & Work*, *21*(1), 3–20. https://doi.org/10.1007/s10111-018-0484-0

Castro de, F. (2020). fitmethis, MATLAB Central File Exchange (Version 1.5.2). Retrieved from https://de.mathworks.com/matlabcentral/fileexchange/40167-fitmethis on 7/6/2020

Catanzariti, J.-F., Guyot, M.-A., Massot, C., Khenioui, H., Agnani, O., & Donzé, C. (2016). Evaluation of motion sickness susceptibility by motion sickness susceptibility questionnaire in adolescents with idiopathic scoliosis: A case-control study. *European Spine Journal: Official Publication of the European Spine Society, the European Spinal Deformity Society, and the European Section of the Cervical Spine Research Society*, *25*(2), 438–443. https://doi.org/10.1007/s00586-015-4060-5

Cha, Y.-H., Brodsky, J., Ishiyama, G., Sabatti, C., & Baloh, R. W. (2008). Clinical features and associated syndromes of mal de debarquement. *Journal of Neurology*, *255*(7), 1038–1044. https://doi.org/10.1007/s00415-008-0837-3

Cha, Y.-H., & Cui, Y. (2013). Rocking dizziness and headache: A two-way street. *Cephalalgia: An International Journal of Headache*, *33*(14), 1160–1169. https://doi.org/10.1177/0333102413487999

Cha, Y.-H., Deblieck, C., & Wu, A. D. (2016). Double-Blind Sham-Controlled Crossover Trial of Repetitive Transcranial Magnetic Stimulation for Mal de Debarquement Syndrome. *Otology & Neurotology: Official Publication of the American Otological Society, American Neurotology Society [and] European Academy of Otology and Neurotology*, *37*(6), 805–812. https://doi.org/10.1097/MAO.0000000000001045

Cha, Y.-H., Urbano, D., & Pariseau, N. (2016). Randomized Single Blind Sham Controlled Trial of Adjunctive Home-Based tDCS after rTMS for Mal De Debarquement Syndrome: Safety, Efficacy, and Participant Satisfaction Assessment. *Brain Stimulation*, *9*(4), 537–544. https://doi.org/10.1016/j.brs.2016.03.016

Chatziastros, A. (2003). *Visuelle Kontrolle der Lokomotion* (Dissertation). Justus-Liebig-University Gießen, Gießen, Germany.

Chen, L., Deng, H., Cui, H., Fang, J., Zuo, Z., Deng, J., . . . Zhao, L. (2018). Inflammatory responses and inflammation-associated diseases in organs. *Oncotarget*, *9*(6), 7204–7218. https://doi.org/10.18632/oncotarget.23208

Chen, Y.-C., Hung, T.-H., Tseng, T.-C., Hsieh, C. C., Chen, F.-C., & Stoffregen, T. A. (2012). Pre-bout standing body sway differs between adult boxers who do and do not report post-bout motion sickness. *PloS One*, *7*(10), e46136. https://doi.org/10.1371/journal.pone.0046136

Cheung, B. S., & Hofer, K. (2001). Coriolis-induced cutaneous blood flow increase in the forearm and calf. *Brain Research Bulletin*, *54*(6), 609–618. https://doi.org/10.1016/s0361-9230(01)00463-4

Cheung, B. S., Money, K. E., & Jacobs, I. (1990). Motion sickness susceptibility and aerobic fitness: A longitudinal study. *Aviation, Space, and Environmental Medicine*, *61*(3), 201–204.

Cheung, B. S., Money, K. E., Kohl, R. L., & Kinter, L. B. (1992). Investigation of anti-motion sickness drugs in the squirrel monkey. *Journal of Clinical Pharmacology*, *32*(2), 163–175. https://doi.org/10.1002/j.1552-4604.1992.tb03822.x

Cheung, B. S., & Nakashima, A. (2006). *A review on the effects of frequency of oscilation on motion sickness: Technical Report*. Defence R&D Canada Toronto TR 2006-229. Retrieved from https://apps.dtic.mil/dtic/tr/fulltext/u2/a472991.pdf on 3/13/2021

Cheung, B. S., Nakashima, A. M., & Hofer, K. D. (2011). Various anti-motion sickness drugs and core body temperature changes. *Aviation, Space, and Environmental Medicine*, *82*(4), 409–415. https://doi.org/10.3357/asem.2903.2011

Chu, H., Li, M.-H., Huang, Y.-C., & Lee, S.-Y. (2013). Simultaneous transcutaneous electrical nerve stimulation mitigates simulator sickness symptoms in healthy adults: A crossover study. *BMC Complementary and Alternative Medicine*, *13*, 84. https://doi.org/10.1186/1472-6882-13-84

Chu, H., Li, M.-H., Juan, S.-H., & Chiou, W.-Y. (2012). Effects of transcutaneous electrical nerve stimulation on motion sickness induced by rotary chair: A crossover study. *Journal of Alternative and Complementary Medicine (New York, N.Y.)*, *18*(5), 494–500. https://doi.org/10.1089/acm.2011.0366

Claremont, C. A. (1931). The psychology of sea-sickness. *Psyche*. (11), 86–90.

Clarke, A. H. (2008). Zu Funktionsprüfung der Otoithenorgane. In H. Scherer (Ed.), *Der Gleichgewichtssinn: Neues aus Forschung und Klinik 6. Hennig Symposium* (pp. 3–15). Vienna: Springer.

Classen, S., Hwangbo, S. W., Mason, J., Wersal, J., Rogers, J., & Sisiopiku, V. P. (2021). Older Drivers' Motion and Simulator Sickness before and after Automated Vehicle Exposure. *Safety*, *7*(2), 26. https://doi.org/10.3390/safety7020026

Clément, G., & Reschke, M. F. (2018). Relationship between motion sickness susceptibility and vestibulo-ocular reflex gain and phase. *Journal of Vestibular Research: Equilibrium and Orientation*, *28*(3-4), 295–304. https://doi.org/10.3233/VES-180632.

Cohen, B., Dai, M., Ogorodnikov, D., Laurens, J., Raphan, T., Müller, P., . . . Straumann, D. (2011). Motion sickness on tilting trains. *FASEB Journal: Official Publication of the Federation of American Societies for Experimental Biology*, *25*(11), 3765–3774. https://doi.org/10.1096/fj.11-184887

Cohen, B., Dai, M., & Raphan, T. (2003). The critical role of velocity storage in production of motion sickness. *Annals of the New York Academy of Sciences*, *1004*, 359–376. https://doi.org/10.1196/annals.1303.034

Cohen, H. (1996). Mild mal de debarquement after sailing. *Annals of the New York Academy of Sciences*, *781*, 598–600. https://doi.org/10.1111/j.1749-6632.1996.tb15734.x

Cohen, J. (1988). *Statistical power analysis for the behavioral sciences* (2nd ed.). Hillsdale, New Jersey: Lawrence Erlbaum Associates.

Contini, D., Zampini, V., Tavazzani, E., Magistretti, J., Russo, G., Prigioni, I., & Masetto, S. (2012). Intercellular K^+ accumulation depolarizes Type I vestibular hair cells and their associated afferent nerve calyx. *Neuroscience*, *227*, 232–246. https://doi.org/10.1016/j.neuroscience.2012.09.051

Costa, F., Lavin, P., Robertson, D., & Biaggioni, I. (1995). Effect of neurovestibular stimulation on autonomic regulation. *Clinical Autonomic Research: Official Journal of the Clinical Autonomic Research Society*, *5*(5), 289–293. https://doi.org/10.1007/BF01818894

Covanis, A. (2006). Panayiotopoulos syndrome: A benign childhood autonomic epilepsy frequently imitating encephalitis, syncope, migraine, sleep disorder, or gastroenteritis. *Pediatrics*, *118*(4), 1237-1243. https://doi.org/10.1542/peds.2006-0623

Cowings, P. S., Naifeh, K. H., & Toscano, W. B. (1990). The stability of individual patterns of autonomic responses to motion sickness stimulation. *Aviation, Space, and Environmental Medicine*, *61*(5), 399–405.

Cowings, P. S., Toscano, W. B., DeRoshia, C., & Tauso, R. (2001). Effects of Command and Control Vehicle (C2V) operational environment on soldier health and performance. *Human Performance in Extreme Environments: The Journal of the Society for Human Performance in Extreme Environments*, *5*(2), 66–91.

Cox, D. R., & Snell, E. J. (1999). *Analysis of binary data* (2nd ed., 1st CRC Press reprint). *Monographs on statistics and applied probability: Vol. 32*. Boca Raton, Florida: Chapman & Hall.

Cullen, K. E. (2012). The vestibular system: Multimodal integration and encoding of self-motion for motor control. *Trends in Neurosciences*, *35*(3), 185–196. https://doi.org/10.1016/j.tins.2011.12.001

Cuomo-Granston, A. (2009). *Pain, motion sickness and migraine: Effects on symptoms and scalp blood flow* (Dissertation). Murdoch University, Perth, Australia.

Cuomo-Granston, A., & Drummond, P. D. (2010). Migraine and motion sickness: What is the link? *Progress in Neurobiology*, *91*(4), 300–312. https://doi.org/10.1016/j.pneurobio.2010.04.001

Curry, C., Li, R., Peterson, N., & Stoffregen, T. A. (2020). Cybersickness in Virtual Reality Head-Mounted Displays: Examining the Influence of Sex Differences and Vehicle Control. *International Journal of Human–Computer Interaction*, *59*(5), 1–7. https://doi.org/10.1080/10447318.2020.1726108

Curthoys, I. S., Blanks, R. H., & Markham, C. H. (1977). Semicircular canal functional anatomy in cat, guinea pig and man. *Acta Oto-Laryngologica*, *83*(3-4), 258–265. https://doi.org/10.3109/00016487709128843

Curthoys, I. S., Markham, C. H., & Curthoys, E. J. (1977). Semicircular duct and ampulla dimensions in cat, guinea pig and man. *Journal of Morphology*, *151*(1), 17–34. https://doi.org/10.1002/jmor.1051510103

D'Amore, F., & Qiu, Y. (2021). Vibration Transmission at Seat Cushion and Sitting Comfort in Next-Generation Cars. In N. L. Black, W. P. Neumann, & I. Noy (Eds.), *Lecture Notes in Networks and Systems. Proceedings of the 21st Congress of the International Ergonomics Association (IEA 2021)* (Vol. 221, pp. 615–622). Cham: Springer International Publishing. https://doi.org/10.1007/978-3-030-74608-7_75

Dai, M., Kunin, M., Raphan, T., & Cohen, B. (2003). The relation of motion sickness to the spatial-temporal properties of velocity storage. *Experimental Brain Research*, *151*(2), 173–189. https://doi.org/10.1007/s00221-003-1479-4

Dai, M., Raphan, T., & Cohen, B. (2007). Labyrinthine lesions and motion sickness susceptibility. *Experimental Brain Research*, *178*(4), 477–487. https://doi.org/10.1007/s00221-006-0759-1

Dai, M., Raphan, T., & Cohen, B. (2011). Prolonged reduction of motion sickness sensitivity by visual-vestibular interaction. *Experimental Brain Research*, *210*(3-4), 503–513. https://doi.org/10.1007/s00221-011-2548-8

Daimler AG (2016, December 22). *Mercedes-Benz at CES 2017: Connected, Autonomous, Shared & Service and Electric Drive* [Press release]. Stuttgart/Las Vegas. Retrieved from https://media.daimler.com/marsMediaSite/de/instance/ko/Mercedes-Benz-auf-der-CES-2017-Vernetzt-autonom-flexibel-und-elektrisch.xhtml?oid=15098223 on 6/2/2021

Daimler AG (2020). *Image database, development data, and CAD drawings* [Internal documents]. Sindelfingen, Germany.

D'Amour, S., Bos, J. E., & Keshavarz, B. (2017). The efficacy of airflow and seat vibration on reducing visually induced motion sickness. *Experimental Brain Research*, *235*(9), 2811–2820. https://doi.org/10.1007/s00221-017-5009-1

Davis, J. R., Vanderploeg, J. M., Santy, P. A., Jennings, R. T., & Stewart, D. F. (1988). Space motion sickness during 24 flights of the space shuttle. *Aviation, Space, and Environmental Medicine*, *59*(12), 1185–1189.

Decker, M. (2009). *Beurteilung der Querdynamik von Personenkraftwagen* (Dissertation). Technical University of Munich - TUM, Munich, Germany.

Deepak, D. T., Kranthi, K. B. L., & Reddy R, M. (2021). Subjective vestibular test findings in individuals with motion sickness. *International Journal of Scientific Research*, 63–65. https://doi.org/10.36106/ijsr/8119713

Denise, P., Vouriot, A., Normand, H., Golding, J. F., & Gresty, M. A. (2009). Effect of temporal relationship between respiration and body motion on motion sickness. *Autonomic Neuroscience: Basic & Clinical*, *151*(2), 142–146. https://doi.org/10.1016/j.autneu.2009.06.007

Denuelle, M., Fabre, N., Payoux, P., Chollet, F., & Geraud, G. (2007). Hypothalamic activation in spontaneous migraine attacks. *Headache*, *47*(10), 1418–1426. https://doi.org/10.1111/j.1526-4610.2007.00776.x

Dettmann, A., Hartwich, F., Roßner, P., Beggiato, M., Felbel, K., Krems, J., & Bullinger, A. C. (2021). Comfort or Not? Automated Driving Style and User Characteristics Causing Human Discomfort in Automated Driving. *International Journal of Human–Computer Interaction*, *37*(4), 331–339. https://doi.org/10.1080/10447318.2020.1860518

Diagne, M., Valla, J., Delfini, C., Buisseret-Delmas, C., & Buisseret, P. (2006). Trigeminovestibular and trigeminospinal pathways in rats: Retrograde tracing compared with glutamic acid decarboxylase and glutamate immunohistochemistry. *The Journal of Comparative Neurology*, *496*(6), 759–772. https://doi.org/10.1002/cne.20964

Diamond, S. G., & Markham, C. H. (1992). Validating the hypothesis of otolith asymmetry as a cause of space motion sickness. *Annals of the New York Academy of Sciences*, *656*, 725–731. https://doi.org/10.1111/j.1749-6632.1992.tb25250.x

Diels, C., & Bos, J. E. (2015). *Design guidelines to minimise self-driving carsickness* (Automated Vehicles Symposium). Michigan. https://doi.org/10.13140/RG.2.1.1309.4244

Diels, C., & Bos, J. E. (2016). Self-driving carsickness. *Applied Ergonomics*, *53 (B)*, 374–382. https://doi.org/10.1016/j.apergo.2015.09.009

Diels, C., Bos, J. E., Hottelart, K., & Reilhac, P. (2016). Motion Sickness in Automated Vehicles: The Elephant in the Room. In G. Meyer (Ed.), *Lecture Notes in Mobility. Road Vehicle Automation 3* (pp. 121–129). Cham: Springer International Publishing.

Diels, C., Ukai, K., & Howarth, P. A. (2007). Visually induced motion sickness with radial displays: Effects of gaze angle and fixation. *Aviation, Space, and Environmental Medicine*, *78*(7), 659–665.

Diener, H. C., Wist, E. R., Dichgans, J., & Brandt, T. (1976). The spatial frequency effect on perceived velocity. *Vision Research*, *16*(2), 169-176. https://doi.org/10.1016/0042-6989(76)90094-8

Dimiccoli, M., Girard, B., Berthoz, A., & Bennequin, D. (2013). Striola magica. A functional explanation of otolith geometry. *Journal of Computational Neuroscience*, *35*(2), 125–154. https://doi.org/10.1007/s10827-013-0444-x

Dix, M. R., & Hood, J. D. (Eds.) (1984). *A Wiley medical publication. Vertigo.* Chichester: Wiley.

DiZio, P., Ekchian, J., Kaplan, J. [Janna], Ventura, J., Graves, W., Giovanardi, M., . . . Lackner, J. R. (2018). An Active Suspension System for Mitigating Motion Sickness and Enabling Reading in a Car. *Aerospace Medicine and Human Performance*, *89*(9), 822–829. https://doi.org/10.3357/AMHP.5012.2018

Dobie, T. G. (2019). *Motion Sickness: A Motion Adaptation Syndrome. Springer Series on Naval Architecture, Marine Engineering, Shipbuilding and Shipping: Vol. 6*. Cham: Springer International Publishing. https://doi.org/10.1007/978-3-319-97493-4

Dobie, T. G., McBride, D., & May, J. (2001). The effects of age and sex on susceptibility to motion sickness. *Aviation, Space, and Environmental Medicine*, *72*(1), 13–20.

Domeyer, J. E., Cassavaugh, N. D., & Backs, R. W. (2013). The use of adaptation to reduce simulator sickness in driving assessment and research. *Accident; Analysis and Prevention*, *53*, 127–132. https://doi.org/10.1016/j.aap.2012.12.039

Donohew, B. E. (2006). *Motion sickness with lateral and roll oscillation* (Dissertation). University of Southampton, Southampton, United Kingdom.

Donohew, B. E., & Griffin, M. J. (2004). Motion sickness: Effect of the frequency of lateral oscillation. *Aviation, Space, and Environmental Medicine*, *75*(8), 649–656.

Donohew, B. E., & Griffin, M. J. (2007). Low frequency motions and motion sickness on a tilting train. *Proceedings of the Institution of Mechanical Engineers, Part F: Journal of Rail and Rapid Transit*, *221*(1), 125–133. https://doi.org/10.1243/09544097JRRT80

Doweck, I., Gordon, C. R., Shlitner, A., Spitzer, O., Gonen, A., Binah, O., . . . Shupak, A. (1997). Alterations in R–R variability associated with experimental motion sickness. *Journal of the Autonomic Nervous System*, *67*(1-2), 31–37. https://doi.org/10.1016/s0165-1838(97)00090-8

Drummond, P. D. (2006). Tryptophan depletion increases nausea, headache and photophobia in migraine sufferers. *Cephalalgia: An International Journal of Headache*, *26*(10), 1225–1233. https://doi.org/10.1111/j.1468-2982.2006.01212.x

Drummond, P. D., & Granston, A. (2004). Facial pain increases nausea and headache during motion sickness in migraine sufferers. *Brain: A Journal of Neurology*, *127*(3), 526–534. https://doi.org/10.1093/brain/awh061

Drummond, P. D., & Woodhouse, A. (1993). Painful stimulation of the forehead increases photophobia in migraine sufferers. *Cephalalgia: An International Journal of Headache*, *13*(5), 321–324. https://doi.org/10.1046/j.1468-2982.1993.1305321.x

Dutia, M. B., & Hunter, M. J. (1985). The sagittal vestibulocollic reflex and its interaction with neck proprioceptive afferents in the decerebrate cat. *The Journal of Physiology*, *359*, 17–29. https://doi.org/10.1113/jphysiol.1985.sp015572

Eatock, R. A., & Songer, J. E. (2011). Vestibular hair cells and afferents: Two channels for head motion signals. *Annual Review of Neuroscience*, *34*, 501–534. https://doi.org/10.1146/annurev-neuro-061010-113710

Eckstein, L. (2014a). *Longitudinal Dynamics of Vehicles: Transportation Systems, Vehilce Forces, Power Train, Brakes, Driving Performance & Consumption* (7th ed.). *Schriftenreihe Automobiltechnik*. Aachen: fka Forschungsgesellschaft Kraftfahrwesen.

Eckstein, L. (2014b). *Vertical and Lateral Dynamics of Vehicles: Suspension Systems, Driving Behaviour, Steering, Axle Design* (10th ed.). *Schriftenreihe Automobiltechnik: Vol. 141*. Aachen: fka Forschungsgesellschaft Kraftfahrwesen.

Eckstein, L. (2014c). *Structural Design of Vehicles: Design & Package, Manufacturing & Joining Techniques, Lightweight & Durability, Passive Safety, Pedestrian Protection* (4th ed.). *Schriftenreihe Automobiltechnik: Vol. 153*. Aachen: fka Forschungsgesellschaft Kraftfahrwesen.

Enz, A. (2007). Muscarinic Acetylcholine Receptors. In *xPharm: The Comprehensive Pharmacology Reference* (pp. 1–6). Elsevier. https://doi.org/10.1016/B978-0080 55232-3.60209-0

Ernstberger, U., Thöne, O., & Weissinger, J. (2020). Im Mittelpunkt steht der Mensch. *Sonderprojekte ATZ/MTZ*, *25*, 8–11. https://doi.org/10.1007/s41491-020-0072-5

Esquibel, D. (2021). Anatomy of the Eye [Webpage]. Retrieved from http://www.desertvisionoptometry.com/eyecare-articles/eye-anatomy on 5/30/2021

Estes, M. S., Blanks, R. H., & Markham, C. H. (1975). Physiologic characteristics of vestibular first-order canal neurons in the cat. I. Response plane determination and resting discharge characteristics. *Journal of Neurophysiology*, *38*(5), 1232–1249. https://doi.org/10.1152/jn.1975.38.5.1232

Eulenburg, P. zu, Ruehl, R. M., Runge, P., & Dieterich, M. (2017). Ageing-related changes in the cortical processing of otolith information in humans. *The European Journal of Neuroscience*, *46*(12), 2817–2825. https://doi.org/10.1111/ejn.13755

Eversmann, T., Gottsmann, M., E. Uhlich, Ulbrecht, G., & Scriba, P. C. (1978). Streß-induzierte Sekretionsänderungen hypophysärer Hormone. *Wehrmedizinische Monatsschrift*, *22*(6), 161–166.

Ezure, K., Cohen, M. S., & Wilson, V. J. (1983). Response of cat semicircular canal afferents to sinusoidal polarizing currents: Implications for input-output properties of second-order neurons. *Journal of Neurophysiology*, *49*(3), 639–648. https://doi.org/10.1152/jn.1983.49.3.639

Faber, E. S. L., & Sah, P. (2007). Functions of SK channels in central neurons. *Clinical and Experimental Pharmacology & Physiology*, *34*(10), 1077–1083. https://doi.org/10.1111/j.1440-1681.2007.04725.x

Fademrecht, L., Bülthoff, I., & La Rosa, S. de (2016). Action recognition in the visual periphery. *Journal of Vision*, *16*(3), 33. https://doi.org/10.1167/16.3.33

Farkhatdinov, I., Michalska, H., Berthoz, A., & Hayward, V. (2019a). Gravito-inertial ambiguity resolved through head stabilization. *Proceedings of Royal Society: A Mathematical, Physical, and Engineering Sciences.* Advance online publication. https://doi.org/10.1098/rspa.2018.0010

Farkhatdinov, I., Michalska, H., Berthoz, A., & Hayward, V. (2019b). Review of Anthropomorphic Head Stabilisation and Verticality Estimation in Robots. In G. Venture, J.-P. Laumond, & B. Watier (Eds.), *Springer Tracts in Advanced Robotics. Biomechanics of Anthropomorphic Systems* (Vol. 124, pp. 185–209). Cham: Springer International Publishing. https://doi.org/10.1007/978-3-319-93870-7_9

Farmer, A. D., Al Omran, Y., Aziz, Q., & Andrews, P. L. (2014). The role of the parasympathetic nervous system in visually induced motion sickness: Systematic review and meta-analysis. *Experimental Brain Research*, *232*(8), 2665–2673. https://doi.org/10.1007/s00221-014-3964-3

Fenzl, M., & Schlegel, C. (2010). Herzratenvariabilität – Diagnosemittel für die Gesundheit: altersbezogene Effektgrössen. *Schweizerische Zeitschrift Für Sportmedizin Und Sporttraumatologie*, *58*(4), 134–140. Retrieved from https://sgsm.ch/fileadmin/user_upload/Zeitschrift/58-2010-4/HR_Fenzl.pdf on 3/23/2021

Fernández, C., & Goldberg, J. M. (1976a). Physiology of peripheral neurons innervating otolith organs of the squirrel monkey. 1st Response to static tilts and to long-duration centrifugal force. *Journal of Neurophysiology*, *39*(5), 970–984. https://doi.org/10.1152/jn.1976.39.5.970

Fernández, C., & Goldberg, J. M. (1976b). Physiology of peripheral neurons innervating otolith organs of the squirrel monkey. 3rd Response dynamics. *Journal of Neurophysiology*, *39*(5), 996–1008. https://doi.org/10.1152/jn.1976.39.5.996

Fernández, C., Goldberg, J. M., & Abend, W. K. (1972). Response to static tilts of peripheral neurons innervating otolith organs of the squirrel monkey. *Journal of Neurophysiology*, *35*(6), 978–987. https://doi.org/10.1152/jn.1972.35.6.978

Festner, M., Baumann, H., & Schramm, D. (2016). Der Einfluss fahrfremder Tätigkeiten und Manöverlängsdynamik auf die Komfort- und Sicherheitswahrnehmungn beim hochautomatisierten Fahren: Ein Argument für die Adaptivität automatisierter Fahrfunktionen. In *VDI-Berichte: Vol. 2288. 32th VDI/VW-Gemeinschaftstagung: Fahrerassistenz und automatisiertes Fahren*. Düsseldorf: VDI Verlag.

Fetter, M. (2007). Vestibulo-ocular reflex. *Developments in Ophthalmology*, *40*, 35–51. https://doi.org/10.1159/000100348

Fetter, M. (2010). Elektrookulographie - Vestibuläres System. *Das Neurophysiologie-Labor*, *32*(3), 129–140. https://doi.org/10.1016/j.neulab.2010.04.005

Fettiplace, R., & Fuchs, P. A. (1999). Mechanisms of hair cell tuning. *Annual Review of Physiology*, *61*, 809–834. https://doi.org/10.1146/annurev.physiol.61.1.809

Fettiplace, R., & Hackney, C. M. (2006). The sensory and motor roles of auditory hair cells. *Nature Reviews. Neuroscience*, *7*(1), 19–29. https://doi.org/10.1038/nrn1828

Field, A. P., Miles, J., & Field, Z. (2012). *Discovering statistics using R*. London: Sage.

Fiorillo, I., Song, Y., Smulders, M., Vink, P., & Naddeo, A. (2021). Flat Cushion vs Shaped Cushion: Comparison in Terms of Pressure Distribution and Postural Perceived Discomfort. In N. L. Black, W. P. Neumann, & I. Noy (Eds.), *Lecture Notes in Networks and Systems. Proceedings of the 21st Congress of the International Ergonomics Association (IEA 2021)* (Vol. 220, pp. 247–254). Cham: Springer International Publishing. https://doi.org/10.1007/978-3-030-74605-6_31

Fitch, G. M., Hankey, J. M., Kleiner, B. M., & Dingus, T. A. (2011). Driver comprehension of multiple haptic seat alerts intended for use in an integrated collision avoidance system. *Transportation Research Part F: Traffic Psychology and Behaviour*, *14*(4), 278–290. https://doi.org/10.1016/j.trf.2011.02.001

Flanagan, M. B., May, J. G., & Dobie, T. G. (2005). Sex differences in tolerance to visually-induced motion sickness. *Aviation, Space, and Environmental Medicine*, *76*(7), 642–646.

Fletcher, T. D. (2012). QuantPsyc: Quantitative Psychology Tools (R package version 1.5). Retrieved from https://cran.r-project.org/web/packages/QuantPsyc/index.html on 5/29/2021

Flöchinger, B. (2012). Kinetosen. In T. Jelinek (Ed.), *Kursbuch Reisemedizin*. Stuttgart: Georg Thieme Verlag. https://doi.org/10.1055/b-0034-42111

Forbes, J., & Das, J. M. (2021). *Anatomy, Head and Neck, Atlantoaxial Joint*. Treasure Island, Florida.

Forge, A., Li, L., Corwin, J. T., & Nevill, G. (1993). Ultrastructural evidence for hair cell regeneration in the mammalian inner ear. *Science (New York, N.Y.)*, *259*(5101), 1616–1619. https://doi.org/10.1126/science.8456284

Förstberg, J. (2000a). Influence from horizontal and/or roll motion on nausea and motion sickness: Experiments in a moving vehicle simulator. Retrieved from https://pdfs.semanticscholar.org/666a/b95e2f0c743c50a7b386e199c40f73b937 80.pdf?_ga=2.131280655.1625022043.1587949347-1083432856.1557338421 on 6/3/2021

Förstberg, J. (2000b). *Ride comfort and motion sickness in tilting trains: Human responses to motion environments in train and simulator experiments* (Dissertation). Royal Insitute of Technology, Stockholm, Sweden.

Förstberg, J., Andersson, E., & Ledin, T. (1998). Influence of different conditions for tilt compensation on symptoms of motion sickness in tilting trains. *Brain Research Bulletin*, *47*(5), 525–535. https://doi.org/10.1016/s0361-9230(98)00097-5

Fox, J. (2019). polycor: Polychoric and Polyserial Correlations (R package version 0.7-10). Retrieved from https://cran.r-project.org/package=polycor on 5/29/2021

Fox, J., Weisberg, S., Price, B., Adler, D., Bates, D., Baud-Bovy, G., . . . R Core Team (2020). car: Companion to Applied Regression (R package version 3.0-10). Retrieved from https://cran.r-project.org/package=car on 5/29/2021

Frett, T., Green, D. A., Arz, M., Noppe, A., Petrat, G., Kramer, A., . . . Jordan, J. (2020). Motion sickness symptoms during jumping exercise on a short-arm centrifuge. *PloS One*, *15*(6), e0234361. https://doi.org/10.1371/journal.pone.0234361

Fuchs, P. A., & Parsons, T. D. (2006). The Synaptic Physiology of Hair Cells. In R. A. Eatock, R. R. Fay, & A. N. Popper (Eds.), *Springer Handbook of Auditory Research. Vertebrate Hair Cells* (Vol. 27, pp. 249–312). New York: Springer-Verlag. https://doi.org/10.1007/0-387-31706-6_6

Fukuda, T. (1976). Postural behaviour and motion sickness. *Acta Oto-Laryngologica*, *81*(3-4), 237–241. https://doi.org/10.3109/00016487609119955

Fulvio, J. M., Ji, M., & Rokers, B. (2021). Variations in visual sensitivity predict motion sickness in virtual reality. *Entertainment Computing*, *38*, 100423. https://doi.org/10.1016/j.entcom.2021.100423

Gagnon, R. W. C., & Kline, D. W. (2003). Senescent effects on binocular summation for contrast sensitivity and spatial interval acuity. *Current Eye Research*, *27*(5), 315–321. https://doi.org/10.1076/ceyr.27.5.315.17225

Gastaldi, L., Pastorelli, S., & Sorli, M. (2009). Vestibular apparatus: dynamic model of the semicircular canals. *WIT Transactions on Biomedicine and Health*. (13), 223–234.

Gastwirth, J. L., Gel, Y. R., Hui, W., Lyubchich, V., Miao, W., & Noguchi, K. (2020). lawstat: Tools for Biostatistics, Public Policy, and Law (R package version 3.4). Retrieved from https://cran.r-project.org/package=lawstat on 5/29/2021

Géléoc, G. S. G., & Holt, J. R. (2003). Developmental acquisition of sensory transduction in hair cells of the mouse inner ear. *Nature Neuroscience*, *6*(10), 1019–1020. https://doi.org/10.1038/nn1120

Gerteis, A. K. S. (2014). *Psychologische Einflussfaktoren kardialer Aktivität: Signals of Safety versus Rumination (kombinierte Feld- und Laboruntersuchung)* (Dissertation). Karl-Franzens-University of Graz, Graz, Austria.

Gianaros, P. J., Muth, E. R., Mordkoff, J. T., Levine, M. E., & Stern, R. M. (2001). A questionnaire for the assessment of the multiple dimensions of motion sickness. *Aviation, Space, and Environmental Medicine*, *72*(2), 115–119.

Gianaros, P. J., Quigley, K. S., Muth, E. R., Levine, M. E., Vasko, R. C., & Stern, R. M. (2003). Relationship between temporal changes in cardiac parasympathetic activity and motion sickness severity. *Psychophysiology*, *40*(1), 39–44.

Gibson, J. (1950). *The perception of the visual world*. Boston, Massachusetts: The Riverside Press, Houghton-Mifflin Company.

Gibson, J. (1962). Observations on active touch. *Psychological Review*, *69*, 477–491. https://doi.org/10.1037/h0046962

Giugliano, D., Ceriello, A., & Esposito, K. (2008). Glucose metabolism and hyperglycemia. *The American Journal of Clinical Nutrition*, *87*(1), 217S-222S. https://doi.org/10.1093/ajcn/87.1.217S

Giv, H. H. (2013). Directional short-time Fourier transform. *Journal of Mathematical Analysis and Applications*, *399*(1), 100–107. https://doi.org/10.1016/j.jmaa.2012.09.053

Goadsby, P. J. (2007). Migraine. In *Comprehensive Medicinal Chemistry II* (pp. 369–379). Elsevier. https://doi.org/10.1016/B0-08-045044-X/00176-0

Goldberg, J. M. (2016). Vestibular Inputs: The Vestibular System. In D. W. Pfaff & N. D. Volkow (Eds.), *Neuroscience in the 21st Century* (Vol. 31, pp. 1007–1054). New York: Springer. https://doi.org/10.1007/978-1-4939-3474-4_30

Goldberg, J. M., & Cullen, K. E. (2011). Vestibular control of the head: Possible functions of the vestibulocollic reflex. *Experimental Brain Research*, *210*(3-4), 331–345. https://doi.org/10.1007/s00221-011-2611-5

Goldberg, J. M., Desmadryl, G., Baird, R. A., & Fernández, C. (1990). The vestibular nerve of the chinchilla. 4th Discharge properties of utricular afferents. *Journal of Neurophysiology*, *63*(4), 781–790. https://doi.org/10.1152/jn.1990.63.4.781

Goldberg, J. M., & Fernández, C. (1971). Physiology of peripheral neurons innervating semicircular canals of the squirrel monkey. 1st Resting discharge and response to constant angular accelerations. *Journal of Neurophysiology*, *34*(4), 635–660. https://doi.org/10.1152/jn.1971.34.4.635

Goldberg, J. M., & Fernández, C. (1977). Conduction times and background discharge of vestibular afferents. *Brain Research*, *122*(3), 545–550. https://doi.org/10.1016/0006-8993(77)90465-6

Goldberg, J. M., & Fernández, C. (1980). Efferent vestibular system in the squirrel monkey: Anatomical location and influence on afferent activity. *Journal of Neurophysiology*, *43*(4), 986–1025. https://doi.org/10.1152/jn.1980.43.4.986

Goldberg, J. M., Wilson, V. J., Cullen, K. E., Angelaki, D. E., Broussard, D. M., Büttner-Ennever, J. A., . . . Minor, L. B. (2012). *The vestibular system: A sixth sense*. Oxford: Oxford University Press.

Goldberger, A. L. (1991). Is the normal heartbeat chaotic or homeostatic? *News in Physiological Sciences: An International Journal of Physiology Produced Jointly by the International Union of Physiological Sciences and the American Physiological Society*, *6*, 87–91. https://doi.org/10.1152/physiologyonline.1991.6.2.87

Golding, J. F. (1992). Phasic skin conductance activity and motion sickness. *Aviation, Space, and Environmental Medicine*, *63*(3), 165–171.

Golding, J. F. (1998). Motion sickness susceptibility questionnaire revised and its relationship to other forms of sickness. *Brain Research Bulletin*, *47*(5), 507–516. https://doi.org/10.1016/s0361-9230(98)00091-4

Golding, J. F. (2006). Predicting individual differences in motion sickness susceptibility by questionnaire. *Personality and Individual Differences*, *41*(2), 237–248. https://doi.org/10.1016/j.paid.2006.01.012

Golding, J. F., Bles, W., Bos, J. E., Haynes, T., & Gresty, M. A. (2003). Motion sickness and tilts of the inertial force environment: Active suspension systems vs. Active passengers. *Aviation, Space, and Environmental Medicine*, *74*(3), 220–227.

Golding, J. F., Doolan, K., Acharya, A., Tribak, M., & Gresty, M. A. (2012). Cognitive cues and visually induced motion sickness. *Aviation, Space, and Environmental Medicine*, *83*(5), 477–482. https://doi.org/10.3357/asem.3095.2012

Golding, J. F., Kadzere, P., & Gresty, M. A. (2005). Motion sickness susceptibility fluctuates through the menstrual cycle. *Aviation, Space, and Environmental Medicine*, *76*(10), 970–973.

Golding, J. F., & Kerguelen, M. (1992). A comparison of the nauseogenic potential of low-frequency vertical versus horizontal linear oscillation. *Aviation, Space, and Environmental Medicine*, *63*(6), 491–497.

Golding, J. F., & Markey, H. M. (1996). Effect of frequency of horizontal linear oscillation on motion sickness and somatogravic illusion. *Aviation, Space, and Environmental Medicine*, *67*(2), 121–126.

Golding, J. F., Markey, H. M., & Stott, J. R. (1995). The Effects of Motion Direction, Body Axis, and Posture on Motion Sickness Induced by Low Frequency Linear Oscillation. *Aviation, Space, and Environmental Medicine*, *66*(11), 1046–1051.

Golding, J. F., Prosyanikova, O., Flynn, M., & Gresty, M. A. (2011). The effect of smoking nicotine tobacco versus smoking deprivation on motion sickness. *Autonomic Neuroscience: Basic & Clinical*, *160*(1-2), 53–58. https://doi.org/10.1016/j.autneu.2010.09.009

Golding, J. F., Rafiq, A., & Keshavarz, B. (2021). Predicting Individual Susceptibility to Visually Induced Motion Sickness by Questionnaire. *Frontiers in Virtual Reality*, *2*. https://doi.org/10.3389/frvir.2021.576871

Goldstein, E. B., Ritter, M., & Herbst, G. (2002). *Wahrnehmungspsychologie* (2. german ed.). *Spektrum Lehrbuch*. Heidelberg Berlin: Spektrum Akademischer Verlag.

Golowko, K., Mugele, P., & Zimmer, D. (2017). Neue Möglichkeiten der Innenraumgestaltung. *ATZ Extra*, *22*(S3), 42–45. https://doi.org/10.1007/s35778-017-0030-3

Gordon, C. R., Spitzer, O., Doweck, I., Melamed, Y., & Shupak, A. (1995). Clinical features of mal de debarquement: Adaptation and habituation to sea conditions. *Journal of Vestibular Research*, *5*(5), 363–369.

Gordon, C. R., Spitzer, O., Shupak, A., & Doweck, I. (1992). Survey of mal de debarquement. *BMJ (Clinical Research Ed.)*, *304*(6826), 544. https://doi.org/10.1136/bmj.304.6826.544

Gottselig, L. (2019). *Fahrzeugkonzepte der Zukunft: Einflüsse der Sitzausrichtung und Außensicht auf das Wohlbefinden von Fahrzeugpassagieren bei Nebentätigkeiten* (Master´s thesis). Technical University of Berlin, Berlin, Germany.

Graybiel, A., Kennedy, R. S., Knoblock, E., Guedry, F., Mertz, W. E., McLoed, M. E., . . . Fregly, A. (1965). Effects of exposure to a rotating environment (10 rpm) on four aviators for a period of twelve days. *Aerospace Medicine*, *36*, 733–754.

Graybiel, A., & Knepton, J. (1976). Sopite syndrome: A sometimes sole manifestation of motion sickness. *Aviation, Space, and Environmental Medicine*, *47*(8), 873–882.

Graybiel, A., & Lackner, J. R. (1980). Evaluation of the relationship between motion sickness symptomatology and blood pressure, heart rate, and body temperature. *Aviation, Space, and Environmental Medicine*, *51*(3), 211–214.

Graybiel, A., Wood, C. D., Miller, E. F., & Cramer, D. B. (1968). Diagnostic criteria for grading the severity of acute motion sickness. *Aerospace Medicine*, *39*(5), 453–455.

Griffin, M. J. (1990). *Handbook of Human Vibration*: Acadademic Press. https://doi.org/10.1016/C2009-0-02730-5

Griffin, M. J., & Howarth, H. (2000). *Motion sickness history questionnaire*. Southampton, United Kingdom. Retrieved from Insitiute of Sound and Vibration Research website: https://eprints.soton.ac.uk/10465/1/Pub1228.pdf on 4/27/2020

Griffin, M. J., & Newman, M. M. (2004). An experimental study of low-frequency motion in cars. *Proceedings of the Institution of Mechanical Engineers, Part D: Journal of Automobile Engineering*, *218*(11), 1231–1238. https://doi.org/10.1243/0954407042580093

Grosjean, P., Ibanez, F., & Etienne, M. (2018). pastecs: Package for Analysis of Space-Time Ecological Serie (R package version 1.3.21). Retrieved from https://cran.r-project.org/web/packages/pastecs/pastecs.pdf on 5/29/2021

Grubbs, F. E. (1969). Procedures for Detecting Outlying Observations in Samples. *Technometrics*, *11*(1). https://doi.org/10.2307/1266761

Grunfeld, E., & Gresty, M. A. (1998). Relationship between motion sickness, migraine and menstruation in crew members of a "round the world" yacht race. *Brain Research Bulletin*, *47*(5), 433–436. https://doi.org/10.1016/s0361-9230(98)00099-9

Grunfeld, E., Shallo-Hoffmann, J. A., Cassidy, L., Okada, T., Faldon, M., Acheson, J. F., & Bronstein, A. M. (2003). Vestibular perception in patients with acquired ophthalmoplegia. *Neurology*, *60*(12), 1993–1995. https://doi.org/10.1212/01.wnl.0000067992.17185.60

Guo, C. C. T., Chen, D. J. Z., Wei, I. Y., So, R. H. Y., & Cheung, R. T. F. (2017). Correlations between individual susceptibility to visually induced motion sickness and decaying time constant of after-nystagmus. *Applied Ergonomics*, *63*, 1–8. https://doi.org/10.1016/j.apergo.2017.03.011

Hainich, R., Drewitz, U., Ihme, K., Lauermann, J., Niedling, M., & Oehl, M. (2021). Evaluation of a Human–Machine Interface for Motion Sickness Mitigation Utilizing Anticipatory Ambient Light Cues in a Realistic Automated Driving Setting. *Information*, *12*(4), 176. https://doi.org/10.3390/info12040176

Hamann, K.-F. (1994). Physiologie und Pathophysiologie des vestibulären Systems. In H. H. Naumann, J. Helms, C. Herberhold, & E. Kastenbauer (Eds.), *Oto-Rhino-Laryngologie in Klink und Praxis* (pp. 260–297). Stuttgart, New York: Georg Thieme Verlag.

Happee, R., Bruijn, E. de, Forbes, P. A., & van der Helm, F. C. T. (2017). Dynamic head-neck stabilization and modulation with perturbation bandwidth investigated using a multisegment neuromuscular model. *Journal of Biomechanics*, *58*, 203–211. https://doi.org/10.1016/j.jbiomech.2017.05.005

Harrell, F. E., JR. (2021). Hmisc: Harrell Miscellaneous (R package version 4.5-0). Retrieved from https://cran.r-project.org/web/packages/Hmisc/index.html on 5/29/2021

Harthorn, T., Bretz, F., Westfall, Peter, Heiberger, Richard M., Schuetzenmeister, A., & Scheibe, S. (2021). multcomp: Simultaneous Inference in General Parametric Models (R package version 1.4-17). Retrieved from https://cran.r-project.org/package=multcomp on 5/29/2021

Harthorn, T., Zeileis, A., Farebrother, R. W., Cummins, C., & Millo, Goivanni, Mitchel, David (2020). lmtest: Testing Linear Regression Models (R package version 0.9-38). Retrieved from https://cran.r-project.org/web/packages/lmtest/lmtest.pdf on 7/11/2021

Hasler, W. L., Kim, M. S., Chey, W. D., Stevenson, V., Stein, B., & Owyang, C. (1995). Central cholinergic and alpha-adrenergic mediation of gastric slow wave dysrhythmias evoked during motion sickness. *The American Journal of Physiology*, *268*(4 Pt 1), G 539-547. https://doi.org/10.1152/ajpgi.1995.268.4.G539

Hatton, G. I. (2009). Magnocellular Neurosecretory System: Organization, Plasticity, Model Peptidergic Neurons. In *Encyclopedia of Neuroscience* (pp. 623–633). Elsevier. https://doi.org/10.1016/B978-008045046-9.01181-5

Häusler, R. (1995). Ski sickness. *Acta Oto-Laryngologica*, *115*(1), 1–2. https://doi.org/10.3109/00016489509133337

Hecht, T., Feldhütter, A., Draeger, K., & Bengler, K. (2020). What Do You Do? An Analysis of Non-driving Related Activities During a 60 Minutes Conditionally Automated Highway Drive. In T. Ahram, R. Taiar, S. Colson, & A. Choplin (Eds.), *Advances in intelligent systems and computing. Human Interaction and Emerging Technologies* (Vol. 1018, pp. 28–34). Cham: Springer International Publishing. https://doi.org/10.1007/978-3-030-25629-6_5

Heer, M., & Paloski, W. H. (2006). Space motion sickness: Incidence, etiology, and countermeasures. *Autonomic Neuroscience: Basic & Clinical*, *129*(1-2), 77–79. https://doi.org/10.1016/j.autneu.2006.07.014

Heinrich, D. (2016). *Modellierung des Fahrerverhaltens zur Ermittlung von Bauteilbelastungen im Fahrzeugantriebsstrang* (Dissertation). Karlsruhe Institute of Technology - KIT, Karlsruhe, Germany.

Heißing, B., Kudritzki, D., Schindlmaister, R., & Mauter, G. (2000). Menschgerechte Auslegung des dynamischen Verhaltens von Pkw. In H. Bubb (Ed.), *Beiträge der Herbstkonferenz der Gesellschaft für Arbeitswissenschaft. Ergonomie und Verkehrssicherheit* (p. 97). München: Herbert Utz.

Helling, K., Hausmann, S., Clarke, A. H., & Scherer, H. (2003). Experimentally induced motion sickness in fish: Possible role of the otolith organs. *Acta Oto-Laryngologica*, *123*(4), 488–492. https://doi.org/10.1080/00365540210000028121

Hemingway, A. (1944). Cold sweating in motion sickness. *The American Journal of Physiology*, *141*(2), 172–175. https://doi.org/10.1152/ajplegacy.1944.141.2.172

Henriques, I. F., Douglas de Oliveira, D. W., Oliveira-Ferreira, F., & Andrade, P. M. O. (2014). Motion sickness prevalence in school children. *European Journal of Pediatrics*, *173*(11), 1473–1482. https://doi.org/10.1007/s00431-014-2351-1

Hepp, K., Henn, V., Vilis, T., & Cohen, B. (1989). Brainstem regions related to saccade generation. *Reviews of Oculomotor Research*, *3*, 105–212.

Herrnberger, L. (2015). *Molecular analysis of plasmalemma vesicle-associated protein and its biological functions in the mammalian vascular endothelium* (Dissertation). University of Regensburg, Regensburg. https://doi.org/10.5283/epub.30379

Herzberger, N., Schwalm, M., Reske, M., Woopen, T., & Eckstein, L. (2019). *Mobilitätskonzepte der Zukunft - Ergebnisse einer Befragung von 619 Personen in Deutschland im Rahmen des Projekts UNICARagil.* https://doi.org/10.18154/RWTH-2018-231975

Hilbig, R., Anken, R. H., Bauerle, A., & Rahmann, H. (2002). Susceptibility to motion sickness in fish: A parabolic aircraft flight study. *Journal of Gravitational Physiology: A Journal of the International Society for Gravitational Physiology*, *9*(1), 29-30.

Hill, L. K., & Siebenbrock, A. (2009). Are all measures created equal? Heart rate variability and respiration. *Biomedical Sciences Instrumentation*, *45*, 71–76.

Hlavac, M. (2018). stargazer: Well-Formatted Regression and Summary Statistics Tables (R package version 5.2.2). Retrieved from https://cran.r-project.org/web/packages/stargazer/stargazer.pdf on 5/29/2021

Hoffer, M. E., Gottshall, K., Kopke, R. D., Weisskopf, P., Moore, R., Allen, K. A., & Wester, D. (2003). Vestibular testing abnormalities in individuals with motion sickness. *Otology & Neurotology: Official Publication of the American Otological Society, American Neurotology Society [and] European Academy of Otology and Neurotology*, *24*(4), 633–636. https://doi.org/10.1097/00129492-200307000-00017

Holder, D. (2021). Systematic analysis of changing vehicle exterior dimensions and relevant vehilce proportions. *Proceedings of the Design Society*, *1*, 2921–2930. https://doi.org/10.1017/pds.2021.553

Holmes, S. R., & Griffin, M. J. (2001). Correlation Between Heart Rate and the Severity of Motion Sickness Caused by Optokinetic Stimulation. *Journal of Psychophysiology*, *15*(1), 35–42. https://doi.org/10.1027//0269-8803.15.1.35

Holmes, S. R., King, S. [Stuart], Rollin Scott, J. R., & Clemes, S. (2002). Facial Skin Pallor Increases During Motion Sickness. *Journal of Psychophysiology*, *16*(3), 150–157. https://doi.org/10.1027//0269-8803.16.3.150

Holt, J. R., & Corey, D. P. (2000). Two mechanisms for transducer adaptation in vertebrate hair cells. *Proceedings of the National Academy of Sciences*, *97*(22), 11730–11735. https://doi.org/10.1073/pnas.97.22.11730

Home, R. (1978). Binocular summation: A study of contrast sensitivity, visual acuity and recognition. *Vision Research*, *18*(5), 579–585. https://doi.org/10.1016/0042-6989(78)90206-7

Horn, A. (2003). *Diagnostik der Herzfrequenzvariabilität in der Sportmedizin: Rahmenbedingungen und methodische Grundlagen* (Dissertation). Ruhr-University Bochum, Bochum, Germany.

Hosmer, D. W., & Lemeshow, S. (1989). *Applied logistic regression*. New York: Wiley.

Howard, I. P., & Rogers, B. J. (2002). *Depth Perception: Basic Mechanisms*. *Seeing in depth: Vol. 2*. Toronto: Porteous.

Howarth, H. V. C., & Griffin, M. J. (2003). Effect of roll oscillation frequency on motion sickness. *Aviation, Space, and Environmental Medicine*, *74*(4), 326–331.

Hromatka, B. S., Tung, J. Y., Kiefer, A. K., Do, C. B., Hinds, D. A., & Eriksson, N. (2015). Genetic variants associated with motion sickness point to roles for inner ear development, neurological processes and glucose homeostasis. *Human Molecular Genetics*, *24*(9), 2700–2708. https://doi.org/10.1093/hmg/ddv028

Hu, S., Grant, W. F., Stern, R. M., & Koch, K. L. (1991). Motion sickness severity and physiological correlates during repeated exposures to a rotating optokinetic drum. *Aviation, Space, and Environmental Medicine*, *62*(4), 308–314.

Hudelmaier, J. (2003). *Sichtanalyse im PKW unter Berücksichtigung von Bewegung und individuellen Körpercharakteristika* (Dissertation). Technical University of Munich - TUM, Munich, Germany.

Hudspeth, A. J., & Corey, D. P. (1977). Sensitivity, polarity, and conductance change in the response of vertebrate hair cells to controlled mechanical stimuli. *Proceedings of the National Academy of Sciences*, *74*(6), 2407–2411. https://doi.org/10.1073/pnas.74.6.2407

Huppert, D., Benson, J., & Brandt, T. (2017). A Historical View of Motion Sickness - A Plague at Sea and on Land, Also with Military Impact. *Frontiers in Neurology*, *8*, 114. https://doi.org/10.3389/fneur.2017.00114

Huppert, D., Grill, E., & Brandt, T. (2019). Survey of motion sickness susceptibility in children and adolescents aged 3 months to 18 years. *Journal of Neurology*, *266*(Suppl 1), 65–73. https://doi.org/10.1007/s00415-019-09333-w

Huterer, M., & Cullen, K. E. (2002). Vestibuloocular reflex dynamics during high-frequency and high-acceleration rotations of the head on body in rhesus monkey. *Journal of Neurophysiology*, *88*(1), 13–28. https://doi.org/10.1152/jn.2002.88.1.13

Huysduynen, H. H. an, Terken, J., Meschtscherjakov, A., Eggen, B., & Tscheligi, M. (2017). Ambient Light and Its Influence on Driving Experience. In A. Löcken, S. Boll, I. Politis, S. Osswald, R. Schroeter, D. Large, . . . N. Broy (Eds.), *Proceedings of the 9th International Conference on Automotive User Interfaces and Interactive Vehicular Applications Adjunct* (pp. 293–301). New York: ACM Press.

Igarashi, M., O-Uchi, T., & Alford, B. R. (1981). Volumetric and dimensional measurements of vestibular structures in the squirrel monkey. *Acta Oto-Laryngologica*, *91*(5-6), 437–444. https://doi.org/10.3109/00016488109138525

IPG Automotive (2021). Advanced Driver Assistance Systems: Added comfort and safety for every road user [Webpage]. Retrieved from https://ipg-automotive.com/cn/areas-of-application/adas/ on 5/29/2021

Irsch, K., & Guyton, D. L. (2009). Anatomy of Eyes. In S. Z. Li & A. Jain (Eds.), *Encyclopedia of Biometrics* (pp. 11–16). Boston, Massachusetts: Springer US. https://doi.org/10.1007/978-0-387-73003-5_253

Irwin, J. A. (1881). The Pathology of Sea-Sickness. *The Lancet*, *118*(3039), 907–909. https://doi.org/10.1016/S0140-6736(02)38129-7

Islam, R., Lee, Y., Jaloli, M., Muhammad, I., Zhu, D., Rad, P., . . . Quarles, J. (2020). Automatic Detection and Prediction of Cybersickness Severity using Deep Neural Networks from user's Physiological Signals. In *2020 IEEE International Symposium on Mixed and Augmented Reality (ISMAR)* (pp. 400–411). IEEE. https://doi.org/10.1109/ISMAR50242.2020.00066

ISO 15622:2018-09. *Intelligent transport systems - Adaptive cruise control systems - Performance requirements and test procedures*. (ISO 15622:2010).

ISO 2631-1:1997-05. *Mechanical vibration and shock - Evaluation of human exposure to whole-body vibration*. (ISO 2631-1:1985).

Isu, N., Hasegawa, T., Takeuchi, I. & Morimoto, A. (2014). Quantitative analysis of time-course development of motion sickness caused by in-vehicle video watching. *Displays*, *35(2)*, 90–97. https://10.1016/j.displa.2014.01.003

Isu, N., Shimizu, T., & Sugata, K. (2001). Mechanics of Coriolis stimulus and inducing factors of motion sickness. *Uchu Seibutsu Kagaku*, *15*(4), 414–419.

Iurato, S., Luctano, L., Pannese, E., & Reale, E. (1972). Efferent Vestibular Fibers in Mammals: Morphological and Histochemical Aspects. In A. Brodal & O. Pompeiano (Eds.), *Progress in Brain Research. Basic aspects of central vestibular mechanisms* (Vol. 37, pp. 429–443). Amsterdam, New York: Elsevier. https://doi.org/10.1016/S0079-6123(08)63917-5

Jacobi, C., & Paul, T. (Eds.) (1991). *Bulimia und Anorexia nervosa: Ursachen und Therapie*. Berlin, Heidelberg: Springer. https://doi.org/10.1007/978-3-642-76461-5

Jacobs, K. M. (2011). Somatosensory System. In J. S. Kreutzer, J. DeLuca, & B. Caplan (Eds.), *Encyclopedia of Clinical Neuropsychology* (pp. 2320–2324). New York: Springer. https://doi.org/10.1007/978-0-387-79948-3_359

Jaeger, R., & Haslwanter, T. (2004). Otolith responses to dynamical stimuli: Results of a numerical investigation. *Biological Cybernetics*, *90*(3), 165–175. https://doi.org/10.1007/s00422-003-0456-0

Jan, M. M., Camfield, P. R., Gordon, K., & Camfield, C. S. (1997). Vomiting after mild head injury is related to migraine. *The Journal of Pediatrics*, *130*(1), 134–137. https://doi.org/10.1016/s0022-3476(97)70322-6

Jarisch, R., Weyer, D., Ehlert, E., Koch, C. H., Pinkowski, E., Jung, P., . . . Koch, A. (2014). Impact of oral vitamin C on histamine levels and seasickness. *Journal of Vestibular Research: Equilibrium & Orientation*, *24*(4), 281–288. https://doi.org/10.3233/VES-140509

Jarosch, O., & Bengler, K. (2019). Rating of Take-Over Performance in Conditionally Automated Driving Using an Expert-Rating System. In N. Stanton (Ed.), *Advances in intelligent systems and computing. Advances in Human Aspects of Transportation* (Vol. 786, pp. 283–294). Cham: Springer International Publishing. https://doi.org/10.1007/978-3-319-93885-1_26

Jennings, R. T., Davis, J. R., & Santy, P. A. (1988). Comparison of aerobic fitness and space motion sickness during the shuttle program. *Aviation, Space, and Environmental Medicine*, *59*(5), 448–451.

Johnson, W. H., Sunahara, F. A., & Landolt, J. P. (1993). Motion sickness, vascular changes accompanying pseudo-coriolis-induced nausea. *Aviation, Space, and Environmental Medicine*, *64*(5), 367–369.

Jones, M. L. H., Ebert, S., & Reed, M. (2019). Sensations Associated with Motion Sickness Response during Passenger Vehicle Operations on a Test Track. In *SAE Technical Paper Series*. Warrendale, Pennsylvania: SAE International. https://doi.org/10.4271/2019-01-0687

Jurisch, M., Holzapfel, C., & Buck, C. (2020). The influence of active suspension systems on motion sickness of vehicle occupants. In *2020 IEEE 23rd International Conference on Intelligent Transportation Systems (ITSC)* (pp. 1–6). IEEE. https://doi.org/10.1109/ITSC45102.2020.9294311

Kachar, B., Parakkal, M., Kurc, M., Zhao, Y., & Gillespie, P. G. (2000). High-resolution structure of hair-cell tip links. *Proceedings of the National Academy of Sciences*, *97*(24), 13336–13341. https://doi.org/10.1073/pnas.97.24.13336

Kaplan, I. (1964). Motion Sickness on Railroads. *Industrial Medicine & Surgery*, *33*, 648–651.

Karjanto, J., Yusof, N. M., Wang, C., Terken, J., Delbressine, F., & Rauterberg, M. (2018). The effect of peripheral visual feedforward system in enhancing situation awareness and mitigating motion sickness in fully automated driving. *Transportation Research Part F: Traffic Psychology and Behaviour*, *58*, 678–692. https://doi.org/10.1016/j.trf.2018.06.046

Kato, K., & Kitazaki, S. (2006). A Study for Understanding Carsickness Based on the Sensory Conflict Theory. In *SAE Technical Paper Series*. Warrendale, Pennsylvania: SAE International. https://doi.org/10.4271/2006-01-0096

Katz, B. J., & Digre, K. B. (2016). Diagnosis, pathophysiology, and treatment of photophobia. *Survey of Ophthalmology*, *61*(4), 466–477. https://doi.org/10.1016/j.survophthal.2016.02.001

Kayan, A., & Hood, J. D. (1984). Neuro-otological manifestations of migraine. *Brain: A Journal of Neurology*, *107*(4), 1123–1142. https://doi.org/10.1093/brain/107.4.1123

Keirstead, S. A., & Rose, P. K. (1988). Structure of the intraspinal projections of single, identified muscle spindle afferents from neck muscles of the cat. *The Journal of Neuroscience*, *8*(9), 3413–3426. https://doi.org/10.1523/JNEUROSCI.08-09-03413.1988

Kellogg, R. S., Kennedy, R. S., & Graybiel, A. (1965). Motion sickness symptomatology of of labyrinthine defective and normal subjects during zero gravity maneuvers. *Aerospace Medicine*, *36*, 315–318.

Kennedy, R. S., Graybiel, A., McDonough, R. C., & Beckwith, F. D. (1968). Symptomatology under storm conditions in the North Atlantic in control subjects and in persons with bilateral labyrinthine defects. *Acta Oto-Laryngologica*, *66*(6), 533–540. https://doi.org/10.3109/00016486809126317

Kennedy, R. S., Lane, N. E., Berbaum, K. S., & Lilienthal, M. G. (1993). Simulator Sickness Questionnaire: An Enhanced Method for Quantifying Simulator Sickness. *The International Journal of Aviation Psychology*, *3*(3), 203–220. https://doi.org/10.1207/s15327108ijap0303_3

Keshavarz, B. (2016). Exploring Behavioral Methods to Reduce Visually Induced Motion Sickness in Virtual Environments. In S. Lackey & R. Shumaker (Eds.), *Lecture notes in computer science. Virtual, Augmented and Mixed Reality* (Vol. 9740, pp. 147–155). Cham: Springer International Publishing. https://doi.org/10.1007/978-3-319-39907-2_14

Keshavarz, B., & Hecht, H. (2011). Validating an efficient method to quantify motion sickness. *Human Factors*, *53*(4), 415–426. https://doi.org/10.1177/0018720811403736

Keshavarz, B., & Hecht, H. (2014). Pleasant music as a countermeasure against visually induced motion sickness. *Applied Ergonomics*, *45*(3), 521–527. https://doi.org/10.1016/j.apergo.2013.07.009

Keshavarz, B., Hecht, H., & Lawson, B. (2014). Visually Induced Motion Sickness: Causes, Characteristics, and Countermeasures. In K. Hale & K. Stanney (Eds.), *Human Factors and Ergonomics. Handbook of Virtual Environments* (2nd ed., Vol. 20143245, pp. 647–698). Boca Raton, Florida: CRC Press. https://doi.org/10.1201/b17360-32

Keshavarz, B., Hecht, H., & Zschutschke, L. (2011). Intra-visual conflict in visually induced motion sickness. *Displays*, *32*(4), 181–188. https://doi.org/10.1016/j.displa.2011.05.009

Keshavarz, B., Murovec, B., Mohanathas, N., & Golding, J. F. (2021). The Visually Induced Motion Sickness Susceptibility Questionnaire (VIMSSQ): Estimating Individual Susceptibility to Motion Sickness-Like Symptoms When Using Visual Devices. *Human Factors.* Advance online publication. https://doi.org/10.1177/00187208211008687

Keshavarz, B., Phillip-Muller, A. E., Hemmerich, W., Riecke, B. E., & Campos, J. L. (2018). The effect of visual motion stimulus characteristics on vection and visually induced motion sickness. *Displays.* Advance online publication. https://doi.org/10.1016/j.displa.2018.07.005

Keshavarz, B., Riecke, B. E., Hettinger, L. J., & Campos, J. L. (2015). Vection and visually induced motion sickness: How are they related? *Frontiers in Psychology*, *6*, 472. https://doi.org/10.3389/fpsyg.2015.00472

Keshavarz, B., Saryazdi, R., Campos, J. L., & Golding, J. F. (2019). Introducing the VIMSSQ: Measuring susceptibility to visually induced motion sickness. *Proceedings of the Human Factors and Ergonomics Society Annual Meeting*, *63*(1), 2267–2271. https://doi.org/10.1177/1071181319631216

Keshavarz, B., Stelzmann, D., Paillard, A., & Hecht, H. (2015). Visually induced motion sickness can be alleviated by pleasant odors. *Experimental Brain Research*, *233*(5), 1353–1364. https://doi.org/10.1007/s00221-015-4209-9

Kilincsoy, U., Wagner, A., Bengler, K., Bubb, H., & Vink, P. (2014). Comfortable rear seat postures preferred by car passengers. In T. Ahram, W. Karwowski & T. Marek (Ed.), *Proceedings of the 5th International Conference on Applied Human Factors and Ergonomics (AHFE)* (pp. 823–831).

King, S. [Stephen] (2015). *Mr. Mercedes: Novel* (Hodder & Stoughton). München: Heyne.

King, S. [Susan], Priesol, A. J., Davidi, S. E., Merfeld, D. M., Ehtemam, F., & Lewis, R. F. (2019). Self-motion perception is sensitized in vestibular migraine: Pathophysiologic and clinical implications. *Scientific Reports*, *9*(1), 14323. https://doi.org/10.1038/s41598-019-50803-y

Klosterhalfen, S., Kellermann, S., Pan, F., Stockhorst, U., Hall, G., & Enck, P. (2005). Effects of ethnicity and gender on motion sickness susceptibility. *Aviation, Space, and Environmental Medicine*, *76*(11), 1051–1057.

Koch, A., Cascorbi, I., Westhofen, M., Dafotakis, M., Klapa, S., & Kuhtz-Buschbeck, J. P. (2018). The Neurophysiology and Treatment of Motion Sickness. *Deutsches Arzteblatt International*, *115*(41), 687–696. https://doi.org/10.3238/arztebl.2018.0687

Koch, A., Last, J., Klapa, S., Tillmans, F., Koch, I., & Kähler, W. (2016). Seekrankheit – aktuelle Aspekte eines alten Leidens. *Wehrmedizinische Monatsschrift*, *60*(2), 68–71.

Koch, K. L., Stern, R. M., Vasey, M. W., Seaton, J. F., Demers, L. M., & Harrison, T. S. (1990). Neuroendocrine and gastric myoelectrical responses to illusory self-motion in humans. *The American Journal of Physiology*, *258*(2 Pt 1), E304-E310. https://doi.org/10.1152/ajpendo.1990.258.2.E304

Koch, T. (2020). *Objektivierung und Quantifizierung der Kopfdynamik in verschiedenen Körperlagen im Umfeld zukünftiger Fahrzeugkonzepte* (Research project). University of Stuttgart, Stuttgart, Germany.

Kohl, R. L. (1985). Endocrine correlates of susceptibility to motion sickness. *Aviation, Space, and Environmental Medicine*, *56*(12), 1158–1165.

Kohl, R. L. (1993). Autonomic function and plasma catecholamines following stressful sensory stimuli. *Aviation, Space, and Environmental Medicine*, *64*(10), 921–927.

Kohl, R. L., & Homick, J. L. (1983). Motion sickness: A modulatory role for the central cholinergic nervous system. *Neuroscience & Biobehavioral Reviews*, *7*(1), 73–85. https://doi.org/10.1016/0149-7634(83)90008-8

Köhler, A.-L., Pelzer, J., Seidel, K., & Ladwig, S. (2019). Sitting Postures and Activities in Autonomous Vehicles – New Requirements towards Occupant Safety. *Proceedings of the Human Factors and Ergonomics Society Annual Meeting*, *63*(1), 1874–1878. https://doi.org/10.1177/1071181319631327

Kolev, O. I., Möller, C., Nilsson, G., & Tibbling, L. (1997). Responses in skin microcirculation to vestibular stimulation before and during motion sickness. *The Canadian Journal of Neurological Sciences. Le Journal Canadien Des Sciences Neurologiques*, *24*(1), 53–57. https://doi.org/10.1017/s0317167100021090

Komsta, L. (2015). moments: Moments, cumulants, skewness, kurtosis and related tests (R package version 0.14). Retrieved from https://cran.r-project.org/package=moments on 5/29/2021

Kondrachuk, A. V. (2001). Models of the dynamics of otolithic membrane and hair cell bundle mechanics. *Journal of Vestibular Research*, *11*(1), 33–42.

Koslucher, F. C., Haaland, E. J., & Stoffregen, T. A. (2014). Body load and the postural precursors of motion sickness. *Gait & Posture*, *39*(1), 606–610. https://doi.org/10.1016/j.gaitpost.2013.09.016

Kreiman, J., Antoñanzas-Barroso, N., & Gerratt, B. R. (2010). Integrated software for analysis and synthesis of voice quality. *Behavior Research Methods*, *42*(4), 1030–1041. https://doi.org/10.3758/BRM.42.4.1030

Kreiman, J., Gerratt, B. R., & Antoñanzas-Barroso, N. (2001). *Analysis and Synthesis of Pathological Voice Quality*. Los Angeles. Retrieved from University of California, School of Medicine, Division of Head Neck Surgery website: https://www.uclahealth.org/head-neck-surgery/workfiles/Laryngeal%20Voice%20Research/Software/Analysis%20and%20Synthesis%20of%20Pathological%20Voice%20Quality.pdf on 7/6/2020

Kufver, B., & Förstberg, J. (2001). *Research on the specific aspects of tilting*. *VTI särtryck: 347, A*. Linköping: Swedish National Road and Transport Research Institute.

Kuiper, O. X., Bos, J. E., & Diels, C. (2018). Looking forward: In-vehicle auxiliary display positioning affects carsickness. *Applied Ergonomics*, *68*, 169–175. https://doi.org/10.1016/j.apergo.2017.11.002

Kuiper, O. X., Bos, J. E., Schmidt, E. A., Diels, C., & Wolter, S. (2020). Knowing What's Coming: Unpredictable Motion Causes More Motion Sickness. *Human Factors*, *62*(8), 1339–1348. https://doi.org/10.1177/0018720819876139

Kyriakidis, M., Happee, R., & Winter, J. de (2015). Public opinion on automated driving: Results of an international questionnaire among 5000 respondents. *Transportation Research Part F: Traffic Psychology and Behaviour*, *32*, 127–140. https://doi.org/10.1016/j.trf.2015.04.014

Laboissière, R., Letievant, J.-C., Ionescu, E., Barraud, P.-A., Mazzuca, M., & Cian, C. (2015). Relationship between Spectral Characteristics of Spontaneous Postural Sway and Motion Sickness Susceptibility. *PloS One*, *10*(12), e0144466. https://doi.org/10.1371/journal.pone.0144466

LaCaille, L., Patino-Fernandez, A. M., Monaco, J., Ding, D., Upchurch Sweeney, C. R., Butler, C. D., . . . Söderback, I. (2013). Electrodermal Activity (EDA). In M. D. Gellman & J. R. Turner (Eds.), *Springer reference. Encyclopedia of Behavioral Medicine* (pp. 666–669). New York: Springer. https://doi.org/10.1007/978-1-4419-1005-9_13

Lachenmayr, B., Buser, A., & Keller, O. (1996). Sehstörungen als Unfallursache. *Bericht Der Bundesanstalt Für Straßenwesen (BASt)*, *65*. Retrieved from https://bast.opus.hbz-nrw.de/opus45-bast/frontdoor/deliver/index/docId/2293/file/M92_15.pdf on 6/3/2021

Lackner, J. R. (2014). Motion sickness: More than nausea and vomiting. *Experimental Brain Research*, *232*(8), 2493–2510. https://doi.org/10.1007/s00221-014-4008-8

Lackner, J. R., & DiZio, P. (2006). Space motion sickness. *Experimental Brain Research*, *175*(3), 377–399. https://doi.org/10.1007/s00221-006-0697-y

Lamb, S., & Kwok, K. C. S. (2015). Mssq-Short Norms May Underestimate Highly Susceptible Individuals: Updating the MSSQ-Short Norms. *Human Factors*, *57*(4), 622–633. https://doi.org/10.1177/0018720814555862

Langheim, J. (Ed.) (2016). *Lecture Notes in Mobility*. *Energy Consumption and Autonomous Driving*. Cham: Springer International Publishing. https://doi.org/10.1007/978-3-319-19818-7

Lasker, D. M., Han, G. C., Park, H. J., & Minor, L. B. (2008). Rotational responses of vestibular-nerve afferents innervating the semicircular canals in the C57BL/6 mouse. *JARO: Journal of the Association for Research in Otolaryngology*, *9*(3), 334–348. https://doi.org/10.1007/s10162-008-0120-4

Laurens, J., & Angelaki, D. E. (2011). The functional significance of velocity storage and its dependence on gravity. *Experimental Brain Research*, *210*(3-4), 407–422. https://doi.org/10.1007/s00221-011-2568-4

Lavin, P. (2014). Ophthalmoplegia. In *Encyclopedia of the Neurological Sciences* (pp. 651–652). Elsevier. https://doi.org/10.1016/B978-0-12-385157-4.00146-9

Lawrence, M. A. (2016). ez: Easy Analysis and Visualization of Factorial Experiments (R package version 4.4-0). Retrieved from https://cran.r-project.org/web/packages/ez/ez.pdf on 5/29/2021

Lawson, B. (2014). Motion Sickness Symptomatology and Origins. In K. Hale & K. Stanney (Eds.), *Human Factors and Ergonomics. Handbook of Virtual Environments* (2nd ed., pp. 532–587). Boca Raton, Florida: CRC Press.

Lawther, A., & Griffin, M. J. (1986). The motion of a ship at sea and the consequent motion sickness amongst passengers. *Ergonomics*, *29*(4), 535–552. https://doi.org/10.1080/00140138608968289

Lawther, A., & Griffin, M. J. (1987). Prediction of the incidence of motion sickness from the magnitude, frequency, and duration of vertical oscillation. *The Journal of the Acoustical Society of America*, *82*(3), 957–966. https://doi.org/10.1121/1.395295

Lawther, A., & Griffin, M. J. (1988). A survey of the occurrence of motion sickness amongst passengers at sea. *Aviation, Space, and Environmental Medicine*, *59*(5), 399–406.

Le, V. C., Jones, M. L. H., Kinnaird, C., Barone, V. J., Bao, T., & Sienko, K. H. (2020). Standing balance of vehicle passengers: The effect of vehicle motion, task performance on post-drive balance. *Gait & Posture*, *82*, 189–195. https://doi.org/10.1016/j.gaitpost.2020.08.123

Lederer, L., & Kidera, G. (1954). Passenger comfort in commercial air travel with reference to motion sickness. *International Record of Medicine and General Practice Clinics*, *167*(12), 661–668.

Lederman, S. J., & Jones, L. A. (2011). Tactile and Haptic Illusions. *IEEE Transactions on Haptics*, *4*(4), 273–294. https://doi.org/10.1109/TOH.2011.2

Lee, S., & Kaylie, D. M. (2013). Balance (Anatomy: Labyrinth and Otoliths). In S. E. Kountakis (Ed.), *Encyclopedia of Otolaryngology, Head and Neck Surgery* (pp. 229–236). Berlin, Heidelberg: Springer. https://doi.org/10.1007/978-3-642-23499-6_650

Lehnert, K. (2018). *Einflüsse zukünftiger Interieurkonzepte autonomer Fahrzeuge auf das menschliche Wohlbefinden* (Master´s thesis). Technical University of Berlin, Berlin, Germany.

Levine, M. E., Chillas, J. C., Stern, R. M., & Knox, G. W. (2000). The effects of seroto-nin (5-HT3) receptor antagonists on gastric tachyarrhythmia and the symptoms of motion sickness. *Aviation, Space, and Environmental Medicine*, *71*(11), 1111–1114.

Levine, M. E., Muth, E. R., Williamson, M. J., & Stern, R. M. (2004). Protein-predomi-nant meals inhibit the development of gastric tachyarrhythmia, nausea and the symptoms of motion sickness. *Alimentary Pharmacology and Therapeutics*, *19*(5), 583–590. https://doi.org/10.1111/j.1365-2036.2004.01885.x

Lewis, R. F. (2004). Frequency-specific mal de debarquement. *Neurology*, *63*(10), 1983–1984. https://doi.org/10.1212/01.wnl.0000144701.94530.6a

Li, Y. [Yan], Liu, A., & Ding, L. (2019). Machine learning assessment of visually in-duced motion sickness levels based on multiple biosignals. *Biomedical Signal Processing and Control*, *49*, 202–211. https://doi.org/10.1016/j.bspc.2018.12.007

Liao, K., Walker, M. F., Joshi, A. C., Reschke, M., Strupp, M., Wagner, J., & Leigh, R. J. (2010). The linear vestibulo-ocular reflex, locomotion and falls in neurological disorders. *Restorative Neurology and Neuroscience*, *28*(1), 91–103. https://doi.org/10.3233/RNN-2010-0507

Lien, H.-C., Sun, W. M., Chen, Y.-H., Kim, H., Hasler, W., & Owyang, C. (2003). Ef-fects of ginger on motion sickness and gastric slow-wave dysrhythmias induced by circular vection. *American Journal of Physiology. Gastrointestinal and Liver Physiology*, *284*(3), G481-G489. https://doi.org/10.1152/ajpgi.00164.2002

Lindsay, P. H., & Norman, D. A. (1973). *Human information processing: An introduc-tion to psychology* (4th ed.). New York: Acadademic Press.

Lisberger, S. G., & Fuchs, A. F. (1978). Role of primate flocculus during rapid behavioral modification of vestibuloocular reflex. 1st Purkinje cell activity during visually guided horizontal smooth-pursuit eye movements and passive head rotation. *Jour-nal of Neurophysiology*, *41*(3), 733–763. https://doi.org/10.1152/jn.1978.41.3.733

Liu, C.-S. J., Bryan, R. N., Miki, A., Woo, J. H., Liu, G. T., & Elliott, M. A. (2006). Magnocellular and parvocellular visual pathways have different blood oxygen level-dependent signal time courses in human primary visual cortex. *AJNR: Amer-ican Journal of Neuroradiology*, *27*(8), 1628–1634.

Liu, P., Guo, Q., Ren, F., Wang, L., & Xu, Z. [Zhigang] (2019). Willingness to pay for self-driving vehicles: Influences of demographic and psychological factors. *Trans-portation Research Part C: Emerging Technologies*, *100*, 306–317. https://doi.org/10.1016/j.trc.2019.01.022

Liu, P., & Xu, Z. [Zhigang] (2019). Self-driving Vehicles: Do Their Risks Outweigh Their Benefits? In H. Krömker (Ed.), *Lecture notes in computer science. HCI in Mobility, Transport, and Automotive Systems* (Vol. 11596, pp. 26–34). Cham: Springer International Publishing. https://doi.org/10.1007/978-3-030-22666-4_2

Liu, R., Xu, M., Zhang, Y., Peli, E., & Hwang, A. D. (2020). A Pilot Study on Electroencephalogram-based Evaluation of Visually Induced Motion Sickness. *Journal of Imaging Science and Technology*. Advance online publication. https://doi.org/10.2352/J.ImagingSci.Technol.2020.64.2.020501

Löfgren, S., Thaung, J., & Lopes, C. (2013). Laser pointers and Eye injuries: An analysis of reported cases. Retrieved from https://www.stralsakerhetsmyndigheten.se/contentassets/0afc07d8bc5740e3884b7924b01cbd6d/201330-laser-pointers-and-eye-injuries---an-analysis-of-reported-cases on 6/4/2021

Lokossou, A., Metanbou, S., Gondry-Jouet, C., & Balédent, O. (2020). Extracranial versus intracranial hydro-hemodynamics during aging: A PC-MRI pilot cross-sectional study. *Fluids and Barriers of the CNS*, *17*(1). https://doi.org/10.1186/s12987-019-0163-4

Longatti, P., Porzionato, A., Basaldella, L., Fiorindi, A., Caro, P. de, & Feletti, A. (2015). The human area postrema: Clear-cut silhouette and variations shown in vivo. *Journal of Neurosurgery*, *122*(5), 989–995. https://doi.org/10.3171/2014.11.JNS14482

Lopez, I., Ishiyama, G., Tang, Y., Tokita, J., Baloh, R. W., & Ishiyama, A. (2005). Regional estimates of hair cells and supporting cells in the human crista ampullaris. *Journal of Neuroscience Research*, *82*(3), 421–431. https://doi.org/10.1002/jnr.20652

Lorenz, S. (2011). *Assistenzsystem zur Optimierung des Sitzkomforts* (Dissertation). Technical University of Munich - TUM, Munich, Germany.

Lozupone, E., & Favia, A. (1990). The structure of the trabeculae of cancellous bone. 2. Long bones and mastoid. *Calcified Tissue International*, *46*(6), 367–372. https://doi.org/10.1007/BF02554966

Lubeck, A. J., Bos, J. E., & Stins, J. F. (2015). Motion in images is essential to cause motion sickness symptoms, but not to increase postural sway. *Displays*, *38*, 55–61. https://doi.org/10.1016/j.displa.2015.03.001

Luccarelli, M., Matt, D. T., & Spena, Paquale Russo, Lienkamp, Markus (2014). Purpose Design for Electric Cars - Parameters Defining Exterior Vehicle Proportions In: CoFAT Conference on Future Automotive Technology. Retrieved from https://mediatum.ub.tum.de/doc/1226669/1226669.pdf on 7/12/2021

Lueg, B. (2019). Seen-Sucht nach Süden: Die oberitalienischen Seen - Film von Barbara Lueg. Retrieved from https://www.zdf.de/dokumentation/dokumentation-sonstige/seensucht-oberitalienische-seen-100.html on 4/10/2021

Luo, D., Ganesh, S., & Koolaard, J. (2020). predictmeans: Calculate Predicted Means for Linear Models (R package version 1.0.4). Retrieved from https://cran.r-project.org/package=predictmeans on 5/29/2021

Lysakowski, A., Minor, L. B., Fernández, C., & Goldberg, J. M. (1995). Physiological identification of morphologically distinct afferent classes innervating the cristae ampullares of the squirrel monkey. *Journal of Neurophysiology*, *73*(3), 1270–1281. https://doi.org/10.1152/jn.1995.73.3.1270

Magnus, R. (1924). *Körperstellung: Experimentell-Physiologische Untersuchungen über die Einzelnen bei der Körperstellung in Tätigkeit Tretenden Reflexe, über ihr Zusammenwirken und ihre Störungen. Monographien aus dem Gesamtgebiete der Physiologie der Pflanzen und der Tiere*. Berlin, Heidelberg: Springer. https://doi.org/10.1007/978-3-662-25478-3

Maier, C. (2018). *Methodik zur Quantifizierung der Kopfdynamik von Passagieren im Fahrzeug* (Bachelor´s thesis). Trier University of Applied Sciences, Trier, Germany.

Malhotra, A., Minja, F. J., Crum, A., & Burrowes, D. (2011). Ocular anatomy and cross-sectional imaging of the eye. *Seminars in Ultrasound, CT, and MR*, *32*(1), 2–13. https://doi.org/10.1053/j.sult.2010.10.009

Mallinson, A. I. (2011). *Visual Vestibular Mismatch: A poorly understood presentation of balance system disease* (Dissertation). Maastricht University, Maastricht, The Netherlands.

Manning, G. W., & Stewart, G. W. (1949). Effect of body position on incidence of motion sickness. *Journal of Applied Physiology*, *1*(9), 619–628. https://doi.org/10.1152/jappl.1949.1.9.619

Mansfield, N. J. (2005). *Human response to vibration*. Boca Raton, Florida: CRC Press.

Marchant-Forde, R. M., Marlin, D. J., & Marchant-Forde, J. N. (2004). Validation of a cardiac monitor for measuring heart rate variability in adult female pigs: Accuracy, artefacts and editing. *Physiology & Behavior*, *80*(4), 449–458. https://doi.org/10.1016/j.physbeh.2003.09.007

Marchetti, G. M., Drton, M., & Sadeghi, K. (2020). ggm: Graphical Markov Models with Mixed Graphs (R package version 2.5). Retrieved from https://cran.r-project.org/package=ggm on 5/29/2021

Marcus, D. A., Furman, J. M., & Balaban, C. D. (2005). Motion sickness in migraine sufferers. *Expert Opinion on Pharmacotherapy*, *6*(15), 2691–2697. https://doi.org/10.1517/14656566.6.15.2691

Marlinski, V., Plotnik, M., & Goldberg, J. M. (2004). Efferent actions in the chinchilla vestibular labyrinth. *JARO: Journal of the Association for Research in Otolaryngology*, *5*(2), 126–143. https://doi.org/10.1007/s10162-003-4029-7

Matchock, R. L., Levine, M. E., Gianaros, P. J., & Stern, R. M. (2008). Susceptibility to nausea and motion sickness as a function of the menstrual cycle. *Women's Health Issues: Official Publication of the Jacobs Institute of Women's Health*, *18*(4), 328–335. https://doi.org/10.1016/j.whi.2008.01.006.

Matsangas, P., & McCauley, M. E. (2014). Sopite syndrome: A revised definition. *Aviation, Space, and Environmental Medicine*, *85*(6), 672–673. https://doi.org/10.3357/ASEM.3891.2014

Matsangas, P., McCauley, M. E., & Becker, W. (2014). The effect of mild motion sickness and sopite syndrome on multitasking cognitive performance. *Human Factors*, *56*(6), 1124–1135. https://doi.org/10.1177/0018720814522484

Matthews, T., Dey, A. K., Mankoff, J., Carter, S., & Rattenbury, T. (2004). A toolkit for managing user attention in peripheral displays. In S. K. Feiner & J. A. Landay (Eds.), *Proceedings of the 17th annual ACM symposium on User interface software and technology* (pp. 247–256). New York: ACM Press. https://doi.org/10.1145/1029632.1029676

Maxton, G. P., & Wormald, J. (2009). *Time for a Model Change: Re-engineering the Global Automotive Industry*: Cambridge University Press. https://doi.org/10.1017/CBO9780511488535

McCauley, M. E., Royal, J. W., Wylie, C. D., O´Hanlon, J., & Mackie, R. R. (1976). *Motion Sickness Incidence: Exploratory Studies of Habituation, Pitch and Roll, and the Refinement of a Mathematical Model*. Santa Barbara, California. Retrieved from Human Factors Research website: https://trid.trb.org/view/399367 on 3/19/2021

McGrath, J., Roy, P., & Perrin, B. J. (2017). Stereocilia morphogenesis and maintenance through regulation of actin stability. *Seminars in Cell & Developmental Biology*, *65*, 88–95. https://doi.org/10.1016/j.semcdb.2016.08.017

McGuinness, J. (2014). *Implications of potassium channel heterogeneity for model of vestibulo-ocular reflex response fidelity* (Dissertation). University of Stirling, Stirling, United Kingdom.

McIntosh, I. B. (1998). Motion sickness - questions and answers. *Journal of Travel Medicine*, *5*(2), 89–91. https://doi.org/10.1111/j.1708-8305.1998.tb00470.x

Megighian, D., & Martini, A. (1980). Motion sickness and space sickness: Clinical and experimental findings. *ORL: Journal for Oto-Rhino-Laryngology and Its Related Specialties*, *42*(4), 185–195. https://doi.org/10.1159/000275493

Meissner, K., Enck, P., Muth, E. R., Kellermann, S., & Klosterhalfen, S. (2009). Cortisol levels predict motion sickness tolerance in women but not in men. *Physiology & Behavior*, *97*(1), 102–106. https://doi.org/10.1016/j.physbeh.2009.02.007

Mekjavic, I. B., Tipton, M. J., Gennser, M., & Eiken, O. (2001). Motion sickness potentiates core cooling during immersion in humans. *The Journal of Physiology*, *535*(2), 619–623. https://doi.org/10.1111/j.1469-7793.2001.00619.x

Menétrey, D., & Basbaum, A. I. (1987). Spinal and trigeminal projections to the nucleus of the solitary tract: A possible substrate for somatovisceral and viscerovisceral reflex activation. *The Journal of Comparative Neurology*, *255*(3), 439–450. https://doi.org/10.1002/cne.902550310

Merendino, K. A., & Dillard, D. H. (1955). The concept of sphincter substitution by an interposed jejunal segment for anatomic and physiologic abnormalities at the esophagogastric junction; with special reference to reflux esophagitis, cardiospasm and esophageal varices. *Annals of Surgery*, *142*(3), 486–506. https://doi.org/10.1097/00000658-195509000-00015

Merrell, A. J., & Kardon, G. (2013). Development of the diaphragm - a skeletal muscle essential for mammalian respiration. *The FEBS Journal*, *280*(17), 4026–4035. https://doi.org/10.1111/febs.12274

Meschtscherjakov, A., Strumegger, S., & Trösterer, S. (2019). Bubble Margin: Motion Sickness Prevention While Reading on Smartphones in Vehicles. In D. Lamas, F. Loizides, L. Nacke, H. Petrie, M. Winckler, & P. Zaphiris (Eds.), *Lecture notes in computer science. Human-Computer Interaction – INTERACT 2019* (Vol. 11747, pp. 660–677). Cham: Springer International Publishing. https://doi.org/10.1007/978-3-030-29384-0_39

Middlekauff, H. R., & Mark, A. L. (1998). The treatment of heart failure: The role of neurohumoral activation. *Internal Medicine (Tokyo, Japan)*, *37*(2), 112–122. https://doi.org/10.2169/internalmedicine.37.112

Miksch, M. [Markus], Steiner, M., Miksch, M. [Michael], & Meschtscherjakov, A. (2016). Motion Sickness Prevention System (MSPS). In P. Green, B. Pfleging, A. L. Kun, Y. Liang, A. Meschtscherjakov, & P. Fröhlich (Eds.), *Proceedings of the 8th International Conference on Automotive User Interfaces and Interactive Vehicular Applications* (pp. 147–152). New York: ACM Press. https://doi.org/10.1145/3004323.3004340

Miller, E. F., & Graybiel, A. (1970). A provocative test for grading susceptibility to motion sickness yielding a single numerical score. *Acta Oto-Laryngologica. Supplementum*, *274*, 1–20.

Mitchelson, F. (1992a). Pharmacological agents affecting emesis. A review (Part I). *Drugs*, *43*(3), 295–315. https://doi.org/10.2165/00003495-199243030-00002

Mitchelson, F. (1992b). Pharmacological agents affecting emesis. A review (Part II). *Drugs*, *43*(4), 443–463. https://doi.org/10.2165/00003495-199243040-00003

Mo, F.-F., Qin, H.-H., Wang, X.-L., Shen, Z.-L., Xu, Z. [Zheng], Wang, K.-H., . . . Li, M. (2012). Acute hyperglycemia is related to gastrointestinal symptoms in motion sickness: An experimental study. *Physiology and Behavior*, *105*(2), 394–401. https://doi.org/10.1016/j.physbeh.2011.08.024

Mogilner, A. (2006). On the edge: Modeling protrusion. *Current Opinion in Cell Biology*, *18*(1), 32–39. https://doi.org/10.1016/j.ceb.2005.11.001

Mok, D., Ro, A., Cadera, W., Crawford, J. D., & Vilis, T. (1992). Rotation of Listing's plane during vergence. *Vision Research*, *32*(11), 2055–2064. https://doi.org/10.1016/0042-6989(92)90067-s

Money, K. E. (1970). Motion sickness. *Physiological Reviews*, *50*(1), 1–39. https://doi.org/10.1152/physrev.1970.50.1.1

Money, K. E., Bonen, L., Beatty, J. D., Kuehn, L. A., Sokoloff, M., & Weaver, R. S. (1971). Physical properties of fluids and structures of vestibular apparatus of the pigeon. *The American Journal of Physiology*, *220*(1), 140–147. https://doi.org/10.1152/ajplegacy.1971.220.1.140

Money, K. E., & Wood, J. D. (1970). *Neural mechanisms underlying the symptomatology of motion sickness*. *Symposium on the Role of the Vestibular Organs in Space Exploration*. Washington, D.C.: National Academies Press. https://doi.org/10.17226/18593

Monzack, E. L., & Cunningham, L. L. (2013). Lead roles for supporting actors: Critical functions of inner ear supporting cells. *Hearing Research*, *303*, 20–29. https://doi.org/10.1016/j.heares.2013.01.008

Morrison, T. R., Dobie, T. G., Willems, G. C., & Endler, J. L. (1991). *Ship Roll Stabilization and Human Performance*. New Orleans, Lousiana. Retrieved from Naval Biodynamics Laboratory website: https://apps.dtic.mil/dtic/tr/fulltext/u2/a232721 .pdf on 3/13/2021

Morrow, G. R. (1985). The effect of a susceptibility to motion sickness on the side effects of cancer chemotherapy. *Cancer*, *55*(12), 2766–2770. https://doi.org/10.1002/ 1097-0142(19850615)55:12<2766::aid-cncr2820551207>3.0.co;2-7

Moskowitz, M. A. (1984). The neurobiology of vascular head pain. *Annals of Neurology*, *16*(2), 157–168. https://doi.org/10.1002/ana.410160202

Moskowitz, M. A. (1993). Neurogenic inflammation in the pathophysiology and treatment of migraine. *Neurology*, *43*(6 Suppl 3), 16-20.

Mu, Y.-T., Chien, W.-C., & Wu, F.-G. (2020). Providing Peripheral Trajectory Information to Avoid Motion Sickness During the In-car Reading Tasks. In T. Ahram, W. Karwowski, S. Pickl, & R. Taiar (Eds.), *Advances in intelligent systems and computing* (pp. 216–222). Cham: Springer International Publishing. https://doi.org/10.1007/978-3-030-27928-8_33

Mueller, M., & Verhagen, J. H. G. (1988). A New Quantitative Model of Total Endolymph Flow in the System of Semicircular Ducts. *Journal of Theoretical Biology*, *134*, 473–501.

Mullen, T. J., Berger, R. D., Oman, C. M., & Cohen, R. J. (1998). Human heart rate variability relation is unchanged during motion sickness. *Journal of Vestibular Research*, *8*(1), 95–105.

Muragushi, Y., Fukui, K., Asaga, Y., & Ono, E. (2006). Development of Human Sensitivity Evaluation System for Vehicle Dynamics. In *31th International FISITA World Automotive Congress,* Yokohama, Japan.

Murdin, L., Golding, J. F., & Bronstein, A. (2011). Managing motion sickness. *BMJ (Clinical Research Ed.)*, *343*. https://doi.org/10.1136/bmj.d7430

Muth, E. R., Walker, A. D., & Fiorello, M. (2006). Effects of Uncoupled Motion on Performance. *Human Factors*, *48*(3), 600–607. https://doi.org/10.1518/001872 006778606750

Mutschler, H. (2007). *Menschmodelle bei niedrigen Beschleunigungen* (Dissertation). Eberhard-Karls-University of Tübingen, Tübingen, Germany.

Nachum, Z., Shupak, A., Letichevsky, V., Ben-David, J., Tal, D., Tamir, A., . . . Luntz, M. (2004). Mal de debarquement and posture: Reduced reliance on vestibular and visual cues. *The Laryngoscope*, *114*(3), 581–586. https://doi.org/10. 1097/00005537-200403000-00036

Nagelkerke, N. J. D. (1991). A note on a general definition of the coefficient of determination. *Biometrika*, *78*(3), 691–692. https://doi.org/10.1093/BIOMET/78.3.691

Nalivaiko, E., Davis, S. L., Blackmore, K. L., Vakulin, A., & Nesbitt, K. V. (2015). Cybersickness provoked by head-mounted display affects cutaneous vascular tone, heart rate and reaction time. *Physiology & Behavior*, *151*, 583–590. https://doi.org/10.1016/j.physbeh.2015.08.043

Nalivaiko, E., Rudd, J. A., & So, R. H. (2014). Motion sickness, nausea and thermoregulation: The "toxic" hypothesis. *Temperature (Austin, Tex.)*, *1*(3), 164–171. https://doi.org/10.4161/23328940.2014.982047

Narra, P., & Zinger, D. S. (2004). An effective LED dimming approach. In *39th IAS Annual Meeting - IEEE Industry Applications Conference* (pp. 1671–1676). IEEE. https://doi.org/10.1109/IAS.2004.1348695

Nedresky, D., & Singh, G. (2021). *Physiology, Luteinizing Hormone*. Treasure Island, Florida.

Neuwirth, E. (2014). RColorBrewer: color schemes for maps (and other graphics) designed by Cynthia Brewer (R package version 1.1-2). Retrieved from http://cran.uni-muenster.de/web/packages/RColorBrewer/RColorBrewer.pdf on 5/29/2021

Nicogossian, A. E., & Parker, J. F. (1982). *Space physiology and medicine* (No. NASA SP-447). Retrieved from NASA Technical Reports Server website: https://ntrs.nasa.gov/archive/nasa/casi.ntrs.nasa.gov/19830017078.pdf on 4/28/2020

Nobel, G., Tribukait, A., Mekjavic, I. B., & Eiken, O. (2010). Histaminergic and cholinergic neuron systems in the impairment of human thermoregulation during motion sickness. *Brain Research Bulletin*, *82*(3-4), 193–200. https://doi.org/10.1016/j.brainresbull.2010.04.004

Nooij, S. A. E., & Bos, J. E. (2007). Sickness induced by head movements after different centrifugal Gx-loads and durations. *Journal of Vestibular Research*, *17*(5-6), 323–332.

Nooij, S. A. E., Pretto, P., & Bülthoff, H. H. (2018). More vection means more velocity storage activity: A factor in visually induced motion sickness? *Experimental Brain Research*, *236*(11), 3031–3041. https://doi.org/10.1007/s00221-018-5340-1

Nooij, S. A. E., Pretto, P., Oberfeld, D., Hecht, H., & Bülthoff, H. H. (2017). Vection is the main contributor to motion sickness induced by visual yaw rotation: Implications for conflict and eye movement theories. *PloS One*, *12*(4), e0175305. https://doi.org/10.1371/journal.pone.0175305

Nooij, S. A. E., Vanspauwen, R., Bos, J. E., & Wuyts, F. L. (2011). A re-investigation of the role of utricular asymmetries in Space Motion Sickness. *Journal of Vestibular Research: Equilibrium & Orientation*, *21*(3), 141–151. https://doi.org/10.3233/VES-2011-0400

Nordhoff, S., Kyriakidis, M., van Arem, B., & Happee, R. (2019). A multi-level model on automated vehicle acceptance (MAVA): a review-based study. *Theoretical Issues in Ergonomics Science*, *20*(6), 682–710. https://doi.org/10.1080/14639 22X.2019.1621406

Nwagwu, V., Patel, R., & Okudo, J. (2015). Mal de Debarquement Syndrome: A Rare Entity-A Case Report and Review of the Literature. *Case Reports in Otolaryngology*, *2015*, 918475. https://doi.org/10.1155/2015/918475

O´Hanlon, J., & McCauley, M. E. (1974). Motion Sickness Incidence as a Function of Vertical Sinusoidal Motion. *Aerospace Medicine*, 366–369.

Obrist, D. (2011). *Fluid Mechanics of the Inner Ear* (Habilitation). Swiss Federal Institute of Technology in Zürich, Zürich, Switzerland.

Okada, T., Grunfeld, E., Shallo-Hoffmann, J., & Bronstein, A. M. (1999). Vestibular perception of angular velocity in normal subjects and in patients with congenital nystagmus. *Brain: A Journal of Neurology*, *122 (Pt 7)*, 1293–1303. https://doi.org/10.1093/brain/122.7.1293

Olofsson, V. (2015). Flip Run Second Wave (Version 1.0.2). Retrieved from https://flip-run-second-wave.soft112.com/ on 3/23/2021

Oman, C. M. (1998). Sensory conflict theory and space sickness: Our changing perspective. *Journal of Vestibular Research*, *8*(1), 51–56.

Oman, C. M. (2012). Are evolutionary hypotheses for motion sickness "just-so" stories? *Journal of Vestibular Research: Equilibrium & Orientation*, *22*(2), 117–127. https://doi.org/10.3233/VES-2011-0432

Oman, C. M., & Cullen, K. E. (2014). Brainstem processing of vestibular sensory exafference: Implications for motion sickness etiology. *Experimental Brain Research*, *232*(8), 2483–2492. https://doi.org/10.1007/s00221-014-3973-2

Oman, C. M., & Young, L. R. (1972). The physiological range of pressure difference and cupula deflections in the human semicircular canal. Theoretical considerations. *Acta Oto-Laryngologica*, *74*(5), 324–331. https://doi.org/10.3109/00016487209 128458

Oosterveld (1995). Motion Sickness. *Journal of Travel Medicine*, *2*(3), 182–185. https://doi.org/10.1111/j.1708-8305.1995.tb00649.x

Open Street Maps (2020). *Mercedes Benz plant in Sindelfingen: Test track "Einfahrbahn"*. Open Database License ODbL (https://opendatacommons.org/licenses/odbl/). Retrieved from https://www.openstreetmap.de/karte.html?zoom =15&lat=48.69807&lon=8.98535&layers=B000TT on 5/29/2021

ORBIS - Daimler AG (2020). *Software for patents database and analyses* [Internal documents provided by M. Lierheimer]. Sindelfingen, Deutschland.

Ormsby, C. (1974). *Model of human dynamic orientation* (Dissertation). Massachusetts Institute of Technology, Cambridge, United States.

Ossig, J., Cramer, S., & Bengler, K. (2021). Concept of an Ontology for Automated Vehicle Behavior in the Context of Human-Centered Research on Automated Driving Styles. *Information*, *12*(1), 21. https://doi.org/10.3390/info12010021

Otten, M., & Wittkowske, S. (2014). *Mobilität für die Zukunft: Interdisziplinäre und (fach-)didaktische Herausforderungen* (1st ed.). *In Bewegung: Vol. 3*. Bielefeld: Bertelsmann W.

Pagani, M., Lombardi, F., Guzzetti, S., Sandrone, G., Rimoldi, O., Malfatto, G., . . . Malliani, A. (1984). Power spectral density of heart rate variability as an index of sympatho-vagal interaction in normal and hypertensive subjects. *Journal of Hypertension. Supplement: Official Journal of the International Society of Hypertension*, *2*(3), 383-385.

Paillard, A. C., Lamôré, M., Etard, O., Millot, J.-L., Jacquot, L., Denise, P., & Quarck, G. (2014). Is there a relationship between odors and motion sickness? *Neuroscience Letters*, *566*, 326–330. https://doi.org/10.1016/j.neulet.2014.02.049

Paillard, A. C., Quarck, G., Paolino, F., Denise, P., Paolino, M., Golding, J. F., & Ghulyan-Bedikian, V. (2013). Motion sickness susceptibility in healthy subjects and vestibular patients: Effects of gender, age and trait-anxiety. *Journal of Vestibular Research: Equilibrium & Orientation*, *23*(4-5), 203–209. https://doi.org/10.3233/VES-130501

Pan, L., Qi, R., Xiao, S., Mao, Y., Su, Y., Xu, R., . . . Cai, Y. (2020). *Predictive ability of motion sickness susceptibility questionnaire for seasickness individual difference in Chinese military personnel.* https://doi.org/10.21203/rs.3.rs-20259/v1

Pardhan, S. (1996). A comparison of binocular summation in young and older patients. *Current Eye Research*, *15*(3), 315–319. https://doi.org/10.3109/02713689609007626

Park, A. H., & Hu, S. (1999). Gender differences in motion sickness history and susceptibility to optokinetic rotation-induced motion sickness. *Aviation, Space, and Environmental Medicine*, *70*(11), 1077–1080.

Pasini, B. (2019). *Die Tochter des Gutsverwalters: Die Vorgeschichte zum Roman Bella Stella* (1st ed.). Reinbek: Rowohlt E-Book.

Pasquier, F., Denise, P., Gauthier, A., Bessot, N., & Quarck, G. (2019). Impact of Galvanic Vestibular Stimulation on Anxiety Level in Young Adults. *Frontiers in Systems Neuroscience*, *13:14*. https://doi.org/10.3389/fnsys.2019.00014

Peng, G. C., Hain, T. C., & Peterson, B. W. (1996). A dynamical model for reflex activated head movements in the horizontal plane. *Biological Cybernetics*, *75*(4), 309–319. https://doi.org/10.1007/s004220050297

Perrin, P., Lion, A., Bosser, G., Gauchard, G., & Meistelman, C. (2013). Motion Sickness in Rally Car Co-Drivers. *Aviation, Space, and Environmental Medicine*, *84*(5), 473–477. https://doi.org/10.3357/ASEM.3523.2013

Persson, R. (2008). *Motion sickness in tilting trains - Description and analysis of the present knowledge*. Literature study. Stockholm. Retrieved from Swedish National Road and Transport Research Institute website: https://www.semanticscholar.org/paper/Motion-sickness-in-tilting-trains%3A-description-and-Persson/f421be3d80272e9604ff63b37f5b9c9bbd45167c on 6/4/2021

Pham Xuan, R., Xiong, Y., Brietzke, A., & Marker, S. (2021). Thermal infrared imaging based facial temperature in comparison to ear temperature during a real-driving scenario. *Journal of Thermal Biology*, *96*, 102806. https://doi.org/10.1016/j.jtherbio.2020.102806

Pickles, J. O., Comis, S. D., & Osborne, M. P. (1984). Cross-links between stereocilia in the guinea pig organ of Corti, and their possible relation to sensory transduction. *Hearing Research*, *15*(2), 103–112. https://doi.org/10.1016/0378-5955(84)90041-8

Pinheiro, J., Bates, D., DebRoy, S., Sarkar, D., & R Core Team (2018). nlme: Linear and Nonlinear Mixed Effects Models (R package version 3.1-137). Retrieved from https://CRAN.R-project.org/package=nlme on 5/29/2021

Pleuvry, B. J. (2004). Receptors, agonists and antagonists. *Anaesthesia & Intensive Care Medicine*, *5*(10), 350–352. https://doi.org/10.1383/anes.5.10.350.52312

Preber, L. (1958). Vegetative reactions in caloric and rotatory tests; a clinical study with special reference to motion sickness. *Acta Oto-Laryngologica. Supplementum*, *114*, 1–119.

Probst, T., Krafczyk, S., Bchele, W., & Brandt, T. (1982). Visuelle Prävention der Bewegungskrankheit im Auto. *Archiv Für Psychiatrie Und Nervenkrankheiten*, *231*(5), 409–421. https://doi.org/10.1007/BF00342721

Propper, R. E., Bonato, F., Ward, L., & Sumner, K. (2018). Findings of an effect of gender, but not handedness, on self-reported motion sickness propensity. *BioPsychoSocial Medicine*, *12*(1), 3221. https://doi.org/10.1186/s13030-018-0121-4

Proske, U., & Gandevia, S. C. (2012). The proprioceptive senses: Their roles in signaling body shape, body position and movement, and muscle force. *Physiological Reviews*, *92*(4), 1651–1697. https://doi.org/10.1152/physrev.00048.2011

R Core Team (2018). stats: R statistical functions (R package version 4.0.2). Retrieved from https://stat.ethz.ch/R-manual/R-patched/library/stats/html/stats-package.html on 5/29/2021

Rabbitt, R. D., Breneman, K. D., King, C., Yamauchi, A. M., Boyle, R., & Highstein, S. M. (2009). Dynamic displacement of normal and detached semicircular canal cupula. *JARO: Journal of the Association for Research in Otolaryngology*, *10*(4), 497–509. https://doi.org/10.1007/s10162-009-0174-y

Raphan, T., Matsuo, V., & Cohen, B. (1979). Velocity storage in the vestibulo-ocular reflex arc (VOR). *Experimental Brain Research*, *35*(2), 229–248. https://doi.org/10.1007/bf00236613

Rawat, N., Connor, C. W., Jones, J. A., Kozlovskaya, I. B., & Sullivan, P. (2002). The correlation between aerobic fitness and motion sickness susceptibility. *Aviation, Space, and Environmental Medicine*, *73*(3), 216–218.

Reason, J. T. (1978). Motion sickness adaptation: a neural mismatch model. *Journal of the Royal Society of Medicine*, *71*, 819–829.

Reason, J. T., & Brand, J. J. (1975). *Motion sickness*. London: Academic Press.

Reavley, C. M., Golding, J. F., Cherkas, L. F., Spector, T. D., & MacGregor, A. J. (2006). Genetic influences on motion sickness susceptibility in adult women: A classical twin study. *Aviation, Space, and Environmental Medicine*, *77*(11), 1148–1152.

Reed, M. P., Ebert, S. M., & Jones, M. L. H. (2019a). Comfortable Head and Neck Postures in Reclined Seating for Use in Automobile Head Rest Design. In *SAE Technical Paper Series*. Warrendale, Pennsylvania: SAE International. https://doi.org/10.4271/2019-01-0408

Reed, M. P., Ebert, S. M., & Jones, M. L. H. (2019b). Posture and belt fit in reclined passenger seats. *Traffic Injury Prevention*, *20*(1), 38-42. https://doi.org/10.1080/15389588.2019.1630733

Reuler, J. B. (1978). Hypothermia: Pathophysiology, clinical settings, and management. *Annals of Internal Medicine*, *89*(4), 519–527. https://doi.org/10.7326/0003-4819-89-4-519

Revelle, W. (2021). psych: Procedures for Psychological, Psychometric, and Personality (R package version 2.1.3). Retrieved from https://cran.r-project.org/web/packages/psych/psych.pdf on 5/29/2021

Riccio, G. E., & Stoffregen, T. A. (1988). Affordances as constraints on the control of stance. *Human Movement Science*, *7*(2-4), 265–300. https://doi.org/10.1016/0167-9457(88)90014-0

Riccio, G. E., & Stoffregen, T. A. (1991). An ecological Theory of Motion Sickness and Postural Instability. *Ecological Psychology*, *3*(3), 195–240. https://doi.org/10.1207/s15326969eco0303_2

Richter, E. (1980). Quantitative study of human Scarpa's ganglion and vestibular sensory epithelia. *Acta Oto-Laryngologica*, *90*(3-4), 199–208. https://doi.org/10.3109/00016488009131716

Ringland, R. F., & Stapleford, R. L. (1972). Motion cue effects on pilot tracking. *7th Annual Conference on Manual Control*, 327–338.

Robinson, D. A. (1976). Adaptive gain control of vestibuloocular reflex by the cerebellum. *Journal of Neurophysiology*, *39*(5), 954–969. https://doi.org/10.1152/jn.1976.39.5.954

Roche-Cerasi, I. (2019). Public acceptance of driverless shuttles in Norway. *Transportation Research Part F: Traffic Psychology and Behaviour*, *66*, 162–183. https://doi.org/10.1016/j.trf.2019.09.002

Rockwell, T. H. (1972). Eye movement analysis of visual information acquisition in driving: an overview. *6th Australian Road Research Board (ARRB) Conference*, *6*(3), 316–331.

Rosenberg, W. von, Chanwimalueang, T., Adjei, T., Jaffer, U., Goverdovsky, V., & Mandic, D. P. (2017). Resolving Ambiguities in the LF/HF Ratio:. *Frontiers in Physiology*, *8*, 360. https://doi.org/10.3389/fphys.2017.00360

Rubin, H. J. (1942). Airsickness in a primary Air Force training detachment. *Journal Aviaton Medicine*. (13), 272–276.

Russomano, T., da Rosa, M., & Dos Santos, M. A. (2019). Space motion sickness: A common neurovestibular dysfunction in microgravity. *Neurology India*, *67*(Supplement), 214-218. https://doi.org/10.4103/0028-3886.259127

SAE J1100:2009-11. *Motor Vehicle Dimensions*. (SAE J1100:1973).

SAE J182:2020-11. *Motor Vehicle Fiducial Marks and Three-Dimensional Reference System*. (SAE J182:1970).

SAE J3016:2021-04. *Taxonomy and Definitions for Terms Related to Driving Automation Systems for On-Road Motor Vehicles*. (SAE J3016:2014).

Salter, S., Diels, C., Herriotts, P., Kanarachos, S., & Thake, D. (2019). Motion sickness in automated vehicles with forward and rearward facing seating orientations. *Applied Ergonomics*, *78*, 54–61. https://doi.org/10.1016/j.apergo.2019.02.001

Salva, P., Molier, J., & Gourinat, Y. Toward a three-dimensional finite-element model of the human inner ear angular accelerometers sensors. *International Journal for Computational Vision and Biomechanics*, *2*(3), 149–156. Retrieved from https://hal.archives-ouvertes.fr/hal-01852241 on 6/5/2021

Saruchi, S. '., Zamzuri, H., Hassan, N., & Ariff, M. H. M. (2018). Modeling of head movements towards lateral acceleration direction via system identification for motion sickness study. In *2018 International Conference on Information and Communications Technology (ICOIACT)* (pp. 633–638). IEEE. https://doi.org/10.1109/ICOIACT.2018.8350749

Sawabe, T., Kanbara, M., & Hagita, N. (2017). Diminished reality for acceleration stimulus: Motion sickness reduction with vection for autonomous driving. In *2017 IEEE Virtual Reality (VR)* (pp. 277–278). IEEE.

Sawada, Y., Itaguchi, Y., Hayashi, M., Aigo, K., Miyagi, T., Miki, M., . . . Miyazaki, M. (2020). Effects of synchronised engine sound and vibration presentation on visually induced motion sickness. *Scientific Reports*, *10*(1), 7553. https://doi.org/10.1038/s41598-020-64302-y

Schega, L., Hamacher, D., Böckelmann, I., Huckauf, A., Mecke, R., Grubert, J., & Tümler J. (2010). Vergleich von Messverfahren zur Analyse der Herzfrequenzvariabilität (HRV). *Deutsche Zeitschrift Für Sportmedizin*, *61*(12), 17–21.

Schmäl, F. (2013). Neuronal mechanisms and the treatment of motion sickness. *Pharmacology*, *91*(3-4), 229–241. https://doi.org/10.1159/000350185

Schmäl, F., & Stoll, W. (2000). Kinetosen. *HNO*, *48*(5), 346–356. https://doi.org/10.1007/s001060050579

Schmidt, E. A., Kuiper, O. X., Wolter, S., Diels, C., & Bos, J. E. (2020). An international survey on the incidence and modulating factors of carsickness. *Transportation Research Part F: Traffic Psychology and Behaviour*, *71*, 76–87. https://doi.org/10.1016/j.trf.2020.03.012

Schmidt, S., Amereller, M., Franz, M., Kaiser, R., & Schwirtz, A. (2014). A literature review on optimum and preferred joint angles in automotive sitting posture. *Applied Ergonomics*, *45*(2), 247–260. https://doi.org/10.1016/j.apergo.2013.04.009

Schmidtke, H. (1975). *Handbuch der Ergonomie: (HdE): mit ergonomischen Konstruktionsrichtlinien*. Munich: W. Zuerl.

Schneck, M. E., Haegerstöm-Portnoy, G., Lott, L. A., & Brabyn, J. A. (2010). Monocular vs. Binocular measurement of spatial vision in elders. *Optometry and Vision Science: Official Publication of the American Academy of Optometry*, *87*(8), 526–531. https://doi.org/10.1097/OPX.0b013e3181e61a88

Schneider, E., Glasauer, S., & Dieterich, M. (2002). Comparison of human ocular torsion patterns during natural and galvanic vestibular stimulation. *Journal of Neurophysiology*, *87*(4), 2064–2073. https://doi.org/10.1152/jn.00558.2001

Schneider, S., Brümmer, V., Göbel, S., Carnahan, H., Dubrowski, A., & Strüder, H. K. (2007). Parabolic flight experience is related to increased release of stress hormones. *European Journal of Applied Physiology*, *100*(3), 301–308. https://doi.org/10.1007/s00421-007-0433-8

Schoettle, B., & Sivak, M. (2014). *A Survey of public opinion about autonomous and self-driving vehicles in the US, the UK and Australia* (UMTRI-2014-21). Michigan. Retrieved from The University of Michigan - Transportation Research Institute website: https://deepblue.lib.umich.edu/handle/2027.42/108384 on 2/4/2021

Schünke, M., Voll, M., Wesker, K. H., Schulte, E., & Schumacher, U. (2009). Innenohr: Gleichgewichtsorgan. In Prometheus LernAtlas - Kopf, Hals und Neuroanatomie (Ed.) (5th ed.). Stuttgart: Thieme. Retrieved from https://eref.thieme.de/cockpits/clAna0001/0/coAna00079/4-9970 on 3/14/2021

Schvarcz, E., Palmer, M., Aman, J., Horowitz, M., Stridsberg, M., & Berne, C. (1997). Physiological hyperglycemia slows gastric emptying in normal subjects and patients with insulin-dependent diabetes mellitus. *Gastroenterology*, *113*(1), 60–66. https://doi.org/10.1016/s0016-5085(97)70080-5

Schwarz, U., Busettini, C., & Miles, F. A. (1989). Ocular responses to linear motion are inversely proportional to viewing distance. *Science (New York, N.Y.)*, *245*(4924), 1394–1396. https://doi.org/10.1126/science.2506641

Seemungal, B. M., Glasauer, S., Gresty, M. A., & Bronstein, A. M. (2007). Vestibular perception and navigation in the congenitally blind. *Journal of Neurophysiology*, *97*(6), 4341–4356. https://doi.org/10.1152/jn.01321.2006

Seifert, A. (2016). Ganzkörperschwingungen: Eine Herausforderung in der Sitzentwicklung [Webpage]. Retrieved from https://www.vdi-wissensforum.de/news/ganz koerperschwingungen-eine-herausforderung-in-der-sitzentwicklung/ on 6/5/2021

Seppelt, B., Reimer, B., Russo, L., Mehler, B., Fisher, J., & Friedman, D. (2018). *Towards a human-centric Taxonomy of Automation Types*. Cambridge. Retrieved from Massachusetts Institute of Technology website: https://agelab.mit.edu/system/files/2018-12/mit-cr_consumer_facing_automation_types_taxonomy_white _paper_dec_20181.pdf on 3/17/2021

Shaffer, F., & Ginsberg, J. P. (2017). An Overview of Heart Rate Variability Metrics and Norms. *Frontiers in Public Health*, *5*(258). https://doi.org/10.3389/fpubh.2017. 00258

Shupak, A., & Gordon, C. R. (2006). Motion sickness: Advances in pathogenesis, prediction, prevention, and treatment. *Aviation, Space, and Environmental Medicine*, *77*(12), 1213–1223.

Shyrokau, B., Wang, D., Savitski, D., Hoepping, K., & Ivanov, V. (2015). Vehicle motion control with subsystem prioritization. *Mechatronics*, *30*, 297–315. https://doi.org/10.1016/j.mechatronics.2014.11.004

Silberstein, G. B. (2001). Tumour-stromal interactions. Role of the stroma in mammary development. *Breast Cancer Research*, *3*(4), 218–223. https://doi.org/10. 1186/bcr299

Simjanoska, M., Gjoreski, M., Gams, M., & Madevska Bogdanova, A. (2018). Non-Invasive Blood Pressure Estimation from ECG Using Machine Learning Techniques. *Sensors (Basel, Switzerland)*, *18*(4). https://doi.org/10.3390/s18041160

Sivak, M., & Schoettle, B. (2015). *Motion Sickness in self-driving vehicles* (UMTRI-2015-12). Michigan. Retrieved from The University of Michigan - Transportation Research Institute website: https://deepblue.lib.umich.edu/handle/2027.42/111 747 on 3/23/2020

Slattery, E. L., Oshima, K., Heller, S., & Warchol, M. E. (2014). Cisplatin exposure damages resident stem cells of the mammalian inner ear. *Developmental Dynamics: An Official Publication of the American Association of Anatomists*, *243*(10), 1328–1337. https://doi.org/10.1002/dvdy.24150

Smyth, J., Birrell, S., Woodman, R., & Jennings, P. (2021). Exploring the utility of EDA and skin temperature as individual physiological correlates of motion sickness. *Applied Ergonomics*, *92*, 103315. https://doi.org/10.1016/j.apergo.2020.103315

Smyth, J., Jennings, P., Bennett, P., & Birrell, S. (2021). A novel method for reducing motion sickness susceptibility through training visuospatial ability - A two-part study. *Applied Ergonomics*, *90*, 103264. https://doi.org/10.1016/j.apergo.2020. 103264

Smyth, J., Jennings, P., & Birrell, S. (2020). Are You Sitting Comfortably? How Current Self-driving Car Concepts Overlook Motion Sickness, and the Impact It Has on Comfort and Productivity. In N. Stanton (Ed.), *Advances in intelligent systems and computing. Advances in Human Factors of Transportation* (Vol. 964, pp. 387–399). Cham: Springer International Publishing. https://doi.org/10.1007/978-3-030-20503-4_36

Smyth, J., Jennings, P., Mouzakitis, A., & Birrell, S. (2018). Too Sick to Drive: How Motion Sickness Severity Impacts Human Performance. *21st International Conference on Intelligent Transportation Systems (ITSC)*, 1787–1793. https://doi.org/10.1109/ITSC.2018.8569572

Somisetty, S., & M Das, J. (2020). *StatPearls: Neuroanatomy, Vestibulo-ocular Reflex*. Treasure Island (FL).

Sony Pictures (2018). Who Wants to Be a Millionaire? (Version 23.02) [App store]. Retrieved from https://apps.apple.com/us/app/who-wants-to-be-a-millionaire/id1418794453#?platform=ipad on 6/5/2021

Soto, E., Vega, R., & Seseña, E. (2013). Neuropharmacological basis of vestibular system disorder treatment. *Journal of Vestibular Research: Equilibrium & Orientation*, *23*(3), 119–137. https://doi.org/10.3233/VES-130494

Stankovic, A. S., Alvarenga, D. L., Coleman Daniels, V. R., Simmons, R. G., Buckey, J. C., & Putcha, L. (2019). Intranasal Scopolamine for Motion Sickness. *Aerospace Medicine and Human Performance*, *90*(11), 917–924. https://doi.org/10.3357/AMHP.5456.2019

Stanley, E. (2015). The Vestibular System and Our Sense of Equilibrium (Chapter 12) [Webpage]. Retrieved from https://docplayer.net/50569289-The-vestibular-system-and-our-sense-of-equilibrium.html on 3/14/2021

Stanney, K., Fidopiastis, C., & Foster, L. (2020). Virtual Reality Is Sexist: But It Does Not Have to Be. *Frontiers in Robotics and AI*, *7*, 197. https://doi.org/10.3389/frobt.2020.00004

Stanney, K. M., Kennedy, R. S., & Drexler, J. M. (1997). Cybersickness is Not Simulator Sickness. *Proceedings of the Human Factors and Ergonomics Society Annual Meeting*, *41*(2), 1138–1142. https://doi.org/10.1177/107118139704100292

Steinhausen, W. (1931). Über den Nachweis der Bewegung der Cupula in der intakten Bogengangsampulle des Labyrinthes bei der natürlichen rotatorischen und calorischen Reizung. *Pflügers Archiv Für Die Gesamte Physiologie Des Menschen Und Der Tiere*, *228*(1), 322–328. https://doi.org/10.1007/BF01755501

Steinhausen, W. (1935). Über die durch die Otolithen ausgelösten Kräfte. *Pflügers Archiv Für Die Gesamte Physiologie Des Menschen Und Der Tiere*, *235*(1), 538–544. https://doi.org/10.1007/BF01764210

Stelling, D., Hermes, M., Huelmann, G., Mittelstädt, J., Niedermeier, D., Schudlik, K., & Duda, H. (2021). Individual differences in the temporal progression of motion sickness and anxiety: The role of passengers' trait anxiety and motion sickness history. *Ergonomics*, 1–10. https://doi.org/10.1080/00140139.2021.1886334

Stern, R. M., Hu, S., LeBlanc, R., & Koch, K. L. (1993). Chinese hyper-susceptibility to vection-induced motion sickness. *Aviation, Space, and Environmental Medicine*, *64*(9 Pt 1), 827–830.

Stern, R. M., & Koch, K. L. (1996). Motion Sickness and Differential Susceptibility. *Current Directions in Psychological Science*, *5*(4), 115–120. https://doi.org/10.1111/1467-8721.ep11452777

Stevens, S. S. (1957). On the psychophysical law. *Psychological Review*, *64*(3), 153–181. https://doi.org/10.1037/h0046162

Stevens, S. S. (1961). To Honor Fechner and Repeal His Law: A power function, not a log function, describes the operating characteristic of a sensory system. *Science (New York, N.Y.)*, *133*(3446), 80–86. https://doi.org/10.1126/science.133.3446.80

Stewart, J. (1971). Human perception of angular acceleration and implications in motion simulation. *Journal of Aircraft*, *8*(4), 248–253. https://doi.org/10.2514/3.44263

Stoffregen, T. A., Chen, F.-C., Varlet, M., Alcantara, C., & Bardy, B. G. (2013). Getting Your Sea Legs. *PloS One*, *8*(6), e66949. https://doi.org/10.1371/journal.pone.0066949

Stoffregen, T. A., & Riccio, G. E. (1988). An ecological theory of orientation and the vestibular system. *Psychological Review*, *95*(1), 3–14. https://doi.org/10.1037/0033-295X.95.1.3

Stone, W. B. (2017). *Psychometric evaluation of the Simulator Sickness Questionnaire as a measure of cybersickness* (Dissertation). Iowa State University, Iowa, United States.

Stott, J. R. (1986). Mechanisms and treatment of aviation sickness. In C. J. Davis, G. V. Lake-Rakaar, & D. G. Grahame-Smith (Eds.), *Nausea and Vomiting: Mechanisms and Treatment* (pp. 110–129). Berlin: Springer.

Strömberg, H., Bligård, L.-O., & Karlsson, M. (2019). HMI of Autonomous Vehicles - More Than Meets the Eye. In S. Bagnara, R. Tartaglia, S. Albolino, T. Alexander, & Y. Fujita (Eds.), *Advances in intelligent systems and computing. Proceedings of the 20th Congress of the International Ergonomics Association (IEA 2018)* (Vol. 823, pp. 359–368). Cham: Springer International Publishing. https://doi.org/10.1007/978-3-319-96074-6_39

Sugita, N., Yoshizawa, M., Abe, M., Tanaka, A., Watanabe, T., Chiba, S., . . . Nitta, S. (2007). Evaluation of adaptation to visually induced motion sickness based on the maximum cross-correlation between pulse transmission time and heart rate. *Journal of Neuroengineering and Rehabilitation*, *4*, 35. https://doi.org/10.1186/1743-0003-4-35

Szentagothai, J. (1950). The elementary vestibulo-ocular reflex arc. *Journal of Neurophysiology*, *13*(6), 395–407. https://doi.org/10.1152/jn.1950.13.6.395

Takeda, N., Morita, M., Hasegawa, S., Horii, A., Kubo, T., & Matsunaga, T. (1993). Neuropharmacology of motion sickness and emesis. A review. *Acta Oto-Laryngologica. Supplementum*, *501*, 10–15. https://doi.org/10.3109/0001648930912 6205

Takeda, N., Morita, M., Horii, A., Nishiike, S., Kitahara, T., & Uno, A. (2001). Neural mechanisms of motion sickness. *JMI: The Journal of Medical Investigation*, *48* (1-2), 44–59.

Takeda, N., Morita, M., Kubo, T., Yamatodani, A., Watanabe, T., Wada, H., & Matsunaga, T. (1986). Histaminergic mechanism of motion sickness. Neurochemical and neuropharmacological studies in rats. *Acta Oto-Laryngologica*, *101*(5-6), 416–421. https://doi.org/10.3109/00016488609108626

Tal, D., Domachevsky, L., Bar, R., Adir, Y., & Shupak, A. (2005). Inner ear decompression sickness and mal de debarquement. *Otology & Neurotology: Official Publication of the American Otological Society, American Neurotology Society [and] European Academy of Otology and Neurotology*, *26*(6), 1204–1207. https://doi.org/10.1097/01.mao.0000181180.39872.80

Tal, D., Hershkovitz, D., Kaminski-Graif, G., Wiener, G., Samuel, O., & Shupak, A. (2013). Vestibular evoked myogenic potentials and habituation to seasickness. *Clinical Neurophysiology: Official Journal of the International Federation of Clinical Neurophysiology*, *124*(12), 2445–2449. https://doi.org/10.1016/j.clinph. 2013.05.016

Tal, D., Shemy, S., Kaminski-Graif, G., Wiener, G., & Hershkovitz, D. (2016). Vestibular evoked myogenic potentials and motion sickness medications. *Clinical Neurophysiology: Official Journal of the International Federation of Clinical Neurophysiology*, *127*(6), 2350–2354. https://doi.org/10.1016/j.clinph.2016.03. 010

Tal, D., Wiener, G., & Shupak, A. (2014). Mal de debarquement, motion sickness and the effect of an artificial horizon. *Journal of Vestibular Research: Equilibrium & Orientation*, *24*(1), 17–23. https://doi.org/10.3233/VES-130505.

Tan, H. Z. (2000). Perceptual user interfaces: haptic interfaces. *Communications of the ACM*, *43*(3), 40–41. https://doi.org/10.1145/330534.330537

Taylor, N. B. G., Hunter, J., & Johnson, W. H. (1957). Antidiuresis as a measurmeent of laboratory induced motion sickness. *Canadian Journal of Biochemistry and Physiology*, *35*(11), 1017–1027. https://doi.org/10.1139/o57-117

Taylor, R. R., Jagger, D. J., Saeed, S. R., Axon, P., Donnelly, N., Tysome, J., . . . Forge, A. (2015). Characterizing human vestibular sensory epithelia for experimental studies: New hair bundles on old tissue and implications for therapeutic interventions in ageing. *Neurobiology of Aging*, *36*(6), 2068–2084. https://doi.org/10.1016/j.neurobiolaging.2015.02.013

Teitelbaum, P. (2002). Mal de debarquement syndrome: A case report. *Journal of Travel Medicine*, *9*(1), 51–52. https://doi.org/10.2310/7060.2002.23951

Thomaier, M. (2008). *Optimierung der NVH-Eigenschaften von Pkw-Fahrwerkstrukturen mittels Active-Vibration-Control* (Dissertation). Technical University of Darmstadt, Darmstadt, Germany.

Thornton, W., & Bonato, F. (2017). *The Human Body and Weightlessness: Operational Effects, Problems and Countermeasures*. Cham: Springer International Publishing. https://doi.org/10.1007/978-3-319-32829-4

Timpe, K.-P., Jürgensohn, T., & Kolrep, H. (2000). *Mensch-Maschine-Systemtechnik: Konzepte, Modellierung, Gestaltung, Evaluation* (1st ed.). Düsseldorf: Symposion Publishing.

Todosiev, E. P. (1963). *The action-point model of the driver-vehicle system* (Dissertation). Ohio State University, Ohio, United States.

Treisman, M. (1977). Motion sickness: An evolutionary hypothesis. *Science (New York, N.Y.)*, *197*(4302), 493–495. https://doi.org/10.1126/science.301659

Trincker, D. (1962). The transformation of mechanical stimulus into nervous excitation by the labyrinthine receptors. *Symposia of the Society for Experimental Biology*. (16), 289–316.

Turner, M., & Griffin, M. J. (1999a). Motion sickness in public road transport: Passenger behavior and susceptibility. *Ergonomics*, *42*(3), 444–461. https://doi.org/10.1080/001401399185586

Turner, M., & Griffin, M. J. (1999b). Motion sickness in public road transport: The effect of driver, route and vehicle. *Ergonomics*, *42*(12), 1646–1664. https://doi.org/10.1080/001401399184730

Turner, M., Griffin, M. J., & Holland, I. (2000). Airsickness and aircraft motion during short-haul flights. *Aviation, Space, and Environmental Medicine*, *71*(12), 1181–1189.

Tuthill, J. C., & Azim, E. (2018). Proprioception. *Current Biology*, *28*(5), R194-R203. https://doi.org/10.1016/j.cub.2018.01.064

Tyler, D. B., & Bard, P. (1949). Motion sickness. *Physiological Reviews*, *29*(4), 311–369. https://doi.org/10.1152/physrev.1949.29.4.311

Udal, A., & Kukk, V. (2012). An Engineering Approach to Time-Frequency Uncertainty Criteria. *Electronics and Electrical Engineering*, *117*(1). https://doi.org/10.5755/j01.eee.117.1.1043

Ueno, M., Ogawa, T., Nakagiri, S., Arisawa, T., Mino, Y., Oyama, K., . . . Ohta, T. (1986). Studies on motion sickness caused by high curve speed railway vehicles. Evaluation of the swing and its effects on passengers and conductors. *Sangyo Igaku. Japanese Journal of Industrial Health*, *28*(4), 266–274. https://doi.org/10.1539/joh1959.28.266

Uijtdehaage, S. H., Stern, R. M., & Koch, K. L. (1992). Effects of eating on vection-induced motion sickness, cardiac vagal tone, and gastric myoelectric activity. *Psychophysiology*, *29*(2), 193–201. https://doi.org/10.1111/j.1469-8986.1992.tb01685.x

Un-Noor, F., Padmanaban, S., Mihet-Popa, L., Mollah, M., & Hossain, E. (2017). A Comprehensive Study of Key Electric Vehicle (EV) Components, Technologies, Challenges, Impacts, and Future Direction of Development. *Energies*, *10*(8), 1217. https://doi.org/10.3390/en10081217

Urciuoli, A., Zanolli, C., Beaudet, A., Dumoncel, J., Santos, F., Moyà-Solà, S., & Alba, D. M. (2020). The evolution of the vestibular apparatus in apes and humans. *ELife*, *9.* https://doi.org/10.7554/elife.51261

Van Buskirk, W. C., Watts, R. G., & Liu, Y. K. (1976). The fluid mechanics of the semicircular canals. *Journal of Fluid Mechanics*, *78*(1), 87–98. https://doi.org/10.1017/S0022112076002346

Van Ombergen, A., van Rompaey, V., Maes, L. K., van de Heyning, P. H., & Wuyts, F. L. (2016). Mal de debarquement syndrome: A systematic review. *Journal of Neurology*, *263*(5), 843–854. https://doi.org/10.1007/s00415-015-7962-6

Van Someren, E. J. (2011). Age-Related Changes in Thermoreception and Thermoregulation. In *Handbook of the Biology of Aging* (pp. 463–478). Elsevier. https://doi.org/10.1016/B978-0-12-378638-8.00022-1

Vastola, M. (2016) US 9,392,970 B2. Biotelemetry system. United States Patent and Trademark Office.

VDI 2057-1:2017-08. *Human exposure to mechanical vibrations - Whole-body vibration*. (VDI 2057:1987).

Ventre-Dominey, J., Luyat, M., Denise, P., & Darlot, C. (2008). Motion sickness induced by otolith stimulation is correlated with otolith-induced eye movements. *Neuroscience*, *155*(3), 771–779. https://doi.org/10.1016/j.neuroscience.2008.05.057

Villard, S. J., Flanagan, M. B., Albanese, G. M., & Stoffregen, T. A. (2008). Postural instability and motion sickness in a virtual moving room. *Human Factors*, *50*(2), 332–345. https://doi.org/10.1518/001872008X250728

Vincent, M., & Hadjikhani, N. (2007). The cerebellum and migraine. *Headache*, *47*(6), 820–833. https://doi.org/10.1111/j.1526-4610.2006.00715.x

Vogel, H., Kohlhaas, R., & Baumgarten, R. J. von (1982). Dependence of motion sickness in automobiles on the direction of linear acceleration. *European Journal of Applied Physiology and Occupational Physiology*, *48*(3), 399–405. https://doi.org/10.1007/BF00430230

Vollrath, M. A., Kwan, K. Y., & Corey, D. P. (2007). The micromachinery of mechanotransduction in hair cells. *Annual Review of Neuroscience*, *30*, 339–365. https://doi.org/10.1146/annurev.neuro.29.051605.112917

Wada, T. (2016). Motion sickness in automated vehicles. In J. Edelmann, M. Plöchl, & P. E. Pfeffer (Eds.), *Advanced Vehicle Control AVEC'16* (Vol. 71, pp. 169–176). Leiden, The Netherlands: CRC Press. https://doi.org/10.1201/9781315265285

Wada, T., Fujisawa, S., & Doi, S. (2018). Analysis of driver's head tilt using a mathematical model of motion sickness. *International Journal of Industrial Ergonomics*, *63*, 89–97. https://doi.org/10.1016/j.ergon.2016.11.003

Wada, T., Konno, H., Fujisawa, S., & Doi, S. (2012). Can passengers' active head tilt decrease the severity of carsickness? Effect of head tilt on severity of motion sickness in a lateral acceleration environment. *Human Factors*, *54*(2), 226–234. https://doi.org/10.1177/0018720812436584

Wada, T., & Yoshida, K. (2016). Effect of passengers' active head tilt and opening/closure of eyes on motion sickness in lateral acceleration environment of cars. *Ergonomics*, *59*(8), 1050–1059. https://doi.org/10.1080/00140139.2015.1109713

Waele, C. de, Mühlethaler, M., & Vidal, P. P. (1995). Neurochemistry of the central vestibular pathways. *Brain Research Reviews*, *20*(1), 24–46. https://doi.org/10.1016/0165-0173(94)00004-9

Walberg, F. (1972). Cerebellovestibular Relations: Anatomy. In A. Brodal & O. Pompeiano (Eds.), *Progress in Brain Research. Basic aspects of central vestibular mechanisms* (Vol. 37, pp. 361–376). Amsterdam, New York: Elsevier. https://doi.org/10.1016/S0079-6123(08)63913-8

Waldfahrer, F. (2008). Medikamentöse Prophylaxe von Kinetosen. In H. Scherer (Ed.), *Der Gleichgewichtssinn: Neues aus Forschung und Klinik 6. Hennig Symposium* (Vol. 178, pp. 135–147). Vienna: Springer. https://doi.org/10.1007/978-3-211-75432-0_16

Walter, H. J., Li, R., Munafo, J., Curry, C., Peterson, N., & Stoffregen, T. A. (2019). Unstable coupling of body sway with imposed motion precedes visually induced motion sickness. *Human Movement Science*, *64*, 389–397. https://doi.org/10.1016/j.humov.2019.03.006

Wan, G., Corfas, G., & Stone, J. S. (2013). Inner ear supporting cells: Rethinking the silent majority. *Seminars in Cell & Developmental Biology*, *24*(5), 448–459. https://doi.org/10.1016/j.semcdb.2013.03.009

Wan, S., & Browning, K. N. (2008). Glucose increases synaptic transmission from vagal afferent central nerve terminals via modulation of 5-HT3 receptors. *American Journal of Physiology. Gastrointestinal and Liver Physiology*, *295*(5), 1050-1057. https://doi.org/10.1152/ajpgi.90288.2008

Warren, W. H., Kay, B. A., Zosh, W. D., Duchon, A. P., & Sahuc, S. (2001). Optic flow is used to control human walking. *Nature Neuroscience*, *4*(2), 213–216. https://doi.org/10.1038/84054

Waxenbaum, J. A., Reddy, V., & Bordoni, B. (2021). *Anatomy, Head and Neck, Cervical Nerves*. Treasure Island, Florida.

Weech, S., Wall, T., & Barnett-Cowan, M. (2020). Reduction of cybersickness during and immediately following noisy galvanic vestibular stimulation. *Experimental Brain Research*, *238*(2), 427–437. https://doi.org/10.1007/s00221-019-05718-5

Wersäll, J., & Bagger-Sjöbäck, D. (1974). Morphology of the Vestibular Sense Organ. In D. Bagger-Sjöbäck, A. Brodal, B. Cohen, G. F. Dohlman, J. M. Fredrickson, R. R. Gacek, . . . J. Wersäll (Eds.), *Handbook of Sensory Physiology. Vestibular System Part 1: Basic Mechanisms* (6 / 1, pp. 123–170). Berlin, Heidelberg: Springer. https://doi.org/10.1007/978-3-642-65942-3_4

Whinnery, J. E., & Parnell, M. J. (1987). The effects of long-term aerobic conditioning on +Gz tolerance. *Aviation, Space, and Environmental Medicine*, *58*(3), 199–204.

Wickham, H. (2007). Reshaping Data with the reshape Package. *Journal of Statistical Software*, *21*(12), 1–20. https://doi.org/10.18637/jss.v021.i12

Wickham, H. (2016). *ggplot2: Elegrant graphics for data analysis* (2nd edition). *Use R!* New York: Springer.

Wickham, H., François, R., Henry, L., & Müller, K. (2021). dplyr: A Grammar of Data Manipulation (R package version 1.0.6). Retrieved from https://cran.r-project.org/package=dplyr on 5/29/2021

William, J. (1881). Sense of Diziness in deaf-muts. *Mind*, *os-VI*(23), 412–413. https://doi.org/10.1093/mind/os-VI.23.412

Williamson, M. J., Thomas, M. J., & Stern, R. M. (2004). The contribution of expectations to motion sickness symptoms and gastric activity. *Journal of Psychosomatic Research*, *56*(6), 721–726. https://doi.org/10.1016/S0022-3999(03)00130-2

Wilson, V. J., & Melvill Jones, G. (1979). *Mammalian vestibular physiology*. New York: Plenum Press.

Wilson, W. D. (1997). Travel sickness in cattle. *The Veterinary Record*, *140*(3), 76.

Winkel, K. N. de, Pretto, P., Nooij, S. A. E., Cohen, I., & Bülthoff, H. H. (2021). Efficacy of augmented visual environments for reducing sickness in autonomous vehicles. *Applied Ergonomics*, *90*, 103282. https://doi.org/10.1016/j.apergo.2020.103282

Winter, J. C. F. de, & Hancock, P. A. (2021). Why human factors science is demonstrably necessary: Historical and evolutionary foundations. *Ergonomics*, 1–17. https://doi.org/10.1080/00140139.2021.1905882

Wolf, H. J. (2009). *Ergonomische Untersuchung des Lenkgefühls an Personenkraftwagen* (Dissertation). Technical University of Munich - TUM, Munich, Germany.

Wolfe, J. W. (1968). Evidence for control of nystagmic habituation by folium-tuber vermis and fastigial nuclei. *Acta Oto-Laryngologica*, Suppl 231:1-48.

Wood, C. D. (1966). Clinical Effectiveness of Anti-motion-Sickness Drugs. *JAMA*, *198*(11), 1155. https://doi.org/10.1001/jama.1966.03110240063024

Woopen, T., Eckstein, L., Kowalewski, S., Moormann, D., Maurer, M., Ernst, R., . . . Hecker, C. (2018). Unicaragil - Disruptive modulare Architektur für agile, automatisierte Fahrzeugkonzepte. In L. Eckstein & S. Pischinger (Eds.), *27th Aachen Colloquium Automobile and Engine Technology* (pp. 663–694). https://doi.org/10. 18154/RWTH-2018-229909

Wotring, V. E. (2012). Gastrointestinal System. In V. E. Wotring (Ed.), *SpringerBriefs in Space Development. Space Pharmacology* (pp. 51–64). Boston, Massachusetts: Springer US. https://doi.org/10.1007/978-1-4614-3396-5_7

Yagi, T., Simpson, N. E., & Markham, C. H. (1977). The relationship of conduction velocity to other physiological properties of the cat's horizontal canal neurons. *Experimental Brain Research*, *30*(4), 587–600. https://doi.org/10.1007/BF00237647

Yang, S., Schlieski, T., Selmins, B., Cooper, S. C., Doherty, R. A., Corriveau, P. J., & Sheedy, J. E. (2012). Stereoscopic viewing and reported perceived immersion and symptoms. *Optometry and Vision Science: Official Publication of the American Academy of Optometry*, *89*(7), 1068–1080. https://doi.org/10.1097/OPX.0b013 e31825da430.

Yang, Y., Fleischer, M., & Bengler, K. (2020). Chicken or Egg Problem? New Challenges and Proposals of Digital Human Modeling and Interior Development of Automated Vehicles. In M. Di Nicolantonio, E. Rossi, & T. Alexander (Eds.), *Advances in intelligent systems and computing. Advances in Additive Manufacturing, Modeling Systems and 3D Prototyping* (Vol. 975, pp. 453–463). Cham: Springer International Publishing. https://doi.org/10.1007/978-3-030-20216-3_42

Yang, Y., Klinkner, J. N., & Bengler, K. (2019). How Will the Driver Sit in an Automated Vehicle? – The Qualitative and Quantitative Descriptions of Non-Driving Postures (NDPs) When Non-Driving-Related-Tasks (NDRTs). In S. Bagnara, R. Tartaglia, S. Albolino, T. Alexander, & Y. Fujita (Eds.), *Proceedings of the 20th Congress of the International Ergonomics Association (IEA 2018)* (pp. 409–420). Cham: Springer International Publishing.

Yates, B. J., Grélot, L., Kerman, I. A., Balaban, C. D., Jakus, J., & Miller, A. D. (1994). Organization of vestibular inputs to nucleus tractus solitarius and adjacent structures in cat brain stem. *The American Journal of Physiology*, *267*(4 Pt 2), R974-83. https://doi.org/10.1152/ajpregu.1994.267.4.R974

Yates, B., Miller, A., & Lucot, J. (1998). Physiological basis and pharmacology of motion sickness: an update. *Brain Research Bulletin*, *47*(5), 395–406. https://doi.org/10.1016/s0361-9230(98)00092-6

Young, L. R., & Meiry, J. L. (1968). A revised dynamic otolith model. *Aerospace Medicine*, *39*(6), 606–608.

Yu, Y.-H., Lai, P.-C., Ko, L.-W., Chuang, C.-H., Kuo, B.-C., & Lin, C.-T. (2010). An EEG-based classification system of Passenger's motion sickness level by using feature extraction/selection technologies. In *The 2010 International Joint Conference on Neural Networks (IJCNN)* (pp. 1–6). IEEE. https://doi.org/10.1109/ IJCNN.2010.5596739

Yusof, N. M. (2019). *Comfort in autonomous car: mitigating motion sickness by enhancing situation awareness through haptic displays* (Dissertation). Eindhoven University of Technology, Eindhoven, The Netherlands.

Yusof, N. M., Karjanto, J., Terken, J. M. B., Delbressine, F. L. M., & Rauterberg, G. W. M. (2020). Gaining Situation Awareness through a Vibrotactile Display to Mitigate Motion Sickness in Fully-Automated Driving Cars. *IJAME: International Journal of Automotive and Mechanical Engineering*, *17*(1), 7771–7783.

Zaidi, M., Khan, A., Sharma, A., Ataebiekov, I., Hadelia, E., Korkmaz, F., . . . Lizneva, D. (2020). Regulation of Bone Mass and Body Composition by Anterior Pituitary Hormones. In *Encyclopedia of Bone Biology* (pp. 503–518). Elsevier. https://doi.org/10.1016/B978-0-12-801238-3.62238-9

Zimatkin, S. M., & Anichtchik, O. V. (1999). Alcohol-histamine interactions. *Alcohol and Alcoholism*, *34*(2), 141–147. https://doi.org/10.1093/alcalc/34.2.141

Zink, M. D., Brüser, C., Winnersbach, P., Napp, A., Leonhardt, S., Marx, N., . . . Mischke, K. (2015). Heartbeat Cycle Length Detection by a Ballistocardiographic Sensor in Atrial Fibrillation and Sinus Rhythm. *BioMed Research International*, 840356. https://doi.org/10.1155/2015/840356

Zuniga, M. G., Dinkes, R. E., Davalos-Bichara, M., Carey, J. P., Schubert, M. C., King, W. M., . . . Agrawal, Y. (2012). Association between hearing loss and saccular dysfunction in older individuals. *Otology & Neurotology: Official Publication of the American Otological Society, American Neurotology Society [and] European Academy of Otology and Neurotology*, *33*(9), 1586–1592. https://doi.org/10.1097/MAO.0b013e31826bedbc

Zwerling, I. (1947). Psychological factors in susceptibility to motion sickness. *The Journal of Psychology*, *23*(2), 219–239. https://doi.org/10.1080/00223980.1947.9917332

17 Appendix

A. Applied R Packages for Data Processing and Statistical Analyses

- R statistical functions "stats" by R Core Team (2018)
- Computing sample size and power just as data processing "Hmisc" by Harrell (2021)
- Tool for biostatistics, public policiy, and law "lawstat" by Gastwirth et al. (2020)
- Calculate moments, kurtosis, and skewness "moments" by Komsta (2015)
- Simult. inference in general parametric models "multcomp" by Harthorn et al. (2021)
- Formatting regressions and summarize statistcs "stargazer" by Hlavac (2018)
- Companion to applied regression "car" by Fox et al. (2020)
- Computes polychoric and polyserial correlations "polycor" by Fox (2019)
- Linear and non-linear mixed effects models "nlme" by Pinheiro et al. (2018)
- Linear mixed effects models using "lme4" by Bates et al. (2015)
- Diagnostics in checking linear regression models "lmtest" by Harthorn et al. (2020)
- Marginalization, conditioning, fitting by max. Likl. "ggm" by Marchetti et al. (2020)
- Diagnose and inference from linear models "predictmeans" by Luo et al. (2020)
- Data screening and estimating power "QuantPsyc" by Fletcher (2012)
- Visualization package "ggplot2" by Wickham (2016)
- Colour schemes for maps and other graphics "RColorBrewer" by Neuwirth (2014)
- Easy analysis and visualization of factorial experiments "ez" by Lawrence (2016)
- Convert data between long and wide format with "reshape2" by Wickham (2007)
- A grammar of data manipulation "dplyr" by Wickham et al. (2021)
- Analysis of space-time ecological series "pastecs" by Grosjean et al. (2018)
- Numerous methods for and operations on matrices "Matrix" by Bates et al. (2021)
- Psychological, psychometric, and personality research "psych" by Revelle (2021)

B. Pharmacological Drug Ingestion to Alleviate Motion Sickness

Based on Benson (2002, p. 1075)

Drug	Route	Adult Dose	Time of onset	Duration of Action [h]
Scopolamine	Oral	0.3-0.6 mg	30 min	4
Scopolamine	Injection	0.1-0.2 mg	15 min	4
Scopolamine	Patch	One	6-8 h	72
Promethazine	Oral	25-50 mg	2 h	15
Promethazine	Injection	25 mg	15 min	15
Promethazine	Suppository	25 mg	1 h	15
Dimenhydrinate	Oral	50-100 mg	2 h	8
Dimenhydrinate	Injection	50 mg	15 min	8
Cylizine	Oral	50 mg	2 h	6
Cylizine	Injection	50 mg	15 min	6
Meclizine	Oral	25-50 mg	2 h	8
Buclizine	Oral	50 mg	1 h	6
Cinnarizine	Oral	15-30 mg	4 h	8

C. Physiological Measures

| Responses to motion sickness	State	Reference (selection)
CARDIOVASCULAR		
Changes in blood pressure and pulse rate		
Tone of arterial portion of capillaries in the nail bed	Increase	(Money, 1970; Reason & Brand, 1975) as adapted and cited in (Nicogossian & Parker, 1982, p. 143); (Dobie, 2019, p. 16)
Diameter of retinal vessels	Decrease	(Money, 1970; Reason & Brand, 1975) as adapted and cited in (Nicogossian & Parker, 1982, p. 143); (Dobie, 2019, p. 16)
Peripheral circulation, especially in the scalp	Decrease	(Money, 1970; Reason & Brand, 1975) as adapted and cited in (Nicogossian & Parker, 1982, p. 143); (Dobie, 2019, p. 16)
Muscle blood flow	Increase	(Money, 1970; Reason & Brand, 1975) as adapted and cited in (Nicogossian & Parker, 1982, p. 143); (Dobie, 2019, p. 16)
RESPIRATION		
Alterations in respiratory rate	Increase	(Money, 1970; Reason & Brand, 1975) as adapted and cited in (Nicogossian & Parker, 1982, p. 143); (Dobie, 2019, p. 16)
Sighing or yawning	Increase	(Money, 1970; Reason & Brand, 1975) as adapted and cited in (Nicogossian & Parker, 1982, p. 143); (Dobie, 2019, p. 16)
GASTROINTESTINAL		
Gastric intestinal tone and secretion	Inhibition	(Money, 1970; Reason & Brand, 1975) as adapted and cited in (Nicogossian & Parker, 1982, p. 143); (Dobie, 2019, p. 16)
Salivation, Bleching	Increase	(Money, 1970; Reason & Brand, 1975) as adapted and cited in (Nicogossian & Parker, 1982, p. 143); (Dobie, 2019, p. 16)
Epigastric discomfort or awareness	Increase	(Money, 1970; Reason & Brand, 1975) as adapted and cited in (Nicogossian & Parker, 1982, p. 143); (Dobie, 2019, p. 16)
BODY FLUIDS		
Blood		
Hemoglobin concentration	Increase	(Money, 1970; Reason & Brand, 1975) as adapted and cited in (Nicogossian & Parker, 1982, p. 143); (Dobie, 2019, p. 16)
Lactic dehydrogenase concentration (LDH)	Change	(Money, 1970; Reason & Brand, 1975) as adapted and cited in (Nicogossian & Parker, 1982, p. 143); (Dobie, 2019, p. 16)
$PaCO_2$ levels in arterial blood (hyperventilation)	Decrease	(Money, 1970; Reason & Brand, 1975) as adapted and cited in (Nicogossian & Parker, 1982, p. 143); (Dobie, 2019, p. 16)
pH concentration	Increase	(Money, 1970; Reason & Brand, 1975) as adapted and cited in (Nicogossian & Parker, 1982, p. 143); (Dobie, 2019, p. 16)
Concentration of eosinophils	Decrease	(Money, 1970; Reason & Brand, 1975) as adapted and cited in (Nicogossian & Parker, 1982, p. 143); (Dobie, 2019, p. 16)
Plasma proteins	Increase	(Money, 1970; Reason & Brand, 1975) as adapted and cited in (Nicogossian & Parker, 1982, p. 143); (Dobie, 2019, p. 16)
Urine		
17-hydroxycorticosteroids	Increase	(Money, 1970; Reason & Brand, 1975) as adapted and cited in (Nicogossian & Parker, 1982, p. 143); (Dobie, 2019, p. 16)
Catecholamines	Increase	(Money, 1970; Reason & Brand, 1975) as adapted and cited in (Nicogossian & Parker, 1982, p. 143); (Dobie, 2019, p. 16)
Antidiuretic hormone (ADH)	Increase	(Eversmann et al., 1978)
Growth hormone (hGH)	Increase	(Eversmann et al., 1978)
Prolactin (hPRL)	Increase	(Eversmann et al., 1978)
Cortisol	Increase	(Eversmann et al., 1978)

The table continues on the next page.

THERMOREGULATION		
Extremities	Decrease	(Money, 1970; Reason & Brand, 1975) as adapted and cited in (Nicogossian & Parker, 1982, p. 143); (Dobie, 2019, p. 16)
Thermogenesis	Decrease	(Nalivaiko et al., 2014)
Electrodermal activity – tonic skin conductance	Increase	(Golding, 1992)
PERCEPTION SYSTEM		
Visual system		
Dilated pupils during emesis	Increase	(Money, 1970; Reason & Brand, 1975) as adapted and cited in (Nicogossian & Parker, 1982, p. 143); (Dobie, 2019, p. 16)
Size of pupils	Decrease	(Money, 1970; Reason & Brand, 1975) as adapted and cited in (Nicogossian & Parker, 1982, p. 143); (Dobie, 2019, p. 16)
Ocular balance	Decrease	(Money, 1970; Reason & Brand, 1975) as adapted and cited in (Nicogossian & Parker, 1982, p. 143); (Dobie, 2019, p. 16)
Proprioceptive system		
Postural sway	Increase	(Laboissière et al., 2015; Walter et al., 2019)
Occipital, parietal, and somatosensory brain area		
Power of alpha (8-13 Hz) and theta band (4-7 Hz)	Increase	(R. Liu et al., 2020; Yu et al., 2010)
Olfactoric		
Sensitivity to odors	Increase	(Paillard et al., 2014)

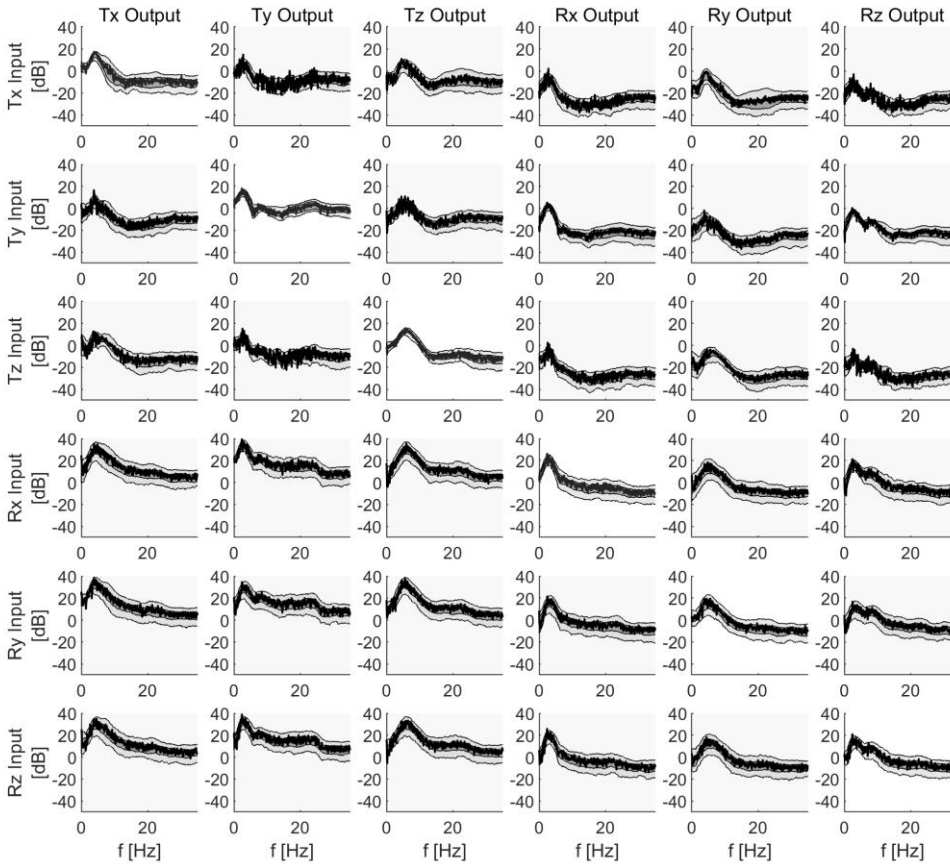## D. Transfer Function – 6 DoF and Uniaxial Excitation

Transfer function 75% and 95% percentile - Sitting Position 25% Excitation (6 DoF)
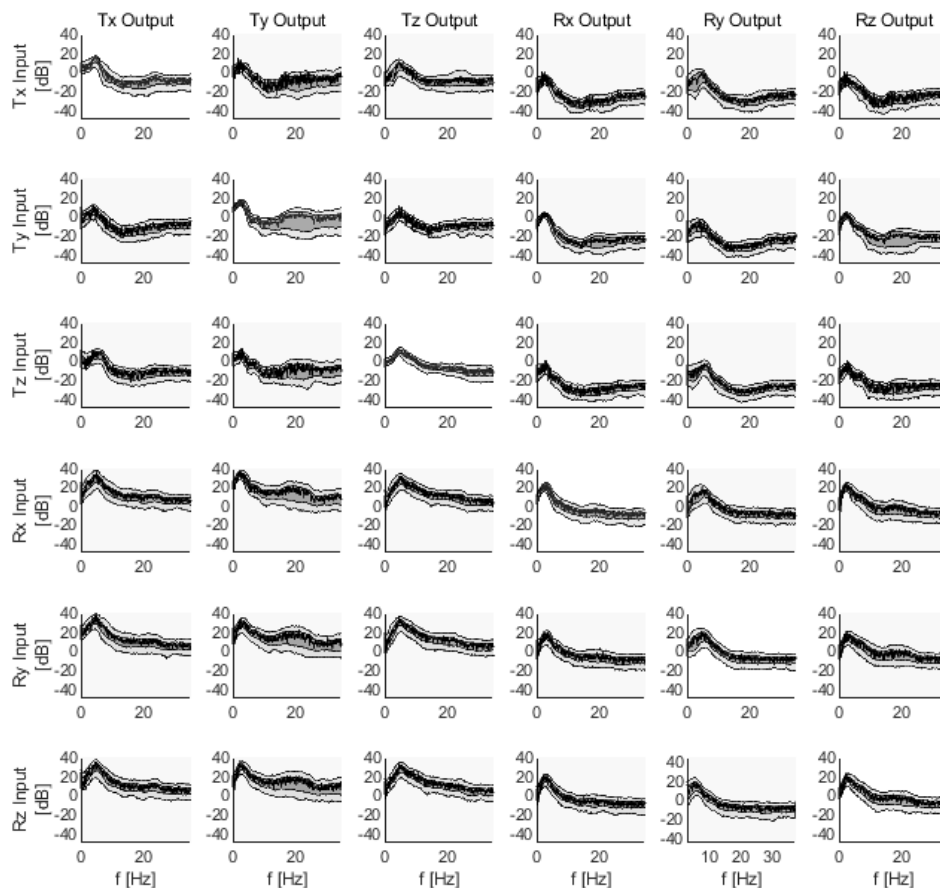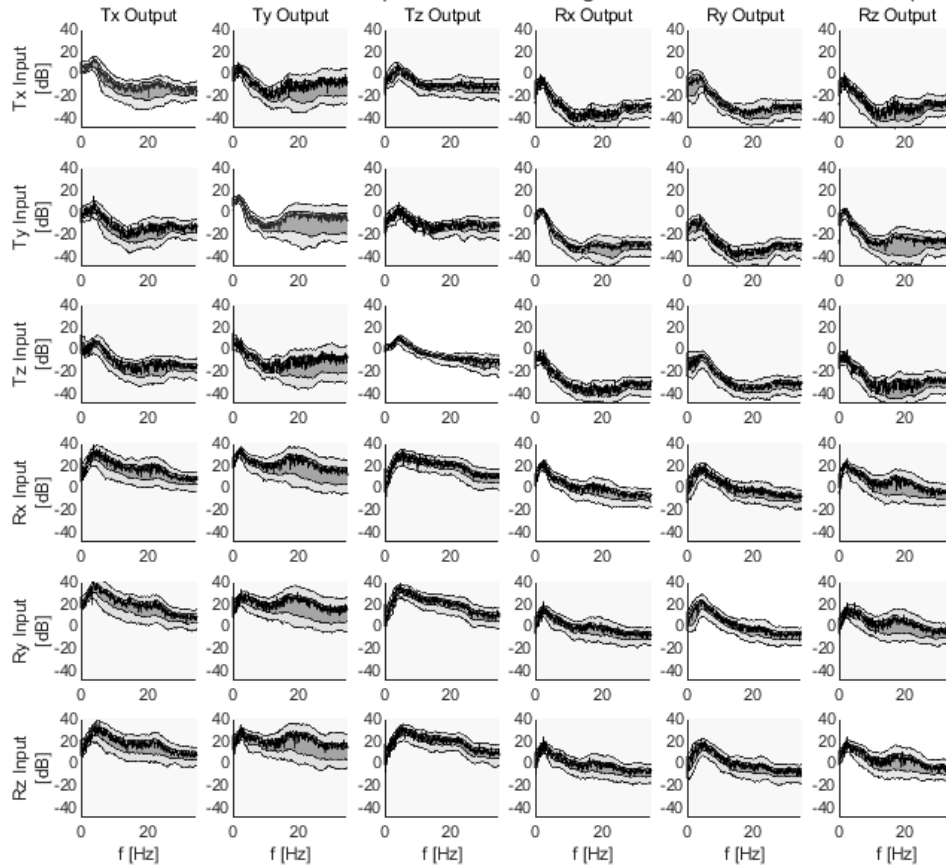
Transfer function 75% and 95% percentile - Reclined Position 25% Excitation (6 DoF)
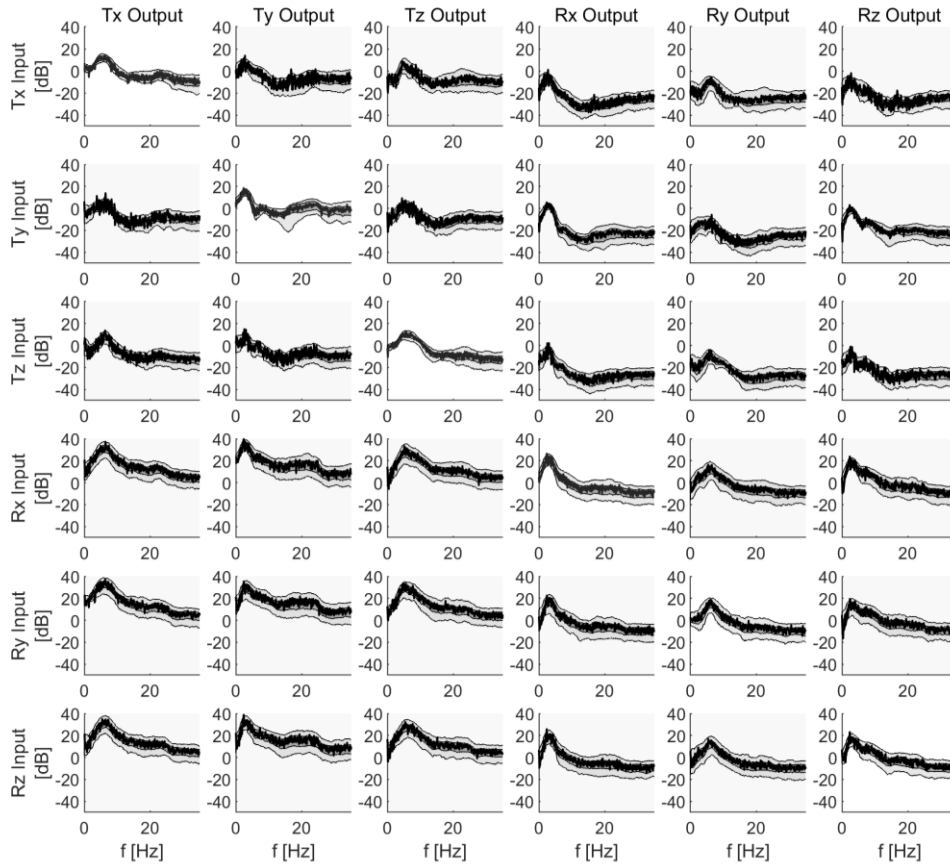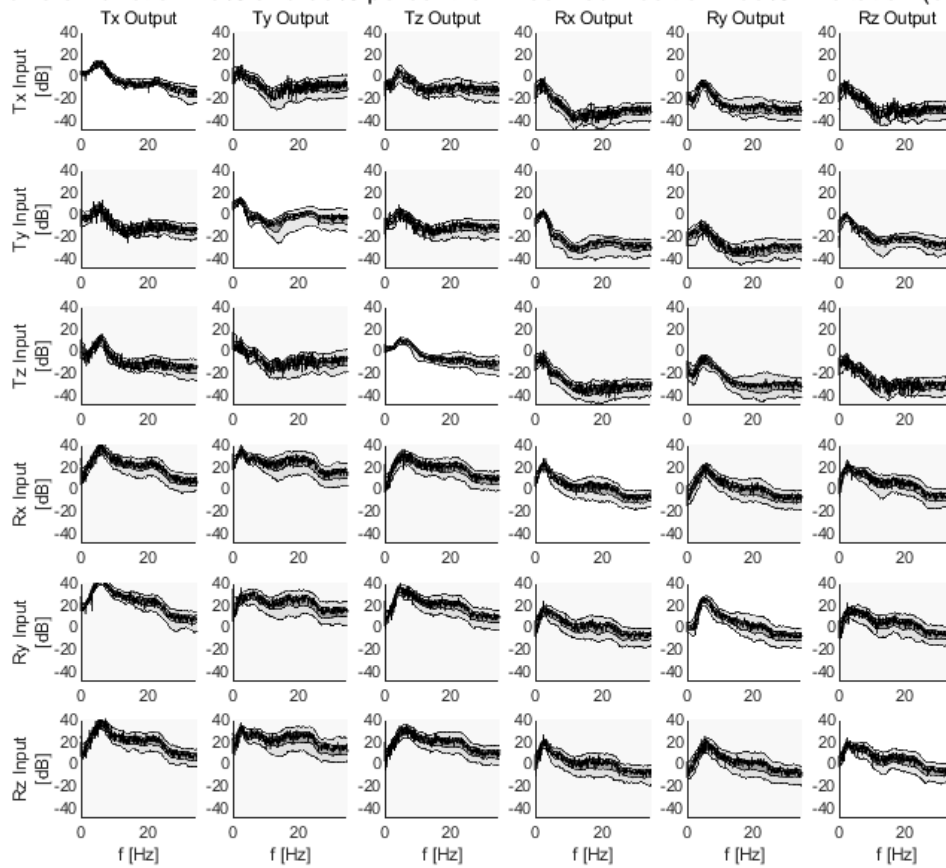

Transfer function 75% and 95% percentile - Lying Position 25% Excitation (6 DoF)
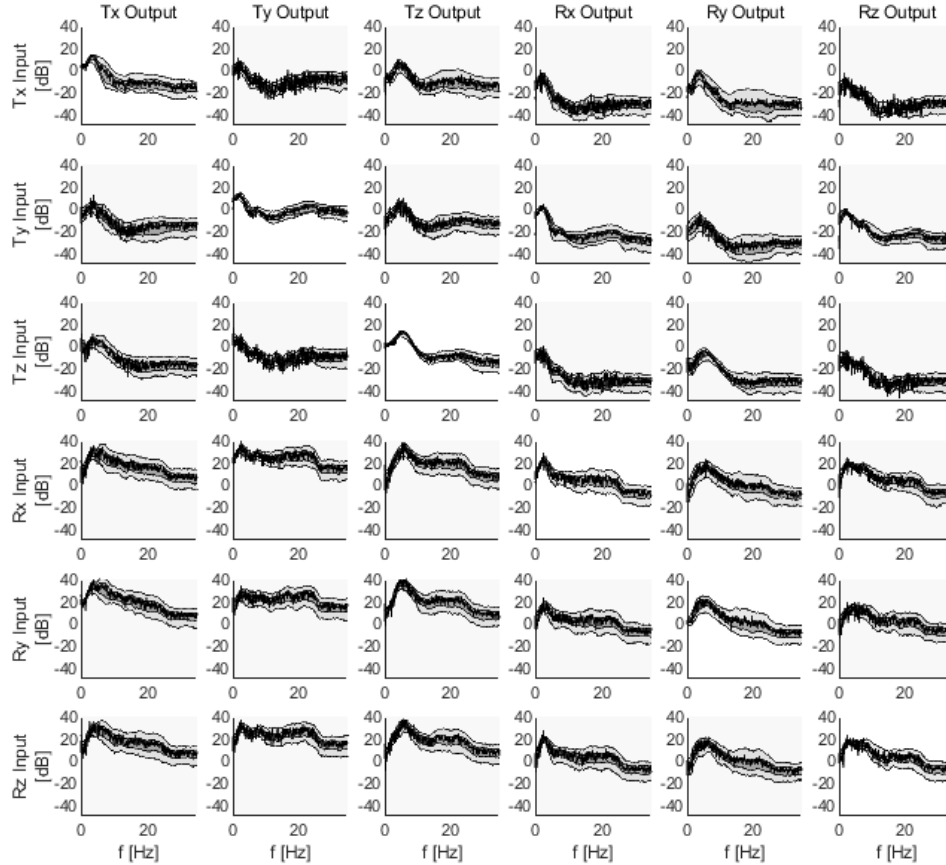
Transfer function 75% and 95% percentile - Sitting Position 100% Excitation (6 DoF)

Transfer function 75% and 95% percentile - Reclined Position 100% Excitation (6 DoF)

Transfer function 75% and 95% percentile - Lying Position 100% Excitation (6 DoF)

Transfer function 75% and 95% percentile - Sitting Position 200% Excitation (6 DoF)
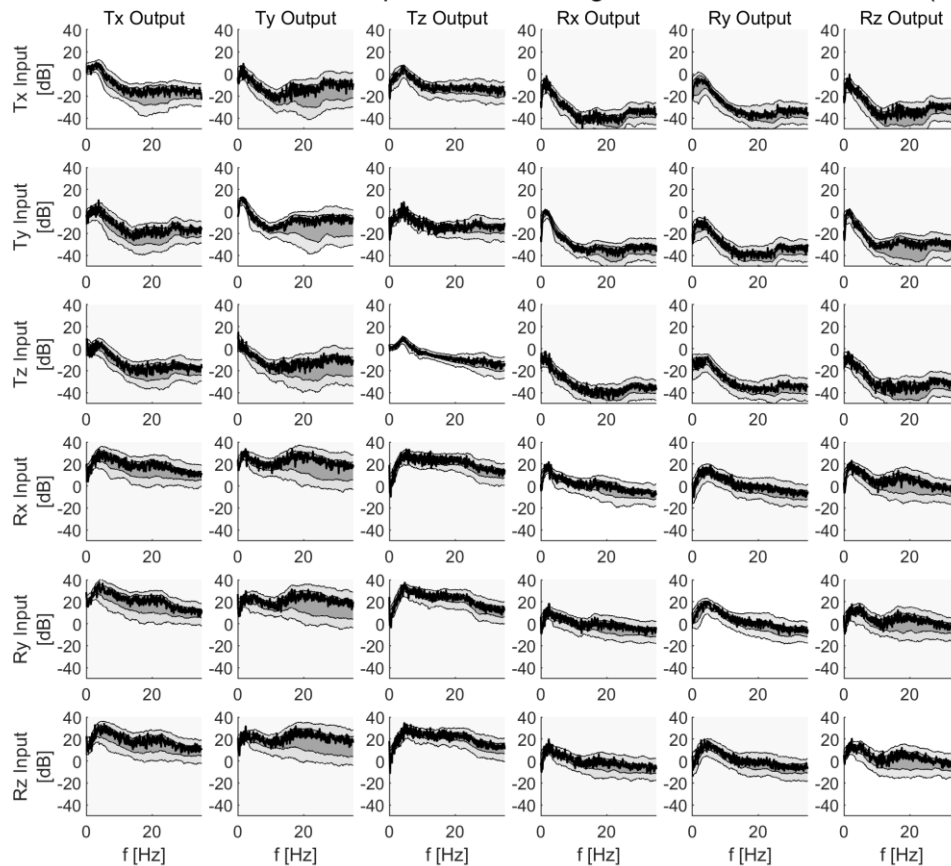
238

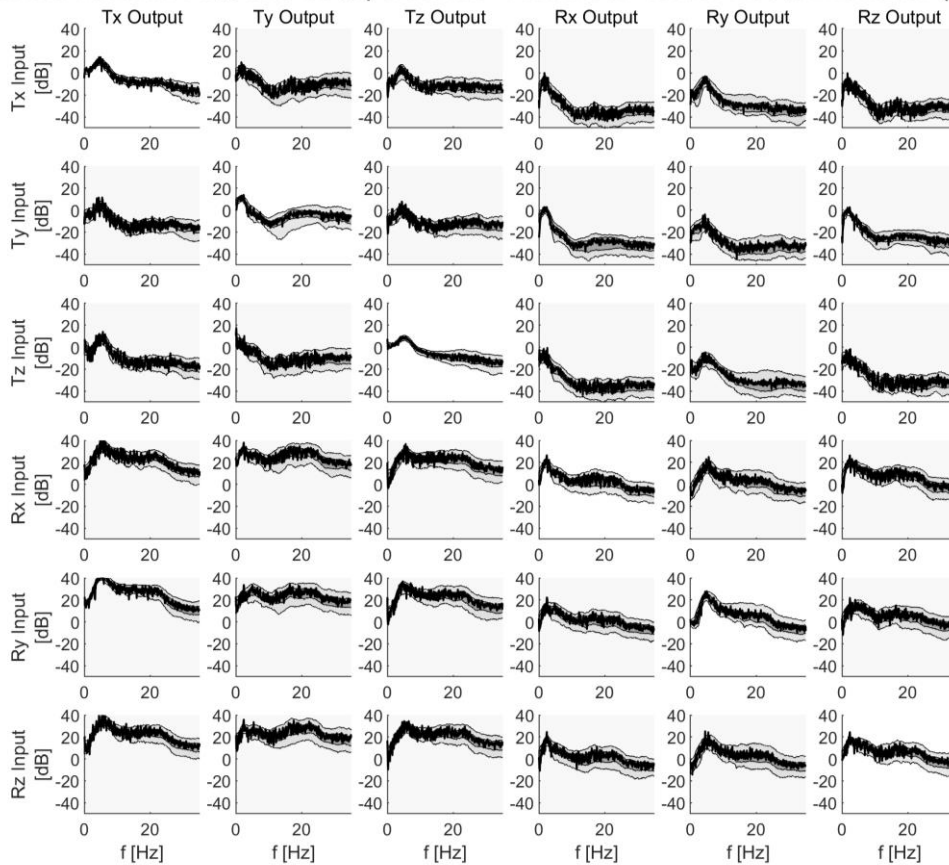Transfer function 75% and 95% percentile - Reclined Position 200% Excitation (6 DoF)

Transfer function 75% and 95% percentile - Lying Position 200% Excitation (6 DoF)
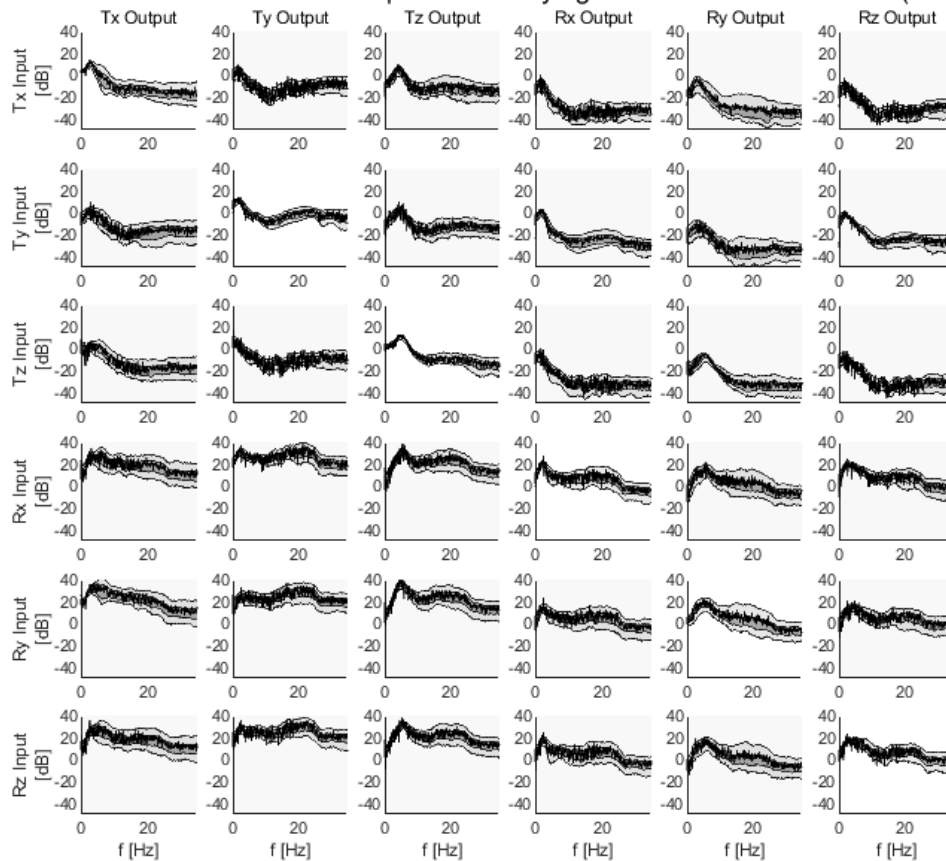
Transfer function 75% and 95% percentile - Sitting Position 25% Excitation (uniaxial)

Transfer function 75% and 95% percentile - Reclined Position 25% Excitation (uniaxial)

Transfer function 75% and 95% percentile - Lying Position 25% Excitation (uniaxial)

Transfer function 75% and 95% percentile - Sitting Position 100% Excitation (uniaxial)
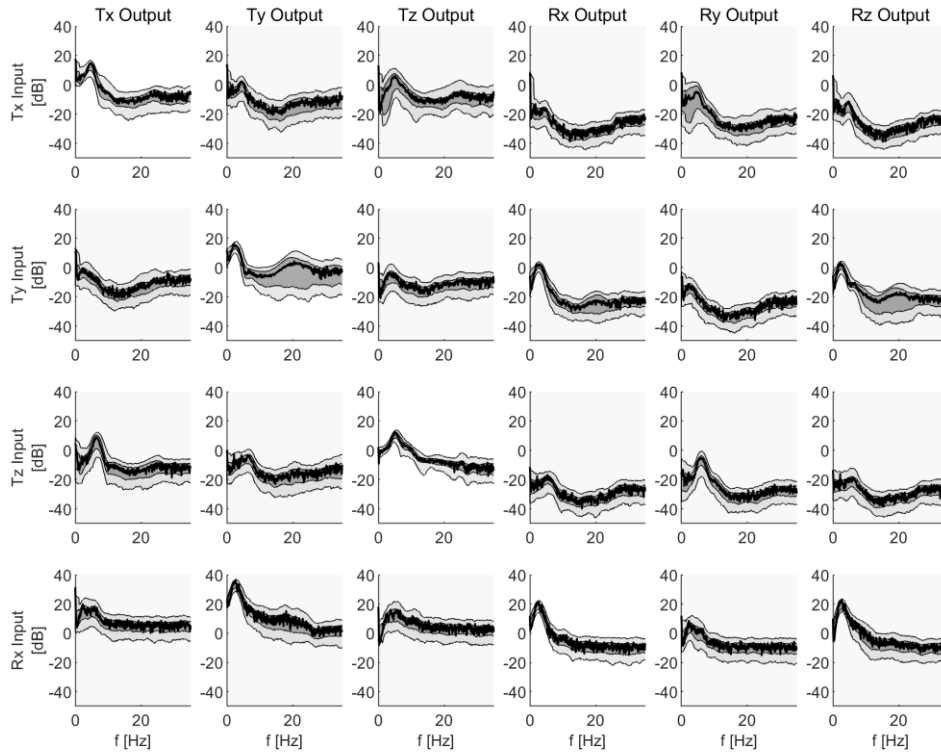
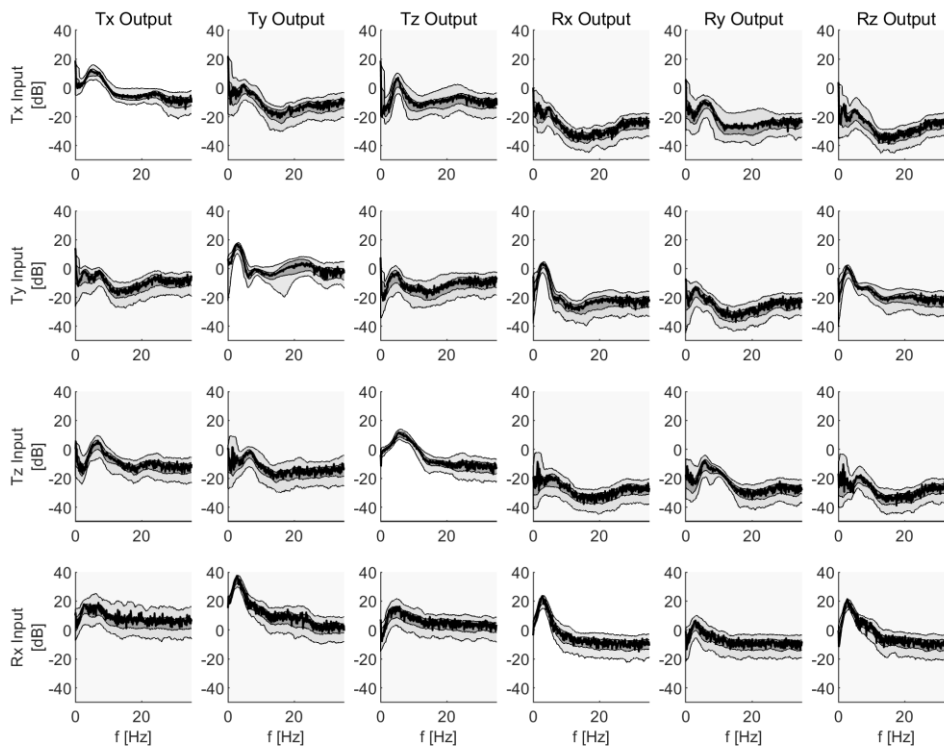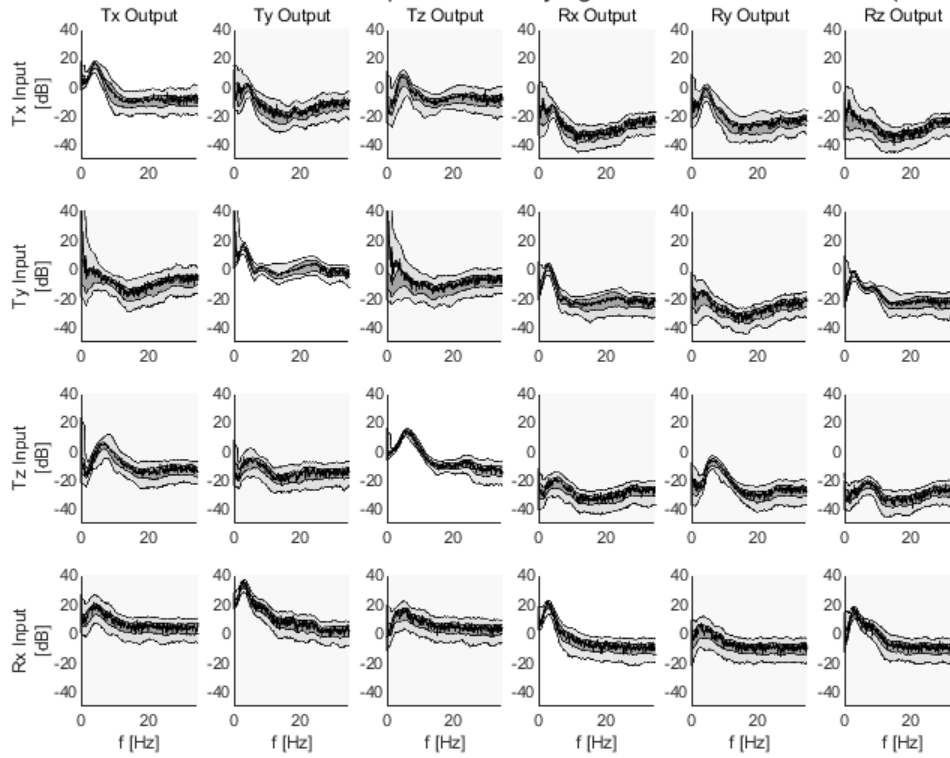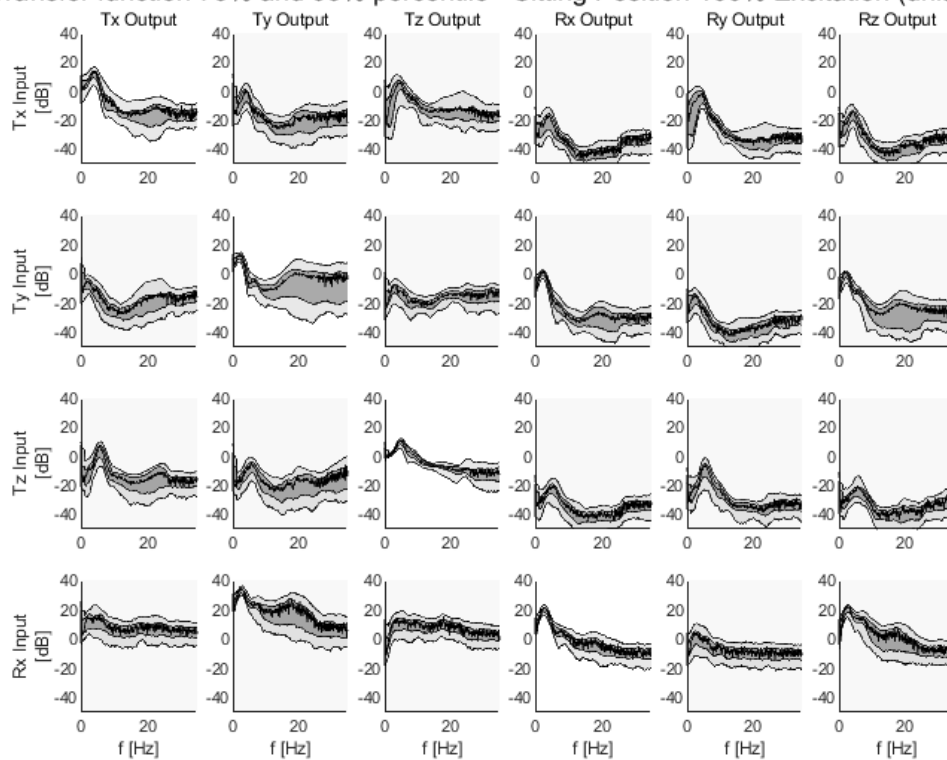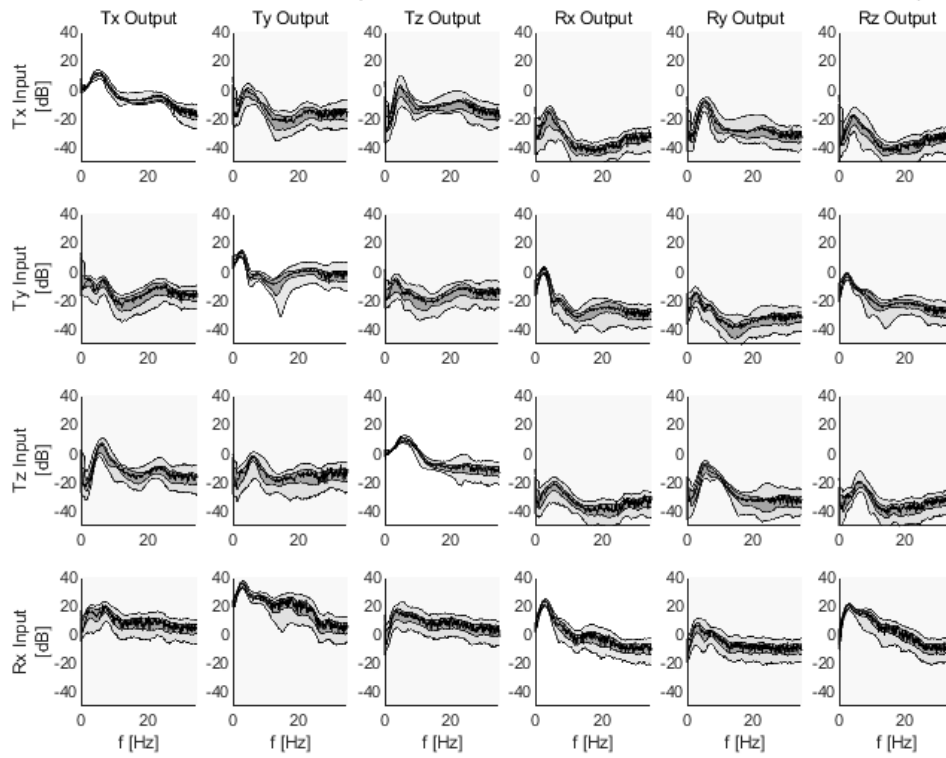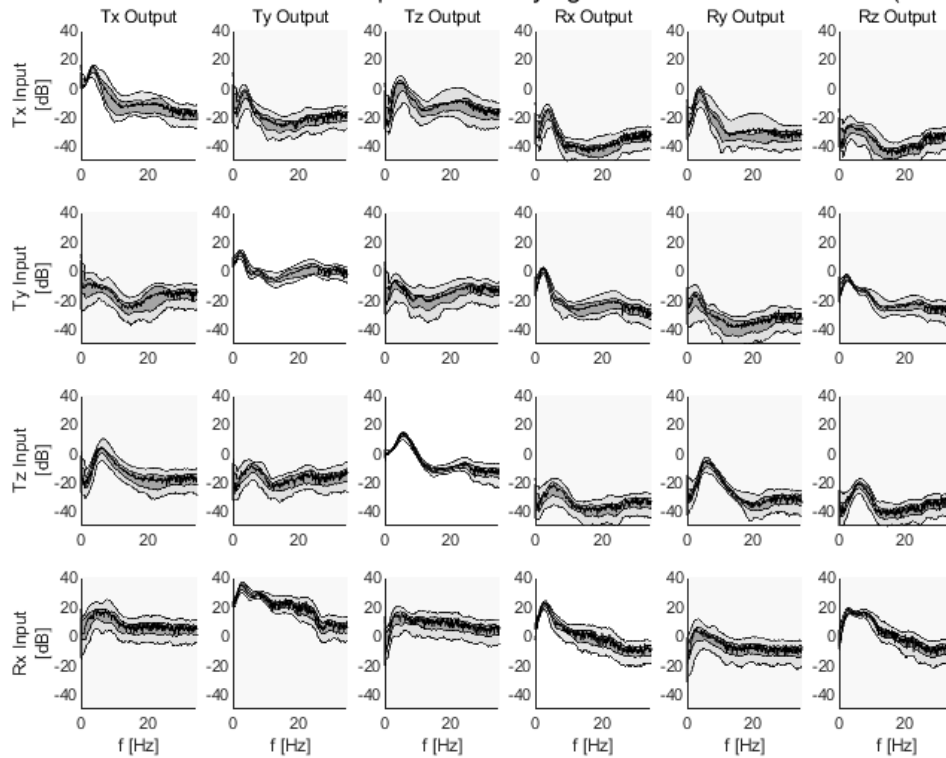Transfer function 75% and 95% percentile - Reclined Position 100% Excitation (uniaxial)

Transfer function 75% and 95% percentile - Lying Position 100% Excitation (uniaxial)

E. Declaration of Consent and Selection of Questionnaires

<u>Volunteer Information Sheet and Declaration of Consent</u>

Sehr geehrte Damen und Herren,
hiermit bitten wir Sie an einer wissenschaftlichen Studie zum Thema Reisekrankheit, auch bekannt unter den Begrifflichkeiten Kinetose bzw. Motion Sickness, im Kontext autonomer Fahrszenarien teilzunehmen. Wir freuen uns, dass Sie sich für dieses Forschungsprojekt interessieren!

Der folgende Text dient dazu, Sie über das Ziel der Untersuchung sowie das genaue Vorgehen zu informieren. Wie Sie bereits wissen, besteht die Studie aus <u>zwei/drei Fahrversuchen</u>, die an zwei bzw. drei separaten Tagen stattfinden werden. Die Termine wurden vorab mit Ihnen vereinbart.

Bitte lesen Sie sich die Informationen aufmerksam durch. Wenn Sie Fragen haben, beantworten wir diese gerne. Anschließend werden wir Sie bitten, uns durch Ihre Unterschrift Ihre Einwilligung zur Teilnahme zu geben und Ihre Kenntnisnahme von der vorliegenden Information zu bestätigen. Auf Wunsch erhalten Sie eine Kopie der Einwilligungserklärung. Zudem kann die Einwilligungserklärung jederzeit widerrufen werden.

Die Durchführung der Studie erfolgt durch den Fachbereich Ergonomie bei der Daimler AG in Sindelfingen. Versuchsleiter ist Dominique Bohrmann:

Dominique Bohrmann M.Eng.	Fachabteilung Ergonomie – Daimler AG
E-Mail: dominique.bohrmann@daimler.com	E-Mail: ██████████████████
Daimler AG	Daimler AG
70546 Stuttgart Deutschland	70546 Stuttgart Deutschland

Ziel und Zweck des Experiments
Die Gewährleistung des körperlichen Wohlbefindens der Insassen autonomer Fahrzeuge ist eine wichtige Ergonomie-Aufgabe, die im Zuge der aktuellen technischen Entwicklungen weiter an Bedeutung gewinnt. Ziel der Studie ist es, Faktoren zu ermitteln, welche das subjektive Erleben einer autonomen Fahrsituation in Form von Reisekrankheitssymptomen beeinflussen. Darüber hinaus stellt das Auftreten möglicher Symptome ein potentielles Risiko bei einer Übernahmeaufforderung des Fahrzeuges dar. Je nach Wohlbefinden und körperlichen Zustand ist es denkbar, dass die Fahrtüchtigkeit und/oder Reaktionsfähigkeit des Fahrers eingeschränkt ist. Die gewonnenen Erkenntnisse der Untersuchung können somit genutzt werden, um gezielte Maßnahmen im Sinne eines Komfort- und Sicherheitsgewinns zu ergreifen.

Ablauf, Dauer und Inhalt des Experiments
Sie werden als Mitfahrer/in im hinteren Bereich einer Mercedes-Benz V-Klasse Platz nehmen. Der Versuch dauert inkl. Vor- und Nachbefragung ca. 90 bis 120 Minuten. Während einer 20-minütigen Fahrt werden Sie die Aufgabe bekommen einem Tablet zu lesen. Die Fahrt ist in 4 Abschnitte à 5 Minuten aufgeteilt. Während jedes Fahrzyklus werden Sie, neben der Leseaufgabe, einen Reaktionstest durchführen. Beim Reaktionstest ertönt in zufälligen Abständen ein akustisches Signal, auf dieses reagieren Sie so schnell wie möglich durch einen Tastendruck der Leertaste vor Ihnen. Wir bitten Sie, sich ganz auf den Lesestoff zu konzentrieren und die Leseaufgabe nur zu unterbrechen, wenn Sie das akustische Signal des Reaktionstests hören, nach dem Tastendruck konzentrieren Sie sich wieder auf den Lesestoff. In regelmäßigen Abständen erscheinen auf dem Tablet Fragen bezüglich Ihres Befindens.

> **Um die Aussagekraft der Ergebnisse zu maximieren, bitten wir Sie, die vorgegebene Körperhaltung während der Fahrt bestmöglich bei zu behalten.**

Datenerfassende Systeme

Neben der subjektiven Auskunft über Ihr aktuelles Wohlbefinden (Motion Sickness Assessment Questionnaire bzw. Fast Motion Sickness Scale) und Anfälligkeit bzgl. Reisekrankheit (Motion Sickness Susceptibility Questionnaire) fließen darüber hinaus physiologische Maße in die Erhebung mit ein. Messgeräte zur Erfassung der Herzfrequenz, der Hautleitfähigkeit und Körperkerntemperatur werden dafür vor der Fahrt an Ihrem Oberkörper und an ihrem Ohr befestigt. Ziel ist es ihr aktuelles Wohlbefinden anhand physiologischer Messgrößen zu objektivieren und zu quantifizieren. Um zu untersuchen, ob mit steigender Reisekrankheit die Leistungsfähigkeit abnimmt und ggfs. die Fahrtüchtigkeit eingeschränkt ist, werden Sie während den Fahrten einen Reaktionstest durchführen. Mit Ihrem Einverständnis wird Ihre Versuchsteilnahme auf Video aufgezeichnet, um die Kopfbewegung bzw. Kopfpose im Raum sowie ein Verhaltenscluster zur Versuchsüberwachung zu erfassen. Diese Information soll als Prädiktor für die Entwicklung des Komfortempfindens dienen.

Wir werden Ihnen vor und nach der Fahrt jeweils einen Fragebogen vorlegen. Bitte beantworten Sie die Fragen ehrlich und möglichst intuitiv – das heißt ohne langes Nachdenken. Sollten Sie selbst Fragen haben, können Sie diese natürlich jederzeit stellen.

Risiken, die mit einer Teilnahme verbunden sind

Da der Fahrversuch auf einem Prüfgelände stattfindet und ein geübter Fahrer zum Einsatz kommt, wird das Gefährdungsrisiko einer üblichen Fahrt im realen Straßenverkehr nicht überschritten. In Abhängigkeit der individuellen Anfälligkeit kann es sein, dass während der Durchführung des Fahrversuchs Symptome von Kinetose (Reisekrankheit) auftreten. Unter diesen Umständen bitten wir Sie, den Versuch unverzüglich abzubrechen.

Hintergrundwissen: Kinetose (Reisekrankheit)

Kinetose beschreibt eine Symptommanifestation, die bei passiven Bewegungsexpositionen auftreten kann und sich durch verschiedene Ausprägungsformen von Müdigkeit, Desinteresse, Kopfschmerzen, Schwindel, Unwohlsein und/oder Übelkeit auszeichnet. Symptome können über Minuten bis Stunden nach der Bewegungsexposition andauern.

Ein Ausschluss von der Studie erfolgt:
- unter Einfluss von Alkohol, Drogen und wahrnehmungs/bewegungsbeeinträchtigenden Medikamenten,
- wenn das System aus physiologischen Aspekten nicht angewendet werden kann,
- bei Personen unter 18 Jahren und sonstigen schutzbedürftigen Personengruppen, z.B. Schwangere oder
- Vorerkrankungen des Vestibularapparates und/oder des Herz-Kreislaufsystems bestehen.

Freiwilligkeit

Die Teilnahme am Experiment ist freiwillig. Sie können dieses jederzeit ohne Angabe von Gründen und ohne Nachteile beenden. Bei Unklarheiten und Fragen wenden Sie sich gerne an die Versuchsleitenden. Bei Unwohlsein oder Schmerzen brechen Sie den Versuch bitte umgehend ab. Eine verschuldensunabhängige Versicherung wurde nicht abgeschlossen. Sie führen die Versuche daher auf eigene Verantwortung durch.

Persönlicher Nutzen

Es besteht kein persönlicher Nutzen für Sie.

Informationen zum Datenschutz

In dieser Studie ist die Fachabteilung Ergonomie der Daimler AG für die Datenverarbeitung verantwortlich. Ihre Daten werden ausschließlich im Rahmen der Dissertation von Dominique Bohrmann zum Themenkomplex der Reisekrankheit verwendet. Dazu gehören personenidentifizierende Daten wie Name, Anschrift und sensible personenbezogene Gesundheits- bzw. Physiodaten sowie Video- und Fotodaten. Alle unmittelbar Ihre Person identifizierenden Daten, wie Name, Geburtsdatum, Anschrift werden durch einen Identifizierungscode ersetzt (pseudonymisiert). Pseudonymisierung bedeutet, dass persönliche und Versuchs-/Interviewdaten getrennt aufbewahrt werden. Des Weiteren versichern wir Ihnen, dass diese Daten auch nicht wieder zusammengeführt werden. Dies schließt eine Identifizierung Ihrer Person durch Unbefugte weitgehend aus. Sollten Sie einverstanden sein, dass Ihre Teilnahme auf Video oder Foto aufgezeichnet bzw. dokumentiert wird, so wird Ihr Gesicht (sofern es auf den Aufnahmen zu erkennen ist) umgehend nach Abschluss der Studienauswertung unkenntlich gemacht oder das gesamte Video- und Fotomaterial gelöscht. Die physiologischen Daten, Leistungskennwerte, Beschleunigungsdaten, Verhaltens- sowie Fragebogenergebnisse und soweit vorhanden Video- und Fotomaterial werden weiterverarbeitet, ausgewertet und in Form von wissenschaftlichen Abhandlungen anonymisiert veröffentlicht. Anonymisierung bedeutet, dass aus den Daten nicht, oder nur mit unverhältnismäßig hohem Aufwand, auf die Person zurückgeschlossen werden kann.

Ihre Daten werden unter Einhalt der Datenschutzbestimmungen auf einem Passwort gesicherten Laufwerk gespeichert, auf das ausschließlich die Versuchsleitung Zugriff hat. Die Daten werden in Anlehnung an die Vorschriften der „guten wissenschaftlichen Praxis" der TU München nach Ablauf von 10 Jahren gelöscht.

Die Einwilligung zur Verarbeitung Ihrer Daten ist freiwillig, Sie können jederzeit die Einwilligung ohne Angabe von Gründen und ohne Nachteile für Sie widerrufen. Sie haben das Recht, Auskunft über die Sie betreffenden Daten zu erhalten, auch in Form einer unentgeltlichen Kopie. Darüber hinaus können Sie die Berichtigung oder Löschung Ihrer Daten verlangen. Wenden Sie sich in diesen Fällen an den Verantwortlichen der Studie Dominique Bohrmann.

Im Falle einer Beschwerde wenden Sie sich an:

Teamleiter Ergonomie
E-Mail: ████████████████
Daimler AG
70546 Stuttgart Deutschland

Oder an:

Landesamt für Datenschutzaufsicht
Promenade 27
91522 Ansbach
Tel.: 0981/53-1300
Fax: 0981/53-981300
E-Mail: poststelle@lda.bayern.de

_____   _____

Ort, Datum   Unterschrift Versuchsleiter

Einwilligungserklärung

Hiermit willige ich, _____, ein, an der Untersuchung zum Thema Reisekrankheit bei hochautomatisierten Fahrszenarien, unter der Leitung von Dominique Bohrmann, teilzunehmen. Ich habe die Probandeninformation und Einwilligungserklärung gelesen, verstanden und bestätige mit meiner Unterschrift, dass ich an dieser Untersuchung freiwillig teilnehme. Zudem bestätige ich hiermit, dass ich weder chronische Herz-Kreislauf-Beschwerden noch Erkrankungen des Gleichgewichtsorgans besitze oder weitere beschriebene Ausschlusskriterien der Probandeninformation erfülle.

Außerdem willige ich der beschriebenen Vorgehensweise der Datenverarbeitung ein. Mit der Pseudonymisierung sowie Speicherung der erhobenen Daten (Physiologische Messdaten, Leistungskennwerte, Fragebogenergebnisse, Verhaltensmessungen, Beschleunigungsdaten und sofern eine Zustimmung erfolgt die Video- und Fotomaterial) und mit der in der Probandeninformation beschriebenen Weiterverarbeitung der Daten bin ich einverstanden. Mir ist bekannt, dass bei der Versuchsfahrt Ausprägungen von Reisekrankheit auftreten können und die mit einem Fahrversuch verbundenen Unfallrisiken bestehen. Die Teilnahme am Experiment erfolgt auf eigenes Risiko. Alle meine Fragen wurden beantwortet und ich habe derzeit keine weiteren Fragen mehr. Sollten sich während der Untersuchung Fragen ergeben, kann ich mich jederzeit an den Versuchsleiter wenden. Zudem willige ich ein, dass meine Daten erhoben und 10 Jahre gespeichert und genutzt werden können.

_____, _____

Ort, Datum   Unterschrift

Einwilligung zur Aufzeichnung von Video- und Fotomaterial

Mit der folgenden Unterschrift willige ich ein, dass im Rahmen der Versuchsdokumentation Video- und Fotoaufnahmen von mir gemacht werden. Diese dienen in erster Linie zur Plausibilisierung von Versuchsdaten (z.B. falls Unstimmigkeiten auftreten) und zur Analyse von Verhaltens- und Bewegungsmuster

_____, _____

Ort, Datum   Unterschrift

Einwilligung zur Veröffentlichung

Ich stimme zu, dass die im Rahmen der Messung und Versuchsdokumentation von mir gemachten Daten, Video- und Fotodaten für die Veröffentlichung der Forschungsergebnisse verwendet werden dürfen. Dabei werde ich so weit wie möglich unkenntlich gemacht, sodass kein Rückschluss auf mich als Person möglich ist

_____, _____

Ort, Datum   Unterschrift

Auf Wunsch erhalten Sie eine Kopie der Einwilligungserklärung!
Die Einwilligungserklärung kann jederzeit widerrufen werden!

Motion Sickness Susceptiblity Questionnaire (MSSQ) – Short Form

Fragebogen zur Anfälligkeit für Bewegungskrankheit (MSSQ-Short)

Mit diesem Fragebogen wollen wir herausfinden, wie anfällig Sie für Bewegungskrankheit sind und bei welchen Arten von Bewegung diese am meisten auftritt. Mit Krankheit ist in diesem Falle gemeint, dass Sie sich unwohl fühlen, Ihnen übel wird oder Sie sich tatsächlich übergeben müssen.

1.   Ihre KINDHEITS-Erfahrungen (vor dem 12. Lebensjahr)

Bitte geben Sie für jede der folgenden Transportarten oder Aktivitäten an, **wie häufig** Ihnen dabei als KIND (vor dem 12. Lebensjahr) **übel** wurde oder Sie sich **unwohl** fühlten.

 (Bitte setzen Sie ein Kreuz in der entsprechenden Zelle.)

	nie	selten	manchmal	häufig	keine Erfahrung
Autos					
Busse					
Züge					
Flugzeuge					
Kleine Boote					
Schiffe, z.B. Kanalfähren					
Schaukeln auf Spielplätzen					
Karussells auf Spielplätzen					
Achterbahnen					

2.   Ihre Erfahrungen der LETZTEN 10 JAHRE (ungefähr)

Bitte geben Sie für jede der folgenden Transportarten oder Aktivitäten an, **wie häufig** Ihnen dabei in den (ungefähr) LETZTEN 10 JAHREN **übel** wurde oder Sie sich **unwohl** fühlten.

(Bitte setzen Sie ein Kreuz in der entsprechenden Zelle.)

	nie	selten	manchmal	häufig	keine Erfahrung
Autos					
Busse					
Züge					
Flugzeuge					
Kleine Boote					
Schiffe, z.B. Kanalfähren					
Schaukeln auf Spielplätzen					
Karussells auf Spielplätzen					
Achterbahnen					

Motion Sickness Assessment Questionnaire (MASQ) and Fast Motion Sickness Scale (FMS)

Fragebogen zur Bewegungskrankheit (MSAQ)   Uhrzeit_____

Bitte bewerten Sie anhand der untenstehenden Skala, wie genau die folgenden Aussagen Ihre Erfahrung beschreiben.

überhaupt nicht 1——2——3——4——5——6——7——8——9 sehr stark

	1	2	3	4	5	6	7	8	9
1. Ich hatte ein unangenehmes Gefühl im Magen	☐	☐	☐	☐	☐	☐	☐	☐	☐
2. Ich fühlte mich schwach	☐	☐	☐	☐	☐	☐	☐	☐	☐
3. Ich fühlte mich verärgert/gereizt	☐	☐	☐	☐	☐	☐	☐	☐	☐
4. Ich fühlte mich schwitzig	☐	☐	☐	☐	☐	☐	☐	☐	☐
5. Ich fühlte mich unwohl	☐	☐	☐	☐	☐	☐	☐	☐	☐
6. Ich fühlte mich schwindelig	☐	☐	☐	☐	☐	☐	☐	☐	☐
7. Ich fühlte mich schläfrig	☐	☐	☐	☐	☐	☐	☐	☐	☐
8. Ich fühlte mich feuchtkühl/schwitzte kalt	☐	☐	☐	☐	☐	☐	☐	☐	☐
9. Ich fühlte mich verwirrt/desorientiert	☐	☐	☐	☐	☐	☐	☐	☐	☐
10. Ich fühlte mich müde/ermüdet	☐	☐	☐	☐	☐	☐	☐	☐	☐
11. Mir wurde übel	☐	☐	☐	☐	☐	☐	☐	☐	☐
12. Ich fühlte mich erhitzt/warm	☐	☐	☐	☐	☐	☐	☐	☐	☐
13. Ich fühlte mich benommen	☐	☐	☐	☐	☐	☐	☐	☐	☐
14. Ich hatte das Gefühl, mich zu drehen	☐	☐	☐	☐	☐	☐	☐	☐	☐
15. Ich hatte das Gefühl, mich gleich zu übergeben	☐	☐	☐	☐	☐	☐	☐	☐	☐
16. Ich fühlte mich unruhig	☐	☐	☐	☐	☐	☐	☐	☐	☐

Start Baseline_____   **Ende Baseline**_____

Abfrage FMS alle 5 min von Beginn an

FMS Baseline

Uhrzeit_____   Temperatur_____°C

Wie übel ist Ihnen jetzt im Moment auf einer Skala von 0-20, wobei 0 keine Übelkeit bedeutet und 20 starke Übelkeit?

0—1—2—3—4—5—6—7—8—9—10—11—12—13—14—15—16—17—18—19—20

Uhrzeit_____   Temperatur_____°C

Wie übel ist Ihnen jetzt im Moment auf einer Skala von 0-20, wobei 0 keine Übelkeit bedeutet und 20 starke Übelkeit?

0—1—2—3—4—5—6—7—8—9—10—11—12—13—14—15—16—17—18—19—20

Uhrzeit_____   Temperatur_____°C

Wie übel ist Ihnen jetzt im Moment auf einer Skala von 0-20, wobei 0 keine Übelkeit bedeutet und 20 starke Übelkeit?

0—1—2—3—4—5—6—7—8—9—10—11—12—13—14—15—16—17—18—19—20

Uhrzeit_____   Temperatur_____°C

Wie übel ist Ihnen jetzt im Moment auf einer Skala von 0-20, wobei 0 keine Übelkeit bedeutet und 20 starke Übelkeit?

0—1—2—3—4—5—6—7—8—9—10—11—12—13—14—15—16—17—18—19—20

Uhrzeit_____   Temperatur_____°C

Wie übel ist Ihnen jetzt im Moment auf einer Skala von 0-20, wobei 0 keine Übelkeit bedeutet und 20 starke Übelkeit?

0—1—2—3—4—5—6—7—8—9—10—11—12—13—14—15—16—17—18—19—20

FMS bei Abbruch

Uhrzeit_____   Temperatur_____°C

Wie übel ist Ihnen jetzt im Moment auf einer Skala von 0-20, wobei 0 keine Übelkeit bedeutet und 20 starke Übelkeit?

0—1—2—3—4—5—6—7—8—9—10—11—12—13—14—15—16—17—18—19—20

Performance Measurment – BDPQ-test

Anmerkungen. Die Buchstabenfolgen wurden im Original in Schriftgröße 20 (Calibri) gedruckt. Es wurden acht Versionen erstellt, das folgende Beispiel entspricht dem Übungsbogen.

Bitte markieren Sie alle Buchstaben b, wenn diesen der Buchstabe q folgt.

Sie haben 1 Minute Zeit für diese Aufgabe. Bitte arbeiten Sie so schnell Sie können und achten Sie gleichzeitig darauf, so wenige Fehler wie möglich zu machen.

Bitte markieren Sie nach Ablauf der Zeit die genaue Stelle in der Zeile, bis zu der Sie gekommen sind mit einem Strich.

Beispiel:

d b b p d p q d b <u>b</u> q p b b p p p b p p d d b b b p <u>b</u> q d p p <u>b</u> q b| d q

q	d	q	p	b	b
d	q	b	d	q	p
p	b	b	b	d	q
b	d	p	d	b	p
b	p	p	b	d	p
p	q	p	q	p	d
q	b	p	q	b	d
q	p	p	q	b	q
q	d	d	q	d	p
p	d	b	d	d	q
q	b	q	b	q	p
d	b	p	p	d	b
p	d	b	d	q	p
b	p	d	d	p	q
b	b	b	p	b	b
d	q	q	b	p	d
p	q	b	d	q	p
p	q	p	b	q	q
b	p	p	p	d	b
b	q	b	b	d	d
d	d	p	p	q	q
p	d	d	d	b	b
q	b	q	d	b	p
b	p	q	d	b	p
q	b	p	q	q	p
q	p	b	d	d	b
d	q	q	p	q	q
q	d	p	d	p	q
q	b	d	p	q	p
b	b	b	q		

- Extract -